

# NISTIR 8271 DRAFT SUPPLEMENT

## Face Recognition Vendor Test (FRVT) Part 2: Identification

Patrick Grother  
Mei Ngan  
Kayee Hanaoka  
*Information Access Division  
Information Technology Laboratory*

This document is a draft supplement of [NIST Interagency Report 8271](#)

2021/10/28

# NISTIR 8271 DRAFT SUPPLEMENT

## Face Recognition Vendor Test (FRVT) Part 2: Identification

Patrick Grother  
Mei Ngan  
Kayee Hanaoka  
*Information Access Division  
Information Technology Laboratory*

This document is a draft supplement of [NIST Interagency Report 8271](#)

October 2021



U.S. Department of Commerce  
*Gina M. Raimondo, Secretary*

National Institute of Standards and Technology  
*James K. Olthoff, Performing the Non-Exclusive Functions and Duties of the Under Secretary of Commerce for Standards and  
Technology & Director, National Institute of Standards and Technology*

## RELEASE NOTES

**2021-10-28:** The 1:N track of the FRVT remains open.

- ▷ This document is the ninth draft update to [NIST Interagency Report 8271](#). It includes results for algorithms recently submitted by three first-time participants (20Face, Fujitsu Research and Development Center, and Vision-Box), and five returning participants (Alchera, Gorilla Technology, Tevian, Thales-Cogent, and Visidon). Visidon
- ▷ Both the main [1:N results page](#) and the small-gallery [paperless travel page](#) have been updated.

**2021-09-21:** The 1:N track of the FRVT remains open. Three news items:

- ▷ This document is the tenth draft update to [NIST Interagency Report 8271](#). It includes results for algorithms recently submitted by six first-time developers: Cubox, Fincore, HyperVerge, Qnap Security, Staqu Technologies, and Tripleize (Aize, 3-ize).
- ▷ It includes results also for four returning developers: Cognitec Systems, Incode Technologies, Innovatrics, Neurotechnology, and Rank One Computing.

**2021-08-02:** The 1:N track of the FRVT remains open. Three news items:

- ▷ This document is the ninth draft update to [NIST Interagency Report 8271](#). It includes results for algorithms recently submitted by eight participants: Cyberlink Corp, NEC Corp, N-Tech Lab, Realnetworks Inc., Sensetime Group, Veridas Digital, Viettel Group, and Vigilant Solutions.
- ▷ Algorithms submitted since July 24 will be included in the next update scheduled for September 9, 2021.
- ▷ A new report, NIST Interagency Report 8381 - FRVT Part 7: Identification for Paperless Travel and Immigration, has been released [[PDF](#), [webpage](#)]. It documents the use of FRVT 1:N algorithms in positive access control and immigration status update travel applications where the enrolled population size is as low as 420 people for aircraft boarding, and 42 000 for an airport security line. These population sizes are much smaller than those used in the main [1:N evaluation](#). Going forward, we will update the report and webpage with results for new algorithms.

**2021-07-07:** The 1:N track of the FRVT remains open. One update:

- ▷ This document is the eighth draft update to [NIST Interagency Report 8271](#). It include results for an algorithm from one participant: Kakao Enterprises.

**2021-06-22:** The 1:N track of the FRVT remains open. Three updates:

- ▷ This is the seventh draft of the update to [NIST Interagency Report 8271](#). It includes results for algorithms from three new participants: Line Corporation, Rendip, and Samsung S1 Corp.
- ▷ We have also added results for algorithms from five returning developers: Imagus Technology, Kneron, Tevian, Visidon, and Xforward AI Technology.
- ▷ The algorithm-specific report cards (examples: [1](#), [2](#), and [3](#)) now include figures showing how low threshold values can be used to reduce candidate list lengths for human review, while (usually) elevating miss rates (FNIR) only modestly. The reports also feature some minor additions and clarifications.

**2021-03-26:** The 1:N track of the FRVT remains open. Three updates:

- ▷ This is the sixth draft of the update to [NIST Interagency Report 8271](#). It includes results for algorithms from three returning developers: Neurotechnology, Guangzhou Pixel Solutions, and Tech5 SA.
- ▷ We have added results on the webpage and in the report for a new ageing dataset in which border crossing photos are searched against a gallery of border crossing photos collected between 10 and 15 years prior to the mated search photos. See section [2](#) for a description of the images. Table [1](#) has a new entry describing the experiment.

- ▷ We will mostly discontinue running the mugshot ageing test, reserving it for algorithms that show high accuracy on the new border-crossing set.

**2021-03-26:** Regarding the fifth draft of the update to [NIST Interagency Report 8271](#):

- ▷ In addition have added results for first algorithms from two new participants: Viettel Group and Veridas Digital Authentication Solutions.
- ▷ We have added results for algorithms from two returning developers: Idemia and Cognitec Systems.
- ▷ In addition to the report, the [results page](#) and its hyperlinked [report cards](#) have been updated.

**2021-02-08:** Regarding the fourth draft of the update to [NIST Interagency Report 8271](#):

- ▷ We have added results for eight algorithms submitted by eight developers: Cyberlink, Dermalog, Imagus, Paravision, Sensetime, Trueface, Vigilant Solutions, and X-Forward AI. With the exception of Trueface, all of these developers have participated previously.
- ▷ We anticipate updating this report again in the first week of March 2021.
- ▷ The main [results page](#) has been revised with tabs for the investigative and lights-out identification tables, and a new tab dedicated to speed and resource consumption.
- ▷ The report cards (example [here](#)) hyperlinked from the [results page](#) have been revised to improve content and format.

**2020-12-14:** Regarding third draft of the update to [NIST Interagency Report 8271](#):

- ▷ We have added results for fifteen algorithms submitted by thirteen developers. The four first-time participants are: Acer, Akurat Satu Indonesia, Canon, and Xforward AI Technology. The ten returning developers are: AllGoVision, Cyberlink Corp, Dahua Technology, Deepglint, Guangzhou Pixel Solutions, IIT Vision, Innovatrics, Rank One Computing, Scanovate, Sensetime Group, Synesis, and VisionLabs.
- ▷ We have added two new datasets to the evaluation: First a set of “visa-border” photos, representing search of an airport immigration lane photo against a database of closely ISO standard portraits; second a “visa-kiosk” set representing search of a photo collected in a registered traveller kiosk against the same ISO portrait gallery. The images are described in section 2.1.
- ▷ As in previous reports, we include results for searching mugshots against a mugshot gallery containing a single image of each of 12 million people. However we have suspending running searches against a gallery in which multiple lifetime photos per person are present, because this is computationally expensive. We retain a N = 3 million search test dedicated to ageing in which mugshots taken up to 18 years after the first photograph are searched - see Table 6.
- ▷ Tables containing computational resource information, Table 2 . . . , now include duration of the finalization step, in which search algorithms can, at their option, build fast-search data structures.
- ▷ We have linked revised per-algorithm PDF report cards from the main [results page](#).
- ▷ We have regenerated all figures and tables to drop algorithms submitted before June 2018. Results for prior algorithms appear in [archived editions](#) of this report.
- ▷ Going forward, we anticipate producing more frequent updates to this report. Developers may submit one algorithm to this evaluation every four calendar months.

**2020-03-24:** Regarding the second draft of the update to [NIST Interagency Report 8271](#):

- ▷ Adds results for three algorithms from three developers, Dermalog, Innovatrics, and Synesis.
- ▷ Adds Table 6 on ageing showing the increase in false negative rates with time elapsed between two photos. Some of the results were contained in graphs in prior editions of this report, but the table adds results for some newly submitted algorithms.

- ▷ Adjusts frontal mugshot results (for recent and lifetime consolidated galleries) to include the effect of removing some images that should not have been included in image test sets. These images were mostly profile views, images of tattoos containing faces, images of faces on tee shirts, and images of photographs on walls behind the intended subject. This affects many tables and reduces false negative identification rates for all algorithms. The reduction is larger for “recent” enrollments than for “lifetime consolidated” ones with the consequence that accuracy on recent images is now superior.

**2020-02-26:** Regarding the first draft of the update to [NIST Interagency Report 8271](#):

- ▷ Adds results for 38 algorithms from 31 different developers, eleven of whom are entirely new to the 1:N track of FRVT. These are Allgovision, Cyberlink, Deepsea Tencent, Farbar F8, Imperial College London, Intsys MSU, Kedacom, Kneron, Pixelall, and Scanovate.

## DISCLAIMER

Specific hardware and software products identified in this report were used in order to perform the evaluations described in this document. In no case does identification of any commercial product, trade name, or vendor, imply recommendation or endorsement by the National Institute of Standards and Technology, nor does it imply that the products and equipment identified are necessarily the best available for the purpose.

## INSTITUTIONAL REVIEW BOARD

The National Institute of Standards and Technology's Research Protections Office reviewed the protocol for this project and determined it is not human subjects research as defined in Department of Commerce Regulations, 15 CFR 27, also known as the Common Rule for the Protection of Human Subjects (45 CFR 46, Subpart A).

## ACKNOWLEDGMENTS

The authors are grateful for the support and collaboration of the the Department of Homeland Security's Science & Technology Directorate (S&T), Office of Biometric Identity Management (OBIM), and Customs and Border Protection (CBP).

Additionally, the authors are grateful to staff in the NIST Biometrics Research Laboratory for infrastructure supporting rapid evaluation of algorithms.

## Executive Summary

This document is a draft revision of the September 2019 report [NIST Interagency Report 8271](#). That report gave extensive documentation of face recognition applied to mugshots. This report extends that by adding more two more challenging datasets containing images with serious departures from canonical frontal image standards. The report also adds results for algorithms submitted to NIST since in 2019 and 2020. The algorithms, which implement one-to-many identification of faces appearing in two-dimensional images, are prototypes from the research and development laboratories of mostly commercial suppliers, and are submitted to NIST as compiled black-box libraries implementing a NIST-specified C++ test interface. The report therefore does not describe how algorithms operate. The report lists accuracy results alongside developer names and will therefore be useful for comparison of face recognition algorithms and assessment of absolute capability. The report is accompanied by a [webpage](#) with sortable results.

The evaluation uses six datasets: frontal mugshots, profile view mugshots, desktop webcam photos, visa-like immigration application photos, immigration lane photos, and registered traveler kiosk photos. These datasets are sequestered at NIST, meaning that developers do not have access to them for training or testing. This aspect is important because face recognition algorithms are very often deployed without the developer having access to the customers image data. A possible exception to this would be in a cloud-based application where the operational image data is uploaded to a cloud operated by a face recognition developer.

The major result in NIST IR 8271 was that massive gains in accuracy have been achieved in the years 2013 to 2018 and these far exceed improvements made in the prior period, 2010 to 2013. While the industry gains were broad - at least 30 developers' algorithms outperformed the most accurate algorithm from late 2013, there remains a wide range of capability. While this report shows accuracy gains only over the period 2018-2020, the most accurate algorithm reported here is substantially more accurate than anything reported in NIST IR 8271. This is evidence that face recognition development continues apace, and that FRVT reports are but a snapshot of contemporary capability.

From discussion with developers, the accuracy gains stem from the adoption of deep convolutional neural networks. As such, face recognition has undergone an industrial revolution, with algorithms increasingly tolerant of poorly illuminated and other low quality images, and poorly posed subjects. One related result is that a few algorithms correctly match side-view photographs to galleries of frontal photos, with search accuracy approaching that of the best c. 2010 algorithms operating on purely frontal images. The capability to recognize under a 90-degree change in viewpoint - pose invariance - has been a long-sought milestone in face recognition research.

With good quality portrait photos, the most accurate algorithms will find matching entries, when present, in galleries containing 12 million individuals, with rank one miss rates of approaching 0.1%. The remaining errors are in large part attributable to long-run ageing, facial injury and poor image quality. Given this impressive achievement - close to perfect recognition - an advocate might claim that cooperative face recognition is a solved problem, a statement that can be refuted with the following context and caveats:

- ▷ **Mugshots vs. less constrained captures:** The low error rates reported here are attained using mostly excellent cooperative live-capture mugshot images collected with an attendant present. Recognition in other circumstances, particularly those without a dedicated photographic environment and human or automated quality control checks, will lead to declines in accuracy. This is documented here for side-view images, poorer quality webcam images, and, particularly, for newly introduced ATM-style kiosk photos that were not originally intended for automated face recognition. In this case, recognition error rates are much higher, often in excess of 20% even with the more accurate algorithms which variously remain intolerant of face cropping (at image edge) and of large downward head pitch.
- ▷ **Algorithm accuracy spectrum:** Recognition accuracy is very strongly dependent on the algorithm and, more

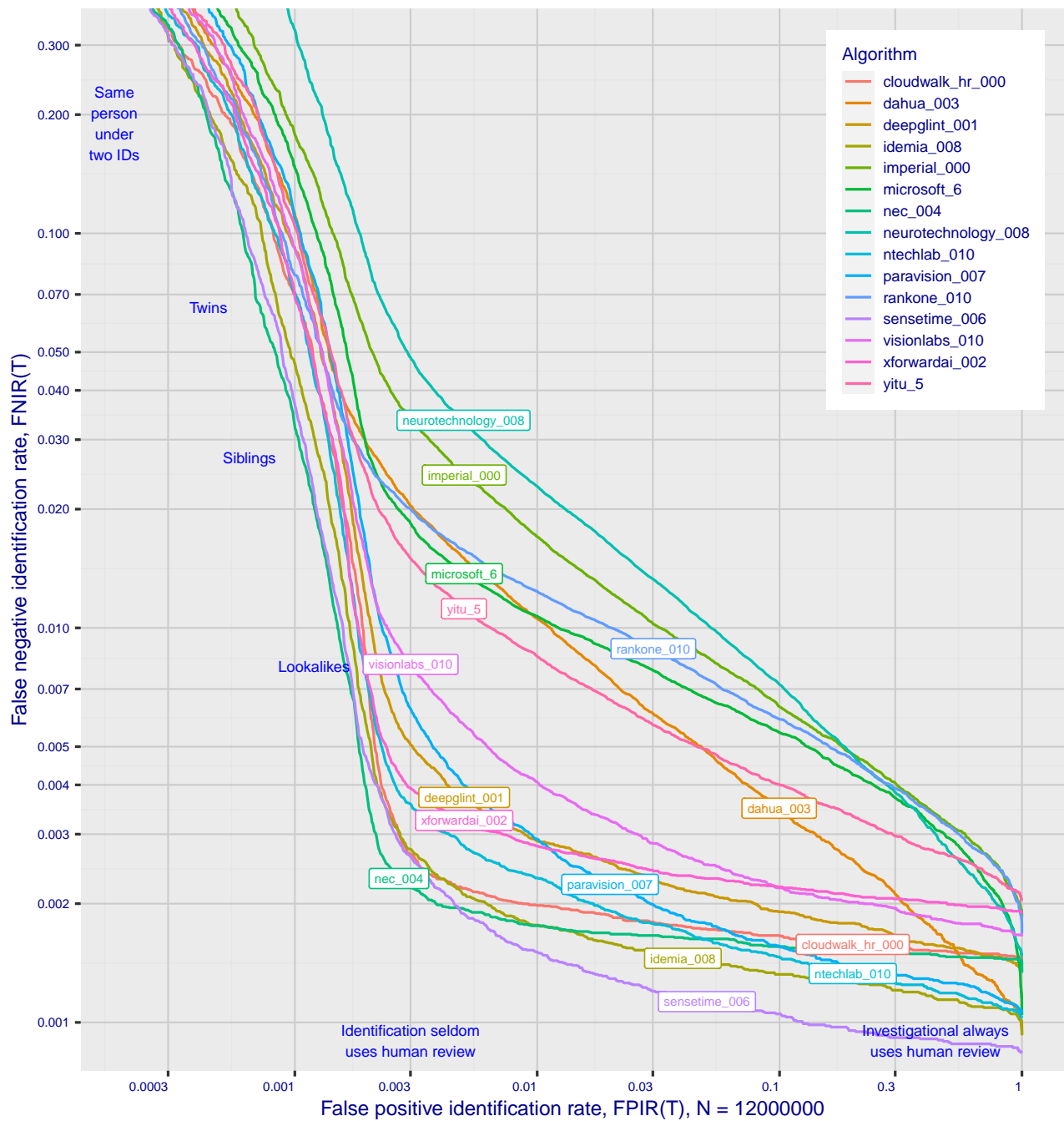


Figure 1: Identification miss rates across the false positive range.  $N = 12$  million individuals are enrolled with one recent image.

generally, on the developer of the algorithm. False negative error rates in a particular scenario range from a few tenths of one percent to beyond fifty percent. This is tabulated exhaustively later: For example Table 9 shows accuracy across datasets. Figure 1 here compares algorithms on mugshot searches in a consolidated gallery of 12 million subjects and 12 million photos. Many algorithms do not achieve the low error rates noted above, and while many of those may still be useful and valuable to end-users, only the most accurate excel on poor quality images and those collected long after the initial enrollment sample.

▷ **Versioning:** While results for up to ten algorithms from each developer are reported here, the intra-provider

accuracy variations are usually smaller than the inter-provider variations. That said different versions give an order of magnitude fewer misses. Some developers demonstrate speed-accuracy tradeoffs<sup>1</sup>. See Figs. 18, 19.

- ▷ **Low similarity scores:** In thousands of mugshot cases the correct gallery image is returned at rank 1 but its similarity score is nevertheless low, below some operationally required score threshold. This is not so important when face recognition is used for “lead generation” in investigational applications because human reviewers are specifically required to review potentially long candidate lists and the threshold is effectively 0. In applications where search volumes are higher and labor is not available to review the results from searches, a higher threshold must be applied. This reduces the length of candidate lists and false positive identification rates at the expense of increased false negative miss rates. The tradeoff between the two error rates is reported extensively later.
- ▷ **Population size:** As the number of enrolled subjects grows, some mates are displaced from rank one, decreasing accuracy. As tabulated later for N up to 12 million, false negative rates generally rise slowly with population size. This enables use of face recognition in very large populations. However in most positive and negative identification applications<sup>2</sup>, a score threshold is set to limit the rate at which non-mate searches produce false positives. This has the consequence that some mated searches will report the mate below threshold, i.e. a miss, even if it is at rank 1. The utility of this is that many non-mated searches will return no candidate identities at all. As the error-tradeoff characteristic shows, investigational miss rates on the right side are very low but then rise steadily (in the center region) as threshold is increased to support “lights-out” applications, and ultimately rise quickly (left side) as discussed below. Thus, if we demand that just one in one thousand non-mate searches produce any false positives, the most accurate algorithms there (Sensetime-004 and NEC-3) would fail on between 3 and 5% of mated searches. Even though the graph shows results for the most accurate algorithms, all but two would fail to find the mate in more than 8% of mated searches. While the two most accurate algorithms produce a relatively flat error tradeoff until the threshold is raised to limit false positives to about 1 in 400 non-mated searches<sup>3</sup>

Thereafter, as the threshold is raised to further reduce false positives, miss rates rise rapidly. This means that low false positive identification rates are inaccessible with these algorithms, a result that does not apply for ten-finger identification algorithms. The rapid rise occurs because the lower mate scores are mixed with very high non-mate scores, the low scores from poor image quality and ageing, the high non-mates from the presence of lookalikes persons (doppelgangers), twins (discussed next) and, ultimately, the presence of a few unconsolidated subjects i.e. persons present under multiple IDs.

- ▷ **False negatives from ageing:** A large source of error in long-run applications where subjects are not re-enrolled on a set schedule is ageing. Changes in facial appearance increase with the time elapsed between photographs. These will depress similarity scores and eventually cause false negatives. All faces age and while this usually proceeds in a graceful and progressive manner, drug use can accelerate this [28]. Elective surgery may be effective in delaying it although this has not been formally quantified with face recognition. As ageing is essentially unavoidable, it can only be mitigated by scheduled re-capture, as in passport re-issuance. To quantify ageing effects, we used the more accurate algorithms to enroll the earliest image of 3.1 million adults and then search

<sup>1</sup>For example, NEC-0 prepares templates much faster than NEC-2 but gives twenty times more misses. Dermalog-5 executes a template search much more quickly than Dermalog-6 but is also much less accurate.

<sup>2</sup>In a positive identification application such as a registered traveler system, a user is making an implicit claim to be enrolled in the system - most users will be. In a negative application, such as with deportees, the implicit claim is that the subject is not enrolled - most will not be.

<sup>3</sup>The gallery size here is 12 million people, one image per person. Given 331 201 non-mated searches, an exhaustive implementation of one-too-many search would execute almost 4 trillion comparisons. At a false positive identification rate of 0.0025 the number of false positives is, to first order, 828 corresponding to single-comparison false match rate of  $828 / 4 \text{ trillion} = 2.1 \cdot 10^{-10}$  i.e. about 1 in 5 billion. Strictly this FMR computation is meaningful only for algorithms that implement 1:N search using N 1:1 comparisons, which is not always the case.

with 10.3 million newer photos taken up to 18 years after the the initial enrollment photo. Figure 2 puts ageing into context by contrasting it with the increase in false negatives that occurs when the number of individuals in an enrollment database becomes larger and the chance of a false positive increases such that higher thresholds may become necessary<sup>4</sup>.

The Figure shows, from to bottom, increases in false negative identification rates (FNIR) with the algorithm being tested. This applies to increases due to  $N$  on the left side, and increases due to ageing on the right side. The relative spacing of the dots shows that for all algorithms the dependency of FNIR on  $N$  (up to 12 million) is considerably less than on  $\Delta T$  (up to 18 years).

In the inset table, accuracy is seen to degrade progressively with time, as mate scores decline and non-mates displace mates from rank 1 position. More accurate algorithms tend to be less sensitive to ageing. The more accurate algorithms give fewer errors after 18 years of ageing than middle tier algorithms give after four. Note also we do not quantify an ageing rate - more formal methods [2] borrowed from the longitudinal analysis literature have been published for doing so (given suitable repeated measures data). See Figures 60, 81 and 91.

<sup>4</sup>Some algorithms implement strategies to automatically adjust scores to account for increased population size. This relieves the system owner of having to increase thresholds as  $N$  increases.

This publication is available free of charge from: <https://doi.org/10.6028/NIST.IR.8271>

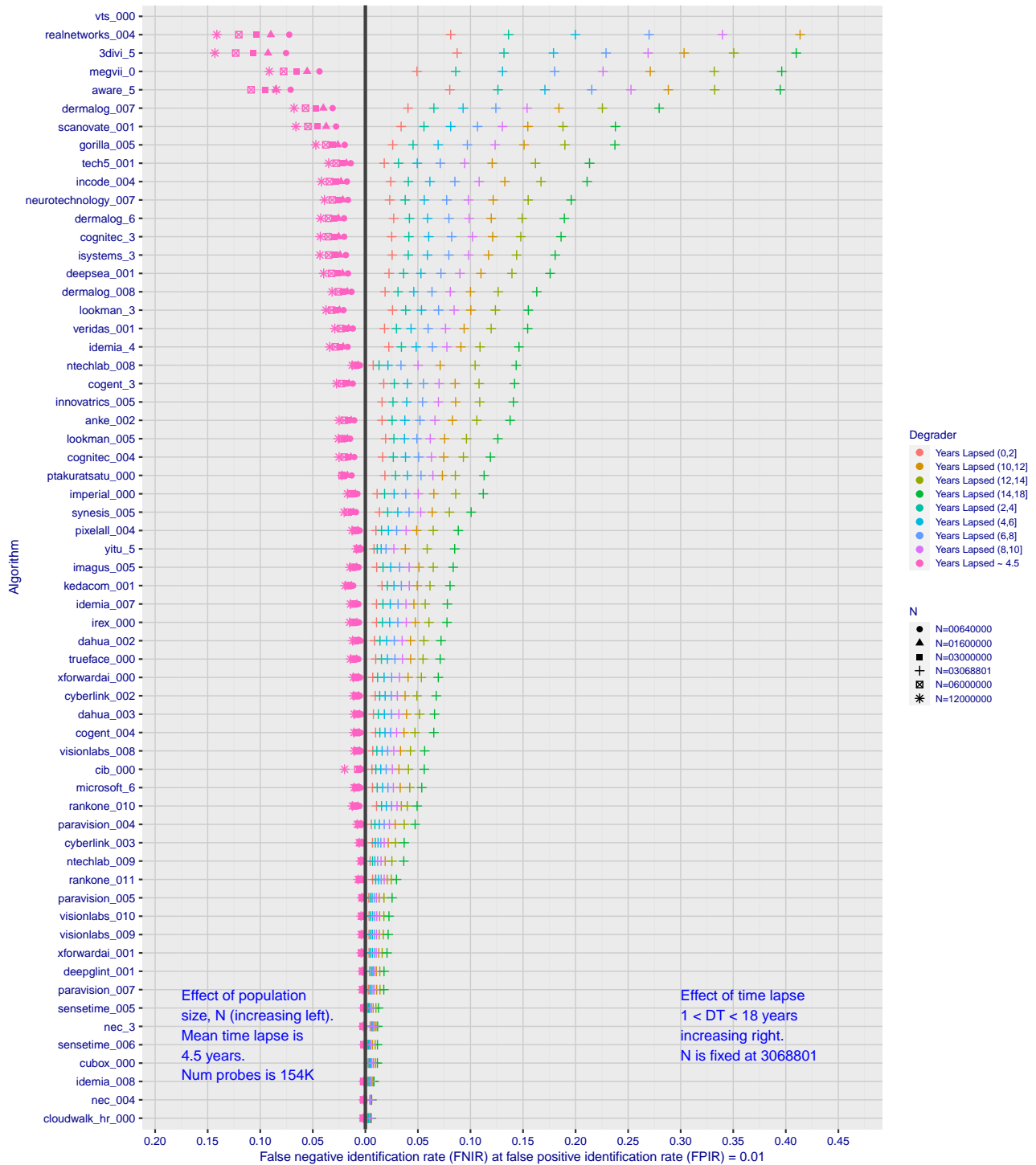


Figure 2: Identification miss rates as a function of enrolled population size,  $N$ , and time-lapse,  $\Delta T$ .

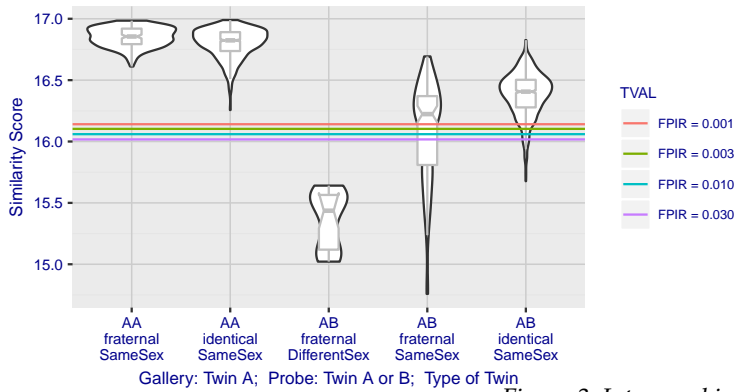


Figure 3: Intra- and inter-twin scores

- ▷ **False positives from twins:** By enrolling 640 000 mugshots, adding photos of one twin, and then searching photos of those subjects and their twin the inset figure shows, for one typical algorithm, the similarity is generally greater when searching twins against themselves (A) than when searching twins against their sibling (B) but very often still above even stringent thresholds i.e. those corresponding to one in one thousand searches producing a false positive. Thus twins will very often produce a high-scoring non-match on a candidate list and a false alarm in an online identification system. The plot of Fig. 3 shows that fraternal twins are sometimes correctly rejected at those thresholds - including most different sex twins (at center). Figure ?? shows substantially similar behavior for all algorithms tested. In an investigative search, a twin would typically appear at rank 1, or rank 2 if their sibling happened to also be the gallery. Twins (and triplets etc.) constituted 3.3% of all live births [17] in recent years<sup>5</sup>, and because that number is higher today than when the individuals in current adult databases were born, the false positives that arise from twins are now, and will increasingly be, an operational problem. Relative to the United States, twins are born with considerable regional variation. For example they are much less common in East Asia, and much more common in Sub-Saharan Africa [21].

The presence of twins in the mugshot database is inevitable given its size, around 12.3 million people. As this is not an insignificant sample of the domestic United States population, people with other familial ties will be present also. The data was collected over an extended period and because location information is not available, we are unable to estimate the proportion of the domestic population that is present in the dataset. However, if we assume twins are neither more or less disposed to arrest than the general population, we can estimate that hundreds of thousands of individuals in the dataset are twins. This will affect false positive rates because we randomly set aside 331 201 individuals for nonmate searches, and some proportion of those will be twins with siblings in the gallery.

- ▷ **Database integrity:** An operational error rate should be added to all false negative rates in this report reflecting the proportion of images in a real database that are un-matchable. Such anomalies arise from images that: do not contain a face; include multiple persons; cannot be decoded; are rotated by 90° or 180°; depict a face on clothing; and others introduced by a long tail of various clerical errors. While the mugshot trials in this report have been constructed to minimize such effects, they are a real problem in actual operations.

This report is being updated continuously as new algorithms are submitted to FRVT, and run on new datasets. Participation in the [one-to-many identification track](#) is independent of participation in the [one-to-one verification track](#) of FRVT.

<sup>5</sup>See the CDC's National Vital Statistics Report for 2017: <https://www.cdc.gov/nchs/data/nvsr/nvsr67/nvsr67.08-508.pdf>

## Scope and Context

**Audience:** This report is intended for developers, integrators, end users, policy makers and others who have some familiarity with biometrics applications. The methods and metrics documented here will be of interest to organizations engaged in tests of face recognition algorithms. Some of these have been incorporated in the ISO/IEC 19795 Part 1 Biometric Testing and Reporting Framework standard, now nearing [publication](#).

**Prior benchmarks:** Automated face recognition accuracy has improved massively in the two decades since initial commercialization of the various technologies. NIST has tracked that improvement through its conduct of regular independent, free, open, and public evaluations. These have fostered improvements in the state of the art. This report serves as an update to the [NIST Interagency Report 8271](#) on performance of face identification algorithms, published in September 2019.

**Demographics:** In December 2019, NIST published a first report on demographic dependencies in face recognition, [NIST Interagency Report 8280](#) that documented age, sex and race differentials in one-to-one and one-to-many false positive and false negative rates.

**Scope:** NIST IR 8271 documented recognition results for four databases containing in excess of 30.2 million still photographs of 14.4 million individuals. That constituted the largest public and independent evaluation of face recognition ever conducted. It includes results for accuracy, speed, investigative vs. identification applications, scalability to large populations, use of multiple images per person, images of cooperative and non-cooperative subjects.

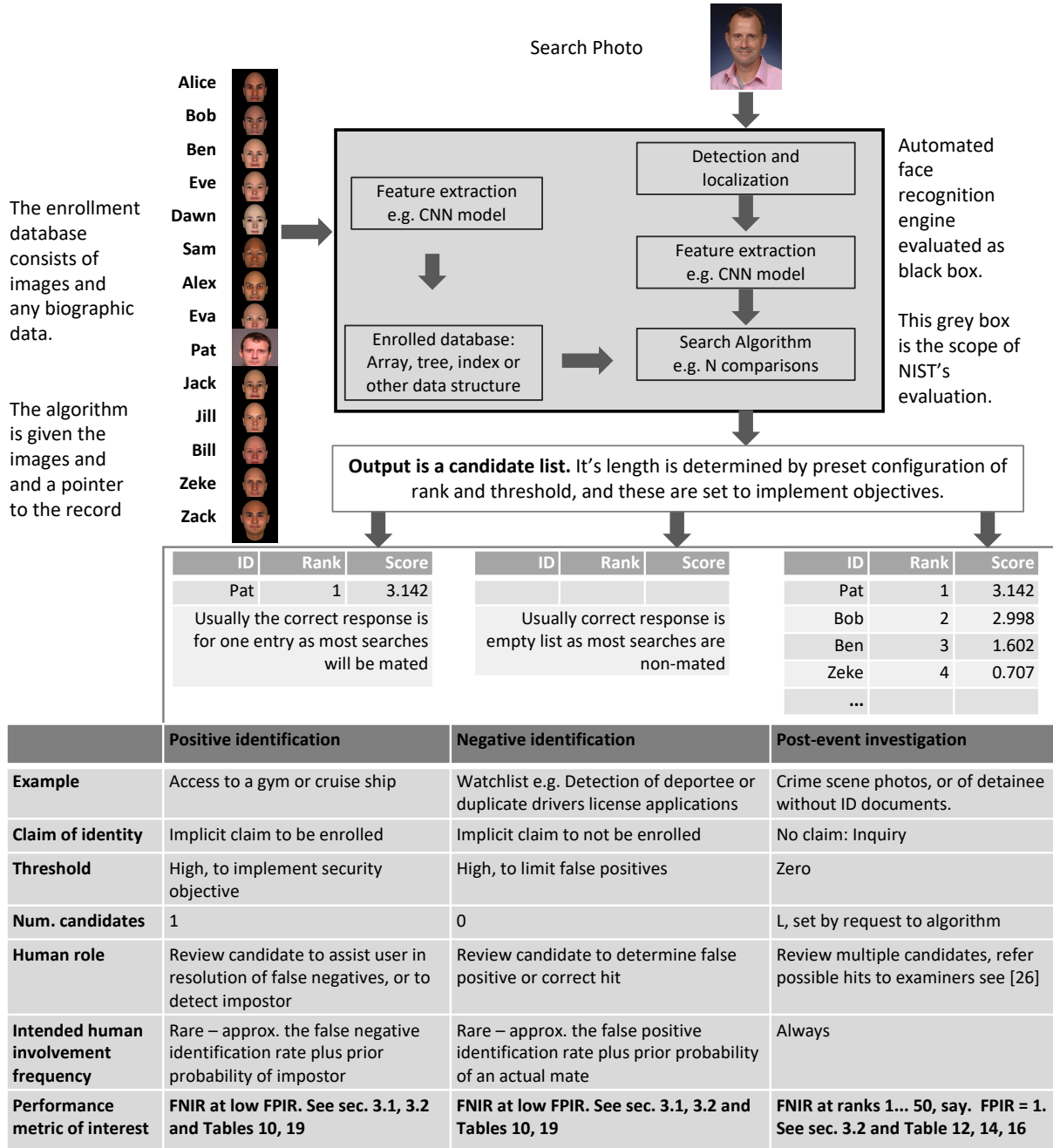
The report also includes results for ageing, recognition of twins, and recognition of profile-view images against frontal galleries. It otherwise does not address causes of recognition failure, neither image-specific problems nor subject-specific factors including demographics. Separate reports on demographic dependencies in face recognition will be published in the future. Additionally out of scope are: performance of live [human-in-the-loop transactional systems](#) like automated border control gates; human recognition accuracy as used in forensic applications; and recognition of persons in video sequences (which NIST evaluated separately [9]). Some of those applications share core matching technologies that *are* tested in this report.

**Images:** Five kinds of images are employed; these are either compared with images of the same kind, or against others from different capture environments as follows. The primary dataset is a set of law enforcement mugshot images (Fig. 5) which are enrolled and then searched with three kinds of images: other mugshots (i.e. within-domain); profile-view photographs (90 degree cross-view); and lower quality webcam images (Fig. 6) collected in similar detention operations (cross-domain). Additionally we compare high quality visa-like photos collected in immigration offices, with: medium quality border crossing images collected in primary immigration lanes; poor quality images collected in ATM-like registered traveller kiosks.

**Participation and industry coverage:** The report includes performance figures for prototype algorithms from the research laboratories of commercial developers and a few universities. This represents a substantial majority of the face recognition industry, but only a tiny minority of the academic community. Participation was open worldwide. While there is no charge for participation, developers incur some software engineering expense in implementing their algorithms behind the NIST application programming interface (API). The test is a black-box test where the function of the algorithm, and the intellectual property associated with it, is hidden inside pre-compiled libraries.

**Recent technology development:** Most face recognition research with deep convolutional neural networks (CNNs) has been aimed at achieving invariance to pose, illumination and expression variations that characterize photojournalism and social media images. The initial research [18, 22] employed large numbers of images of relatively few ( $\sim 10^4$ ) individuals to learn invariance. Inevitably much larger populations ( $\sim 10^7$ ) were employed for training [11, 20] but the benchmark, Labeled Faces in the Wild with (essentially) an equal error rate metric [12], represents an easy task,

one-to-one verification at very high false match rates. While a larger scale identification benchmark duly followed, Megaface [15], its primary metric, rank one hit rate, contrasts with the high threshold discrimination task required in most large-population applications of face recognition, namely credential de-duplication, and background checks. There, identification in galleries containing up to  $10^8$  individuals must be performed using a) very few images per individual and b) stringent thresholds to afford very low false positive identification rates. This track of FRVT was launched to measure the capability of the new technologies, including in these two cases. FRVT has included open-set identification tests since 2002, reporting both false negative and positive identification rates [7].



**Performance metrics for applications:** This report documents the performance of one-to-many face recognition algorithms. The word "performance" here refers to recognition accuracy and computational resource usage, as measured

by executing those algorithms on massive sequestered datasets.

This report includes extensive tabulation of recognition error rates germane to the main use-cases for face search technology. The Figure below, inspired by the Figure 1 in [23] differentiates different applications of the technology. The last row directs readers to the main tables relevant to those applications, respectively threshold-based and rank-based metrics that are special cases of the metrics given in section 3. The terms negative identification and positive identification are taken from the [ISO/IEC 2382-37:2017](#) standardized biometrics vocabulary.

The algorithms are specifically configured for these applications by setting thresholds and candidate list lengths. Both rank-based metrics and threshold-based metrics include tradeoffs. In investigation, overall accuracy will be reduced if labor is only available to review a few candidates from the automated system. Note that when a fixed number of candidates are returned, the false positive identification rate of the automated face recognition engine will be 100%, because a probe image of anyone not enrolled will still return candidates. In identification applications where false positives must be limited to satisfy reviewer labor availability or a security objective, higher false negative rates are implied. This report includes extensive quantification of this threshold-based tradeoff. See Sec. 3

**Template diversity:** The FRVT is designed to evaluate black-box technologies with the consequence that the templates that hold features extracted from face images are entirely proprietary opaque binary data that embed considerable intellectual property of the developer. Despite migration to CNN-based technologies there is no consensus on the optimal feature vector dimension. This is evidenced by template sizes ranging from below 100 bytes to more than four kilobytes. This diversity of approaches, suggests there is no prospect of a standard template something that would require a common feature set to be extracted from faces. Interoperability in automated face recognition remains solidly based on images and documentary standards for those, in particular the ICAO portrait [27] specification deriving from the ISO/IEC 19794-5 Token frontal [24] standard, which are similar to certain ANSI/NIST Type 10 [26] formats.

**Training:** The algorithms submitted to NIST have been developed using image datasets that developers do not disclose. The development will often include application of machine learning techniques and will additionally involve iterative training and testing cycles. NIST itself does not perform any training and does not refine or alter the algorithm in any way. Thus the model, data files, and libraries that define an algorithm are fixed for the duration of the tests. This reflects typical operational reality where recognition software, once installed, is fixed and constant until upgraded. This situation persists because on-site training of algorithms on customer data is atypical essentially because training is not a turnkey process.

**Automated search and human review:** Virtually all applications using automated face search require human review of the outputs at some frequency: Always for investigational applications; rarely in positive identification applications, after rejection (false or otherwise); and rarely in negative identification applications, after an alarm (false or otherwise). The human role is usually to compare a reference image with the query image or the live-subject if present, to render either a definitive decision on “exclusion” (different subjects), or “identification” (same subject), or a declaration that one or both images have “no value” and that no decision can be made. Note that automated face recognition algorithms are not built to do exclusion - low scores from a face comparison arise from different faces *and* poor quality images of the same face.

Human reviewers make recognition errors [5, 19, 25] and are sensitive to image acquisition and quality. Accurate human review is supported by high resolution - as specified in the Type 50, 51 acquisition profiles of the ANSI/NIST Type 10 record [26], and by multiple non-frontal views as specified in the same standard. These often afford views of the ear. Organizations involved in image collection should consider supporting human adjudication by collecting high-resolution frontal and non-frontal views, preparing low resolution versions for automated face recognition [24], and retaining both for any subsequent resolution of candidate matches. Along these lines, the [ISO/IEC Joint Technical](#)

Committee 1 subcommittee 37 on biometrics has just initiated projects on image quality assessment and face-aware capture.

## Release Notes

**FRVT Activities:** Since February 2017, NIST has been evaluating one-to-one verification algorithms on an ongoing basis. NIST then restarted FRVT's one-to-many track in February 2018, inviting participants to send up to prototype algorithms. Both tracks allows developers to submit updated algorithms to NIST at any time but no more frequently than four calendar months. This more closely aligns development and evaluation schedules. Results are posted to the web within a few weeks of submission. Details and full report are linked from the [Ongoing FRVT site](#).

**FRVT Reports:** The results of the FRVT appear in the series NIST Interagency Reports tabulated below. The reports were developed separately and released on different schedules. In prior years NIST has mostly reported FRVT results as a single report; this had the disadvantage that results from completed sub-studies were not published until all other studies were complete.

Date	Link	Title	No.
2014-03-20	<a href="#">PDF</a>	FRVT Performance of Automated Age Estimation Algorithms	7995
2015-04-20	<a href="#">PDF</a>	Face Recognition Vendor Test (FRVT) Performance of Automated Gender Classification Algorithms	8052
2014-05-21	<a href="#">PDF</a>	FRVT Performance of face identification algorithms	8009
2017-03-07	<a href="#">PDF</a>	Face In Video Evaluation (FIVE) Face Recognition of Non-Cooperative Subjects	8173
2017-11-23	<a href="#">PDF</a>	The 2017 IARPA Face Recognition Prize Challenge (FRPC)	8197
2018-11-27	<a href="#">PDF</a>	Face Recognition Vendor Test - Part 2: Identification	8271
2019-09-11	<a href="#">PDF</a>	Face Recognition Vendor Test - Part 2: Identification	8271
2019-12-11	<a href="#">PDF</a>	Face Recognition Vendor Test - Part 3: Demographic Effects	8280
2020-01-03	<a href="#">WWW</a>	Face Recognition Vendor Test (FRVT) - Part 1 Verification	Draft

Details appear on pages linked from <https://www.nist.gov/programs-projects/face-projects>.

**Appendices:** This report is accompanied by appendices which present exhaustive results on a per-algorithm basis. These are machine-generated and are included because the authors believe that visualization of such data is broadly informative and vital to understanding the context of the report.

**Typesetting:** Virtually all of the tabulated content in this report was produced automatically. This involved the use of scripting tools to generate directly type-settable  $\text{\LaTeX}$  content. This improves timeliness, flexibility, maintainability, and reduces transcription errors.

**Graphics:** Many of the Figures in this report were produced using the `ggplot2` package running under `R`, the capabilities of which extend beyond those evident in this document.

# Contents

<b>Release Notes</b>	<b>1</b>
<b>Disclaimer</b>	<b>4</b>
<b>Institutional Review Board</b>	<b>4</b>
<b>Acknowledgments</b>	<b>4</b>
<b>Executive Summary</b>	<b>5</b>
<b>Scope and Context</b>	<b>11</b>
<b>Release Notes</b>	<b>15</b>
<b>1 Introduction</b>	<b>17</b>
<b>2 Evaluation datasets</b>	<b>18</b>
<b>3 Performance metrics</b>	<b>24</b>
<b>4 Results</b>	<b>40</b>
<b>Appendices</b>	<b>74</b>
<b>A Accuracy on large-population FRVT 2018 mugshots</b>	<b>74</b>
<b>B Effect of time-lapse: Accuracy after face ageing</b>	<b>119</b>
<b>C Effect of enrolling multiple images</b>	<b>215</b>
<b>D Accuracy with poor quality webcam images</b>	<b>222</b>
<b>E Accuracy for profile-view to frontal recognition</b>	<b>232</b>
<b>F Search duration</b>	<b>236</b>
<b>G Gallery Insertion Timing</b>	<b>243</b>

# 1 Introduction

One-to-many identification represents the largest market for face recognition technology. Algorithms are used across the world in a diverse range of biometric applications: detection of duplicates in databases, detection of fraudulent applications for credentials such as passports and driving licenses, token-less access control, surveillance, social media tagging, lookalike discovery, criminal investigation, and forensic clustering.

This report contains a breadth of performance measurements relevant to many applications. Performance here refers to accuracy and resource consumption. In most applications, the core accuracy of a facial recognition algorithm is the most important performance variable. Resource consumption will be important also as it drives the amount of hardware, power, and cooling necessary to accommodate high volume workflows. Algorithms consume processing time, they require computer memory, and their static template data requires storage space. This report documents these variables.

## 1.1 Open-set searches

FRVT tested open-set identification algorithms. Real-world applications are almost always “open-set”, meaning that some searches have an enrolled mate, but some do not. For example, some subjects have truly not been issued a visa or drivers license before; some law enforcement searches are from first-time arrestees<sup>6</sup>. In an “open-set” application, algorithms make no prior assumption about whether or not to return a high-scoring result, and for a mated search, the ideal behaviour is that the search produces the correct mate at high score and first rank. For a non-mate search, the ideal behavior is that the search produces zero high-scoring candidates.

Many academic benchmarks execute only closed-set searches. The proportion of mates found in the rank one position is the default accuracy metric. This hit rate metric ignores the score with which a mate is found; weak hits count as much as strong hits. This ignores the real-world imperative that in many applications it is necessary to elevate a threshold to reduce the number of false positives.

<sup>6</sup>Operationally closed-set applications are rare because it is usually not the case that all searches have an enrolled mate. One counter-example, however, is a cruise ship in which all passengers are enrolled and all searches should produce exactly one identity. Another example is forensic identification of dental records from an aircraft crash.

## 2 Evaluation datasets

This report documents accuracy for four kinds of images - mugshots, webcam, profiles and wild - as described in the following sections.

### 2.1 Immigration-related images

This report includes benchmark tests sharing a common enrollment of high quality frontal portrait images collected while subject make applications for various immigration benefits. We then search that with two kinds of images, webcam images collected during in-bound immigration and also images collected from registered travelers using a ATM-style kiosk. These are described below and depicted in Figure 4.



Figure 4: Example photos.

- ▷ **Application reference photos:** The images are collected in an attended interview setting using dedicated capture equipment and lighting. The images, at size 300x300 pixels, are smaller than normally indicated by ISO. The images are all high-quality frontal portraits collected in immigration offices and with a white background. As such, potential quality related drivers of high false match rates (such as blur) can be expected to be absent. The images are encoded as ISO/IEC 10918-1 i.e. JPEG. Older images had a compression ration of about 16:1, while newer images, since 2010, are more lightly compressed at 4:1. When these images are provided as input into the algorithm, they are labeled with the type “iso”. This report enrols 1 600 000 application images, one per person.
- ▷ **Border crossing photos:** Most images are have width 320 and height 240 pixels. They are JPEG compressed at 16:1 i.e. filesize just below 15KB. The images present challenges for face recognition in that subjects often exhibit non-zero yaw and pitch (associated with the rotational degrees of freedom of the camera mount), low contrast (due to varying and intense background lights), and poor spatial resolution (due to inexpensive cameras). There are often subjects standing in the background, usually at very low resolution (see Figure 4b). In such cases, algorithms should detect all faces and determine which is the largest and most centered. When these images are provided as input into the algorithm, they are labeled with the type “wild”.
- ▷ **Kiosk photos:** These photos were collected from subjects whose attention was focused on interaction with an immigration kiosk. They images were not intended for use with automated face recognition. The camera is situated above a display which the user touches, and is triggered either without directing the subject to look at it, or without waiting for the subject to comply. The images are therefore characterized by pitch-down pose, sometimes exceeding 45 degrees, as in Figure 4c. Yaw-angle variation is mild, with most images close to frontal. The images

have width 320 pixels and height 240 pixels and therefore tall individuals are sometimes cropped. This is often just above the eyes and can occur at the nose or mouth. Conversely, short individuals are sometimes cropped such that only the top part of the face is visible. In a quite small number of cases, there other subjects standing just behind the primary subject such that algorithms should detect all faces and determine which is the largest and most centered. Background ceiling lighting is often visible and this sometimes leads to under-exposure of the face. When these images are provided as input into the algorithm, they are labeled with the type “wild”.

## 2.2 Law enforcement images

The main mugshot dataset used is referred to as the FRVT 2018 set. This set was collected over the period 2002 to 2017 in routine United States law enforcement operations. This set yields three subsets

- ▷ **Mugshots:** Mugshots comprise about 86% of the database. They have reasonable compliance with the ANSI/NIST ITL1-2011 Type 10 standard’s subject acquisition profiles levels 10-20 for frontal images [26]. The most common departure from the standard’s requirements is the presence of mild pose variations around frontal - the images of Figure 5 are typical. The images vary in size, with many being 480x600 pixels with JPEG compression applied to produce filesizes of between 18 and 36KB with many images outside this range, implying that about 0.5 bits are being encoded per pixel. When these images are provided as input into the algorithm, they are labeled with the type “mugshot”. Example images appear in Fig. 5

NIST Interagency Report 8238 includes a comparison of this set of mugshots with the smaller and easier sets of mugshots used in tests run in 2010 and 2014.

- ▷ **Profile images:** Profile-view images have been collected in law enforcement for more than 100 years, as human capability is improved with orthogonal information. The profile images used in this report were collected during the same session as the frontal mugshot photograph, in the same standardized photographic setup. These would not therefore be used with automated face recognition. A small subset, 200 000 images, were set aside for testing. When these images are provided as input into the algorithm, they are labeled with the type “wild”. Example images appear in Fig. 7
- ▷ **Webcam images:** The remaining 14% of the images were collected using an inexpensive webcam attached to a flexible operator-directed mount. These images are all of size 240x240 pixels, that are in considerable violation of most quality-related clauses of all face recognition standards. As evident in the figure, the most common defects are non-frontal pose (associated with the rotational degrees of freedom of the camera mount), low contrast (due to varying and intense background lights), and poor spatial resolution (due to inexpensive camera optics) - see examples in Fig 6. The images are overly JPEG compressed, to between 4 and 7KB, implying that only 0.5 to 1 bits are being encoded per color pixel. When these images are provided as input into the algorithm, they are labeled with the type “wild”. Example images appear in Fig. 6

These are drawn from NIST Special Database 32 which may be downloaded [here](#).

These images were partitioned in galleries and probesets for the various experiment listed in Table 1.

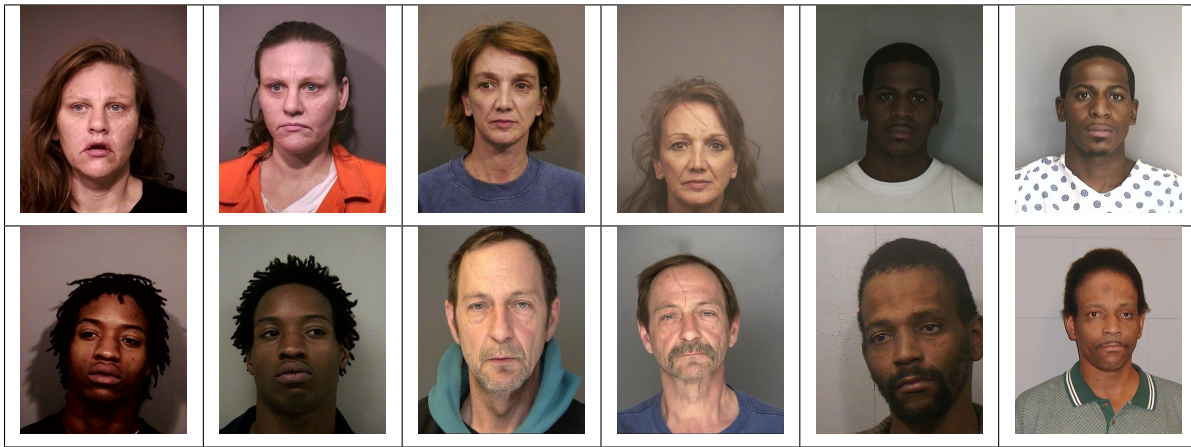


Figure 5: Six mated mugshot pairs representative of the FRVT-2014 (LEO) and FRVT-2018 datasets. The images are collected live, i.e. not scanned from paper. Image source: NIST Special Database 32 the Multiple Encounter Deceased Subjects dataset.



Figure 6: Twelve webcam images representative of probes against the FRVT-2018 mugshot gallery. The first eight images are four mated pairs. Such images present challenges to recognition including pose, non-uniform illumination, low contrast, compression, cropping, and low spatial sampling rate. Image source: NIST Special Database 32 the Multiple Encounter Deceased Subjects dataset.



Figure 7: **[Profile views]** The three images are a frontal enrollment, subsequent frontal probe, and same-session ninety degree profile view. While collection of both frontal and profile views has been typical in law enforcement for more than a century, the recognition of profile to frontal views has essentially been impossible. However, reasonably high accuracy results is now possible - see section E.

Image				
Encounter	1	...	$K_i - 1$	$K_i$
Capture Time	$T_1$	...	$T_{K_i - 1}$	$T_{K_i}$
Role RECENT	Not used	Not used	Enrolled	Search
Role LIFETIME	Enrolled	Enrolled	Enrolled	Search

Figure 8: Depiction of the “recent” and “lifetime” enrollment types. Image source: NIST Special Database 32

## 2.3 Enrollment strategies

Many operational applications include collection and enrollment of biometric data from subjects on more than one occasion. This might be done on a regular basis, as might occur in credential (re-)issuance, or irregularly, as might happen in a criminal recidivist situation [4]. The number of images per person will depend on the application area. In civil identity credentialing (e.g. passports, driver’s licenses), the images will be acquired approximately uniformly over time (e.g. ten years for a passport). While the distribution of dates for such images of a person might be assumed uniform, a number of factors might undermine this assumption<sup>7</sup>. In criminal applications, the number of images would depend on the number of arrests. The distribution of dates for arrest records for a person (i.e. the recidivism distribution) has been modeled using the exponential distribution but is recognized to be more complicated<sup>8</sup>.

In any case, the 2010 NIST evaluation of face recognition showed that considerable accuracy benefits accrue with retention and use of *all* historical images [6].

To this end, the FRVT API document provides  $K \geq 1$  images of an individual to the enrollment software. The software is tasked with producing a single proprietary undocumented “black-box” template<sup>9</sup> from the  $K$  images. This affords the algorithm an ability to generate a *model* of the individual, rather than to simply extract features from each image on a sequential basis.

As depicted in Figure 8, the  $i$ -th individual in the FRVT 2018 dataset has  $K_i$  images. These are labelled as  $x_k$  for  $k = 1 \dots K_i$  in chronological order of capture date. To measure the utility of having multiple enrollment images, this report evaluates three kinds of enrollment:

- ▷ **Recent:** Only the second most recent image,  $x_{K_i - 1}$  is enrolled. This strategy of enrollment mimics the operational policy of retaining the imagery from the most recent encounter. This might be done operationally to ameliorate the effects of face ageing. Obviously retaining only the most recent image should only be done if the identity of the person is trusted to be correct. For example, in an access control situation retention of the most recent successful *authentication* image would be hazardous if it could be a false positive.
- ▷ **Lifetime-consolidated:** All but the most recent image are enrolled,  $x_1 \dots x_{K_i - 1}$ . This subject-centric strategy might be adopted if quality variations exist where an older image might be more suitable for matching, despite the ageing effect.

<sup>7</sup>For example, a person might skip applying for a passport for one cycle, letting it expire. In addition, a person might submit identical images (from the same photography session) to consecutive passport applications at five year intervals.

<sup>8</sup>A number of distributions have been considered to model recidivism, see for example [3].

<sup>9</sup>There are no formal face template standards. Template standards only exist for fingerprint minutiae - see ISO/IEC 19794-2:2011.

**RECENT**



Num. people, N = 6  
Num. images, M = 6

For each of N enrollees, the algorithm is given only the most recent photo.

Operational situation:  
Typical when old images are not, or cannot be, retained, or (rarely) if prior images are too old to be valuable.

Accuracy computation: False negative unless the enrolled mate is returned within top R ranks and at or above threshold.

**LIFETIME CONSOLIDATED**



Num. people, N = 6  
Num. images, M = 9

For each enrollee, the algorithm is given all photos from all historical encounters. The algorithm is able to fuse information from all images of a person

Operational situation:  
Typical when, say, fingerprints are available and precise de-duplication is possible.  
  
The result is a consolidated **person-centric** database.

**LIFETIME UNCONSOLIDATED**



Num. people, N = 6  
Num. images, M = 9

For each of N enrollees, the algorithm is given all photos from all historical encounters but as separate images, so that the algorithm is not aware that some images are of the same ID.

Operational situation:  
This is typical when ID is not known when an image is collected, or is uncertain.  
  
The result is an unconsolidated **event-based** database.

Accuracy computation: False negative unless any of the enrolled mates are returned within top R ranks and at or above threshold.

This publication is available free of charge from: <https://doi.org/10.6028/NIST.IR.8271>

**Figure 9: Enrollment strategies.** The figure shows the three kinds of enrollment databases examined in this report. Image source: NIST Special Database 32

		ENROLLMENT			SEARCH				
		TYPE SEE	POPULATION		MATE		NON-MATE		
		SECTION 2.3	FILTER	N-SUBJECTS	N-IMAGES	N-SUBJECTS	N-IMAGES	N-SUBJECTS	N-IMAGES
<b>Mugshot trials from enrollment of single images</b>									
1	RECENT	NATURAL	640 000	640 000	154 549	154 549	331 254	331 254	
2	RECENT	NATURAL	1 600 000	1 600 000					
3	RECENT	NATURAL	3 000 000	3 000 000					
4	RECENT	NATURAL	6 000 000	6 000 000					
5	RECENT	NATURAL	12 000 000	12 000 000					
<b>Cross-domain</b>									
13	MUGSHOTS AS ON ROW 2				82 106 WEBCAM	82 106 WEBCAM	331 254 WEBCAM	331 254 WEBCAM	
<b>Cross-view</b>									
14	MUGSHOTS AS ON ROW 2				100 000 PROFILE	100 000 PROFILE	100 000 PROFILE	100 000 PROFILE	
<b>Mugshot ageing</b>									
17	OLDEST	NATURAL	3 068 801	3 068 801	2 853 221	10 951 064	0	0	
<b>Border crossing ageing</b>									
17	OLDEST	NATURAL	1 600 000	1 600 000	1 922 437	1 922 437	1 920 000	1 920 000	
<b>Visa-border</b>									
19	PRIOR	NATURAL	1 600 000 VISA	1 600 000 VISA	80 000 BORDER	80 000 BORDER	80 000 BORDER	80 000 BORDER	
20	VISA AS ON ROW 18				21 016 BORDER	21 016 BORDER	21 016 BORDER	21 016 BORDER	

Table 1: **Enrollment and search sets.** Each row summarizes one identification trial. Unless stated otherwise, all entries refer to mugshot images. The term “natural” means that subjects were selected without heed to demographics, i.e. in the distribution native to this dataset. The probe images were collected in a different calendar year to the enrollment image. Missing values in rows 2-12 are the same as in row 1.

- ▷ **Lifetime-unconsolidated:** Again all but the most recent image are enrolled  $x_1 \dots x_{K_i-1}$  but now separately, with different identifiers, such that the algorithm is not aware that the images are from the same face. This kind of event- or encounter-centric enrollment is very common when operational constraints preclude reliable consolidation of the historical encounters into a single identity. This aspect also prevents the recognition algorithm from a) building a holistic model of identity (as is common in speaker recognition systems) and b) implementing fusion, for example template-level fusion of feature vectors, or post-search score-level fusion. The result is that searches will typically yield more than one image of a person in the top ranks. This has consequences for appropriate metrics, as detailed in section 3.2.1

NIST first evaluated this kind of enrollment in mid 2018, and the results tables include some comparison of accuracy available from all three enrollment styles.

In all cases, the most recent image,  $x_{K_i}$ , is reserved as the search image. For the 1.6 million subject enrollment partition of the FRVT 2018 data,  $1 \leq K_i \leq 33$  with  $K_i = 1$  in 80.1% of the individuals,  $K_i = 2$  in 13.4%,  $K_i = 3$  in 3.7%,  $K_i = 4$  in 1.4%,  $K_i = 5$  in 0.6%,  $K_i = 6$  in 0.3%, and  $K_i > 6$  is 0.2% for everyone else. This distribution is substantially dependent on United States recidivism rates.

We did not evaluate the case of retaining only the highest quality image, since automated quality assessment is out of scope for this report. We do not anticipate that such strategies will prove beneficial when the quality assessment apparatus is imperfect and unvalidated.

### 3 Performance metrics

This section gives specific definitions for accuracy and timing metrics. Tests of open-set biometric algorithms must quantify frequency of two error conditions:

- ▷ **False positives:** Type I errors occur when search data from a person who has never been seen before is incorrectly associated with one or more enrollees' data.
- ▷ **Misses:** Type II errors arise when a search of an enrolled person's biometric does not return the correct identity.

Many practitioners prefer to talk about "hit rates" instead of "miss rates" - the first is simply one minus the other as detailed below. Sections 3.1 and 3.2 define metrics for the Type I and Type II performance variables.

Additionally, because recognition algorithms sometimes fail to produce a template from an image, or fail to execute a one-to-many search, the occurrence of such events must be recorded. Further because algorithms might elect to not produce a template from, for example, a poor quality image, these failure rates must be combined with the recognition error rates to support algorithm comparison. This is addressed in section 3.5.

Finally, section 3.7 discusses measurement of computation duration, and section 3.8 addresses the uncertainty associated with various measurements. Template size measurement is included with the results.

#### 3.1 Quantifying false positives

It is typical for a search to be conducted into an enrolled population of  $N$  identities, and for the algorithm to be configured to return the closest  $L$  candidate identities. These candidates are ranked by their score, in descending order, with all scores required to be greater than or equal to zero. A human analyst might examine either all  $L$  candidates, or just the top  $R \leq L$  identities, or only those with score greater than threshold,  $T$ . The workload associated with such examination is discussed later, in 3.6.

False alarm performance is quantified in two related ways. These express how many searches produces false positives, and then, how many false positives are produced in a search.

**False positive identification rate:** The first quantity, FPIR, is the proportion of non-mate searches that produce an adverse outcome:

$$\text{FPIR}(N, T) = \frac{\text{Num. non-mate searches where one or more enrolled candidates are returned with score at or above threshold}}{\text{Num. non-mate searches attempted.}} \quad (1)$$

Under this definition, FPIR can be computed from the highest non-mate candidate produced in a search - it is not necessary to consider candidates at rank 2 and above. FPIR is the primary measure of Type I errors in this report.

**Selectivity:** However, note that in any given search, several non-mate may be returned above threshold. In order to quantify such events, a second quantity, selectivity (SEL), is defined as the *number* of non-mates returned on a candidate list, averaged over all searches.

$$\text{SEL}(N, T) = \frac{\text{Num. non-mate enrolled candidates returned with score at or above threshold}}{\text{Num. non-mate searches attempted.}} \quad (2)$$

where  $0 \leq \text{SEL}(N, T) \leq L$ . Both of these metrics are useful operationally. FPIR is useful for targeting how often an

adverse false positive outcome can occur, while SEL as a number is related to workload associated with adjudicating candidate lists. The relationship between the two quantities is complicated - it depends on whether an algorithm concentrates the false alarms in the results of a few searches or whether it disburses them across many. This was detailed in FRVT 2014, NISTIR 8009. It has not yet been detailed in FRVT 2018.

### 3.2 Quantifying hits and misses

If  $L$  candidates are returned in a search, a shorter candidate list can be prepared by taking the top  $R \leq L$  candidates for which the score is above some threshold,  $T \geq 0$ . This reduction of the candidate list is done because thresholds may be applied, and only short lists might be reviewed (according to policy or labor availability, for example). It is useful then to state accuracy in terms of  $R$  and  $T$ , so we define a “miss rate” with the general name **false negative identification rate** (FNIR), as follows:

$$\text{FNIR}(N, R, T) = \frac{\text{Num. mate searches with enrolled mate found outside top R ranks or score below threshold}}{\text{Num. mate searches attempted}} \quad (3)$$

This formulation is simple for evaluation in that it does not distinguish between causes of misses. Thus a mate that is not reported on a candidate list is treated the same as a miss arising from face finding failure, algorithm intolerance of poor quality, or software crashes. Thus if the algorithm fails to produce a candidate list, either because the search failed, or because a search template was not made, the result is regarded as a miss, adding to FNIR.

*Hit rates, and true positive identification rates:* While FNIR states the “miss rate” as how often the correct candidate is either not above threshold or not at good rank, many communities prefer to talk of “hit rates”. This is simply the **true positive identification rate** (TPIR) which is the complement of FNIR giving a positive statement of how often mated searches are successful:

$$\text{TPIR}(N, R, T) = 1 - \text{FNIR}(N, R, T) \quad (4)$$

This report does not report true positive “hit” rates, preferring false negative miss rates for two reasons. First, costs rise linearly with error rates. For example, if we double FNIR in an access control system, then we double user inconvenience and delay. If we express that as decrease of TPIR from, say 98.5% to 97%, then we mentally have to invert the scale to see a doubling in costs. More subtly, readers don’t perceive differences in numbers near 100% well, becoming inured to the “high nineties” effect where numbers close to 100 are perceived indifferently.

**Reliability** is a corresponding term, typically being identical to TPIR, and often cited in automated (fingerprint) identification system (AFIS) evaluations.

An important special case is the **cumulative match characteristic** (CMC) which summarizes accuracy of mated-searches only. It ignores similarity scores by relaxing the threshold requirement, and just reports the fraction of mated searches returning the mate at rank  $R$  or better.

$$\text{CMC}(N, R) = 1 - \text{FNIR}(N, R, 0) \quad (5)$$

We primarily cite the complement of this quantity,  $\text{FNIR}(N, R, 0)$ , the fraction of mates *not* in the top  $R$  ranks.

The **rank one hit rate** is the fraction of mated searches yielding the correct candidate at best rank, i.e.  $\text{CMC}(N, 1)$ . While this quantity is the most common summary indicator of an algorithm’s efficacy, it is not dependent on similarity scores, so it does not distinguish between strong (high scoring) and weak hits. It also ignores that an adjudicating reviewer is often willing to look at many candidates.

### 3.2.1 False negative rates for unconsolidated galleries

As detailed in section 2.3 a common type of gallery, here referred to as the lifetime unconsolidate type, is populated with all images of an individual without any association between them. That is, the gallery construction algorithm is not provided with any ID labels that would support processing of a person's images jointly. This contrasts with the lifetime consolidate type where an algorithm may explicitly fuse features from multiple images of a person, or select a best image. In such cases, where the number of enrolled images is a random variable, we define two false negative rates as follows.

The first demands that the algorithm place any of the  $K_i$  mates in the top  $R \geq 1$  ranks. The proportion of searches for which this does not occur forms a false negative identification rate:

$$\text{FNIR}_{\text{any}}(N, R, T) = 1 - \frac{\text{Num. mate searches where any enrolled mate is found in the top R ranks and at-or-above threshold}}{\text{Num. mate searches attempted.}} \quad (6)$$

The second demands that the algorithm place all  $K_i$  mates in the top  $R \geq K_i$  ranks. The proportion of searches for which this does not occur forms a false negative identification rate:

$$\text{FNIR}_{\text{all}}(N, R, T) = 1 - \frac{\text{Num. mate searches where all enrolled mates are found in the top R ranks and at-or-above threshold}}{\text{Num. mate searches attempted.}} \quad (7)$$

Placing all mates in the top ranks is a more difficult task than correctly retrieving any image, so it holds that:  $\text{FNIR}_{\text{all}} \geq \text{FNIR}_{\text{any}}$ . This is evident in the results presented for November 2018 algorithms in Tables starting at ??.

The information retrieval community might prefer to compute and plot *precision* and *recall*; this is a valid approach, but we advance the two metrics above because they relate to our normal definition of consolidated FNIR, and they cover the two extreme use-cases of wanting any hit vs. all hits.

### 3.3 DET interpretation

In biometrics, a false negative occurs when an algorithm fails to match two samples of one person – a Type II error. Correspondingly, a false positive occurs when samples from two persons are improperly associated – a Type I error.

Matches are declared by a biometric system when the native comparison score from the recognition algorithm meets some threshold. Comparison scores can be either similarity scores, in which case higher values indicate that the samples are more likely to come from the same person, or dissimilarity scores, in which case higher values indicate different people. Similarity scores are traditionally computed by fingerprint and face recognition algorithms, while dissimilarities are used in iris recognition. In some cases, the dissimilarity score is a distance possessing metric properties. In any case, scores can be either mate scores, coming from a comparison of one person's samples, or nonmate scores, coming from comparison of different persons' samples.

The words "genuine" or "authentic" are synonyms for mate, and the word "impostor" is used as a synonym for non-mate. The words "mate" and "nonmate" are traditionally used in identification applications (such as law enforcement search, or background checks) while genuine and impostor are used in verification applications (such as access control).

An error tradeoff characteristic represents the tradeoff between Type II and Type I classification errors. For identification this plots false negative vs. false positive identification rates i.e. FNIR vs. FPIR parametrically with T. Such plots

are often called detection error tradeoff (DET) characteristics or receiver operating characteristic (ROC). These serve the same function – to show error tradeoff – but differ, for example, in plotting the complement of an error rate (e.g. TPIR = 1 – FNIR) and in transforming the axes, most commonly using logarithms, to show multiple decades of FPIR. More rarely, the function might be the inverse of the Gaussian cumulative distribution function.

The slides of Figures 10 through 15 discuss presentation and interpretation of DETs used in this document for reporting face identification accuracy. Further detail is provided in formal biometrics testing standards, see the various parts of ISO/IEC 19795 Biometrics Testing and Reporting. More terms, including and beyond those to do with accuracy, appear in ISO/IEC 2382-37 Information technology – Vocabulary – Part 37: Harmonized biometric vocabulary.

2021/10/28  
 13:44:33  
 FNIR(N, R, T) = False neg. identification rate  
 FPIR(N, T) = False pos. identification rate  
 N = Num. enrolled subjects  
 R = Num. candidates examined  
 T = Threshold  
 T = 0 → Investigation  
 T > 0 → Identification

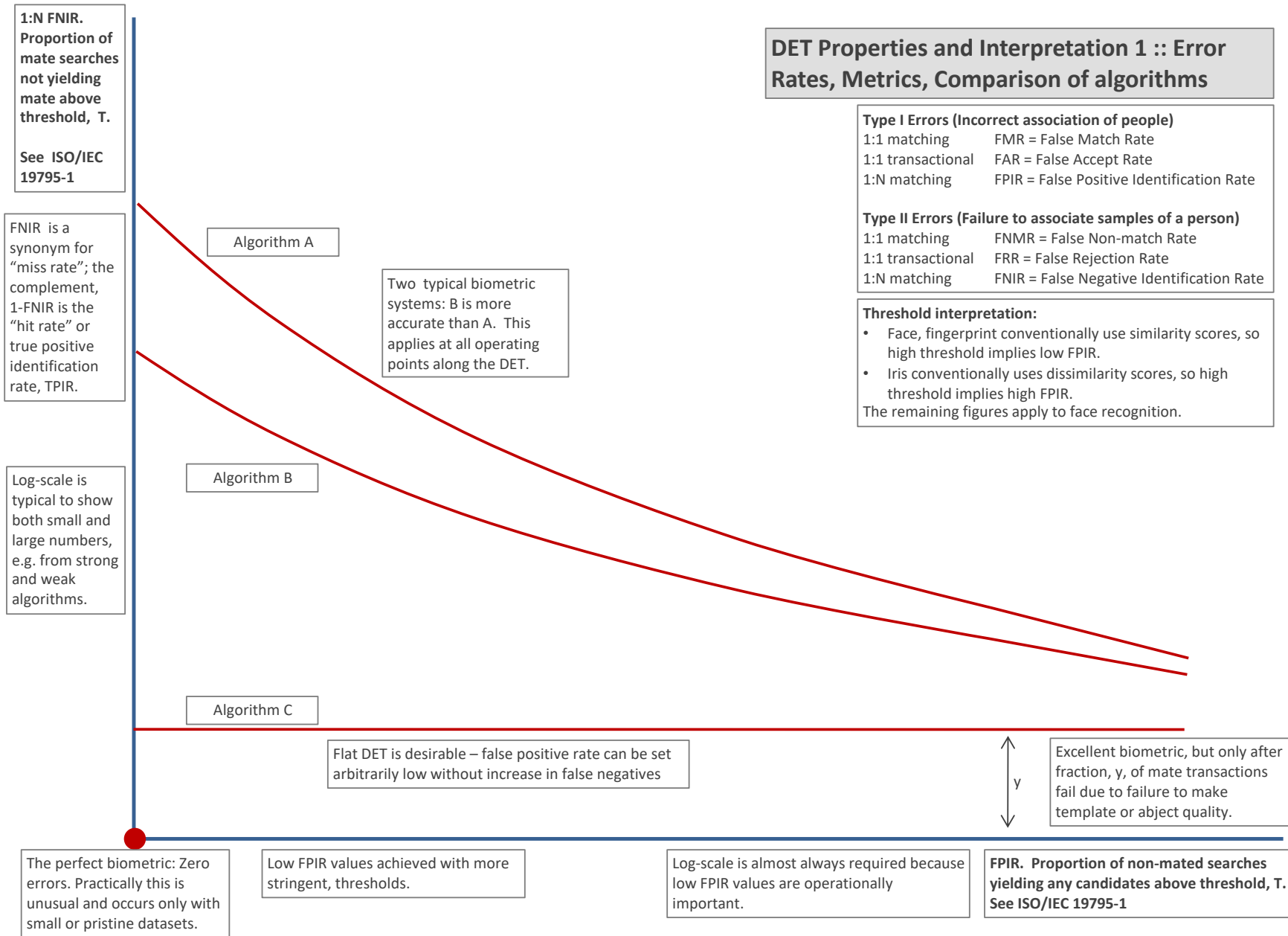


Figure 10: DET as the primary performance reporting mechanism.

2021/10/28  
 FNIR(N, R, T) =  
 FP(R, T) =  
 False neg. identification rate  
 False pos. identification rate  
 N = Num. enrolled subjects  
 R = Num. candidates examined  
 T = Threshold  
 T = 0 → Investigation  
 T > 0 → Identification

FRVT - FACE RECOGNITION VENDOR TEST - IDENTIFICATION

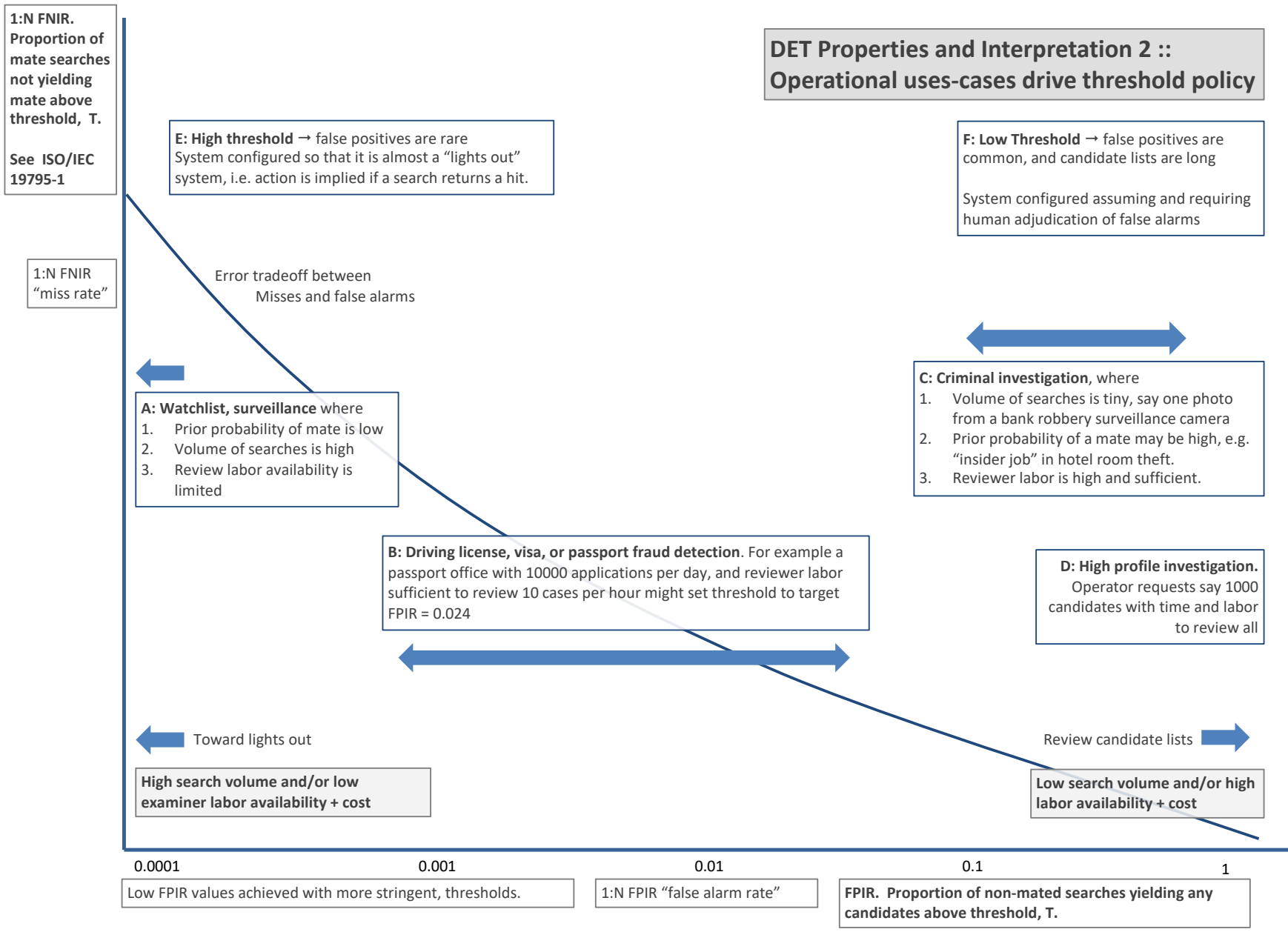


Figure 11: DET as the primary performance reporting mechanism.

2021/10/28  
 FNIR(N, R, T) =  
 FPR(N, T) =  
 False neg. identification rate  
 False pos. identification rate  
 N = Num. enrolled subjects  
 R = Num. candidates examined  
 T = Threshold  
 T = 0 → Investigation  
 T > 0 → Identification

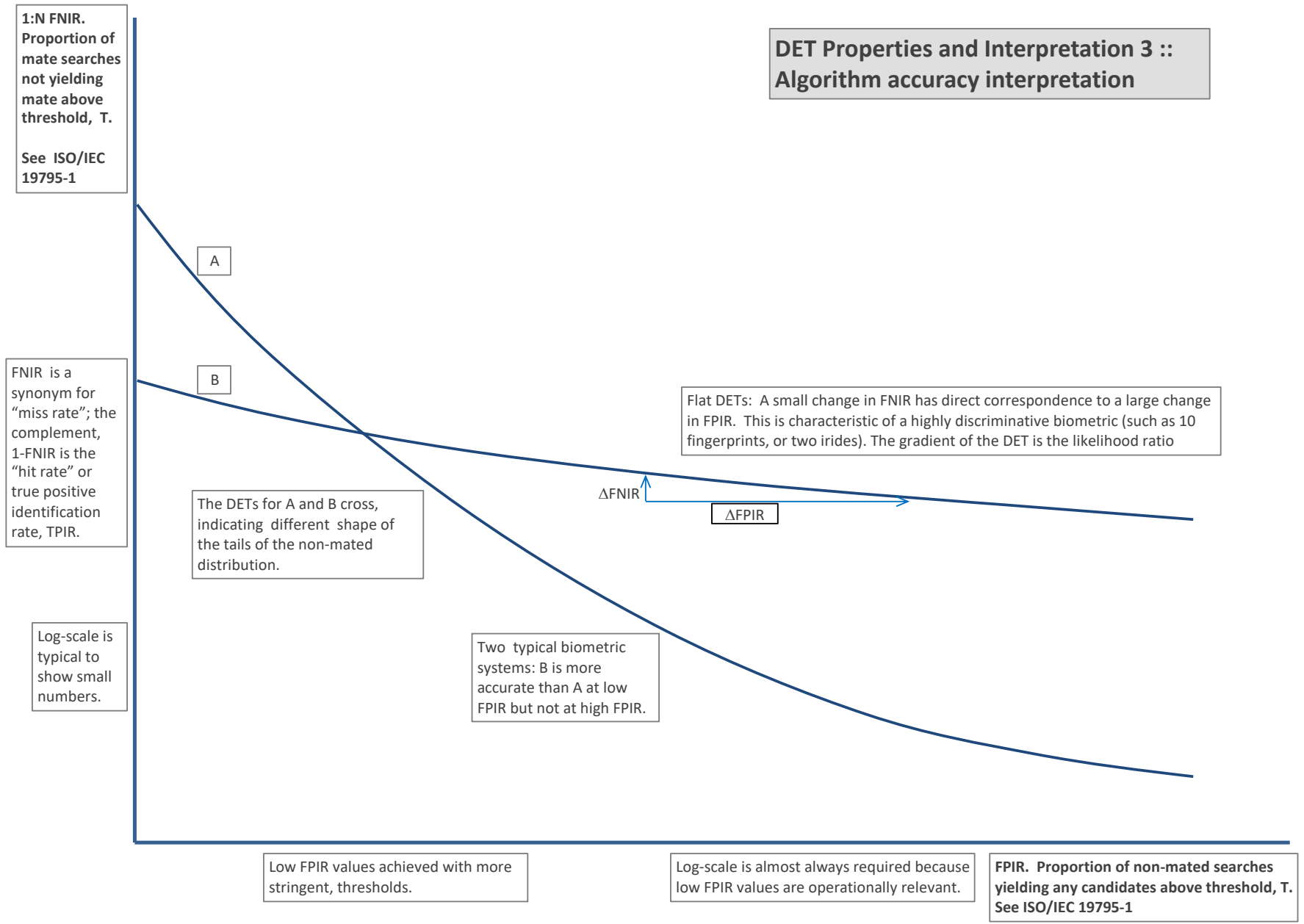


Figure 12: DET as the primary performance reporting mechanism.

2021/10/28  
 13:44:33  
 FNIR(N, R, T) =  
 FPFR(N, T) =  
 False neg. identification rate  
 False pos. identification rate  
 N = Num. enrolled subjects  
 R = Num. candidates examined  
 T = Threshold  
 T = 0 → Investigation  
 T > 0 → Identification

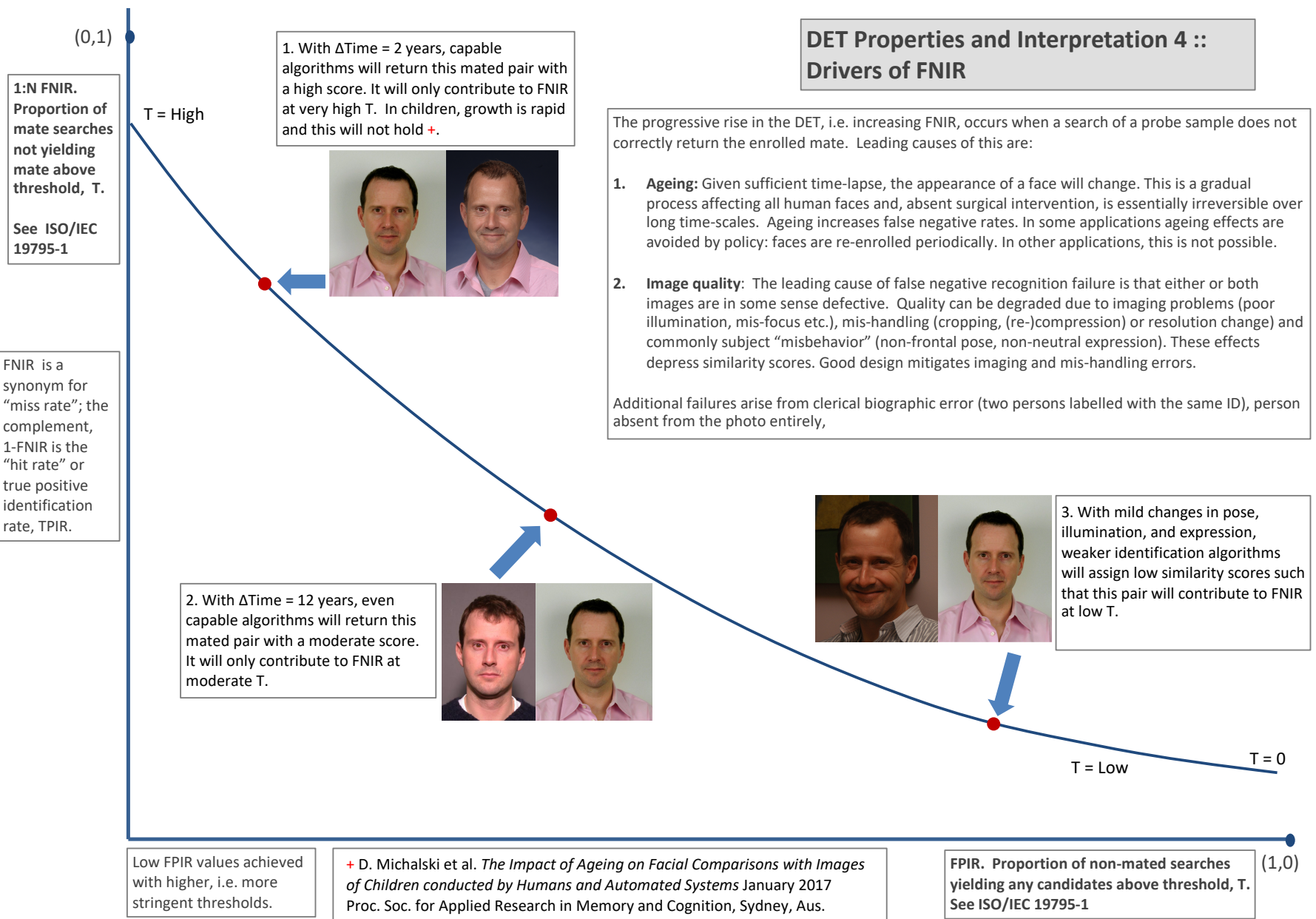


Figure 13: DET as the primary performance reporting mechanism.

2021/10/28  
 13:44:33  
 FNIR(N, R, T) =  
 FPIR(N, T) =  
 False neg. identification rate  
 False pos. identification rate  
 N = Num. enrolled subjects  
 R = Num. candidates examined  
 T = Threshold  
 T = 0 → Investigation  
 T > 0 → Identification

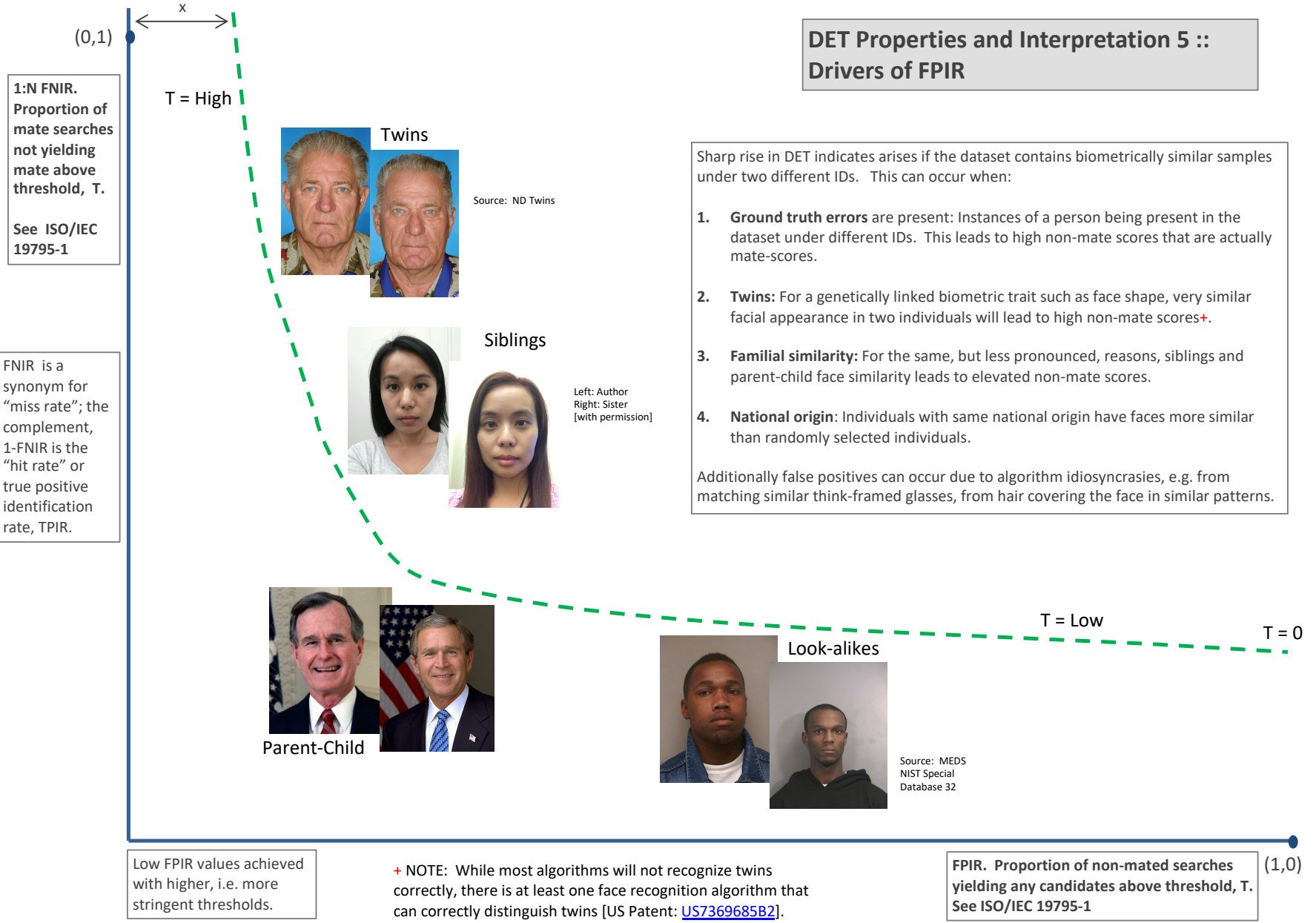


Figure 14: DET as the primary performance reporting mechanism.

2021/10/28  
 13:44:33  
 FNIR(N, R, T) = False neg. identification rate  
 FPIR(N, T) = False pos. identification rate  
 N = Num. enrolled subjects  
 R = Num. candidates examined  
 T = Threshold  
 T = 0 → Investigation  
 T > 0 → Identification

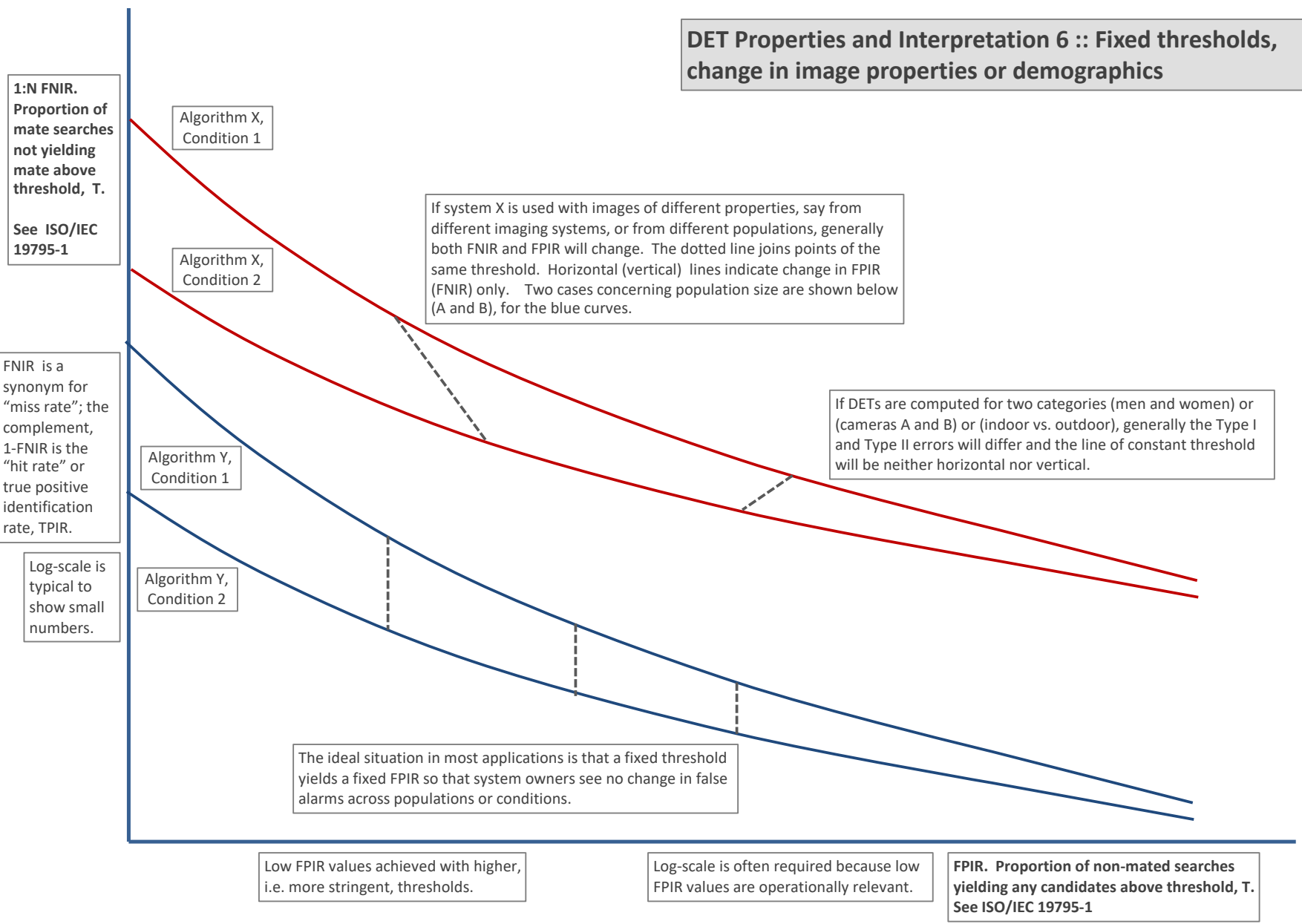


Figure 15: DET as the primary performance reporting mechanism.

2021/10/28  
 13:44:33  
 FNIR(N, R, T) = False neg. identification rate  
 FPIR(N, T) = False pos. identification rate  
 N = Num. enrolled subjects  
 R = Num. candidates examined  
 T = Threshold  
 T = 0 → Investigation  
 T > 0 → Identification

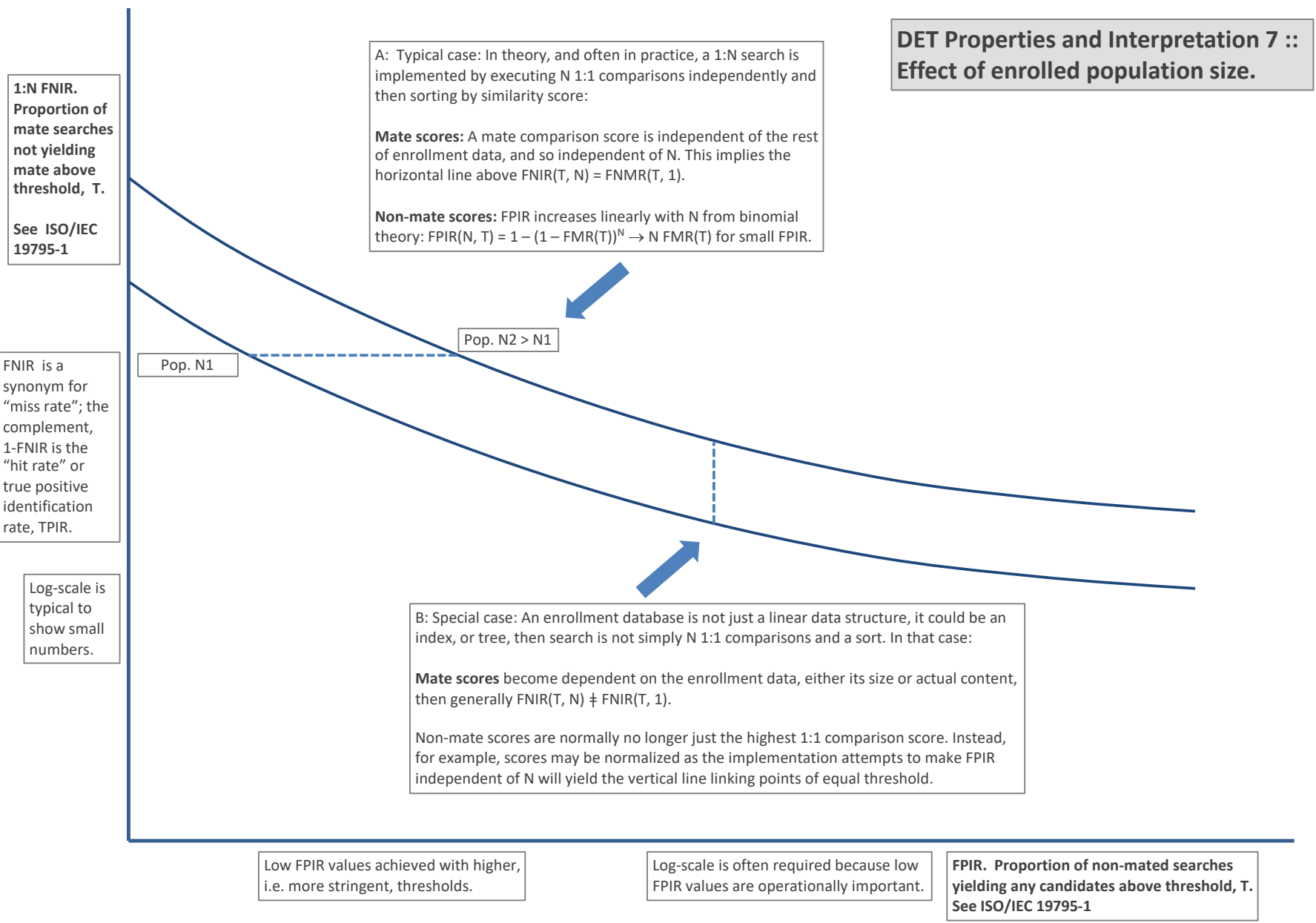


Figure 16: DET as the primary performance reporting mechanism.

2021/10/28  
 13:44:33  
 FNIR(N, R, T) = False neg. identification rate  
 FPIR(N, T) = False pos. identification rate  
 N = Num. enrolled subjects  
 R = Num. candidates examined  
 T = Threshold  
 T = 0 → Investigation  
 T > 0 → Identification

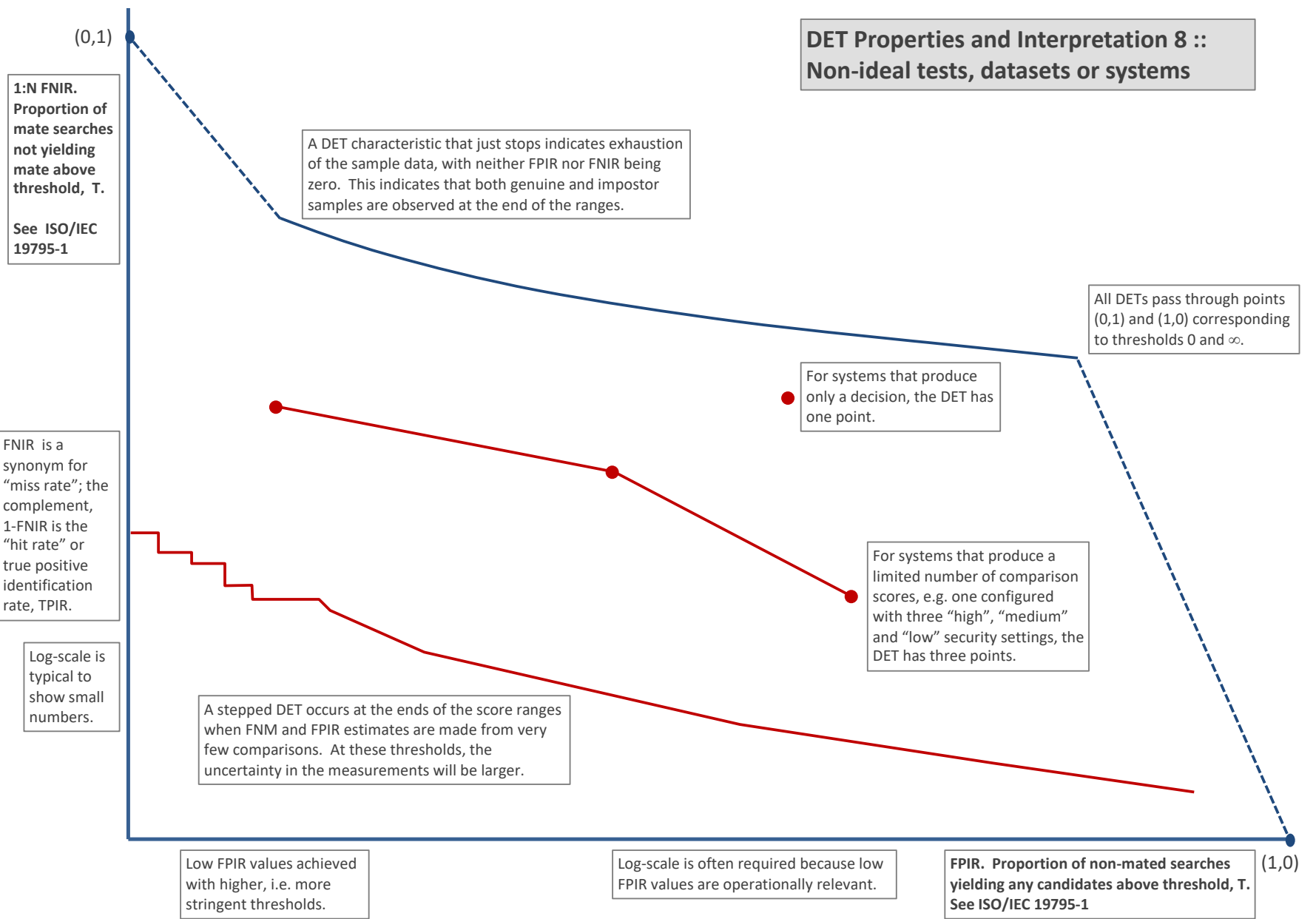


Figure 17: DET as the primary performance reporting mechanism.

### 3.4 Best practice testing requires execution of searches with and without mates

FRVT embeds 1:N searches of two kinds: Those for which there is an enrolled mate, and those for which there is not. The respective numbers for these types of searches appear in Table 1. However, it is common to conduct only mated searches<sup>10</sup>. The cumulative match characteristic is computed from candidate lists produced in mated searches. Even if the CMC is the only metric of interest, the actual trials executed in a test should nevertheless include searches for which no mate exists. As detailed in Table 1 the FRVT reserved disjoint populations of subjects for executing true non-mate searches.

### 3.5 Failure to extract features

During enrollment some algorithms fail to convert a face image to a template. The proportion of failures is the failure-to-enroll rate, denoted by FTE. Similarly, some search images are not converted to templates. The corresponding proportion is termed failure-to-extract, denoted by FTX.

We do not report FTX because we assume that the same underlying algorithm is used for template generation for enrollment and search.

Failure to extract rates are incorporated into FNIR and FPIR measurements as follows.

- ▷ **Enrollment templates:** Any failed enrollment is regarded as producing a zero length template. Algorithms are required by the API [10] to transparently process zero length templates. The effect of template generation failure on search accuracy depends on whether subsequent searches are mated, or non-mated: Mated searches will fail giving elevated FNIR; non-mated searches will not produce false positives so, to first order, FPIR will be reduced by a factor of  $1 - \text{FTE}$ .
- ▷ **Search templates and 1:N search:** In cases where the algorithm fails to produce a search template from input imagery, the result is taken to be a candidate list whose entries have no hypothesized identities and zero score. The effect of template generation failure on search accuracy depends on whether searches are mated, or non-mated: Mated searches will fail giving elevated FNIR; Non-mated searches will not produce false positives, so FPIR will be reduced. Thus given a measurement of false negative and positive rates made over only those where failures-to-extract did not occur, those rates - call them  $\text{FNIR}^\dagger$  and  $\text{FPIR}^\dagger$  - could be adjusted by an explicit measurement of FTX as follows

$$\text{FNIR} = \text{FTX} + (1 - \text{FTX})\text{FNIR}^\dagger \quad (8)$$

$$\text{FPIR} = (1 - \text{FTX})\text{FPIR}^\dagger \quad (9)$$

This approach is the correct treatment for positive-identification applications such as access control where cooperative users are enrolled and make attempts at recognition. This approach is not appropriate to negative identification applications, such as visa fraud detection, in which hostile individuals may attempt to evade detection by submitting poor quality samples. In those cases, template generation failures should be investigated as though a false alarm had occurred.

<sup>10</sup>For example, the [Megaface benchmark](#). This is bad practice for several reasons: First, if a developer knows, or can reasonably assume, that a mate always exists, then unrealistic gaming of the test is possible. A second reason is that it does not put FPIR on equal footing with FNIR and that matters because in most applications, not all searches have mates - not everyone has been previously enrolled in a driving license issuance or a criminal justice system - so addressing between-class separation becomes necessary.

### 3.6 Fixed length candidate lists, threshold independent workload

Suppose an automated face identification algorithm returns  $L$  candidates, and a human reviewer is retained to examine up to  $R$  candidates, where  $R \leq L$  might be set by policy, preference or labor availability. For now, assume also that the reviewer is not provided with, or ignores, similarity scores, and thresholds are not applied. Given the algorithm typically places mates at low (good) ranks, the number of candidates a reviewer can be expected to review can be derived as follows. Note that the reviewer will:

- ▷ Always inspect the first ranked image Frac. reviewed = 1
- ▷ Then inspect those candidates where mate not confirmed at rank 1 Frac. reviewed = 1-CMC(1)
- ▷ Then inspect those candidates where mate not confirmed at rank 1 or 2 Frac. reviewed = 1-CMC(2)

etc. Thus if the reviewer will stop after a maximum of  $R$  candidates, the expected number of candidate reviews is

$$M(R) = 1 + (1 - CMC(1)) + (1 - CMC(2)) + \dots + (1 - CMC(R - 1)) \quad (10)$$

$$= R - \sum_{r=1}^{R-1} CMC(r) \quad (11)$$

A recognition algorithm that front-loads the cumulative match characteristic will offer reduced workload for the reviewer. This workload is defined only over the searches for which a mate exists. In the cases where there truly is no mate, the reviewer would review all  $R$  candidates. Thus, if the proportion of searches for which a mate does exist is  $\beta$ , which in the law enforcement context would be the recidivism rate [3], the full expression for workload becomes:

$$M(R) = \beta \left( R - \sum_{r=1}^{R-1} CMC(r) \right) + (1 - \beta)R \quad (12)$$

$$= R - \beta \sum_{r=1}^{R-1} CMC(r) \quad (13)$$

### 3.7 Timing measurement

Algorithms were submitted to NIST as implementations of the application programming interface(API) specified by NIST in the Evaluation Plan [10]. The API includes functions for initialization, template generation, finalization, search, gallery insert, and gallery delete. Two template generation functions are required, one for the preparation of an enrollment template, and one for a search template.

In NIST's test harness, all functions were wrapped by calls to the C++ `std::chrono::high resolution clock` which on the dedicated timing machine counts 1ns clock ticks. Precision is somewhat worse than that however.

## 3.8 Uncertainty estimation

### 3.8.1 Random error

This study leverages operational datasets for measurement of recognition error rates. This affords several advantages. First, large numbers of searches are conducted (see Table 1) giving precision to the measurements. Moreover, for the two mugshot datasets, these do not involve reuse of individuals so binomial statistics can be expected to apply to recognition error counts. In that case, an observed count of a particular recognition outcome (i.e. a false negative or false positive) in  $M$  trials will sustain 95% confidence that the actual error rate is no larger than some value.

As an example, the minimum number of mugshot searches conducted in this report is  $M = 154\,549$ , and for an observed FNIR around 0.002, the measurement supports a conclusion that the actual FNIR is no higher than 0.00228 at 99% confidence level. On the false positive side, we tabulate FNIR at FPIR values as low as 0.001. Given estimates based on 331\,254 non-mate trials, the actual FPIR values will be below 0.00115 at 99% confidence. In conclusion, large scale evaluation, without reuse of subjects, supports tight uncertainty bounds on the measured error rates.

### 3.8.2 Systematic error

The FRVT 2018 dataset includes anomalies discovered as a result of inspecting images involved in recognition failures from the most accurate algorithms. Two kinds of failure occur: False negatives (which, for the purpose here, include failures to make templates) and false positives.

**False negative errors:** We reviewed 600 false negative pairs for which either or both of the leading two algorithms did not put the correct mate in the top 50 candidates. Given 154\,549 searches, this number represents 0.39% of the total, resulting in FNIR  $\sim 0.0039$ . Of the 600 pairs:

- ▷ **A: Poor quality:** About 20% of the pairs included images of very low quality, often greyscale, low resolution, blurred, low contrast, partially cropped, interlaced, or noisy scans of paper images. Additionally, in a few cases, the face is injured or occluded by bandages or heavy cosmetics.
- ▷ **B: Ground truth identity label bugs:** About 15% of the pairs are not actually mated. We only assigned this outcome when a pair is clearly not mated.
- ▷ **C: Profile views:** About 35% included an image of a profile (side) view of the face, or, more rarely, an image that was rotated 90 degrees in-plane (roll).
- ▷ **D: Tattoos:** About 30% included an image of a tattoo that contained a face image. These arise from mis-labelling in the parent dataset metadata.
- ▷ **E: Ageing:** There is considerable time-lapse between the two captures.

All these estimates are approximate. Of these, the tattoo and mislabeled images can never be matched. These constitute an accuracy floor in the sample implying that FNIR cannot be below 0.0018<sup>11</sup>. The profile-views, low-quality images, and images with considerable ageing can, in principle, be successfully matched - indeed some algorithms do so - so are not part of the accuracy floor.

<sup>11</sup>This value is the sum of two partial false negative rates:  $\text{FNIR}_B = 0.15 * 0.0039$  plus  $\text{FNIR}_D = 0.3 * 0.0039$

For the microsoft-4 algorithm the lowest miss rate from (recent entry in Table 21) is FNIR(640 000, 50, 0) = 0.0018. This is close to the value estimated from the inspection of misses. It is below the 0.0039 figure because the algorithm does match some profile and poor quality images, that the yitu-2 algorithm does not.

For many tables (e.g. Table 21), the FNIR values obtained for the FRVT-2018 mugshots could be corrected by reducing them by 0.0018. The best values would then be indistinct from zero. The results in this report *were not* adjusted to account for this systematic error.

**False positive errors:** As shown in Figure 1 and discussed in Figure 14 many of the DET characteristics in this report exhibit a pronounced turn upward at low false positive rates. The shape can be caused by identity labelling errors in the ground truth of a dataset, specifically persons present in the database under two IDs such that some proportion of non-mate pairs are actually mated. To look for such possibilities, we merged the highest 1000 non-mate pairs produced by three different algorithms which resulted in 1839 unique pairs. This constitutes 0.56% of all non-mate searches. We assert that it is *very* difficult for human reviewers to assign the pairs into the following three categories: twins; doppelgangers; or ground-truth errors (instances of the same person under two IDs). Given this difficulty we made no attempt to correct any possible ground truth errors except by removing 57 pairs in the following categories:

- ▷ **A: Profile views:** Thirteen pairs included one or two profile-view images. As described in Figure 168, these can cause false positives.
- ▷ **B: Same-session photographs:** For twelve pairs, the images were identical or trivially altered (e.g. cropped) versions of the same photo. These were present under a different ID likely due to some clerical or procedural mistake.
- ▷ **C: Tattoos of faces:** There were fourteen instances of tattoo photographs that contained faces causing false matches.
- ▷ **D: T-shirt faces:** There were six instances of T-shirt photographs (of Bob Marley and Che Guevara) being detected instead of the face and causing false positives.
- ▷ **E: Background faces:** There were twelve instances of one subject appearing in the background of two otherwise correct portrait photos.

Note we did not remove any images where there was a chance that the pair was actually a different person.

In any case, the results in this report have not been adjusted for this systematic error.

## 4 Results

This section gives extensive results for algorithms submitted to FRVT 2018. Three page “report cards” for each algorithm are contained in a [separate supplement](#). Performance metrics were described in section 3. The main results are summarized in tabular form with more exhaustive data included as DET, CMC and related graphs in appendices as follows:

- ▷ The three tables 2-4 list algorithms alongside full developer names, acceptance date, size of the provided configuration data, template size and generation time, and search duration data.
  - The **template generation duration** is most important to applications that require fast response. For example, an eGate taking more than two seconds to produce a template might be unacceptable. Note that GPUs may be of utility in expediting this operation for some algorithms, though at additional expense. Two additional factors should be considered<sup>1213</sup>.
  - The **search duration** is the time taken for a search of a search template into a gallery of  $N$  enrollment templates. This performance variable, together with the volume of searches, is influential on the amount of hardware needed to sustain an operational deployment. This is measured here with the algorithm running on a single core of a contemporary CPU. Search is most simply implemented as  $N$  computations of a distance metric followed by a sort operation to find the closest enrollments. However, considerable optimization of this process is possible, up to and including fast-search algorithms that, by various means, avoid computation of all  $N$  distances.
  - The **template size** is the size of the extracted feature vector (or vectors) and any needed header information. Large template sizes may be influential on bus or network bandwidth, storage requirements, and on search duration. While the template itself is an opaque data blob, the feature dimensionality might be estimated by assuming a four-bytes-per-float encoding. There is a wide range of encodings. For the more accurate algorithm, sizes range from 256 bytes to about 2KB bytes, indicating essentially no consensus on face modeling and template design.
  - The **template size multiplier** column shows how, given  $k$  input images, the size of the template grows. Most implementations internally extract features from each image and concatenate them, and implement some score-level fusion logic during search. Other implementations, including many of the most accurate algorithms, produce templates whose size does not grow with  $k$ . This could be achieved via selection of the best quality image - but this is not optimal in handling ageing where the oldest image could be the best quality. Another mechanism would be feature-level fusion where information is fused from all  $k$  inputs. In any case, as a black-box test, the fusion scheme is proprietary and unknown.
  - The size of the **configuration data** is the total size of all files resident in a vendor-provided directory that contains arbitrary read-only files such as parameters, recognition models (e.g. caffe). Generally a large value for this quantity may prohibit the use of the algorithm on a resource-constrained device.

<sup>12</sup>The FRVT 2018 API prohibited threading, so some gains from parallelism may be available on multiple-cores or multiple processors, if the feature extraction code could be distributed across them.

<sup>13</sup>Note also that factors of two or more may be realizable by exploiting modern vector processing instructions on CPUs. It is not clear in our measurements whether all developers exploited Intel’s AVX2 instructions, for example. Our machine was so equipped, but we insisted that the same compiled library should also run on older machines lacking that instruction. The more sophisticated implementations may have detected AVX2 presence and branched accordingly. The less sophisticated may be defaulted to the reduced instruction set. Readers should see the FRVT 2018 API document for the specific chip details.

▷ Tables 21-22 report core rank-based accuracy for mugshot images. The population size is limited to  $N = 1.6$  million identities because this is the largest gallery size on which all algorithms were executed. Notable observations from these tables are as follows:

- **Accuracy gains since 2018:** NIST Interagency Report 8238 documented massive gains over those reported in the FRVT 2014 report, NIST Interagency Report 8009. Further gains are documented in this report. Comparing the most accurate algorithm in November 2018, NEC-3, the value of  $\text{FNIR}(N, L, T)$  reduced from 0.0031 to 0.0024 for the Sensetime-004 algorithm with  $N = 12$  million recent images. The tables show broader gains: many developers have made advances since 2018 with between two and five-fold reduction in errors.
- **Wide range in accuracy:** The rank-1 miss rates vary from  $\text{FNIR}(N, 1, 0) = 0.0012$  for sensetime-004 up to about 0.5 for the very fast but inaccurate microfocus-x algorithms. Among the developers who are superior to NEC in 2013, the range is from 0.002 to 0.035 for camvi-3. This large accuracy range is consistent with the buyer-beware maxim, and indicates that face recognition software is far from being commoditized.

▷ Tables 25-26 report threshold-based error rates,  $\text{FNIR}(N, L, T)$ , for  $N = 1.6$  million for mugshot-mugshot accuracy on FRVT 2014, FRVT 2018, and also (in pink) mugshot-webcam accuracy using FRVT 2018 enrollments. Notable observations from these tables are as follows:

- **Order of magnitude accuracy gains since 2014:** As with rank-based results, the gains in accuracy are substantial, though somewhat reduced. At  $\text{FPIR} = 0.01$ , the best improvement over NEC in 2014 is a 27 fold reduction in FNIR using the NEC.2 algorithm. At  $\text{FPIR} = 0.001$ , the largest gain is a six-fold reduction in FNIR via the NEC.3 algorithm.
- **Broad gains across the industry:** About 19 companies realize accuracy better than the NEC benchmark from 2014. This is somewhat lower than the 28 developers who succeeded on the rank-1 metric. This may be due to the ubiquity of, and emphasis on, the rank-1 metric in many published algorithm development papers.
- **Webcam images:** Searches of webcam images give  $\text{FNIR}(N, T)$  values around 2 to 3 times higher than mugshot searches. Notably the leading developers with mugshots are approximately the same with poorer quality webcams. But some developers e.g. Camvi, Megvii, TongYi, and Neurotechnology do improve their relative rankings on webcams, perhaps indicating their algorithms were tailored to less constrained images.

▷ Tables 15, 18, 19 and show, respectively, high-threshold, rank 1, and rank 50 FNIR values for all algorithms performing searches into five different gallery sizes,  $N = 640\,000$ ,  $N = 1\,600\,000$ ,  $N = 3\,000\,000$ ,  $N = 6\,000\,000$  and  $12\,000\,000$ . The  $\text{FPIR} = 0.001$  table is included to inform high-volume duplicate detection applications. The Rank-1 table is included as a primary accuracy indicator. The Rank-50 table is included to inform agencies who routinely produce 50 candidates for human-review. The notable results are:

- **Slow growth in rank-based miss rates:**  $\text{FNIR}(N, R)$  generally grows as a power law,  $aN^b$ . From the straight lines of many graphs of Figure 20 this is clearly a reasonable model for most, but not all, algorithms. The coefficient  $a$  can be interpreted as FNIR in a gallery of size 1. The more important coefficient  $b$  indicates scalability, and often,  $b \ll 1$ , implies very benign growth in FNIR. The coefficients of the models appear in the Tables 18 and 19.
- **Slow growth in threshold-based miss rates:**  $\text{FNIR}(N, T)$  also generally grows as a power law,  $aN^b$  except at the high threshold values corresponding to low FPIR values. This is visible in the plots of Figure 36 which

show straight lines except for  $FPIR = 0.001$ , which increase more rapidly with  $N$  above 3 000 000. Each trace in those figures shows  $FNIR(N, T)$  at fixed  $FPIR$  with both  $N$  and  $T$  varying. Thus at large  $N$ , it is usually necessary to elevate  $T$  to maintain fixed  $FPIR$ . This causes increased  $FNIR$ . Why that would no-longer obey a power-law is not known. However, if we expect large galleries to contain individuals with familial relations to the non-mate search images - in the most extreme case, twins - then suppression of false positives becomes more difficult. This is discussed in the Figures starting at Fig. 10

- ▷ Figure ?? shows false positives from twins against their enrolled siblings, broken out by type of twin: fraternal or identical. The Figure is based on the enrollment of 104 single images on one of a pair of twins, and then the search of 2354 second images. Note that the dataset is heavily skewed towards identical twins which is not representative of the true population. There is also a skew towards same sex fraternal twin pairs compared to different sex fraternal twin pairs again not representative of the true population.

The notable results are:

- For all algorithms tested, the 1087 mated searches (Twin A vs. Twin A) produce scores almost always above typical operational thresholds, with (not shown) matches at rank 1. The images are of good quality, so this is the result expected from the rest of this report.
- For the 1066 identical twin searches (AB), almost all produce the twin at rank 1, with a few producing the mate at further down the candidate lists rank and low score.
- For the 169 fraternal searches (AB) from same sex pairs, most algorithms give a large number of very high scores, implying false positives at all thresholds. However, there there are long tails containing lower scores that are correctly below threshold. In general, scores that are higher in this distribution are all rank 1 whereas the lower scores have much higher ranks.
- (Not shown) Of the 169, there are 24 fraternal searches (AB) involving different sex twins. Here most algorithms correctly report scores well below the lowest threshold, and usually not on the candidate list at all.

2021/10/28  
 FNIR(N, R, T) = False neg. identification rate  
 FPIR(N, T) = False pos. identification rate  
 N = Num. enrolled subjects  
 R = Num. candidates examined  
 T = Threshold  
 T = 0 → Investigation  
 T > 0 → Identification

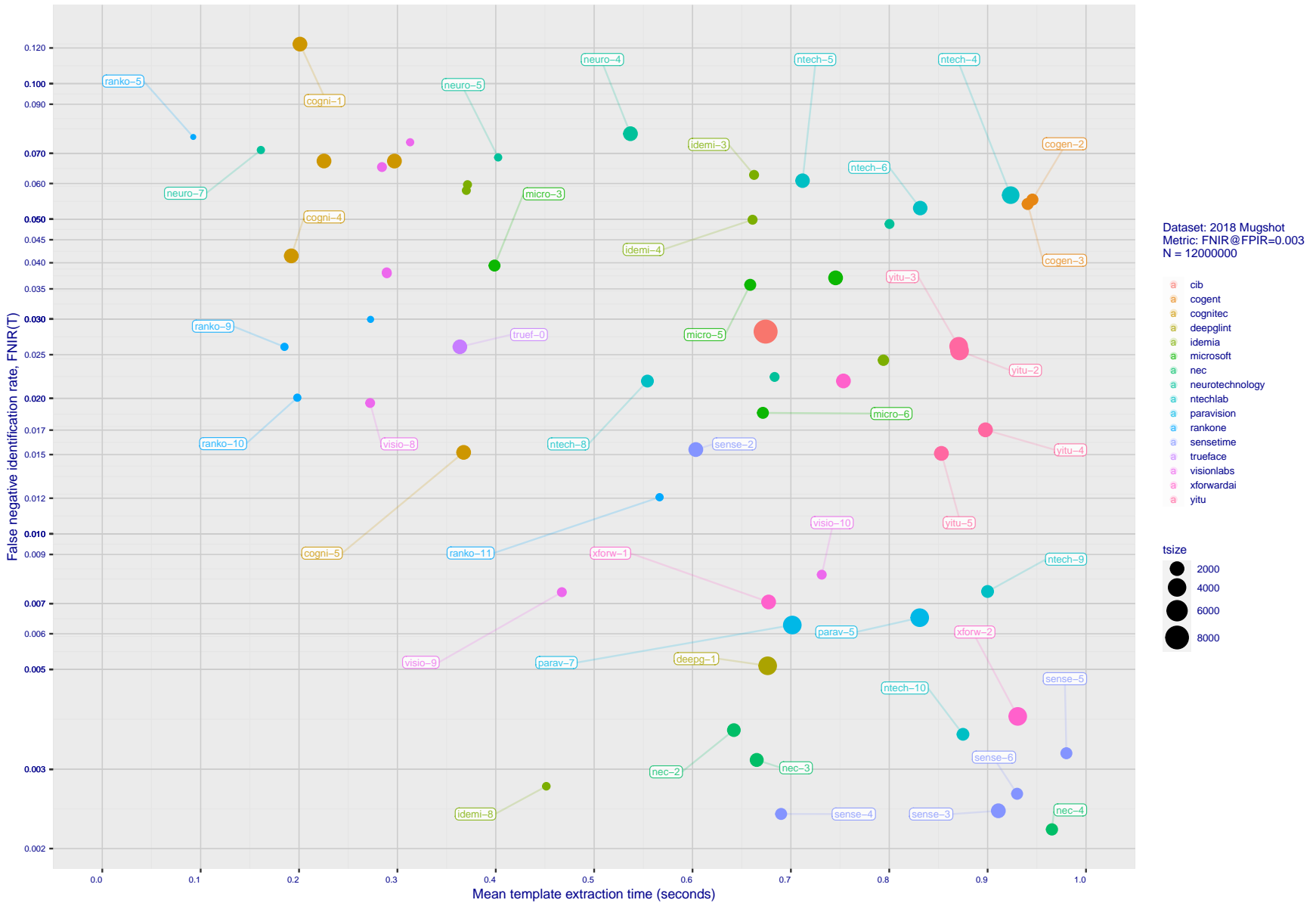


Figure 18: **[Mugshot Dataset] Speed-accuracy tradeoff.** For developers of the more accurate algorithms the plot shows the tradeoff of high-threshold recognition misses,  $FNIR(N, N, T)$  for  $FPIR(N, T) = 0.003$ , and template generation time. Developers are coded by color. Template size is encoded by the size of the circle. Some labels are quite distant from the respective point, to avoid superposing text. Without any other influences, the assumption would be that taking time to localize the face, and extract features, would lead to better accuracy. The most notable result, for NEC, is that their slower algorithms are much more accurate than the version that extract features in fewer than 90 milliseconds.

2021/10/28  
13:44:33

FNIR(N, R, T) =  
FP(R, T) =

False neg. identification rate  
False pos. identification rate

N = Num. enrolled subjects  
R = Num. candidates examined

T = Threshold

T = 0 → Investigation  
T > 0 → Identification

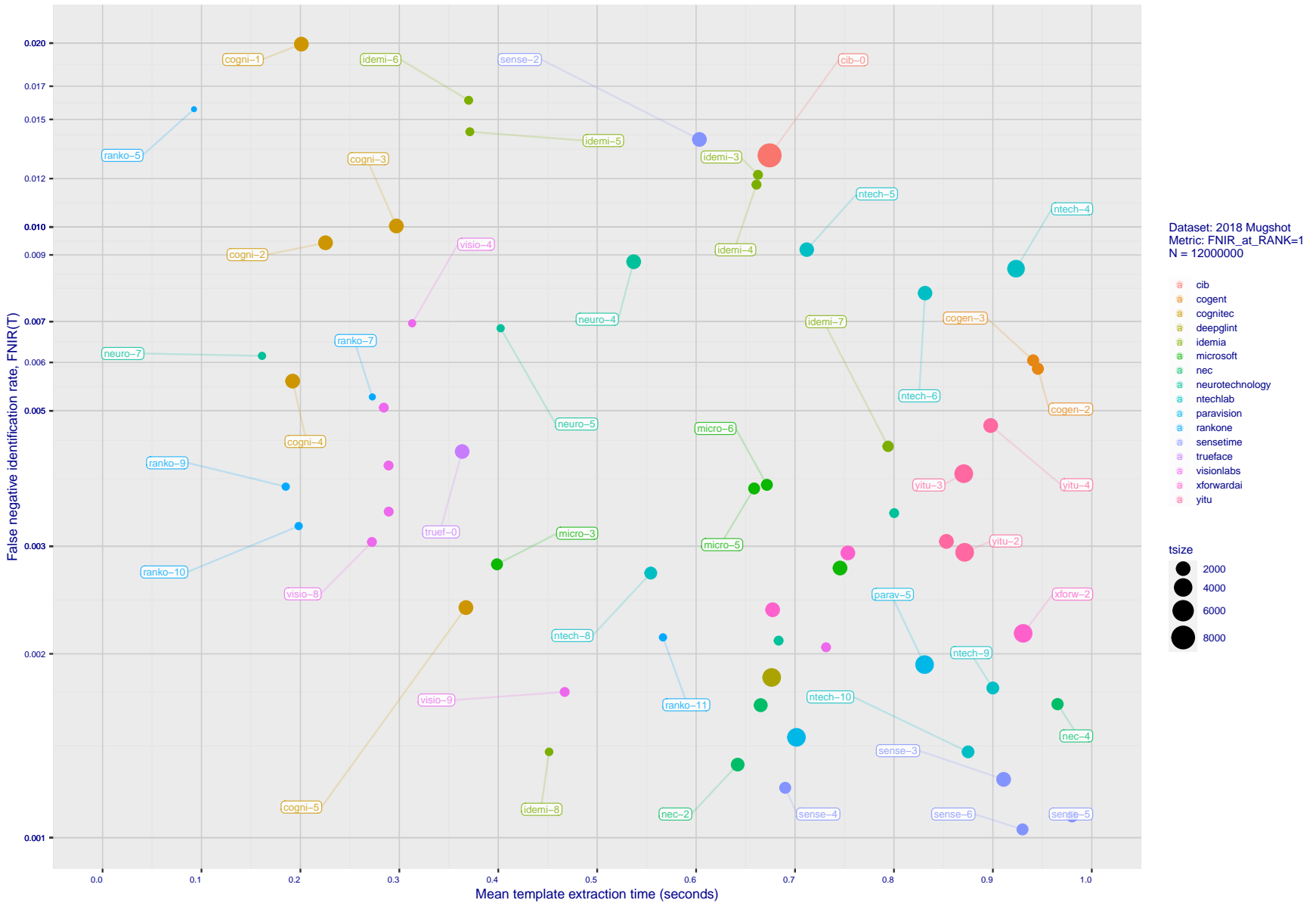


Figure 19: [Mugshot Dataset] Speed-accuracy tradeoff. For developers of the more accurate algorithms the plot shows the tradeoff of rank-one recognition miss-rates,  $FNIR(N, 1, 0)$ , and template generation time. Developers are coded by color. Template size is encoded by the size of the circle. Some labels are quite distant from the respective point, to avoid superposing text. Without any other influences, the assumption would be that taking time to localize the face, and extract features, would lead to better accuracy. This occurs for NEC with their slower algorithm being much accurate than the version that extract features in fewer than 90 milliseconds.

2021/10/28  
 FNIR(N, R, T) = False neg. identification rate  
 13:44:33 FPR(N, T) = False pos. identification rate  
 R = Num. candidates examined  
 T = Threshold  
 T = 0 → Investigation  
 T > 0 → Identification

	DEVELOPER FULL NAME	SHORT NAME	SEQ. NUM.	VALIDATION DATE	CONFIG <sup>1</sup> DATA (MB)	LIB <sup>1</sup> DATA (MB)	TEMPLATE GENERATION		FINALIZE <sup>2</sup> TIME (S)	SEARCH DURATION <sup>5</sup> MILLISEC					POWER LAW (μs)	
							SIZE (B)	MULT <sup>3</sup>		L=1	L=50	L=50	L=50	L=50		L=50
										N=1.6M	N=1.6M	N=1.6M	N=3M	N=6M	N=12M	
1	20Face	20face	000	2021-10-01	112	319	<sup>120</sup> 2048	-	<sup>10</sup> 236	<sup>48</sup> 9	<sup>(169)</sup> 6355	<sup>(171)</sup> 6341	-	-	-	-
2	3Divi	3divi	5	2018-10-26	186	51	<sup>163</sup> 4096	k	<sup>92</sup> 638	<sup>137</sup> 28	<sup>(78)</sup> 538	<sup>(78)</sup> 537	<sup>(72)</sup> 1377	<sup>(69)</sup> 2614	<sup>(65)</sup> 5530	<sup>113</sup> 0.07N <sup>1.1</sup>
3	3Divi	3divi	6	2018-10-26	187	51	<sup>33</sup> 528	k	<sup>93</sup> 640	<sup>24</sup> 5	<sup>(11)</sup> 33	<sup>(12)</sup> 33	-	-	-	-
4	Acer Incorporated	acer	000	2020-08-12	35	67	<sup>28</sup> 512	-	<sup>18</sup> 198	<sup>14</sup> 4	<sup>(52)</sup> 295	<sup>(53)</sup> 295	<sup>(44)</sup> 623	<sup>(63)</sup> 2302	<sup>(58)</sup> 4915	<sup>140</sup> 0.00N <sup>1.3</sup>
5	Akurat Satu Indonesia	ptakuratsatu	000	2020-10-23	0	572	<sup>34</sup> 538	-	<sup>171</sup> 905	<sup>180</sup> 28633	<sup>(6)</sup> 15	<sup>(6)</sup> 16	<sup>(6)</sup> 17	<sup>(5)</sup> 17	<sup>(4)</sup> 17	<sup>3</sup> 6827.74N <sup>0.1</sup>
6	Alchera Inc	alchera	2	2018-10-30	7	14	<sup>81</sup> 2048	k	<sup>6</sup> 114	<sup>163</sup> 3	<sup>(149)</sup> 2923	<sup>(152)</sup> 2929	-	-	-	-
7	Alchera Inc	alchera	3	2018-10-30	251	14	<sup>115</sup> 2048	k	<sup>76</sup> 531	<sup>164</sup> 63	<sup>(150)</sup> 2955	<sup>(153)</sup> 2956	<sup>(130)</sup> 6546	<sup>(131)</sup> 15013	<sup>(131)</sup> 35262	<sup>135</sup> 0.10N <sup>1.2</sup>
8	Alchera Inc	alchera	004	2021-09-17	476	24	<sup>117</sup> 2048	-	<sup>156</sup> 853	<sup>148</sup> 35	<sup>(170)</sup> 6657	<sup>(176)</sup> 6851	-	-	-	-
9	Alivia / Innovation Sys	isystems	3	2018-10-30	350	784	<sup>126</sup> 2048	1	<sup>147</sup> 825	<sup>110</sup> 16	<sup>(64)</sup> 385	<sup>(65)</sup> 389	<sup>(58)</sup> 979	<sup>(57)</sup> 1822	<sup>(84)</sup> 9348	<sup>141</sup> 0.00N <sup>1.3</sup>
10	AllGoVision	allgovision	000	2019-07-30	168	150	<sup>98</sup> 2048	k	<sup>48</sup> 404	<sup>66</sup> 12	<sup>(153)</sup> 3226	<sup>(156)</sup> 3193	<sup>(128)</sup> 6129	<sup>(128)</sup> 12449	<sup>(128)</sup> 25835	<sup>62</sup> 1.40N <sup>1.0</sup>
11	AllGoVision	allgovision	001	2020-07-14	283	126	<sup>124</sup> 2048	-	<sup>136</sup> 777	<sup>72</sup> 13	<sup>(152)</sup> 3174	<sup>(155)</sup> 3183	<sup>(127)</sup> 6073	<sup>(126)</sup> 12284	<sup>(127)</sup> 25701	<sup>60</sup> 1.42N <sup>1.0</sup>
12	Anke Investments	anke	0	2018-10-30	779	27	<sup>151</sup> 2072	k	<sup>58</sup> 429	<sup>108</sup> 16	<sup>(89)</sup> 675	<sup>(94)</sup> 748	<sup>(77)</sup> 1483	<sup>(76)</sup> 2968	<sup>(70)</sup> 6148	<sup>84</sup> 0.21N <sup>1.1</sup>
13	Anke Investments	anke	1	2018-10-30	779	27	<sup>150</sup> 2072	k	<sup>54</sup> 430	<sup>102</sup> 15	<sup>(94)</sup> 707	<sup>(97)</sup> 769	-	-	-	-
14	Anke Investments	anke	002	2019-06-27	341	401	<sup>142</sup> 2056	k	<sup>88</sup> 623	<sup>81</sup> 13	<sup>(88)</sup> 624	<sup>(89)</sup> 682	<sup>(69)</sup> 1306	<sup>(65)</sup> 2403	<sup>(62)</sup> 5082	<sup>53</sup> 0.30N <sup>1.0</sup>
15	Aware	aware	5	2018-10-30	368	27	<sup>159</sup> 3100	k	<sup>141</sup> 792	<sup>146</sup> 34	<sup>(15)</sup> 98	<sup>(18)</sup> 203	<sup>(16)</sup> 371	<sup>(12)</sup> 252	<sup>13</sup> 4.13N <sup>0.7</sup>	
16	Aware	aware	6	2018-10-30	368	27	<sup>2</sup> 124	k	<sup>140</sup> 789	<sup>2</sup> 2	<sup>(30)</sup> 158	<sup>(30)</sup> 162	-	-	-	-
17	Ayonix	ayonix	1	2018-10-29	74	2	<sup>83</sup> 1036	k	<sup>2</sup> 12	<sup>61</sup> 11	<sup>(48)</sup> 279	<sup>(49)</sup> 279	-	-	-	-
18	Ayonix	ayonix	2	2018-10-30	74	2	<sup>52</sup> 1036	1	<sup>1</sup> 11	<sup>87</sup> 14	<sup>(47)</sup> 279	<sup>(48)</sup> 276	<sup>(38)</sup> 535	<sup>(34)</sup> 1087	<sup>(34)</sup> 2284	<sup>69</sup> 0.11N <sup>1.0</sup>
19	Camvi Technologies	camvitech	4	2018-10-30	233	220	<sup>44</sup> 1024	1	<sup>108</sup> 686	<sup>144</sup> 31	<sup>(12)</sup> 33	<sup>(11)</sup> 32	<sup>(10)</sup> 38	<sup>(9)</sup> 40	<sup>(7)</sup> 48	<sup>4</sup> 8492.66N <sup>0.1</sup>
20	Camvi Technologies	camvitech	5	2018-10-30	257	220	<sup>42</sup> 1024	1	<sup>122</sup> 751	<sup>142</sup> 31	<sup>(10)</sup> 31	<sup>(9)</sup> 30	-	-	-	-
21	Canon Inc	cib	000	2020-10-19	426	127	<sup>181</sup> 8196	-	<sup>102</sup> 674	<sup>168</sup> 113	<sup>(154)</sup> 3589	<sup>(158)</sup> 3604	<sup>(131)</sup> 6738	<sup>(129)</sup> 13495	<sup>(129)</sup> 27114	<sup>25</sup> 2.33N <sup>1.0</sup>
22	Cloudwalk - Hengrui AI Technology	hr	000	2021-02-10	501	392	<sup>107</sup> 2048	-	<sup>172</sup> 905	<sup>95</sup> 15	<sup>(49)</sup> 282	<sup>(47)</sup> 276	<sup>(37)</sup> 539	<sup>(42)</sup> 1268	<sup>(48)</sup> 3177	<sup>117</sup> 0.03N <sup>1.1</sup>
23	Cognitec Systems GmbH	cognitec	2	2018-10-30	463	26	<sup>139</sup> 2052	k	<sup>18</sup> 225	<sup>132</sup> 27	<sup>(138)</sup> 1733	<sup>(137)</sup> 1763	<sup>(117)</sup> 3660	<sup>(115)</sup> 7279	<sup>(113)</sup> 13895	<sup>57</sup> 0.83N <sup>1.0</sup>
24	Cognitec Systems GmbH	cognitec	3	2018-10-30	465	26	<sup>138</sup> 2052	k	<sup>29</sup> 297	<sup>106</sup> 16	<sup>(134)</sup> 1719	<sup>(138)</sup> 1791	<sup>(116)</sup> 3638	<sup>(114)</sup> 7277	<sup>(117)</sup> 14904	<sup>76</sup> 0.66N <sup>1.0</sup>
25	Cognitec Systems GmbH	cognitec	004	2021-03-08	384	60	<sup>131</sup> 2052	-	<sup>13</sup> 192	<sup>79</sup> 13	<sup>(133)</sup> 1673	<sup>(135)</sup> 1727	<sup>(107)</sup> 2904	<sup>(105)</sup> 5801	<sup>(103)</sup> 11707	<sup>22</sup> 1.15N <sup>1.0</sup>
26	Cognitec Systems GmbH	cognitec	005	2021-07-30	460	61	<sup>129</sup> 2052	-	<sup>36</sup> 367	<sup>48</sup> 9	<sup>(126)</sup> 1556	<sup>(127)</sup> 1551	<sup>(109)</sup> 2916	<sup>(113)</sup> 6561	<sup>(114)</sup> 13958	<sup>90</sup> 0.38N <sup>1.1</sup>
27	Cubox	cubox	000	2021-08-24	529	298	<sup>96</sup> 2048	-	<sup>174</sup> 917	<sup>54</sup> 10	<sup>(158)</sup> 3646	<sup>(160)</sup> 4076	<sup>(133)</sup> 7605	<sup>(132)</sup> 15871	-	<sup>83</sup> 1.16N <sup>1.1</sup>
28	Cyberlink Corp	cyberlink	000	2019-06-12	217	93	<sup>133</sup> 2052	1	<sup>98</sup> 654	<sup>140</sup> 30	<sup>(91)</sup> 696	<sup>(91)</sup> 701	<sup>(73)</sup> 1379	<sup>(70)</sup> 2639	<sup>(72)</sup> 6214	<sup>71</sup> 0.28N <sup>1.0</sup>
29	Cyberlink Corp	cyberlink	001	2019-10-07	459	102	<sup>132</sup> 2052	1	<sup>51</sup> 423	<sup>138</sup> 28	<sup>(92)</sup> 698	<sup>(90)</sup> 700	<sup>(71)</sup> 1350	<sup>(103)</sup> 5524	<sup>(106)</sup> 12031	<sup>139</sup> 0.00N <sup>1.3</sup>
30	Cyberlink Corp	cyberlink	002	2020-07-31	333	109	<sup>176</sup> 4140	-	<sup>123</sup> 724	<sup>172</sup> 6875	<sup>(123)</sup> 1353	<sup>(157)</sup> 3198	<sup>(129)</sup> 6138	<sup>(125)</sup> 12205	<sup>(111)</sup> 13106	<sup>16</sup> 16.71N <sup>0.8</sup>
31	Cyberlink Corp	cyberlink	003	2021-01-05	333	100	<sup>179</sup> 6212	-	<sup>111</sup> 691	<sup>150</sup> 35	<sup>(73)</sup> 488	<sup>(92)</sup> 723	<sup>(75)</sup> 1415	<sup>(74)</sup> 2886	<sup>(66)</sup> 5643	<sup>99</sup> 0.12N <sup>1.1</sup>
32	Cyberlink Corp	cyberlink	004	2021-07-16	371	100	<sup>178</sup> 6212	-	<sup>123</sup> 728	<sup>128</sup> 23	<sup>(74)</sup> 492	<sup>(77)</sup> 504	<sup>(59)</sup> 923	<sup>(47)</sup> 1448	<sup>(50)</sup> 3350	<sup>19</sup> 0.73N <sup>0.9</sup>
33	Dahua Technology Co Ltd	dahua	0	2018-10-29	276	167	<sup>125</sup> 2048	k	<sup>41</sup> 374	<sup>122</sup> 22	-	<sup>(45)</sup> 258	-	-	-	-
34	Dahua Technology Co Ltd	dahua	1	2018-10-29	276	167	<sup>122</sup> 2048	k	<sup>39</sup> 369	<sup>134</sup> 28	-	<sup>(44)</sup> 257	<sup>(42)</sup> 602	<sup>(40)</sup> 1202	<sup>(46)</sup> 3007	<sup>124</sup> 0.02N <sup>1.2</sup>
35	Dahua Technology Co Ltd	dahua	002	2019-12-02	607	137	<sup>88</sup> 2048	k	<sup>107</sup> 685	<sup>121</sup> 19	<sup>(40)</sup> 243	<sup>(46)</sup> 269	<sup>(65)</sup> 1189	<sup>(75)</sup> 2950	<sup>(78)</sup> 6732	<sup>145</sup> 0.00N <sup>1.5</sup>
36	Dahua Technology Co Ltd	dahua	003	2020-11-18	889	154	<sup>116</sup> 2048	-	<sup>122</sup> 723	<sup>114</sup> 18	<sup>(50)</sup> 283	<sup>(43)</sup> 249	<sup>(32)</sup> 468	<sup>(32)</sup> 935	<sup>(30)</sup> 1871	<sup>26</sup> 0.16N <sup>1.0</sup>
37	Deepglint	deepglint	001	2019-11-15	448	265	<sup>161</sup> 4096	-	<sup>108</sup> 676	<sup>147</sup> 35	<sup>(90)</sup> 677	<sup>(125)</sup> 1495	<sup>(81)</sup> 1724	<sup>(72)</sup> 2747	<sup>(73)</sup> 6246	<sup>14</sup> 25.27N <sup>0.8</sup>
38	Dermalog	dermalog	5	2018-10-26	0	440	<sup>3</sup> 128	1	<sup>75</sup> 528	<sup>171</sup> 3155	<sup>(1)</sup> 0	<sup>(1)</sup> 0	<sup>(1)</sup> 0	<sup>(1)</sup> 0	<sup>(1)</sup> 0	<sup>5</sup> 66.21N <sup>0.2</sup>
39	Dermalog	dermalog	6	2018-10-26	0	453	<sup>15</sup> 256	1	<sup>72</sup> 507	<sup>3</sup> 2	<sup>(27)</sup> 142	<sup>(27)</sup> 144	<sup>(23)</sup> 269	<sup>(22)</sup> 531	<sup>(21)</sup> 1294	<sup>77</sup> 0.05N <sup>1.0</sup>
40	Dermalog	dermalog	007	2020-02-12	0	424	<sup>4</sup> 128	1	<sup>58</sup> 410	<sup>1</sup> 1	<sup>(20)</sup> 98	<sup>(17)</sup> 96	<sup>(20)</sup> 218	<sup>(18)</sup> 429	<sup>(18)</sup> 1013	<sup>106</sup> 0.10N <sup>1.1</sup>
41	Dermalog	dermalog	008	2021-01-25	0	531	<sup>22</sup> 512	-	<sup>38</sup> 370	<sup>16</sup> 4	<sup>(58)</sup> 335	<sup>(40)</sup> 246	<sup>(31)</sup> 462	<sup>(31)</sup> 924	<sup>(29)</sup> 1849	<sup>29</sup> 0.15N <sup>1.0</sup>
42	FarBar Inc	f8	001	2019-10-03	266	19	<sup>128</sup> 2048	k	<sup>148</sup> 810	<sup>84</sup> 14	-	-	-	-	-	-
43	Fincore Ltd	fincore	000	2021-08-18	250	224	<sup>99</sup> 2048	-	<sup>61</sup> 475	<sup>49</sup> 9	<sup>(83)</sup> 562	<sup>(82)</sup> 560	-	-	-	-
44	Fujitsu Research and Development Center	fujitsulab	000	2021-10-12	497	337	<sup>47</sup> 1032	-	<sup>179</sup> 945	<sup>26</sup> 5	<sup>(132)</sup> 1668	<sup>(131)</sup> 1657	<sup>(113)</sup> 3140	<sup>(110)</sup> 6320	<sup>(109)</sup> 12723	<sup>52</sup> 0.78N <sup>1.0</sup>
45	Gorilla Technology	gorilla	2	2018-10-29	91	1252	<sup>59</sup> 1132	k	<sup>33</sup> 338	<sup>130</sup> 24	<sup>(28)</sup> 145	<sup>(28)</sup> 146	<sup>(24)</sup> 293	<sup>(23)</sup> 612	<sup>(25)</sup> 1509	<sup>104</sup> 0.02N <sup>1.1</sup>
46	Gorilla Technology	gorilla	3	2018-10-26	94	1252	<sup>152</sup> 2156	k	<sup>78</sup> 559	<sup>176</sup> 12020	-	<sup>(141)</sup> 2047	-	-	-	-
47	Gorilla Technology	gorilla	004	2020-01-06	182	1244	<sup>153</sup> 2192	k	<sup>43</sup> 388	<sup>152</sup> 41	<sup>(51)</sup> 286	<sup>(52)</sup> 285	<sup>(66)</sup> 1191	<sup>(66)</sup> 2416	<sup>(61)</sup> 5036	<sup>138</sup> 0.00N <sup>1.3</sup>
48	Gorilla Technology	gorilla	005	2021-02-22	306	1420	<sup>160</sup> 8288	-	<sup>6</sup> 483	<sup>166</sup> 78	<sup>(98)</sup> 802	<sup>(98)</sup> 799	<sup>(78)</sup> 1514	<sup>(86)</sup> 4454	<sup>(80)</sup> 8820	<sup>126</sup> 0.05N <sup>1.2</sup>
49	Gorilla Technology	gorilla	006	2021-09-30	377	691	<sup>182</sup> 8336	-	<sup>132</sup> 767	<sup>167</sup> 99	<sup>(129)</sup> 1626	<sup>(128)</sup> 1612	<sup>(94)</sup> 2422	<sup>(85)</sup> 4422	<sup>(85)</sup> 9363	<sup>51</sup> 0.59N <sup>1.0</sup>
50	Guangzhou Pixel Solutions Co Ltd	pixelall	002	2019-07-01	0	165	<sup>154</sup> 2560	k	<sup>12</sup> 190	<sup>99</sup> 15	<sup>(121)</sup> 1296	<sup>(122)</sup> 1334	<sup>(100)</sup> 2526	<sup>(95)</sup> 5136	<sup>(99)</sup> 11045	<sup>70</sup> 0.52N <sup>1.0</sup>
51	Guangzhou Pixel Solutions Co Ltd	pixelall	003	2019-11-05	0	690	<sup>155</sup> 2560	k	<sup>116</sup> 703	<sup>127</sup> 22	<sup>(118)</sup> 1273	<sup>(119)</sup> 1307	<sup>(97)</sup> 2474	<sup>(96)</sup> 5198	<sup>(100)</sup> 11141	<sup>78</sup> 0.46N <sup>1.0</sup>
52	Guangzhou Pixel Solutions Co Ltd	pixelall	004	2020-07-02	0	538	<sup>157</sup> 2560	k	<sup>55</sup> 449	<sup>113</sup> 17	<sup>(117)</sup> 1259	<sup>(118)</sup> 1300	<sup>(96)</sup> 2465	<sup>(101)</sup> 5492	<sup>(101)</sup> 11	

2021/10/28  
 FN(R/N, R, T) =  
 13:44:33 FPR(N, T) =  
 False neg. identification rate  
 R = Num. candidates examined  
 T = Threshold  
 T = 0 → Investigation  
 T > 0 → Identification

	DEVELOPER FULL NAME	SHORT NAME	SEQ. NUM.	VALIDATION DATE	CONFIG <sup>1</sup> DATA (MB)	LIB <sup>1</sup> DATA (MB)	TEMPLATE GENERATION			FINALIZE <sup>2</sup> TIME (S)		SEARCH DURATION <sup>5</sup> MILLISEC						POWER LAW (μs)
							SIZE (B)	MULT <sup>3</sup>	TIME (MS) <sup>4</sup>	N=1.6M	N=1.6M	N=1.6M	N=3M	N=6M	N=12M			
																L=1	L=50	
53	Guangzhou Pixel Solutions Co Ltd	pixelall	005	2021-03-23	0	717	<sup>156</sup> 2560	-	<sup>153</sup> 840	<sup>60</sup> 11	<sup>(128)</sup> 1606	<sup>(126)</sup> 1528	<sup>(102)</sup> 2609	<sup>(92)</sup> 4926	<sup>(104)</sup> 11770	<sup>(84)</sup> 44.0.73N <sup>1.0</sup>		
54	Hikvision Research Institute	hikvision	5	2018-10-29	593	9	<sup>64</sup> 1408	1	<sup>85</sup> 607	<sup>105</sup> 16	<sup>(103)</sup> 883	<sup>(104)</sup> 895	<sup>(84)</sup> 1908	<sup>(79)</sup> 3792	<sup>(86)</sup> 9387	<sup>(114)</sup> 0.10N <sup>1.1</sup>		
55	Hikvision Research Institute	hikvision	6	2018-10-29	593	9	<sup>63</sup> 1408	1	<sup>85</sup> 598	<sup>107</sup> 16	<sup>(101)</sup> 871	<sup>(103)</sup> 877	-	-	-	-		
56	HyperVerge Inc	hyperverge	001	2021-08-11	1791	212	<sup>45</sup> 1024	-	<sup>152</sup> 845	<sup>25</sup> 5	<sup>(93)</sup> 705	<sup>(88)</sup> 681	<sup>(70)</sup> 1346	<sup>(71)</sup> 2681	<sup>(67)</sup> 5680	<sup>59</sup> 0.32N <sup>1.0</sup>		
57	Idemia	idemia	5	2018-10-29	417	48	<sup>21</sup> 352	1	<sup>40</sup> 371	<sup>25</sup> 5	<sup>(24)</sup> 137	<sup>(25)</sup> 138	<sup>(29)</sup> 437	<sup>(28)</sup> 724	<sup>(26)</sup> 1630	<sup>132</sup> 0.01N <sup>1.2</sup>		
58	Idemia	idemia	6	2018-10-29	417	48	<sup>20</sup> 352	1	<sup>39</sup> 370	<sup>24</sup> 4	<sup>(25)</sup> 137	<sup>(24)</sup> 138	<sup>(30)</sup> 442	<sup>(30)</sup> 827	<sup>(27)</sup> 1646	<sup>134</sup> 0.01N <sup>1.2</sup>		
59	Idemia	idemia	007	2020-01-17	738	113	<sup>40</sup> 860	1	<sup>142</sup> 794	<sup>85</sup> 14	<sup>(29)</sup> 151	<sup>(29)</sup> 152	<sup>(47)</sup> 683	<sup>(49)</sup> 1481	<sup>(47)</sup> 3022	<sup>143</sup> 0.00N <sup>1.4</sup>		
60	Idemia	idemia	008	2021-03-15	378	65	<sup>19</sup> 300	-	<sup>57</sup> 451	<sup>12</sup> 3	<sup>(23)</sup> 132	<sup>(23)</sup> 131	<sup>(21)</sup> 247	<sup>(20)</sup> 501	<sup>(19)</sup> 1013	<sup>41</sup> 0.07N <sup>1.0</sup>		
61	Imagus Technology Pty Ltd	imagus	005	2021-01-15	222	311	<sup>127</sup> 2048	-	<sup>137</sup> 786	<sup>83</sup> 14	<sup>(39)</sup> 236	<sup>(56)</sup> 313	<sup>(45)</sup> 651	<sup>(45)</sup> 1361	<sup>(36)</sup> 2461	<sup>112</sup> 0.03N <sup>1.1</sup>		
62	Imagus Technology Pty Ltd	imagus	006	2021-05-27	248	369	<sup>111</sup> 2048	-	<sup>170</sup> 904	<sup>50</sup> 9	<sup>(56)</sup> 317	<sup>(39)</sup> 234	<sup>(33)</sup> 499	<sup>(43)</sup> 1273	<sup>(39)</sup> 2727	<sup>131</sup> 0.01N <sup>1.2</sup>		
63	Imperial College London	imperial	000	2019-08-28	461	15	<sup>37</sup> 2048	1	<sup>85</sup> 577	<sup>71</sup> 13	<sup>(61)</sup> 360	<sup>(64)</sup> 379	<sup>(79)</sup> 1626	<sup>(82)</sup> 4057	<sup>(97)</sup> 10291	<sup>146</sup> 0.00N <sup>1.5</sup>		
64	Incode Technologies Inc	incode	2	2018-10-29	71	31	<sup>30</sup> 2048	1	<sup>29</sup> 289	<sup>104</sup> 15	<sup>(69)</sup> 411	<sup>(66)</sup> 404	-	-	-	-		
65	Incode Technologies Inc	incode	3	2018-10-29	133	31	<sup>85</sup> 2048	1	<sup>114</sup> 697	<sup>94</sup> 15	<sup>(68)</sup> 408	<sup>(69)</sup> 412	<sup>(52)</sup> 847	<sup>(50)</sup> 1608	<sup>(56)</sup> 4486	<sup>108</sup> 0.05N <sup>1.1</sup>		
66	Incode Technologies Inc	incode	004	2019-06-24	254	50	<sup>82</sup> 2048	1	<sup>64</sup> 475	<sup>64</sup> 12	<sup>(62)</sup> 365	<sup>(63)</sup> 378	<sup>(78)</sup> 1482	<sup>(52)</sup> 1660	<sup>(45)</sup> 2954	<sup>87</sup> 0.12N <sup>1.1</sup>		
67	Incode Technologies Inc	incode	005	2021-07-29	259	21	<sup>91</sup> 2048	-	<sup>69</sup> 500	<sup>53</sup> 10	<sup>(55)</sup> 316	<sup>(73)</sup> 454	<sup>(66)</sup> 890	<sup>(58)</sup> 1843	<sup>(53)</sup> 3640	<sup>98</sup> 0.07N <sup>1.1</sup>		
68	Innovatrics	innovatrics	4	2018-10-30	0	400	<sup>57</sup> 1076	k	<sup>44</sup> 399	<sup>173</sup> 10902	<sup>(5)</sup> 8	<sup>(4)</sup> 8	<sup>(4)</sup> 11	<sup>(2)</sup> 9	<sup>(3)</sup> 13	<sup>9</sup> 668.38N <sup>0.2</sup>		
69	Innovatrics	innovatrics	005	2019-09-30	0	455	<sup>36</sup> 538	1	<sup>142</sup> 827	<sup>175</sup> 11897	<sup>(4)</sup> 8	<sup>(5)</sup> 8	<sup>(3)</sup> 9	<sup>(3)</sup> 9	<sup>(2)</sup> 9	<sup>1</sup> 4055.65N <sup>0.1</sup>		
70	Innovatrics	innovatrics	007	2021-08-16	175	58	<sup>35</sup> 538	-	<sup>137</sup> 777	<sup>86</sup> 14	<sup>(19)</sup> 97	<sup>(20)</sup> 100	<sup>(16)</sup> 188	<sup>(17)</sup> 378	<sup>(16)</sup> 788	<sup>20</sup> 0.09N <sup>1.0</sup>		
71	IrexAI	irex	000	2021-02-09	724	46	<sup>158</sup> 3080	-	<sup>154</sup> 844	<sup>120</sup> 19	<sup>(87)</sup> 616	<sup>(85)</sup> 600	<sup>(62)</sup> 1120	<sup>(68)</sup> 2477	<sup>(68)</sup> 5863	<sup>93</sup> 0.13N <sup>1.1</sup>		
72	Kakao Enterprise	kakao	000	2021-06-23	404	124	<sup>137</sup> 2052	-	<sup>152</sup> 835	<sup>38</sup> 8	<sup>(38)</sup> 213	<sup>(37)</sup> 215	<sup>(34)</sup> 510	<sup>(33)</sup> 971	<sup>(31)</sup> 1955	<sup>95</sup> 0.05N <sup>1.1</sup>		
73	Kedacom International Pte	kedacom	001	2019-09-16	239	36	<sup>17</sup> 292	1	<sup>71</sup> 507	<sup>4</sup> 2	<sup>(96)</sup> 764	<sup>(95)</sup> 760	<sup>(85)</sup> 1940	<sup>(77)</sup> 2983	<sup>(74)</sup> 6623	<sup>73</sup> 0.31N <sup>1.0</sup>		
74	Kneron	kneron	000	2020-03-03	366	13	<sup>100</sup> 2048	k	<sup>74</sup> 523	<sup>76</sup> 13	<sup>(146)</sup> 2535	<sup>(149)</sup> 2506	<sup>(129)</sup> 4752	<sup>(123)</sup> 9696	<sup>(128)</sup> 20926	<sup>74</sup> 0.95N <sup>1.0</sup>		
75	Kneron	kneron	001	2021-06-10	270	69	<sup>115</sup> 2048	-	<sup>62</sup> 472	<sup>49</sup> 9	<sup>(114)</sup> 2690	<sup>(151)</sup> 2642	-	-	-	-		
76	Line Corporation	line	000	2021-06-02	138	397	<sup>78</sup> 2048	-	<sup>65</sup> 481	<sup>38</sup> 8	<sup>(161)</sup> 5433	<sup>(165)</sup> 5418	<sup>(136)</sup> 10144	-	-	<sup>24</sup> 3.65N <sup>1.0</sup>		
77	Lomonosov Moscow State University	intsysmsu	000	2019-08-19	375	168	<sup>94</sup> 2048	1	<sup>86</sup> 614	<sup>77</sup> 13	<sup>(71)</sup> 430	<sup>(71)</sup> 431	<sup>(55)</sup> 860	<sup>(53)</sup> 1730	<sup>(64)</sup> 5353	<sup>122</sup> 0.03N <sup>1.1</sup>		
78	Lookman Electroplast Industries	lookman	3	2018-10-28	203	24	<sup>18</sup> 292	1	<sup>32</sup> 336	<sup>11</sup> 3	<sup>(95)</sup> 739	<sup>(93)</sup> 745	<sup>(74)</sup> 1394	<sup>(73)</sup> 2817	<sup>(77)</sup> 8286	<sup>102</sup> 0.13N <sup>1.1</sup>		
79	Lookman Electroplast Industries	lookman	4	2018-10-28	184	24	<sup>37</sup> 548	1	<sup>38</sup> 320	<sup>14</sup> 4	<sup>(105)</sup> 981	<sup>(106)</sup> 998	-	-	-	-		
80	Lookman Electroplast Industries	lookman	005	2019-09-16	239	36	<sup>38</sup> 548	1	<sup>70</sup> 506	<sup>14</sup> 4	<sup>(106)</sup> 1005	<sup>(107)</sup> 1008	<sup>(101)</sup> 2597	<sup>(100)</sup> 5446	<sup>(81)</sup> 8939	<sup>100</sup> 0.19N <sup>1.1</sup>		
81	Megvii/Face++	megvii	1	2018-10-28	1703	41	<sup>165</sup> 4096	1	<sup>90</sup> 631	<sup>145</sup> 32	<sup>(79)</sup> 552	<sup>(83)</sup> 561	<sup>(68)</sup> 1222	<sup>(64)</sup> 2321	<sup>(69)</sup> 5968	<sup>107</sup> 0.08N <sup>1.1</sup>		
82	Megvii/Face++	megvii	2	2018-10-28	1735	42	<sup>171</sup> 4096	1	<sup>91</sup> 635	<sup>143</sup> 31	<sup>(80)</sup> 553	<sup>(80)</sup> 558	-	-	-	-		
83	MicroFocus	microfocus	5	2018-10-29	94	26	<sup>12</sup> 256	k	<sup>22</sup> 262	<sup>7</sup> 2	<sup>(35)</sup> 182	<sup>(34)</sup> 186	<sup>(27)</sup> 354	<sup>(27)</sup> 708	<sup>(23)</sup> 1425	<sup>38</sup> 0.11N <sup>1.0</sup>		
84	MicroFocus	microfocus	6	2018-10-29	94	26	<sup>10</sup> 256	k	<sup>22</sup> 262	<sup>9</sup> 2	<sup>(36)</sup> 183	<sup>(33)</sup> 186	-	-	-	-		
85	Microsoft	microsoft	5	2018-10-29	381	155	<sup>43</sup> 1024	1	<sup>92</sup> 658	<sup>62</sup> 11	<sup>(127)</sup> 1606	<sup>(132)</sup> 1673	<sup>(112)</sup> 3076	<sup>(109)</sup> 6302	<sup>(112)</sup> 13160	<sup>50</sup> 0.79N <sup>1.0</sup>		
86	Microsoft	microsoft	6	2018-10-29	478	155	<sup>41</sup> 1024	1	<sup>100</sup> 671	<sup>98</sup> 15	<sup>(130)</sup> 1642	<sup>(130)</sup> 1618	<sup>(118)</sup> 3710	<sup>(111)</sup> 6401	<sup>(110)</sup> 12892	<sup>66</sup> 0.68N <sup>1.0</sup>		
87	N-Tech Lab	ntech	5	2018-10-30	1685	113	<sup>78</sup> 1940	k	<sup>120</sup> 711	<sup>161</sup> 55	<sup>(42)</sup> 243	<sup>(42)</sup> 246	<sup>(36)</sup> 538	<sup>(35)</sup> 1100	<sup>(42)</sup> 2867	<sup>118</sup> 0.02N <sup>1.1</sup>		
88	N-Tech Lab	ntech	6	2018-10-30	1686	117	<sup>76</sup> 1940	k	<sup>151</sup> 831	<sup>162</sup> 63	<sup>(41)</sup> 243	<sup>(41)</sup> 246	<sup>(38)</sup> 546	<sup>(36)</sup> 1104	<sup>(43)</sup> 2873	<sup>120</sup> 0.02N <sup>1.1</sup>		
89	N-Tech Lab	ntechlab	007	2019-06-25	2450	51	<sup>160</sup> 3348	k	<sup>143</sup> 795	<sup>165</sup> 73	<sup>(65)</sup> 393	<sup>(70)</sup> 427	<sup>(60)</sup> 780	<sup>(56)</sup> 1768	<sup>(52)</sup> 3499	<sup>72</sup> 0.16N <sup>1.0</sup>		
90	N-Tech Lab	ntechlab	008	2020-01-06	1111	51	<sup>61</sup> 1300	k	<sup>77</sup> 554	<sup>151</sup> 36	<sup>(34)</sup> 179	<sup>(31)</sup> 184	<sup>(26)</sup> 341	<sup>(26)</sup> 683	<sup>(22)</sup> 1395	<sup>36</sup> 0.11N <sup>1.0</sup>		
91	N-Tech Lab	ntechlab	009	2021-03-01	1208	42	<sup>62</sup> 1300	-	<sup>169</sup> 899	<sup>149</sup> 35	<sup>(33)</sup> 178	<sup>(32)</sup> 184	<sup>(25)</sup> 336	<sup>(25)</sup> 676	<sup>(28)</sup> 1704	<sup>88</sup> 0.05N <sup>1.1</sup>		
92	N-Tech Lab	ntechlab	010	2021-06-24	351	213	<sup>60</sup> 1280	-	<sup>164</sup> 874	<sup>27</sup> 6	<sup>(72)</sup> 440	<sup>(72)</sup> 435	<sup>(51)</sup> 821	<sup>(51)</sup> 1645	<sup>(49)</sup> 3337	<sup>45</sup> 0.22N <sup>1.0</sup>		
93	NEC	nec	2	2018-10-30	705	35	<sup>71</sup> 1616	k	<sup>94</sup> 642	<sup>117</sup> 18	<sup>(66)</sup> 405	<sup>(68)</sup> 409	<sup>(60)</sup> 1072	<sup>(54)</sup> 1755	<sup>(55)</sup> 4255	<sup>109</sup> 0.06N <sup>1.1</sup>		
94	NEC	nec	3	2018-10-30	774	110	<sup>72</sup> 1712	k	<sup>98</sup> 665	<sup>123</sup> 21	<sup>(3)</sup> 7	<sup>(3)</sup> 7	<sup>(5)</sup> 14	<sup>(8)</sup> 40	<sup>(9)</sup> 82	<sup>127</sup> 0.00N <sup>1.2</sup>		
95	NEC	nec	004	2021-07-19	971	63	<sup>182</sup> 1104	-	<sup>182</sup> 965	<sup>29</sup> 7	<sup>(59)</sup> 349	<sup>(59)</sup> 351	<sup>(46)</sup> 662	<sup>(44)</sup> 1330	<sup>(38)</sup> 2685	<sup>39</sup> 0.20N <sup>1.0</sup>		
96	Neurotechnology	neurotech	5	2018-10-30	266	53	<sup>9</sup> 256	k	<sup>42</sup> 402	<sup>8</sup> 2	<sup>(99)</sup> 835	<sup>(100)</sup> 839	<sup>(80)</sup> 1690	<sup>(78)</sup> 3219	<sup>(82)</sup> 8955	<sup>94</sup> 0.19N <sup>1.1</sup>		
97	Neurotechnology	neurotech	6	2018-10-30	564	53	<sup>11</sup> 256	k	<sup>121</sup> 726	<sup>6</sup> 2	<sup>(100)</sup> 839	<sup>(101)</sup> 842	-	-	-	-		
98	Neurotechnology	neurotech	007	2019-10-03	57	51	<sup>8</sup> 256	k	<sup>7</sup> 161	<sup>5</sup> 2	<sup>(110)</sup> 1118	<sup>(111)</sup> 1110	<sup>(89)</sup> 2143	<sup>(84)</sup> 4397	<sup>(83)</sup> 9045	<sup>49</sup> 0.55N <sup>1.0</sup>		
99	Neurotechnology	neurotechnology	008	2021-03-22	355	49	<sup>32</sup> 514	-	<sup>144</sup> 800	<sup>18</sup> 4	<sup>(113)</sup> 1167	<sup>(114)</sup> 1149	<sup>(91)</sup> 2266	<sup>(89)</sup> 4573	<sup>(90)</sup> 9586	<sup>55</sup> 0.55N <sup>1.0</sup>		
100	Neurotechnology	neurotechnology	009	2021-09-01	246	82	<sup>31</sup> 513	-	<sup>106</sup> 683	<sup>19</sup> 3	<sup>(108)</sup> 1035	<sup>(109)</sup> 1049	<sup>(87)</sup> 1977	<sup>(83)</sup> 4270	<sup>(78)</sup> 8756	<sup>82</sup> 0.32N <sup>1.1</sup>		
101	Newland Computer Co Ltd	newland	2	2018-10-30	96	27	<sup>95</sup> 2048	-	<sup>158</sup> 855	<sup>100</sup> 15	<sup>(173)</sup> 8741	<sup>(178)</sup> 8854	<sup>(147)</sup> 17892	<sup>(144)</sup> 39356	-	<sup>105</sup> 1.32N <sup>1.1</sup>		
102	Noblis	noblis	1	2018-10-30	114	176	<sup>80</sup> 2048	1	<sup>12</sup> 206	<sup>96</sup> 15	<sup>(119)</sup> 1273	<sup>(117)</sup> 1272	-	-	-	-		
103	Noblis	noblis	2	2018-10-30	153	176	<sup>177</sup> 6144	1	<sup>73</sup> 517	<sup>154</sup> 43	<sup>(149)</sup> 2513	<sup>(150)</sup> 2522	<sup>(126)</sup> 5649	<sup>(127)</sup> 12432	<sup>(133)</sup> 44262	<sup>136</sup> 0.04N <sup>1.3</sup>		
104	Paravision (EverAI)	everai	2	2018-10-30	224	304	<sup>88</sup> 2048	1	<sup>38</sup> 366	<sup>141</sup> 30	<sup>(46)</sup> 278	<sup>(51)</sup> 283	-	-	-	-		

Notes	
1	Configuration size does not capture static data present in libraries. Libraries are included but the size also includes any ancillary libraries for image processing (e.g. openCV) or numerical computation (e.g. blas).
2	Finalization is the processing of converting N = 1600000 templates into a searchable data structure an operation which can be a simple copy, or the building of an index or tree, for example. The duration of the operation may be data dependent, and may not be linear in the number of input templates.
3	This multiplier expresses the increase in template size when k images are passed to the template generation function.
4	All durations are measured on Intel®Xeon®CPU E5-2630 v4 @ 2.20GHz processors. Estimates are made by wrapping the API function call in calls to std::chrono::high_resolution_clock which on the machine in (3) counts 1ns clock ticks. Precision is somewhat worse than that however.
5	Search durations are measured as in the prior note. The power-law model in the final column mostly fits the empirical results in Figure 169. However in certain cases the model is not correct and should not be used numerically.

Table 3: Summary of algorithms and properties included in this report. The blue superscripts give ranking for the quantity in that column. Missing search durations, denoted by “-”, are absent because those runs were not executed, usually because we did not run on the larger galleries. Caution: The power-law model is sometimes an incorrect model. It is included here only to show broad sublinear behavior, which is flagged in green. The models should not be used for prediction.

	DEVELOPER FULL NAME	SHORT NAME	SEQ. NUM.	VALIDATION DATE	CONFIG <sup>1</sup> DATA (MB)	LIB <sup>1</sup> DATA (MB)	TEMPLATE GENERATION			FINALIZE <sup>2</sup> TIME (S)	SEARCH DURATION <sup>5</sup> MILLISEC					
							SIZE (B)	MULT <sup>3</sup>	TIME (MS) <sup>4</sup>		L=1	L=50	L=50	L=50	L=50	POWER LAW (μs)
											N=1.6M	N=1.6M	N=1.6M	N=3M	N=6M	
105	Paravision (EverAI)	everai	3	2018-10-30	438	304	<sup>101</sup> 2048	1	<sup>121</sup> 717	<sup>136</sup> 28	<sup>(45)</sup> 278	<sup>(60)</sup> 281	<sup>(39)</sup> 572	<sup>(37)</sup> 1146	<sup>(33)</sup> 2278	<sup>67</sup> 0.12N <sup>1.0</sup>
106	Paravision (EverAI)	everai-paravision	004	2019-06-19	527	128	<sup>168</sup> 4096	1	<sup>101</sup> 672	<sup>157</sup> 45	<sup>(81)</sup> 559	<sup>(81)</sup> 559	<sup>(103)</sup> 2611	<sup>(112)</sup> 6445	<sup>(115)</sup> 14519	<sup>144</sup> 0.00N <sup>1.5</sup>
107	Paravision (EverAI)	paravision	005	2019-12-11	543	154	<sup>169</sup> 4096	1	<sup>150</sup> 830	<sup>159</sup> 48	<sup>(82)</sup> 561	<sup>(84)</sup> 564	<sup>(59)</sup> 1056	<sup>(61)</sup> 2298	<sup>(59)</sup> 4966	<sup>85</sup> 0.16N <sup>1.1</sup>
108	Paravision (EverAI)	paravision	007	2021-02-01	529	235	<sup>168</sup> 4096	-	<sup>115</sup> 701	<sup>160</sup> 48	<sup>(84)</sup> 569	<sup>(79)</sup> 558	<sup>(61)</sup> 1086	<sup>(59)</sup> 2111	<sup>(54)</sup> 4254	<sup>18</sup> 1.11N <sup>0.9</sup>
109	Qnap Security	qnap	000	2021-07-28	182	15	<sup>87</sup> 2048	-	<sup>58</sup> 457	<sup>49</sup> 9	<sup>(115)</sup> 1231	<sup>(136)</sup> 1763	-	-	-	-
110	Quantasoft	quantasoft	1	2018-10-30	276	452	<sup>90</sup> 2048	k	<sup>42</sup> 385	<sup>26</sup> 6	<sup>(174)</sup> 15422	<sup>(179)</sup> 14858	<sup>(145)</sup> 14717	-	<sup>(121)</sup> 18323	-
111	Rank One Computing	rankone	4	2018-10-09	0	101	<sup>85</sup>	k	<sup>3</sup> 36	<sup>30</sup> 7	<sup>(21)</sup> 101	<sup>(21)</sup> 101	<sup>(17)</sup> 190	-	-	<sup>23</sup> 0.07N <sup>1.0</sup>
112	Rank One Computing	rankone	5	2018-10-24	0	101	<sup>5133</sup>	k	<sup>4</sup> 92	<sup>31</sup> 7	<sup>(26)</sup> 140	<sup>(26)</sup> 144	<sup>(22)</sup> 266	<sup>(21)</sup> 525	<sup>(20)</sup> 1049	<sup>21</sup> 0.11N <sup>1.0</sup>
113	Rank One Computing	rankone	006	2019-06-03	0	133	<sup>7</sup> 165	k	<sup>21</sup> 245	<sup>35</sup> 8	-	-	-	-	-	-
114	Rank One Computing	rankone	007	2019-11-12	0	137	<sup>6</sup> 165	k	<sup>24</sup> 272	<sup>33</sup> 7	<sup>(22)</sup> 116	<sup>(22)</sup> 115	<sup>(19)</sup> 215	<sup>(19)</sup> 439	<sup>(17)</sup> 877	<sup>37</sup> 0.07N <sup>1.0</sup>
115	Rank One Computing	rankone	009	2020-06-26	0	105	<sup>14260</sup>	k	<sup>11</sup> 185	<sup>59</sup> 11	<sup>(16)</sup> 95	<sup>(18)</sup> 96	<sup>(14)</sup> 181	<sup>(14)</sup> 362	<sup>(15)</sup> 727	<sup>28</sup> 0.06N <sup>1.0</sup>
116	Rank One Computing	rankone	010	2020-11-05	0	135	<sup>16261</sup>	-	<sup>14</sup> 198	<sup>55</sup> 10	<sup>(17)</sup> 95	<sup>(15)</sup> 95	<sup>(13)</sup> 178	<sup>(13)</sup> 357	<sup>(14)</sup> 714	<sup>27</sup> 0.06N <sup>1.0</sup>
117	Rank One Computing	rankone	011	2021-08-27	0	175	<sup>15261</sup>	-	<sup>79</sup> 566	<sup>39</sup> 8	<sup>(18)</sup> 96	<sup>(16)</sup> 95	<sup>(15)</sup> 183	<sup>(15)</sup> 370	<sup>(13)</sup> 714	<sup>34</sup> 0.06N <sup>1.0</sup>
118	Realnetworks Inc	realnetworks	2	2018-10-30	105	104	<sup>175</sup> 4104	k	<sup>20</sup> 241	<sup>135</sup> 28	<sup>(137)</sup> 2008	<sup>(142)</sup> 2048	<sup>(120)</sup> 4194	<sup>(119)</sup> 8642	<sup>(118)</sup> 15035	<sup>43</sup> 1.08N <sup>1.0</sup>
119	Realnetworks Inc	realnetworks	003	2019-06-12	93	102	<sup>74</sup> 1848	k	<sup>10</sup> 173	<sup>70</sup> 13	<sup>(112)</sup> 1145	<sup>(112)</sup> 1132	<sup>(88)</sup> 2142	<sup>(97)</sup> 5241	<sup>(98)</sup> 10495	<sup>97</sup> 0.21N <sup>1.1</sup>
120	Realnetworks Inc	realnetworks	004	2019-10-17	94	102	<sup>73</sup> 1848	1	<sup>5</sup> 171	<sup>58</sup> 11	<sup>(111)</sup> 1143	<sup>(113)</sup> 1137	<sup>(90)</sup> 2149	<sup>(91)</sup> 4740	<sup>(93)</sup> 9693	<sup>81</sup> 0.36N <sup>1.0</sup>
121	Realnetworks Inc	realnetworks	005	2021-06-23	168	209	<sup>143</sup> 2056	-	<sup>31</sup> 332	<sup>41</sup> 9	<sup>(131)</sup> 1654	<sup>1616</sup>	<sup>(111)</sup> 3030	<sup>(107)</sup> 6068	<sup>(112)</sup> 12134	<sup>31</sup> 1.01N <sup>1.0</sup>
122	Remark Holdings	remarkai	000	2019-06-12	234	1092	<sup>84</sup> 2048	k	<sup>95</sup> 650	<sup>69</sup> 12	<sup>(165)</sup> 5776	<sup>(167)</sup> 5703	<sup>(138)</sup> 11604	<sup>(143)</sup> 32133	<sup>(142)</sup> 91436	<sup>137</sup> 0.05N <sup>1.3</sup>
123	Remark Holdings	remarkai	0	2018-10-30	187	847	<sup>119</sup> 2048	k	<sup>81</sup> 593	<sup>89</sup> 14	<sup>(164)</sup> 5685	<sup>(168)</sup> 5723	-	-	-	-
124	Remark Holdings	remarkai	1	2018-10-30	187	847	<sup>110</sup> 2048	k	<sup>52</sup> 427	<sup>93</sup> 14	<sup>(163)</sup> 5680	<sup>(169)</sup> 5761	<sup>(141)</sup> 12475	<sup>(140)</sup> 28726	<sup>(140)</sup> 59618	<sup>128</sup> 0.37N <sup>1.2</sup>
125	Rendip	rendip	000	2021-05-21	0	416	<sup>102</sup> 2048	-	<sup>166</sup> 890	<sup>47</sup> 9	<sup>(43)</sup> 249	<sup>(61)</sup> 368	<sup>(49)</sup> 697	<sup>(48)</sup> 1452	<sup>(44)</sup> 2926	<sup>91</sup> 0.08N <sup>1.1</sup>
126	Samsung SI Corp	s1	000	2021-06-03	257	196	<sup>166</sup> 4096	-	<sup>159</sup> 865	<sup>122</sup> 20	<sup>(171)</sup> 6715	<sup>(175)</sup> 6794	<sup>(144)</sup> 13032	<sup>(140)</sup> 26372	<sup>(139)</sup> 55723	<sup>65</sup> 2.82N <sup>1.0</sup>
127	Scanovate Ltd	scanovate	000	2020-01-15	250	446	<sup>102</sup> 2048	-	<sup>117</sup> 705	<sup>91</sup> 14	<sup>(125)</sup> 1419	<sup>(124)</sup> 1412	<sup>(110)</sup> 3008	<sup>(124)</sup> 5167	<sup>(105)</sup> 12012	<sup>129</sup> 0.10N <sup>1.2</sup>
128	Scanovate Ltd	scanovate	001	2020-09-10	250	446	<sup>102</sup> 2048	-	<sup>103</sup> 675	<sup>75</sup> 13	<sup>(122)</sup> 1321	<sup>(121)</sup> 1320	<sup>(98)</sup> 2502	<sup>(94)</sup> 5047	<sup>(95)</sup> 101663	<sup>46</sup> 0.65N <sup>1.0</sup>
129	Sensetime Group	sensetime	0	2018-10-30	525	6	<sup>174</sup> 4104	k	<sup>113</sup> 693	<sup>153</sup> 41	<sup>(75)</sup> 498	<sup>(74)</sup> 501	<sup>(67)</sup> 1212	<sup>(60)</sup> 2281	<sup>(60)</sup> 5032	<sup>103</sup> 0.09N <sup>1.1</sup>
130	Sensetime Group	sensetime	1	2018-10-30	525	6	<sup>172</sup> 4104	k	<sup>89</sup> 628	<sup>158</sup> 48	<sup>(77)</sup> 516	<sup>(75)</sup> 502	<sup>(63)</sup> 1146	<sup>(62)</sup> 2301	<sup>(57)</sup> 4765	<sup>101</sup> 0.09N <sup>1.1</sup>
131	Sensetime Group	sensetime	002	2019-06-03	523	6	<sup>143</sup> 2056	k	<sup>84</sup> 603	<sup>115</sup> 18	<sup>(60)</sup> 359	<sup>(62)</sup> 370	<sup>(83)</sup> 1897	<sup>(87)</sup> 5048	<sup>(89)</sup> 9543	<sup>107</sup> 0.00N <sup>1.5</sup>
132	Sensetime Group	sensetime	003	2019-12-02	769	76	<sup>144</sup> 2056	1	<sup>173</sup> 910	<sup>119</sup> 19	<sup>(159)</sup> 4885	<sup>(164)</sup> 4989	<sup>(140)</sup> 12325	<sup>(137)</sup> 24712	<sup>(135)</sup> 49445	<sup>111</sup> 0.67N <sup>1.1</sup>
133	Sensetime Group	sensetime	004	2020-08-10	456	29	<sup>50</sup> 1032	-	<sup>110</sup> 690	<sup>68</sup> 12	<sup>(144)</sup> 2490	<sup>(142)</sup> 2477	<sup>(124)</sup> 4654	<sup>(122)</sup> 9402	<sup>(125)</sup> 19651	<sup>48</sup> 1.22N <sup>1.0</sup>
134	Sensetime Group	sensetime	005	2020-12-17	631	39	<sup>51</sup> 1032	-	<sup>183</sup> 980	<sup>57</sup> 11	<sup>(142)</sup> 2459	<sup>(159)</sup> 9939	<sup>(132)</sup> 7398	<sup>(130)</sup> 14768	<sup>(124)</sup> 19016	<sup>17</sup> 14.03N <sup>0.9</sup>
135	Sensetime Group	sensetime	006	2021-07-26	526	54	<sup>49</sup> 1032	-	<sup>175</sup> 929	<sup>34</sup> 7	<sup>(141)</sup> 2414	<sup>(146)</sup> 2422	<sup>(122)</sup> 4527	<sup>(120)</sup> 9128	<sup>(122)</sup> 18640	<sup>40</sup> 1.35N <sup>1.0</sup>
136	Shaman Software	shaman	6	2018-10-26	0	200	<sup>121</sup> 2048	k	<sup>118</sup> 706	<sup>90</sup> 14	<sup>(86)</sup> 603	<sup>(86)</sup> 612	-	-	-	-
137	Shaman Software	shaman	7	2018-10-26	0	200	<sup>101</sup> 2048	k	<sup>119</sup> 707	<sup>92</sup> 14	<sup>(85)</sup> 602	<sup>(87)</sup> 614	<sup>(64)</sup> 1187	<sup>(67)</sup> 2448	<sup>(63)</sup> 5083	<sup>68</sup> 0.25N <sup>1.0</sup>
138	Shanghai Yitu Technology	yitu	4	2018-10-30	219	136	<sup>147</sup> 2070	1	<sup>168</sup> 897	<sup>156</sup> 45	<sup>(120)</sup> 1288	<sup>(116)</sup> 1203	<sup>(95)</sup> 2440	<sup>(98)</sup> 5241	<sup>(92)</sup> 9671	<sup>64</sup> 0.52N <sup>1.0</sup>
139	Shanghai Yitu Technology	yitu	5	2018-10-30	2043	136	<sup>148</sup> 2070	1	<sup>157</sup> 853	<sup>155</sup> 44	<sup>(116)</sup> 1237	<sup>(115)</sup> 1199	<sup>(99)</sup> 2513	<sup>(93)</sup> 5013	<sup>(91)</sup> 9620	<sup>61</sup> 0.55N <sup>1.0</sup>
140	Smilart	smilart	4	2018-10-30	65	89	<sup>23</sup> 512	k	<sup>8</sup> 167	<sup>17</sup> 4	<sup>(175)</sup> 16137	<sup>(180)</sup> 15633	-	-	-	-
141	Smilart	smilart	5	2018-10-30	562	89	<sup>108</sup> 2048	k	<sup>56</sup> 450	<sup>88</sup> 14	-	-	-	-	-	-
142	Stagu Technologies	stagu	000	2021-08-30	1018	690	<sup>170</sup> 4096	-	<sup>148</sup> 826	<sup>131</sup> 24	<sup>(160)</sup> 4950	<sup>(163)</sup> 4933	-	-	-	-
143	Synesis	synesis	3	2018-10-30	237	150	<sup>167</sup> 4096	k	<sup>5</sup> 99	<sup>139</sup> 29	<sup>(97)</sup> 789	<sup>(99)</sup> 801	<sup>(86)</sup> 1941	<sup>(81)</sup> 3888	<sup>(79)</sup> 8810	<sup>119</sup> 0.07N <sup>1.1</sup>
144	Synesis	synesis	003	2019-07-04	143	17	<sup>114</sup> 2048	k	<sup>17</sup> 211	<sup>65</sup> 12	<sup>(76)</sup> 507	<sup>(76)</sup> 502	<sup>(92)</sup> 2297	<sup>(88)</sup> 4564	<sup>(87)</sup> 9452	<sup>142</sup> 0.00N <sup>1.4</sup>
145	Synesis	synesis	005	2020-09-08	494	24	<sup>173</sup> 4104	-	<sup>130</sup> 756	<sup>129</sup> 24	<sup>(102)</sup> 877	<sup>(102)</sup> 865	<sup>(114)</sup> 3182	<sup>(90)</sup> 4658	<sup>(94)</sup> 9750	<sup>130</sup> 0.06N <sup>1.2</sup>
146	Tech5 SA	tech5	001	2019-08-19	1394	116	<sup>65</sup> 1536	k	<sup>165</sup> 887	<sup>52</sup> 10	<sup>(63)</sup> 383	<sup>(96)</sup> 766	<sup>(105)</sup> 2767	<sup>(108)</sup> 6149	<sup>(71)</sup> 6178	<sup>110</sup> 0.12N <sup>1.1</sup>
147	Tech5 SA	tech5	002	2021-04-07	727	112	<sup>30</sup> 513	-	<sup>178</sup> 940	<sup>13</sup> 4	<sup>(158)</sup> 4682	<sup>(174)</sup> 6689	<sup>(142)</sup> 12541	<sup>(138)</sup> 25145	<sup>(137)</sup> 50239	<sup>30</sup> 4.18N <sup>1.0</sup>
148	Tencent Deepsea Lab	deepsea	001	2019-07-29	250	323	<sup>79</sup> 2048	1	<sup>127</sup> 737	<sup>67</sup> 12	<sup>(107)</sup> 1021	<sup>(108)</sup> 1020	<sup>(106)</sup> 2774	<sup>(104)</sup> 5767	<sup>(108)</sup> 12341	<sup>133</sup> 0.06N <sup>1.2</sup>
149	Tevean	tevean	5	2018-10-30	773	15	<sup>112</sup> 2048	1	<sup>49</sup> 405	<sup>97</sup> 15	<sup>(67)</sup> 405	<sup>(67)</sup> 408	<sup>(53)</sup> 854	<sup>(55)</sup> 1757	<sup>(51)</sup> 3380	<sup>80</sup> 0.14N <sup>1.0</sup>
150	Tevean	tevean	006	2021-04-16	769	19	<sup>48</sup> 1032	-	<sup>82</sup> 597	<sup>51</sup> 10	<sup>(53)</sup> 295	<sup>(54)</sup> 295	<sup>(40)</sup> 578	<sup>(39)</sup> 1187	<sup>(41)</sup> 2741	<sup>92</sup> 0.06N <sup>1.1</sup>
151	Tevean	tevean	007	2021-10-12	703	19	<sup>46</sup> 1032	-	<sup>134</sup> 777	<sup>21</sup> 4	<sup>(54)</sup> 297	<sup>(55)</sup> 298	<sup>(41)</sup> 579	<sup>(38)</sup> 1179	<sup>(55)</sup> 2418	<sup>75</sup> 0.11N <sup>1.0</sup>
152	Thales	cogent	2	2018-10-30	681	39	<sup>58</sup> 1043	k	<sup>180</sup> 945	<sup>133</sup> 27	<sup>(138)</sup> 2017	<sup>(144)</sup> 2144	<sup>(121)</sup> 4298	<sup>(118)</sup> 8472	<sup>(120)</sup> 16429	<sup>47</sup> 1.08N <sup>1.0</sup>
153	Thales	cogent	3	2018-10-30	681	39	<sup>55</sup> 1043	k	<sup>177</sup> 940	<sup>49</sup> 9	<sup>(114)</sup> 1230	<sup>(120)</sup> 1311	<sup>(104)</sup> 2687	<sup>(99)</sup> 5398	<sup>(96)</sup> 10184	<sup>56</sup> 0.62N <sup>1.0</sup>
154	Thales	cogent	004	2021-02-10	1376	59	<sup>141</sup> 2053	-	<sup>181</sup> 947	<sup>82</sup> 14	<sup>(148)</sup> 2903	<sup>(139)</sup> 1911	<sup>(115)</sup> 3566	<sup>(116)</sup> 7498	<sup>(119)</sup> 16370	<sup>79</sup> 0.64N <sup>1.0</sup>
155	Thales	cogent	005	2021-09-13	1043	56	<sup>59</sup> 1062	-	<sup>133</sup> 769	<sup>25</sup> 5	<sup>(104)</sup> 912	<sup>(105)</sup> 996	<sup>(82)</sup> 1872	<sup>(80)</sup> 3845	<sup>(76)</sup> 7555	<sup>58</sup> 0.44N <sup>1.0</sup>
156	TigerIT Americas LLC	tiger	2	2018-10-29	416	518	<sup>140</sup> 2052	k	<sup>60</sup> 461	<sup>101</sup> 15	<sup>(136)</sup> 1816	<sup>(140)</sup> 1921	<sup>(119)</sup> 3833	<sup>(117)</sup> 7526	<sup>(116)</sup> 14820	<sup>63</sup> 0.83N <sup>1.0</sup>

Notes

- Configuration size does not capture static data present in libraries. Libraries are included but the size also includes any ancillary libraries for image processing (e.g. openCV) or numerical computation (e.g. blas).
- Finalization is the processing of converting N = 1600000 templates into a searchable data structure operation which can be a simple copy, or the building of an index or tree, for example. The duration of the operation may be data dependent, and may not be linear in the number of input templates.
- This multiplier expresses the increase in template size when k images are passed to the template generation function.
- All durations are measured on Intel®Xeon®CPU E5-2630 v4 @ 2.20GHz processors. Estimates are made by wrapping the API function call in calls to std::chrono::high\_resolution\_clock which on the machine in (3) counts 1ns clock ticks. Precision is somewhat worse than that however.
- Search durations are measured as in the prior note. The power-law model in the final column mostly fits the empirical results in Figure 169. However in certain cases the model is not correct and should not be used numerically.

2021/10/28  
 FN(R,N,R,T) = False neg. identification rate  
 FPR(N,T) = False pos. identification rate  
 N = Num. enrolled subjects  
 R = Num. candidates examined  
 T = Threshold  
 T > 0 → Identification

Table 4: Summary of algorithms and properties included in this report. The blue superscripts give ranking for the quantity in that column. Missing search durations, denoted by “-”, are absent because those runs were not executed, usually because we did not run on the larger galleries. Caution: The power-law model is sometimes an incorrect model. It is included here only to show broad sublinear behavior, which is flagged in green. The models should not be used for prediction.

	DEVELOPER	SHORT NAME	SEQ. NUM.	VALIDATION DATE	CONFIG <sup>1</sup> DATA (MB)	LIB <sup>1</sup> DATA (MB)	TEMPLATE GENERATION			FINALIZE <sup>2</sup> TIME (S)	SEARCH DURATION <sup>5</sup> MILLISEC						POWER LAW ( $\mu s$ )
							SIZE (B)	MULT <sup>3</sup>	TIME (MS) <sup>4</sup>		L=1 N=1.6M	L=50 N=1.6M	L=50 N=3M	L=50 N=6M	L=50 N=12M		
157	TigerIT Americas LLC	tiger	3	2018-10-30	416	518	<sup>130</sup> 2052	k	<sup>59</sup> 461	<sup>182</sup> 37431	<sup>(57)</sup> 191	<sup>(38)</sup> 189	-	-	-	-	-
158	Toshiba	toshiba	0	2018-10-30	961	105	<sup>70</sup> 1548	k	<sup>163</sup> 876	<sup>63</sup> 12	<sup>(168)</sup> 6153	<sup>(170)</sup> 6236	<sup>(139)</sup> 12221	<sup>(139)</sup> 25355	<sup>(136)</sup> 49448	<sup>125</sup> 0.36	$N^{1.2}$
159	Toshiba	toshiba	1	2018-10-30	961	105	<sup>147</sup> 2060	k	<sup>162</sup> 875	<sup>183</sup> 44701	<sup>(167)</sup> 6007	<sup>(172)</sup> 6355	-	-	-	-	-
160	Tripleize	aize	001	2021-08-06	262	150	<sup>92</sup> 2048	-	<sup>46</sup> 402	<sup>44</sup> 9	<sup>(151)</sup> 3087	<sup>(154)</sup> 3080	-	-	-	-	-
161	Trueface.ai	trueface	000	2021-01-27	247	119	<sup>77</sup> 2000	-	<sup>34</sup> 363	<sup>73</sup> 13	<sup>(44)</sup> 271	<sup>(58)</sup> 327	<sup>(43)</sup> 614	<sup>(41)</sup> 1239	<sup>(37)</sup> 2678	<sup>54</sup> 0.15	$N^{1.0}$
162	Veridas Digital Authentication Solutions S.L.	veridas	001	2021-03-05	347	875	<sup>121</sup> 2048	-	<sup>160</sup> 872	<sup>74</sup> 13	<sup>(162)</sup> 5493	<sup>(166)</sup> 5469	<sup>(137)</sup> 10350	<sup>(135)</sup> 20655	<sup>(132)</sup> 41264	<sup>32</sup> 3.40	$N^{1.0}$
163	Veridas Digital Authentication Solutions S.L.	veridas	002	2021-07-06	347	870	<sup>113</sup> 2048	-	<sup>164</sup> 877	<sup>56</sup> 10	<sup>(57)</sup> 322	<sup>(57)</sup> 325	<sup>(48)</sup> 685	<sup>(46)</sup> 1365	<sup>(40)</sup> 2730	<sup>86</sup> 0.09	$N^{1.1}$
164	Viettel Group	vt	000	2021-03-12	250	257	<sup>89</sup> 2048	-	<sup>68</sup> 492	<sup>170</sup> 2295	<sup>(2)</sup> 4	<sup>(2)</sup> 4	<sup>(11)</sup> 11	-	-	<sup>12</sup> 0.61	$N^{0.6}$
165	Viettel Group	vt	001	2021-07-16	352	600	<sup>86</sup> 2048	-	<sup>167</sup> 891	<sup>125</sup> 21	<sup>(143)</sup> 2477	<sup>(148)</sup> 2487	<sup>(123)</sup> 4644	<sup>(121)</sup> 9313	<sup>(123)</sup> 18713	<sup>33</sup> 1.53	$N^{1.0}$
166	Vigilant Solutions	vigilant	5	2018-10-30	335	122	<sup>67</sup> 1544	k	<sup>131</sup> 762	<sup>118</sup> 19	-	<sup>(134)</sup> 1720	-	-	-	-	-
167	Vigilant Solutions	vigilant	6	2018-10-30	337	122	<sup>69</sup> 1544	k	<sup>146</sup> 816	<sup>124</sup> 21	-	-	-	-	-	-	-
168	Vigilant Solutions	vigilantsolutions	007	2021-01-08	340	51	<sup>68</sup> 1544	-	<sup>87</sup> 616	<sup>112</sup> 16	<sup>(124)</sup> 1354	<sup>(123)</sup> 1352	<sup>(108)</sup> 2911	<sup>(106)</sup> 5966	<sup>(102)</sup> 11466	<sup>96</sup> 0.27	$N^{1.1}$
169	Vigilant Solutions	vigilantsolutions	008	2021-07-23	340	51	<sup>66</sup> 1544	-	<sup>47</sup> 403	<sup>78</sup> 13	<sup>(109)</sup> 1062	<sup>(110)</sup> 1061	<sup>(93)</sup> 2330	<sup>(102)</sup> 5520	<sup>(88)</sup> 9499	<sup>115</sup> 0.11	$N^{1.1}$
170	Visidon	visidon	1	2018-10-30	166	42	<sup>134</sup> 2052	k	<sup>99</sup> 667	<sup>103</sup> 15	<sup>(156)</sup> 4370	<sup>(162)</sup> 4472	<sup>(134)</sup> 8454	<sup>(133)</sup> 17262	<sup>(130)</sup> 34288	<sup>42</sup> 2.40	$N^{1.0}$
171	Visidon	vd	002	2021-05-18	248	42	<sup>136</sup> 2052	-	<sup>109</sup> 687	<sup>40</sup> 9	<sup>(139)</sup> 2089	<sup>(145)</sup> 2336	-	-	-	-	-
172	Visidon	vd	003	2021-10-12	497	43	<sup>135</sup> 2052	-	<sup>112</sup> 692	<sup>37</sup> 8	<sup>(140)</sup> 2095	<sup>(143)</sup> 2082	-	-	-	-	-
173	Visiob-Box	visionbox	000	2021-09-17	252	274	<sup>146</sup> 2059	-	<sup>66</sup> 481	<sup>111</sup> 16	<sup>(70)</sup> 422	<sup>(60)</sup> 359	<sup>(54)</sup> 855	<sup>(24)</sup> 631	<sup>(32)</sup> 2096	<sup>15</sup> 2.46	$N^{0.8}$
174	VisionLabs	visionlabs	6	2018-10-30	360	17	<sup>29</sup> 512	1	<sup>28</sup> 289	<sup>179</sup> 20290	<sup>(13)</sup> 36	<sup>(13)</sup> 36	<sup>(11)</sup> 39	<sup>(10)</sup> 44	<sup>(8)</sup> 53	<sup>8</sup> 3211.93	$N^{0.2}$
175	VisionLabs	visionlabs	7	2018-10-30	360	17	<sup>28</sup> 512	1	<sup>27</sup> 289	<sup>181</sup> 34666	<sup>(14)</sup> 63	<sup>(14)</sup> 63	<sup>(12)</sup> 72	<sup>(12)</sup> 80	<sup>(10)</sup> 115	<sup>10</sup> 2076.32	$N^{0.2}$
176	VisionLabs	visionlabs	008	2019-06-18	348	17	<sup>26</sup> 512	1	<sup>25</sup> 272	<sup>177</sup> 12747	<sup>(8)</sup> 23	<sup>(6)</sup> 29	<sup>(7)</sup> 26	<sup>(6)</sup> 29	<sup>(5)</sup> 33	<sup>6</sup> 2539.61	$N^{0.2}$
177	VisionLabs	visionlabs	009	2020-08-04	689	20	<sup>24</sup> 512	-	<sup>61</sup> 467	<sup>178</sup> 13245	<sup>(9)</sup> 23	<sup>(8)</sup> 29	<sup>(8)</sup> 34	<sup>(11)</sup> 71	<sup>(11)</sup> 145	<sup>11</sup> 8.88	$N^{0.6}$
178	VisionLabs	visionlabs	010	2021-02-05	1042	20	<sup>27</sup> 512	-	<sup>126</sup> 731	<sup>174</sup> 11837	<sup>(7)</sup> 21	<sup>(10)</sup> 32	<sup>(9)</sup> 36	<sup>(7)</sup> 39	<sup>(6)</sup> 43	<sup>7</sup> 3183.79	$N^{0.2}$
179	Vocord	vocord	5	2018-10-30	1035	185	<sup>39</sup> 768	k	<sup>137</sup> 780	<sup>32</sup> 7	<sup>(31)</sup> 158	<sup>(36)</sup> 204	<sup>(28)</sup> 383	<sup>(29)</sup> 767	<sup>(24)</sup> 1466	<sup>35</sup> 0.12	$N^{1.0}$
180	Vocord	vocord	6	2018-10-30	1035	185	<sup>183</sup> 10240	k	<sup>138</sup> 785	<sup>169</sup> 243	<sup>(32)</sup> 170	<sup>(38)</sup> 216	-	-	-	-	-
181	Xforward AI Technology	xforwardai	000	2020-07-24	236	171	<sup>106</sup> 2048	-	<sup>129</sup> 753	<sup>80</sup> 13	<sup>(157)</sup> 4603	<sup>(177)</sup> 7647	<sup>(146)</sup> 15723	<sup>(136)</sup> 23900	<sup>(138)</sup> 53729	<sup>116</sup> 0.56	$N^{1.1}$
182	Xforward AI Technology	xforwardai	001	2021-01-21	332	50	<sup>103</sup> 2048	-	<sup>105</sup> 677	<sup>109</sup> 16	<sup>(166)</sup> 5887	<sup>(161)</sup> 4384	<sup>(135)</sup> 8798	<sup>(134)</sup> 18553	<sup>(134)</sup> 48993	<sup>123</sup> 0.32	$N^{1.1}$
183	Xforward AI Technology	xforwardai	002	2021-05-24	691	50	<sup>164</sup> 4096	-	<sup>176</sup> 930	<sup>118</sup> 18	<sup>(172)</sup> 6957	<sup>(173)</sup> 6400	<sup>(143)</sup> 12659	<sup>(142)</sup> 31077	<sup>(141)</sup> 65158	<sup>121</sup> 0.52	$N^{1.1}$

Notes	
1	Configuration size does not capture static data present in libraries. Libraries are included but the size also includes any ancillary libraries for image processing (e.g. openCV) or numerical computation (e.g. blas).
2	Finalization is the processing of converting $N = 1600000$ templates into a searchable data structure an operation which can be a simple copy, or the building of an index or tree, for example. The duration of the operation may be data dependent, and may not be linear in the number of input templates.
3	This multiplier expresses the increase in template size when $k$ images are passed to the template generation function.
4	All durations are measured on Intel®Xeon®CPU E5-2630 v4 @ 2.20GHz processors. Estimates are made by wrapping the API function call in calls to <code>std::chrono::high_resolution_clock</code> which on the machine in (3) counts 1ns clock ticks. Precision is somewhat worse than that however.
5	Search durations are measured as in the prior note. The power-law model in the final column mostly fits the empirical results in Figure 169. However in certain cases the model is not correct and should not be used numerically.

Table 5: Summary of algorithms and properties included in this report. The blue superscripts give ranking for the quantity in that column. Missing search durations, denoted by “-”, are absent because those runs were not executed, usually because we did not run on the larger galleries. Caution: The power-law model is sometimes an incorrect model. It is included here only to show broad sublinear behavior, which is flagged in green. The models should not be used for prediction.

2021/10/28  
13:44:33

FNIR(N, R, T) = False neg. identification rate  
FPR(N, T) = False pos. identification rate  
N = Num. enrolled subjects  
R = Num. candidates examined

T = Threshold

T = 0 → Investigation  
T > 0 → Identification

#	MISS RATES ALGORITHM	INVESTIGATION, FNIR(N, R = 1, T = 0)								IDENTIFICATION, FNIR(N, R = L, T ≥ 0) FOR FPIR = 0.001							
		(0, 2]	(2, 4]	(4, 6]	(6, 8]	(8, 10]	(10, 12]	(12, 14]	(14, 18]	(0, 2]	(2, 4]	(4, 6]	(6, 8]	(8, 10]	(10, 12]	(12, 14]	(14, 18]
1	3DIVI-005	<sup>97</sup> 0.0207	<sup>96</sup> 0.0304	<sup>96</sup> 0.0415	<sup>96</sup> 0.0533	<sup>96</sup> 0.0646	<sup>96</sup> 0.0735	<sup>96</sup> 0.0884	<sup>97</sup> 0.1148	<sup>100</sup> 0.1580	<sup>97</sup> 0.2316	<sup>97</sup> 0.3033	<sup>97</sup> 0.3740	<sup>97</sup> 0.4285	<sup>97</sup> 0.4742	<sup>98</sup> 0.5329	<sup>96</sup> 0.5975
2	ANKE-000	<sup>94</sup> 0.0162	<sup>94</sup> 0.0245	<sup>94</sup> 0.0333	<sup>94</sup> 0.0428	<sup>94</sup> 0.0515	<sup>94</sup> 0.0615	<sup>94</sup> 0.0780	<sup>95</sup> 0.1028	<sup>95</sup> 0.1132	<sup>95</sup> 0.1761	<sup>95</sup> 0.2402	<sup>95</sup> 0.3057	<sup>94</sup> 0.3640	<sup>94</sup> 0.4200	<sup>94</sup> 0.4928	<sup>94</sup> 0.5680
3	ANKE-002	<sup>48</sup> 0.0055	<sup>49</sup> 0.0074	<sup>49</sup> 0.0090	<sup>48</sup> 0.0103	<sup>47</sup> 0.0116	<sup>48</sup> 0.0135	<sup>47</sup> 0.0162	<sup>46</sup> 0.0202	<sup>55</sup> 0.0329	<sup>55</sup> 0.0560	<sup>55</sup> 0.0843	<sup>56</sup> 0.1169	<sup>56</sup> 0.1481	<sup>56</sup> 0.1820	<sup>56</sup> 0.2280	<sup>56</sup> 0.2831
4	AWARE-005	<sup>105</sup> 0.0328	<sup>105</sup> 0.0519	<sup>105</sup> 0.0712	<sup>105</sup> 0.0910	<sup>105</sup> 0.1078	<sup>105</sup> 0.1235	<sup>105</sup> 0.1457	<sup>105</sup> 0.1831	<sup>105</sup> 0.3605	<sup>106</sup> 0.4949	<sup>106</sup> 0.5948	<sup>106</sup> 0.6783	<sup>107</sup> 0.7393	<sup>107</sup> 0.7905	<sup>107</sup> 0.8408	<sup>108</sup> 0.8831
5	AWARE-006	<sup>105</sup> 0.0702	<sup>105</sup> 0.1110	<sup>105</sup> 0.1502	<sup>107</sup> 0.1899	<sup>107</sup> 0.2253	<sup>110</sup> 0.2614	<sup>105</sup> 0.3045	<sup>105</sup> 0.3659								
6	AYONIX-002	<sup>112</sup> 0.3360	<sup>113</sup> 0.4389	<sup>113</sup> 0.5144	<sup>113</sup> 0.5814	<sup>113</sup> 0.6340	<sup>113</sup> 0.6818	<sup>113</sup> 0.7297	<sup>114</sup> 0.7774	<sup>109</sup> 0.8288	<sup>110</sup> 0.9013	<sup>110</sup> 0.9375	<sup>110</sup> 0.9603	<sup>110</sup> 0.9744	<sup>111</sup> 0.9837	<sup>111</sup> 0.9893	<sup>111</sup> 0.9927
7	CAMVI-004	<sup>108</sup> 0.0623	<sup>108</sup> 0.0944	<sup>108</sup> 0.1243	<sup>108</sup> 0.1548	<sup>107</sup> 0.1812	<sup>107</sup> 0.2056	<sup>107</sup> 0.2344	<sup>105</sup> 0.2672	<sup>90</sup> 0.0810	<sup>90</sup> 0.1267	<sup>89</sup> 0.1721	<sup>87</sup> 0.2203	<sup>87</sup> 0.2619	<sup>85</sup> 0.3040	<sup>84</sup> 0.3543	<sup>80</sup> 0.4124
8	CAMVI-005	<sup>110</sup> 0.0849	<sup>110</sup> 0.1255	<sup>110</sup> 0.1631	<sup>110</sup> 0.1989	<sup>110</sup> 0.2298	<sup>109</sup> 0.2585	<sup>108</sup> 0.2915	<sup>108</sup> 0.3246								
9	CIB-000	<sup>13</sup> 0.0022	<sup>13</sup> 0.0030	<sup>14</sup> 0.0037	<sup>14</sup> 0.0044	<sup>16</sup> 0.0049	<sup>16</sup> 0.0057	<sup>16</sup> 0.0069	<sup>16</sup> 0.0062	<sup>24</sup> 0.0139	<sup>25</sup> 0.0240	<sup>26</sup> 0.0373	<sup>27</sup> 0.0525	<sup>27</sup> 0.0689	<sup>25</sup> 0.0859	<sup>25</sup> 0.1109	<sup>25</sup> 0.1454
10	CLOUDWALK-HR-000	<sup>7</sup> 0.0019	<sup>6</sup> 0.0024	<sup>7</sup> 0.0029	<sup>6</sup> 0.0032	<sup>5</sup> 0.0032	<sup>4</sup> 0.0036	<sup>7</sup> 0.0041	<sup>7</sup> 0.0020	<sup>7</sup> 0.0029	<sup>7</sup> 0.0041	<sup>7</sup> 0.0054	<sup>7</sup> 0.0064	<sup>7</sup> 0.0073	<sup>7</sup> 0.0085	<sup>7</sup> 0.0102	<sup>7</sup> 0.0112
11	COGENT-000	<sup>88</sup> 0.0128	<sup>89</sup> 0.0184	<sup>91</sup> 0.0250	<sup>91</sup> 0.0327	<sup>92</sup> 0.0407	<sup>90</sup> 0.0488	<sup>88</sup> 0.0611	<sup>88</sup> 0.0794	<sup>76</sup> 0.0559	<sup>78</sup> 0.0923	<sup>76</sup> 0.1342	<sup>76</sup> 0.1812	<sup>75</sup> 0.2243	<sup>74</sup> 0.2675	<sup>74</sup> 0.3240	<sup>76</sup> 0.3992
12	COGENT-001	<sup>90</sup> 0.0128	<sup>90</sup> 0.0184	<sup>92</sup> 0.0250	<sup>92</sup> 0.0327	<sup>91</sup> 0.0407	<sup>91</sup> 0.0488	<sup>88</sup> 0.0611	<sup>89</sup> 0.0794	<sup>77</sup> 0.0559	<sup>77</sup> 0.0923	<sup>76</sup> 0.1342	<sup>76</sup> 0.1812	<sup>74</sup> 0.2243	<sup>73</sup> 0.2675	<sup>73</sup> 0.3240	<sup>74</sup> 0.3992
13	COGENT-002	<sup>68</sup> 0.0081	<sup>65</sup> 0.0105	<sup>62</sup> 0.0123	<sup>63</sup> 0.0137	<sup>61</sup> 0.0157	<sup>61</sup> 0.0175	<sup>61</sup> 0.0175	<sup>59</sup> 0.0280	<sup>68</sup> 0.0499	<sup>66</sup> 0.0827	<sup>66</sup> 0.1207	<sup>66</sup> 0.1639	<sup>66</sup> 0.2037	<sup>65</sup> 0.2432	<sup>66</sup> 0.2972	<sup>67</sup> 0.3638
14	COGENT-003	<sup>70</sup> 0.0082	<sup>66</sup> 0.0108	<sup>64</sup> 0.0128	<sup>66</sup> 0.0145	<sup>67</sup> 0.0168	<sup>67</sup> 0.0191	<sup>68</sup> 0.0239	<sup>65</sup> 0.0312	<sup>70</sup> 0.0582	<sup>70</sup> 0.0971	<sup>70</sup> 0.1417	<sup>70</sup> 0.1918	<sup>70</sup> 0.2380	<sup>80</sup> 0.2836	<sup>80</sup> 0.3440	<sup>80</sup> 0.4207
15	COGENT-004	<sup>85</sup> 0.0066	<sup>82</sup> 0.0080	<sup>44</sup> 0.0085	<sup>38</sup> 0.0080	<sup>36</sup> 0.0083	<sup>34</sup> 0.0092	<sup>34</sup> 0.0106	<sup>34</sup> 0.0130	<sup>66</sup> 0.0410	<sup>64</sup> 0.0720	<sup>64</sup> 0.1099	<sup>64</sup> 0.1539	<sup>63</sup> 0.1974	<sup>66</sup> 0.2443	<sup>66</sup> 0.3043	<sup>69</sup> 0.3757
16	COGNITEC-000	<sup>104</sup> 0.0265	<sup>102</sup> 0.0423	<sup>105</sup> 0.0588	<sup>105</sup> 0.0757	<sup>105</sup> 0.0894	<sup>101</sup> 0.1014	<sup>101</sup> 0.1169	<sup>100</sup> 0.1381	<sup>96</sup> 0.1522	<sup>96</sup> 0.2330	<sup>98</sup> 0.3051	<sup>98</sup> 0.3751	<sup>98</sup> 0.4300	<sup>98</sup> 0.4779	<sup>99</sup> 0.5307	<sup>99</sup> 0.5913
17	COGNITEC-001	<sup>92</sup> 0.0149	<sup>93</sup> 0.0228	<sup>93</sup> 0.0312	<sup>93</sup> 0.0399	<sup>93</sup> 0.0479	<sup>93</sup> 0.0546	<sup>92</sup> 0.0656	<sup>90</sup> 0.0806	<sup>92</sup> 0.0963	<sup>92</sup> 0.1562	<sup>92</sup> 0.2157	<sup>92</sup> 0.2771	<sup>92</sup> 0.3287	<sup>92</sup> 0.3771	<sup>93</sup> 0.4343	<sup>94</sup> 0.4959
18	COGNITEC-002	<sup>76</sup> 0.0101	<sup>79</sup> 0.0138	<sup>80</sup> 0.0170	<sup>80</sup> 0.0201	<sup>80</sup> 0.0237	<sup>79</sup> 0.0264	<sup>77</sup> 0.0309	<sup>76</sup> 0.0389	<sup>71</sup> 0.0517	<sup>70</sup> 0.0879	<sup>71</sup> 0.1269	<sup>72</sup> 0.1707	<sup>70</sup> 0.2098	<sup>67</sup> 0.2463	<sup>65</sup> 0.2919	<sup>65</sup> 0.3535
19	COGNITEC-003	<sup>77</sup> 0.0104	<sup>80</sup> 0.0140	<sup>81</sup> 0.0174	<sup>81</sup> 0.0205	<sup>81</sup> 0.0238	<sup>80</sup> 0.0266	<sup>78</sup> 0.0311	<sup>78</sup> 0.0401	<sup>74</sup> 0.0504	<sup>69</sup> 0.0855	<sup>68</sup> 0.1235	<sup>68</sup> 0.1662	<sup>67</sup> 0.2045	<sup>64</sup> 0.2403	<sup>64</sup> 0.2854	<sup>64</sup> 0.3451
20	COGNITEC-004	<sup>69</sup> 0.0073	<sup>62</sup> 0.0099	<sup>61</sup> 0.0118	<sup>58</sup> 0.0130	<sup>58</sup> 0.0147	<sup>61</sup> 0.0163	<sup>56</sup> 0.0189	<sup>55</sup> 0.0239	<sup>56</sup> 0.0325	<sup>55</sup> 0.0548	<sup>51</sup> 0.0798	<sup>50</sup> 0.1074	<sup>49</sup> 0.1325	<sup>50</sup> 0.1591	<sup>49</sup> 0.1952	<sup>48</sup> 0.2414
21	CUBOX-000	<sup>4</sup> 0.0019	<sup>4</sup> 0.0024	<sup>4</sup> 0.0028	<sup>4</sup> 0.0031	<sup>4</sup> 0.0032	<sup>3</sup> 0.0037	<sup>3</sup> 0.0044	<sup>4</sup> 0.0027	<sup>4</sup> 0.0039	<sup>4</sup> 0.0059	<sup>4</sup> 0.0083	<sup>5</sup> 0.0111	<sup>5</sup> 0.0141	<sup>5</sup> 0.0185	<sup>5</sup> 0.0252	<sup>5</sup> 0.0339
22	CYBERLINK-002	<sup>48</sup> 0.0055	<sup>44</sup> 0.0068	<sup>40</sup> 0.0075	<sup>34</sup> 0.0078	<sup>31</sup> 0.0084	<sup>31</sup> 0.0094	<sup>32</sup> 0.0107	<sup>30</sup> 0.0114	<sup>31</sup> 0.0180	<sup>31</sup> 0.0302	<sup>30</sup> 0.0460	<sup>31</sup> 0.0643	<sup>32</sup> 0.0837	<sup>32</sup> 0.1058	<sup>31</sup> 0.1370	<sup>31</sup> 0.1787
23	CYBERLINK-003	<sup>26</sup> 0.0041	<sup>33</sup> 0.0052	<sup>26</sup> 0.0057	<sup>24</sup> 0.0058	<sup>24</sup> 0.0061	<sup>26</sup> 0.0068	<sup>26</sup> 0.0078	<sup>25</sup> 0.0078	<sup>18</sup> 0.0109	<sup>19</sup> 0.0259	<sup>20</sup> 0.0356	<sup>20</sup> 0.0468	<sup>20</sup> 0.0574	<sup>20</sup> 0.0787	<sup>21</sup> 0.1072	
24	DAHUA-002	<sup>29</sup> 0.0035	<sup>27</sup> 0.0047	<sup>27</sup> 0.0058	<sup>26</sup> 0.0067	<sup>27</sup> 0.0074	<sup>26</sup> 0.0082	<sup>26</sup> 0.0100	<sup>26</sup> 0.0108	<sup>29</sup> 0.0169	<sup>34</sup> 0.0294	<sup>30</sup> 0.0449	<sup>29</sup> 0.0635	<sup>29</sup> 0.0817	<sup>30</sup> 0.1013	<sup>29</sup> 0.1291	<sup>29</sup> 0.1638
25	DAHUA-003	<sup>18</sup> 0.0026	<sup>18</sup> 0.0036	<sup>18</sup> 0.0043	<sup>19</sup> 0.0050	<sup>19</sup> 0.0055	<sup>18</sup> 0.0062	<sup>22</sup> 0.0080	<sup>19</sup> 0.0073	<sup>28</sup> 0.0160	<sup>29</sup> 0.0280	<sup>28</sup> 0.0432	<sup>28</sup> 0.0615	<sup>28</sup> 0.0794	<sup>29</sup> 0.0987	<sup>29</sup> 0.1270	<sup>26</sup> 0.1587
26	DEEPLINT-001	<sup>16</sup> 0.0024	<sup>15</sup> 0.0032	<sup>15</sup> 0.0037	<sup>12</sup> 0.0040	<sup>12</sup> 0.0043	<sup>16</sup> 0.0049	<sup>14</sup> 0.0060	<sup>14</sup> 0.0052	<sup>12</sup> 0.0058	<sup>11</sup> 0.0119	<sup>11</sup> 0.0155	<sup>11</sup> 0.0199	<sup>12</sup> 0.0249	<sup>11</sup> 0.0338	<sup>11</sup> 0.0463	
27	DEESEA-001	<sup>69</sup> 0.0081	<sup>69</sup> 0.0116	<sup>72</sup> 0.0149	<sup>75</sup> 0.0182	<sup>75</sup> 0.0216	<sup>76</sup> 0.0260	<sup>80</sup> 0.0332	<sup>80</sup> 0.0432	<sup>62</sup> 0.0458	<sup>63</sup> 0.0752	<sup>63</sup> 0.1086	<sup>62</sup> 0.1460	<sup>62</sup> 0.1812	<sup>62</sup> 0.2186	<sup>62</sup> 0.2663	<sup>61</sup> 0.3213
28	DERMALOG-006	<sup>81</sup> 0.0113	<sup>81</sup> 0.0142	<sup>77</sup> 0.0163	<sup>76</sup> 0.0183	<sup>73</sup> 0.0200	<sup>72</sup> 0.0218	<sup>70</sup> 0.0251	<sup>68</sup> 0.0329	<sup>74</sup> 0.0545	<sup>72</sup> 0.0889	<sup>72</sup> 0.1271	<sup>71</sup> 0.1697	<sup>69</sup> 0.2090	<sup>68</sup> 0.2498	<sup>68</sup> 0.3028	<sup>68</sup> 0.3670
29	DERMALOG-007	<sup>87</sup> 0.0125	<sup>87</sup> 0.0170	<sup>87</sup> 0.0214	<sup>87</sup> 0.0264	<sup>86</sup> 0.0309	<sup>85</sup> 0.0356	<sup>86</sup> 0.0432	<sup>86</sup> 0.0579	<sup>91</sup> 0.0910	<sup>91</sup> 0.1453	<sup>91</sup> 0.2009	<sup>91</sup> 0.2602	<sup>91</sup> 0.3134	<sup>91</sup> 0.3649	<sup>90</sup> 0.4289	<sup>91</sup> 0.5007
30	DERMALOG-008	<sup>51</sup> 0.0057	<sup>51</sup> 0.0077	<sup>53</sup> 0.0095	<sup>53</sup> 0.0110	<sup>52</sup> 0.0128	<sup>54</sup> 0.0148	<sup>55</sup> 0.0180	<sup>54</sup> 0.0223	<sup>69</sup> 0.0501	<sup>68</sup> 0.0850	<sup>69</sup> 0.1247	<sup>70</sup> 0.1692	<sup>71</sup> 0.2105	<sup>70</sup> 0.2541	<sup>70</sup> 0.3102	<sup>70</sup> 0.3762
31	GORILLA-002	<sup>99</sup> 0.0213	<sup>99</sup> 0.0359	<sup>100</sup> 0.0528	<sup>100</sup> 0.0716	<sup>102</sup> 0.0895	<sup>102</sup> 0.1088	<sup>102</sup> 0.1367	<sup>102</sup> 0.1765	<sup>102</sup> 0.1828	<sup>103</sup> 0.2787	<sup>103</sup> 0.3654	<sup>103</sup> 0.4485	<sup>103</sup> 0.5168	<sup>103</sup> 0.5823	<sup>103</sup> 0.6508	<sup>103</sup> 0.7180
32	GORILLA-005	<sup>37</sup> 0.0044	<sup>46</sup> 0.0070	<sup>57</sup> 0.0102	<sup>61</sup> 0.0136	<sup>66</sup> 0.0170	<sup>70</sup> 0.0204	<sup>73</sup> 0.0272	<sup>75</sup> 0.0373	<sup>76</sup> 0.0566	<sup>80</sup> 0.0973	<sup>81</sup> 0.1432	<sup>81</sup> 0.1937	<sup>80</sup> 0.2398	<sup>82</sup> 0.2862	<sup>81</sup> 0.3437	<sup>81</sup> 0.4150
33	IDEMIA-003	<sup>80</sup> 0.0110	<sup>85</sup> 0.0151	<sup>85</sup> 0.0196	<sup>84</sup> 0.0238	<sup>83</sup> 0.0281	<sup>83</sup> 0.0313	<sup>85</sup> 0.0368	<sup>82</sup> 0.0504	<sup>86</sup> 0.0717	<sup>88</sup> 0.1147	<sup>85</sup> 0.1614	<sup>85</sup> 0.2113	<sup>84</sup> 0.2553	<sup>84</sup> 0.2976	<sup>83</sup> 0.3537	<sup>83</sup> 0.4334
34	IDEMIA-004	<sup>79</sup> 0.0107	<sup>83</sup> 0.0148	<sup>84</sup> 0.0192	<sup>83</sup> 0.0233	<sup>82</sup> 0.0277	<sup>82</sup> 0.0367	<sup>83</sup> 0.0512	<sup>57</sup> 0.0373	<sup>54</sup> 0.0587	<sup>53</sup> 0.0833	<sup>52</sup> 0.1100	<sup>51</sup> 0.1340	<sup>49</sup> 0.1580	<sup>46</sup> 0.1911	<sup>47</sup> 0.2482	
35	IDEMIA-005	<sup>83</sup> 0.0118	<sup>86</sup> 0.0167	<sup>89</sup> 0.0218	<sup>88</sup> 0.0270	<sup>87</sup> 0.0317	<sup>86</sup> 0.0357	<sup>85</sup> 0.0425	<sup>85</sup> 0.0579	<sup>64</sup> 0.0440	<sup>63</sup> 0.0689	<sup>59</sup> 0.0964	<sup>58</sup> 0.1254	<sup>57</sup> 0.1513	<sup>55</sup> 0.1762	<sup>50</sup> 0.2113	<sup>50</sup> 0.2698
36	IDEMIA-006	<sup>86</sup> 0.0124	<sup>88</sup> 0.0171	<sup>88</sup> 0.0218	<sup>86</sup> 0.0263	<sup>86</sup> 0.0302	<sup>84</sup> 0.0321	<sup>81</sup> 0.0356	<sup>81</sup> 0.0471	<sup>61</sup> 0.0409	<sup>58</sup> 0.0620	<sup>56</sup> 0.0850	<sup>51</sup> 0.1097	<sup>48</sup> 0.1309	<sup>43</sup> 0.1486	<sup>41</sup> 0.1738	<sup>40</sup> 0.2200
37	IDEMIA-007	<sup>46</sup> 0.0050	<sup>47</sup> 0.0071	<sup>47</sup> 0.0089	<sup>49</sup> 0.0106	<sup>50</sup> 0.0124	<sup>50</sup> 0.0142	<sup>50</sup> 0.0171	<sup>52</sup> 0.0220	<sup>31</sup> 0.0202	<sup>35</sup> 0.0335	<sup>33</sup> 0.0491	<sup>32</sup> 0.0663	<sup>30</sup> 0.0825	<sup>29</sup> 0.0999	<sup>28</sup> 0.1240	<sup>26</sup> 0.1645
38	IDEMIA-008	<sup>4</sup> 0.0018	<sup>3</sup> 0.0024	<sup>3</sup> 0.0029	<sup>3</sup> 0.0032	<sup>3</sup> 0.0035	<sup>4</sup> 0.0039	<sup>4</sup> 0.0046	<sup>5</sup> 0.0033	<sup>3</sup> 0.0034	<sup>3</sup> 0.0051	<sup>3</sup> 0.0069	<sup>3</sup> 0.0087	<sup>3</sup> 0.0102	<sup>4</sup> 0.0123	<sup>3</sup> 0.0146	<sup>3</sup> 0.0186
39	IMAGUS-005	<sup>34</sup> 0.0039	<sup>32</sup> 0.0052	<sup>30</sup> 0.0061	<sup>28</sup> 0.0067	<sup>29</sup> 0.0077	<sup>29</sup> 0.0088	<sup>29</sup> 0.0103	<sup>29</sup> 0.0109	<sup>38</sup> 0							

#	MISS RATES ALGORITHM	INVESTIGATION, FNIR(N, R = 1, T = 0)								IDENTIFICATION, FNIR(N, R = L, T ≥ 0) FOR FPIR = 0.001							
		(0, 2]	(2, 4]	(4, 6]	(6, 8]	(8, 10]	(10, 12]	(12, 14]	(14, 18]	(0, 2]	(2, 4]	(4, 6]	(6, 8]	(8, 10]	(10, 12]	(12, 14]	(14, 18]
45	IREX-000	<sup>23</sup> 0.0031	<sup>23</sup> 0.0042	<sup>23</sup> 0.0051	<sup>25</sup> 0.0060	<sup>25</sup> 0.0068	<sup>25</sup> 0.0080	<sup>26</sup> 0.0095	<sup>29</sup> 0.0107	<sup>51</sup> 0.0313	<sup>51</sup> 0.0539	<sup>52</sup> 0.0815	<sup>55</sup> 0.1137	<sup>54</sup> 0.1442	<sup>54</sup> 0.1755	<sup>55</sup> 0.2181	<sup>52</sup> 0.2718
46	ISYSTEMS-002	<sup>75</sup> 0.0101	<sup>78</sup> 0.0135	<sup>79</sup> 0.0169	<sup>78</sup> 0.0197	<sup>79</sup> 0.0228	<sup>76</sup> 0.0256	<sup>76</sup> 0.0304	<sup>77</sup> 0.0398	<sup>89</sup> 0.0779	<sup>89</sup> 0.1258	<sup>90</sup> 0.1759	<sup>89</sup> 0.2299	<sup>89</sup> 0.2758	<sup>88</sup> 0.3204	<sup>88</sup> 0.3763	<sup>88</sup> 0.4401
47	ISYSTEMS-003	<sup>74</sup> 0.0089	<sup>68</sup> 0.0115	<sup>68</sup> 0.0139	<sup>68</sup> 0.0158	<sup>69</sup> 0.0177	<sup>69</sup> 0.0198	<sup>68</sup> 0.0234	<sup>62</sup> 0.0303	<sup>83</sup> 0.0647	<sup>83</sup> 0.1056	<sup>83</sup> 0.1502	<sup>83</sup> 0.1986	<sup>82</sup> 0.2402	<sup>78</sup> 0.2819	<sup>77</sup> 0.3351	<sup>76</sup> 0.3976
48	KEDACOM-001	<sup>82</sup> 0.0116	<sup>74</sup> 0.0130	<sup>66</sup> 0.0135	<sup>59</sup> 0.0133	<sup>56</sup> 0.0135	<sup>49</sup> 0.0141	<sup>43</sup> 0.0151	<sup>40</sup> 0.0176	<sup>40</sup> 0.0241	<sup>40</sup> 0.0360	<sup>38</sup> 0.0513	<sup>33</sup> 0.0689	<sup>33</sup> 0.0866	<sup>33</sup> 0.1060	<sup>29</sup> 0.1327	<sup>26</sup> 0.1694
49	LOOKMAN-003	<sup>85</sup> 0.0123	<sup>82</sup> 0.0144	<sup>76</sup> 0.0158	<sup>69</sup> 0.0168	<sup>71</sup> 0.0178	<sup>65</sup> 0.0188	<sup>58</sup> 0.0212	<sup>60</sup> 0.0260	<sup>63</sup> 0.0438	<sup>64</sup> 0.0687	<sup>60</sup> 0.0978	<sup>40</sup> 0.1296	<sup>59</sup> 0.1581	<sup>55</sup> 0.1879	<sup>57</sup> 0.2294	<sup>53</sup> 0.2756
50	LOOKMAN-005	<sup>81</sup> 0.0118	<sup>76</sup> 0.0134	<sup>69</sup> 0.0142	<sup>65</sup> 0.0144	<sup>60</sup> 0.0150	<sup>59</sup> 0.0160	<sup>50</sup> 0.0176	<sup>49</sup> 0.0213	<sup>50</sup> 0.0310	<sup>40</sup> 0.0480	<sup>40</sup> 0.0698	<sup>45</sup> 0.0954	<sup>45</sup> 0.1216	<sup>45</sup> 0.1491	<sup>45</sup> 0.1890	<sup>40</sup> 0.2381
51	MICROFOCUS-005	<sup>114</sup> 0.4269	<sup>114</sup> 0.5527	<sup>114</sup> 0.6355	<sup>115</sup> 0.7024	<sup>115</sup> 0.7503	<sup>115</sup> 0.7876	<sup>115</sup> 0.8234	<sup>116</sup> 0.8601	<sup>110</sup> 0.8338	<sup>111</sup> 0.9113	<sup>111</sup> 0.9468	<sup>111</sup> 0.9667	<sup>111</sup> 0.9771	<sup>110</sup> 0.9836	<sup>110</sup> 0.9880	<sup>110</sup> 0.9924
52	MICROSOFT-003	<sup>29</sup> 0.0034	<sup>31</sup> 0.0050	<sup>32</sup> 0.0064	<sup>31</sup> 0.0078	<sup>34</sup> 0.0092	<sup>34</sup> 0.0107	<sup>35</sup> 0.0135	<sup>39</sup> 0.0166	<sup>49</sup> 0.0288	<sup>49</sup> 0.0503	<sup>49</sup> 0.0763	<sup>49</sup> 0.1067	<sup>53</sup> 0.1359	<sup>52</sup> 0.1680	<sup>51</sup> 0.2116	<sup>48</sup> 0.2644
53	MICROSOFT-004	<sup>25</sup> 0.0032	<sup>26</sup> 0.0047	<sup>25</sup> 0.0060	<sup>31</sup> 0.0075	<sup>34</sup> 0.0087	<sup>34</sup> 0.0103	<sup>34</sup> 0.0131	<sup>39</sup> 0.0159	<sup>46</sup> 0.0268	<sup>47</sup> 0.0470	<sup>47</sup> 0.0716	<sup>47</sup> 0.1007	<sup>47</sup> 0.1291	<sup>51</sup> 0.1610	<sup>49</sup> 0.2052	<sup>48</sup> 0.2590
54	MICROSOFT-005	<sup>24</sup> 0.0031	<sup>25</sup> 0.0047	<sup>34</sup> 0.0066	<sup>42</sup> 0.0084	<sup>42</sup> 0.0103	<sup>46</sup> 0.0131	<sup>46</sup> 0.0164	<sup>44</sup> 0.0185	<sup>42</sup> 0.0243	<sup>44</sup> 0.0432	<sup>44</sup> 0.0658	<sup>43</sup> 0.0913	<sup>44</sup> 0.1172	<sup>42</sup> 0.1476	<sup>44</sup> 0.1874	<sup>40</sup> 0.2272
55	MICROSOFT-006	<sup>25</sup> 0.0032	<sup>30</sup> 0.0049	<sup>33</sup> 0.0065	<sup>41</sup> 0.0081	<sup>41</sup> 0.0096	<sup>41</sup> 0.0117	<sup>40</sup> 0.0144	<sup>38</sup> 0.0160	<sup>22</sup> 0.0134	<sup>23</sup> 0.0233	<sup>24</sup> 0.0346	<sup>22</sup> 0.0462	<sup>21</sup> 0.0578	<sup>22</sup> 0.0713	<sup>22</sup> 0.0903	<sup>21</sup> 0.1156
56	NEC-000	<sup>56</sup> 0.0195	<sup>58</sup> 0.0316	<sup>58</sup> 0.0445	<sup>58</sup> 0.0581	<sup>57</sup> 0.0699	<sup>56</sup> 0.0817	<sup>56</sup> 0.0998	<sup>56</sup> 0.1237	<sup>88</sup> 0.0759	<sup>88</sup> 0.1245	<sup>88</sup> 0.1729	<sup>88</sup> 0.2240	<sup>88</sup> 0.2671	<sup>87</sup> 0.3117	<sup>83</sup> 0.3639	<sup>88</sup> 0.4348
57	NEC-001	<sup>103</sup> 0.0246	<sup>101</sup> 0.0382	<sup>99</sup> 0.0524	<sup>99</sup> 0.0672	<sup>100</sup> 0.0793	<sup>100</sup> 0.0904	<sup>99</sup> 0.1076	<sup>99</sup> 0.1317	<sup>93</sup> 0.1019	<sup>96</sup> 0.1623	<sup>93</sup> 0.2214	<sup>93</sup> 0.2834	<sup>93</sup> 0.3341	<sup>93</sup> 0.3844	<sup>93</sup> 0.4400	<sup>92</sup> 0.5183
58	NEC-002	<sup>26</sup> 0.0033	<sup>21</sup> 0.0041	<sup>17</sup> 0.0043	<sup>14</sup> 0.0045	<sup>13</sup> 0.0049	<sup>15</sup> 0.0056	<sup>10</sup> 0.0061	<sup>15</sup> 0.0066	<sup>11</sup> 0.0090	<sup>11</sup> 0.0111	<sup>10</sup> 0.0131	<sup>9</sup> 0.0149	<sup>9</sup> 0.0171	<sup>8</sup> 0.0217	<sup>8</sup> 0.0247	<sup>5</sup> 0.0267
59	NEC-003	<sup>30</sup> 0.0036	<sup>25</sup> 0.0046	<sup>23</sup> 0.0051	<sup>23</sup> 0.0055	<sup>23</sup> 0.0059	<sup>19</sup> 0.0067	<sup>19</sup> 0.0077	<sup>21</sup> 0.0073	<sup>9</sup> 0.0056	<sup>9</sup> 0.0076	<sup>9</sup> 0.0091	<sup>7</sup> 0.0105	<sup>6</sup> 0.0119	<sup>6</sup> 0.0137	<sup>5</sup> 0.0162	<sup>3</sup> 0.0209
60	NEC-004	<sup>23</sup> 0.0039	<sup>23</sup> 0.0045	<sup>21</sup> 0.0047	<sup>17</sup> 0.0046	<sup>13</sup> 0.0044	<sup>12</sup> 0.0046	<sup>12</sup> 0.0052	<sup>9</sup> 0.0036	<sup>7</sup> 0.0046	<sup>3</sup> 0.0057	<sup>0.0063</sup>	<sup>1</sup> 0.0069	<sup>1</sup> 0.0076	<sup>1</sup> 0.0090	<sup>1</sup> 0.0105	<sup>0</sup> 0.0105
61	NEUROTECHNOLOGY-003	<sup>100</sup> 0.0234	<sup>100</sup> 0.0379	<sup>101</sup> 0.0549	<sup>106</sup> 0.0682	<sup>99</sup> 0.0720	<sup>97</sup> 0.0747	<sup>97</sup> 0.0886	<sup>96</sup> 0.1066	<sup>108</sup> 0.6802	<sup>108</sup> 0.8187	<sup>109</sup> 0.8920	<sup>109</sup> 0.9355	<sup>109</sup> 0.9594	<sup>109</sup> 0.9738	<sup>109</sup> 0.9828	<sup>109</sup> 0.9885
62	NEUROTECHNOLOGY-004	<sup>76</sup> 0.0104	<sup>77</sup> 0.0134	<sup>75</sup> 0.0156	<sup>72</sup> 0.0173	<sup>71</sup> 0.0195	<sup>71</sup> 0.0212	<sup>69</sup> 0.0245	<sup>66</sup> 0.0320	<sup>82</sup> 0.0642	<sup>81</sup> 0.1015	<sup>80</sup> 0.1426	<sup>78</sup> 0.1881	<sup>77</sup> 0.2299	<sup>76</sup> 0.2722	<sup>75</sup> 0.3269	<sup>74</sup> 0.3943
63	NEUROTECHNOLOGY-005	<sup>70</sup> 0.0089	<sup>69</sup> 0.0116	<sup>69</sup> 0.0136	<sup>67</sup> 0.0152	<sup>65</sup> 0.0173	<sup>65</sup> 0.0196	<sup>64</sup> 0.0233	<sup>60</sup> 0.0306	<sup>75</sup> 0.0556	<sup>74</sup> 0.0913	<sup>73</sup> 0.1315	<sup>73</sup> 0.1766	<sup>73</sup> 0.2192	<sup>72</sup> 0.2617	<sup>71</sup> 0.3174	<sup>71</sup> 0.3843
64	NEUROTECHNOLOGY-007	<sup>68</sup> 0.0078	<sup>64</sup> 0.0103	<sup>63</sup> 0.0124	<sup>64</sup> 0.0140	<sup>62</sup> 0.0161	<sup>62</sup> 0.0185	<sup>61</sup> 0.0225	<sup>60</sup> 0.0290	<sup>81</sup> 0.0641	<sup>84</sup> 0.1069	<sup>84</sup> 0.1546	<sup>84</sup> 0.2075	<sup>85</sup> 0.2572	<sup>86</sup> 0.3081	<sup>87</sup> 0.3713	<sup>87</sup> 0.4421
65	NOBLIS-002	<sup>111</sup> 0.1520	<sup>111</sup> 0.2419	<sup>111</sup> 0.3296	<sup>112</sup> 0.4114	<sup>112</sup> 0.4856	<sup>112</sup> 0.5528	<sup>112</sup> 0.6061	<sup>112</sup> 0.6532	<sup>112</sup> 0.9984	<sup>112</sup> 0.9996	<sup>112</sup> 0.9998	<sup>112</sup> 0.9999	<sup>112</sup> 0.9999	<sup>112</sup> 1.0000	<sup>112</sup> 1.0000	<sup>112</sup> 1.0000
66	NTECHLAB-003	<sup>64</sup> 0.0078	<sup>75</sup> 0.0131	<sup>80</sup> 0.0202	<sup>89</sup> 0.0295	<sup>90</sup> 0.0405	<sup>92</sup> 0.0543	<sup>93</sup> 0.0761	<sup>94</sup> 0.1035	<sup>60</sup> 0.0491	<sup>74</sup> 0.0881	<sup>78</sup> 0.1384	<sup>82</sup> 0.1985	<sup>86</sup> 0.2594	<sup>89</sup> 0.3270	<sup>89</sup> 0.4065	<sup>88</sup> 0.4891
67	NTECHLAB-004	<sup>60</sup> 0.0068	<sup>60</sup> 0.0110	<sup>78</sup> 0.0167	<sup>85</sup> 0.0239	<sup>88</sup> 0.0330	<sup>90</sup> 0.0447	<sup>93</sup> 0.0641	<sup>95</sup> 0.0759	<sup>59</sup> 0.0379	<sup>60</sup> 0.0688	<sup>61</sup> 0.1108	<sup>65</sup> 0.1629	<sup>72</sup> 0.2192	<sup>81</sup> 0.2846	<sup>86</sup> 0.3657	<sup>88</sup> 0.4524
68	NTECHLAB-006	<sup>58</sup> 0.0056	<sup>61</sup> 0.0095	<sup>71</sup> 0.0148	<sup>82</sup> 0.0218	<sup>84</sup> 0.0301	<sup>87</sup> 0.0413	<sup>89</sup> 0.0591	<sup>91</sup> 0.0814	<sup>55</sup> 0.0349	<sup>59</sup> 0.0636	<sup>60</sup> 0.1023	<sup>63</sup> 0.1506	<sup>65</sup> 0.2024	<sup>71</sup> 0.2617	<sup>76</sup> 0.3374	<sup>80</sup> 0.4185
69	NTECHLAB-007	<sup>36</sup> 0.0044	<sup>12</sup> 0.0066	<sup>48</sup> 0.0089	<sup>56</sup> 0.0118	<sup>59</sup> 0.0159	<sup>66</sup> 0.0189	<sup>71</sup> 0.0255	<sup>71</sup> 0.0342	<sup>42</sup> 0.0256	<sup>44</sup> 0.0450	<sup>47</sup> 0.0705	<sup>48</sup> 0.1012	<sup>50</sup> 0.1334	<sup>51</sup> 0.1692	<sup>52</sup> 0.2170	<sup>53</sup> 0.2752
70	NTECHLAB-008	<sup>19</sup> 0.0025	<sup>20</sup> 0.0038	<sup>25</sup> 0.0052	<sup>30</sup> 0.0074	<sup>43</sup> 0.0104	<sup>51</sup> 0.0146	<sup>69</sup> 0.0236	<sup>72</sup> 0.0348	<sup>25</sup> 0.0143	<sup>29</sup> 0.0267	<sup>31</sup> 0.0459	<sup>36</sup> 0.0733	<sup>39</sup> 0.1062	<sup>41</sup> 0.1469	<sup>48</sup> 0.2044	<sup>51</sup> 0.2698
71	NTECHLAB-009	<sup>12</sup> 0.0022	<sup>14</sup> 0.0031	<sup>15</sup> 0.0038	<sup>16</sup> 0.0045	<sup>18</sup> 0.0055	<sup>21</sup> 0.0067	<sup>24</sup> 0.0088	<sup>26</sup> 0.0100	<sup>17</sup> 0.0073	<sup>17</sup> 0.0117	<sup>17</sup> 0.0170	<sup>17</sup> 0.0238	<sup>18</sup> 0.0319	<sup>18</sup> 0.0419	<sup>18</sup> 0.0577	<sup>19</sup> 0.0833
72	PARAVISION-002	<sup>52</sup> 0.0058	<sup>57</sup> 0.0083	<sup>59</sup> 0.0111	<sup>62</sup> 0.0137	<sup>64</sup> 0.0162	<sup>64</sup> 0.0187	<sup>64</sup> 0.0229	<sup>61</sup> 0.0295								
73	PARAVISION-003	<sup>43</sup> 0.0048	<sup>43</sup> 0.0067	<sup>50</sup> 0.0090	<sup>51</sup> 0.0109	<sup>53</sup> 0.0128	<sup>54</sup> 0.0148	<sup>54</sup> 0.0178	<sup>51</sup> 0.0219	<sup>56</sup> 0.0354	<sup>57</sup> 0.0618	<sup>58</sup> 0.0931	<sup>59</sup> 0.1290	<sup>60</sup> 0.1625	<sup>60</sup> 0.1964	<sup>60</sup> 0.2408	<sup>57</sup> 0.2924
74	PARAVISION-004	<sup>15</sup> 0.0024	<sup>16</sup> 0.0032	<sup>16</sup> 0.0040	<sup>15</sup> 0.0047	<sup>17</sup> 0.0053	<sup>17</sup> 0.0061	<sup>17</sup> 0.0073	<sup>18</sup> 0.0072	<sup>19</sup> 0.0118	<sup>22</sup> 0.0209	<sup>23</sup> 0.0327	<sup>23</sup> 0.0465	<sup>23</sup> 0.0613	<sup>23</sup> 0.0779	<sup>23</sup> 0.1008	<sup>23</sup> 0.1285
75	PARAVISION-005	<sup>11</sup> 0.0021	<sup>12</sup> 0.0028	<sup>12</sup> 0.0035	<sup>13</sup> 0.0041	<sup>15</sup> 0.0046	<sup>15</sup> 0.0054	<sup>15</sup> 0.0067	<sup>17</sup> 0.0070	<sup>11</sup> 0.0057	<sup>12</sup> 0.0093	<sup>12</sup> 0.0144	<sup>14</sup> 0.0207	<sup>15</sup> 0.0278	<sup>15</sup> 0.0368	<sup>16</sup> 0.0508	<sup>16</sup> 0.0715
76	PARAVISION-007	<sup>9</sup> 0.0019	<sup>7</sup> 0.0025	<sup>6</sup> 0.0029	<sup>8</sup> 0.0033	<sup>8</sup> 0.0036	<sup>8</sup> 0.0042	<sup>9</sup> 0.0049	<sup>9</sup> 0.0030	<sup>10</sup> 0.0057	<sup>13</sup> 0.0094	<sup>14</sup> 0.0144	<sup>13</sup> 0.0206	<sup>14</sup> 0.0275	<sup>14</sup> 0.0357	<sup>14</sup> 0.0485	<sup>14</sup> 0.0652
77	PIXELALL-002	<sup>71</sup> 0.0085	<sup>72</sup> 0.0119	<sup>70</sup> 0.0147	<sup>71</sup> 0.0172	<sup>72</sup> 0.0198	<sup>73</sup> 0.0225	<sup>73</sup> 0.0270	<sup>73</sup> 0.0349	<sup>96</sup> 0.1193	<sup>96</sup> 0.1900	<sup>96</sup> 0.2601	<sup>96</sup> 0.3332	<sup>96</sup> 0.3955	<sup>96</sup> 0.4565	<sup>96</sup> 0.5268	<sup>96</sup> 0.6030
78	PIXELALL-003	<sup>45</sup> 0.0050	<sup>41</sup> 0.0063	<sup>38</sup> 0.0072	<sup>35</sup> 0.0077	<sup>32</sup> 0.0085	<sup>32</sup> 0.0095	<sup>33</sup> 0.0113	<sup>31</sup> 0.0119	<sup>43</sup> 0.0248	<sup>43</sup> 0.0418	<sup>42</sup> 0.0622	<sup>42</sup> 0.0861	<sup>42</sup> 0.1104	<sup>39</sup> 0.1364	<sup>39</sup> 0.1723	<sup>38</sup> 0.2167
79	PIXELALL-004	<sup>47</sup> 0.0049	<sup>39</sup> 0.0063	<sup>39</sup> 0.0072	<sup>36</sup> 0.0079	<sup>35</sup> 0.0089	<sup>36</sup> 0.0103	<sup>36</sup> 0.0127	<sup>35</sup> 0.0146	<sup>37</sup> 0.0211	<sup>39</sup> 0.0360	<sup>41</sup> 0.0553	<sup>41</sup> 0.0792	<sup>38</sup> 0.1045	<sup>38</sup> 0.1317	<sup>38</sup> 0.1700	<sup>41</sup> 0.2246
80	PTAKURATSATU-000	<sup>53</sup> 0.0061	<sup>54</sup> 0.0082	<sup>54</sup> 0.0097	<sup>52</sup> 0.0109	<sup>48</sup> 0.0120	<sup>45</sup> 0.0131	<sup>41</sup> 0.0146	<sup>43</sup> 0.0180	<sup>58</sup> 0.0375	<sup>56</sup> 0.0596	<sup>54</sup> 0.0842	<sup>54</sup> 0.1116	<sup>52</sup> 0.1357	<sup>48</sup> 0.1553	<sup>42</sup> 0.1820	<sup>41</sup> 0.2326
81	RANKONE-002	<sup>58</sup> 0.0212	<sup>57</sup> 0.0313	<sup>57</sup> 0.0431	<sup>57</sup> 0.0562	<sup>98</sup> 0.0712	<sup>99</sup> 0.0881	<sup>100</sup> 0.1130	<sup>101</sup> 0.1543	<sup>94</sup> 0.1111	<sup>94</sup> 0.1707	<sup>94</sup> 0.2305	<sup>94</sup> 0.2968	<sup>95</sup> 0.3646	<sup>95</sup> 0.4345	<sup>95</sup> 0.5172	<sup>96</sup> 0.6110
82	RANKONE-004	<sup>107</sup> 0.0424	<sup>106</sup> 0.0643	<sup>106</sup> 0.0875	<sup>106</sup> 0.1127	<sup>106</sup> 0.1364	<sup>104</sup> 0.1579	<sup>104</sup> 0.1914	<sup>104</sup> 0.2378	<sup>108</sup> 0.1855	<sup>102</sup> 0.2681	<sup>102</sup> 0.3431	<sup>100</sup> 0.4155	<sup>100</sup> 0.4785	<sup>99</sup> 0.5350	<sup>99</sup> 0.5980	<sup>98</sup> 0.6722
83	RANKONE-005	<sup>91</sup> 0.0136	<sup>92</sup> 0.0192	<sup>90</sup> 0.0246	<sup>80</sup> 0.0303	<sup>89</sup> 0.0362											

#	MISS RATES ALGORITHM	INVESTIGATION, FNIR(N, R = 1, T = 0)								IDENTIFICATION, FNIR(N, R = L, T ≥ 0) FOR FPIR = 0.001							
		(0, 2]	(2, 4]	(4, 6]	(6, 8]	(8, 10]	(10, 12]	(12, 14]	(14, 18]	(0, 2]	(2, 4]	(4, 6]	(6, 8]	(8, 10]	(10, 12]	(12, 14]	(14, 18]
89	REALNETWORKS-003	<sup>102</sup> 0.0245	<sup>104</sup> 0.0437	<sup>104</sup> 0.0686	<sup>108</sup> 0.0975	<sup>105</sup> 0.1312	<sup>106</sup> 0.1719	<sup>106</sup> 0.2294	<sup>107</sup> 0.2907	<sup>99</sup> 0.1468	<sup>99</sup> 0.2370	<sup>100</sup> 0.3313	<sup>102</sup> 0.4269	<sup>102</sup> 0.5142	<sup>105</sup> 0.5979	<sup>104</sup> 0.6815	<sup>104</sup> 0.7567
90	REALNETWORKS-004	<sup>101</sup> 0.0244	<sup>103</sup> 0.0428	<sup>103</sup> 0.0663	<sup>104</sup> 0.0939	<sup>104</sup> 0.1251	<sup>105</sup> 0.1634	<sup>105</sup> 0.2170	<sup>106</sup> 0.2785	<sup>98</sup> 0.1484	<sup>100</sup> 0.2377	<sup>99</sup> 0.3303	<sup>101</sup> 0.4249	<sup>101</sup> 0.5106	<sup>102</sup> 0.5924	<sup>103</sup> 0.6758	<sup>103</sup> 0.7534
91	SCANOVATE-001	<sup>67</sup> 0.0079	<sup>71</sup> 0.0117	<sup>74</sup> 0.0151	<sup>77</sup> 0.0185	<sup>77</sup> 0.0221	<sup>79</sup> 0.0259	<sup>79</sup> 0.0321	<sup>79</sup> 0.0427	<sup>89</sup> 0.0727	<sup>87</sup> 0.1169	<sup>86</sup> 0.1650	<sup>86</sup> 0.2115	<sup>83</sup> 0.2528	<sup>80</sup> 0.2925	<sup>80</sup> 0.3437	<sup>79</sup> 0.4084
92	SENSETIME-002	<sup>95</sup> 0.0186	<sup>91</sup> 0.0191	<sup>83</sup> 0.0183	<sup>74</sup> 0.0179	<sup>69</sup> 0.0173	<sup>47</sup> 0.0133	<sup>25</sup> 0.0089	<sup>15</sup> 0.0059	<sup>39</sup> 0.0220	<sup>24</sup> 0.0236	<sup>18</sup> 0.0237	<sup>18</sup> 0.0240	<sup>12</sup> 0.0245	<sup>19</sup> 0.0219	<sup>9</sup> 0.0195	<sup>6</sup> 0.0222
93	SENSETIME-003	<sup>10</sup> 0.0021	<sup>11</sup> 0.0028	<sup>10</sup> 0.0031	<sup>7</sup> 0.0033	<sup>5</sup> 0.0035	<sup>7</sup> 0.0040	<sup>7</sup> 0.0047	<sup>7</sup> 0.0033	<sup>9</sup> 0.0046	<sup>3</sup> 0.0064	<sup>6</sup> 0.0076	<sup>4</sup> 0.0086	<sup>4</sup> 0.0101	<sup>3</sup> 0.0122	<sup>4</sup> 0.0155	<sup>4</sup> 0.0196
94	SENSETIME-004	<sup>3</sup> 0.0016	<sup>3</sup> 0.0022	<sup>3</sup> 0.0025	<sup>3</sup> 0.0028	<sup>3</sup> 0.0030	<sup>3</sup> 0.0035	<sup>4</sup> 0.0043	<sup>3</sup> 0.0025	<sup>4</sup> 0.0036	<sup>4</sup> 0.0052	<sup>3</sup> 0.0066	<sup>3</sup> 0.0081	<sup>3</sup> 0.0099	<sup>3</sup> 0.0126	<sup>6</sup> 0.0169	<sup>7</sup> 0.0230
95	SENSETIME-005	<sup>2</sup> 0.0015	<sup>2</sup> 0.0020	<sup>2</sup> 0.0024	<sup>2</sup> 0.0026	<sup>2</sup> 0.0029	<sup>3</sup> 0.0035	<sup>3</sup> 0.0043	<sup>3</sup> 0.0028	<sup>2</sup> 0.0036	<sup>2</sup> 0.0059	<sup>8</sup> 0.0089	<sup>9</sup> 0.0128	<sup>10</sup> 0.0177	<sup>11</sup> 0.0240	<sup>12</sup> 0.0345	<sup>12</sup> 0.0493
96	SENSETIME-006	<sup>1</sup> 0.0015	<sup>1</sup> 0.0019	<sup>1</sup> 0.0022	<sup>1</sup> 0.0025	<sup>1</sup> 0.0027	<sup>2</sup> 0.0033	<sup>1</sup> 0.0040	<sup>2</sup> 0.0021	<sup>2</sup> 0.0031	<sup>4</sup> 0.0068	<sup>6</sup> 0.0097	<sup>7</sup> 0.0132	<sup>8</sup> 0.0184	<sup>10</sup> 0.0262	<sup>10</sup> 0.0359	
97	SIAT-002	<sup>116</sup> 0.8309	<sup>116</sup> 0.8310	<sup>116</sup> 0.8311	<sup>116</sup> 0.8306	<sup>116</sup> 0.8296	<sup>116</sup> 0.8302	<sup>116</sup> 0.8300	<sup>115</sup> 0.8301	<sup>111</sup> 0.8340	<sup>109</sup> 0.8368	<sup>108</sup> 0.8404	<sup>108</sup> 0.8445	<sup>108</sup> 0.8480	<sup>108</sup> 0.8532	<sup>108</sup> 0.8595	<sup>107</sup> 0.8691
98	SYNESIS-003	<sup>88</sup> 0.0125	<sup>84</sup> 0.0151	<sup>82</sup> 0.0174	<sup>79</sup> 0.0199	<sup>76</sup> 0.0223	<sup>74</sup> 0.0240	<sup>74</sup> 0.0279	<sup>69</sup> 0.0331	<sup>84</sup> 0.0658	<sup>82</sup> 0.1052	<sup>82</sup> 0.1483	<sup>81</sup> 0.1968	<sup>81</sup> 0.2399	<sup>79</sup> 0.2834	<sup>76</sup> 0.3405	<sup>78</sup> 0.4046
99	SYNESIS-005	<sup>39</sup> 0.0044	<sup>36</sup> 0.0058	<sup>36</sup> 0.0070	<sup>39</sup> 0.0080	<sup>36</sup> 0.0091	<sup>29</sup> 0.0103	<sup>35</sup> 0.0125	<sup>36</sup> 0.0152	<sup>43</sup> 0.0262	<sup>44</sup> 0.0444	<sup>44</sup> 0.0666	<sup>44</sup> 0.0923	<sup>43</sup> 0.1156	<sup>40</sup> 0.1399	<sup>40</sup> 0.1736	<sup>39</sup> 0.2185
100	TECH5-001	<sup>56</sup> 0.0061	<sup>60</sup> 0.0093	<sup>65</sup> 0.0128	<sup>70</sup> 0.0171	<sup>76</sup> 0.0221	<sup>81</sup> 0.0289	<sup>84</sup> 0.0412	<sup>84</sup> 0.0560	<sup>85</sup> 0.0660	<sup>86</sup> 0.1156	<sup>89</sup> 0.1733	<sup>90</sup> 0.2385	<sup>90</sup> 0.2998	<sup>90</sup> 0.3629	<sup>92</sup> 0.4424	<sup>93</sup> 0.5284
101	TOSHIBA-001	<sup>72</sup> 0.0086	<sup>73</sup> 0.0119	<sup>73</sup> 0.0150	<sup>74</sup> 0.0178	<sup>74</sup> 0.0209	<sup>75</sup> 0.0241	<sup>75</sup> 0.0292	<sup>74</sup> 0.0365								
102	TRUEFACE-000	<sup>35</sup> 0.0043	<sup>35</sup> 0.0057	<sup>29</sup> 0.0061	<sup>27</sup> 0.0067	<sup>26</sup> 0.0073	<sup>27</sup> 0.0084	<sup>27</sup> 0.0097	<sup>25</sup> 0.0099	<sup>34</sup> 0.0200	<sup>36</sup> 0.0338	<sup>37</sup> 0.0504	<sup>34</sup> 0.0705	<sup>34</sup> 0.0904	<sup>34</sup> 0.1112	<sup>35</sup> 0.1401	<sup>32</sup> 0.1792
103	VERIDAS-001	<sup>57</sup> 0.0063	<sup>55</sup> 0.0083	<sup>55</sup> 0.0099	<sup>55</sup> 0.0113	<sup>59</sup> 0.0132	<sup>53</sup> 0.0148	<sup>54</sup> 0.0184	<sup>50</sup> 0.0219	<sup>60</sup> 0.0403	<sup>60</sup> 0.0684	<sup>61</sup> 0.1012	<sup>61</sup> 0.1386	<sup>61</sup> 0.1741	<sup>61</sup> 0.2113	<sup>61</sup> 0.2611	<sup>62</sup> 0.3233
104	VISIONLABS-004	<sup>42</sup> 0.0048	<sup>45</sup> 0.0069	<sup>51</sup> 0.0091	<sup>54</sup> 0.0111	<sup>54</sup> 0.0130	<sup>56</sup> 0.0152	<sup>55</sup> 0.0187	<sup>57</sup> 0.0242	<sup>73</sup> 0.0540	<sup>76</sup> 0.0916	<sup>77</sup> 0.1358	<sup>77</sup> 0.1855	<sup>78</sup> 0.2303	<sup>77</sup> 0.2745	<sup>76</sup> 0.3312	<sup>72</sup> 0.3913
105	VISIONLABS-005	<sup>38</sup> 0.0044	<sup>38</sup> 0.0063	<sup>42</sup> 0.0081	<sup>43</sup> 0.0095	<sup>46</sup> 0.0109	<sup>44</sup> 0.0125	<sup>45</sup> 0.0187	<sup>68</sup> 0.0479	<sup>68</sup> 0.0812	<sup>67</sup> 0.1212	<sup>69</sup> 0.1664	<sup>68</sup> 0.2078	<sup>68</sup> 0.2473	<sup>68</sup> 0.2999	<sup>68</sup> 0.3577	
106	VISIONLABS-006	<sup>25</sup> 0.0035	<sup>29</sup> 0.0048	<sup>31</sup> 0.0061	<sup>29</sup> 0.0069	<sup>28</sup> 0.0077	<sup>28</sup> 0.0087	<sup>30</sup> 0.0105	<sup>33</sup> 0.0120	<sup>47</sup> 0.0273	<sup>46</sup> 0.0465	<sup>46</sup> 0.0702	<sup>46</sup> 0.0970	<sup>46</sup> 0.1228	<sup>44</sup> 0.1486	<sup>45</sup> 0.1847	<sup>43</sup> 0.2295
107	VISIONLABS-008	<sup>20</sup> 0.0028	<sup>19</sup> 0.0037	<sup>20</sup> 0.0047	<sup>21</sup> 0.0053	<sup>22</sup> 0.0058	<sup>20</sup> 0.0067	<sup>23</sup> 0.0081	<sup>24</sup> 0.0085	<sup>28</sup> 0.0143	<sup>26</sup> 0.0241	<sup>27</sup> 0.0373	<sup>26</sup> 0.0519	<sup>26</sup> 0.0677	<sup>24</sup> 0.0850	<sup>24</sup> 0.1104	<sup>24</sup> 0.1444
108	VISIONLABS-009	<sup>8</sup> 0.0020	<sup>8</sup> 0.0026	<sup>9</sup> 0.0030	<sup>9</sup> 0.0034	<sup>10</sup> 0.0038	<sup>10</sup> 0.0044	<sup>11</sup> 0.0052	<sup>12</sup> 0.0046	<sup>14</sup> 0.0065	<sup>15</sup> 0.0105	<sup>15</sup> 0.0156	<sup>15</sup> 0.0217	<sup>16</sup> 0.0289	<sup>16</sup> 0.0368	<sup>15</sup> 0.0499	<sup>15</sup> 0.0681
109	VISIONLABS-010	<sup>8</sup> 0.0020	<sup>8</sup> 0.0025	<sup>8</sup> 0.0030	<sup>10</sup> 0.0034	<sup>9</sup> 0.0036	<sup>9</sup> 0.0043	<sup>9</sup> 0.0051	<sup>13</sup> 0.0047	<sup>16</sup> 0.0069	<sup>16</sup> 0.0113	<sup>16</sup> 0.0170	<sup>16</sup> 0.0238	<sup>17</sup> 0.0316	<sup>17</sup> 0.0411	<sup>17</sup> 0.0557	<sup>17</sup> 0.0740
110	VTS-000	<sup>115</sup> 0.5878	<sup>115</sup> 0.6312	<sup>115</sup> 0.6602	<sup>114</sup> 0.6863	<sup>114</sup> 0.7073	<sup>114</sup> 0.7246	<sup>114</sup> 0.7458	<sup>113</sup> 0.7747	<sup>107</sup> 0.5929	<sup>107</sup> 0.6397	<sup>107</sup> 0.6729	<sup>107</sup> 0.7034	<sup>106</sup> 0.7279	<sup>106</sup> 0.7493	<sup>105</sup> 0.7739	<sup>105</sup> 0.8076
111	XFORWARDAI-000	<sup>19</sup> 0.0027	<sup>17</sup> 0.0034	<sup>19</sup> 0.0044	<sup>20</sup> 0.0052	<sup>20</sup> 0.0058	<sup>23</sup> 0.0067	<sup>21</sup> 0.0079	<sup>22</sup> 0.0076	<sup>27</sup> 0.0157	<sup>30</sup> 0.0281	<sup>29</sup> 0.0443	<sup>30</sup> 0.0635	<sup>31</sup> 0.0834	<sup>31</sup> 0.1050	<sup>30</sup> 0.1330	<sup>30</sup> 0.1714
112	XFORWARDAI-001	<sup>14</sup> 0.0023	<sup>10</sup> 0.0028	<sup>11</sup> 0.0034	<sup>11</sup> 0.0037	<sup>11</sup> 0.0039	<sup>11</sup> 0.0045	<sup>10</sup> 0.0052	<sup>11</sup> 0.0043	<sup>13</sup> 0.0060	<sup>14</sup> 0.0096	<sup>13</sup> 0.0144	<sup>12</sup> 0.0200	<sup>13</sup> 0.0260	<sup>13</sup> 0.0334	<sup>13</sup> 0.0435	<sup>13</sup> 0.0586
113	YITU-002	<sup>59</sup> 0.0066	<sup>56</sup> 0.0083	<sup>52</sup> 0.0094	<sup>43</sup> 0.0101	<sup>46</sup> 0.0121	<sup>55</sup> 0.0150	<sup>60</sup> 0.0223	<sup>67</sup> 0.0328	<sup>58</sup> 0.0189	<sup>33</sup> 0.0317	<sup>34</sup> 0.0494	<sup>38</sup> 0.0750	<sup>40</sup> 0.1066	<sup>46</sup> 0.1494	<sup>58</sup> 0.2171	<sup>59</sup> 0.2958
114	YITU-003	<sup>62</sup> 0.0072	<sup>59</sup> 0.0089	<sup>56</sup> 0.0100	<sup>50</sup> 0.0107	<sup>51</sup> 0.0125	<sup>57</sup> 0.0153	<sup>62</sup> 0.0226	<sup>70</sup> 0.0334	<sup>38</sup> 0.0194	<sup>34</sup> 0.0321	<sup>35</sup> 0.0500	<sup>40</sup> 0.0756	<sup>41</sup> 0.1071	<sup>47</sup> 0.1500	<sup>54</sup> 0.2177	<sup>60</sup> 0.2964
115	YITU-004	<sup>54</sup> 0.0061	<sup>50</sup> 0.0075	<sup>43</sup> 0.0081	<sup>40</sup> 0.0081	<sup>38</sup> 0.0092	<sup>38</sup> 0.0107	<sup>46</sup> 0.0154	<sup>48</sup> 0.0207	<sup>21</sup> 0.0125	<sup>21</sup> 0.0204	<sup>22</sup> 0.0314	<sup>24</sup> 0.0469	<sup>25</sup> 0.0671	<sup>29</sup> 0.0955	<sup>35</sup> 0.1421	<sup>37</sup> 0.2006
116	YITU-005	<sup>60</sup> 0.0067	<sup>53</sup> 0.0080	<sup>46</sup> 0.0087	<sup>43</sup> 0.0085	<sup>40</sup> 0.0094	<sup>39</sup> 0.0108	<sup>45</sup> 0.0151	<sup>47</sup> 0.0204	<sup>20</sup> 0.0124	<sup>20</sup> 0.0198	<sup>21</sup> 0.0308	<sup>21</sup> 0.0462	<sup>24</sup> 0.0667	<sup>28</sup> 0.0953	<sup>34</sup> 0.1418	<sup>35</sup> 0.1930

**Table 8: Accuracy for the FRVT 2018 mugshot sets under ageing.** The second row shows the time lapse between gallery and subsequent probe images, in years. The first two columns identify the algorithm. The next 8 values give rank-based FNIR with  $R = 1$ ,  $T = 0$  and  $FPIR = 1$ . All these are relevant to investigational uses where candidates from all searches would need human review. The second 8 values give threshold-based FNIR with  $T \geq 0$ ,  $FPIR = 0.001$  and no rank criterion. The shaded cells indicate the three most accurate algorithms for that elapsed time. The gallery size is 3068801. The total number of searches is 10951064.

2021/10/28  
 FNIR(N, R, T) = False neg. identification rate  
 FPIR(N, T) = False pos. identification rate  
 N = Num. enrolled subjects  
 R = Num. candidates examined  
 T = Threshold  
 T = 0 → Investigation  
 T > 0 → Identification

#	ALGORITHM	INVESTIGATION MODE						IDENTIFICATION MODE						FAILURE TO EXTRACT					
		RANK ONE MISS RATE, FNIR(N, 0, 1)						HIGH T → FPIR = 0.001, FNIR(N, T, L)						FEATURES					
		N=1.6M						N=1.6M											
		GALLERY	MUGSHOT	MUGSHOT	MUGSHOT	VISA	BORDER	VISA	MUGSHOT	MUGSHOT	MUGSHOT	VISA	BORDER	VISA	MUGSHOT	MUGSHOT	MUGSHOT	VISA	BORDER
PROBE	MUGSHOT	WEBCAM	PROFILE	BORDER	BOR <sub>1</sub> 10YR	KIOSK	MUGSHOT	WEBCAM	PROFILE	BORDER	BOR <sub>1</sub> 10YR	KIOSK	MUGSHOT	WEBCAM	PROFILE	BORDER	BOR <sub>1</sub> 10YR	KIOSK	
1	20FACE-000	<sup>219</sup> 0.055	<sup>200</sup> 0.085	<sup>111</sup> 0.736	<sup>135</sup> 0.056	<sup>62</sup> 0.239	<sup>130</sup> 0.243	<sup>206</sup> 0.348	<sup>208</sup> 0.450	<sup>181</sup> 1.000	<sup>138</sup> 0.424	<sup>60</sup> 0.772	<sup>134</sup> 0.938	0.000	0.000	0.000			0.000
2	3DIVI-003	<sup>219</sup> 0.083	<sup>215</sup> 0.206		<sup>147</sup> 0.141		<sup>153</sup> 0.474	<sup>215</sup> 0.400	<sup>213</sup> 0.626		<sup>149</sup> 0.605		<sup>122</sup> 0.821	0.002	0.005				
3	3DIVI-004	<sup>179</sup> 0.018	<sup>188</sup> 0.062		<sup>129</sup> 0.035		<sup>134</sup> 0.279	<sup>187</sup> 0.169	<sup>193</sup> 0.343		<sup>129</sup> 0.277		<sup>102</sup> 0.607	0.002	0.005				
4	3DIVI-005	<sup>181</sup> 0.018	<sup>187</sup> 0.062	<sup>157</sup> 0.930	<sup>163</sup> 0.821		<sup>135</sup> 0.279	<sup>184</sup> 0.166	<sup>191</sup> 0.339	<sup>115</sup> 0.996	<sup>154</sup> 0.864		<sup>101</sup> 0.597	0.002	0.005			0.442	
5	3DIVI-006	<sup>191</sup> 0.024	<sup>195</sup> 0.074		<sup>131</sup> 0.047		<sup>143</sup> 0.312	<sup>186</sup> 0.168	<sup>191</sup> 0.342		<sup>130</sup> 0.283		<sup>105</sup> 0.615	0.002	0.005				
6	ACER-000	<sup>157</sup> 0.011	<sup>151</sup> 0.036	<sup>138</sup> 0.827	<sup>116</sup> 0.025		<sup>118</sup> 0.209	<sup>177</sup> 0.146	<sup>171</sup> 0.246	<sup>73</sup> 0.981	<sup>124</sup> 0.201		<sup>89</sup> 0.490	0.000	0.000	0.042			
7	AIZE-001	<sup>116</sup> 0.006	<sup>116</sup> 0.022	<sup>103</sup> 0.683	<sup>105</sup> 0.016	<sup>33</sup> 0.050	<sup>102</sup> 0.165	<sup>140</sup> 0.077	<sup>131</sup> 0.143	<sup>96</sup> 0.994	<sup>100</sup> 0.101	<sup>51</sup> 0.364	<sup>74</sup> 0.387	0.001	0.001	0.047			0.000
8	ALCHERA-000	<sup>172</sup> 0.016	<sup>175</sup> 0.047	<sup>143</sup> 0.870	<sup>130</sup> 0.046		<sup>140</sup> 0.292	<sup>174</sup> 0.138	<sup>151</sup> 0.216	<sup>130</sup> 0.999	<sup>119</sup> 0.176		<sup>118</sup> 0.803	0.006	0.014	0.328			
9	ALCHERA-001	<sup>243</sup> 0.987	<sup>241</sup> 1.000		<sup>167</sup> 1.000		<sup>187</sup> 1.000	<sup>242</sup> 0.999	<sup>244</sup> 1.000		<sup>199</sup> 1.000		<sup>183</sup> 1.000	0.006	0.013	0.324			
10	ALCHERA-002	<sup>230</sup> 0.095	<sup>212</sup> 0.166	<sup>170</sup> 0.954	<sup>162</sup> 0.668		<sup>151</sup> 0.446	<sup>222</sup> 0.486	<sup>213</sup> 0.591	<sup>152</sup> 1.000	<sup>183</sup> 0.827		<sup>119</sup> 0.811	0.001	0.002	0.106			
11	ALCHERA-003	<sup>156</sup> 0.010	<sup>149</sup> 0.035	<sup>111</sup> 0.741	<sup>106</sup> 0.016		<sup>116</sup> 0.206	<sup>178</sup> 0.155	<sup>141</sup> 0.239	<sup>141</sup> 0.999	<sup>118</sup> 0.172		<sup>86</sup> 0.464	0.001	0.002	0.106			
12	ALCHERA-004	<sup>156</sup> 0.011	<sup>154</sup> 0.038	<sup>51</sup> 0.345	<sup>107</sup> 0.017	<sup>39</sup> 0.088	<sup>91</sup> 0.144	<sup>214</sup> 0.394	<sup>208</sup> 0.529	<sup>92</sup> 0.991	<sup>139</sup> 0.424	<sup>58</sup> 0.708	<sup>38</sup> 0.546	0.001	0.001	0.046			0.000
13	ALLGOVISION-000	<sup>145</sup> 0.011	<sup>145</sup> 0.033	<sup>148</sup> 0.894	<sup>112</sup> 0.021		<sup>137</sup> 0.282	<sup>152</sup> 0.088	<sup>146</sup> 0.166	<sup>89</sup> 0.990	<sup>103</sup> 0.117		<sup>95</sup> 0.526	0.002	0.003	0.122			
14	ALLGOVISION-001	<sup>145</sup> 0.009	<sup>160</sup> 0.038	<sup>99</sup> 0.661	<sup>111</sup> 0.021		<sup>128</sup> 0.241	<sup>157</sup> 0.102	<sup>161</sup> 0.221	<sup>79</sup> 0.986	<sup>113</sup> 0.150		<sup>90</sup> 0.491	0.001	0.001	0.042			
15	ANKE-000	<sup>172</sup> 0.013	<sup>155</sup> 0.038	<sup>160</sup> 0.931	<sup>233</sup> 1.000		<sup>194</sup> 1.000	<sup>162</sup> 0.117	<sup>160</sup> 0.220	<sup>97</sup> 0.994	<sup>171</sup> 1.000		<sup>173</sup> 1.000	0.000	0.001	0.080			
16	ANKE-001	<sup>171</sup> 0.013	<sup>156</sup> 0.038	<sup>163</sup> 0.946	<sup>173</sup> 1.000		<sup>221</sup> 1.000	<sup>166</sup> 0.119	<sup>159</sup> 0.220	<sup>102</sup> 0.994	<sup>228</sup> 1.000		<sup>240</sup> 1.000	0.000	0.001	0.080			
17	ANKE-002	<sup>76</sup> 0.003	<sup>81</sup> 0.016	<sup>76</sup> 0.522	<sup>56</sup> 0.005		<sup>70</sup> 0.119	<sup>83</sup> 0.032	<sup>71</sup> 0.079	<sup>50</sup> 0.948	<sup>56</sup> 0.034		<sup>47</sup> 0.245	0.001	0.001	0.049			
18	AWARE-003	<sup>191</sup> 0.031	<sup>201</sup> 0.090	<sup>180</sup> 0.966	<sup>153</sup> 0.316		<sup>139</sup> 0.290	<sup>170</sup> 0.128	<sup>188</sup> 0.298	<sup>77</sup> 0.984	<sup>140</sup> 0.428		<sup>96</sup> 0.530	0.004	0.003	0.874			
19	AWARE-004	<sup>214</sup> 0.068	<sup>214</sup> 0.176	<sup>189</sup> 0.976	<sup>145</sup> 0.122		<sup>149</sup> 0.414	<sup>200</sup> 0.269	<sup>203</sup> 0.509	<sup>155</sup> 1.000	<sup>135</sup> 0.397		<sup>120</sup> 0.816	0.003	0.003	0.776			
20	AWARE-005	<sup>198</sup> 0.031	<sup>189</sup> 0.067	<sup>190</sup> 0.978	<sup>133</sup> 0.048		<sup>142</sup> 0.308	<sup>209</sup> 0.364	<sup>172</sup> 0.253	<sup>158</sup> 1.000	<sup>128</sup> 0.255		<sup>130</sup> 0.916	0.001	0.002	0.189			
21	AWARE-006	<sup>210</sup> 0.070	<sup>208</sup> 0.128	<sup>190</sup> 0.983	<sup>144</sup> 0.111		<sup>150</sup> 0.421	<sup>201</sup> 0.276	<sup>198</sup> 0.398	<sup>149</sup> 0.999	<sup>183</sup> 0.368		<sup>112</sup> 0.749	0.001	0.002	0.189			
22	AYONIX-000	<sup>231</sup> 0.450	<sup>236</sup> 0.685	<sup>201</sup> 0.996	<sup>161</sup> 0.607		<sup>164</sup> 0.867	<sup>231</sup> 0.811	<sup>231</sup> 0.998	<sup>120</sup> 0.998	<sup>158</sup> 0.954		<sup>142</sup> 0.982	0.010	0.031	0.939			
23	AYONIX-001	<sup>231</sup> 0.341	<sup>229</sup> 0.527	<sup>191</sup> 0.993	<sup>166</sup> 0.994		<sup>162</sup> 0.778	<sup>233</sup> 0.824	<sup>229</sup> 0.920	<sup>145</sup> 0.999	<sup>162</sup> 0.999		<sup>139</sup> 0.969	0.010	0.031	0.939			
24	AYONIX-002	<sup>235</sup> 0.341	<sup>230</sup> 0.527	<sup>196</sup> 0.993	<sup>157</sup> 0.464		<sup>161</sup> 0.778	<sup>232</sup> 0.824	<sup>226</sup> 0.920	<sup>147</sup> 0.999	<sup>155</sup> 0.915		<sup>138</sup> 0.969	0.010	0.031	0.939			
25	CAMVI-003	<sup>201</sup> 0.052	<sup>202</sup> 0.090	<sup>151</sup> 0.911	<sup>141</sup> 0.093		<sup>146</sup> 0.360	<sup>135</sup> 0.071	<sup>121</sup> 0.132	<sup>58</sup> 0.970	<sup>102</sup> 0.114		<sup>77</sup> 0.402	0.006	0.013	0.675			
26	CAMVI-004	<sup>207</sup> 0.047	<sup>196</sup> 0.077	<sup>114</sup> 0.744	<sup>140</sup> 0.072		<sup>141</sup> 0.296	<sup>136</sup> 0.072	<sup>123</sup> 0.136	<sup>143</sup> 0.999	<sup>39</sup> 0.100		<sup>116</sup> 0.787	0.000	0.000	0.000			
27	CAMVI-005	<sup>213</sup> 0.065	<sup>206</sup> 0.103	<sup>116</sup> 0.746	<sup>142</sup> 0.098		<sup>156</sup> 0.341	<sup>156</sup> 0.099	<sup>153</sup> 0.179	<sup>151</sup> 1.000	<sup>114</sup> 0.156		<sup>150</sup> 0.999	0.000	0.000	0.000			
28	CIB-000	<sup>25</sup> 0.002	<sup>10</sup> 0.008	<sup>11</sup> 0.100	<sup>11</sup> 0.002	<sup>17</sup> 0.011	<sup>7</sup> 0.069	<sup>35</sup> 0.012	<sup>31</sup> 0.045	<sup>164</sup> 1.000	<sup>31</sup> 0.017	<sup>24</sup> 0.141	<sup>187</sup> 0.894	0.000	0.000	0.000			0.000
29	CLOUDWALK-HR-000	<sup>21</sup> 0.001	<sup>22</sup> 0.010	<sup>3</sup> 0.064	<sup>8</sup> 0.002	<sup>4</sup> 0.006	<sup>2</sup> 0.057	<sup>6</sup> 0.002	<sup>3</sup> 0.013	<sup>1</sup> 0.133	<sup>5</sup> 0.005	<sup>3</sup> 0.033	<sup>5</sup> 0.099	0.001	0.000	0.042			0.000
30	COGENT-000	<sup>156</sup> 0.010	<sup>173</sup> 0.046	<sup>181</sup> 0.965				<sup>113</sup> 0.053	<sup>129</sup> 0.140	<sup>108</sup> 0.995				0.000	0.000	0.000			
31	COGENT-001	<sup>155</sup> 0.010	<sup>172</sup> 0.046	<sup>181</sup> 0.965				<sup>112</sup> 0.053	<sup>129</sup> 0.140	<sup>107</sup> 0.995				0.000	0.000	0.000			
32	COGENT-002	<sup>91</sup> 0.004	<sup>106</sup> 0.020	<sup>153</sup> 0.925				<sup>99</sup> 0.044	<sup>98</sup> 0.098	<sup>119</sup> 0.998				0.000	0.000	0.000			
33	COGENT-003	<sup>91</sup> 0.004	<sup>110</sup> 0.021	<sup>160</sup> 0.939				<sup>104</sup> 0.046	<sup>98</sup> 0.095	<sup>121</sup> 0.998				0.000	0.000	0.000			
34	COGENT-004	<sup>51</sup> 0.002	<sup>35</sup> 0.013	<sup>151</sup> 0.922	<sup>48</sup> 0.004	<sup>32</sup> 0.019	<sup>65</sup> 0.113	<sup>84</sup> 0.033	<sup>40</sup> 0.051	<sup>117</sup> 0.997	<sup>38</sup> 0.022	<sup>22</sup> 0.126	<sup>84</sup> 0.456	0.000	0.000	0.000			0.000
35	COGENT-005	<sup>31</sup> 0.002	<sup>29</sup> 0.010	<sup>21</sup> 0.126	<sup>12</sup> 0.002	<sup>15</sup> 0.010	<sup>71</sup> 0.120	<sup>25</sup> 0.009	<sup>28</sup> 0.037	<sup>85</sup> 0.989	<sup>21</sup> 0.011	<sup>15</sup> 0.082	<sup>128</sup> 0.905	0.000	0.000	0.000			0.000
36	COGNITEC-000	<sup>195</sup> 0.025	<sup>184</sup> 0.059	<sup>178</sup> 0.964				<sup>182</sup> 0.161	<sup>188</sup> 0.303	<sup>93</sup> 0.992				0.003	0.002	0.924			
37	COGNITEC-001	<sup>163</sup> 0.012	<sup>147</sup> 0.034	<sup>173</sup> 0.958				<sup>158</sup> 0.102	<sup>163</sup> 0.230	<sup>196</sup> 1.000				0.003	0.002	0.924			
38	COGNITEC-002	<sup>119</sup> 0.006	<sup>132</sup> 0.025	<sup>167</sup> 0.949				<sup>115</sup> 0.053	<sup>152</sup> 0.178	<sup>163</sup> 1.000				0.003	0.002	0.924			
39	COGNITEC-003	<sup>123</sup> 0.006	<sup>131</sup> 0.025	<sup>159</sup> 0.930				<sup>111</sup> 0.053	<sup>141</sup> 0.162	<sup>165</sup> 1.000				0.004	0.002	0.878			
40	COGNITEC-004	<sup>86</sup> 0.003	<sup>80</sup> 0.016	<sup>138</sup> 0.813	<sup>98</sup> 0.013	<sup>36</sup> 0.057	<sup>90</sup> 0.143	<sup>82</sup> 0.031	<sup>91</sup> 0.097	<sup>86</sup> 0.990	<sup>88</sup> 0.068	<sup>50</sup> 0.316	<sup>36</sup> 0.288	0.002	0.001	0.635			0.006
41	COGNITEC-005	<sup>31</sup> 0.002	<sup>27</sup> 0.010	<sup>108</sup> 0.713	<sup>113</sup> 0.021	<sup>31</sup> 0.037	<sup>67</sup> 0.115	<sup>27</sup> 0.010	<sup>31</sup> 0.041	<sup>228</sup> 1.000	<sup>63</sup> 0.041	<sup>29</sup> 0.157	<sup>31</sup> 0.179	0.002	0.001	0.614			0.017
42	CUBOX-000	<sup>16</sup> 0.001	<sup>25</sup> 0.010	<sup>6</sup> 0.058	<sup>6</sup> 0.002	<sup>2</sup> 0.004	<sup>1</sup> 0.049	<sup>11</sup> 0.003	<sup>12</sup> 0.019	<sup>2</sup> 0.168	<sup>2</sup> 0.004	<sup>2</sup> 0.028	<sup>1</sup> 0.073	0.001	0.000	0.042			0.000
43	CYBERLINK-000	<sup>91</sup> 0.004	<sup>104</sup> 0.020	<sup>108</sup> 0.717	<sup>80</sup> 0.007		<sup>83</sup> 0.134	<sup>121</sup> 0.056	<sup>108</sup> 0.116	<sup>110</sup> 0.995	<sup>86</sup> 0.063		<sup>69</sup> 0.339	0.001	0.001	0.063			
44	CYBERLINK-001	<sup>91</sup> 0.004	<sup>93</sup> 0.018	<sup>110</sup> 0.731	<sup>75</sup> 0.007		<sup>82</sup> 0.133	<sup>116</sup> 0.054	<sup>105</sup> 0.109	<sup>106</sup> 0.995	<sup>83</sup> 0.062		<sup>106</sup> 0.65						

#	ALGORITHM	INVESTIGATION MODE						IDENTIFICATION MODE						FAILURE TO EXTRACT					
		RANK ONE MISS RATE, FNIR(N, 0, 1)						HIGH T → FPIR = 0.001, FNIR(N, T, L)						FEATURES					
		N=1.6M						N=1.6M											
GALLERY	MUGSHOT	MUGSHOT	MUGSHOT	VISA	BORDER	VISA	MUGSHOT	MUGSHOT	MUGSHOT	VISA	BORDER	VISA	MUGSHOT	MUGSHOT	MUGSHOT	VISA	BORDER	KIOSK	
PROBE	MUGSHOT	WEBCAM	PROFILE	BORDER	BOR <sub>L</sub> 10YR	KIOSK	MUGSHOT	WEBCAM	PROFILE	BORDER	BOR <sub>L</sub> 10YR	KIOSK	MUGSHOT	WEBCAM	PROFILE	BORDER	BOR <sub>L</sub> 10YR	KIOSK	
47	CYBERLINK-004	<sup>35</sup> 0.002	<sup>44</sup> 0.011	<sup>65</sup> 0.423	<sup>27</sup> 0.003	<sup>16</sup> 0.011	<sup>51</sup> 0.104	<sup>25</sup> 0.007	<sup>29</sup> 0.036	<sup>188</sup> 1.000	<sup>21</sup> 0.013	<sup>19</sup> 0.109	<sup>137</sup> 0.954	0.000	0.000	0.011		0.000	
48	DAHUA-000	<sup>149</sup> 0.009	<sup>134</sup> 0.026					<sup>145</sup> 0.086	<sup>124</sup> 0.135					0.004	0.003				
49	DAHUA-001	<sup>127</sup> 0.007	<sup>126</sup> 0.024	<sup>107</sup> 0.703				<sup>158</sup> 0.073	<sup>116</sup> 0.122	<sup>71</sup> 0.980				0.002	0.002	0.346			
50	DAHUA-002	<sup>42</sup> 0.002	<sup>44</sup> 0.012	<sup>47</sup> 0.304	<sup>24</sup> 0.003		<sup>29</sup> 0.084	<sup>44</sup> 0.015	<sup>36</sup> 0.046	<sup>25</sup> 0.638	<sup>28</sup> 0.017		<sup>24</sup> 0.159	0.001	0.000	0.099			
51	DAHUA-003	<sup>10</sup> 0.001	<sup>7</sup> 0.007	<sup>33</sup> 0.206	<sup>9</sup> 0.002	<sup>12</sup> 0.009	<sup>11</sup> 0.073	<sup>46</sup> 0.014	<sup>31</sup> 0.041	<sup>21</sup> 0.579	<sup>23</sup> 0.013	<sup>14</sup> 0.081	<sup>17</sup> 0.134	0.000	0.000	0.000		0.000	
52	DEEPLINT-001	<sup>19</sup> 0.001	<sup>6</sup> 0.007	<sup>32</sup> 0.200	<sup>29</sup> 0.002		<sup>13</sup> 0.073	<sup>12</sup> 0.003	<sup>7</sup> 0.014	<sup>150</sup> 1.000	<sup>8</sup> 0.006		<sup>23</sup> 0.159	0.000	0.000	0.038			
53	DEESEA-001	<sup>102</sup> 0.004	<sup>78</sup> 0.016	<sup>136</sup> 0.814	<sup>87</sup> 0.010		<sup>89</sup> 0.140	<sup>103</sup> 0.046	<sup>98</sup> 0.101	<sup>78</sup> 0.985	<sup>92</sup> 0.077		<sup>89</sup> 0.326	0.000	0.001	0.047			
54	DERMALOG-003	<sup>283</sup> 0.126	<sup>217</sup> 0.217		<sup>152</sup> 0.296		<sup>156</sup> 0.560	<sup>221</sup> 0.482	<sup>217</sup> 0.655		<sup>152</sup> 0.677		<sup>125</sup> 0.870	0.002	0.002	0.103			
55	DERMALOG-004	<sup>223</sup> 0.125	<sup>216</sup> 0.215	<sup>158</sup> 0.930	<sup>146</sup> 0.135		<sup>157</sup> 0.467	<sup>220</sup> 0.480	<sup>218</sup> 0.657	<sup>111</sup> 0.995	<sup>148</sup> 0.603		<sup>124</sup> 0.856	0.001	0.002	0.107			
56	DERMALOG-005	<sup>174</sup> 0.015	<sup>153</sup> 0.037	<sup>106</sup> 0.701	<sup>151</sup> 0.242		<sup>147</sup> 0.384	<sup>151</sup> 0.088	<sup>137</sup> 0.154	<sup>88</sup> 0.990	<sup>131</sup> 0.300		<sup>104</sup> 0.614	0.001	0.002	0.102			
57	DERMALOG-006	<sup>140</sup> 0.008	<sup>130</sup> 0.024	<sup>97</sup> 0.619	<sup>88</sup> 0.010		<sup>98</sup> 0.155	<sup>110</sup> 0.052	<sup>101</sup> 0.105	<sup>72</sup> 0.981	<sup>81</sup> 0.059		<sup>66</sup> 0.318	0.003	0.006	0.181			
58	DERMALOG-007	<sup>148</sup> 0.009	<sup>135</sup> 0.027	<sup>101</sup> 0.675	<sup>102</sup> 0.014		<sup>102</sup> 0.170	<sup>144</sup> 0.086	<sup>135</sup> 0.152	<sup>87</sup> 0.990	<sup>98</sup> 0.099		<sup>100</sup> 0.557	0.001	0.002	0.102			
59	DERMALOG-008	<sup>80</sup> 0.003	<sup>71</sup> 0.015	<sup>76</sup> 0.516	<sup>71</sup> 0.007	<sup>48</sup> 0.029	<sup>89</sup> 0.139	<sup>101</sup> 0.045	<sup>87</sup> 0.094	<sup>175</sup> 1.000	<sup>78</sup> 0.057	<sup>51</sup> 0.382	<sup>135</sup> 0.940	0.000	0.000	0.002		0.000	
60	EYDEEA-003	<sup>218</sup> 0.080	<sup>210</sup> 0.148	<sup>176</sup> 0.960	<sup>143</sup> 0.101		<sup>147</sup> 0.379	<sup>211</sup> 0.388	<sup>210</sup> 0.543	<sup>109</sup> 0.994	<sup>146</sup> 0.570		<sup>117</sup> 0.792	0.001	0.003	0.161			
61	F8-001	<sup>167</sup> 0.012		<sup>100</sup> 0.669	<sup>212</sup> 1.000		<sup>189</sup> 1.000	<sup>183</sup> 0.166		<sup>129</sup> 0.998				0.004	1.000	0.158			
62	FINCORE-000	<sup>158</sup> 0.011	<sup>148</sup> 0.034	<sup>122</sup> 0.767	<sup>123</sup> 0.032	<sup>60</sup> 0.117	<sup>111</sup> 0.191	<sup>173</sup> 0.134	<sup>158</sup> 0.217	<sup>160</sup> 1.000	<sup>120</sup> 0.187	<sup>59</sup> 0.598	<sup>85</sup> 0.458	0.000	0.001	0.043		0.000	
63	FUJITSULAB-000	<sup>58</sup> 0.002	<sup>62</sup> 0.014	<sup>66</sup> 0.440	<sup>47</sup> 0.004	<sup>35</sup> 0.023	<sup>42</sup> 0.098	<sup>59</sup> 0.021	<sup>50</sup> 0.056		<sup>40</sup> 0.024	<sup>34</sup> 0.177	<sup>46</sup> 0.240	0.000	0.001	0.016		0.000	
64	GLORY-000	<sup>228</sup> 0.178	<sup>223</sup> 0.320	<sup>200</sup> 0.994	<sup>150</sup> 0.228		<sup>152</sup> 0.678	<sup>210</sup> 0.367	<sup>211</sup> 0.547	<sup>105</sup> 0.995	<sup>142</sup> 0.453		<sup>123</sup> 0.839	0.011	0.013	0.985			
65	GLORY-001	<sup>225</sup> 0.127	<sup>220</sup> 0.267	<sup>195</sup> 0.992	<sup>147</sup> 0.178		<sup>151</sup> 0.594	<sup>203</sup> 0.305	<sup>209</sup> 0.537	<sup>94</sup> 0.993	<sup>137</sup> 0.408		<sup>121</sup> 0.819	0.011	0.013	0.988			
66	GORILLA-001	<sup>211</sup> 0.060	<sup>203</sup> 0.095	<sup>162</sup> 0.936	<sup>138</sup> 0.069		<sup>143</sup> 0.329	<sup>216</sup> 0.406	<sup>205</sup> 0.453	<sup>171</sup> 1.000	<sup>143</sup> 0.468		<sup>217</sup> 1.000	0.001	0.001	0.069			
67	GORILLA-002	<sup>186</sup> 0.020	<sup>169</sup> 0.040	<sup>118</sup> 0.753	<sup>117</sup> 0.027		<sup>123</sup> 0.214	<sup>190</sup> 0.188	<sup>179</sup> 0.268	<sup>171</sup> 1.000	<sup>127</sup> 0.250		<sup>153</sup> 1.000	0.001	0.001	0.069			
68	GORILLA-003	<sup>199</sup> 0.036	<sup>191</sup> 0.077	<sup>137</sup> 0.821	<sup>132</sup> 0.048		<sup>132</sup> 0.265	<sup>204</sup> 0.318	<sup>200</sup> 0.434	<sup>239</sup> 1.000	<sup>136</sup> 0.407		<sup>189</sup> 1.000	0.001	0.001	0.069			
69	GORILLA-004	<sup>124</sup> 0.006	<sup>127</sup> 0.024	<sup>105</sup> 0.697	<sup>91</sup> 0.012		<sup>102</sup> 0.162	<sup>154</sup> 0.089	<sup>145</sup> 0.160	<sup>52</sup> 0.959	<sup>108</sup> 0.135		<sup>81</sup> 0.438	0.000	0.001	0.042			
70	GORILLA-005	<sup>85</sup> 0.003	<sup>94</sup> 0.018	<sup>34</sup> 0.209	<sup>67</sup> 0.006		<sup>71</sup> 0.124	<sup>125</sup> 0.058	<sup>129</sup> 0.142	<sup>29</sup> 0.700	<sup>96</sup> 0.088		<sup>64</sup> 0.315	0.000	0.000	0.040			
71	GORILLA-006	<sup>37</sup> 0.002	<sup>47</sup> 0.012	<sup>20</sup> 0.122	<sup>34</sup> 0.003	<sup>29</sup> 0.018	<sup>51</sup> 0.105	<sup>74</sup> 0.027	<sup>81</sup> 0.089	<sup>20</sup> 0.531	<sup>44</sup> 0.028	<sup>33</sup> 0.166	<sup>40</sup> 0.218	0.000	0.000	0.041		0.000	
72	HIK-003	<sup>184</sup> 0.012	<sup>138</sup> 0.027	<sup>104</sup> 0.689	<sup>94</sup> 0.012		<sup>92</sup> 0.151	<sup>159</sup> 0.103	<sup>139</sup> 0.158	<sup>56</sup> 0.969	<sup>111</sup> 0.142		<sup>83</sup> 0.445	0.000	0.000	0.048			
73	HIK-004	<sup>161</sup> 0.011	<sup>136</sup> 0.027	<sup>113</sup> 0.743	<sup>92</sup> 0.012		<sup>92</sup> 0.152	<sup>157</sup> 0.099	<sup>136</sup> 0.153	<sup>63</sup> 0.976	<sup>109</sup> 0.137		<sup>80</sup> 0.434	0.000	0.000	0.048			
74	HIK-005	<sup>106</sup> 0.005	<sup>83</sup> 0.017	<sup>82</sup> 0.535	<sup>77</sup> 0.007		<sup>62</sup> 0.111	<sup>96</sup> 0.044	<sup>70</sup> 0.077	<sup>148</sup> 0.999	<sup>87</sup> 0.068		<sup>97</sup> 0.541	0.000	0.000	0.000			
75	HIK-006	<sup>107</sup> 0.005	<sup>82</sup> 0.017	<sup>83</sup> 0.535			<sup>108</sup> 0.047	<sup>108</sup> 0.047	<sup>78</sup> 0.086	<sup>183</sup> 1.000				0.000	0.000	0.000			
76	HYPERVERGE-001	<sup>14</sup> 0.001	<sup>36</sup> 0.011	<sup>8</sup> 0.067	<sup>5</sup> 0.002	<sup>5</sup> 0.007	<sup>4</sup> 0.061	<sup>16</sup> 0.004	<sup>25</sup> 0.031	<sup>5</sup> 0.220	<sup>11</sup> 0.007	<sup>9</sup> 0.053	<sup>7</sup> 0.101	0.001	0.000	0.041		0.000	
77	IDEMIA-003	<sup>130</sup> 0.007	<sup>146</sup> 0.034	<sup>171</sup> 0.958	<sup>108</sup> 0.018		<sup>127</sup> 0.210	<sup>108</sup> 0.047	<sup>145</sup> 0.165		<sup>105</sup> 0.123		<sup>115</sup> 0.766	0.000	0.000	0.041			
78	IDEMIA-004	<sup>126</sup> 0.007	<sup>144</sup> 0.032	<sup>166</sup> 0.947	<sup>109</sup> 0.018		<sup>119</sup> 0.210	<sup>92</sup> 0.037	<sup>112</sup> 0.118	<sup>62</sup> 0.973	<sup>104</sup> 0.123		<sup>114</sup> 0.766	0.000	0.000	0.041			
79	IDEMIA-005	<sup>139</sup> 0.008	<sup>161</sup> 0.039	<sup>189</sup> 0.954	<sup>114</sup> 0.021		<sup>124</sup> 0.217	<sup>98</sup> 0.044	<sup>134</sup> 0.150	<sup>66</sup> 0.978	<sup>106</sup> 0.130		<sup>126</sup> 0.879	0.000	0.000	0.041			
80	IDEMIA-006	<sup>152</sup> 0.010	<sup>193</sup> 0.072	<sup>184</sup> 0.969	<sup>119</sup> 0.030		<sup>131</sup> 0.253	<sup>95</sup> 0.043	<sup>163</sup> 0.226	<sup>74</sup> 0.982	<sup>112</sup> 0.144		<sup>110</sup> 0.733	0.000	0.000	0.041			
81	IDEMIA-007	<sup>72</sup> 0.003	<sup>75</sup> 0.015	<sup>244</sup> 1.000	<sup>68</sup> 0.006	<sup>50</sup> 0.036	<sup>79</sup> 0.131	<sup>52</sup> 0.018	<sup>48</sup> 0.055	<sup>193</sup> 1.000	<sup>74</sup> 0.052	<sup>36</sup> 0.182	<sup>218</sup> 1.000	0.000	0.000	0.040		0.000	
82	IDEMIA-008	<sup>6</sup> 0.001	<sup>3</sup> 0.007	<sup>12</sup> 0.079	<sup>4</sup> 0.001	<sup>7</sup> 0.007	<sup>15</sup> 0.075	<sup>5</sup> 0.002	<sup>5</sup> 0.013	<sup>4</sup> 0.204	<sup>4</sup> 0.005	<sup>5</sup> 0.036	<sup>9</sup> 0.106	0.000	0.000	0.040		0.000	
83	IMAGUS-002	<sup>231</sup> 0.220	<sup>221</sup> 0.301	<sup>194</sup> 0.988				<sup>224</sup> 0.749	<sup>222</sup> 0.816	<sup>184</sup> 1.000				0.004	0.008	0.550			
84	IMAGUS-003	<sup>236</sup> 0.356	<sup>222</sup> 0.513	<sup>198</sup> 0.993				<sup>238</sup> 0.807	<sup>223</sup> 0.909	<sup>167</sup> 1.000				0.004	0.008	0.550			
85	IMAGUS-005	<sup>48</sup> 0.002	<sup>46</sup> 0.012	<sup>49</sup> 0.319	<sup>66</sup> 0.006	<sup>34</sup> 0.022	<sup>81</sup> 0.132	<sup>55</sup> 0.018	<sup>58</sup> 0.066	<sup>39</sup> 0.838	<sup>46</sup> 0.029	<sup>32</sup> 0.161	<sup>43</sup> 0.231	0.000	0.000	0.000		0.000	
86	IMAGUS-006	<sup>82</sup> 0.002	<sup>59</sup> 0.014	<sup>46</sup> 0.293	<sup>40</sup> 0.004	<sup>33</sup> 0.019	<sup>63</sup> 0.112	<sup>57</sup> 0.019	<sup>61</sup> 0.069	<sup>46</sup> 0.897	<sup>45</sup> 0.028	<sup>31</sup> 0.161	<sup>81</sup> 0.260	0.000	0.000	0.000		0.000	
87	IMPERIAL-000	<sup>70</sup> 0.002	<sup>72</sup> 0.015	<sup>45</sup> 0.280	<sup>53</sup> 0.004		<sup>41</sup> 0.097	<sup>69</sup> 0.026	<sup>60</sup> 0.068	<sup>133</sup> 0.999	<sup>64</sup> 0.042		<sup>48</sup> 0.245	0.000	0.000	0.000			
88	INCODE-000	<sup>208</sup> 0.049	<sup>208</sup> 0.100	<sup>168</sup> 0.951				<sup>203</sup> 0.310	<sup>198</sup> 0.420	<sup>128</sup> 0.998				0.001	0.004	0.173			
89	INCODE-001	<sup>177</sup> 0.017	<sup>174</sup> 0.046	<sup>119</sup> 0.762				<sup>193</sup> 0.212	<sup>182</sup> 0.296	<sup>179</sup> 1.000				0.001	0.004	0.173			
90	INCODE-002	<sup>181</sup> 0.018	<sup>176</sup> 0.048	<sup>140</sup> 0.843				<sup>189</sup> 0.184	<sup>180</sup> 0.269	<sup>95</sup> 0.993				0.000	0.001	0.066			
91	INCODE-003	<sup>169</sup> 0.013	<sup>163</sup> 0.040	<sup>120</sup> 0.764				<sup>185</sup> 0.167	<sup>176</sup> 0.264	<sup>146</sup> 0.999				0.000	0.0				

#	ALGORITHM	INVESTIGATION MODE						IDENTIFICATION MODE						FAILURE TO EXTRACT					
		RANK ONE MISS RATE, FNIR(N, 0, 1)						HIGH T → FPIR = 0.001, FNIR(N, T, L)						FEATURES					
		N=1.6M						N=1.6M											
GALLERY	MUGSHOT	MUGSHOT	MUGSHOT	VISA	BORDER	VISA	MUGSHOT	MUGSHOT	MUGSHOT	VISA	BORDER	VISA	MUGSHOT	MUGSHOT	MUGSHOT	VISA	BORDER	KIOSK	
PROBE	MUGSHOT	WEBCAM	PROFILE	BORDER	BOR <sub>L</sub> 10YR	KIOSK	MUGSHOT	WEBCAM	PROFILE	BORDER	BOR <sub>L</sub> 10YR	KIOSK	MUGSHOT	WEBCAM	PROFILE	BORDER	BOR <sub>L</sub> 10YR	KIOSK	
93	INC005-005	<sup>36</sup> 0.002	<sup>40</sup> 0.011	<sup>46</sup> 0.147	<sup>19</sup> 0.002	<sup>22</sup> 0.013	<sup>22</sup> 0.079	<sup>31</sup> 0.011	<sup>48</sup> 0.043	<sup>18</sup> 0.528	<sup>30</sup> 0.017	<sup>25</sup> 0.145	<sup>21</sup> 0.155	0.000	0.000	0.042	0.000		
94	INNOVATRICS-002	<sup>205</sup> 0.045	<sup>194</sup> 0.074	<sup>14</sup> 0.853				<sup>198</sup> 0.234	<sup>18</sup> 0.310	<sup>185</sup> 1.000				0.000	0.001	0.046			
95	INNOVATRICS-003	<sup>193</sup> 0.026	<sup>179</sup> 0.055	<sup>14</sup> 0.845				<sup>194</sup> 0.221	<sup>183</sup> 0.297	<sup>156</sup> 1.000				0.000	0.001	0.046			
96	INNOVATRICS-004	<sup>168</sup> 0.012	<sup>165</sup> 0.040	<sup>172</sup> 0.958				<sup>172</sup> 0.132	<sup>162</sup> 0.222	<sup>70</sup> 0.980				0.000	0.001	0.046			
97	INNOVATRICS-005	<sup>71</sup> 0.002	<sup>67</sup> 0.014	<sup>64</sup> 0.407	<sup>55</sup> 0.005		<sup>59</sup> 0.109	<sup>85</sup> 0.034	<sup>46</sup> 0.089	<sup>40</sup> 0.846	<sup>70</sup> 0.047		<sup>40</sup> 0.251	0.000	0.001	0.041			
98	INNOVATRICS-007	<sup>38</sup> 0.002	<sup>39</sup> 0.011	<sup>41</sup> 0.248	<sup>22</sup> 0.002	<sup>24</sup> 0.013	<sup>17</sup> 0.077	<sup>36</sup> 0.133	<sup>41</sup> 0.051	<sup>29</sup> 0.743	<sup>29</sup> 0.017	<sup>17</sup> 0.093	<sup>20</sup> 0.154	0.000	0.001	0.041		0.000	
99	INTSYSMSU-000	<sup>220</sup> 0.146	<sup>125</sup> 0.023	<sup>90</sup> 0.562	<sup>139</sup> 0.072		<sup>80</sup> 0.132	<sup>240</sup> 0.998	<sup>235</sup> 1.000	<sup>154</sup> 1.000	<sup>161</sup> 0.999		<sup>151</sup> 0.999	0.000	0.000	0.050			
100	IREX-000	<sup>105</sup> 0.004	<sup>18</sup> 0.010	<sup>100</sup> 0.681	<sup>18</sup> 0.002	<sup>19</sup> 0.012	<sup>25</sup> 0.082	<sup>78</sup> 0.028	<sup>54</sup> 0.060	<sup>51</sup> 0.957	<sup>69</sup> 0.044	<sup>48</sup> 0.302	<sup>29</sup> 0.170	0.000	0.000	0.042		0.000	
101	ISYSTEMS-002	<sup>125</sup> 0.006	<sup>133</sup> 0.026	<sup>14</sup> 0.844				<sup>142</sup> 0.078	<sup>116</sup> 0.126	<sup>118</sup> 0.998				0.002	0.002	0.142			
102	ISYSTEMS-003	<sup>113</sup> 0.005	<sup>122</sup> 0.023	<sup>125</sup> 0.791				<sup>126</sup> 0.059	<sup>104</sup> 0.107	<sup>157</sup> 1.000				0.002	0.002	0.142			
103	KAKAO-000	<sup>20</sup> 0.001	<sup>31</sup> 0.011	<sup>19</sup> 0.119	<sup>21</sup> 0.002	<sup>21</sup> 0.013	<sup>19</sup> 0.078	<sup>46</sup> 0.015	<sup>48</sup> 0.056	<sup>14</sup> 0.468	<sup>33</sup> 0.019	<sup>23</sup> 0.141	<sup>22</sup> 0.158	0.000	0.000	0.041		0.000	
104	KEDACOM-001	<sup>135</sup> 0.008	<sup>150</sup> 0.036	<sup>18</sup> 0.972	<sup>125</sup> 0.034		<sup>125</sup> 0.237	<sup>65</sup> 0.023	<sup>68</sup> 0.072	<sup>81</sup> 0.986	<sup>77</sup> 0.055		<sup>60</sup> 0.305	0.000	0.000	0.000			
105	KNERON-000	<sup>120</sup> 0.006	<sup>137</sup> 0.027	<sup>88</sup> 0.552	<sup>118</sup> 0.028		<sup>114</sup> 0.195							0.000	0.000	0.000			
106	KNERON-001	<sup>196</sup> 0.030	<sup>235</sup> 0.621	<sup>40</sup> 0.237	<sup>148</sup> 0.144	<sup>61</sup> 0.207	<sup>136</sup> 0.280							0.000	0.000	0.000		0.000	
107	LINE-000	<sup>58</sup> 0.002	<sup>60</sup> 0.014	<sup>38</sup> 0.223	<sup>59</sup> 0.005	<sup>46</sup> 0.029	<sup>55</sup> 0.107	<sup>81</sup> 0.031	<sup>91</sup> 0.095		<sup>68</sup> 0.046	<sup>47</sup> 0.278	<sup>106</sup> 1.000	0.000	0.000	0.000		0.000	
108	LOOKMAN-003	<sup>141</sup> 0.009	<sup>159</sup> 0.038		<sup>128</sup> 0.035		<sup>12</sup> 0.239	<sup>97</sup> 0.044	<sup>107</sup> 0.112		<sup>95</sup> 0.084		<sup>70</sup> 0.355	0.000	0.000	0.000			
109	LOOKMAN-004	<sup>146</sup> 0.009	<sup>162</sup> 0.039	<sup>188</sup> 0.973				<sup>100</sup> 0.045	<sup>103</sup> 0.105	<sup>64</sup> 0.977				0.000	0.000	0.000			
110	LOOKMAN-005	<sup>138</sup> 0.008	<sup>152</sup> 0.036	<sup>18</sup> 0.972	<sup>122</sup> 0.035		<sup>128</sup> 0.237	<sup>80</sup> 0.030	<sup>87</sup> 0.086	<sup>67</sup> 0.978	<sup>84</sup> 0.062		<sup>61</sup> 0.308	0.000	0.000	0.000			
111	MEGVII-001	<sup>163</sup> 0.012	<sup>90</sup> 0.017		<sup>186</sup> 1.000			<sup>137</sup> 0.072	<sup>96</sup> 0.097					0.002	0.000				
112	MEGVII-002	<sup>168</sup> 0.012	<sup>92</sup> 0.017	<sup>67</sup> 0.450	<sup>236</sup> 1.000			<sup>141</sup> 0.077	<sup>93</sup> 0.096	<sup>128</sup> 0.998				0.002	0.000	0.033			
113	MICROFOCUS-003	<sup>243</sup> 0.594	<sup>239</sup> 0.781		<sup>164</sup> 0.708		<sup>166</sup> 0.907	<sup>236</sup> 0.931	<sup>234</sup> 0.979		<sup>160</sup> 0.982		<sup>146</sup> 0.991	0.001	0.005				
114	MICROFOCUS-004	<sup>241</sup> 0.576	<sup>238</sup> 0.758		<sup>163</sup> 0.701		<sup>165</sup> 0.904	<sup>241</sup> 0.999	<sup>232</sup> 0.975		<sup>159</sup> 0.974		<sup>144</sup> 0.989	0.001	0.005				
115	MICROFOCUS-005	<sup>237</sup> 0.424	<sup>233</sup> 0.601		<sup>159</sup> 0.494		<sup>160</sup> 0.777	<sup>234</sup> 0.835	<sup>228</sup> 0.928		<sup>157</sup> 0.935		<sup>143</sup> 0.985	0.001	0.005				
116	MICROFOCUS-006	<sup>238</sup> 0.427	<sup>232</sup> 0.583		<sup>158</sup> 0.490		<sup>163</sup> 0.782	<sup>228</sup> 0.978	<sup>227</sup> 0.923		<sup>156</sup> 0.923		<sup>140</sup> 0.971	0.001	0.005				
117	MICROSOFT-003	<sup>48</sup> 0.002	<sup>50</sup> 0.012		<sup>44</sup> 0.004		<sup>60</sup> 0.109	<sup>76</sup> 0.028	<sup>88</sup> 0.091		<sup>88</sup> 0.036		<sup>45</sup> 0.233	0.000	0.001				
118	MICROSOFT-004	<sup>24</sup> 0.001	<sup>49</sup> 0.012		<sup>37</sup> 0.004		<sup>61</sup> 0.109	<sup>70</sup> 0.026	<sup>74</sup> 0.087		<sup>54</sup> 0.033		<sup>41</sup> 0.222	0.000	0.001				
119	MICROSOFT-005	<sup>45</sup> 0.002	<sup>35</sup> 0.011	<sup>25</sup> 0.144	<sup>31</sup> 0.003		<sup>43</sup> 0.099	<sup>68</sup> 0.070	<sup>63</sup> 0.070	<sup>22</sup> 0.587	<sup>42</sup> 0.027		<sup>32</sup> 0.180	0.000	0.001	0.049			
120	MICROSOFT-006	<sup>50</sup> 0.002	<sup>43</sup> 0.011	<sup>28</sup> 0.150	<sup>41</sup> 0.004		<sup>45</sup> 0.100	<sup>32</sup> 0.012	<sup>28</sup> 0.037	<sup>9</sup> 0.386	<sup>51</sup> 0.032		<sup>30</sup> 0.178	0.000	0.001	0.049			
121	NEC-000	<sup>174</sup> 0.017	<sup>167</sup> 0.041	<sup>175</sup> 0.959	<sup>115</sup> 0.025		<sup>129</sup> 0.243	<sup>144</sup> 0.079	<sup>138</sup> 0.140	<sup>68</sup> 0.979			<sup>88</sup> 0.474	0.001	0.002	0.890			
122	NEC-001	<sup>187</sup> 0.021	<sup>180</sup> 0.056	<sup>185</sup> 0.967	<sup>124</sup> 0.033		<sup>133</sup> 0.277	<sup>161</sup> 0.106	<sup>195</sup> 0.197	<sup>80</sup> 0.986	<sup>107</sup> 0.133		<sup>87</sup> 0.468	0.005	0.003	0.934			
123	NEC-002	<sup>3</sup> 0.001	<sup>15</sup> 0.009	<sup>38</sup> 0.363	<sup>36</sup> 0.003		<sup>68</sup> 0.117	<sup>10</sup> 0.003	<sup>13</sup> 0.020	<sup>144</sup> 0.999	<sup>15</sup> 0.008		<sup>108</sup> 0.676	0.000	0.001	0.041			
124	NEC-003	<sup>13</sup> 0.001	<sup>23</sup> 0.010	<sup>37</sup> 0.352	<sup>40</sup> 0.004	<sup>20</sup> 0.013	<sup>72</sup> 0.120	<sup>8</sup> 0.002	<sup>11</sup> 0.017	<sup>36</sup> 0.824	<sup>16</sup> 0.008	<sup>6</sup> 0.036	<sup>107</sup> 0.668	0.000	0.001	0.041		0.001	
125	NEC-004	<sup>7</sup> 0.001	<sup>14</sup> 0.009	<sup>84</sup> 0.538	<sup>30</sup> 0.003	<sup>9</sup> 0.007	<sup>14</sup> 0.075	<sup>3</sup> 0.002	<sup>4</sup> 0.013	<sup>24</sup> 0.622	<sup>3</sup> 0.004	<sup>6</sup> 0.019	<sup>6</sup> 0.100	0.000	0.001	0.041		0.001	
126	NEUROTECHNOLOGY-003	<sup>188</sup> 0.022	<sup>168</sup> 0.042	<sup>177</sup> 0.961				<sup>227</sup> 0.636	<sup>178</sup> 0.266	<sup>189</sup> 1.000				0.000	0.001	0.131			
127	NEUROTECHNOLOGY-004	<sup>115</sup> 0.006	<sup>103</sup> 0.020	<sup>183</sup> 0.970				<sup>131</sup> 0.063	<sup>109</sup> 0.117	<sup>100</sup> 0.994				0.000	0.001	0.131			
128	NEUROTECHNOLOGY-005	<sup>101</sup> 0.004	<sup>129</sup> 0.024	<sup>147</sup> 0.893				<sup>119</sup> 0.054	<sup>141</sup> 0.130	<sup>122</sup> 0.998				0.000	0.000	0.030			
129	NEUROTECHNOLOGY-006	<sup>182</sup> 0.018	<sup>171</sup> 0.045	<sup>56</sup> 0.606				<sup>199</sup> 0.249	<sup>197</sup> 0.418					0.000	0.000				
130	NEUROTECHNOLOGY-007	<sup>98</sup> 0.004	<sup>109</sup> 0.021	<sup>128</sup> 0.796	<sup>86</sup> 0.009		<sup>110</sup> 0.180	<sup>130</sup> 0.062	<sup>149</sup> 0.173	<sup>162</sup> 1.000	<sup>132</sup> 0.339		<sup>154</sup> 1.000	0.001	0.001	0.041			
131	NEUROTECHNOLOGY-008	<sup>57</sup> 0.002	<sup>66</sup> 0.014	<sup>68</sup> 0.457	<sup>46</sup> 0.004	<sup>37</sup> 0.023	<sup>47</sup> 0.101	<sup>114</sup> 0.053	<sup>73</sup> 0.080	<sup>168</sup> 1.000	<sup>57</sup> 0.035	<sup>48</sup> 0.293	<sup>37</sup> 0.203	0.000	0.001	0.052		0.001	
132	NEUROTECHNOLOGY-009	<sup>48</sup> 0.001	<sup>33</sup> 0.011	<sup>41</sup> 0.179	<sup>14</sup> 0.002	<sup>23</sup> 0.013	<sup>21</sup> 0.079	<sup>47</sup> 0.015	<sup>44</sup> 0.052	<sup>23</sup> 0.588	<sup>34</sup> 0.020	<sup>28</sup> 0.153	<sup>26</sup> 0.165	0.001	0.000	0.046		0.000	
133	NEWLAND-002	<sup>217</sup> 0.079	<sup>207</sup> 0.117	<sup>161</sup> 0.936				<sup>218</sup> 0.438	<sup>204</sup> 0.466	<sup>137</sup> 0.999				0.007	0.012	0.200			
134	NOBLIS-001	<sup>231</sup> 0.249	<sup>228</sup> 0.522	<sup>197</sup> 0.993				<sup>243</sup> 1.000	<sup>239</sup> 1.000	<sup>178</sup> 1.000				0.000	0.000	0.000			
135	NOBLIS-002	<sup>229</sup> 0.179	<sup>225</sup> 0.392	<sup>191</sup> 0.982				<sup>239</sup> 0.997	<sup>241</sup> 1.000	<sup>170</sup> 1.000				0.000	0.000	0.000			
136	NTECHLAB-003	<sup>121</sup> 0.006	<sup>119</sup> 0.023	<sup>74</sup> 0.504				<sup>117</sup> 0.054	<sup>110</sup> 0.118	<sup>38</sup> 0.837				0.000	0.000	0.040			
137	NTECHLAB-004	<sup>111</sup> 0.005	<sup>99</sup> 0.019	<sup>71</sup> 0.506	<sup>82</sup> 0.008		<sup>76</sup> 0.129	<sup>93</sup> 0.041	<sup>102</sup> 0.105	<sup>37</sup> 0.833	<sup>76</sup> 0.053		<sup>55</sup> 0.263	0.000	0.000	0.040			
138	NTECHLAB-005	<sup>108</sup> 0.005	<sup>95</sup> 0.018	<sup>59</sup> 0.367	<sup>84</sup> 0.008		<sup>69</sup> 0.118	<sup>94</sup> 0.042	<sup>100</sup> 0.102	<sup>32</sup> 0.771	<sup>90</sup> 0.073		<sup>58</sup> 0.294	0.000	0.000	0.040			

Table 11: Miss rates by dataset: At left, rank 1 miss rates relevant to investigations; at right, with threshold set to target FPIR = 0.01 for higher volume, low prior, uses. Yellow indicates most accurate algorithm. Throughout blue superscripts indicate the rank of the algorithm for that column.

2021/10/28 FNIR(N, R, T) = False neg. identification rate N = Num. enrolled subjects T = Threshold  
 13:44:33 FPIR(N, T) = False pos. identification rate R = Num. candidates examined T > 0 → Investigation  
 T > 0 → Identification

#	ALGORITHM	INVESTIGATION MODE										IDENTIFICATION MODE					FAILURE TO EXTRACT				
		RANK ONE MISS RATE, FNIR(N, 0, 1)										HIGH T → FPIR = 0.001, FNIR(N, T, L)					FEATURES				
		N=1.6M										N=1.6M									
		GALLERY	MUGSHOT	MUGSHOT	MUGSHOT	VISA	BORDER	VISA	MUGSHOT	MUGSHOT	MUGSHOT	VISA	BORDER	VISA	MUGSHOT	MUGSHOT	MUGSHOT	VISA	BORDER	KIOSK	
PROBE	MUGSHOT	WEBCAM	PROFILE	BORDER	BOR <sub>2</sub> 10YR	KIOSK	MUGSHOT	WEBCAM	PROFILE	BORDER	BOR <sub>2</sub> 10YR	KIOSK	MUGSHOT	WEBCAM	PROFILE	BORDER	BOR <sub>2</sub> 10YR	KIOSK			
139	NTECHLAB-006	<sup>181</sup> 0.004	<sup>87</sup> 0.017	<sup>36</sup> 0.347	<sup>74</sup> 0.007	<sup>66</sup> 0.113	<sup>88</sup> 0.037	<sup>88</sup> 0.094	<sup>31</sup> 0.754	<sup>79</sup> 0.057		<sup>82</sup> 0.260	0.000	0.000	0.040						
140	NTECHLAB-007	<sup>74</sup> 0.003	<sup>51</sup> 0.012	<sup>30</sup> 0.326	<sup>52</sup> 0.004	<sup>56</sup> 0.107	<sup>67</sup> 0.026	<sup>59</sup> 0.067	<sup>30</sup> 0.750	<sup>52</sup> 0.032		<sup>42</sup> 0.223	0.000	0.000	0.042						
141	NTECHLAB-008	<sup>26</sup> 0.002	<sup>19</sup> 0.010	<sup>29</sup> 0.157	<sup>35</sup> 0.003	<sup>30</sup> 0.084	<sup>41</sup> 0.014	<sup>35</sup> 0.045	<sup>19</sup> 0.529	<sup>35</sup> 0.033		<sup>33</sup> 0.183	0.000	0.000	0.044						
142	NTECHLAB-009	<sup>11</sup> 0.001	<sup>8</sup> 0.008	<sup>23</sup> 0.138	<sup>13</sup> 0.002	<sup>25</sup> 0.013	<sup>13</sup> 0.074	<sup>19</sup> 0.005	<sup>15</sup> 0.022	<sup>25</sup> 0.015	<sup>20</sup> 0.109	<sup>18</sup> 0.142	0.000	0.000	0.041		0.001				
143	NTECHLAB-010	<sup>9</sup> 0.001	<sup>11</sup> 0.008	<sup>14</sup> 0.085	<sup>7</sup> 0.002	<sup>10</sup> 0.008	<sup>3</sup> 0.057	<sup>9</sup> 0.003	<sup>0</sup> 0.015	<sup>7</sup> 0.252	<sup>3</sup> 0.007	<sup>11</sup> 0.059	<sup>3</sup> 0.098	0.001	0.001	0.043		0.000			
144	PARAVISION-000	<sup>183</sup> 0.019	<sup>158</sup> 0.038	<sup>81</sup> 0.534	<sup>156</sup> 0.423	<sup>155</sup> 0.529	<sup>153</sup> 0.089	<sup>147</sup> 0.170	<sup>139</sup> 0.999	<sup>144</sup> 0.470		<sup>133</sup> 0.926	0.000	0.000	0.000						
145	PARAVISION-001	<sup>94</sup> 0.004	<sup>107</sup> 0.020	<sup>31</sup> 0.329	<sup>153</sup> 0.414	<sup>154</sup> 0.484	<sup>107</sup> 0.049	<sup>120</sup> 0.128	<sup>131</sup> 0.999	<sup>141</sup> 0.444		<sup>111</sup> 0.739	0.000	0.000	0.000						
146	PARAVISION-002	<sup>99</sup> 0.004	<sup>113</sup> 0.022	<sup>53</sup> 0.335	<sup>103</sup> 0.015	<sup>106</sup> 0.175	<sup>108</sup> 0.050	<sup>113</sup> 0.119	<sup>75</sup> 0.983	<sup>93</sup> 0.080		<sup>91</sup> 0.497	0.000	0.000	0.032						
147	PARAVISION-003	<sup>48</sup> 0.003	<sup>100</sup> 0.019	<sup>42</sup> 0.252	<sup>104</sup> 0.015	<sup>103</sup> 0.167	<sup>86</sup> 0.035	<sup>92</sup> 0.096	<sup>101</sup> 0.994	<sup>80</sup> 0.058		<sup>89</sup> 0.296	0.000	0.000	0.032						
148	PARAVISION-004	<sup>38</sup> 0.002	<sup>28</sup> 0.010	<sup>18</sup> 0.104	<sup>64</sup> 0.006	<sup>64</sup> 0.112	<sup>30</sup> 0.010	<sup>30</sup> 0.038	<sup>169</sup> 1.000	<sup>32</sup> 0.018		<sup>129</sup> 0.908	0.000	0.000	0.032						
149	PARAVISION-005	<sup>24</sup> 0.002	<sup>20</sup> 0.010	<sup>11</sup> 0.079	<sup>76</sup> 0.007	<sup>54</sup> 0.106	<sup>15</sup> 0.004	<sup>16</sup> 0.024	<sup>69</sup> 0.980	<sup>20</sup> 0.011		<sup>15</sup> 0.132	0.000	0.000	0.038						
150	PARAVISION-007	<sup>9</sup> 0.001	<sup>9</sup> 0.008	<sup>6</sup> 0.066	<sup>58</sup> 0.005	<sup>14</sup> 0.010	<sup>46</sup> 0.101	<sup>14</sup> 0.004	<sup>17</sup> 0.025	<sup>182</sup> 1.000	<sup>18</sup> 0.009	<sup>21</sup> 0.113	<sup>169</sup> 1.000	0.000	0.000	0.000		0.000			
151	PIXELALL-002	<sup>102</sup> 0.005	<sup>115</sup> 0.022	<sup>133</sup> 0.810	<sup>90</sup> 0.011	<sup>111</sup> 0.187	<sup>160</sup> 0.105	<sup>195</sup> 0.388	<sup>174</sup> 1.000	<sup>147</sup> 0.602		<sup>229</sup> 1.000	0.000	0.000	0.000						
152	PIXELALL-003	<sup>56</sup> 0.002	<sup>65</sup> 0.014	<sup>73</sup> 0.515	<sup>74</sup> 0.006	<sup>94</sup> 0.151	<sup>62</sup> 0.022	<sup>66</sup> 0.073	<sup>153</sup> 1.000	<sup>61</sup> 0.037		<sup>99</sup> 0.554	0.000	0.000	0.000						
153	PIXELALL-004	<sup>54</sup> 0.002	<sup>69</sup> 0.015	<sup>59</sup> 0.523	<sup>61</sup> 0.005	<sup>96</sup> 0.152	<sup>54</sup> 0.018	<sup>74</sup> 0.079	<sup>166</sup> 1.000	<sup>72</sup> 0.051		<sup>147</sup> 0.994	0.000	0.000	0.000						
154	PIXELALL-005	<sup>48</sup> 0.002	<sup>34</sup> 0.011	<sup>44</sup> 0.264	<sup>93</sup> 0.012	<sup>43</sup> 0.028	<sup>92</sup> 0.146	<sup>34</sup> 0.012	<sup>39</sup> 0.050	<sup>172</sup> 1.000	<sup>43</sup> 0.027	<sup>39</sup> 0.203	<sup>132</sup> 1.000	0.000	0.000	0.000		0.000			
155	PTAKURATSATU-000	<sup>38</sup> 0.003	<sup>86</sup> 0.017	<sup>34</sup> 0.605	<sup>60</sup> 0.005	<sup>41</sup> 0.027	<sup>52</sup> 0.105	<sup>87</sup> 0.037	<sup>118</sup> 0.124	<sup>48</sup> 0.924	<sup>69</sup> 0.046	<sup>41</sup> 0.206	<sup>44</sup> 0.232	0.000	0.001	0.039		0.000			
156	QNAP-000	<sup>136</sup> 0.008	<sup>140</sup> 0.027	<sup>77</sup> 0.522	<sup>100</sup> 0.013	<sup>54</sup> 0.054	<sup>99</sup> 0.158	<sup>171</sup> 0.129	<sup>169</sup> 0.238	<sup>188</sup> 1.000	<sup>121</sup> 0.191	<sup>56</sup> 0.539	<sup>149</sup> 0.998	0.001	0.000	0.054		0.000			
157	QUANTASOFT-001	<sup>234</sup> 0.218	<sup>237</sup> 0.727					<sup>223</sup> 0.639						0.000	0.000						
158	RANKONE-002	<sup>184</sup> 0.019	<sup>192</sup> 0.071					<sup>164</sup> 0.118	<sup>174</sup> 0.261				0.000	0.000							
159	RANKONE-003	<sup>184</sup> 0.019	<sup>190</sup> 0.068					<sup>165</sup> 0.118	<sup>173</sup> 0.255				0.000	0.000							
160	RANKONE-004	<sup>205</sup> 0.041	<sup>209</sup> 0.141					<sup>191</sup> 0.193	<sup>199</sup> 0.426				0.000	0.000							
161	RANKONE-005	<sup>158</sup> 0.009	<sup>166</sup> 0.041	<sup>198</sup> 0.986				<sup>127</sup> 0.059	<sup>150</sup> 0.173	<sup>123</sup> 0.998			0.000	0.000	0.489						
162	RANKONE-006	<sup>112</sup> 0.005		<sup>130</sup> 0.797				<sup>89</sup> 0.037		<sup>65</sup> 0.977			0.002		0.167						
163	RANKONE-007	<sup>88</sup> 0.003	<sup>98</sup> 0.019	<sup>127</sup> 0.796				<sup>64</sup> 0.022	<sup>89</sup> 0.095	<sup>55</sup> 0.967			0.001	0.001	0.102						
164	RANKONE-009	<sup>66</sup> 0.002	<sup>53</sup> 0.013	<sup>85</sup> 0.549	<sup>63</sup> 0.006		<sup>84</sup> 0.134	<sup>30</sup> 0.018	<sup>68</sup> 0.076	<sup>32</sup> 0.969	<sup>82</sup> 0.062		<sup>68</sup> 0.328	0.000	0.000	0.000					
165	RANKONE-010	<sup>60</sup> 0.002	<sup>21</sup> 0.010	<sup>60</sup> 0.374	<sup>57</sup> 0.005	<sup>40</sup> 0.027	<sup>74</sup> 0.126	<sup>39</sup> 0.014	<sup>52</sup> 0.058	<sup>34</sup> 0.802	<sup>75</sup> 0.052	<sup>43</sup> 0.208	<sup>50</sup> 0.259	0.000	0.000	0.000		0.000			
166	RANKONE-011	<sup>20</sup> 0.002	<sup>41</sup> 0.011	<sup>37</sup> 0.223	<sup>39</sup> 0.004	<sup>31</sup> 0.019	<sup>28</sup> 0.082	<sup>24</sup> 0.009	<sup>37</sup> 0.048		<sup>60</sup> 0.037	<sup>36</sup> 0.182	<sup>141</sup> 0.977	0.000	0.000	0.000		0.000			
167	REALNETWORKS-000	<sup>204</sup> 0.040	<sup>199</sup> 0.078					<sup>197</sup> 0.234	<sup>189</sup> 0.319				0.001	0.000							
168	REALNETWORKS-001	<sup>203</sup> 0.040	<sup>198</sup> 0.078					<sup>196</sup> 0.234	<sup>190</sup> 0.319				0.001	0.000							
169	REALNETWORKS-002	<sup>205</sup> 0.039	<sup>197</sup> 0.078					<sup>195</sup> 0.231	<sup>188</sup> 0.315				0.001	0.000							
170	REALNETWORKS-003	<sup>191</sup> 0.024	<sup>186</sup> 0.062	<sup>123</sup> 0.771	<sup>122</sup> 0.031		<sup>117</sup> 0.209	<sup>181</sup> 0.159	<sup>177</sup> 0.266	<sup>122</sup> 0.998	<sup>116</sup> 0.164		<sup>92</sup> 0.500	0.001	0.000	0.009					
171	REALNETWORKS-004	<sup>189</sup> 0.024	<sup>183</sup> 0.059	<sup>129</sup> 0.797	<sup>121</sup> 0.031		<sup>122</sup> 0.213	<sup>180</sup> 0.158	<sup>176</sup> 0.263	<sup>140</sup> 0.999	<sup>117</sup> 0.170		<sup>103</sup> 0.613	0.001	0.000	0.009					
172	REALNETWORKS-005	<sup>48</sup> 0.002	<sup>36</sup> 0.013	<sup>46</sup> 0.433	<sup>56</sup> 0.004	<sup>36</sup> 0.023	<sup>48</sup> 0.102	<sup>75</sup> 0.028	<sup>67</sup> 0.074	<sup>39</sup> 0.971	<sup>39</sup> 0.037	<sup>43</sup> 0.223	<sup>39</sup> 0.215	0.000	0.000	0.006		0.000			
173	REMARKAI-000	<sup>143</sup> 0.009	<sup>143</sup> 0.030					<sup>169</sup> 0.128	<sup>156</sup> 0.203				0.000	0.001							
174	REMARKAI-000	<sup>90</sup> 0.003	<sup>96</sup> 0.018	<sup>98</sup> 0.660	<sup>81</sup> 0.008		<sup>93</sup> 0.148	<sup>120</sup> 0.055	<sup>114</sup> 0.120	<sup>138</sup> 0.999	<sup>89</sup> 0.069		<sup>109</sup> 0.717	0.000	0.000	0.000					
175	REMARKAI-002	<sup>141</sup> 0.008	<sup>142</sup> 0.029	<sup>131</sup> 0.802				<sup>168</sup> 0.124	<sup>154</sup> 0.196	<sup>91</sup> 0.991			0.000	0.001	0.017						
176	RENDIP-000	<sup>27</sup> 0.002	<sup>70</sup> 0.015	<sup>64</sup> 0.424	<sup>69</sup> 0.006	<sup>42</sup> 0.028	<sup>31</sup> 0.084	<sup>33</sup> 0.012	<sup>53</sup> 0.059	<sup>45</sup> 0.894	<sup>36</sup> 0.022	<sup>39</sup> 0.185	<sup>27</sup> 0.167	0.000	0.000	0.041		0.000			
177	S1-000	<sup>68</sup> 0.002	<sup>85</sup> 0.017	<sup>43</sup> 0.258	<sup>62</sup> 0.005	<sup>39</sup> 0.025	<sup>34</sup> 0.090	<sup>77</sup> 0.028	<sup>76</sup> 0.085	<sup>185</sup> 1.000	<sup>71</sup> 0.047	<sup>202</sup> 1.000	<sup>247</sup> 1.000	0.000	0.000	0.040		0.000			
178	SCANOVATE-000	<sup>111</sup> 0.005	<sup>170</sup> 0.045	<sup>89</sup> 0.560	<sup>126</sup> 0.035		<sup>121</sup> 0.211	<sup>134</sup> 0.067	<sup>170</sup> 0.240	<sup>44</sup> 0.893	<sup>125</sup> 0.215		<sup>76</sup> 0.400	0.000	0.001	0.057					
179	SCANOVATE-001	<sup>114</sup> 0.005	<sup>164</sup> 0.040	<sup>46</sup> 0.585	<sup>120</sup> 0.031		<sup>109</sup> 0.178	<sup>145</sup> 0.081	<sup>164</sup> 0.227	<sup>47</sup> 0.911	<sup>122</sup> 0.192		<sup>79</sup> 0.404	0.000	0.001	0.044					
180	SENSETIME-000	<sup>60</sup> 0.002	<sup>77</sup> 0.016	<sup>30</sup> 0.528				<sup>60</sup> 0.021	<sup>36</sup> 0.063	<sup>231</sup> 1.000			0.004	0.000	0.042						
181	SENSETIME-001	<sup>63</sup> 0.002	<sup>76</sup> 0.016					<sup>63</sup> 0.022	<sup>37</sup> 0.064				0.004	0.000							
182	SENSETIME-002	<sup>172</sup> 0.014	<sup>101</sup> 0.020	<sup>61</sup> 0.384	<sup>89</sup> 0.011		<sup>50</sup> 0.104	<sup>42</sup> 0.015	<sup>21</sup> 0.028	<sup>99</sup> 0.994	<sup>50</sup> 0.032		<sup>94</sup> 0.523	0.009	0.000	0.040					
183	SENSETIME-003	<sup>4</sup> 0.001	<sup>4</sup> 0.007	<sup>2</sup> 0.150	<sup>23</sup> 0.003		<sup>35</sup> 0.091	<sup>4</sup> 0.002	<sup>1</sup> 0.012	<sup>15</sup> 0.477	<sup>14</sup> 0.008		<sup>16</sup> 0.133	0.000	0.000	0.041					
184	SENSETIME-004	<sup>3</sup> 0.001	<sup>5</sup> 0.007	<sup>10</sup> 0.072	<sup>17</sup> 0.002		<sup>32</sup> 0.084	<sup>1</sup> 0.002	<sup>3</sup> 0.013	<sup>6</sup> 0.229	<sup>7</sup> 0.006		<sup>12</sup> 0.113	0.000	0.000	0.041					

Table 12: Miss rates by dataset: At left, rank 1 miss rates relevant to investigations; at

#	ALGORITHM	INVESTIGATION MODE						IDENTIFICATION MODE						FAILURE TO EXTRACT					
		RANK ONE MISS RATE, FNIR(N, 0, 1)						HIGH T → FPIR = 0.001, FNIR(N, T, L)						FEATURES					
		N=1.6M						N=1.6M											
GALLERY	MUGSHOT	MUGSHOT	MUGSHOT	VISA	BORDER	VISA	MUGSHOT	MUGSHOT	MUGSHOT	VISA	BORDER	VISA	MUGSHOT	MUGSHOT	MUGSHOT	VISA	BORDER	KIOSK	
PROBE	MUGSHOT	WEBCAM	PROFILE	BORDER	BOR <sub>2</sub> 10YR	KIOSK	MUGSHOT	WEBCAM	PROFILE	BORDER	BOR <sub>2</sub> 10YR	KIOSK	MUGSHOT	WEBCAM	PROFILE	BORDER	BOR <sub>2</sub> 10YR	KIOSK	
185	SENSETIME-005	<sup>2</sup> 0.001	<sup>2</sup> 0.006	<sup>2</sup> 0.059	<sup>14</sup> 0.002	<sup>8</sup> 0.007	<sup>24</sup> 0.082	<sup>7</sup> 0.002	<sup>2</sup> 0.014	<sup>3</sup> 0.173	<sup>10</sup> 0.007	<sup>8</sup> 0.104	0.000	0.000	0.041		0.000		
186	SENSETIME-006	<sup>1</sup> 0.001	<sup>1</sup> 0.006	<sup>1</sup> 0.055	<sup>1</sup> 0.001	<sup>1</sup> 0.004	<sup>3</sup> 0.064	<sup>2</sup> 0.002	<sup>2</sup> 0.012	<sup>125</sup> 0.998	<sup>1</sup> 0.004	<sup>4</sup> 0.034	<sup>2</sup> 0.093	0.000	0.000	0.025		0.000	
187	SHAMAN-003	<sup>224</sup> 0.124	<sup>213</sup> 0.172					<sup>219</sup> 0.451	<sup>213</sup> 0.597				0.020	0.011					
188	SHAMAN-004	<sup>224</sup> 0.222	<sup>222</sup> 0.319					<sup>226</sup> 0.615	<sup>220</sup> 0.754				0.020	0.011					
189	SHAMAN-006	<sup>286</sup> 0.040	<sup>182</sup> 0.058	<sup>163</sup> 0.938				<sup>175</sup> 0.141	<sup>186</sup> 0.237	<sup>60</sup> 0.972			0.020	0.011	0.869				
190	SHAMAN-007	<sup>20</sup> 0.040	<sup>181</sup> 0.057					<sup>176</sup> 0.141	<sup>169</sup> 0.240				0.020	0.010					
191	SIAT-001	<sup>40</sup> 0.002	<sup>224</sup> 0.333		<sup>51</sup> 0.004		<sup>44</sup> 0.099	<sup>48</sup> 0.018	<sup>194</sup> 0.365		<sup>48</sup> 0.031		0.000	0.000					
192	SIAT-002	<sup>41</sup> 0.002	<sup>226</sup> 0.446		<sup>154</sup> 0.348		<sup>49</sup> 0.102	<sup>61</sup> 0.022	<sup>205</sup> 0.478		<sup>134</sup> 0.372	<sup>132</sup> 0.923	0.000	0.000					
193	SMILART-004	<sup>248</sup> 0.965	<sup>240</sup> 0.974					<sup>237</sup> 0.968	<sup>233</sup> 0.976				0.011	0.013					
194	SMILART-005												0.011	0.013					
195	STAGU-000	<sup>192</sup> 0.007	<sup>105</sup> 0.020	<sup>96</sup> 0.613	<sup>110</sup> 0.020	<sup>55</sup> 0.055	<sup>100</sup> 0.159	<sup>128</sup> 0.062	<sup>201</sup> 0.443	<sup>159</sup> 1.000	<sup>145</sup> 0.535	<sup>61</sup> 0.961	<sup>197</sup> 1.000	0.000	0.000	0.000		0.000	
196	SYNESIS-003	<sup>228</sup> 0.170	<sup>218</sup> 0.235					<sup>224</sup> 0.582	<sup>210</sup> 0.646				0.006	0.015					
197	SYNESIS-003	<sup>129</sup> 0.016	<sup>123</sup> 0.023	<sup>130</sup> 0.827	<sup>96</sup> 0.013		<sup>86</sup> 0.136	<sup>132</sup> 0.065	<sup>117</sup> 0.123	<sup>53</sup> 0.960	<sup>91</sup> 0.075		<sup>63</sup> 0.314	0.000	0.001	0.063			
198	SYNESIS-005	<sup>142</sup> 0.009	<sup>54</sup> 0.013	<sup>115</sup> 0.744	<sup>33</sup> 0.003		<sup>36</sup> 0.092	<sup>66</sup> 0.025	<sup>64</sup> 0.072	<sup>76</sup> 0.984	<sup>53</sup> 0.032		<sup>38</sup> 0.214	0.001	0.000	0.135			
199	TECH5-001	<sup>98</sup> 0.004	<sup>84</sup> 0.017	<sup>92</sup> 0.584	<sup>74</sup> 0.007		<sup>59</sup> 0.107	<sup>122</sup> 0.057	<sup>229</sup> 0.935	<sup>186</sup> 1.000	<sup>126</sup> 0.244		<sup>148</sup> 0.994	0.000	0.000	0.006			
200	TECH5-002	<sup>75</sup> 0.003	<sup>32</sup> 0.011	<sup>48</sup> 0.312	<sup>32</sup> 0.003	<sup>47</sup> 0.029	<sup>33</sup> 0.089	<sup>73</sup> 0.027	<sup>62</sup> 0.070	<sup>35</sup> 0.805	<sup>62</sup> 0.039	<sup>40</sup> 0.205	<sup>82</sup> 0.440	0.001	0.000	0.041		0.000	
201	TEVIAN-003	<sup>179</sup> 0.015	<sup>177</sup> 0.052					<sup>188</sup> 0.177	<sup>184</sup> 0.298				0.001	0.002					
202	TEVIAN-004	<sup>160</sup> 0.011	<sup>157</sup> 0.038					<sup>163</sup> 0.117	<sup>151</sup> 0.176				0.001	0.002					
203	TEVIAN-005	<sup>133</sup> 0.007	<sup>141</sup> 0.028	<sup>69</sup> 0.467				<sup>150</sup> 0.087	<sup>131</sup> 0.144	<sup>54</sup> 0.962			0.001	0.002	0.116				
204	TEVIAN-006	<sup>68</sup> 0.002	<sup>37</sup> 0.011	<sup>24</sup> 0.123	<sup>26</sup> 0.003	<sup>26</sup> 0.013	<sup>10</sup> 0.071	<sup>28</sup> 0.010	<sup>24</sup> 0.032	<sup>10</sup> 0.425	<sup>26</sup> 0.016	<sup>16</sup> 0.093	<sup>136</sup> 0.951	0.001	0.000	0.062		0.000	
205	TEVIAN-007	<sup>39</sup> 0.002	<sup>17</sup> 0.009	<sup>16</sup> 0.093	<sup>10</sup> 0.002	<sup>15</sup> 0.009	<sup>6</sup> 0.067	<sup>21</sup> 0.005	<sup>14</sup> 0.022	<sup>8</sup> 0.301	<sup>13</sup> 0.065	<sup>15</sup> 0.122	0.000	0.000	0.062		0.000		
206	TIGER-000	<sup>212</sup> 0.062	<sup>204</sup> 0.095					<sup>213</sup> 0.390	<sup>206</sup> 0.500				0.000	0.000					
207	TIGER-002	<sup>117</sup> 0.006	<sup>121</sup> 0.023	<sup>74</sup> 0.514				<sup>147</sup> 0.086	<sup>140</sup> 0.158	<sup>135</sup> 0.999			0.000	0.000	0.056				
208	TIGER-003	<sup>116</sup> 0.006	<sup>120</sup> 0.023					<sup>146</sup> 0.086	<sup>141</sup> 0.158				0.000	0.000					
209	TONGYITRANS-000	<sup>128</sup> 0.007	<sup>118</sup> 0.022					<sup>139</sup> 0.074	<sup>108</sup> 0.112				0.003	0.001					
210	TONGYITRANS-001	<sup>129</sup> 0.007	<sup>117</sup> 0.022					<sup>133</sup> 0.066	<sup>99</sup> 0.101				0.003	0.001					
211	TOSHIBA-000	<sup>108</sup> 0.004	<sup>111</sup> 0.022	<sup>121</sup> 0.766				<sup>129</sup> 0.062	<sup>111</sup> 0.118	<sup>109</sup> 0.995			0.000	0.000	0.070				
212	TOSHIBA-001	<sup>109</sup> 0.005	<sup>114</sup> 0.022					<sup>124</sup> 0.058	<sup>86</sup> 0.092				0.000	0.000					
213	TRUEFACE-000	<sup>87</sup> 0.003	<sup>87</sup> 0.014	<sup>39</sup> 0.230	<sup>78</sup> 0.007	<sup>38</sup> 0.024	<sup>30</sup> 0.092	<sup>83</sup> 0.018	<sup>85</sup> 0.062	<sup>41</sup> 0.882	<sup>47</sup> 0.030	<sup>38</sup> 0.194	<sup>35</sup> 0.188	0.001	0.001	0.047		0.003	
214	VD-000	<sup>240</sup> 0.474	<sup>231</sup> 0.551					<sup>235</sup> 0.917	<sup>231</sup> 0.946				0.011	0.013					
215	VD-001	<sup>195</sup> 0.028	<sup>178</sup> 0.053					<sup>192</sup> 0.201	<sup>181</sup> 0.281				0.005	0.001					
216	VD-002	<sup>191</sup> 0.010	<sup>139</sup> 0.027	<sup>146</sup> 0.893	<sup>99</sup> 0.013	<sup>52</sup> 0.050	<sup>107</sup> 0.176	<sup>143</sup> 0.079	<sup>133</sup> 0.148	<sup>112</sup> 0.996	<sup>97</sup> 0.095	<sup>52</sup> 0.367	<sup>72</sup> 0.372	0.004	0.003	0.156		0.002	
217	VD-003	<sup>134</sup> 0.008	<sup>112</sup> 0.022	<sup>124</sup> 0.773	<sup>83</sup> 0.008	<sup>49</sup> 0.030	<sup>87</sup> 0.137	<sup>102</sup> 0.046	<sup>97</sup> 0.100	<sup>136</sup> 0.999	<sup>73</sup> 0.051	<sup>44</sup> 0.244	<sup>65</sup> 0.315	0.003	0.003	0.144		0.002	
218	VERIDAS-001	<sup>78</sup> 0.003	<sup>63</sup> 0.014	<sup>87</sup> 0.550	<sup>70</sup> 0.006	<sup>45</sup> 0.028	<sup>78</sup> 0.131	<sup>91</sup> 0.037	<sup>75</sup> 0.082	<sup>82</sup> 0.987	<sup>66</sup> 0.044	<sup>45</sup> 0.266	<sup>55</sup> 0.264	0.000	0.002	0.093		0.001	
219	VERIDAS-002	<sup>77</sup> 0.003	<sup>64</sup> 0.014	<sup>86</sup> 0.550	<sup>71</sup> 0.006	<sup>44</sup> 0.028	<sup>77</sup> 0.131	<sup>90</sup> 0.037	<sup>74</sup> 0.082	<sup>83</sup> 0.987	<sup>65</sup> 0.044	<sup>46</sup> 0.266	<sup>54</sup> 0.264	0.000	0.002	0.093		0.001	
220	VIGILANTSOLUTIONS-003	<sup>215</sup> 0.069	<sup>211</sup> 0.151	<sup>174</sup> 0.958				<sup>217</sup> 0.408	<sup>219</sup> 0.660	<sup>132</sup> 0.999			0.000	0.001	0.127				
221	VIGILANTSOLUTIONS-004	<sup>223</sup> 0.125	<sup>219</sup> 0.244	<sup>195</sup> 0.965				<sup>223</sup> 0.549	<sup>223</sup> 0.817	<sup>114</sup> 0.996			0.000	0.001	0.127				
222	VIGILANTSOLUTIONS-005	<sup>147</sup> 0.009	<sup>152</sup> 0.920					<sup>212</sup> 0.388	<sup>176</sup> 1.000				0.000	0.001	0.127				
223	VIGILANTSOLUTIONS-006	<sup>193</sup> 0.010		<sup>193</sup> 0.921				<sup>207</sup> 0.353	<sup>173</sup> 1.000				0.000	0.001	0.127				
224	VIGILANTSOLUTIONS-007	<sup>89</sup> 0.003	<sup>88</sup> 0.017	<sup>156</sup> 0.925	<sup>97</sup> 0.013	<sup>57</sup> 0.068	<sup>105</sup> 0.175	<sup>75</sup> 0.028	<sup>80</sup> 0.088	<sup>113</sup> 0.996	<sup>94</sup> 0.081	<sup>54</sup> 0.371	<sup>75</sup> 0.391	0.000	0.001	0.127		0.001	
225	VIGILANTSOLUTIONS-008	<sup>82</sup> 0.003	<sup>89</sup> 0.017	<sup>151</sup> 0.913	<sup>101</sup> 0.014	<sup>38</sup> 0.072	<sup>108</sup> 0.178	<sup>58</sup> 0.021	<sup>49</sup> 0.077	<sup>134</sup> 0.999	<sup>101</sup> 0.104	<sup>55</sup> 0.398	<sup>93</sup> 0.511	0.000	0.001	0.127		0.001	
226	VISIONBOX-000	<sup>47</sup> 0.002	<sup>38</sup> 0.011	<sup>117</sup> 0.752	<sup>54</sup> 0.005	<sup>25</sup> 0.017	<sup>20</sup> 0.078	<sup>51</sup> 0.018	<sup>31</sup> 0.057	<sup>90</sup> 0.990	<sup>39</sup> 0.023	<sup>27</sup> 0.146	<sup>25</sup> 0.162	0.000	0.001	0.043		0.001	
227	VISIONLABS-004	<sup>76</sup> 0.003	<sup>102</sup> 0.020	<sup>54</sup> 0.343				<sup>123</sup> 0.058	<sup>142</sup> 0.159	<sup>43</sup> 0.890			0.001	0.001	0.046				
228	VISIONLABS-005	<sup>47</sup> 0.002	<sup>97</sup> 0.019	<sup>52</sup> 0.334				<sup>109</sup> 0.050	<sup>132</sup> 0.147	<sup>42</sup> 0.888			0.001	0.001	0.046				
229	VISIONLABS-006	<sup>44</sup> 0.002	<sup>74</sup> 0.015	<sup>36</sup> 0.211	<sup>42</sup> 0.004		<sup>40</sup> 0.096	<sup>72</sup> 0.027	<sup>84</sup> 0.090	<sup>26</sup> 0.672			0.001	0.001	0.051				
230	VISIONLABS-007	<sup>38</sup> 0.002	<sup>73</sup> 0.015	<sup>35</sup> 0.211	<sup>35</sup> 0.004		<sup>39</sup> 0.095	<sup>71</sup> 0.027	<sup>83</sup> 0.090	<sup>27</sup> 0.672	<sup>49</sup> 0.031	<sup>34</sup> 0.185	0.001	0.001	0.051				

Table 13: Miss rates by dataset: At left, rank 1 miss rates relevant to investigations; at right, with threshold set to target FPIR = 0.01 for higher volume, low prior, uses. Yellow indicates most accurate algorithm. Throughout blue superscripts indicate the rank of the algorithm for that column.

2021/10/28  
13:44:33

FNIR(N, R, T) =  
FPIR(N, T) =

False neg. identification rate  
False pos. identification rate

N = Num. enrolled subjects  
R = Num. candidates examined

T = Threshold

T = 0 → Investigation  
T > 0 → Identification

#	ALGORITHM	INVESTIGATION MODE						IDENTIFICATION MODE						FAILURE TO EXTRACT					
		RANK ONE MISS RATE, FNIR(N, 0, 1)						HIGH T → FPIR = 0.001, FNIR(N, T, L)						FEATURES					
		N=1.6M						N=1.6M											
	GALLERY	MUGSHOT	MUGSHOT	MUGSHOT	VISA	BORDER	VISA	MUGSHOT	MUGSHOT	MUGSHOT	VISA	BORDER	VISA	MUGSHOT	MUGSHOT	MUGSHOT	VISA	BORDER	KIOSK
	PROBE	MUGSHOT	WEBCAM	PROFILE	BORDER	BOR <sub>1</sub> 10YR	KIOSK	MUGSHOT	WEBCAM	PROFILE	BORDER	BOR <sub>1</sub> 10YR	KIOSK	MUGSHOT	WEBCAM	PROFILE	BORDER	BOR <sub>1</sub> 10YR	KIOSK
231	VISIONLABS-008	<sup>85</sup> 0.002	<sup>48</sup> 0.014	<sup>24</sup> 0.141	<sup>15</sup> 0.002		<sup>25</sup> 0.081	<sup>37</sup> 0.013	<sup>45</sup> 0.051	<sup>16</sup> 0.481	<sup>27</sup> 0.017		<sup>19</sup> 0.151	0.001	0.000	0.075			
232	VISIONLABS-009	<sup>8</sup> 0.001	<sup>13</sup> 0.008	<sup>15</sup> 0.091	<sup>3</sup> 0.001		<sup>9</sup> 0.071	<sup>17</sup> 0.005	<sup>18</sup> 0.025	<sup>35</sup> 0.799	<sup>17</sup> 0.008		<sup>11</sup> 0.113	0.000	0.000	0.060			
233	VISIONLABS-010	<sup>15</sup> 0.001	<sup>38</sup> 0.010	<sup>9</sup> 0.069	<sup>7</sup> 0.001	<sup>3</sup> 0.006	<sup>8</sup> 0.069	<sup>20</sup> 0.005	<sup>20</sup> 0.027		<sup>12</sup> 0.008	<sup>10</sup> 0.055	<sup>10</sup> 0.109	0.000	0.000	0.040		0.000	
234	VOCORD-003	<sup>122</sup> 0.006	<sup>128</sup> 0.024	<sup>132</sup> 0.804	<sup>137</sup> 0.061		<sup>112</sup> 0.188	<sup>167</sup> 0.122	<sup>138</sup> 0.155	<sup>124</sup> 0.998	<sup>119</sup> 0.157		<sup>78</sup> 0.404	0.001	0.011	0.425			
235	VOCORD-004	<sup>137</sup> 0.008	<sup>108</sup> 0.021	<sup>126</sup> 0.792	<sup>95</sup> 0.012		<sup>75</sup> 0.127	<sup>208</sup> 0.355	<sup>148</sup> 0.173	<sup>161</sup> 1.000	<sup>123</sup> 0.193		<sup>145</sup> 0.991	0.000	0.000	0.000			
236	VOCORD-005	<sup>131</sup> 0.007	<sup>124</sup> 0.023	<sup>134</sup> 0.812	<sup>134</sup> 0.055		<sup>115</sup> 0.206	<sup>176</sup> 0.158	<sup>122</sup> 0.130	<sup>116</sup> 0.997	<sup>110</sup> 0.138		<sup>73</sup> 0.381	0.001	0.009	0.554			
237	VOCORD-006	<sup>246</sup> 1.000	<sup>242</sup> 1.000	<sup>225</sup> 1.000	<sup>247</sup> 1.000		<sup>206</sup> 1.000	<sup>244</sup> 1.000	<sup>246</sup> 1.000	<sup>218</sup> 1.000	<sup>183</sup> 1.000		<sup>161</sup> 1.000	0.001	0.009	0.554			
238	VTS-000	<sup>242</sup> 0.594	<sup>234</sup> 0.608	<sup>149</sup> 0.909	<sup>160</sup> 0.607	<sup>63</sup> 0.724	<sup>159</sup> 0.739	<sup>225</sup> 0.598	<sup>214</sup> 0.619	<sup>143</sup> 0.999	<sup>150</sup> 0.613	<sup>59</sup> 0.760	<sup>113</sup> 0.761	0.000	0.001	0.047		0.000	
239	VTS-001	<sup>25</sup> 0.002	<sup>24</sup> 0.010	<sup>30</sup> 0.167	<sup>65</sup> 0.006	<sup>30</sup> 0.018	<sup>18</sup> 0.077	<sup>38</sup> 0.013	<sup>42</sup> 0.051	<sup>58</sup> 0.994	<sup>37</sup> 0.022	<sup>25</sup> 0.141	<sup>36</sup> 0.192	0.000	0.000	0.040		0.000	
240	XFORWARDAI-000	<sup>61</sup> 0.002	<sup>61</sup> 0.014	<sup>14</sup> 0.089	<sup>43</sup> 0.004	<sup>27</sup> 0.015	<sup>38</sup> 0.094	<sup>43</sup> 0.015	<sup>47</sup> 0.053	<sup>12</sup> 0.440	<sup>35</sup> 0.021	<sup>30</sup> 0.159	<sup>28</sup> 0.169	0.000	0.000	0.000		0.000	
241	XFORWARDAI-001	<sup>55</sup> 0.002	<sup>52</sup> 0.013	<sup>7</sup> 0.067	<sup>29</sup> 0.003	<sup>11</sup> 0.009	<sup>26</sup> 0.082	<sup>18</sup> 0.005	<sup>22</sup> 0.028	<sup>13</sup> 0.448	<sup>19</sup> 0.008	<sup>12</sup> 0.062	<sup>14</sup> 0.123	0.000	0.000	0.000		0.000	
242	XFORWARDAI-002	<sup>49</sup> 0.002	<sup>48</sup> 0.012	<sup>3</sup> 0.059	<sup>23</sup> 0.002	<sup>6</sup> 0.007	<sup>16</sup> 0.077	<sup>12</sup> 0.003	<sup>10</sup> 0.016	<sup>17</sup> 0.525	<sup>6</sup> 0.005	<sup>7</sup> 0.041	<sup>4</sup> 0.099	0.000	0.000	0.000		0.000	
243	YISHENG-001	<sup>194</sup> 0.027	<sup>188</sup> 0.060		<sup>136</sup> 0.058		<sup>138</sup> 0.287	<sup>205</sup> 0.346	<sup>221</sup> 0.808		<sup>151</sup> 0.666		<sup>131</sup> 0.919	0.002	0.005				
244	YITU-002	<sup>43</sup> 0.002	<sup>26</sup> 0.010					<sup>49</sup> 0.018	<sup>38</sup> 0.049					0.000	0.000				
245	YITU-003	<sup>81</sup> 0.003	<sup>70</sup> 0.016					<sup>36</sup> 0.019	<sup>45</sup> 0.052					0.003	0.001				
246	YITU-004	<sup>12</sup> 0.001	<sup>15</sup> 0.008	<sup>144</sup> 0.866				<sup>26</sup> 0.010	<sup>19</sup> 0.027	<sup>46</sup> 0.936				0.000	0.000	0.000			
247	YITU-005	<sup>63</sup> 0.002	<sup>68</sup> 0.014					<sup>20</sup> 0.010	<sup>25</sup> 0.032					0.003	0.001				

Table 14: Miss rates by dataset: At left, rank 1 miss rates relevant to investigations; at right, with threshold set to target FPIR = 0.01 for higher volume, low prior, uses. Yellow indicates most accurate algorithm. Throughout blue superscripts indicate the rank of the algorithm for that column.

2021/10/28  
13:44:33

FNIR(N, R, T) =  
FPIR(N, T) =

False neg. identification rate  
False pos. identification rate

N = Num. enrolled subjects  
R = Num. candidates examined

T = Threshold

T = 0 → Investigation  
T > 0 → Identification

MISSES BELOW THRESHOLD, T		ENROL MOST RECENT				
FNIR(N, T > 0, R > L)		DATASET: FRVT 2018 MUGSHOTS				
#	ALGORITHM	N=0.64M	N=1.6M	N=3.0M	N=6.0M	N=12.0M
1	3DIVI-005	<sup>184</sup> 0.1358	<sup>184</sup> 0.1664	<sup>158</sup> 0.1915	<sup>149</sup> 0.2370	<sup>143</sup> 0.3054
2	ACER-000	<sup>178</sup> 0.1185	<sup>177</sup> 0.1455	<sup>153</sup> 0.1714	<sup>143</sup> 0.2074	<sup>136</sup> 0.2537
3	ALCHERA-003	<sup>176</sup> 0.1176	<sup>178</sup> 0.1553	<sup>154</sup> 0.1853	<sup>150</sup> 0.2409	<sup>151</sup> 0.3553
4	ALLGOVISION-000	<sup>151</sup> 0.0688	<sup>182</sup> 0.0881	<sup>156</sup> 0.1084	<sup>128</sup> 0.1389	<sup>116</sup> 0.2129
5	ALLGOVISION-001	<sup>157</sup> 0.0785	<sup>187</sup> 0.1017	<sup>143</sup> 0.1218	<sup>135</sup> 0.1584	<sup>123</sup> 0.2273
6	ANKE-000	<sup>163</sup> 0.0942	<sup>162</sup> 0.1169	<sup>148</sup> 0.1404	<sup>140</sup> 0.1776	<sup>137</sup> 0.2559
7	ANKE-002	<sup>83</sup> 0.0229	<sup>83</sup> 0.0318	<sup>84</sup> 0.0406	<sup>79</sup> 0.0605	<sup>70</sup> 0.1466
8	AWARE-003	<sup>173</sup> 0.1098	<sup>170</sup> 0.1283	<sup>149</sup> 0.1447	<sup>138</sup> 0.1768	<sup>128</sup> 0.2364
9	AWARE-005	<sup>211</sup> 0.3389	<sup>207</sup> 0.3643	<sup>167</sup> 0.3993	<sup>158</sup> 0.4526	<sup>135</sup> 0.2531
10	AYONIX-002	<sup>233</sup> 0.7862	<sup>232</sup> 0.8242	<sup>171</sup> 0.8508	<sup>163</sup> 0.8704	<sup>159</sup> 0.8939
11	CAMVI-004	<sup>109</sup> 0.0367	<sup>136</sup> 0.0716	<sup>131</sup> 0.0983	<sup>152</sup> 0.2508	<sup>140</sup> 0.2701
12	CIB-000	<sup>34</sup> 0.0086	<sup>35</sup> 0.0125	<sup>36</sup> 0.0160	<sup>42</sup> 0.0303	<sup>56</sup> 0.1251
13	CLOUDWALK-HR-000	<sup>7</sup> 0.0019	<sup>6</sup> 0.0020	<sup>4</sup> 0.0023	<sup>8</sup> 0.0072	<sup>11</sup> 0.0701
14	COGENT-000	<sup>128</sup> 0.0430	<sup>113</sup> 0.0527	<sup>112</sup> 0.0695	<sup>114</sup> 0.1133	<sup>108</sup> 0.1960
15	COGENT-001	<sup>125</sup> 0.0430	<sup>112</sup> 0.0527	<sup>113</sup> 0.0695	<sup>113</sup> 0.1133	<sup>105</sup> 0.1960
16	COGENT-002	<sup>95</sup> 0.0322	<sup>99</sup> 0.0444	<sup>99</sup> 0.0610	<sup>111</sup> 0.1116	<sup>118</sup> 0.2180
17	COGENT-003	<sup>96</sup> 0.0328	<sup>104</sup> 0.0463	<sup>110</sup> 0.0683	<sup>121</sup> 0.1294	<sup>130</sup> 0.2445
18	COGENT-004	<sup>80</sup> 0.0210	<sup>84</sup> 0.0331	<sup>94</sup> 0.0527	<sup>116</sup> 0.1138	<sup>115</sup> 0.2119
19	COGENT-005	<sup>26</sup> 0.0064	<sup>25</sup> 0.0091	<sup>26</sup> 0.0123	<sup>41</sup> 0.0303	<sup>52</sup> 0.1233
20	COGNITEC-000	<sup>186</sup> 0.1377	<sup>182</sup> 0.1606	<sup>157</sup> 0.1870	<sup>145</sup> 0.2176	<sup>142</sup> 0.2831
21	COGNITEC-001	<sup>159</sup> 0.0807	<sup>158</sup> 0.1017	<sup>142</sup> 0.1214	<sup>131</sup> 0.1513	<sup>121</sup> 0.2238
22	COGNITEC-002	<sup>119</sup> 0.0406	<sup>115</sup> 0.0531	<sup>106</sup> 0.0666	<sup>99</sup> 0.0935	<sup>101</sup> 0.1874
23	COGNITEC-003	<sup>117</sup> 0.0400	<sup>111</sup> 0.0526	<sup>102</sup> 0.0650	<sup>95</sup> 0.0895	<sup>94</sup> 0.1772
24	COGNITEC-004	<sup>82</sup> 0.0222	<sup>82</sup> 0.0313	<sup>80</sup> 0.0388	<sup>74</sup> 0.0540	<sup>38</sup> 0.1103
25	COGNITEC-005	<sup>25</sup> 0.0063	<sup>27</sup> 0.0096	<sup>30</sup> 0.0144	<sup>36</sup> 0.0287	<sup>25</sup> 0.0967
26	CYBERLINK-000	<sup>121</sup> 0.0414	<sup>121</sup> 0.0565	<sup>116</sup> 0.0707	<sup>107</sup> 0.1031	<sup>112</sup> 0.2050
27	CYBERLINK-001	<sup>111</sup> 0.0392	<sup>116</sup> 0.0536	<sup>111</sup> 0.0695	<sup>104</sup> 0.0973	<sup>95</sup> 0.1794
28	CYBERLINK-002	<sup>40</sup> 0.0105	<sup>43</sup> 0.0148	<sup>47</sup> 0.0202	<sup>58</sup> 0.0399	<sup>57</sup> 0.1255
29	CYBERLINK-003	<sup>23</sup> 0.0056	<sup>25</sup> 0.0077	<sup>24</sup> 0.0100	<sup>25</sup> 0.0235	<sup>53</sup> 0.1237
30	CYBERLINK-004	<sup>22</sup> 0.0051	<sup>22</sup> 0.0071	<sup>23</sup> 0.0102	<sup>21</sup> 0.0199	<sup>59</sup> 0.1269
31	DAHUA-001	<sup>140</sup> 0.0569	<sup>138</sup> 0.0727	<sup>128</sup> 0.0878	<sup>117</sup> 0.1148	<sup>100</sup> 0.1867
32	DAHUA-002	<sup>45</sup> 0.0108	<sup>44</sup> 0.0151	<sup>43</sup> 0.0191	<sup>38</sup> 0.0291	<sup>47</sup> 0.1153
33	DAHUA-003	<sup>38</sup> 0.0100	<sup>40</sup> 0.0139	<sup>41</sup> 0.0180	<sup>39</sup> 0.0296	<sup>41</sup> 0.1130
34	DEEPLINT-001	<sup>13</sup> 0.0027	<sup>13</sup> 0.0033	<sup>13</sup> 0.0043	<sup>14</sup> 0.0121	<sup>23</sup> 0.0922
35	DEEPLINT-001	<sup>105</sup> 0.0347	<sup>103</sup> 0.0462	<sup>98</sup> 0.0586	<sup>93</sup> 0.0802	<sup>91</sup> 0.1708
36	DERMALOG-005	<sup>159</sup> 0.0700	<sup>151</sup> 0.0880	<sup>138</sup> 0.1144	<sup>134</sup> 0.1578	<sup>131</sup> 0.2451
37	DERMALOG-006	<sup>114</sup> 0.0395	<sup>110</sup> 0.0517	<sup>102</sup> 0.0659	<sup>103</sup> 0.0973	<sup>93</sup> 0.1745
38	DERMALOG-007	<sup>152</sup> 0.0691	<sup>149</sup> 0.0863	<sup>137</sup> 0.1107	<sup>130</sup> 0.1504	<sup>126</sup> 0.2299
39	DERMALOG-008	<sup>101</sup> 0.0338	<sup>101</sup> 0.0455	<sup>101</sup> 0.0626	<sup>108</sup> 0.1060	<sup>124</sup> 0.2276
40	FUJITSULAB-000	<sup>59</sup> 0.0148	<sup>59</sup> 0.0206	<sup>63</sup> 0.0277	<sup>76</sup> 0.0541	<sup>92</sup> 0.1739
41	GORILLA-002	<sup>190</sup> 0.1539	<sup>190</sup> 0.1880	<sup>161</sup> 0.2184	<sup>153</sup> 0.2596	<sup>150</sup> 0.3398
42	GORILLA-004	<sup>154</sup> 0.0699	<sup>154</sup> 0.0892	<sup>134</sup> 0.1048	<sup>126</sup> 0.1370	<sup>109</sup> 0.1969
43	GORILLA-005	<sup>130</sup> 0.0453	<sup>125</sup> 0.0583	<sup>119</sup> 0.0704	<sup>105</sup> 0.0974	<sup>71</sup> 0.1474
44	GORILLA-006	<sup>75</sup> 0.0196	<sup>74</sup> 0.0275	<sup>69</sup> 0.0331	<sup>68</sup> 0.0516	<sup>40</sup> 0.1113
45	HIK-003	<sup>160</sup> 0.0828	<sup>159</sup> 0.1028	<sup>142</sup> 0.1202	<sup>133</sup> 0.1525	<sup>133</sup> 0.2480
46	HIK-004	<sup>158</sup> 0.0796	<sup>155</sup> 0.0988	<sup>137</sup> 0.1147	<sup>129</sup> 0.1474	<sup>134</sup> 0.2483
47	HIK-005	<sup>93</sup> 0.0312	<sup>96</sup> 0.0436	<sup>97</sup> 0.0560	<sup>97</sup> 0.0911	<sup>117</sup> 0.2129
48	HYPERVERGE-001	<sup>16</sup> 0.0033	<sup>16</sup> 0.0045	<sup>16</sup> 0.0059	<sup>12</sup> 0.0117	<sup>18</sup> 0.0872
49	IDEMIA-003	<sup>105</sup> 0.0346	<sup>106</sup> 0.0471	<sup>120</sup> 0.0892	<sup>155</sup> 0.2789	<sup>154</sup> 0.4311
50	IDEMIA-004	<sup>92</sup> 0.0300	<sup>92</sup> 0.0373	<sup>86</sup> 0.0447	<sup>80</sup> 0.0617	<sup>89</sup> 0.1635
51	IDEMIA-005	<sup>108</sup> 0.0360	<sup>98</sup> 0.0440	<sup>92</sup> 0.0537	<sup>92</sup> 0.0764	<sup>102</sup> 0.1915
52	IDEMIA-006	<sup>106</sup> 0.0351	<sup>95</sup> 0.0433	<sup>93</sup> 0.0525	<sup>89</sup> 0.0734	<sup>119</sup> 0.2201
53	IDEMIA-007	<sup>53</sup> 0.0136	<sup>52</sup> 0.0181	<sup>48</sup> 0.0228	<sup>51</sup> 0.0357	<sup>68</sup> 0.1402
54	IDEMIA-008	<sup>5</sup> 0.0016	<sup>5</sup> 0.0019	<sup>6</sup> 0.0024	<sup>4</sup> 0.0053	<sup>6</sup> 0.0470
55	IMAGUS-005	<sup>54</sup> 0.0137	<sup>55</sup> 0.0185	<sup>58</sup> 0.0237	<sup>52</sup> 0.0368	<sup>34</sup> 0.1067
56	IMAGUS-006	<sup>55</sup> 0.0137	<sup>57</sup> 0.0190	<sup>56</sup> 0.0244	<sup>56</sup> 0.0396	<sup>48</sup> 0.1159
57	IMPERIAL-000	<sup>69</sup> 0.0187	<sup>69</sup> 0.0259	<sup>77</sup> 0.0358	<sup>88</sup> 0.0733	<sup>96</sup> 0.1794
58	INCODE-003	<sup>183</sup> 0.1324	<sup>185</sup> 0.1672	<sup>159</sup> 0.1961	<sup>148</sup> 0.2345	<sup>143</sup> 0.3123
59	INCODE-004	<sup>118</sup> 0.0403	<sup>118</sup> 0.0538	<sup>106</sup> 0.0662	<sup>98</sup> 0.0917	<sup>86</sup> 0.1619
60	INCODE-005	<sup>31</sup> 0.0083	<sup>31</sup> 0.0113	<sup>31</sup> 0.0145	<sup>26</sup> 0.0247	<sup>20</sup> 0.0912
61	INNOVATRICS-007	<sup>36</sup> 0.0093	<sup>36</sup> 0.0125	<sup>34</sup> 0.0159	<sup>29</sup> 0.0259	<sup>35</sup> 0.1092
62	INTSYSMSU-000	<sup>241</sup> 0.9982	<sup>240</sup> 0.9984	<sup>176</sup> 0.9985	<sup>166</sup> 0.9987	<sup>162</sup> 0.9988
63	IREX-000	<sup>72</sup> 0.0190	<sup>75</sup> 0.0280	<sup>81</sup> 0.0391	<sup>84</sup> 0.0677	<sup>74</sup> 0.1479
64	ISYSTEMS-002	<sup>142</sup> 0.0584	<sup>142</sup> 0.0783	<sup>130</sup> 0.0973	<sup>127</sup> 0.1373	<sup>125</sup> 0.2295
65	ISYSTEMS-003	<sup>122</sup> 0.0438	<sup>126</sup> 0.0590	<sup>122</sup> 0.0807	<sup>119</sup> 0.1259	<sup>127</sup> 0.2357
66	KAKAO-000	<sup>46</sup> 0.0109	<sup>46</sup> 0.0151	<sup>46</sup> 0.0196	<sup>46</sup> 0.0324	<sup>27</sup> 0.1010
67	KEDACOM-001	<sup>66</sup> 0.0181	<sup>65</sup> 0.0227	<sup>58</sup> 0.0265	<sup>61</sup> 0.0422	<sup>65</sup> 0.1340
68	LOOKMAN-003	<sup>105</sup> 0.0346	<sup>97</sup> 0.0437	<sup>93</sup> 0.0514	<sup>87</sup> 0.0724	<sup>87</sup> 0.1620
69	LOOKMAN-005	<sup>84</sup> 0.0240	<sup>80</sup> 0.0301	<sup>76</sup> 0.0356	<sup>67</sup> 0.0512	<sup>64</sup> 0.1334
70	MEGVII-001	<sup>138</sup> 0.0562	<sup>137</sup> 0.0722	<sup>124</sup> 0.0872	<sup>123</sup> 0.1309	<sup>141</sup> 0.2713
71	MICROFOCUS-005	<sup>239</sup> 0.9732	<sup>234</sup> 0.8354	<sup>175</sup> 0.8555	<sup>164</sup> 0.8755	<sup>160</sup> 0.8954
72	MICROSOFT-003	<sup>76</sup> 0.0198	<sup>76</sup> 0.0278	<sup>76</sup> 0.0356	<sup>73</sup> 0.0538	<sup>80</sup> 0.1539

Table 15: Identification-mode: Effect of N on FNIR at high threshold. Values are threshold-based miss rates i.e. FNIR at FPiR = 0.001 for five enrollment population sizes, N. The right six columns apply for enrollment of one image. Missing entries usually apply because another algorithm from the same developer was run instead. Some developers are missing because less accurate algorithms were not run on galleries with N ≥ 3 000 000. Throughout blue superscripts indicate the rank of the algorithm for that column.

MISSES BELOW THRESHOLD, T		ENROL MOST RECENT				
FNIR(N, T > 0, R > L)		DATASET: FRVT 2018 MUGSHOTS				
#	ALGORITHM	N=0.64M	N=1.6M	N=3.0M	N=6.0M	N=12.0M
73	MICROSOFT-004	<sup>68</sup> 0.0185	<sup>70</sup> 0.0259	<sup>70</sup> 0.0333	<sup>69</sup> 0.0517	<sup>78</sup> 0.1510
74	MICROSOFT-005	<sup>67</sup> 0.0181	<sup>68</sup> 0.0256	<sup>68</sup> 0.0320	<sup>66</sup> 0.0512	<sup>76</sup> 0.1491
75	MICROSOFT-006	<sup>35</sup> 0.0091	<sup>32</sup> 0.0120	<sup>36</sup> 0.0162	<sup>40</sup> 0.0301	<sup>25</sup> 0.1482
76	NEC-000	<sup>146</sup> 0.0637	<sup>144</sup> 0.0789	<sup>129</sup> 0.0933	<sup>118</sup> 0.1163	<sup>104</sup> 0.1941
77	NEC-001	<sup>161</sup> 0.0863	<sup>161</sup> 0.1055	<sup>144</sup> 0.1249	<sup>132</sup> 0.1519	<sup>122</sup> 0.2253
78	NEC-002	<sup>9</sup> 0.0020	<sup>10</sup> 0.0026	<sup>10</sup> 0.0033	<sup>16</sup> 0.0135	<sup>9</sup> 0.0653
79	NEC-003	<sup>10</sup> 0.0021	<sup>8</sup> 0.0024	<sup>7</sup> 0.0028	<sup>6</sup> 0.0059	<sup>8</sup> 0.0540
80	NEC-004	<sup>6</sup> 0.0017	<sup>3</sup> 0.0018	<sup>1</sup> 0.0020	<sup>1</sup> 0.0037	<sup>1</sup> 0.0329
81	NEUROTECHNOLOGY-003	<sup>226</sup> 0.5698	<sup>227</sup> 0.6362	<sup>170</sup> 0.7035	<sup>162</sup> 0.7602	<sup>138</sup> 0.8224
82	NEUROTECHNOLOGY-004	<sup>132</sup> 0.0466	<sup>131</sup> 0.0629	<sup>118</sup> 0.0779	<sup>115</sup> 0.1135	<sup>114</sup> 0.2102
83	NEUROTECHNOLOGY-005	<sup>115</sup> 0.0396	<sup>119</sup> 0.0538	<sup>108</sup> 0.0675	<sup>102</sup> 0.0950	<sup>108</sup> 0.1966
84	NEUROTECHNOLOGY-007	<sup>127</sup> 0.0436	<sup>130</sup> 0.0623	<sup>120</sup> 0.0802	<sup>124</sup> 0.1320	<sup>129</sup> 0.2393
85	NEUROTECHNOLOGY-008	<sup>102</sup> 0.0339	<sup>114</sup> 0.0530	<sup>127</sup> 0.0893	<sup>139</sup> 0.1769	<sup>148</sup> 0.3288
86	NEUROTECHNOLOGY-009	<sup>44</sup> 0.0108	<sup>47</sup> 0.0152	<sup>46</sup> 0.0196	<sup>44</sup> 0.0324	<sup>37</sup> 0.1102
87	NTECHLAB-003	<sup>123</sup> 0.0421	<sup>117</sup> 0.0537	<sup>107</sup> 0.0674	<sup>96</sup> 0.0907	<sup>84</sup> 0.1582
88	NTECHLAB-004	<sup>94</sup> 0.0312	<sup>93</sup> 0.0405	<sup>92</sup> 0.0519	<sup>86</sup> 0.0722	<sup>77</sup> 0.1503
89	NTECHLAB-005	<sup>98</sup> 0.0334	<sup>94</sup> 0.0424	<sup>98</sup> 0.0537	<sup>91</sup> 0.0760	<sup>82</sup> 0.1543
90	NTECHLAB-006	<sup>90</sup> 0.0288	<sup>88</sup> 0.0367	<sup>89</sup> 0.0471	<sup>83</sup> 0.0670	<sup>79</sup> 0.1523
91	NTECHLAB-007	<sup>70</sup> 0.0188	<sup>87</sup> 0.0256	<sup>66</sup> 0.0317	<sup>65</sup> 0.0495	<sup>63</sup> 0.1306
92	NTECHLAB-008	<sup>42</sup> 0.0107	<sup>41</sup> 0.0145	<sup>42</sup> 0.0187	<sup>35</sup> 0.0286	<sup>26</sup> 0.0995
93	NTECHLAB-009	<sup>19</sup> 0.0037	<sup>19</sup> 0.0049	<sup>19</sup> 0.0062	<sup>15</sup> 0.0125	<sup>14</sup> 0.0735
94	NTECHLAB-010	<sup>8</sup> 0.0020	<sup>9</sup> 0.0025	<sup>8</sup> 0.0030	<sup>9</sup> 0.0077	<sup>13</sup> 0.0710
95	PARAVISION-003	<sup>86</sup> 0.0260	<sup>86</sup> 0.0351	<sup>85</sup> 0.0447	<sup>82</sup> 0.0657	<sup>88</sup> 0.1630
96	PARAVISION-004	<sup>28</sup> 0.0074	<sup>30</sup> 0.0101	<sup>29</sup> 0.0136	<sup>32</sup> 0.0267	<sup>38</sup> 0.1256
97	PARAVISION-005	<sup>15</sup> 0.0032	<sup>15</sup> 0.0041	<sup>15</sup> 0.0057	<sup>20</sup> 0.0174	<sup>29</sup> 0.1037
98	PARAVISION-007	<sup>14</sup> 0.0030	<sup>14</sup> 0.0040	<sup>14</sup> 0.0055	<sup>22</sup> 0.0211	<sup>26</sup> 0.1097
99	PIXELALL-002	<sup>156</sup> 0.0716	<sup>160</sup> 0.1052	<sup>151</sup> 0.1475	<sup>151</sup> 0.2489	<sup>153</sup> 0.3904
100	PIXELALL-003	<sup>62</sup> 0.0158	<sup>62</sup> 0.0218	<sup>68</sup> 0.0288	<sup>62</sup> 0.0474	<sup>45</sup> 0.1138
101	PIXELALL-004	<sup>49</sup> 0.0129	<sup>54</sup> 0.0183	<sup>57</sup> 0.0245	<sup>53</sup> 0.0378	<sup>66</sup> 0.1375
102	PIXELALL-005	<sup>34</sup> 0.0087	<sup>34</sup> 0.0121	<sup>38</sup> 0.0171	<sup>27</sup> 0.0250	<sup>31</sup> 0.1052
103	PTAKURATSATU-000	<sup>87</sup> 0.0275	<sup>87</sup> 0.0366	<sup>88</sup> 0.0458	<sup>71</sup> 0.0523	<sup>7</sup> 0.0523
104	QUANTASOFT-001	<sup>228</sup> 0.6387	<sup>228</sup> 0.6387	<sup>169</sup> 0.6387		<sup>156</sup> 0.6387
105	RANKONE-002	<sup>168</sup> 0.0973	<sup>164</sup> 0.1175	<sup>142</sup> 0.1359	<sup>137</sup> 0.1718	<sup>138</sup> 0.2613
106	RANKONE-003	<sup>169</sup> 0.0973	<sup>165</sup> 0.1175	<sup>148</sup> 0.1359	<sup>136</sup> 0.1718	<sup>139</sup> 0.2613
107	RANKONE-005	<sup>133</sup> 0.0473	<sup>127</sup> 0.0592	<sup>114</sup> 0.0700	<sup>100</sup> 0.0944	<sup>110</sup> 0.1998
108	RANKONE-007	<sup>64</sup> 0.0168	<sup>64</sup> 0.0222	<sup>59</sup> 0.0266	<sup>55</sup> 0.0381	<sup>42</sup> 0.1132
109	RANKONE-009	<sup>50</sup> 0.0132	<sup>50</sup> 0.0177	<sup>58</sup> 0.0230	<sup>48</sup> 0.0344	<sup>22</sup> 0.0921
110	RANKONE-010	<sup>41</sup> 0.0106	<sup>39</sup> 0.0136	<sup>39</sup> 0.0174	<sup>31</sup> 0.0265	<sup>16</sup> 0.0785
111	RANKONE-011	<sup>24</sup> 0.0063	<sup>24</sup> 0.0087	<sup>24</sup> 0.0115	<sup>33</sup> 0.0269	<sup>44</sup> 0.1135
112	REALNETWORKS-002	<sup>196</sup> 0.1943	<sup>195</sup> 0.2314	<sup>164</sup> 0.2656	<sup>157</sup> 0.3134	<sup>147</sup> 0.3208
113	REALNETWORKS-003	<sup>182</sup> 0.1300	<sup>181</sup> 0.1594	<sup>158</sup> 0.1858	<sup>146</sup> 0.2246	<sup>144</sup> 0.3076
114	REALNETWORKS-004	<sup>181</sup> 0.1279	<sup>180</sup> 0.1581	<sup>158</sup> 0.1857	<sup>147</sup> 0.2329	<sup>146</sup> 0.3179
115	REALNETWORKS-005	<sup>77</sup> 0.0202	<sup>75</sup> 0.0277	<sup>74</sup> 0.0355	<sup>78</sup> 0.0560	<sup>69</sup> 0.1431
116	REMARKAI-000	<sup>120</sup> 0.0406	<sup>120</sup> 0.0552	<sup>109</sup> 0.0676	<sup>106</sup> 0.1028	<sup>111</sup> 0.2003
117	RENDIP-000	<sup>32</sup> 0.0085	<sup>33</sup> 0.0121	<sup>33</sup> 0.0156	<sup>34</sup> 0.0277	<sup>50</sup> 0.1182
118	s1-000	<sup>79</sup> 0.0204	<sup>77</sup> 0.0279	<sup>79</sup> 0.0382	<sup>81</sup> 0.0630	<sup>90</sup> 0.1707
119	SCANOVATE-000	<sup>134</sup> 0.0498	<sup>134</sup> 0.0667	<sup>121</sup> 0.0804	<sup>110</sup> 0.1097	<sup>89</sup> 0.1109
120	SCANOVATE-001	<sup>145</sup> 0.0630	<sup>145</sup> 0.0815	<sup>132</sup> 0.0993	<sup>120</sup> 0.1292	<sup>107</sup> 0.1960
121	SENSETIME-000	<sup>61</sup> 0.0158	<sup>60</sup> 0.0208	<sup>61</sup> 0.0270	<sup>57</sup> 0.0398	<sup>51</sup> 0.1232
122	SENSETIME-001	<sup>63</sup> 0.0161	<sup>63</sup> 0.0219	<sup>64</sup> 0.0277	<sup>60</sup> 0.0420	<sup>61</sup> 0.1304
123	SENSETIME-002	<sup>57</sup> 0.0146	<sup>42</sup> 0.0148	<sup>38</sup> 0.0153	<sup>24</sup> 0.0234	<sup>10</sup> 0.0657
124	SENSETIME-003	<sup>3</sup> 0.0016	<sup>4</sup> 0.0018	<sup>3</sup> 0.0021	<sup>5</sup> 0.0054	<sup>4</sup> 0.0451
125	SENSETIME-004	<sup>2</sup> 0.0015	<sup>1</sup> 0.0018	<sup>2</sup> 0.0021	<sup>2</sup> 0.0040	<sup>2</sup> 0.0354
126	SENSETIME-005	<sup>4</sup> 0.0016	<sup>7</sup> 0.0022	<sup>9</sup> 0.0031	<sup>11</sup> 0.0089	<sup>5</sup> 0.0454
127	SENSETIME-006	<sup>1</sup> 0.0014	<sup>2</sup> 0.0018	<sup>2</sup> 0.0023	<sup>3</sup> 0.0047	<sup>3</sup> 0.0372
128	SHAMAN-007	<sup>180</sup> 0.1212	<sup>176</sup> 0.1413	<sup>152</sup> 0.1587	<sup>141</sup> 0.1879	<sup>132</sup> 0.2460
129	SIAT-001	<sup>52</sup> 0.0136	<sup>48</sup> 0.0176	<sup>51</sup> 0.0230	<sup>47</sup> 0.0344	<sup>28</sup> 0.1035
130	SIAT-002	<sup>60</sup> 0.0154	<sup>61</sup> 0.0216	<sup>66</sup> 0.0273	<sup>59</sup> 0.0404	<sup>60</sup> 0.1283
131	SYNOPSIS-003	<sup>224</sup> 0.5341	<sup>224</sup> 0.5821	<sup>168</sup> 0.6113	<sup>161</sup> 0.6479	<sup>157</sup> 0.6822
132	SYNOPSIS-003	<sup>135</sup> 0.0499	<sup>132</sup> 0.0652	<sup>122</sup> 0.0804	<sup>109</sup> 0.1095	<sup>103</sup> 0.1916
133	SYNOPSIS-005	<sup>65</sup> 0.0181	<sup>66</sup> 0.0248	<sup>67</sup> 0.0319	<sup>70</sup> 0.0518	<sup>83</sup> 0.1580
134	TECH5-001	<sup>122</sup> 0.0420	<sup>122</sup> 0.0574	<sup>128</sup> 0.0911	<sup>144</sup> 0.2106	<sup>152</sup> 0.3725
135	TECH5-002	<sup>74</sup> 0.0194	<sup>73</sup> 0.0269	<sup>73</sup> 0.0346	<sup>72</sup> 0.0537	<sup>85</sup> 0.1607
136	TEVIAN-005	<sup>153</sup> 0.0692	<sup>150</sup> 0.0873	<sup>136</sup> 0.1066	<sup>122</sup> 0.1301	<sup>98</sup> 0.1840
137	TEVIAN-006	<sup>30</sup> 0.0078	<sup>28</sup> 0.0098	<sup>24</sup> 0.0130	<sup>30</sup> 0.0261	<sup>62</sup> 0.1305
138	TEVIAN-007	<sup>21</sup> 0.0038	<sup>21</sup> 0.0052	<sup>28</sup> 0.0065	<sup>19</sup> 0.0154	<sup>24</sup> 0.0957
139	TIGER-002	<sup>148</sup> 0.0647	<sup>147</sup> 0.0861	<sup>133</sup> 0.1036	<sup>125</sup> 0.1332	<sup>120</sup> 0.2231
140	TOSHIBA-000	<sup>131</sup> 0.0460	<sup>129</sup> 0.0620	<sup>119</sup> 0.0780	<sup>112</sup> 0.1117	<sup>113</sup> 0.2082
141	TRUEFACE-000	<sup>51</sup> 0.0134	<sup>53</sup> 0.0182	<sup>54</sup> 0.0238	<sup>54</sup> 0.0380	<sup>67</sup> 0.1385
142	VD-001	<sup>192</sup> 0.1642	<sup>192</sup> 0.2015	<sup>163</sup> 0.2351	<sup>154</sup> 0.2736	<sup>149</sup> 0.3293
143	VERIDAS-001	<sup>89</sup> 0.0278	<sup>91</sup> 0.0373	<sup>90</sup> 0.0491	<sup>90</sup> 0.0753	<sup>81</sup> 0.1541
144	VERIDAS-002	<sup>88</sup> 0.0278	<sup>90</sup> 0.0373	<sup>78</sup> 0.0373	<sup>64</sup> 0.0491	<sup>15</sup> 0.0753

Table 16: Identification-mode: Effect of N on FNIR at high threshold. Values are threshold-based miss rates i.e. FNIR at FPIR = 0.001 for five enrollment population sizes, N. The right six columns apply for enrollment of one image. Missing entries usually apply because another algorithm from the same developer was run instead. Some developers are missing because less accurate algorithms were not run on galleries with N ≥ 3 000 000. Throughout blue superscripts indicate the rank of the algorithm for that column.

MISSES BELOW THRESHOLD, T		ENROL MOST RECENT				
FNIR(N, T > 0, R > L)		DATASET: FRVT 2018 MUGSHOTS				
#	ALGORITHM	N=0.64M	N=1.6M	N=3.0M	N=6.0M	N=12.0M
145	VIGILANTSOLUTIONS-008	<sup>58</sup> 0.0146	<sup>58</sup> 0.0205	<sup>60</sup> 0.0269	<sup>63</sup> 0.0489	<sup>49</sup> 0.1164
146	VISIONBOX-000	<sup>47</sup> 0.0122	<sup>51</sup> 0.0177	<sup>56</sup> 0.0239		<sup>161</sup> 0.9538
147	VISIONLABS-004	<sup>123</sup> 0.0427	<sup>123</sup> 0.0578	<sup>113</sup> 0.0703	<sup>101</sup> 0.0949	<sup>99</sup> 0.1853
148	VISIONLABS-005	<sup>111</sup> 0.0369	<sup>109</sup> 0.0502	<sup>100</sup> 0.0626	<sup>94</sup> 0.0847	<sup>97</sup> 0.1815
149	VISIONLABS-006	<sup>71</sup> 0.0188	<sup>72</sup> 0.0267	<sup>72</sup> 0.0336	<sup>77</sup> 0.0542	<sup>72</sup> 0.1478
150	VISIONLABS-007	<sup>72</sup> 0.0188	<sup>71</sup> 0.0266	<sup>71</sup> 0.0335	<sup>75</sup> 0.0540	<sup>73</sup> 0.1479
151	VISIONLABS-008	<sup>37</sup> 0.0096	<sup>37</sup> 0.0131	<sup>37</sup> 0.0166	<sup>37</sup> 0.0291	<sup>55</sup> 0.1247
152	VISIONLABS-009	<sup>17</sup> 0.0034	<sup>17</sup> 0.0046	<sup>17</sup> 0.0060	<sup>17</sup> 0.0140	<sup>19</sup> 0.0881
153	VISIONLABS-010	<sup>20</sup> 0.0038	<sup>20</sup> 0.0051	<sup>21</sup> 0.0070	<sup>18</sup> 0.0149	<sup>21</sup> 0.0920
154	VOCORD-005	<sup>177</sup> 0.1179	<sup>179</sup> 0.1577	<sup>160</sup> 0.2183	<sup>156</sup> 0.3122	<sup>155</sup> 0.4490
155	VTS-001	<sup>39</sup> 0.0102	<sup>38</sup> 0.0133	<sup>40</sup> 0.0175	<sup>43</sup> 0.0322	<sup>54</sup> 0.1243
156	XFORWARDAI-000	<sup>43</sup> 0.0107	<sup>45</sup> 0.0151	<sup>44</sup> 0.0195	<sup>45</sup> 0.0324	<sup>32</sup> 0.1057
157	XFORWARDAI-001	<sup>18</sup> 0.0037	<sup>18</sup> 0.0049	<sup>18</sup> 0.0060	<sup>13</sup> 0.0120	<sup>17</sup> 0.0800
158	XFORWARDAI-002	<sup>12</sup> 0.0026	<sup>12</sup> 0.0030	<sup>12</sup> 0.0035	<sup>10</sup> 0.0078	<sup>12</sup> 0.0706
159	YITU-002	<sup>48</sup> 0.0129	<sup>49</sup> 0.0177	<sup>49</sup> 0.0228	<sup>49</sup> 0.0345	<sup>43</sup> 0.1133
160	YITU-003	<sup>56</sup> 0.0138	<sup>56</sup> 0.0185	<sup>50</sup> 0.0236	<sup>50</sup> 0.0353	<sup>46</sup> 0.1148
161	YITU-004	<sup>27</sup> 0.0067	<sup>26</sup> 0.0096	<sup>26</sup> 0.0129	<sup>23</sup> 0.0232	<sup>30</sup> 0.1046
162	YITU-005	<sup>29</sup> 0.0074	<sup>29</sup> 0.0101	<sup>28</sup> 0.0135	<sup>28</sup> 0.0255	<sup>33</sup> 0.1057

Table 17: **Identification-mode: Effect of N on FNIR at high threshold.** Values are threshold-based miss rates i.e. FNIR at FPIR = 0.001 for five enrollment population sizes, N. The right six columns apply for enrollment of one image. Missing entries usually apply because another algorithm from the same developer was run instead. Some developers are missing because less accurate algorithms were not run on galleries with  $N \geq 3\,000\,000$ . Throughout blue superscripts indicate the rank of the algorithm for that column.

MISSES AT GIVEN RANK		ENROL MOST RECENT											
FNIR(N, T = 0, R)		RANK 1					RANK 50						
#	ALGORITHM	N=0.64M	N=1.6M	N=3.0M	N=6.0M	N=12.0M	$aN^b$	N=0.64M	N=1.6M	N=3.0M	N=6.0M	N=12.0M	$aN^b$
1	3DIVI-005	<sup>182</sup> 0.0137	<sup>181</sup> 0.0176	<sup>151</sup> 0.0210	<sup>145</sup> 0.0253	<sup>142</sup> 0.0302	<sup>116</sup> 0.0004 N <sup>0.271 124</sup>	<sup>164</sup> 0.0040	<sup>163</sup> 0.0049	<sup>141</sup> 0.0057	<sup>137</sup> 0.0068	<sup>134</sup> 0.0081	<sup>47</sup> 0.0002 N <sup>0.240 129</sup>
2	ACER-000	<sup>151</sup> 0.0081	<sup>151</sup> 0.0106	<sup>139</sup> 0.0128	<sup>137</sup> 0.0157	<sup>135</sup> 0.0195	<sup>54</sup> 0.0001 N <sup>0.299 148</sup>	<sup>116</sup> 0.0020	<sup>128</sup> 0.0026	<sup>120</sup> 0.0031	<sup>120</sup> 0.0037	<sup>114</sup> 0.0045	<sup>18</sup> 0.0000 N <sup>0.284 142</sup>
3	ALCHERA-003	<sup>147</sup> 0.0079	<sup>154</sup> 0.0104	<sup>137</sup> 0.0123	<sup>136</sup> 0.0147	<sup>133</sup> 0.0180	<sup>72</sup> 0.0002 N <sup>0.278 135</sup>	<sup>144</sup> 0.0027	<sup>144</sup> 0.0032	<sup>126</sup> 0.0035	<sup>123</sup> 0.0042	<sup>117</sup> 0.0048	<sup>51</sup> 0.0002 N <sup>0.199 119</sup>
4	ALLGOVISION-000	<sup>167</sup> 0.0101	<sup>162</sup> 0.0114	<sup>138</sup> 0.0127	<sup>135</sup> 0.0145	<sup>132</sup> 0.0166	<sup>14</sup> 0.0010 N <sup>0.171 67</sup>	<sup>183</sup> 0.0063	<sup>179</sup> 0.0067	<sup>146</sup> 0.0071	<sup>140</sup> 0.0075	<sup>138</sup> 0.0081	<sup>146</sup> 0.0020 N <sup>0.086 78</sup>
5	ALLGOVISION-001	<sup>139</sup> 0.0069	<sup>140</sup> 0.0090	<sup>134</sup> 0.0107	<sup>130</sup> 0.0128	<sup>129</sup> 0.0157	<sup>62</sup> 0.0002 N <sup>0.277 133</sup>	<sup>133</sup> 0.0023	<sup>134</sup> 0.0027	<sup>121</sup> 0.0031	<sup>116</sup> 0.0036	<sup>111</sup> 0.0043	<sup>40</sup> 0.0001 N <sup>0.211 124</sup>
6	ANKE-000	<sup>168</sup> 0.0102	<sup>140</sup> 0.0132	<sup>147</sup> 0.0155	<sup>142</sup> 0.0188	<sup>138</sup> 0.0225	<sup>101</sup> 0.0003 N <sup>0.270 123</sup>	<sup>135</sup> 0.0032	<sup>136</sup> 0.0040	<sup>137</sup> 0.0046	<sup>131</sup> 0.0056	<sup>125</sup> 0.0066	<sup>39</sup> 0.0001 N <sup>0.247 131</sup>
7	ANKE-002	<sup>80</sup> 0.0024	<sup>78</sup> 0.0028	<sup>70</sup> 0.0032	<sup>70</sup> 0.0037	<sup>70</sup> 0.0043	<sup>64</sup> 0.0002 N <sup>0.203 79</sup>	<sup>92</sup> 0.0016	<sup>91</sup> 0.0017	<sup>85</sup> 0.0017	<sup>75</sup> 0.0018	<sup>68</sup> 0.0019	<sup>35</sup> 0.0006 N <sup>0.067 69</sup>
8	AWARE-003	<sup>198</sup> 0.0238	<sup>197</sup> 0.0306	<sup>168</sup> 0.0361	<sup>156</sup> 0.0431	<sup>155</sup> 0.0506	<sup>139</sup> 0.0008 N <sup>0.288 118</sup>	<sup>177</sup> 0.0055	<sup>185</sup> 0.0075	<sup>156</sup> 0.0092	<sup>151</sup> 0.0113	<sup>150</sup> 0.0143	<sup>29</sup> 0.0001 N <sup>0.323 152</sup>
9	AWARE-005	<sup>200</sup> 0.0245	<sup>199</sup> 0.0311	<sup>163</sup> 0.0366	<sup>157</sup> 0.0434	<sup>146</sup> 0.0512	<sup>150</sup> 0.0056 N <sup>0.118 38</sup>	<sup>181</sup> 0.0062	<sup>191</sup> 0.0082	<sup>158</sup> 0.0101	<sup>154</sup> 0.0128	<sup>150</sup> 0.0089	<sup>110</sup> 0.0007 N <sup>0.169 114</sup>
10	AYONIX-002	<sup>234</sup> 0.2935	<sup>235</sup> 0.3414	<sup>193</sup> 0.3736	<sup>165</sup> 0.4101	<sup>161</sup> 0.4465	<sup>160</sup> 0.0440 N <sup>0.143 48</sup>	<sup>233</sup> 0.0950	<sup>235</sup> 0.1274	<sup>173</sup> 0.1524	<sup>164</sup> 0.1828	<sup>160</sup> 0.2150	<sup>148</sup> 0.0023 N <sup>0.279 140</sup>
11	CAMVI-004	<sup>172</sup> 0.0124	<sup>201</sup> 0.0468	<sup>168</sup> 0.0719	<sup>164</sup> 0.2363	<sup>160</sup> 0.2367	<sup>2</sup> 0.0000 N <sup>0.055 162</sup>	<sup>206</sup> 0.0117	<sup>221</sup> 0.0464	<sup>169</sup> 0.0715	<sup>163</sup> 0.2361	<sup>161</sup> 0.2364	<sup>2</sup> 0.0000 N <sup>0.071 162</sup>
12	CIB-000	<sup>27</sup> 0.0014	<sup>26</sup> 0.0015	<sup>23</sup> 0.0017	<sup>27</sup> 0.0019	<sup>123</sup> 0.0131	<sup>3</sup> 0.0000 N <sup>0.638 161</sup>	<sup>30</sup> 0.0012	<sup>30</sup> 0.0012	<sup>30</sup> 0.0012	<sup>29</sup> 0.0012	<sup>148</sup> 0.0122	<sup>3</sup> 0.0000 N <sup>0.647 161</sup>
13	CLOUDWALK-HR-000	<sup>31</sup> 0.0015	<sup>21</sup> 0.0015	<sup>19</sup> 0.0015	<sup>15</sup> 0.0016	<sup>12</sup> 0.0017	<sup>135</sup> 0.0007 N <sup>0.054 9</sup>	<sup>80</sup> 0.0014	<sup>66</sup> 0.0014	<sup>56</sup> 0.0014	<sup>52</sup> 0.0014	<sup>39</sup> 0.0014	<sup>135</sup> 0.0012 N <sup>0.012 12</sup>
14	COAGENT-000	<sup>167</sup> 0.0101	<sup>150</sup> 0.0105	<sup>134</sup> 0.0109	<sup>126</sup> 0.0115	<sup>120</sup> 0.0125	<sup>156</sup> 0.0038 N <sup>0.071 13</sup>	<sup>125</sup> 0.0021	<sup>125</sup> 0.0024	<sup>116</sup> 0.0028	<sup>119</sup> 0.0036	<sup>134</sup> 0.0095	<sup>8</sup> 0.0000 N <sup>0.466 158</sup>
15	COAGENT-001	<sup>166</sup> 0.0101	<sup>150</sup> 0.0105	<sup>134</sup> 0.0109	<sup>125</sup> 0.0115	<sup>121</sup> 0.0125	<sup>152</sup> 0.0038 N <sup>0.071 14</sup>	<sup>124</sup> 0.0021	<sup>122</sup> 0.0024	<sup>115</sup> 0.0028	<sup>118</sup> 0.0036	<sup>134</sup> 0.0095	<sup>8</sup> 0.0000 N <sup>0.466 158</sup>
16	COAGENT-002	<sup>90</sup> 0.0029	<sup>93</sup> 0.0036	<sup>91</sup> 0.0041	<sup>89</sup> 0.0049	<sup>85</sup> 0.0059	<sup>40</sup> 0.0001 N <sup>0.244 110</sup>	<sup>76</sup> 0.0014	<sup>83</sup> 0.0015	<sup>79</sup> 0.0017	<sup>80</sup> 0.0019	<sup>80</sup> 0.0021	<sup>52</sup> 0.0002 N <sup>0.144 108</sup>
17	COAGENT-003	<sup>96</sup> 0.0031	<sup>97</sup> 0.0038	<sup>96</sup> 0.0043	<sup>92</sup> 0.0051	<sup>82</sup> 0.0060	<sup>51</sup> 0.0001 N <sup>0.230 100</sup>	<sup>68</sup> 0.0015	<sup>94</sup> 0.0017	<sup>95</sup> 0.0018	<sup>91</sup> 0.0020	<sup>86</sup> 0.0022	<sup>50</sup> 0.0002 N <sup>0.143 107</sup>
18	COAGENT-004	<sup>95</sup> 0.0018	<sup>95</sup> 0.0020	<sup>95</sup> 0.0022	<sup>90</sup> 0.0025	<sup>42</sup> 0.0026	<sup>80</sup> 0.0002 N <sup>0.199 89</sup>	<sup>69</sup> 0.0013	<sup>64</sup> 0.0014	<sup>60</sup> 0.0014	<sup>55</sup> 0.0015	<sup>48</sup> 0.0015	<sup>99</sup> 0.0007 N <sup>0.060 53</sup>
19	COAGENT-005	<sup>37</sup> 0.0016	<sup>34</sup> 0.0017	<sup>28</sup> 0.0018	<sup>20</sup> 0.0020	<sup>25</sup> 0.0021	<sup>112</sup> 0.0004 N <sup>0.108 30</sup>	<sup>70</sup> 0.0013	<sup>58</sup> 0.0013	<sup>50</sup> 0.0014	<sup>43</sup> 0.0014	<sup>33</sup> 0.0014	<sup>133</sup> 0.0011 N <sup>0.017 20</sup>
20	COGNITEC-000	<sup>193</sup> 0.0195	<sup>192</sup> 0.0252	<sup>159</sup> 0.0297	<sup>154</sup> 0.0352	<sup>150</sup> 0.0417	<sup>132</sup> 0.0006 N <sup>0.259 119</sup>	<sup>173</sup> 0.0050	<sup>177</sup> 0.0065	<sup>153</sup> 0.0077	<sup>150</sup> 0.0097	<sup>147</sup> 0.0122	<sup>56</sup> 0.0001 N <sup>0.305 146</sup>
21	COGNITEC-001	<sup>160</sup> 0.0090	<sup>160</sup> 0.0117	<sup>147</sup> 0.0139	<sup>140</sup> 0.0166	<sup>136</sup> 0.0199	<sup>93</sup> 0.0002 N <sup>0.271 126</sup>	<sup>151</sup> 0.0030	<sup>150</sup> 0.0034	<sup>134</sup> 0.0040	<sup>130</sup> 0.0046	<sup>124</sup> 0.0054	<sup>30</sup> 0.0002 N <sup>0.207 123</sup>
22	COGNITEC-002	<sup>122</sup> 0.0048	<sup>119</sup> 0.0057	<sup>112</sup> 0.0067	<sup>107</sup> 0.0079	<sup>107</sup> 0.0094	<sup>84</sup> 0.0002 N <sup>0.232 102</sup>	<sup>135</sup> 0.0024	<sup>131</sup> 0.0026	<sup>118</sup> 0.0028	<sup>111</sup> 0.0030	<sup>109</sup> 0.0034	<sup>82</sup> 0.0005 N <sup>0.117 94</sup>
23	COGNITEC-003	<sup>124</sup> 0.0053	<sup>123</sup> 0.0062	<sup>115</sup> 0.0072	<sup>112</sup> 0.0085	<sup>110</sup> 0.0100	<sup>99</sup> 0.0003 N <sup>0.222 91</sup>	<sup>145</sup> 0.0030	<sup>123</sup> 0.0032	<sup>114</sup> 0.0035	<sup>110</sup> 0.0037	<sup>115</sup> 0.0008 N <sup>0.098 86</sup>	
24	COGNITEC-004	<sup>86</sup> 0.0027	<sup>86</sup> 0.0032	<sup>86</sup> 0.0037	<sup>84</sup> 0.0045	<sup>82</sup> 0.0056	<sup>31</sup> 0.0001 N <sup>0.253 116</sup>	<sup>67</sup> 0.0013	<sup>67</sup> 0.0014	<sup>67</sup> 0.0015	<sup>68</sup> 0.0017	<sup>64</sup> 0.0019	<sup>60</sup> 0.0002 N <sup>0.123 99</sup>
25	COGNITEC-005	<sup>27</sup> 0.0014	<sup>31</sup> 0.0016	<sup>28</sup> 0.0018	<sup>33</sup> 0.0021	<sup>33</sup> 0.0024	<sup>57</sup> 0.0001 N <sup>0.169 65</sup>	<sup>25</sup> 0.0011	<sup>27</sup> 0.0011	<sup>25</sup> 0.0012	<sup>25</sup> 0.0012	<sup>24</sup> 0.0012	<sup>98</sup> 0.0007 N <sup>0.037 37</sup>
26	CYBERLINK-000	<sup>101</sup> 0.0034	<sup>97</sup> 0.0040	<sup>90</sup> 0.0046	<sup>94</sup> 0.0054	<sup>90</sup> 0.0062	<sup>77</sup> 0.0002 N <sup>0.209 85</sup>	<sup>121</sup> 0.0021	<sup>117</sup> 0.0022	<sup>109</sup> 0.0023	<sup>105</sup> 0.0025	<sup>97</sup> 0.0027	<sup>92</sup> 0.0006 N <sup>0.092 83</sup>
27	CYBERLINK-001	<sup>93</sup> 0.0030	<sup>91</sup> 0.0035	<sup>93</sup> 0.0042	<sup>91</sup> 0.0050	<sup>87</sup> 0.0060	<sup>41</sup> 0.0001 N <sup>0.243 109</sup>	<sup>95</sup> 0.0016	<sup>96</sup> 0.0017	<sup>90</sup> 0.0018	<sup>86</sup> 0.0020	<sup>83</sup> 0.0022	<sup>72</sup> 0.0004 N <sup>0.109 90</sup>
28	CYBERLINK-002	<sup>79</sup> 0.0024	<sup>79</sup> 0.0026	<sup>74</sup> 0.0028	<sup>66</sup> 0.0031	<sup>57</sup> 0.0035	<sup>123</sup> 0.0005 N <sup>0.121 39</sup>	<sup>117</sup> 0.0020	<sup>112</sup> 0.0021	<sup>105</sup> 0.0021	<sup>99</sup> 0.0022	<sup>98</sup> 0.0022	<sup>148</sup> 0.0012 N <sup>0.036 36</sup>
29	CYBERLINK-003	<sup>29</sup> 0.0015	<sup>28</sup> 0.0016	<sup>28</sup> 0.0017	<sup>21</sup> 0.0018	<sup>18</sup> 0.0022	<sup>19</sup> 0.0003 N <sup>0.110 32</sup>	<sup>31</sup> 0.0011	<sup>29</sup> 0.0011	<sup>27</sup> 0.0012	<sup>28</sup> 0.0012	<sup>28</sup> 0.0013	<sup>89</sup> 0.0006 N <sup>0.047 49</sup>
30	CYBERLINK-004	<sup>41</sup> 0.0016	<sup>39</sup> 0.0017	<sup>34</sup> 0.0018	<sup>24</sup> 0.0019	<sup>20</sup> 0.0021	<sup>128</sup> 0.0005 N <sup>0.085 23</sup>	<sup>77</sup> 0.0014	<sup>68</sup> 0.0014	<sup>58</sup> 0.0014	<sup>53</sup> 0.0014	<sup>44</sup> 0.0015	<sup>132</sup> 0.0010 N <sup>0.022 28</sup>
31	DAHUA-001	<sup>125</sup> 0.0053	<sup>127</sup> 0.0067	<sup>119</sup> 0.0079	<sup>117</sup> 0.0093	<sup>114</sup> 0.0112	<sup>69</sup> 0.0002 N <sup>0.256 117</sup>	<sup>143</sup> 0.0027	<sup>137</sup> 0.0029	<sup>122</sup> 0.0031	<sup>113</sup> 0.0034	<sup>109</sup> 0.0038	<sup>86</sup> 0.0005 N <sup>0.121 97</sup>
32	DAHUA-002	<sup>45</sup> 0.0017	<sup>47</sup> 0.0018	<sup>48</sup> 0.0021	<sup>40</sup> 0.0023	<sup>36</sup> 0.0027	<sup>70</sup> 0.0002 N <sup>0.136 33</sup>	<sup>61</sup> 0.0013	<sup>59</sup> 0.0013	<sup>53</sup> 0.0014	<sup>48</sup> 0.0014	<sup>44</sup> 0.0015	<sup>106</sup> 0.0007 N <sup>0.043 46</sup>
33	DAHUA-003	<sup>77</sup> 0.0010	<sup>78</sup> 0.0012	<sup>71</sup> 0.0014	<sup>16</sup> 0.0016	<sup>16</sup> 0.0018	<sup>28</sup> 0.0001 N <sup>0.199 78</sup>	<sup>12</sup> 0.0009	<sup>10</sup> 0.0009	<sup>10</sup> 0.0009	<sup>10</sup> 0.0009	<sup>9</sup> 0.0009	<sup>90</sup> 0.0006 N <sup>0.027 32</sup>
34	DEEPLINK-001	<sup>24</sup> 0.0014	<sup>17</sup> 0.0014	<sup>16</sup> 0.0015	<sup>17</sup> 0.0016	<sup>15</sup> 0.0018	<sup>120</sup> 0.0004 N <sup>0.089 24</sup>	<sup>38</sup> 0.0013	<sup>45</sup> 0.0013	<sup>45</sup> 0.0013	<sup>37</sup> 0.0013	<sup>31</sup> 0.0013	<sup>130</sup> 0.0010 N <sup>0.017 19</sup>
35	DEEPLINK-002	<sup>100</sup> 0.0033	<sup>105</sup> 0.0043	<sup>102</sup> 0.0052	<sup>100</sup> 0.0065	<sup>99</sup> 0.0081	<sup>12</sup> 0.0001 N <sup>0.311 151</sup>	<sup>51</sup> 0.0012	<sup>62</sup> 0.0014	<sup>71</sup> 0.0015	<sup>70</sup> 0.0017	<sup>74</sup> 0.0020	<sup>43</sup> 0.0001 N <sup>0.159 112</sup>
36	DERMALOG-005	<sup>172</sup> 0.0114	<sup>172</sup> 0.0149	<sup>142</sup> 0.0201	<sup>150</sup> 0.0289	<sup>153</sup> 0.0447	<sup>7</sup> 0.0000 N <sup>0.470 160</sup>	<sup>200</sup> 0.0094	<sup>201</sup> 0.0122	<sup>164</sup> 0.0171	<sup>158</sup> 0.0254	<sup>156</sup> 0.0406	<sup>9</sup> 0.0000 N <sup>0.505 159</sup>
37	DERMALOG-006	<sup>149</sup> 0.0075	<sup>149</sup> 0.0081	<sup>129</sup> 0.0086	<sup>118</sup> 0.0093	<sup>111</sup> 0.0104	<sup>19</sup> 0.0017 N <sup>0.290 131</sup>	<sup>182</sup> 0.0062	<sup>176</sup> 0.0063	<sup>144</sup> 0.0064	<sup>136</sup> 0.0065	<sup>129</sup> 0.0068	<sup>153</sup> 0.0043 N <sup>0.028 33</sup>
38	DERMALOG-007	<sup>149</sup> 0.0080	<sup>148</sup> 0.0092	<sup>131</sup> 0.0102	<sup>128</sup> 0.0118	<sup>125</sup> 0.0140	<sup>130</sup> 0.0006 N <sup>0.190 75</sup>	<sup>175</sup> 0.0051	<sup>170</sup> 0.0054	<sup>140</sup> 0.0056	<sup>132</sup> 0.0058	<sup>124</sup> 0.0063	<sup>147</sup> 0.0020 N <sup>0.068 70</sup>
39	DERMALOG-008	<sup>79</sup> 0.0024	<sup>88</sup> 0.0029	<sup>88</sup> 0.0034	<sup>79</sup> 0.0040	<sup>74</sup> 0.0048	<sup>33</sup> 0.0001 N <sup>0.239 107</sup>	<sup>85</sup> 0.0015	<sup>80</sup> 0.0015	<sup>77</sup> 0.0016	<sup>71</sup> 0.0017	<sup>68</sup> 0.0019	<sup>76</sup> 0.0004 N <sup>0.088 79</sup>
40	FUJITSULAB-000	<sup>59</sup> 0.0019	<sup>59</sup> 0.0022	<sup>66</sup> 0.0025	<sup>51</sup> 0.0029	<sup>54</sup> 0.0033	<sup>59</sup> 0.0001 N <sup>0.190 74</sup>	<sup>68</sup> 0.0013	<sup>61</sup> 0.0014	<sup>57</sup> 0.0014	<sup>54</sup> 0.0015	<sup>50</sup> 0.0016	<sup>85</sup> 0.0006 N <sup>0.099 62</sup>
41	GORILLA-002	<sup>184</sup> 0.0147	<sup>186</sup> 0.0197	<sup>155</sup> 0.0238	<sup>149</sup> 0.0288	<sup>147</sup> 0.0351	<sup>103</sup> 0.0003 N <sup>0.295 144</sup>	<sup>154</sup> 0.0032	<sup>158</sup> 0.0041	<sup>139</sup> 0.0049	<sup>135</sup> 0.0062	<sup>132</sup> 0.0080	<sup>19</sup> 0.0000 N <sup>0.315 149</sup>
42	GORILLA-004	<sup>122</sup> 0.0048	<sup>121</sup> 0.0063	<sup>117</sup> 0.0075	<sup>110</sup> 0.0091	<sup>11</sup>							

MISSES AT GIVEN RANK		ENROL MOST RECENT										
FNIR(N, T=0, R)		RANK 1					RANK 50					
#	ALGORITHM	N=0.64M	N=1.6M	N=3.0M	N=6.0M	$aN^b$	N=0.64M	N=1.6M	N=3.0M	N=6.0M	N=12.0M	$aN^b$
73	MICROSOFT-003	<sup>14</sup> 0.0013	<sup>29</sup> 0.0016	<sup>35</sup> 0.0018	<sup>39</sup> 0.0022	<sup>41</sup> 0.0028	<sup>13</sup> 0.0000 N <sup>0.271 127</sup>	<sup>2</sup> 0.0006	<sup>2</sup> 0.0006	<sup>4</sup> 0.0007	<sup>6</sup> 0.0008	<sup>7</sup> 0.0009
74	MICROSOFT-004	<sup>13</sup> 0.0012	<sup>24</sup> 0.0015	<sup>29</sup> 0.0018	<sup>37</sup> 0.0021	<sup>39</sup> 0.0028	<sup>13</sup> 0.0000 N <sup>0.281 136</sup>	<sup>1</sup> 0.0006	<sup>1</sup> 0.0006	<sup>1</sup> 0.0007	<sup>1</sup> 0.0007	<sup>4</sup> 0.0009
75	MICROSOFT-005	<sup>34</sup> 0.0015	<sup>46</sup> 0.0019	<sup>54</sup> 0.0023	<sup>63</sup> 0.0030	<sup>62</sup> 0.0037	<sup>6</sup> 0.0000 N <sup>0.320 153</sup>	<sup>3</sup> 0.0006	<sup>3</sup> 0.0006	<sup>2</sup> 0.0007	<sup>2</sup> 0.0008	<sup>3</sup> 0.0009
76	MICROSOFT-006	<sup>38</sup> 0.0016	<sup>50</sup> 0.0020	<sup>60</sup> 0.0025	<sup>64</sup> 0.0030	<sup>65</sup> 0.0038	<sup>11</sup> 0.0000 N <sup>0.305 149</sup>	<sup>4</sup> 0.0006	<sup>4</sup> 0.0007	<sup>3</sup> 0.0007	<sup>3</sup> 0.0009	<sup>13</sup> 0.0010
77	NEC-000	<sup>178</sup> 0.0131	<sup>178</sup> 0.0170	<sup>150</sup> 0.0203	<sup>144</sup> 0.0244	<sup>141</sup> 0.0294	<sup>109</sup> 0.0003 N <sup>0.276 132</sup>	<sup>150</sup> 0.0029	<sup>155</sup> 0.0038	<sup>138</sup> 0.0048	<sup>134</sup> 0.0059	<sup>129</sup> 0.0074
78	NEC-001	<sup>190</sup> 0.0180	<sup>188</sup> 0.0209	<sup>154</sup> 0.0233	<sup>148</sup> 0.0266	<sup>143</sup> 0.0304	<sup>146</sup> 0.0016 N <sup>0.179 71</sup>	<sup>204</sup> 0.0109	<sup>197</sup> 0.0113	<sup>159</sup> 0.0116	<sup>152</sup> 0.0121	<sup>149</sup> 0.0129
79	NEC-002	<sup>3</sup> 0.0009	<sup>5</sup> 0.0010	<sup>5</sup> 0.0011	<sup>5</sup> 0.0012	<sup>5</sup> 0.0013	<sup>84</sup> 0.0002 N <sup>0.113 36</sup>	<sup>5</sup> 0.0008	<sup>5</sup> 0.0008	<sup>5</sup> 0.0008	<sup>4</sup> 0.0008	<sup>3</sup> 0.0008
80	NEC-003	<sup>18</sup> 0.0013	<sup>17</sup> 0.0014	<sup>13</sup> 0.0015	<sup>13</sup> 0.0016	<sup>9</sup> 0.0016	<sup>123</sup> 0.0005 N <sup>0.099 17</sup>	<sup>41</sup> 0.0012	<sup>32</sup> 0.0012	<sup>29</sup> 0.0012	<sup>27</sup> 0.0012	<sup>23</sup> 0.0012
81	NEC-004	<sup>23</sup> 0.0014	<sup>17</sup> 0.0014	<sup>15</sup> 0.0015	<sup>12</sup> 0.0016	<sup>10</sup> 0.0017	<sup>131</sup> 0.0006 N <sup>0.059 11</sup>	<sup>35</sup> 0.0013	<sup>48</sup> 0.0013	<sup>43</sup> 0.0013	<sup>41</sup> 0.0013	<sup>23</sup> 0.0013
82	NEUROTECHNOLOGY-003	<sup>180</sup> 0.0179	<sup>184</sup> 0.0225	<sup>156</sup> 0.0263	<sup>151</sup> 0.0306	<sup>148</sup> 0.0361	<sup>138</sup> 0.0007 N <sup>0.239 108</sup>	<sup>167</sup> 0.0042	<sup>171</sup> 0.0057	<sup>149</sup> 0.0072	<sup>145</sup> 0.0090	<sup>140</sup> 0.0112
83	NEUROTECHNOLOGY-004	<sup>116</sup> 0.0046	<sup>114</sup> 0.0056	<sup>111</sup> 0.0064	<sup>106</sup> 0.0074	<sup>102</sup> 0.0088	<sup>97</sup> 0.0002 N <sup>0.220 90</sup>	<sup>127</sup> 0.0022	<sup>124</sup> 0.0025	<sup>117</sup> 0.0028	<sup>112</sup> 0.0031	<sup>104</sup> 0.0034
84	NEUROTECHNOLOGY-005	<sup>100</sup> 0.0035	<sup>100</sup> 0.0043	<sup>100</sup> 0.0049	<sup>96</sup> 0.0057	<sup>91</sup> 0.0068	<sup>74</sup> 0.0002 N <sup>0.235 133</sup>	<sup>123</sup> 0.0021	<sup>120</sup> 0.0023	<sup>111</sup> 0.0024	<sup>106</sup> 0.0025	<sup>98</sup> 0.0028
85	NEUROTECHNOLOGY-007	<sup>98</sup> 0.0032	<sup>96</sup> 0.0039	<sup>97</sup> 0.0044	<sup>93</sup> 0.0052	<sup>89</sup> 0.0062	<sup>63</sup> 0.0002 N <sup>0.222 92</sup>	<sup>118</sup> 0.0020	<sup>115</sup> 0.0022	<sup>108</sup> 0.0023	<sup>101</sup> 0.0024	<sup>92</sup> 0.0026
86	NEUROTECHNOLOGY-008	<sup>94</sup> 0.0019	<sup>97</sup> 0.0022	<sup>97</sup> 0.0025	<sup>89</sup> 0.0029	<sup>85</sup> 0.0034	<sup>44</sup> 0.0001 N <sup>0.205 83</sup>	<sup>64</sup> 0.0013	<sup>52</sup> 0.0013	<sup>49</sup> 0.0013	<sup>46</sup> 0.0014	<sup>42</sup> 0.0015
87	NEUROTECHNOLOGY-009	<sup>14</sup> 0.0013	<sup>18</sup> 0.0014	<sup>20</sup> 0.0016	<sup>22</sup> 0.0018	<sup>21</sup> 0.0021	<sup>33</sup> 0.0001 N <sup>0.162 61</sup>	<sup>26</sup> 0.0011	<sup>26</sup> 0.0011	<sup>23</sup> 0.0011	<sup>21</sup> 0.0012	<sup>11</sup> 0.0012
88	NTECHLAB-003	<sup>119</sup> 0.0046	<sup>120</sup> 0.0062	<sup>118</sup> 0.0076	<sup>119</sup> 0.0094	<sup>115</sup> 0.0114	<sup>29</sup> 0.0001 N <sup>0.310 150</sup>	<sup>63</sup> 0.0013	<sup>86</sup> 0.0016	<sup>94</sup> 0.0018	<sup>98</sup> 0.0022	<sup>93</sup> 0.0026
89	NTECHLAB-004	<sup>107</sup> 0.0037	<sup>110</sup> 0.0048	<sup>107</sup> 0.0058	<sup>103</sup> 0.0071	<sup>100</sup> 0.0085	<sup>26</sup> 0.0001 N <sup>0.291 141</sup>	<sup>32</sup> 0.0011	<sup>37</sup> 0.0013	<sup>39</sup> 0.0015	<sup>39</sup> 0.0017	<sup>33</sup> 0.0017
90	NTECHLAB-005	<sup>103</sup> 0.0035	<sup>103</sup> 0.0047	<sup>108</sup> 0.0058	<sup>104</sup> 0.0073	<sup>105</sup> 0.0092	<sup>15</sup> 0.0000 N <sup>0.334 156</sup>	<sup>9</sup> 0.0008	<sup>23</sup> 0.0011	<sup>32</sup> 0.0012	<sup>60</sup> 0.0015	<sup>67</sup> 0.0019
91	NTECHLAB-006	<sup>97</sup> 0.0030	<sup>100</sup> 0.0041	<sup>101</sup> 0.0050	<sup>98</sup> 0.0062	<sup>97</sup> 0.0078	<sup>14</sup> 0.0000 N <sup>0.299 141</sup>	<sup>6</sup> 0.0008	<sup>12</sup> 0.0009	<sup>22</sup> 0.0011	<sup>31</sup> 0.0013	<sup>34</sup> 0.0016
92	NTECHLAB-007	<sup>74</sup> 0.0022	<sup>74</sup> 0.0027	<sup>75</sup> 0.0031	<sup>74</sup> 0.0037	<sup>75</sup> 0.0044	<sup>35</sup> 0.0001 N <sup>0.245 112</sup>	<sup>30</sup> 0.0018	<sup>35</sup> 0.0012	<sup>38</sup> 0.0013	<sup>47</sup> 0.0014	<sup>47</sup> 0.0015
93	NTECHLAB-008	<sup>26</sup> 0.0014	<sup>36</sup> 0.0017	<sup>37</sup> 0.0020	<sup>45</sup> 0.0024	<sup>39</sup> 0.0027	<sup>21</sup> 0.0001 N <sup>0.224 95</sup>	<sup>21</sup> 0.0010	<sup>22</sup> 0.0010	<sup>20</sup> 0.0011	<sup>20</sup> 0.0011	<sup>19</sup> 0.0012
94	NTECHLAB-009	<sup>17</sup> 0.0012	<sup>17</sup> 0.0013	<sup>10</sup> 0.0014	<sup>11</sup> 0.0015	<sup>14</sup> 0.0018	<sup>74</sup> 0.0002 N <sup>0.140 45</sup>	<sup>17</sup> 0.0009	<sup>14</sup> 0.0009	<sup>13</sup> 0.0010	<sup>13</sup> 0.0010	<sup>12</sup> 0.0010
95	NTECHLAB-010	<sup>8</sup> 0.0011	<sup>10</sup> 0.0011	<sup>10</sup> 0.0012	<sup>7</sup> 0.0013	<sup>7</sup> 0.0014	<sup>105</sup> 0.0003 N <sup>0.091 26</sup>	<sup>20</sup> 0.0010	<sup>20</sup> 0.0010	<sup>16</sup> 0.0010	<sup>14</sup> 0.0010	<sup>11</sup> 0.0010
96	PARAVISION-003	<sup>88</sup> 0.0026	<sup>84</sup> 0.0031	<sup>84</sup> 0.0035	<sup>81</sup> 0.0042	<sup>79</sup> 0.0048	<sup>89</sup> 0.0002 N <sup>0.210 86</sup>	<sup>97</sup> 0.0016	<sup>95</sup> 0.0017	<sup>93</sup> 0.0018	<sup>88</sup> 0.0020	<sup>79</sup> 0.0021
97	PARAVISION-004	<sup>34</sup> 0.0015	<sup>28</sup> 0.0016	<sup>28</sup> 0.0017	<sup>25</sup> 0.0019	<sup>22</sup> 0.0021	<sup>114</sup> 0.0003 N <sup>0.111 33</sup>	<sup>60</sup> 0.0013	<sup>51</sup> 0.0013	<sup>44</sup> 0.0013	<sup>36</sup> 0.0013	<sup>26</sup> 0.0014
98	PARAVISION-005	<sup>39</sup> 0.0015	<sup>21</sup> 0.0015	<sup>21</sup> 0.0016	<sup>20</sup> 0.0018	<sup>17</sup> 0.0019	<sup>119</sup> 0.0004 N <sup>0.094 27</sup>	<sup>65</sup> 0.0013	<sup>54</sup> 0.0013	<sup>47</sup> 0.0013	<sup>40</sup> 0.0013	<sup>33</sup> 0.0014
99	PARAVISION-007	<sup>10</sup> 0.0011	<sup>9</sup> 0.0012	<sup>9</sup> 0.0012	<sup>8</sup> 0.0013	<sup>8</sup> 0.0015	<sup>107</sup> 0.0003 N <sup>0.091 25</sup>	<sup>22</sup> 0.0010	<sup>17</sup> 0.0010	<sup>15</sup> 0.0010	<sup>16</sup> 0.0010	<sup>14</sup> 0.0011
100	PIXELALL-002	<sup>109</sup> 0.0037	<sup>108</sup> 0.0045	<sup>103</sup> 0.0052	<sup>99</sup> 0.0062	<sup>95</sup> 0.0075	<sup>57</sup> 0.0002 N <sup>0.238 106</sup>	<sup>102</sup> 0.0017	<sup>108</sup> 0.0019	<sup>104</sup> 0.0021	<sup>102</sup> 0.0024	<sup>85</sup> 0.0027
101	PIXELALL-003	<sup>106</sup> 0.0039	<sup>106</sup> 0.0048	<sup>106</sup> 0.0058	<sup>104</sup> 0.0071	<sup>102</sup> 0.0085	<sup>64</sup> 0.0002 N <sup>0.182 73</sup>	<sup>75</sup> 0.0014	<sup>69</sup> 0.0014	<sup>61</sup> 0.0014	<sup>57</sup> 0.0015	<sup>49</sup> 0.0016
102	PIXELALL-004	<sup>46</sup> 0.0017	<sup>59</sup> 0.0020	<sup>53</sup> 0.0023	<sup>51</sup> 0.0026	<sup>47</sup> 0.0030	<sup>97</sup> 0.0001 N <sup>0.192 76</sup>	<sup>62</sup> 0.0013	<sup>55</sup> 0.0013	<sup>54</sup> 0.0014	<sup>51</sup> 0.0014	<sup>44</sup> 0.0015
103	PIXELALL-005	<sup>40</sup> 0.0018	<sup>46</sup> 0.0019	<sup>38</sup> 0.0020	<sup>36</sup> 0.0021	<sup>31</sup> 0.0024	<sup>125</sup> 0.0005 N <sup>0.098 28</sup>	<sup>89</sup> 0.0015	<sup>85</sup> 0.0016	<sup>75</sup> 0.0016	<sup>64</sup> 0.0016	<sup>55</sup> 0.0016
104	PTAKURATSATU-000	<sup>85</sup> 0.0025	<sup>86</sup> 0.0030	<sup>83</sup> 0.0036	<sup>78</sup> 0.0040	<sup>67</sup> 0.0040	<sup>184</sup> 0.0003 N <sup>0.167 63</sup>	<sup>88</sup> 0.0015	<sup>88</sup> 0.0016	<sup>96</sup> 0.0018	<sup>87</sup> 0.0020	<sup>74</sup> 0.0020
105	QUANTASOFT-001	<sup>238</sup> 0.2177	<sup>238</sup> 0.2177	<sup>192</sup> 0.2177	<sup>158</sup> 0.2177	<sup>163</sup> 0.2177	<sup>1000.0 1</sup>	<sup>236</sup> 0.1116	<sup>232</sup> 0.1116	<sup>171</sup> 0.1116	<sup>158</sup> 0.1116	<sup>163</sup> 0.1116
106	RANKONE-002	<sup>158</sup> 0.0155	<sup>158</sup> 0.0194	<sup>153</sup> 0.0224	<sup>147</sup> 0.0262	<sup>144</sup> 0.0304	<sup>136</sup> 0.0007 N <sup>0.230 99</sup>	<sup>172</sup> 0.0048	<sup>174</sup> 0.0060	<sup>147</sup> 0.0071	<sup>147</sup> 0.0085	<sup>144</sup> 0.0102
107	RANKONE-003	<sup>147</sup> 0.0155	<sup>148</sup> 0.0194	<sup>150</sup> 0.0224	<sup>146</sup> 0.0262	<sup>144</sup> 0.0304	<sup>136</sup> 0.0007 N <sup>0.230 98</sup>	<sup>171</sup> 0.0048	<sup>175</sup> 0.0060	<sup>147</sup> 0.0071	<sup>146</sup> 0.0085	<sup>143</sup> 0.0102
108	RANKONE-005	<sup>148</sup> 0.0075	<sup>150</sup> 0.0094	<sup>135</sup> 0.0110	<sup>131</sup> 0.0132	<sup>128</sup> 0.0156	<sup>96</sup> 0.0003 N <sup>0.251 115</sup>	<sup>144</sup> 0.0026	<sup>145</sup> 0.0032	<sup>131</sup> 0.0036	<sup>126</sup> 0.0043	<sup>118</sup> 0.0050
109	RANKONE-007	<sup>89</sup> 0.0028	<sup>88</sup> 0.0034	<sup>87</sup> 0.0038	<sup>83</sup> 0.0045	<sup>81</sup> 0.0053	<sup>66</sup> 0.0002 N <sup>0.211 87</sup>	<sup>87</sup> 0.0015	<sup>90</sup> 0.0017	<sup>89</sup> 0.0018	<sup>83</sup> 0.0019	<sup>81</sup> 0.0021
110	RANKONE-009	<sup>61</sup> 0.0020	<sup>66</sup> 0.0024	<sup>67</sup> 0.0027	<sup>68</sup> 0.0032	<sup>64</sup> 0.0038	<sup>38</sup> 0.0001 N <sup>0.219 89</sup>	<sup>71</sup> 0.0013	<sup>65</sup> 0.0014	<sup>64</sup> 0.0015	<sup>58</sup> 0.0015	<sup>51</sup> 0.0016
111	RANKONE-010	<sup>68</sup> 0.0020	<sup>68</sup> 0.0022	<sup>68</sup> 0.0025	<sup>58</sup> 0.0029	<sup>53</sup> 0.0032	<sup>48</sup> 0.0002 N <sup>0.164 62</sup>	<sup>82</sup> 0.0014	<sup>75</sup> 0.0015	<sup>70</sup> 0.0015	<sup>62</sup> 0.0016	<sup>57</sup> 0.0017
112	RANKONE-011	<sup>21</sup> 0.0014	<sup>22</sup> 0.0015	<sup>23</sup> 0.0017	<sup>23</sup> 0.0018	<sup>24</sup> 0.0021	<sup>77</sup> 0.0002 N <sup>0.150 51</sup>	<sup>34</sup> 0.0011	<sup>28</sup> 0.0012	<sup>28</sup> 0.0012	<sup>24</sup> 0.0012	<sup>21</sup> 0.0012
113	REALNETWORKS-002	<sup>201</sup> 0.0299	<sup>201</sup> 0.0393	<sup>163</sup> 0.0470	<sup>159</sup> 0.0562	<sup>156</sup> 0.0580	<sup>141</sup> 0.0013 N <sup>0.236 105</sup>	<sup>176</sup> 0.0054	<sup>186</sup> 0.0076	<sup>159</sup> 0.0097	<sup>153</sup> 0.0126	<sup>150</sup> 0.0132
114	REALNETWORKS-003	<sup>191</sup> 0.0183	<sup>191</sup> 0.0242	<sup>158</sup> 0.0291	<sup>153</sup> 0.0352	<sup>152</sup> 0.0423	<sup>115</sup> 0.0004 N <sup>0.250 110</sup>	<sup>166</sup> 0.0041	<sup>166</sup> 0.0054	<sup>143</sup> 0.0064	<sup>144</sup> 0.0080	<sup>142</sup> 0.0101
115	REALNETWORKS-004	<sup>188</sup> 0.0175	<sup>187</sup> 0.0236	<sup>157</sup> 0.0284	<sup>152</sup> 0.0347	<sup>149</sup> 0.0416	<sup>112</sup> 0.0003 N <sup>0.295 143</sup>	<sup>163</sup> 0.0040	<sup>164</sup> 0.0050	<sup>142</sup> 0.0061	<sup>142</sup> 0.0078	<sup>141</sup> 0.0099
116	REALNETWORKS-005	<sup>69</sup> 0.0020	<sup>68</sup> 0.0023	<sup>65</sup> 0.0026	<sup>62</sup> 0.0030	<sup>59</sup> 0.0037	<sup>45</sup> 0.0001 N <sup>0.207 84</sup>	<sup>36</sup> 0.0012	<sup>36</sup> 0.0012	<sup>41</sup> 0.0013	<sup>45</sup> 0.0014	<sup>40</sup> 0.0015
117	REMARKA-000	<sup>87</sup> 0.0027	<sup>90</sup> 0.0034	<sup>90</sup> 0.0040	<sup>88</sup> 0.0048	<sup>84</sup> 0.0058	<sup>30</sup> 0.0001 N <sup>0.260 121</sup>	<sup>83</sup> 0.0014	<sup>82</sup> 0.0015	<sup>78</sup> 0.0016	<sup>73</sup> 0.0018	<sup>71</sup> 0.0020
118	RENDIP-000	<sup>25</sup> 0.0014	<sup>26</sup> 0.0015	<sup>27</sup> 0.0017	<sup>26</sup> 0.0019	<sup>24</sup> 0.0022	<sup>46</sup> 0.0002 N <sup>0.158 56</sup>	<sup>35</sup> 0.0012	<sup>34</sup> 0.0012	<sup>31</sup> 0.0012	<sup>26</sup> 0.0012	<sup>24</sup> 0.0013
119	SI-000	<sup>68</sup> 0.0021	<sup>66</sup> 0.0024	<sup>70</sup> 0.0028	<sup>69</sup> 0.0032	<sup>63</sup> 0.0037	<sup>58</sup> 0.0001 N <sup>0.203 80</sup>	<sup>84</sup> 0.0014	<sup>79</sup> 0.0015	<sup>72</sup> 0.0015	<sup>66</sup> 0.0016	<sup>58</sup> 0.0017
120	SCANOVATE-000	<sup>119</sup> 0.0038	<sup>11</sup>									

This publication is available free of charge from: https://doi.org/10.6028/NIST.IR.8271

MISSES AT GIVEN RANK		ENROL MOST RECENT											
FNIR(N, T= 0, R)		RANK 1					RANK 50						
#	ALGORITHM	N=0.64M	N=1.6M	N=3.0M	N=6.0M	N=12.0M	$\alpha N^b$	N=0.64M	N=1.6M	N=3.0M	N=6.0M	N=12.0M	$\alpha N^b$
145	VERIDAS-002	<sup>75</sup> 0.0023	<sup>77</sup> 0.0028	<sup>69</sup> 0.0028	<sup>67</sup> 0.0032	<sup>61</sup> 0.0037	<sup>100</sup> 0.0003 N <sup>0.158 55</sup>	<sup>78</sup> 0.0014	<sup>72</sup> 0.0015	<sup>63</sup> 0.0015	<sup>59</sup> 0.0015	<sup>53</sup> 0.0016	<sup>113</sup> 0.0007 N <sup>0.047 50</sup>
146	VIGILANTSOLUTIONS-008	<sup>81</sup> 0.0025	<sup>82</sup> 0.0029	<sup>82</sup> 0.0034	<sup>80</sup> 0.0040	<sup>79</sup> 0.0047	<sup>46</sup> 0.0001 N <sup>0.224 94</sup>	<sup>37</sup> 0.0012	<sup>45</sup> 0.0013	<sup>59</sup> 0.0014	<sup>61</sup> 0.0015	<sup>59</sup> 0.0017	<sup>59</sup> 0.0002 N <sup>0.150 103</sup>
147	VISIONBOX-000	<sup>48</sup> 0.0017	<sup>47</sup> 0.0019	<sup>51</sup> 0.0022	<sup>193</sup> 1.0000	<sup>183</sup> 0.9526	<sup>6</sup> 0.0000 N <sup>2.570 163</sup>	<sup>49</sup> 0.0012	<sup>43</sup> 0.0013	<sup>46</sup> 0.0013	<sup>168</sup> 1.0000	<sup>163</sup> 0.9525	<sup>1</sup> 0.0000 N <sup>2.719 163</sup>
148	VISIONLABS-004	<sup>72</sup> 0.0022	<sup>76</sup> 0.0027	<sup>80</sup> 0.0032	<sup>82</sup> 0.0044	<sup>92</sup> 0.0070	<sup>6</sup> 0.0000 N <sup>0.387 157</sup>	<sup>50</sup> 0.0012	<sup>63</sup> 0.0014	<sup>80</sup> 0.0017	<sup>104</sup> 0.0025	<sup>115</sup> 0.0045	<sup>3</sup> 0.0000 N <sup>0.435 156</sup>
149	VISIONLABS-005	<sup>59</sup> 0.0020	<sup>67</sup> 0.0024	<sup>73</sup> 0.0029	<sup>72</sup> 0.0037	<sup>80</sup> 0.0051	<sup>19</sup> 0.0000 N <sup>0.322 154</sup>	<sup>46</sup> 0.0012	<sup>49</sup> 0.0013	<sup>74</sup> 0.0016	<sup>84</sup> 0.0019	<sup>100</sup> 0.0029	<sup>11</sup> 0.0000 N <sup>0.298 144</sup>
150	VISIONLABS-006	<sup>42</sup> 0.0016	<sup>44</sup> 0.0018	<sup>52</sup> 0.0022	<sup>56</sup> 0.0028	<sup>68</sup> 0.0041	<sup>9</sup> 0.0000 N <sup>0.314 152</sup>	<sup>42</sup> 0.0012	<sup>44</sup> 0.0013	<sup>65</sup> 0.0015	<sup>78</sup> 0.0019	<sup>96</sup> 0.0027	<sup>13</sup> 0.0000 N <sup>0.275 138</sup>
151	VISIONLABS-007	<sup>40</sup> 0.0016	<sup>38</sup> 0.0018	<sup>39</sup> 0.0020	<sup>43</sup> 0.0023	<sup>46</sup> 0.0034	<sup>16</sup> 0.0001 N <sup>0.248 113</sup>	<sup>39</sup> 0.0012	<sup>38</sup> 0.0012	<sup>35</sup> 0.0013	<sup>34</sup> 0.0013	<sup>30</sup> 0.0020	<sup>42</sup> 0.0001 N <sup>0.152 109</sup>
152	VISIONLABS-008	<sup>53</sup> 0.0019	<sup>53</sup> 0.0020	<sup>47</sup> 0.0021	<sup>50</sup> 0.0025	<sup>48</sup> 0.0030	<sup>73</sup> 0.0002 N <sup>0.169 64</sup>	<sup>100</sup> 0.0016	<sup>98</sup> 0.0017	<sup>87</sup> 0.0017	<sup>89</sup> 0.0020	<sup>88</sup> 0.0023	<sup>69</sup> 0.0003 N <sup>0.114 93</sup>
153	VISIONLABS-009	<sup>9</sup> 0.0011	<sup>8</sup> 0.0011	<sup>8</sup> 0.0012	<sup>9</sup> 0.0014	<sup>13</sup> 0.0017	<sup>43</sup> 0.0001 N <sup>0.160 60</sup>	<sup>20</sup> 0.0010	<sup>16</sup> 0.0010	<sup>17</sup> 0.0010	<sup>19</sup> 0.0011	<sup>37</sup> 0.0014	<sup>57</sup> 0.0002 N <sup>0.109 89</sup>
154	VISIONLABS-010	<sup>20</sup> 0.0014	<sup>15</sup> 0.0014	<sup>17</sup> 0.0015	<sup>18</sup> 0.0017	<sup>19</sup> 0.0021	<sup>80</sup> 0.0002 N <sup>0.137 44</sup>	<sup>54</sup> 0.0013	<sup>41</sup> 0.0013	<sup>48</sup> 0.0013	<sup>50</sup> 0.0014	<sup>56</sup> 0.0017	<sup>71</sup> 0.0004 N <sup>0.090 82</sup>
155	VOCORD-005	<sup>132</sup> 0.0060	<sup>131</sup> 0.0070	<sup>122</sup> 0.0082	<sup>121</sup> 0.0097	<sup>119</sup> 0.0117	<sup>96</sup> 0.0003 N <sup>0.232 103</sup>	<sup>158</sup> 0.0033	<sup>152</sup> 0.0035	<sup>133</sup> 0.0037	<sup>122</sup> 0.0040	<sup>114</sup> 0.0043	<sup>127</sup> 0.0010 N <sup>0.090 81</sup>
156	VTS-001	<sup>19</sup> 0.0014	<sup>25</sup> 0.0015	<sup>26</sup> 0.0017	<sup>29</sup> 0.0019	<sup>30</sup> 0.0023	<sup>44</sup> 0.0001 N <sup>0.179 72</sup>	<sup>19</sup> 0.0010	<sup>19</sup> 0.0010	<sup>19</sup> 0.0010	<sup>17</sup> 0.0011	<sup>16</sup> 0.0011	<sup>81</sup> 0.0005 N <sup>0.051 55</sup>
157	XFORWARDAI-000	<sup>68</sup> 0.0021	<sup>61</sup> 0.0023	<sup>55</sup> 0.0024	<sup>52</sup> 0.0027	<sup>45</sup> 0.0029	<sup>124</sup> 0.0005 N <sup>0.111 34</sup>	<sup>113</sup> 0.0019	<sup>107</sup> 0.0019	<sup>100</sup> 0.0019	<sup>90</sup> 0.0020	<sup>75</sup> 0.0020	<sup>141</sup> 0.0015 N <sup>0.018 22</sup>
158	XFORWARDAI-001	<sup>62</sup> 0.0020	<sup>55</sup> 0.0020	<sup>45</sup> 0.0021	<sup>38</sup> 0.0022	<sup>32</sup> 0.0024	<sup>140</sup> 0.0009 N <sup>0.085 10</sup>	<sup>112</sup> 0.0019	<sup>106</sup> 0.0019	<sup>98</sup> 0.0019	<sup>82</sup> 0.0019	<sup>68</sup> 0.0019	<sup>145</sup> 0.0018 N <sup>0.004 7</sup>
159	XFORWARDAI-002	<sup>58</sup> 0.0019	<sup>49</sup> 0.0020	<sup>41</sup> 0.0020	<sup>35</sup> 0.0021	<sup>26</sup> 0.0022	<sup>142</sup> 0.0011 N <sup>0.038 5</sup>	<sup>111</sup> 0.0019	<sup>104</sup> 0.0019	<sup>97</sup> 0.0019	<sup>81</sup> 0.0019	<sup>66</sup> 0.0019	<sup>144</sup> 0.0018 N <sup>0.003 6</sup>
160	YITU-002	<sup>38</sup> 0.0016	<sup>43</sup> 0.0018	<sup>46</sup> 0.0021	<sup>46</sup> 0.0024	<sup>46</sup> 0.0029	<sup>32</sup> 0.0001 N <sup>0.213 88</sup>	<sup>18</sup> 0.0009	<sup>21</sup> 0.0010	<sup>18</sup> 0.0010	<sup>18</sup> 0.0011	<sup>17</sup> 0.0012	<sup>70</sup> 0.0004 N <sup>0.073 72</sup>
161	YITU-003	<sup>84</sup> 0.0026	<sup>81</sup> 0.0029	<sup>76</sup> 0.0031	<sup>70</sup> 0.0035	<sup>66</sup> 0.0039	<sup>119</sup> 0.0004 N <sup>0.141 47</sup>	<sup>119</sup> 0.0020	<sup>114</sup> 0.0021	<sup>107</sup> 0.0022	<sup>100</sup> 0.0023	<sup>90</sup> 0.0024	<sup>128</sup> 0.0010 N <sup>0.054 56</sup>
162	YITU-004	<sup>11</sup> 0.0011	<sup>12</sup> 0.0013	<sup>18</sup> 0.0015	<sup>19</sup> 0.0017	<sup>26</sup> 0.0047	<sup>4</sup> 0.0000 N <sup>0.438 158</sup>	<sup>11</sup> 0.0008	<sup>9</sup> 0.0009	<sup>9</sup> 0.0009	<sup>9</sup> 0.0009	<sup>105</sup> 0.0036	<sup>6</sup> 0.0000 N <sup>0.395 155</sup>
163	YITU-005	<sup>73</sup> 0.0022	<sup>63</sup> 0.0023	<sup>59</sup> 0.0025	<sup>53</sup> 0.0027	<sup>49</sup> 0.0031	<sup>126</sup> 0.0005 N <sup>0.113 35</sup>	<sup>114</sup> 0.0020	<sup>109</sup> 0.0020	<sup>103</sup> 0.0020	<sup>92</sup> 0.0020	<sup>77</sup> 0.0020	<sup>143</sup> 0.0017 N <sup>0.012 13</sup>

**Table 20: Investigation-mode: Effect of N on FNIR on recent images** For five enrollment population sizes, N, with T = 0 and FPIR = 1. The left five columns are rank 1 miss rates The right five columns are rank 50 miss rates Missing entries usually apply because another algorithm from the same developer was run instead. Some developers are missing because less accurate algorithms were not run on galleries with N > 1 600 000. Throughout blue superscripts indicate the rank of the algorithm for that column, and yellow highlighting indicates the most accurate value. Caution: The Power-low models are mostly intended to draw attention to the kind of behavior, not as a model to be used for prediction.

MISSES OUTSIDE RANK R		RESOURCE USAGE		ENROL MOST RECENT, N = 1.6M					
FNIR(N, T=0, R)		TEMPLATE		FRVT 2018 MUGSHOTS					
#	ALGORITHM	BYTES	MSEC	R=1	R=5	R=10	R=20	R=50	WORK-10
1	20FACE-000	<sup>144</sup> 2048	<sup>39</sup> 247	<sup>210</sup> 0.0552	<sup>201</sup> 0.0269	<sup>203</sup> 0.0198	<sup>200</sup> 0.0146	<sup>190</sup> 0.0099	<sup>205</sup> 1.275
2	3DIVI-003	<sup>35</sup> 512	<sup>128</sup> 625	<sup>219</sup> 0.0833	<sup>214</sup> 0.0444	<sup>214</sup> 0.0349	<sup>210</sup> 0.0270	<sup>210</sup> 0.0191	<sup>212</sup> 1.447
3	3DIVI-004	<sup>226</sup> 4096	<sup>128</sup> 628	<sup>179</sup> 0.0175	<sup>173</sup> 0.0091	<sup>170</sup> 0.0075	<sup>167</sup> 0.0061	<sup>162</sup> 0.0049	<sup>176</sup> 1.092
4	3DIVI-005	<sup>227</sup> 4096	<sup>135</sup> 653	<sup>180</sup> 0.0176	<sup>173</sup> 0.0091	<sup>168</sup> 0.0074	<sup>166</sup> 0.0061	<sup>163</sup> 0.0049	<sup>177</sup> 1.092
5	3DIVI-006	<sup>49</sup> 528	<sup>137</sup> 653	<sup>190</sup> 0.0240	<sup>196</sup> 0.0171	<sup>199</sup> 0.0160	<sup>201</sup> 0.0154	<sup>200</sup> 0.0148	<sup>195</sup> 1.162
6	ACER-000	<sup>37</sup> 512	<sup>29</sup> 201	<sup>187</sup> 0.0106	<sup>141</sup> 0.0051	<sup>138</sup> 0.0041	<sup>137</sup> 0.0034	<sup>129</sup> 0.0026	<sup>142</sup> 1.053
7	AIZE-001	<sup>143</sup> 2048	<sup>76</sup> 403	<sup>118</sup> 0.0056	<sup>120</sup> 0.0037	<sup>123</sup> 0.0033	<sup>120</sup> 0.0030	<sup>130</sup> 0.0027	<sup>120</sup> 1.035
8	ALCHERA-000	<sup>151</sup> 2048	<sup>43</sup> 263	<sup>175</sup> 0.0161	<sup>184</sup> 0.0124	<sup>189</sup> 0.0117	<sup>194</sup> 0.0111	<sup>190</sup> 0.0105	<sup>183</sup> 1.116
9	ALCHERA-001	<sup>171</sup> 2048	<sup>6</sup> 66	<sup>245</sup> 0.9869	<sup>243</sup> 0.9782	<sup>243</sup> 0.9735	<sup>245</sup> 0.9679	<sup>244</sup> 0.9590	<sup>245</sup> 9.811
10	ALCHERA-002	<sup>146</sup> 2048	<sup>14</sup> 115	<sup>220</sup> 0.0949	<sup>219</sup> 0.0555	<sup>217</sup> 0.0443	<sup>217</sup> 0.0354	<sup>215</sup> 0.0254	<sup>219</sup> 1.544
11	ALCHERA-003	<sup>173</sup> 2048	<sup>116</sup> 548	<sup>154</sup> 0.0104	<sup>144</sup> 0.0054	<sup>144</sup> 0.0045	<sup>144</sup> 0.0038	<sup>144</sup> 0.0032	<sup>146</sup> 1.055
12	ALCHERA-004	<sup>123</sup> 2048	<sup>213</sup> 854	<sup>159</sup> 0.0110	<sup>140</sup> 0.0049	<sup>134</sup> 0.0038	<sup>129</sup> 0.0032	<sup>126</sup> 0.0025	<sup>140</sup> 1.051
13	ALGOVISION-000	<sup>163</sup> 2048	<sup>84</sup> 425	<sup>162</sup> 0.0114	<sup>167</sup> 0.0084	<sup>173</sup> 0.0078	<sup>174</sup> 0.0073	<sup>179</sup> 0.0067	<sup>167</sup> 1.079
14	ALGOVISION-001	<sup>170</sup> 2048	<sup>193</sup> 792	<sup>145</sup> 0.0090	<sup>136</sup> 0.0048	<sup>132</sup> 0.0040	<sup>136</sup> 0.0033	<sup>134</sup> 0.0027	<sup>138</sup> 1.048
15	ANKE-000	<sup>203</sup> 2072	<sup>86</sup> 431	<sup>170</sup> 0.0132	<sup>158</sup> 0.0073	<sup>157</sup> 0.0060	<sup>156</sup> 0.0050	<sup>150</sup> 0.0040	<sup>163</sup> 1.072
16	ANKE-001	<sup>202</sup> 2072	<sup>88</sup> 433	<sup>171</sup> 0.0132	<sup>159</sup> 0.0073	<sup>159</sup> 0.0061	<sup>159</sup> 0.0050	<sup>159</sup> 0.0040	<sup>164</sup> 1.073
17	ANKE-002	<sup>192</sup> 2056	<sup>131</sup> 641	<sup>79</sup> 0.0028	<sup>80</sup> 0.0020	<sup>80</sup> 0.0018	<sup>87</sup> 0.0018	<sup>91</sup> 0.0017	<sup>81</sup> 1.019
18	AWARE-003	<sup>204</sup> 2076	<sup>171</sup> 716	<sup>197</sup> 0.0306	<sup>194</sup> 0.0162	<sup>191</sup> 0.0127	<sup>188</sup> 0.0100	<sup>180</sup> 0.0075	<sup>186</sup> 1.163
19	AWARE-004	<sup>202</sup> 2072	<sup>92</sup> 433	<sup>168</sup> 0.0679	<sup>214</sup> 0.0679	<sup>211</sup> 0.0348	<sup>208</sup> 0.0274	<sup>208</sup> 0.0208	<sup>203</sup> 1.354
20	AWARE-005	<sup>215</sup> 3100	<sup>200</sup> 827	<sup>198</sup> 0.0311	<sup>195</sup> 0.0167	<sup>193</sup> 0.0134	<sup>190</sup> 0.0107	<sup>191</sup> 0.0082	<sup>197</sup> 1.167
21	AWARE-006	<sup>3</sup> 124	<sup>196</sup> 818	<sup>216</sup> 0.0697	<sup>209</sup> 0.0369	<sup>209</sup> 0.0288	<sup>209</sup> 0.0223	<sup>209</sup> 0.0158	<sup>213</sup> 1.371
22	AYONIX-000	<sup>77</sup> 1036	<sup>1</sup> 10	<sup>239</sup> 0.4505	<sup>240</sup> 0.3540	<sup>240</sup> 0.3176	<sup>240</sup> 0.2834	<sup>240</sup> 0.2381	<sup>240</sup> 4.288
23	AYONIX-001	<sup>78</sup> 1036	<sup>1</sup> 12	<sup>234</sup> 0.3414	<sup>234</sup> 0.2338	<sup>234</sup> 0.1977	<sup>235</sup> 0.1652	<sup>234</sup> 0.1274	<sup>234</sup> 3.226
24	AYONIX-002	<sup>80</sup> 1036	<sup>4</sup> 11	<sup>235</sup> 0.3414	<sup>235</sup> 0.2338	<sup>235</sup> 0.1977	<sup>234</sup> 0.1652	<sup>235</sup> 0.1274	<sup>235</sup> 3.226
25	CAMVI-003	<sup>66</sup> 1024	<sup>164</sup> 707	<sup>209</sup> 0.0520	<sup>218</sup> 0.0517	<sup>219</sup> 0.0517	<sup>222</sup> 0.0517	<sup>222</sup> 0.0517	<sup>217</sup> 1.466
26	CAMVI-004	<sup>67</sup> 1024	<sup>173</sup> 718	<sup>207</sup> 0.0468	<sup>210</sup> 0.0465	<sup>218</sup> 0.0465	<sup>219</sup> 0.0464	<sup>221</sup> 0.0464	<sup>214</sup> 1.419
27	CAMVI-005	<sup>63</sup> 1024	<sup>184</sup> 769	<sup>213</sup> 0.0652	<sup>220</sup> 0.0648	<sup>223</sup> 0.0648	<sup>224</sup> 0.0648	<sup>226</sup> 0.0647	<sup>220</sup> 1.584
28	CIB-000	<sup>243</sup> 8196	<sup>143</sup> 674	<sup>26</sup> 0.0015	<sup>27</sup> 0.0013	<sup>28</sup> 0.0012	<sup>30</sup> 0.0012	<sup>30</sup> 0.0012	<sup>29</sup> 1.012
29	CLOUDWALK-HR-000	<sup>128</sup> 2048	<sup>230</sup> 908	<sup>21</sup> 0.0015	<sup>24</sup> 0.0014	<sup>48</sup> 0.0014	<sup>56</sup> 0.0014	<sup>60</sup> 0.0014	<sup>40</sup> 1.013
30	COGENT-000	<sup>47</sup> 525	<sup>117</sup> 551	<sup>186</sup> 0.0105	<sup>178</sup> 0.0096	<sup>183</sup> 0.0095	<sup>181</sup> 0.0095	<sup>181</sup> 0.0095	<sup>181</sup> 1.088
31	COGENT-001	<sup>46</sup> 525	<sup>118</sup> 552	<sup>155</sup> 0.0105	<sup>179</sup> 0.0096	<sup>182</sup> 0.0095	<sup>180</sup> 0.0095	<sup>180</sup> 0.0095	<sup>180</sup> 1.088
32	COGENT-002	<sup>82</sup> 1043	<sup>243</sup> 987	<sup>95</sup> 0.0036	<sup>89</sup> 0.0022	<sup>88</sup> 0.0020	<sup>85</sup> 0.0018	<sup>83</sup> 0.0015	<sup>90</sup> 1.021
33	COGENT-003	<sup>81</sup> 1043	<sup>243</sup> 960	<sup>95</sup> 0.0038	<sup>90</sup> 0.0024	<sup>96</sup> 0.0021	<sup>99</sup> 0.0019	<sup>99</sup> 0.0017	<sup>96</sup> 1.023
34	COGENT-004	<sup>191</sup> 2053	<sup>241</sup> 952	<sup>51</sup> 0.0020	<sup>53</sup> 0.0016	<sup>56</sup> 0.0015	<sup>61</sup> 0.0015	<sup>64</sup> 0.0014	<sup>52</sup> 1.015
35	COGENT-005	<sup>83</sup> 1062	<sup>187</sup> 774	<sup>34</sup> 0.0017	<sup>43</sup> 0.0014	<sup>43</sup> 0.0014	<sup>50</sup> 0.0014	<sup>58</sup> 0.0013	<sup>43</sup> 1.013
36	COGNITEC-000	<sup>180</sup> 2052	<sup>19</sup> 176	<sup>192</sup> 0.0252	<sup>190</sup> 0.0136	<sup>188</sup> 0.0107	<sup>187</sup> 0.0085	<sup>170</sup> 0.0065	<sup>191</sup> 1.136
37	COGNITEC-001	<sup>175</sup> 2052	<sup>30</sup> 202	<sup>163</sup> 0.0117	<sup>151</sup> 0.0062	<sup>150</sup> 0.0051	<sup>152</sup> 0.0042	<sup>150</sup> 0.0034	<sup>151</sup> 1.062
38	COGNITEC-002	<sup>184</sup> 2052	<sup>35</sup> 227	<sup>119</sup> 0.0057	<sup>119</sup> 0.0037	<sup>120</sup> 0.0032	<sup>122</sup> 0.0029	<sup>131</sup> 0.0026	<sup>119</sup> 1.035
39	COGNITEC-003	<sup>176</sup> 2052	<sup>53</sup> 297	<sup>123</sup> 0.0062	<sup>120</sup> 0.0040	<sup>129</sup> 0.0036	<sup>135</sup> 0.0033	<sup>140</sup> 0.0030	<sup>126</sup> 1.039
40	COGNITEC-004	<sup>182</sup> 2052	<sup>26</sup> 192	<sup>86</sup> 0.0032	<sup>80</sup> 0.0020	<sup>74</sup> 0.0018	<sup>69</sup> 0.0015	<sup>69</sup> 0.0014	<sup>84</sup> 1.020
41	COGNITEC-005	<sup>188</sup> 2052	<sup>65</sup> 367	<sup>31</sup> 0.0016	<sup>25</sup> 0.0013	<sup>24</sup> 0.0012	<sup>24</sup> 0.0012	<sup>24</sup> 0.0011	<sup>24</sup> 1.012
42	CUBOX-000	<sup>121</sup> 2048	<sup>233</sup> 918	<sup>16</sup> 0.0014	<sup>34</sup> 0.0014	<sup>43</sup> 0.0014	<sup>51</sup> 0.0014	<sup>60</sup> 0.0014	<sup>33</sup> 1.012
43	CYBERLINK-000	<sup>177</sup> 2052	<sup>158</sup> 699	<sup>97</sup> 0.0040	<sup>108</sup> 0.0028	<sup>112</sup> 0.0026	<sup>114</sup> 0.0024	<sup>110</sup> 0.0022	<sup>107</sup> 1.027
44	CYBERLINK-001	<sup>185</sup> 2052	<sup>87</sup> 433	<sup>91</sup> 0.0035	<sup>90</sup> 0.0023	<sup>94</sup> 0.0021	<sup>90</sup> 0.0018	<sup>90</sup> 0.0017	<sup>92</sup> 1.022
45	CYBERLINK-002	<sup>240</sup> 4140	<sup>180</sup> 738	<sup>73</sup> 0.0026	<sup>91</sup> 0.0023	<sup>102</sup> 0.0022	<sup>108</sup> 0.0021	<sup>112</sup> 0.0021	<sup>88</sup> 1.021
46	CYBERLINK-003	<sup>242</sup> 6212	<sup>157</sup> 696	<sup>28</sup> 0.0016	<sup>28</sup> 0.0013	<sup>29</sup> 0.0013	<sup>29</sup> 0.0012	<sup>29</sup> 0.0012	<sup>30</sup> 1.012
47	CYBERLINK-004	<sup>243</sup> 6212	<sup>179</sup> 738	<sup>33</sup> 0.0017	<sup>47</sup> 0.0015	<sup>54</sup> 0.0015	<sup>58</sup> 0.0014	<sup>60</sup> 0.0014	<sup>45</sup> 1.014
48	DAHUA-000	<sup>152</sup> 2048	<sup>71</sup> 378	<sup>149</sup> 0.0093	<sup>153</sup> 0.0066	<sup>158</sup> 0.0061	<sup>164</sup> 0.0057	<sup>167</sup> 0.0054	<sup>152</sup> 1.062
49	DAHUA-001	<sup>148</sup> 2048	<sup>67</sup> 371	<sup>127</sup> 0.0067	<sup>128</sup> 0.0040	<sup>128</sup> 0.0036	<sup>133</sup> 0.0033	<sup>137</sup> 0.0029	<sup>128</sup> 1.040
50	DAHUA-002	<sup>140</sup> 2048	<sup>159</sup> 699	<sup>42</sup> 0.0018	<sup>46</sup> 0.0015	<sup>51</sup> 0.0014	<sup>50</sup> 0.0014	<sup>50</sup> 0.0013	<sup>46</sup> 1.014
51	DAHUA-003	<sup>158</sup> 2048	<sup>176</sup> 725	<sup>10</sup> 0.0012	<sup>8</sup> 0.0010	<sup>10</sup> 0.0009	<sup>10</sup> 0.0009	<sup>10</sup> 0.0009	<sup>7</sup> 1.009
52	DEEPLINT-001	<sup>222</sup> 4096	<sup>148</sup> 687	<sup>19</sup> 0.0014	<sup>33</sup> 0.0014	<sup>34</sup> 0.0013	<sup>40</sup> 0.0013	<sup>46</sup> 0.0013	<sup>32</sup> 1.012
53	DEEPEA-001	<sup>119</sup> 2048	<sup>190</sup> 780	<sup>102</sup> 0.0043	<sup>80</sup> 0.0022	<sup>78</sup> 0.0018	<sup>74</sup> 0.0016	<sup>68</sup> 0.0014	<sup>93</sup> 1.022
54	DERMALOG-003	<sup>5</sup> 128	<sup>32</sup> 211	<sup>224</sup> 0.1259	<sup>220</sup> 0.0744	<sup>222</sup> 0.0603	<sup>221</sup> 0.0480	<sup>220</sup> 0.0347	<sup>223</sup> 1.731
55	DERMALOG-004	<sup>4</sup> 128	<sup>31</sup> 208	<sup>223</sup> 0.1251	<sup>222</sup> 0.0739	<sup>221</sup> 0.0598	<sup>220</sup> 0.0475	<sup>219</sup> 0.0343	<sup>222</sup> 1.727
56	DERMALOG-005	<sup>7</sup> 128	<sup>110</sup> 532	<sup>174</sup> 0.0149	<sup>187</sup> 0.0129	<sup>190</sup> 0.0125	<sup>196</sup> 0.0123	<sup>201</sup> 0.0122	<sup>184</sup> 1.118
57	DERMALOG-006	<sup>14</sup> 256	<sup>108</sup> 514	<sup>140</sup> 0.0081	<sup>157</sup> 0.0069	<sup>160</sup> 0.0066	<sup>168</sup> 0.0065	<sup>176</sup> 0.0063	<sup>155</sup> 1.063
58	DERMALOG-007	<sup>6</sup> 128	<sup>82</sup> 413	<sup>148</sup> 0.0092	<sup>150</sup> 0.0066	<sup>156</sup> 0.0060	<sup>163</sup> 0.0057	<sup>170</sup> 0.0054	<sup>153</sup> 1.062
59	DERMALOG-008	<sup>32</sup> 512	<sup>66</sup> 370	<sup>80</sup> 0.0029	<sup>79</sup> 0.0020	<sup>77</sup> 0.0018	<sup>77</sup> 0.0017	<sup>80</sup> 0.0015	<sup>80</sup> 1.019
60	EYEDea-003	<sup>79</sup> 1036	<sup>72</sup> 385	<sup>218</sup> 0.0800	<sup>215</sup> 0.0451	<sup>215</sup> 0.0362	<sup>211</sup> 0.0289	<sup>211</sup> 0.0211	<sup>216</sup> 1.448
61	F8-001	<sup>172</sup> 2048	<sup>212</sup> 851	<sup>167</sup> 0.0120	<sup>170</sup> 0.0105	<sup>186</sup> 0.0102	<sup>189</sup> 0.0100	<sup>190</sup> 0.0099	<sup>179</sup> 1.096
62	FINCORE-000	<sup>164</sup> 2048	<sup>98</sup> 477	<sup>138</sup> 0.0108	<sup>143</sup> 0.0052	<sup>140</sup> 0.0042	<sup>139</sup> 0.0034	<sup>132</sup> 0.0026	<sup>144</sup> 1.054
63	FUJITSULAB-000	<sup>74</sup> 1032	<sup>240</sup> 950	<sup>88</sup> 0.0022	<sup>88</sup> 0.0016	<sup>89</sup> 0.0015	<sup>80</sup> 0.0015	<sup>81</sup> 0.0014	<sup>88</sup> 1.015
64	GLORY-000	<sup>30</sup> 418	<sup>15</sup> 160	<sup>228</sup> 0.1781	<sup>220</sup> 0.1391	<sup>230</sup> 0.1266	<sup>230</sup> 0.1154	<sup>230</sup> 0.1007	<sup>229</sup> 2.298
65	GLORY-001	<sup>104</sup> 1726	<sup>78</sup> 405	<sup>225</sup> 0.1268	<sup>220</sup> 0.0967	<sup>223</sup> 0.0869	<sup>226</sup> 0.0778	<sup>220</sup> 0.0673	<sup>225</sup> 1.903
66	GORILLA-001	<sup>205</sup> 2156	<sup>18</sup> 169	<sup>211</sup> 0.0603	<sup>206</sup> 0.0304	<sup>205</sup> 0.0230	<sup>205</sup> 0.0174	<sup>198</sup> 0.0117	<sup>206</sup> 1.309
67	GORILLA-002	<sup>86</sup> 1132	<sup>62</sup> 341	<sup>186</sup> 0.0197	<sup>194</sup> 0.0092	<sup>164</sup> 0.0070	<sup>159</sup> 0.0054	<sup>158</sup> 0.0041	<sup>178</sup> 1.096
68	GORILLA-003	<sup>206</sup> 2156	<sup>120</sup> 563	<sup>199</sup> 0.0361	<sup>192</sup> 0.0146	<sup>187</sup> 0.0106	<sup>181</sup> 0.0078	<sup>160</sup> 0.0054	<sup>194</sup> 1.158
69	GORILLA-004	<sup>207</sup> 2192	<sup>74</sup> 395	<sup>124</sup> 0.0063	<sup>116</sup> 0.0032	<sup>112</sup> 0.0026	<sup>111</sup> 0.0023	<sup>99</sup> 0.0018	<sup>116</sup> 1.033
70	GORILLA-005	<sup>244</sup> 6288	<sup>101</sup> 483	<sup>85</sup> 0.0032	<sup>70</sup> 0.0019	<sup>69</sup> 0.0017	<sup>63</sup> 0.0015	<sup>49</sup> 0.0013	<sup>78</sup> 1.018
71	GORILLA-006	<sup>246</sup> 8336	<sup>183</sup> 768	<sup>37</sup> 0.0017	<sup>24</sup> 0.0013	<sup>22</sup> 0.0012	<sup>23</sup> 0.0012	<sup>24</sup> 0.0011	<sup>27</sup> 1.012
72	HK-003	<sup>92</sup> 1408	<sup>130</sup> 633	<sup>164</sup> 0.0117	<sup>140</sup> 0.0060	<sup>148</sup> 0.0048	<sup>149</sup> 0.0039	<sup>141</sup> 0.0030	<sup>150</sup> 1.061

Table 21: Rank-based accuracy for the FRVT 20

#	MISSES OUTSIDE RANK R FNIR(N, T=0, R) ALGORITHM	RESOURCE USAGE		ENROL MOST RECENT, N = 1.6M FRVT 2018 MUGSHOTS						
		TEMPLATE		R=1	R=5	R=10	R=20	R=50	WORK-10	
		BYTES	MSEC							
73	HIK-004	<sup>87</sup> 1152	<sup>108</sup> 510	<sup>161</sup> 0.0113	<sup>147</sup> 0.0059	<sup>148</sup> 0.0047	<sup>142</sup> 0.0037	<sup>138</sup> 0.0030	<sup>149</sup> 1.060	
74	HIK-005	<sup>91</sup> 1408	<sup>124</sup> 619	<sup>106</sup> 0.0046	<sup>101</sup> 0.0025	<sup>98</sup> 0.0020	<sup>79</sup> 0.0017	<sup>76</sup> 0.0015	<sup>101</sup> 1.025	
75	HIK-006	<sup>93</sup> 1408	<sup>124</sup> 610	<sup>107</sup> 0.0046	<sup>100</sup> 0.0025	<sup>91</sup> 0.0020	<sup>80</sup> 0.0017	<sup>75</sup> 0.0015	<sup>102</sup> 1.025	
76	HYPERVERGE-001	<sup>62</sup> 1024	<sup>211</sup> 846	<sup>14</sup> 0.0014	<sup>26</sup> 0.0013	<sup>41</sup> 0.0013	<sup>37</sup> 0.0013	<sup>30</sup> 0.0013	<sup>23</sup> 1.012	
77	IDEMIA-003	<sup>48</sup> 528	<sup>154</sup> 689	<sup>138</sup> 0.0069	<sup>134</sup> 0.0045	<sup>132</sup> 0.0039	<sup>138</sup> 0.0034	<sup>135</sup> 0.0027	<sup>131</sup> 1.043	
78	IDEMIA-004	<sup>50</sup> 528	<sup>141</sup> 669	<sup>129</sup> 0.0066	<sup>124</sup> 0.0038	<sup>124</sup> 0.0032	<sup>120</sup> 0.0027	<sup>113</sup> 0.0021	<sup>122</sup> 1.038	
79	IDEMIA-005	<sup>28</sup> 352	<sup>69</sup> 374	<sup>139</sup> 0.0081	<sup>132</sup> 0.0044	<sup>130</sup> 0.0036	<sup>132</sup> 0.0032	<sup>140</sup> 0.0030	<sup>134</sup> 1.044	
80	IDEMIA-006	<sup>29</sup> 352	<sup>68</sup> 373	<sup>135</sup> 0.0096	<sup>142</sup> 0.0052	<sup>141</sup> 0.0042	<sup>147</sup> 0.0039	<sup>133</sup> 0.0037	<sup>141</sup> 1.052	
81	IDEMIA-007	<sup>59</sup> 860	<sup>198</sup> 807	<sup>72</sup> 0.0026	<sup>54</sup> 0.0016	<sup>47</sup> 0.0014	<sup>36</sup> 0.0013	<sup>33</sup> 0.0012	<sup>59</sup> 1.015	
82	IDEMIA-008	<sup>27</sup> 300	<sup>91</sup> 451	<sup>6</sup> 0.0011	<sup>7</sup> 0.0009	<sup>9</sup> 0.0009	<sup>11</sup> 0.0009	<sup>11</sup> 0.0009	<sup>5</sup> 1.009	
83	IMAGUS-002	<sup>39</sup> 512	<sup>7</sup> 76	<sup>231</sup> 0.2203	<sup>229</sup> 0.1342	<sup>238</sup> 0.1090	<sup>227</sup> 0.0871	<sup>225</sup> 0.0632	<sup>230</sup> 2.308	
84	IMAGUS-003	<sup>38</sup> 512	<sup>5</sup> 57	<sup>236</sup> 0.3559	<sup>236</sup> 0.2491	<sup>236</sup> 0.2132	<sup>236</sup> 0.1791	<sup>236</sup> 0.1397	<sup>236</sup> 3.363	
85	IMAGUS-005	<sup>110</sup> 2048	<sup>192</sup> 788	<sup>48</sup> 0.0019	<sup>35</sup> 0.0016	<sup>50</sup> 0.0015	<sup>54</sup> 0.0014	<sup>36</sup> 0.0013	<sup>53</sup> 1.015	
86	IMAGUS-006	<sup>145</sup> 2048	<sup>229</sup> 905	<sup>32</sup> 0.0020	<sup>39</sup> 0.0016	<sup>61</sup> 0.0015	<sup>64</sup> 0.0015	<sup>70</sup> 0.0014	<sup>55</sup> 1.015	
87	IMPERIAL-000	<sup>115</sup> 2048	<sup>138</sup> 654	<sup>76</sup> 0.0024	<sup>72</sup> 0.0019	<sup>72</sup> 0.0018	<sup>86</sup> 0.0018	<sup>92</sup> 0.0017	<sup>71</sup> 1.018	
88	INCODE-000	<sup>64</sup> 1024	<sup>24</sup> 190	<sup>208</sup> 0.0489	<sup>203</sup> 0.0261	<sup>202</sup> 0.0204	<sup>202</sup> 0.0160	<sup>199</sup> 0.0117	<sup>203</sup> 1.262	
89	INCODE-001	<sup>154</sup> 2048	<sup>151</sup> 690	<sup>177</sup> 0.0166	<sup>168</sup> 0.0084	<sup>162</sup> 0.0067	<sup>161</sup> 0.0055	<sup>160</sup> 0.0043	<sup>169</sup> 1.086	
90	INCODE-002	<sup>155</sup> 2048	<sup>50</sup> 291	<sup>181</sup> 0.0178	<sup>171</sup> 0.0090	<sup>165</sup> 0.0070	<sup>162</sup> 0.0056	<sup>161</sup> 0.0043	<sup>175</sup> 1.092	
91	INCODE-003	<sup>117</sup> 2048	<sup>161</sup> 704	<sup>169</sup> 0.0129	<sup>153</sup> 0.0064	<sup>151</sup> 0.0051	<sup>150</sup> 0.0040	<sup>143</sup> 0.0031	<sup>157</sup> 1.066	
92	INCODE-004	<sup>153</sup> 2048	<sup>103</sup> 508	<sup>92</sup> 0.0035	<sup>96</sup> 0.0024	<sup>98</sup> 0.0021	<sup>102</sup> 0.0020	<sup>102</sup> 0.0019	<sup>94</sup> 1.023	
93	INCODE-005	<sup>126</sup> 2048	<sup>104</sup> 500	<sup>32</sup> 0.0017	<sup>35</sup> 0.0014	<sup>41</sup> 0.0014	<sup>39</sup> 0.0013	<sup>40</sup> 0.0013	<sup>36</sup> 1.013	
94	INNOVATRICS-002	<sup>82</sup> 530	<sup>41</sup> 255	<sup>208</sup> 0.0451	<sup>208</sup> 0.0342	<sup>211</sup> 0.0322	<sup>213</sup> 0.0308	<sup>215</sup> 0.0297	<sup>210</sup> 1.321	
95	INNOVATRICS-003	<sup>51</sup> 530	<sup>40</sup> 255	<sup>193</sup> 0.0263	<sup>185</sup> 0.0126	<sup>181</sup> 0.0095	<sup>176</sup> 0.0074	<sup>166</sup> 0.0053	<sup>188</sup> 1.129	
96	INNOVATRICS-004	<sup>84</sup> 1076	<sup>48</sup> 406	<sup>168</sup> 0.0123	<sup>152</sup> 0.0063	<sup>149</sup> 0.0050	<sup>151</sup> 0.0040	<sup>146</sup> 0.0032	<sup>156</sup> 1.064	
97	INNOVATRICS-005	<sup>54</sup> 538	<sup>209</sup> 842	<sup>71</sup> 0.0024	<sup>66</sup> 0.0018	<sup>70</sup> 0.0017	<sup>73</sup> 0.0016	<sup>71</sup> 0.0014	<sup>66</sup> 1.017	
98	INNOVATRICS-007	<sup>58</sup> 538	<sup>199</sup> 785	<sup>36</sup> 0.0017	<sup>40</sup> 0.0014	<sup>36</sup> 0.0013	<sup>34</sup> 0.0013	<sup>39</sup> 0.0012	<sup>38</sup> 1.013	
99	INTSYSMSU-000	<sup>122</sup> 2048	<sup>147</sup> 675	<sup>228</sup> 0.1457	<sup>228</sup> 0.1320	<sup>232</sup> 0.1272	<sup>231</sup> 0.1225	<sup>233</sup> 0.1163	<sup>228</sup> 2.203	
100	IREX-000	<sup>214</sup> 3080	<sup>247</sup> 2379	<sup>103</sup> 0.0044	<sup>129</sup> 0.0043	<sup>143</sup> 0.0043	<sup>153</sup> 0.0043	<sup>159</sup> 0.0043	<sup>127</sup> 1.039	
101	ISYSTEMS-002	<sup>120</sup> 2048	<sup>58</sup> 316	<sup>123</sup> 0.0064	<sup>130</sup> 0.0043	<sup>136</sup> 0.0039	<sup>141</sup> 0.0037	<sup>143</sup> 0.0034	<sup>130</sup> 1.041	
102	ISYSTEMS-003	<sup>131</sup> 2048	<sup>214</sup> 856	<sup>112</sup> 0.0052	<sup>125</sup> 0.0039	<sup>132</sup> 0.0036	<sup>140</sup> 0.0034	<sup>147</sup> 0.0033	<sup>121</sup> 1.037	
103	KAKAO-000	<sup>179</sup> 2052	<sup>208</sup> 840	<sup>29</sup> 0.0015	<sup>16</sup> 0.0011	<sup>17</sup> 0.0011	<sup>14</sup> 0.0010	<sup>15</sup> 0.0010	<sup>16</sup> 1.010	
104	KEDACOM-001	<sup>26</sup> 292	<sup>112</sup> 537	<sup>138</sup> 0.0077	<sup>160</sup> 0.0074	<sup>166</sup> 0.0073	<sup>173</sup> 0.0072	<sup>181</sup> 0.0072	<sup>158</sup> 1.067	
105	KNERON-000	<sup>136</sup> 2048	<sup>109</sup> 530	<sup>126</sup> 0.0059	<sup>148</sup> 0.0059	<sup>158</sup> 0.0059	<sup>165</sup> 0.0059	<sup>172</sup> 0.0059	<sup>143</sup> 1.053	
106	KNERON-001	<sup>162</sup> 2048	<sup>97</sup> 468	<sup>198</sup> 0.0295	<sup>205</sup> 0.0295	<sup>210</sup> 0.0295	<sup>212</sup> 0.0295	<sup>214</sup> 0.0295	<sup>204</sup> 1.266	
107	LINE-000	<sup>166</sup> 2048	<sup>59</sup> 482	<sup>39</sup> 0.0022	<sup>51</sup> 0.0015	<sup>45</sup> 0.0014	<sup>32</sup> 0.0013	<sup>31</sup> 0.0012	<sup>31</sup> 1.015	
108	LOOKMAN-003	<sup>29</sup> 292	<sup>63</sup> 342	<sup>144</sup> 0.0088	<sup>164</sup> 0.0078	<sup>172</sup> 0.0076	<sup>178</sup> 0.0075	<sup>184</sup> 0.0074	<sup>161</sup> 1.071	
109	LOOKMAN-004	<sup>57</sup> 548	<sup>39</sup> 325	<sup>146</sup> 0.0091	<sup>165</sup> 0.0079	<sup>171</sup> 0.0076	<sup>177</sup> 0.0075	<sup>183</sup> 0.0073	<sup>162</sup> 1.072	
110	LOOKMAN-005	<sup>59</sup> 548	<sup>107</sup> 514	<sup>138</sup> 0.0080	<sup>162</sup> 0.0075	<sup>169</sup> 0.0074	<sup>175</sup> 0.0073	<sup>182</sup> 0.0072	<sup>159</sup> 1.068	
111	MEGVII-001	<sup>225</sup> 4096	<sup>134</sup> 652	<sup>168</sup> 0.0118	<sup>175</sup> 0.0093	<sup>178</sup> 0.0087	<sup>185</sup> 0.0084	<sup>190</sup> 0.0080	<sup>170</sup> 1.086	
112	MEGVII-002	<sup>228</sup> 4096	<sup>134</sup> 656	<sup>166</sup> 0.0118	<sup>176</sup> 0.0093	<sup>177</sup> 0.0088	<sup>184</sup> 0.0084	<sup>189</sup> 0.0080	<sup>171</sup> 1.087	
113	MICROFOCUS-003	<sup>18</sup> 256	<sup>48</sup> 269	<sup>241</sup> 0.5942	<sup>242</sup> 0.4692	<sup>242</sup> 0.4204	<sup>242</sup> 0.3724	<sup>242</sup> 0.3095	<sup>242</sup> 5.361	
114	MICROFOCUS-004	<sup>21</sup> 256	<sup>47</sup> 270	<sup>241</sup> 0.5763	<sup>241</sup> 0.4519	<sup>241</sup> 0.4026	<sup>241</sup> 0.3560	<sup>241</sup> 0.2957	<sup>241</sup> 5.199	
115	MICROFOCUS-005	<sup>18</sup> 256	<sup>47</sup> 266	<sup>237</sup> 0.4242	<sup>237</sup> 0.3028	<sup>237</sup> 0.2606	<sup>237</sup> 0.2209	<sup>238</sup> 0.1724	<sup>237</sup> 3.861	
116	MICROFOCUS-006	<sup>18</sup> 256	<sup>47</sup> 265	<sup>238</sup> 0.4268	<sup>238</sup> 0.3049	<sup>238</sup> 0.2623	<sup>239</sup> 0.2233	<sup>239</sup> 0.1746	<sup>238</sup> 3.880	
117	MICROSOFT-003	<sup>69</sup> 1024	<sup>77</sup> 404	<sup>29</sup> 0.0016	<sup>11</sup> 0.0010	<sup>9</sup> 0.0009	<sup>3</sup> 0.0008	<sup>2</sup> 0.0006	<sup>11</sup> 1.009	
118	MICROSOFT-004	<sup>161</sup> 2048	<sup>186</sup> 773	<sup>22</sup> 0.0015	<sup>6</sup> 0.0009	<sup>1</sup> 0.0008	<sup>1</sup> 0.0007	<sup>1</sup> 0.0006	<sup>9</sup> 1.009	
119	MICROSOFT-005	<sup>68</sup> 1024	<sup>142</sup> 673	<sup>43</sup> 0.0019	<sup>9</sup> 0.0010	<sup>4</sup> 0.0008	<sup>2</sup> 0.0008	<sup>3</sup> 0.0006	<sup>14</sup> 1.010	
120	MICROSOFT-006	<sup>65</sup> 1024	<sup>158</sup> 695	<sup>38</sup> 0.0020	<sup>17</sup> 0.0011	<sup>11</sup> 0.0010	<sup>4</sup> 0.0008	<sup>4</sup> 0.0007	<sup>18</sup> 1.011	
121	NEC-000	<sup>213</sup> 2592	<sup>8</sup> 82	<sup>178</sup> 0.0170	<sup>170</sup> 0.0086	<sup>161</sup> 0.0066	<sup>158</sup> 0.0052	<sup>155</sup> 0.0038	<sup>172</sup> 1.087	
122	NEC-001	<sup>212</sup> 2592	<sup>9</sup> 88	<sup>187</sup> 0.0209	<sup>191</sup> 0.0141	<sup>192</sup> 0.0128	<sup>195</sup> 0.0119	<sup>197</sup> 0.0113	<sup>190</sup> 1.135	
123	NEC-002	<sup>102</sup> 1616	<sup>138</sup> 653	<sup>3</sup> 0.0010	<sup>3</sup> 0.0009	<sup>3</sup> 0.0008	<sup>6</sup> 0.0008	<sup>5</sup> 0.0008	<sup>3</sup> 1.008	
124	NEC-003	<sup>103</sup> 1712	<sup>158</sup> 690	<sup>13</sup> 0.0014	<sup>23</sup> 0.0012	<sup>20</sup> 0.0012	<sup>31</sup> 0.0012	<sup>32</sup> 0.0012	<sup>20</sup> 1.011	
125	NEC-004	<sup>85</sup> 1104	<sup>244</sup> 967	<sup>17</sup> 0.0014	<sup>31</sup> 0.0013	<sup>39</sup> 0.0013	<sup>41</sup> 0.0013	<sup>48</sup> 0.0013	<sup>31</sup> 1.012	
126	NEUROTECHNOLOGY-003	<sup>116</sup> 2048	<sup>113</sup> 547	<sup>188</sup> 0.0225	<sup>186</sup> 0.0126	<sup>188</sup> 0.0100	<sup>182</sup> 0.0078	<sup>171</sup> 0.0057	<sup>187</sup> 1.125	
127	NEUROTECHNOLOGY-004	<sup>169</sup> 2048	<sup>111</sup> 543	<sup>113</sup> 0.0056	<sup>118</sup> 0.0036	<sup>124</sup> 0.0032	<sup>125</sup> 0.0029	<sup>124</sup> 0.0025	<sup>118</sup> 1.035	
128	NEUROTECHNOLOGY-005	<sup>20</sup> 256	<sup>81</sup> 412	<sup>101</sup> 0.0043	<sup>110</sup> 0.0029	<sup>114</sup> 0.0027	<sup>115</sup> 0.0024	<sup>120</sup> 0.0023	<sup>110</sup> 1.028	
129	NEUROTECHNOLOGY-006	<sup>15</sup> 256	<sup>181</sup> 746	<sup>182</sup> 0.0180	<sup>166</sup> 0.0079	<sup>154</sup> 0.0059	<sup>154</sup> 0.0046	<sup>148</sup> 0.0033	<sup>168</sup> 1.083	
130	NEUROTECHNOLOGY-007	<sup>10</sup> 256	<sup>17</sup> 169	<sup>96</sup> 0.0039	<sup>105</sup> 0.0027	<sup>110</sup> 0.0025	<sup>112</sup> 0.0023	<sup>115</sup> 0.0022	<sup>103</sup> 1.026	
131	NEUROTECHNOLOGY-008	<sup>45</sup> 514	<sup>198</sup> 804	<sup>37</sup> 0.0022	<sup>48</sup> 0.0015	<sup>58</sup> 0.0014	<sup>52</sup> 0.0014	<sup>52</sup> 0.0013	<sup>50</sup> 1.015	
132	NEUROTECHNOLOGY-009	<sup>44</sup> 513	<sup>149</sup> 686	<sup>18</sup> 0.0014	<sup>20</sup> 0.0012	<sup>21</sup> 0.0012	<sup>22</sup> 0.0011	<sup>26</sup> 0.0011	<sup>19</sup> 1.011	
133	NEWLAND-002	<sup>160</sup> 2048	<sup>218</sup> 868	<sup>211</sup> 0.0786	<sup>217</sup> 0.0480	<sup>218</sup> 0.0397	<sup>216</sup> 0.0332	<sup>213</sup> 0.0263	<sup>218</sup> 1.468	
134	NOBLIS-001	<sup>127</sup> 2048	<sup>33</sup> 211	<sup>233</sup> 0.2492	<sup>233</sup> 0.1772	<sup>230</sup> 0.1542	<sup>233</sup> 0.1339	<sup>231</sup> 0.1112	<sup>233</sup> 2.679	
135	NOBLIS-002	<sup>241</sup> 6144	<sup>111</sup> 535	<sup>229</sup> 0.1794	<sup>226</sup> 0.1108	<sup>228</sup> 0.0903	<sup>225</sup> 0.0722	<sup>224</sup> 0.0535	<sup>226</sup> 2.077	
136	NTECHLAB-003	<sup>218</sup> 3484	<sup>203</sup> 831	<sup>121</sup> 0.0062	<sup>112</sup> 0.0029	<sup>109</sup> 0.0023	<sup>100</sup> 0.0019	<sup>86</sup> 0.0016	<sup>115</sup> 1.030	
137	NTECHLAB-004	<sup>217</sup> 3484	<sup>234</sup> 929	<sup>110</sup> 0.0048	<sup>93</sup> 0.0023	<sup>88</sup> 0.0019	<sup>76</sup> 0.0016	<sup>57</sup> 0.0013	<sup>99</sup> 1.024	
138	NTECHLAB-005	<sup>108</sup> 1940	<sup>172</sup> 717	<sup>108</sup> 0.0047	<sup>88</sup> 0.0022	<sup>78</sup> 0.0017	<sup>42</sup> 0.0013	<sup>25</sup> 0.0011	<sup>95</sup> 1.023	
139	NTECHLAB-006	<sup>107</sup> 1940	<sup>209</sup> 841	<sup>100</sup> 0.0041	<sup>71</sup> 0.0019	<sup>59</sup> 0.0015	<sup>26</sup> 0.0012	<sup>12</sup> 0.0009	<sup>83</sup> 1.019	
140	NTECHLAB-007	<sup>216</sup> 3348	<sup>209</sup> 834</							

#	MISSES OUTSIDE RANK R FNIR(N, T=0, R)	RESOURCE USAGE		ENROL MOST RECENT, N = 1.6M						
		TEMPLATE		FRVT 2018 MUGSHOTS						
		BYTES	MSEC	R=1	R=5	R=10	R=20	R=50	WORK-10	
145	PARAVISION-001	<sup>132</sup> 2048	<sup>122</sup> 590	<sup>94</sup> 0.0038	<sup>98</sup> 0.0024	<sup>99</sup> 0.0022	<sup>105</sup> 0.0020	<sup>103</sup> 0.0019	<sup>97</sup> 1.023	
146	PARAVISION-002	<sup>137</sup> 2048	<sup>78</sup> 377	<sup>99</sup> 0.0040	<sup>102</sup> 0.0025	<sup>103</sup> 0.0022	<sup>106</sup> 0.0021	<sup>105</sup> 0.0019	<sup>100</sup> 1.025	
147	PARAVISION-003	<sup>147</sup> 2048	<sup>178</sup> 735	<sup>84</sup> 0.0031	<sup>87</sup> 0.0022	<sup>93</sup> 0.0020	<sup>94</sup> 0.0019	<sup>95</sup> 0.0017	<sup>87</sup> 1.021	
148	PARAVISION-004	<sup>221</sup> 4096	<sup>172</sup> 720	<sup>38</sup> 0.0016	<sup>38</sup> 0.0014	<sup>48</sup> 0.0013	<sup>45</sup> 0.0013	<sup>51</sup> 0.0013	<sup>37</sup> 1.013	
149	PARAVISION-005	<sup>224</sup> 4096	<sup>213</sup> 858	<sup>24</sup> 0.0015	<sup>36</sup> 0.0014	<sup>40</sup> 0.0013	<sup>46</sup> 0.0013	<sup>54</sup> 0.0013	<sup>34</sup> 1.013	
150	PARAVISION-007	<sup>229</sup> 4096	<sup>162</sup> 706	<sup>9</sup> 0.0012	<sup>15</sup> 0.0011	<sup>16</sup> 0.0010	<sup>17</sup> 0.0010	<sup>17</sup> 0.0010	<sup>13</sup> 1.010	
151	PIXELALL-002	<sup>209</sup> 2560	<sup>29</sup> 198	<sup>106</sup> 0.0045	<sup>111</sup> 0.0029	<sup>110</sup> 0.0025	<sup>110</sup> 0.0022	<sup>108</sup> 0.0019	<sup>111</sup> 1.028	
152	PIXELALL-003	<sup>211</sup> 2560	<sup>174</sup> 719	<sup>56</sup> 0.0021	<sup>56</sup> 0.0016	<sup>64</sup> 0.0015	<sup>59</sup> 0.0014	<sup>69</sup> 0.0014	<sup>57</sup> 1.015	
153	PIXELALL-004	<sup>210</sup> 2560	<sup>92</sup> 453	<sup>54</sup> 0.0020	<sup>50</sup> 0.0015	<sup>53</sup> 0.0015	<sup>52</sup> 0.0014	<sup>55</sup> 0.0013	<sup>49</sup> 1.014	
154	PIXELALL-005	<sup>208</sup> 2560	<sup>218</sup> 845	<sup>46</sup> 0.0019	<sup>62</sup> 0.0017	<sup>63</sup> 0.0016	<sup>75</sup> 0.0016	<sup>85</sup> 0.0016	<sup>56</sup> 1.015	
155	PTAKURATSATU-000	<sup>85</sup> 538	<sup>232</sup> 910	<sup>84</sup> 0.0030	<sup>86</sup> 0.0021	<sup>87</sup> 0.0019	<sup>83</sup> 0.0018	<sup>88</sup> 0.0016	<sup>85</sup> 1.020	
156	QNAP-000	<sup>150</sup> 2048	<sup>98</sup> 457	<sup>136</sup> 0.0078	<sup>131</sup> 0.0044	<sup>134</sup> 0.0037	<sup>134</sup> 0.0033	<sup>136</sup> 0.0028	<sup>132</sup> 1.043	
157	QUANTASOFT-001	<sup>142</sup> 2048	<sup>79</sup> 396	<sup>230</sup> 0.2177	<sup>232</sup> 0.1643	<sup>232</sup> 0.1468	<sup>235</sup> 0.1312	<sup>232</sup> 0.1116	<sup>232</sup> 2.539	
158	RANKONE-002	<sup>10</sup> 133	<sup>11</sup> 113	<sup>188</sup> 0.0194	<sup>180</sup> 0.0112	<sup>180</sup> 0.0093	<sup>180</sup> 0.0077	<sup>174</sup> 0.0060	<sup>181</sup> 1.111	
159	RANKONE-003	<sup>8</sup> 133	<sup>13</sup> 114	<sup>184</sup> 0.0194	<sup>181</sup> 0.0112	<sup>178</sup> 0.0093	<sup>179</sup> 0.0077	<sup>175</sup> 0.0060	<sup>180</sup> 1.111	
160	RANKONE-004	<sup>1</sup> 85	<sup>4</sup> 36	<sup>203</sup> 0.0415	<sup>202</sup> 0.0226	<sup>202</sup> 0.0177	<sup>198</sup> 0.0141	<sup>195</sup> 0.0102	<sup>202</sup> 1.225	
161	RANKONE-005	<sup>9</sup> 133	<sup>10</sup> 94	<sup>150</sup> 0.0094	<sup>145</sup> 0.0054	<sup>145</sup> 0.0046	<sup>148</sup> 0.0039	<sup>145</sup> 0.0032	<sup>145</sup> 1.054	
162	RANKONE-006	<sup>12</sup> 165	<sup>42</sup> 261	<sup>112</sup> 0.0050	<sup>115</sup> 0.0030	<sup>113</sup> 0.0027	<sup>113</sup> 0.0024	<sup>111</sup> 0.0021	<sup>114</sup> 1.030	
163	RANKONE-007	<sup>11</sup> 165	<sup>42</sup> 278	<sup>88</sup> 0.0034	<sup>94</sup> 0.0023	<sup>98</sup> 0.0021	<sup>91</sup> 0.0018	<sup>90</sup> 0.0017	<sup>91</sup> 1.022	
164	RANKONE-009	<sup>22</sup> 260	<sup>25</sup> 191	<sup>64</sup> 0.0024	<sup>57</sup> 0.0016	<sup>62</sup> 0.0015	<sup>65</sup> 0.0015	<sup>65</sup> 0.0014	<sup>60</sup> 1.015	
165	RANKONE-010	<sup>23</sup> 261	<sup>28</sup> 200	<sup>60</sup> 0.0022	<sup>64</sup> 0.0018	<sup>66</sup> 0.0016	<sup>71</sup> 0.0015	<sup>73</sup> 0.0015	<sup>63</sup> 1.016	
166	RANKONE-011	<sup>24</sup> 261	<sup>124</sup> 567	<sup>25</sup> 0.0015	<sup>22</sup> 0.0012	<sup>24</sup> 0.0012	<sup>25</sup> 0.0012	<sup>25</sup> 0.0012	<sup>21</sup> 1.011	
167	REALNETWORKS-000	<sup>232</sup> 4100	<sup>37</sup> 244	<sup>203</sup> 0.0402	<sup>201</sup> 0.0195	<sup>197</sup> 0.0149	<sup>195</sup> 0.0111	<sup>188</sup> 0.0077	<sup>201</sup> 1.201	
168	REALNETWORKS-001	<sup>235</sup> 4104	<sup>38</sup> 243	<sup>203</sup> 0.0402	<sup>200</sup> 0.0195	<sup>196</sup> 0.0149	<sup>192</sup> 0.0111	<sup>187</sup> 0.0077	<sup>200</sup> 1.201	
169	REALNETWORKS-002	<sup>233</sup> 4104	<sup>38</sup> 245	<sup>200</sup> 0.0393	<sup>199</sup> 0.0189	<sup>195</sup> 0.0142	<sup>191</sup> 0.0108	<sup>186</sup> 0.0076	<sup>199</sup> 1.195	
170	REALNETWORKS-003	<sup>105</sup> 1848	<sup>21</sup> 178	<sup>194</sup> 0.0242	<sup>183</sup> 0.0117	<sup>178</sup> 0.0090	<sup>172</sup> 0.0070	<sup>168</sup> 0.0054	<sup>183</sup> 1.120	
171	REALNETWORKS-004	<sup>106</sup> 1848	<sup>21</sup> 185	<sup>190</sup> 0.0236	<sup>182</sup> 0.0112	<sup>176</sup> 0.0087	<sup>170</sup> 0.0068	<sup>164</sup> 0.0050	<sup>182</sup> 1.116	
172	REALNETWORKS-005	<sup>192</sup> 2056	<sup>60</sup> 337	<sup>62</sup> 0.0023	<sup>52</sup> 0.0016	<sup>46</sup> 0.0014	<sup>48</sup> 0.0013	<sup>36</sup> 0.0012	<sup>54</sup> 1.015	
173	REMARKAI-000	<sup>130</sup> 2048	<sup>125</sup> 615	<sup>143</sup> 0.0086	<sup>133</sup> 0.0044	<sup>129</sup> 0.0036	<sup>128</sup> 0.0031	<sup>125</sup> 0.0025	<sup>135</sup> 1.045	
174	REMARKAI-000	<sup>125</sup> 2048	<sup>138</sup> 691	<sup>90</sup> 0.0034	<sup>85</sup> 0.0021	<sup>84</sup> 0.0019	<sup>78</sup> 0.0017	<sup>82</sup> 0.0015	<sup>86</sup> 1.020	
175	REMARKAI-002	<sup>118</sup> 2048	<sup>89</sup> 434	<sup>141</sup> 0.0081	<sup>126</sup> 0.0040	<sup>118</sup> 0.0031	<sup>116</sup> 0.0026	<sup>110</sup> 0.0021	<sup>129</sup> 1.041	
176	RENDIP-000	<sup>113</sup> 2048	<sup>225</sup> 894	<sup>27</sup> 0.0015	<sup>25</sup> 0.0013	<sup>27</sup> 0.0012	<sup>28</sup> 0.0012	<sup>34</sup> 0.0012	<sup>28</sup> 1.012	
177	s1-000	<sup>223</sup> 4096	<sup>218</sup> 865	<sup>64</sup> 0.0024	<sup>65</sup> 0.0018	<sup>67</sup> 0.0017	<sup>72</sup> 0.0016	<sup>79</sup> 0.0015	<sup>65</sup> 1.017	
178	SCANOVATE-000	<sup>134</sup> 2048	<sup>167</sup> 712	<sup>111</sup> 0.0050	<sup>104</sup> 0.0026	<sup>100</sup> 0.0022	<sup>89</sup> 0.0018	<sup>84</sup> 0.0015	<sup>106</sup> 1.026	
179	SCANOVATE-001	<sup>138</sup> 2048	<sup>145</sup> 675	<sup>114</sup> 0.0053	<sup>106</sup> 0.0027	<sup>104</sup> 0.0022	<sup>92</sup> 0.0018	<sup>81</sup> 0.0015	<sup>109</sup> 1.028	
180	SENSETIME-000	<sup>237</sup> 4104	<sup>130</sup> 715	<sup>64</sup> 0.0023	<sup>81</sup> 0.0020	<sup>85</sup> 0.0019	<sup>88</sup> 0.0018	<sup>97</sup> 0.0017	<sup>76</sup> 1.018	
181	SENSETIME-001	<sup>236</sup> 4104	<sup>140</sup> 656	<sup>63</sup> 0.0023	<sup>78</sup> 0.0020	<sup>83</sup> 0.0019	<sup>82</sup> 0.0017	<sup>87</sup> 0.0016	<sup>74</sup> 1.018	
182	SENSETIME-002	<sup>194</sup> 2056	<sup>133</sup> 650	<sup>172</sup> 0.0137	<sup>189</sup> 0.0136	<sup>194</sup> 0.0136	<sup>192</sup> 0.0136	<sup>203</sup> 0.0136	<sup>186</sup> 1.122	
183	SENSETIME-003	<sup>195</sup> 2056	<sup>238</sup> 940	<sup>4</sup> 0.0010	<sup>10</sup> 0.0010	<sup>12</sup> 0.0010	<sup>12</sup> 0.0009	<sup>13</sup> 0.0009	<sup>6</sup> 1.009	
184	SENSETIME-004	<sup>73</sup> 1032	<sup>168</sup> 710	<sup>2</sup> 0.0010	<sup>4</sup> 0.0009	<sup>5</sup> 0.0009	<sup>5</sup> 0.0009	<sup>8</sup> 0.0009	<sup>4</sup> 1.008	
185	SENSETIME-005	<sup>71</sup> 1032	<sup>246</sup> 1007	<sup>2</sup> 0.0009	<sup>1</sup> 0.0008	<sup>2</sup> 0.0008	<sup>5</sup> 0.0008	<sup>6</sup> 0.0008	<sup>1</sup> 1.008	
186	SENSETIME-006	<sup>72</sup> 1032	<sup>244</sup> 956	<sup>2</sup> 0.0009	<sup>2</sup> 0.0008	<sup>2</sup> 0.0008	<sup>2</sup> 0.0008	<sup>2</sup> 0.0008	<sup>2</sup> 1.008	
187	SHAMAN-003	<sup>159</sup> 2048	<sup>160</sup> 704	<sup>221</sup> 0.1243	<sup>224</sup> 0.0823	<sup>224</sup> 0.0708	<sup>223</sup> 0.0616	<sup>223</sup> 0.0518	<sup>223</sup> 1.789	
188	SHAMAN-004	<sup>141</sup> 2048	<sup>132</sup> 642	<sup>232</sup> 0.2221	<sup>231</sup> 0.1473	<sup>229</sup> 0.1241	<sup>229</sup> 0.1049	<sup>228</sup> 0.0825	<sup>231</sup> 2.411	
189	SHAMAN-006	<sup>135</sup> 2048	<sup>163</sup> 706	<sup>202</sup> 0.0398	<sup>210</sup> 0.0344	<sup>213</sup> 0.0332	<sup>215</sup> 0.0323	<sup>215</sup> 0.0315	<sup>209</sup> 1.316	
190	SHAMAN-007	<sup>111</sup> 2048	<sup>169</sup> 709	<sup>201</sup> 0.0396	<sup>209</sup> 0.0342	<sup>212</sup> 0.0331	<sup>213</sup> 0.0322	<sup>217</sup> 0.0314	<sup>207</sup> 1.315	
191	SIAT-001	<sup>178</sup> 2052	<sup>208</sup> 842	<sup>40</sup> 0.0018	<sup>39</sup> 0.0014	<sup>40</sup> 0.0013	<sup>22</sup> 0.0012	<sup>25</sup> 0.0011	<sup>39</sup> 1.013	
192	SIAT-002	<sup>174</sup> 2052	<sup>222</sup> 906	<sup>41</sup> 0.0018	<sup>37</sup> 0.0014	<sup>37</sup> 0.0013	<sup>38</sup> 0.0013	<sup>37</sup> 0.0012	<sup>42</sup> 1.013	
193	SMILART-004	<sup>33</sup> 512	<sup>16</sup> 167	<sup>244</sup> 0.9648	<sup>244</sup> 0.9641	<sup>244</sup> 0.9640	<sup>244</sup> 0.9639	<sup>245</sup> 0.9638	<sup>244</sup> 9.678	
194	SMILART-005	<sup>168</sup> 2048	<sup>56</sup> 464						<sup>247</sup> 10.000	
195	STAQU-000	<sup>231</sup> 4096	<sup>192</sup> 827	<sup>132</sup> 0.0071	<sup>150</sup> 0.0060	<sup>155</sup> 0.0057	<sup>160</sup> 0.0055	<sup>165</sup> 0.0053	<sup>142</sup> 1.056	
196	SYNESIS-003	<sup>220</sup> 4096	<sup>11</sup> 103	<sup>227</sup> 0.1700	<sup>227</sup> 0.1172	<sup>227</sup> 0.1047	<sup>228</sup> 0.0953	<sup>229</sup> 0.0869	<sup>227</sup> 2.120	
197	SYNESIS-003	<sup>149</sup> 2048	<sup>34</sup> 215	<sup>176</sup> 0.0162	<sup>193</sup> 0.0160	<sup>198</sup> 0.0160	<sup>203</sup> 0.0160	<sup>208</sup> 0.0160	<sup>192</sup> 1.144	
198	SYNESIS-005	<sup>234</sup> 4104	<sup>180</sup> 772	<sup>142</sup> 0.0085	<sup>169</sup> 0.0085	<sup>174</sup> 0.0085	<sup>186</sup> 0.0085	<sup>192</sup> 0.0085	<sup>166</sup> 1.076	
199	TECH5-001	<sup>94</sup> 1536	<sup>228</sup> 898	<sup>98</sup> 0.0040	<sup>97</sup> 0.0024	<sup>97</sup> 0.0021	<sup>93</sup> 0.0018	<sup>93</sup> 0.0017	<sup>98</sup> 1.024	
200	TECH5-002	<sup>43</sup> 513	<sup>239</sup> 941	<sup>72</sup> 0.0027	<sup>42</sup> 0.0014	<sup>26</sup> 0.0012	<sup>21</sup> 0.0011	<sup>18</sup> 0.0010	<sup>48</sup> 1.014	
201	TEVIAN-003	<sup>129</sup> 2048	<sup>56</sup> 300	<sup>173</sup> 0.0147	<sup>161</sup> 0.0074	<sup>153</sup> 0.0059	<sup>155</sup> 0.0047	<sup>154</sup> 0.0037	<sup>163</sup> 1.075	
202	TEVIAN-004	<sup>163</sup> 2048	<sup>54</sup> 299	<sup>160</sup> 0.0113	<sup>146</sup> 0.0057	<sup>146</sup> 0.0047	<sup>143</sup> 0.0037	<sup>139</sup> 0.0030	<sup>148</sup> 1.058	
203	TEVIAN-005	<sup>156</sup> 2048	<sup>85</sup> 416	<sup>135</sup> 0.0073	<sup>123</sup> 0.0038	<sup>117</sup> 0.0031	<sup>119</sup> 0.0027	<sup>119</sup> 0.0023	<sup>125</sup> 1.038	
204	TEVIAN-006	<sup>76</sup> 1032	<sup>123</sup> 599	<sup>69</sup> 0.0024	<sup>67</sup> 0.0018	<sup>73</sup> 0.0018	<sup>81</sup> 0.0017	<sup>89</sup> 0.0017	<sup>67</sup> 1.017	
205	TEVIAN-007	<sup>75</sup> 1032	<sup>189</sup> 779	<sup>39</sup> 0.0018	<sup>32</sup> 0.0014	<sup>36</sup> 0.0013	<sup>43</sup> 0.0013	<sup>42</sup> 0.0013	<sup>38</sup> 1.013	
206	TIGER-000	<sup>190</sup> 2052	<sup>88</sup> 428	<sup>212</sup> 0.0616	<sup>207</sup> 0.0310	<sup>208</sup> 0.0236	<sup>206</sup> 0.0178	<sup>200</sup> 0.0120	<sup>208</sup> 1.315	
207	TIGER-002	<sup>189</sup> 2052	<sup>92</sup> 464	<sup>117</sup> 0.0056	<sup>113</sup> 0.0029	<sup>109</sup> 0.0024	<sup>96</sup> 0.0019	<sup>78</sup> 0.0015	<sup>112</sup> 1.030	
208	TIGER-003	<sup>183</sup> 2052	<sup>94</sup> 464	<sup>116</sup> 0.0056	<sup>114</sup> 0.0029	<sup>108</sup> 0.0024	<sup>95</sup> 0.0019	<sup>77</sup> 0.0015	<sup>113</sup> 1.030	
209	TONGYITRANS-000	<sup>198</sup> 2070	<sup>21</sup> 190	<sup>128</sup> 0.0069	<sup>121</sup> 0.0038	<sup>124</sup> 0.0032	<sup>122</sup> 0.0029	<sup>120</sup> 0.0026	<sup>122</sup> 1.038	
210	TONGYITRANS-001	<sup>201</sup> 2070	<sup>21</sup> 189	<sup>129</sup> 0.0069	<sup>122</sup> 0.0038	<sup>122</sup> 0.0032	<sup>124</sup> 0.0029	<sup>129</sup> 0.0026	<sup>124</sup> 1.038	
211	TOSHIBA-000	<sup>101</sup> 1548	<sup>238</sup> 930	<sup>104</sup> 0.0045	<sup>103</sup> 0.0026	<sup>103</sup> 0.0022	<sup>103</sup> 0.0020	<sup>101</sup> 0.0018	<sup>108</sup> 1.026	
212	TOSHIBA-001	<sup>197</sup> 2060	<sup>236</sup> 931	<sup>109</sup> 0.0048	<sup>107</sup> 0.0027	<sup>106</sup> 0.0023	<sup>106</sup> 0.0020	<sup>100</sup> 0.0018	<sup>108</sup> 1.027	
213	TRUEFACE-000	<sup>109</sup> 2000	<sup>61</sup> 365	<sup>87</sup> 0.0033	<sup>109</sup> 0.0028	<sup>118</sup> 0.0028	<sup>118</sup> 0.0026	<sup>127</sup> 0.0026	<sup>105</sup> 1.026	
214	VD-000	<sup>70</sup> 1028	<sup>61</sup> 337	<sup>240</sup> 0.4737	<sup>239</sup> 0.3204	<sup>239</sup> 0.2695	<sup>238</sup> 0.2215	<sup>237</sup> 0.1678	<sup>239</sup> 4.058	
215	VD-001	<sup>186</sup> 2052	<sup>156</sup> 695	<sup>195</sup> 0.0276	<sup>198</sup> 0.0181	<sup>200</sup> 0.0162	<sup>199</sup> 0.0146	<sup>202</sup> 0.0130	<sup>198</sup> 1.174	
216	VD-002	<sup>181</sup> 2052	<sup>149</sup> 689	<sup>154</sup> 0.0095	<sup>163</sup> 0.0077	<sup>160</sup> 0.0073	<sup>171</sup> 0.0070	<sup>180</sup> 0.0068	<sup>160</sup> 1.071	

Table 23: Rank-based accuracy for the FRVT 2018 mugshot sets. In columns 3 and 4 are template size and template generation duration. Thereafter values are rank-based FNIR with T = 0 and FPIR = 1. This is appropriate to investigational uses but not those with higher volumes where candidates from all searches would need review

MISSES OUTSIDE RANK R		RESOURCE USAGE		ENROL MOST RECENT, N = 1.6M						
FNIR(N, T=0, R)		TEMPLATE		FRVT 2018 MUGSHOTS						
#	ALGORITHM	BYTES	MSEC	R=1	R=5	R=10	R=20	R=50	WORK-10	
217	VD-003	<sup>187</sup> 2052	<sup>154</sup> 693	<sup>134</sup> 0.0076	<sup>156</sup> 0.0069	<sup>163</sup> 0.0067	<sup>169</sup> 0.0066	<sup>178</sup> 0.0066	<sup>154</sup> 1.063	
218	VERIDAS-001	<sup>112</sup> 2048	<sup>222</sup> 885	<sup>78</sup> 0.0028	<sup>75</sup> 0.0019	<sup>71</sup> 0.0017	<sup>70</sup> 0.0015	<sup>74</sup> 0.0015	<sup>75</sup> 1.018	
219	VERIDAS-002	<sup>112</sup> 2048	<sup>222</sup> 888	<sup>77</sup> 0.0028	<sup>74</sup> 0.0019	<sup>68</sup> 0.0017	<sup>68</sup> 0.0015	<sup>72</sup> 0.0015	<sup>73</sup> 1.018	
220	VIGILANTSOLUTIONS-003	<sup>100</sup> 1544	<sup>201</sup> 832	<sup>212</sup> 0.0694	<sup>212</sup> 0.0349	<sup>207</sup> 0.0262	<sup>207</sup> 0.0201	<sup>203</sup> 0.0140	<sup>212</sup> 1.355	
221	VIGILANTSOLUTIONS-004	<sup>96</sup> 1544	<sup>201</sup> 830	<sup>222</sup> 0.1249	<sup>221</sup> 0.0706	<sup>220</sup> 0.0557	<sup>218</sup> 0.0434	<sup>216</sup> 0.0305	<sup>221</sup> 1.699	
222	VIGILANTSOLUTIONS-005	<sup>98</sup> 1544	<sup>188</sup> 778	<sup>147</sup> 0.0092	<sup>135</sup> 0.0045	<sup>126</sup> 0.0036	<sup>121</sup> 0.0029	<sup>116</sup> 0.0022	<sup>136</sup> 1.046	
223	VIGILANTSOLUTIONS-006	<sup>95</sup> 1544	<sup>201</sup> 834	<sup>151</sup> 0.0099	<sup>137</sup> 0.0048	<sup>133</sup> 0.0038	<sup>127</sup> 0.0030	<sup>118</sup> 0.0022	<sup>139</sup> 1.049	
224	VIGILANTSOLUTIONS-007	<sup>97</sup> 1544	<sup>128</sup> 618	<sup>89</sup> 0.0034	<sup>77</sup> 0.0020	<sup>72</sup> 0.0017	<sup>67</sup> 0.0015	<sup>53</sup> 0.0013	<sup>82</sup> 1.019	
225	VIGILANTSOLUTIONS-008	<sup>99</sup> 1544	<sup>79</sup> 405	<sup>82</sup> 0.0029	<sup>69</sup> 0.0018	<sup>64</sup> 0.0016	<sup>62</sup> 0.0015	<sup>45</sup> 0.0013	<sup>72</sup> 1.018	
226	VISIONBOX-000	<sup>186</sup> 2059	<sup>100</sup> 482	<sup>47</sup> 0.0019	<sup>49</sup> 0.0015	<sup>52</sup> 0.0014	<sup>49</sup> 0.0013	<sup>43</sup> 0.0013	<sup>47</sup> 1.014	
227	VISIONLABS-004	<sup>17</sup> 256	<sup>59</sup> 315	<sup>76</sup> 0.0027	<sup>65</sup> 0.0018	<sup>62</sup> 0.0016	<sup>66</sup> 0.0015	<sup>63</sup> 0.0014	<sup>69</sup> 1.017	
228	VISIONLABS-005	<sup>40</sup> 512	<sup>58</sup> 300	<sup>67</sup> 0.0024	<sup>61</sup> 0.0017	<sup>58</sup> 0.0015	<sup>53</sup> 0.0014	<sup>49</sup> 0.0013	<sup>61</sup> 1.016	
229	VISIONLABS-006	<sup>42</sup> 512	<sup>51</sup> 292	<sup>44</sup> 0.0018	<sup>45</sup> 0.0015	<sup>42</sup> 0.0014	<sup>43</sup> 0.0013	<sup>44</sup> 0.0013	<sup>44</sup> 1.014	
230	VISIONLABS-007	<sup>36</sup> 512	<sup>52</sup> 293	<sup>38</sup> 0.0018	<sup>41</sup> 0.0014	<sup>38</sup> 0.0013	<sup>33</sup> 0.0013	<sup>38</sup> 0.0012	<sup>41</sup> 1.013	
231	VISIONLABS-008	<sup>41</sup> 512	<sup>48</sup> 277	<sup>52</sup> 0.0020	<sup>68</sup> 0.0018	<sup>76</sup> 0.0018	<sup>84</sup> 0.0018	<sup>98</sup> 0.0017	<sup>64</sup> 1.017	
232	VISIONLABS-009	<sup>31</sup> 512	<sup>103</sup> 494	<sup>8</sup> 0.0011	<sup>13</sup> 0.0011	<sup>15</sup> 0.0010	<sup>16</sup> 0.0010	<sup>16</sup> 0.0010	<sup>12</sup> 1.010	
233	VISIONLABS-010	<sup>34</sup> 512	<sup>177</sup> 732	<sup>15</sup> 0.0014	<sup>30</sup> 0.0013	<sup>32</sup> 0.0013	<sup>35</sup> 0.0013	<sup>41</sup> 0.0013	<sup>26</sup> 1.012	
234	VOCORD-003	<sup>61</sup> 896	<sup>169</sup> 714	<sup>122</sup> 0.0062	<sup>117</sup> 0.0035	<sup>119</sup> 0.0030	<sup>117</sup> 0.0026	<sup>121</sup> 0.0023	<sup>117</sup> 1.035	
235	VOCORD-004	<sup>60</sup> 896	<sup>113</sup> 538	<sup>137</sup> 0.0079	<sup>139</sup> 0.0049	<sup>142</sup> 0.0043	<sup>146</sup> 0.0038	<sup>149</sup> 0.0034	<sup>137</sup> 1.048	
236	VOCORD-005	<sup>58</sup> 768	<sup>190</sup> 822	<sup>131</sup> 0.0070	<sup>136</sup> 0.0046	<sup>139</sup> 0.0041	<sup>143</sup> 0.0038	<sup>152</sup> 0.0035	<sup>133</sup> 1.044	
237	VOCORD-006	<sup>247</sup> 10240	<sup>198</sup> 825	<sup>246</sup> 1.0000	<sup>246</sup> 1.0000	<sup>246</sup> 1.0000	<sup>246</sup> 1.0000	<sup>246</sup> 1.0000	<sup>246</sup> 10.000	
238	VTS-000	<sup>167</sup> 2048	<sup>103</sup> 492	<sup>242</sup> 0.5937	<sup>243</sup> 0.5936	<sup>245</sup> 0.5936	<sup>243</sup> 0.5936	<sup>243</sup> 0.5936	<sup>243</sup> 6.343	
239	VTS-001	<sup>124</sup> 2048	<sup>224</sup> 891	<sup>27</sup> 0.0015	<sup>18</sup> 0.0012	<sup>18</sup> 0.0011	<sup>18</sup> 0.0011	<sup>19</sup> 0.0010	<sup>17</sup> 1.011	
240	XFORWARDAI-000	<sup>139</sup> 2048	<sup>182</sup> 768	<sup>61</sup> 0.0023	<sup>82</sup> 0.0020	<sup>89</sup> 0.0020	<sup>101</sup> 0.0019	<sup>107</sup> 0.0019	<sup>77</sup> 1.018	
241	XFORWARDAI-001	<sup>137</sup> 2048	<sup>148</sup> 681	<sup>56</sup> 0.0020	<sup>76</sup> 0.0019	<sup>86</sup> 0.0019	<sup>98</sup> 0.0019	<sup>106</sup> 0.0019	<sup>70</sup> 1.018	
242	XFORWARDAI-002	<sup>230</sup> 4096	<sup>237</sup> 935	<sup>48</sup> 0.0020	<sup>73</sup> 0.0019	<sup>84</sup> 0.0019	<sup>97</sup> 0.0019	<sup>104</sup> 0.0019	<sup>68</sup> 1.017	
243	YISHENG-001	<sup>219</sup> 3704	<sup>73</sup> 387	<sup>194</sup> 0.0265	<sup>188</sup> 0.0130	<sup>185</sup> 0.0102	<sup>183</sup> 0.0080	<sup>173</sup> 0.0059	<sup>189</sup> 1.134	
244	YITU-002	<sup>238</sup> 4138	<sup>210</sup> 870	<sup>48</sup> 0.0018	<sup>21</sup> 0.0012	<sup>19</sup> 0.0011	<sup>19</sup> 0.0011	<sup>21</sup> 0.0010	<sup>23</sup> 1.012	
245	YITU-003	<sup>239</sup> 4138	<sup>220</sup> 871	<sup>81</sup> 0.0029	<sup>92</sup> 0.0023	<sup>101</sup> 0.0022	<sup>109</sup> 0.0021	<sup>114</sup> 0.0021	<sup>89</sup> 1.021	
246	YITU-004	<sup>199</sup> 2070	<sup>231</sup> 910	<sup>12</sup> 0.0013	<sup>5</sup> 0.0009	<sup>8</sup> 0.0009	<sup>9</sup> 0.0009	<sup>8</sup> 0.0009	<sup>8</sup> 1.009	
247	YITU-005	<sup>200</sup> 2070	<sup>216</sup> 861	<sup>61</sup> 0.0023	<sup>84</sup> 0.0021	<sup>92</sup> 0.0020	<sup>104</sup> 0.0020	<sup>109</sup> 0.0020	<sup>79</sup> 1.019	

Table 24: Rank-based accuracy for the FRVT 2018 mugshot sets. In columns 3 and 4 are template size and template generation duration. Thereafter values are rank-based FNIR with T = 0 and FPIR = 1. This is appropriate to investigational uses but not those with higher volumes where candidates from all searches would need review. The next column is a workload statistic, a small value shows an algorithm front-loads mates into the first 10 candidates. Throughout, blue superscripts indicate the rank of the algorithm for that column, and the best value is highlighted in yellow.

This publication is available free of charge from: https://doi.org/10.6028/NIST.IR.8271

#	ALGORITHM	ENROL RECENT MUGSHOT, N = 1.6M									ENROL APPLICATION PORTRAIT, N = 1.6M					
		ENROL: MUGSHOT PROBE: MUGSHOT			ENROL: MUGSHOT PROBE: WEBCAM			ENROL: MUGSHOT PROBE: PROFILE			ENROL: VISA PROBE: BORDER		ENROL: BORDER PROBE: BORDER 10+YR		ENROL: VISA PROBE: KIOSK	
		FPIR=0.0003	FPIR=0.001	FPIR=0.01	FPIR=0.0003	FPIR=0.001	FPIR=0.01	FPIR=0.0003	FPIR=0.001	FPIR=0.01	FPIR=0.001	FPIR=0.01	FPIR=0.001	FPIR=0.01	FPIR=0.001	FPIR=0.01
1	20FACE-000	<sup>199</sup> 0.462	<sup>206</sup> 0.348	<sup>213</sup> 0.230	<sup>209</sup> 0.763	<sup>202</sup> 0.450	<sup>201</sup> 0.301	<sup>173</sup> 1.000	<sup>181</sup> 1.000	<sup>182</sup> 1.000	<sup>138</sup> 0.424	<sup>129</sup> 0.255	<sup>60</sup> 0.772	<sup>61</sup> 0.599	<sup>139</sup> 0.938	<sup>145</sup> 0.836
2	3DIVI-003	<sup>201</sup> 0.482	<sup>215</sup> 0.400	<sup>219</sup> 0.282	<sup>203</sup> 0.685	<sup>215</sup> 0.626	<sup>217</sup> 0.497				<sup>149</sup> 0.605	<sup>149</sup> 0.445			<sup>122</sup> 0.821	<sup>135</sup> 0.717
3	3DIVI-004	<sup>173</sup> 0.256	<sup>191</sup> 0.169	<sup>191</sup> 0.093	<sup>195</sup> 0.400	<sup>193</sup> 0.343	<sup>197</sup> 0.237				<sup>129</sup> 0.277	<sup>132</sup> 0.172			<sup>102</sup> 0.607	<sup>117</sup> 0.485
4	3DIVI-005	<sup>172</sup> 0.255	<sup>184</sup> 0.166	<sup>190</sup> 0.093	<sup>170</sup> 0.395	<sup>191</sup> 0.339	<sup>190</sup> 0.234	<sup>114</sup> 0.998	<sup>115</sup> 0.996	<sup>123</sup> 0.990	<sup>154</sup> 0.864	<sup>156</sup> 0.846			<sup>101</sup> 0.597	<sup>116</sup> 0.484
5	3DIVI-006	<sup>171</sup> 0.253	<sup>186</sup> 0.168	<sup>190</sup> 0.096	<sup>170</sup> 0.403	<sup>192</sup> 0.342	<sup>190</sup> 0.238				<sup>130</sup> 0.283	<sup>133</sup> 0.174			<sup>103</sup> 0.615	<sup>118</sup> 0.490
6	ACER-000	<sup>199</sup> 0.208	<sup>197</sup> 0.146	<sup>180</sup> 0.074	<sup>160</sup> 0.300	<sup>171</sup> 0.246	<sup>170</sup> 0.157	<sup>68</sup> 0.987	<sup>79</sup> 0.981	<sup>87</sup> 0.955	<sup>124</sup> 0.201	<sup>128</sup> 0.114			<sup>89</sup> 0.490	<sup>102</sup> 0.363
7	AIZE-001	<sup>117</sup> 0.127	<sup>140</sup> 0.077	<sup>138</sup> 0.034	<sup>126</sup> 0.187	<sup>130</sup> 0.143	<sup>129</sup> 0.087	<sup>89</sup> 0.995	<sup>96</sup> 0.994	<sup>112</sup> 0.983	<sup>100</sup> 0.101	<sup>102</sup> 0.052	<sup>51</sup> 0.364	<sup>54</sup> 0.216	<sup>74</sup> 0.387	<sup>86</sup> 0.289
8	ALCHERA-000	<sup>164</sup> 0.231	<sup>174</sup> 0.138	<sup>178</sup> 0.070	<sup>148</sup> 0.259	<sup>157</sup> 0.216	<sup>166</sup> 0.146	<sup>123</sup> 0.999	<sup>130</sup> 0.999	<sup>156</sup> 0.996	<sup>119</sup> 0.176	<sup>126</sup> 0.111			<sup>118</sup> 0.803	<sup>112</sup> 0.456
9	ALCHERA-001	<sup>242</sup> 1.000	<sup>242</sup> 0.999	<sup>244</sup> 0.999	<sup>235</sup> 1.000	<sup>244</sup> 1.000	<sup>244</sup> 1.000				<sup>199</sup> 1.000	<sup>177</sup> 1.000			<sup>183</sup> 1.000	<sup>198</sup> 1.000
10	ALCHERA-002	<sup>221</sup> 0.807	<sup>222</sup> 0.486	<sup>222</sup> 0.302	<sup>202</sup> 0.685	<sup>212</sup> 0.591	<sup>212</sup> 0.442	<sup>153</sup> 1.000	<sup>152</sup> 1.000	<sup>169</sup> 0.999	<sup>153</sup> 0.827	<sup>153</sup> 0.770			<sup>119</sup> 0.811	<sup>132</sup> 0.705
11	ALCHERA-003	<sup>195</sup> 0.450	<sup>178</sup> 0.155	<sup>176</sup> 0.070	<sup>148</sup> 0.304	<sup>168</sup> 0.239	<sup>170</sup> 0.152	<sup>148</sup> 1.000	<sup>141</sup> 0.999	<sup>156</sup> 0.997	<sup>118</sup> 0.172	<sup>119</sup> 0.097			<sup>86</sup> 0.464	<sup>101</sup> 0.362
12	ALCHERA-004	<sup>205</sup> 0.520	<sup>214</sup> 0.394	<sup>212</sup> 0.211	<sup>199</sup> 0.642	<sup>208</sup> 0.529	<sup>203</sup> 0.327	<sup>98</sup> 0.995	<sup>92</sup> 0.991	<sup>61</sup> 0.813	<sup>139</sup> 0.424	<sup>138</sup> 0.232	<sup>58</sup> 0.708	<sup>60</sup> 0.515	<sup>98</sup> 0.546	<sup>110</sup> 0.398
13	ALLGOVISION-000	<sup>125</sup> 0.138	<sup>152</sup> 0.088	<sup>157</sup> 0.045	<sup>137</sup> 0.202	<sup>146</sup> 0.166	<sup>157</sup> 0.106	<sup>76</sup> 0.993	<sup>89</sup> 0.990	<sup>111</sup> 0.982	<sup>103</sup> 0.117	<sup>108</sup> 0.066			<sup>99</sup> 0.526	<sup>109</sup> 0.396
14	ALLGOVISION-001	<sup>154</sup> 0.155	<sup>157</sup> 0.102	<sup>163</sup> 0.053	<sup>154</sup> 0.275	<sup>161</sup> 0.221	<sup>165</sup> 0.141	<sup>80</sup> 0.993	<sup>79</sup> 0.986	<sup>76</sup> 0.933	<sup>113</sup> 0.150	<sup>115</sup> 0.081			<sup>98</sup> 0.491	<sup>108</sup> 0.389
15	ANKE-000	<sup>145</sup> 0.184	<sup>162</sup> 0.117	<sup>172</sup> 0.063	<sup>147</sup> 0.256	<sup>160</sup> 0.220	<sup>166</sup> 0.151	<sup>88</sup> 0.995	<sup>97</sup> 0.994	<sup>128</sup> 0.990	<sup>171</sup> 1.000	<sup>203</sup> 1.000			<sup>173</sup> 1.000	<sup>179</sup> 1.000
16	ANKE-001	<sup>143</sup> 0.183	<sup>166</sup> 0.119	<sup>172</sup> 0.063	<sup>148</sup> 0.256	<sup>159</sup> 0.220	<sup>170</sup> 0.151	<sup>98</sup> 0.995	<sup>102</sup> 0.994	<sup>131</sup> 0.992	<sup>228</sup> 1.000	<sup>218</sup> 1.000			<sup>240</sup> 1.000	<sup>243</sup> 1.000
17	ANKE-002	<sup>75</sup> 0.062	<sup>83</sup> 0.032	<sup>82</sup> 0.014	<sup>67</sup> 0.103	<sup>71</sup> 0.079	<sup>79</sup> 0.050	<sup>48</sup> 0.975	<sup>50</sup> 0.948	<sup>56</sup> 0.795	<sup>56</sup> 0.034	<sup>59</sup> 0.018			<sup>47</sup> 0.245	<sup>57</sup> 0.190
18	AWARE-003	<sup>142</sup> 0.174	<sup>170</sup> 0.128	<sup>183</sup> 0.082	<sup>147</sup> 0.351	<sup>185</sup> 0.298	<sup>190</sup> 0.204	<sup>68</sup> 0.987	<sup>77</sup> 0.984	<sup>108</sup> 0.977	<sup>140</sup> 0.428	<sup>142</sup> 0.378			<sup>96</sup> 0.530	<sup>111</sup> 0.443
19	AWARE-004	<sup>187</sup> 0.355	<sup>200</sup> 0.269	<sup>208</sup> 0.175	<sup>191</sup> 0.619	<sup>207</sup> 0.509	<sup>210</sup> 0.375	<sup>151</sup> 1.000	<sup>155</sup> 1.000	<sup>171</sup> 0.999	<sup>135</sup> 0.397	<sup>137</sup> 0.279			<sup>128</sup> 0.816	<sup>127</sup> 0.631
20	AWARE-005	<sup>211</sup> 0.608	<sup>209</sup> 0.364	<sup>188</sup> 0.085	<sup>165</sup> 0.342	<sup>172</sup> 0.253	<sup>170</sup> 0.163	<sup>149</sup> 1.000	<sup>158</sup> 1.000	<sup>170</sup> 0.999	<sup>128</sup> 0.255	<sup>130</sup> 0.122			<sup>130</sup> 0.916	<sup>134</sup> 0.714
21	AWARE-006	<sup>200</sup> 0.475	<sup>201</sup> 0.276	<sup>209</sup> 0.175	<sup>186</sup> 0.466	<sup>196</sup> 0.398	<sup>201</sup> 0.283	<sup>136</sup> 1.000	<sup>149</sup> 0.999	<sup>166</sup> 0.999	<sup>133</sup> 0.368	<sup>136</sup> 0.254			<sup>114</sup> 0.749	<sup>124</sup> 0.623
22	AYONIX-000	<sup>224</sup> 0.846	<sup>231</sup> 0.811	<sup>236</sup> 0.724	<sup>224</sup> 0.956	<sup>230</sup> 0.939	<sup>236</sup> 0.892	<sup>118</sup> 0.998	<sup>120</sup> 0.998	<sup>141</sup> 0.995	<sup>158</sup> 0.954	<sup>158</sup> 0.891			<sup>142</sup> 0.982	<sup>150</sup> 0.959
23	AYONIX-001	<sup>225</sup> 0.875	<sup>233</sup> 0.824	<sup>234</sup> 0.701	<sup>210</sup> 0.946	<sup>225</sup> 0.920	<sup>227</sup> 0.845	<sup>141</sup> 1.000	<sup>145</sup> 0.999	<sup>151</sup> 0.996	<sup>162</sup> 0.998	<sup>162</sup> 0.998			<sup>139</sup> 0.969	<sup>147</sup> 0.926
24	AYONIX-002	<sup>226</sup> 0.876	<sup>232</sup> 0.824	<sup>238</sup> 0.702	<sup>217</sup> 0.946	<sup>226</sup> 0.920	<sup>227</sup> 0.845	<sup>145</sup> 1.000	<sup>147</sup> 0.999	<sup>152</sup> 0.996	<sup>155</sup> 0.915	<sup>154</sup> 0.821			<sup>138</sup> 0.969	<sup>146</sup> 0.926
25	CAMVI-003	<sup>96</sup> 0.094	<sup>135</sup> 0.071	<sup>168</sup> 0.058	<sup>148</sup> 0.152	<sup>123</sup> 0.132	<sup>151</sup> 0.108	<sup>31</sup> 0.979	<sup>38</sup> 0.970	<sup>82</sup> 0.940	<sup>102</sup> 0.114	<sup>130</sup> 0.100			<sup>77</sup> 0.402	<sup>105</sup> 0.377
26	CAMVI-004	<sup>105</sup> 0.107	<sup>136</sup> 0.072	<sup>168</sup> 0.054	<sup>148</sup> 0.240	<sup>125</sup> 0.136	<sup>144</sup> 0.100	<sup>138</sup> 1.000	<sup>143</sup> 0.999	<sup>155</sup> 0.998	<sup>99</sup> 0.100	<sup>119</sup> 0.081			<sup>111</sup> 0.787	<sup>119</sup> 0.507
27	CAMVI-005	<sup>126</sup> 0.139	<sup>156</sup> 0.099	<sup>182</sup> 0.076	<sup>181</sup> 0.451	<sup>153</sup> 0.179	<sup>161</sup> 0.132	<sup>141</sup> 1.000	<sup>151</sup> 1.000	<sup>164</sup> 0.998	<sup>114</sup> 0.156	<sup>127</sup> 0.112			<sup>150</sup> 0.999	<sup>156</sup> 0.983
28	CIB-000	<sup>51</sup> 0.044	<sup>35</sup> 0.012	<sup>31</sup> 0.005	<sup>47</sup> 0.077	<sup>54</sup> 0.045	<sup>33</sup> 0.025	<sup>127</sup> 1.000	<sup>164</sup> 1.000	<sup>178</sup> 1.000	<sup>31</sup> 0.017	<sup>24</sup> 0.008	<sup>23</sup> 0.141	<sup>23</sup> 0.068	<sup>127</sup> 0.894	<sup>120</sup> 0.521
29	CLOUDWALK-HR-000	<sup>5</sup> 0.004	<sup>6</sup> 0.002	<sup>5</sup> 0.002	<sup>4</sup> 0.015	<sup>6</sup> 0.013	<sup>5</sup> 0.012	<sup>1</sup> 0.188	<sup>1</sup> 0.133	<sup>2</sup> 0.095	<sup>5</sup> 0.005	<sup>4</sup> 0.003	<sup>3</sup> 0.033	<sup>4</sup> 0.018	<sup>2</sup> 0.099	<sup>2</sup> 0.075
30	COGENT-000	<sup>130</sup> 0.143	<sup>113</sup> 0.053	<sup>121</sup> 0.029	<sup>118</sup> 0.175	<sup>126</sup> 0.140	<sup>140</sup> 0.100	<sup>96</sup> 0.996	<sup>108</sup> 0.995	<sup>127</sup> 0.991						
31	COGENT-001	<sup>129</sup> 0.143	<sup>112</sup> 0.053	<sup>130</sup> 0.029	<sup>119</sup> 0.175	<sup>127</sup> 0.140	<sup>147</sup> 0.100	<sup>96</sup> 0.996	<sup>107</sup> 0.995	<sup>128</sup> 0.991						
32	COGENT-002	<sup>139</sup> 0.159	<sup>99</sup> 0.044	<sup>97</sup> 0.017	<sup>46</sup> 0.124	<sup>36</sup> 0.098	<sup>100</sup> 0.063	<sup>118</sup> 0.998	<sup>119</sup> 0.998	<sup>137</sup> 0.994						
33	COGENT-003	<sup>157</sup> 0.203	<sup>104</sup> 0.046	<sup>87</sup> 0.016	<sup>81</sup> 0.121	<sup>90</sup> 0.095	<sup>97</sup> 0.061	<sup>118</sup> 0.999	<sup>121</sup> 0.998	<sup>146</sup> 0.995						
34	COGENT-004	<sup>160</sup> 0.209	<sup>84</sup> 0.033	<sup>39</sup> 0.006	<sup>38</sup> 0.067	<sup>40</sup> 0.051	<sup>41</sup> 0.031	<sup>113</sup> 0.998	<sup>117</sup> 0.997	<sup>148</sup> 0.995	<sup>38</sup> 0.022	<sup>37</sup> 0.012	<sup>22</sup> 0.126	<sup>25</sup> 0.072	<sup>84</sup> 0.456	<sup>51</sup> 0.178
35	COGENT-005	<sup>64</sup> 0.050	<sup>25</sup> 0.009	<sup>25</sup> 0.004	<sup>27</sup> 0.050	<sup>29</sup> 0.037	<sup>29</sup> 0.023	<sup>94</sup> 0.996	<sup>85</sup> 0.989	<sup>20</sup> 0.323	<sup>21</sup> 0.011	<sup>19</sup> 0.006	<sup>15</sup> 0.082	<sup>16</sup> 0.043	<sup>128</sup> 0.905	<sup>89</sup> 0.202
36	COGNITEC-000	<sup>163</sup> 0.226	<sup>182</sup> 0.161	<sup>197</sup> 0.095	<sup>188</sup> 0.439	<sup>186</sup> 0.303	<sup>188</sup> 0.200	<sup>93</sup> 0.996	<sup>93</sup> 0.992	<sup>96</sup> 0.971						
37	COGNITEC-001	<sup>155</sup> 0.192	<sup>158</sup> 0.102	<sup>167</sup> 0.053	<sup>231</sup> 0.997	<sup>165</sup> 0.230	<sup>166</sup> 0.135	<sup>188</sup> 1.000	<sup>196</sup> 1.000	<sup>91</sup> 0.965						
38	COGNITEC-002	<sup>113</sup> 0.122	<sup>115</sup> 0.053	<sup>121</sup> 0.025	<sup>229</sup> 0.990	<sup>152</sup> 0.178	<sup>150</sup> 0.101	<sup>218</sup> 1.000	<sup>163</sup> 1.000	<sup>88</sup> 0.956						
39	COGNITEC-003	<sup>100</sup> 0.099	<sup>111</sup> 0.053	<sup>122</sup> 0.025	<sup>141</sup> 0.222	<sup>144</sup> 0.162	<sup>144</sup> 0.100	<sup>150</sup> 1.000	<sup>165</sup> 1.000	<sup>83</sup> 0.946						
40	COGNITEC-004	<sup>69</sup> 0.055	<sup>82</sup> 0.031	<sup>85</sup> 0.014	<sup>88</sup> 0.127	<sup>94</sup> 0.097	<sup>89</sup> 0.058	<sup>88</sup> 0.995	<sup>86</sup> 0.990	<sup>72</sup> 0.919	<sup>88</sup> 0.068	<sup>88</sup> 0.038	<sup>50</sup> 0.316	<sup>33</sup> 0.196	<sup>36</sup> 0.288	<sup>67</sup> 0.218
41	COGNITEC-005	<sup>70</sup> 0.055	<sup>27</sup> 0.010	<sup>24</sup> 0.004	<sup>31</sup> 0.058	<sup>32</sup> 0.041	<sup>29</sup> 0.022	<sup>234</sup> 1.000	<sup>228</sup> 1.000	<sup>67</sup> 0.878	<sup>63</sup> 0.041	<sup>76</sup> 0.028	<sup>29</sup> 0.157	<sup>33</sup> 0.092	<sup>31</sup> 0.179	<sup>36</sup> 0.145
42	CUBOX-000	<sup>8</sup> 0.005	<sup>11</sup> 0.003	<sup>12</sup> 0.002	<sup>12</sup> 0.022	<sup>12</sup> 0.019	<sup>13</sup> 0.014	<sup>4</sup> 0.276	<sup>2</sup> 0.168	<sup>4</sup> 0.104	<sup>2</sup> 0.004	<sup>2</sup> 0.003	<sup>2</sup> 0.028	<sup>2</sup> 0.014	<sup>1</sup> 0.073	<sup>1</sup> 0.062
43	CYBERLINK-000	<sup>123</sup> 0.137	<sup>121</sup> 0.056	<sup>113</sup> 0.023	<sup>113</sup> 0.162	<sup>108</sup> 0.116	<sup>110</sup> 0.070	<sup>107</sup> 0.997	<sup>110</sup> 0.995	<sup>116</sup> 0.981	<sup>86</sup> 0.063	<sup>84</sup> 0.032			<sup>69</sup> 0.339	<sup>75</sup> 0.232
44	CYBERLINK-001	<sup>37</sup> 0.096	<sup>116</sup> 0.054	<sup>111</sup> 0.022	<sup>107</sup> 0.138	<sup>105&lt;/</sup>										

MISSES BELOW THRESHOLD, T		ENROL RECENT MUGSHOT, N = 1.6M															ENROL APPLICATION PORTRAIT, N = 1.6M					
		ENROL: MUGSHOT			ENROL: MUGSHOT			ENROL: MUGSHOT			ENROL: VISA			ENROL: BORDER		ENROL: VISA						
		PROBE: MUGSHOT			PROBE: WEBCAM			PROBE: PROFILE			PROBE: BORDER			PROBE: BORDER 10+YR		PROBE: KIOSK						
#	ALGORITHM	FPIR=0.0003	FPIR=0.001	FPIR=0.01	FPIR=0.0003	FPIR=0.001	FPIR=0.01	FPIR=0.0003	FPIR=0.001	FPIR=0.01	FPIR=0.0003	FPIR=0.001	FPIR=0.01	FPIR=0.001	FPIR=0.01	FPIR=0.001	FPIR=0.01					
47	CYBERLINK-004	<sup>153</sup> 0.188	<sup>22</sup> 0.007	<sup>22</sup> 0.003	<sup>34</sup> 0.063	<sup>27</sup> 0.036	<sup>25</sup> 0.022	<sup>180</sup> 1.000	<sup>180</sup> 1.000	<sup>173</sup> 0.999	<sup>24</sup> 0.013	<sup>22</sup> 0.007	<sup>19</sup> 0.109	<sup>17</sup> 0.050	<sup>137</sup> 0.954	<sup>89</sup> 0.291						
48	DAHUA-000	<sup>119</sup> 0.128	<sup>148</sup> 0.086	<sup>154</sup> 0.045	<sup>124</sup> 0.179	<sup>124</sup> 0.135	<sup>128</sup> 0.083															
49	DAHUA-001	<sup>104</sup> 0.106	<sup>138</sup> 0.073	<sup>142</sup> 0.037	<sup>104</sup> 0.151	<sup>116</sup> 0.122	<sup>110</sup> 0.075	<sup>69</sup> 0.987	<sup>71</sup> 0.980	<sup>77</sup> 0.933												
50	DAHUA-002	<sup>32</sup> 0.026	<sup>44</sup> 0.015	<sup>44</sup> 0.006	<sup>34</sup> 0.060	<sup>36</sup> 0.046	<sup>39</sup> 0.029	<sup>24</sup> 0.681	<sup>25</sup> 0.638	<sup>35</sup> 0.522	<sup>28</sup> 0.017	<sup>29</sup> 0.008			<sup>24</sup> 0.159	<sup>26</sup> 0.125						
51	DAHUA-003	<sup>31</sup> 0.025	<sup>40</sup> 0.014	<sup>35</sup> 0.005	<sup>28</sup> 0.054	<sup>31</sup> 0.041	<sup>31</sup> 0.024	<sup>18</sup> 0.647	<sup>21</sup> 0.579	<sup>27</sup> 0.447	<sup>23</sup> 0.013	<sup>21</sup> 0.006	<sup>14</sup> 0.081	<sup>15</sup> 0.043	<sup>17</sup> 0.134	<sup>16</sup> 0.109						
52	DEEPLINT-001	<sup>13</sup> 0.010	<sup>13</sup> 0.003	<sup>13</sup> 0.002	<sup>7</sup> 0.018	<sup>7</sup> 0.014	<sup>7</sup> 0.010	<sup>159</sup> 1.000	<sup>150</sup> 1.000	<sup>25</sup> 0.503	<sup>8</sup> 0.006	<sup>2</sup> 0.004			<sup>2</sup> 0.159	<sup>12</sup> 0.097						
53	DEESEA-001	<sup>85</sup> 0.073	<sup>103</sup> 0.046	<sup>109</sup> 0.022	<sup>94</sup> 0.129	<sup>98</sup> 0.101	<sup>99</sup> 0.059	<sup>74</sup> 0.988	<sup>78</sup> 0.985	<sup>109</sup> 0.973	<sup>92</sup> 0.077	<sup>99</sup> 0.041			<sup>69</sup> 0.326	<sup>76</sup> 0.251						
54	DERMALOG-003	<sup>207</sup> 0.550	<sup>221</sup> 0.482	<sup>230</sup> 0.360	<sup>206</sup> 0.715	<sup>217</sup> 0.655	<sup>221</sup> 0.526				<sup>152</sup> 0.677	<sup>151</sup> 0.554			<sup>125</sup> 0.870	<sup>142</sup> 0.791						
55	DERMALOG-004	<sup>209</sup> 0.554	<sup>220</sup> 0.480	<sup>225</sup> 0.358	<sup>206</sup> 0.711	<sup>218</sup> 0.657	<sup>210</sup> 0.526	<sup>100</sup> 0.997	<sup>111</sup> 0.995	<sup>130</sup> 0.991	<sup>148</sup> 0.603	<sup>154</sup> 0.458			<sup>124</sup> 0.856	<sup>138</sup> 0.751						
56	DERMALOG-005	<sup>154</sup> 0.189	<sup>151</sup> 0.088	<sup>156</sup> 0.043	<sup>130</sup> 0.201	<sup>137</sup> 0.154	<sup>149</sup> 0.096	<sup>98</sup> 0.996	<sup>88</sup> 0.990	<sup>89</sup> 0.950	<sup>131</sup> 0.300	<sup>138</sup> 0.267			<sup>100</sup> 0.614	<sup>113</sup> 0.459						
57	DERMALOG-006	<sup>99</sup> 0.098	<sup>110</sup> 0.052	<sup>124</sup> 0.026	<sup>100</sup> 0.137	<sup>101</sup> 0.105	<sup>100</sup> 0.067	<sup>74</sup> 0.989	<sup>72</sup> 0.981	<sup>79</sup> 0.933	<sup>81</sup> 0.059	<sup>82</sup> 0.031			<sup>69</sup> 0.318	<sup>71</sup> 0.230						
58	DERMALOG-007	<sup>151</sup> 0.188	<sup>149</sup> 0.086	<sup>148</sup> 0.040	<sup>130</sup> 0.200	<sup>135</sup> 0.152	<sup>137</sup> 0.093	<sup>97</sup> 0.996	<sup>87</sup> 0.990	<sup>85</sup> 0.950	<sup>98</sup> 0.099	<sup>101</sup> 0.052			<sup>100</sup> 0.557	<sup>93</sup> 0.299						
59	DERMALOG-008	<sup>176</sup> 0.268	<sup>101</sup> 0.045	<sup>94</sup> 0.017	<sup>149</sup> 0.231	<sup>87</sup> 0.094	<sup>89</sup> 0.054	<sup>169</sup> 1.000	<sup>175</sup> 1.000	<sup>179</sup> 1.000	<sup>78</sup> 0.057	<sup>78</sup> 0.025	<sup>54</sup> 0.382	<sup>51</sup> 0.158	<sup>130</sup> 0.940	<sup>130</sup> 0.678						
60	EYEDEA-003	<sup>204</sup> 0.509	<sup>211</sup> 0.388	<sup>217</sup> 0.265	<sup>197</sup> 0.625	<sup>210</sup> 0.543	<sup>211</sup> 0.404	<sup>101</sup> 0.997	<sup>103</sup> 0.994	<sup>119</sup> 0.990	<sup>146</sup> 0.570	<sup>145</sup> 0.392			<sup>117</sup> 0.792	<sup>129</sup> 0.658						
61	F8-001	<sup>197</sup> 0.458	<sup>183</sup> 0.166	<sup>139</sup> 0.036				<sup>125</sup> 0.999	<sup>129</sup> 0.998	<sup>149</sup> 0.995												
62	FINCORE-000	<sup>150</sup> 0.187	<sup>173</sup> 0.134	<sup>178</sup> 0.071	<sup>153</sup> 0.267	<sup>158</sup> 0.217	<sup>163</sup> 0.140	<sup>149</sup> 1.000	<sup>180</sup> 1.000	<sup>144</sup> 0.995	<sup>120</sup> 0.187	<sup>125</sup> 0.108	<sup>57</sup> 0.598	<sup>59</sup> 0.418	<sup>88</sup> 0.458	<sup>98</sup> 0.349						
63	FUJITSULAB-000	<sup>168</sup> 0.246	<sup>99</sup> 0.021	<sup>99</sup> 0.008	<sup>44</sup> 0.070	<sup>50</sup> 0.056	<sup>59</sup> 0.035				<sup>40</sup> 0.024	<sup>40</sup> 0.013	<sup>34</sup> 0.177	<sup>37</sup> 0.093	<sup>49</sup> 0.240	<sup>41</sup> 0.156						
64	GLORY-000	<sup>194</sup> 0.441	<sup>210</sup> 0.367	<sup>224</sup> 0.295	<sup>193</sup> 0.586	<sup>211</sup> 0.547	<sup>214</sup> 0.470	<sup>89</sup> 0.995	<sup>105</sup> 0.995	<sup>134</sup> 0.993	<sup>142</sup> 0.453	<sup>144</sup> 0.381			<sup>123</sup> 0.839	<sup>143</sup> 0.795						
65	GLORY-001	<sup>186</sup> 0.355	<sup>202</sup> 0.305	<sup>214</sup> 0.236	<sup>169</sup> 0.582	<sup>209</sup> 0.537	<sup>213</sup> 0.448	<sup>84</sup> 0.994	<sup>94</sup> 0.993	<sup>124</sup> 0.991	<sup>137</sup> 0.408	<sup>141</sup> 0.336			<sup>121</sup> 0.819	<sup>139</sup> 0.753						
66	GORILLA-001	<sup>219</sup> 0.747	<sup>216</sup> 0.406	<sup>214</sup> 0.246	<sup>197</sup> 0.590	<sup>203</sup> 0.453	<sup>203</sup> 0.314	<sup>169</sup> 1.000	<sup>171</sup> 1.000	<sup>184</sup> 1.000	<sup>143</sup> 0.468	<sup>143</sup> 0.299			<sup>217</sup> 1.000	<sup>133</sup> 0.710						
67	GORILLA-002	<sup>175</sup> 0.266	<sup>190</sup> 0.188	<sup>197</sup> 0.106	<sup>169</sup> 0.342	<sup>179</sup> 0.268	<sup>189</sup> 0.170	<sup>168</sup> 1.000	<sup>177</sup> 1.000	<sup>159</sup> 0.993	<sup>127</sup> 0.250	<sup>131</sup> 0.137			<sup>153</sup> 1.000	<sup>115</sup> 0.466						
68	GORILLA-003	<sup>217</sup> 0.694	<sup>204</sup> 0.318	<sup>207</sup> 0.157	<sup>201</sup> 0.684	<sup>200</sup> 0.434	<sup>199</sup> 0.247	<sup>231</sup> 1.000	<sup>239</sup> 1.000	<sup>184</sup> 1.000	<sup>136</sup> 0.407	<sup>134</sup> 0.213			<sup>189</sup> 1.000	<sup>122</sup> 0.562						
69	GORILLA-004	<sup>122</sup> 0.135	<sup>154</sup> 0.089	<sup>151</sup> 0.043	<sup>130</sup> 0.202	<sup>143</sup> 0.160	<sup>146</sup> 0.101	<sup>46</sup> 0.972	<sup>52</sup> 0.959	<sup>69</sup> 0.903	<sup>108</sup> 0.135	<sup>111</sup> 0.072			<sup>81</sup> 0.438	<sup>95</sup> 0.309						
70	GORILLA-005	<sup>94</sup> 0.086	<sup>125</sup> 0.058	<sup>124</sup> 0.026	<sup>129</sup> 0.179	<sup>129</sup> 0.142	<sup>139</sup> 0.088	<sup>25</sup> 0.770	<sup>28</sup> 0.700	<sup>39</sup> 0.553	<sup>96</sup> 0.088	<sup>99</sup> 0.040			<sup>69</sup> 0.315	<sup>68</sup> 0.223						
71	GORILLA-006	<sup>37</sup> 0.046	<sup>74</sup> 0.027	<sup>70</sup> 0.011	<sup>79</sup> 0.118	<sup>81</sup> 0.089	<sup>89</sup> 0.053	<sup>19</sup> 0.602	<sup>20</sup> 0.531	<sup>29</sup> 0.369	<sup>44</sup> 0.028	<sup>44</sup> 0.013	<sup>33</sup> 0.166	<sup>36</sup> 0.093	<sup>40</sup> 0.218	<sup>40</sup> 0.154						
72	HIK-003	<sup>140</sup> 0.159	<sup>189</sup> 0.103	<sup>169</sup> 0.057	<sup>129</sup> 0.190	<sup>139</sup> 0.158	<sup>152</sup> 0.105	<sup>56</sup> 0.980	<sup>56</sup> 0.969	<sup>74</sup> 0.925	<sup>111</sup> 0.142	<sup>113</sup> 0.080			<sup>83</sup> 0.445	<sup>100</sup> 0.359						
73	HIK-004	<sup>136</sup> 0.156	<sup>155</sup> 0.099	<sup>169</sup> 0.054	<sup>124</sup> 0.182	<sup>136</sup> 0.153	<sup>149</sup> 0.101	<sup>61</sup> 0.983	<sup>63</sup> 0.976	<sup>89</sup> 0.947	<sup>109</sup> 0.137	<sup>112</sup> 0.077			<sup>80</sup> 0.434	<sup>99</sup> 0.353						
74	HIK-005	<sup>102</sup> 0.102	<sup>96</sup> 0.044	<sup>94</sup> 0.019	<sup>69</sup> 0.098	<sup>70</sup> 0.077	<sup>74</sup> 0.048	<sup>149</sup> 1.000	<sup>145</sup> 0.999	<sup>169</sup> 0.998	<sup>87</sup> 0.068	<sup>87</sup> 0.036			<sup>97</sup> 0.541	<sup>78</sup> 0.258						
75	HIK-006	<sup>128</sup> 0.142	<sup>105</sup> 0.047	<sup>100</sup> 0.020	<sup>72</sup> 0.111	<sup>78</sup> 0.086	<sup>78</sup> 0.052	<sup>125</sup> 1.000	<sup>183</sup> 1.000	<sup>174</sup> 0.999												
76	HYPERVERGE-001	<sup>11</sup> 0.009	<sup>16</sup> 0.004	<sup>4</sup> 0.002	<sup>44</sup> 0.039	<sup>23</sup> 0.031	<sup>24</sup> 0.020	<sup>9</sup> 0.275	<sup>9</sup> 0.220	<sup>9</sup> 0.146	<sup>11</sup> 0.007	<sup>11</sup> 0.004	<sup>9</sup> 0.053	<sup>11</sup> 0.027	<sup>7</sup> 0.101	<sup>5</sup> 0.083						
77	IDEMIA-003	<sup>208</sup> 0.552	<sup>106</sup> 0.047	<sup>104</sup> 0.021	<sup>245</sup> 1.000	<sup>145</sup> 0.165	<sup>128</sup> 0.079				<sup>215</sup> 1.000	<sup>105</sup> 0.123	<sup>105</sup> 0.061		<sup>115</sup> 0.766	<sup>126</sup> 0.630						
78	IDEMIA-004	<sup>68</sup> 0.055	<sup>92</sup> 0.037	<sup>103</sup> 0.021	<sup>103</sup> 0.144	<sup>112</sup> 0.118	<sup>122</sup> 0.079	<sup>51</sup> 0.976	<sup>62</sup> 0.973	<sup>92</sup> 0.968	<sup>104</sup> 0.123	<sup>104</sup> 0.061			<sup>114</sup> 0.766	<sup>125</sup> 0.630						
79	IDEMIA-005	<sup>82</sup> 0.066	<sup>98</sup> 0.044	<sup>123</sup> 0.026	<sup>123</sup> 0.181	<sup>134</sup> 0.150	<sup>151</sup> 0.102	<sup>55</sup> 0.979	<sup>66</sup> 0.978	<sup>96</sup> 0.973	<sup>106</sup> 0.130	<sup>110</sup> 0.070			<sup>126</sup> 0.879	<sup>136</sup> 0.743						
80	IDEMIA-006	<sup>80</sup> 0.065	<sup>95</sup> 0.043	<sup>124</sup> 0.025	<sup>152</sup> 0.266	<sup>163</sup> 0.226	<sup>173</sup> 0.161	<sup>64</sup> 0.984	<sup>74</sup> 0.982	<sup>109</sup> 0.980	<sup>112</sup> 0.144	<sup>117</sup> 0.090			<sup>110</sup> 0.733	<sup>121</sup> 0.531						
81	IDEMIA-007	<sup>43</sup> 0.035	<sup>52</sup> 0.018	<sup>59</sup> 0.008	<sup>46</sup> 0.073	<sup>48</sup> 0.055	<sup>49</sup> 0.033	<sup>199</sup> 1.000	<sup>193</sup> 1.000	<sup>212</sup> 1.000	<sup>74</sup> 0.052	<sup>76</sup> 0.022	<sup>36</sup> 0.182	<sup>39</sup> 0.109	<sup>218</sup> 1.000	<sup>154</sup> 0.982						
82	IDEMIA-008	<sup>3</sup> 0.004	<sup>3</sup> 0.002	<sup>3</sup> 0.001	<sup>3</sup> 0.016	<sup>3</sup> 0.013	<sup>3</sup> 0.009	<sup>3</sup> 0.276	<sup>4</sup> 0.204	<sup>3</sup> 0.136	<sup>4</sup> 0.005	<sup>3</sup> 0.003	<sup>5</sup> 0.036	<sup>6</sup> 0.019	<sup>9</sup> 0.106	<sup>9</sup> 0.092						
83	IMAGUS-002	<sup>229</sup> 0.908	<sup>229</sup> 0.749	<sup>231</sup> 0.564	<sup>215</sup> 0.944	<sup>222</sup> 0.816	<sup>224</sup> 0.645	<sup>176</sup> 1.000	<sup>184</sup> 1.000	<sup>185</sup> 1.000												
84	IMAGUS-003	<sup>228</sup> 0.898	<sup>230</sup> 0.807	<sup>233</sup> 0.669	<sup>229</sup> 0.954	<sup>224</sup> 0.909	<sup>229</sup> 0.809	<sup>177</sup> 1.000	<sup>167</sup> 1.000	<sup>180</sup> 1.000												
85	IMAGUS-005	<sup>41</sup> 0.034	<sup>55</sup> 0.018	<sup>59</sup> 0.008	<sup>54</sup> 0.088	<sup>58</sup> 0.066	<sup>59</sup> 0.040	<sup>37</sup> 0.926	<sup>39</sup> 0.838	<sup>45</sup> 0.647	<sup>46</sup> 0.029	<sup>51</sup> 0.016	<sup>32</sup> 0.161	<sup>38</sup> 0.094	<sup>43</sup> 0.231	<sup>56</sup> 0.189						
86	IMAGUS-006	<sup>48</sup> 0.039	<sup>57</sup> 0.019	<sup>56</sup> 0.008	<sup>58</sup> 0.093	<sup>61</sup> 0.069	<sup>64</sup> 0.042	<sup>58</sup> 0.980	<sup>46</sup> 0.897	<sup>58</sup> 0.621	<sup>45</sup> 0.028	<sup>47</sup> 0.015	<sup>31</sup> 0.161	<sup>34</sup> 0.092	<sup>51</sup> 0.260	<sup>53</sup> 0.181						
87	IMPERIAL-000	<sup>133</sup> 0.154	<sup>69</sup> 0.026	<sup>65</sup> 0.009	<sup>58</sup> 0.089	<sup>60</sup> 0.068	<sup>61</sup> 0.041	<sup>162</sup> 1.000	<sup>133</sup> 0.999	<sup>144</sup> 0.995	<sup>64</sup> 0.042	<sup>66</sup> 0.020			<sup>48</sup> 0.245	<sup>46</sup> 0.168						
88	INCDE-000	<sup>193</sup> 0.423	<sup>203</sup> 0.310	<sup>210</sup> 0.199	<sup>188</sup> 0.486	<sup>198</sup> 0.420	<sup>203</sup> 0.304	<sup>143</sup> 1.000	<sup>126</sup> 0.998	<sup>139</sup> 0.994												
89	INCDE-001	<sup>183</sup> 0.319	<sup>193</sup> 0.212	<sup>198</sup> 0.112	<sup>169</sup> 0.348	<sup>182</sup> 0.296	<sup>188</sup> 0.198	<sup>170</sup> 1.000	<sup>179</sup> 1.000	<sup>177</sup> 1.000												
90	INCDE-002	<sup>180</sup> 0.285	<sup>189</sup> 0.184	<sup>196</sup> 0.100	<sup>164</sup> 0.333	<sup>180</sup> 0.2																

2021/10/28  
13:44:33

FNIR(N, R, T) =  
FP(R,N, T) =

False neg. identification rate  
False pos. identification rate

N = Num. enrolled subjects  
R = Num. candidates examined

T = Threshold

T = 0 → Investigation  
T > 0 → Identification

MISSES BELOW THRESHOLD, T				ENROL RECENT MUGSHOT, N = 1.6M									ENROL APPLICATION PORTRAIT, N = 1.6M					
#	ALGORITHM	ENROL: MUGSHOT PROBE: MUGSHOT			ENROL: MUGSHOT PROBE: WEBCAM			ENROL: MUGSHOT PROBE: PROFILE			ENROL: VISA PROBE: BORDER		ENROL: BORDER PROBE: BORDER 10+YR		ENROL: VISA PROBE: KIOSK			
		FPIR=0.0003	FPIR=0.001	FPIR=0.01	FPIR=0.0003	FPIR=0.001	FPIR=0.01	FPIR=0.0003	FPIR=0.001	FPIR=0.01	FPIR=0.001	FPIR=0.01	FPIR=0.001	FPIR=0.01	FPIR=0.001	FPIR=0.01		
93	INC005-005	<sup>22</sup> 0.021	<sup>31</sup> 0.011	<sup>29</sup> 0.005	<sup>29</sup> 0.055	<sup>33</sup> 0.043	<sup>34</sup> 0.026	<sup>17</sup> 0.614	<sup>18</sup> 0.528	<sup>24</sup> 0.372	<sup>30</sup> 0.017	<sup>30</sup> 0.009	<sup>26</sup> 0.145	<sup>26</sup> 0.073	<sup>21</sup> 0.155	<sup>19</sup> 0.116		
94	INNOVATRICES-002	<sup>191</sup> 0.379	<sup>198</sup> 0.234	<sup>206</sup> 0.139	<sup>177</sup> 0.403	<sup>181</sup> 0.310	<sup>192</sup> 0.209	<sup>178</sup> 1.000	<sup>185</sup> 1.000	<sup>176</sup> 0.999								
95	INNOVATRICES-003	<sup>183</sup> 0.297	<sup>191</sup> 0.221	<sup>202</sup> 0.132	<sup>171</sup> 0.351	<sup>183</sup> 0.297	<sup>189</sup> 0.203	<sup>152</sup> 1.000	<sup>156</sup> 1.000	<sup>163</sup> 0.998								
96	INNOVATRICES-004	<sup>148</sup> 0.184	<sup>172</sup> 0.132	<sup>181</sup> 0.074	<sup>150</sup> 0.262	<sup>162</sup> 0.222	<sup>167</sup> 0.149	<sup>63</sup> 0.984	<sup>70</sup> 0.980	<sup>97</sup> 0.973								
97	INNOVATRICES-005	<sup>72</sup> 0.057	<sup>85</sup> 0.034	<sup>84</sup> 0.014	<sup>75</sup> 0.114	<sup>82</sup> 0.089	<sup>79</sup> 0.052	<sup>34</sup> 0.890	<sup>40</sup> 0.846	<sup>48</sup> 0.723	<sup>20</sup> 0.047	<sup>69</sup> 0.022			<sup>49</sup> 0.251	<sup>54</sup> 0.182		
98	INNOVATRICES-007	<sup>26</sup> 0.024	<sup>38</sup> 0.013	<sup>36</sup> 0.005	<sup>35</sup> 0.065	<sup>41</sup> 0.051	<sup>42</sup> 0.032	<sup>28</sup> 0.806	<sup>29</sup> 0.743	<sup>35</sup> 0.567	<sup>28</sup> 0.017	<sup>31</sup> 0.009	<sup>17</sup> 0.093	<sup>20</sup> 0.053	<sup>20</sup> 0.154	<sup>25</sup> 0.120		
99	INTSYSMSU-000	<sup>238</sup> 0.999	<sup>240</sup> 0.998	<sup>242</sup> 0.990	<sup>233</sup> 1.000	<sup>235</sup> 1.000	<sup>236</sup> 0.998	<sup>146</sup> 1.000	<sup>154</sup> 1.000	<sup>159</sup> 0.998	<sup>161</sup> 0.999	<sup>161</sup> 0.989			<sup>151</sup> 0.999	<sup>158</sup> 0.988		
100	IREX-000	<sup>83</sup> 0.068	<sup>78</sup> 0.028	<sup>53</sup> 0.008	<sup>64</sup> 0.099	<sup>54</sup> 0.060	<sup>44</sup> 0.032	<sup>70</sup> 0.988	<sup>51</sup> 0.957	<sup>47</sup> 0.680	<sup>67</sup> 0.044	<sup>36</sup> 0.011	<sup>49</sup> 0.302	<sup>23</sup> 0.062	<sup>29</sup> 0.170	<sup>33</sup> 0.135		
101	ISYSTEMS-002	<sup>138</sup> 0.155	<sup>143</sup> 0.078	<sup>135</sup> 0.032	<sup>111</sup> 0.161	<sup>119</sup> 0.126	<sup>125</sup> 0.080	<sup>117</sup> 0.998	<sup>118</sup> 0.998	<sup>133</sup> 0.993								
102	ISYSTEMS-003	<sup>158</sup> 0.204	<sup>129</sup> 0.059	<sup>118</sup> 0.024	<sup>99</sup> 0.135	<sup>104</sup> 0.107	<sup>107</sup> 0.068	<sup>154</sup> 1.000	<sup>157</sup> 1.000	<sup>157</sup> 0.997								
103	KAKAO-000	<sup>39</sup> 0.028	<sup>46</sup> 0.015	<sup>44</sup> 0.006	<sup>45</sup> 0.071	<sup>49</sup> 0.056	<sup>50</sup> 0.034	<sup>11</sup> 0.539	<sup>14</sup> 0.468	<sup>21</sup> 0.327	<sup>33</sup> 0.019	<sup>32</sup> 0.010	<sup>23</sup> 0.141	<sup>29</sup> 0.075	<sup>22</sup> 0.158	<sup>24</sup> 0.120		
104	KEDACOM-001	<sup>36</sup> 0.041	<sup>68</sup> 0.023	<sup>81</sup> 0.013	<sup>61</sup> 0.096	<sup>68</sup> 0.072	<sup>85</sup> 0.054	<sup>73</sup> 0.989	<sup>81</sup> 0.986	<sup>101</sup> 0.973	<sup>71</sup> 0.055	<sup>55</sup> 0.043			<sup>60</sup> 0.305	<sup>80</sup> 0.264		
105	KNERON-000			<sup>137</sup> 0.033			<sup>142</sup> 0.099											
106	KNERON-001			<sup>161</sup> 0.052														
107	LINE-000	<sup>76</sup> 0.062	<sup>81</sup> 0.031	<sup>80</sup> 0.012	<sup>98</sup> 0.132	<sup>91</sup> 0.095	<sup>85</sup> 0.054			<sup>192</sup> 1.000	<sup>68</sup> 0.046	<sup>69</sup> 0.021	<sup>47</sup> 0.278	<sup>50</sup> 0.151	<sup>196</sup> 1.000	<sup>81</sup> 0.268		
108	LOOKMAN-003	<sup>81</sup> 0.066	<sup>99</sup> 0.044	<sup>119</sup> 0.025	<sup>95</sup> 0.131	<sup>107</sup> 0.112	<sup>126</sup> 0.082				<sup>98</sup> 0.084	<sup>106</sup> 0.061			<sup>70</sup> 0.355	<sup>94</sup> 0.304		
109	LOOKMAN-004	<sup>86</sup> 0.074	<sup>108</sup> 0.045	<sup>116</sup> 0.024	<sup>85</sup> 0.123	<sup>110</sup> 0.105	<sup>117</sup> 0.075	<sup>53</sup> 0.979	<sup>64</sup> 0.977	<sup>103</sup> 0.974								
110	LOOKMAN-005	<sup>63</sup> 0.050	<sup>80</sup> 0.030	<sup>90</sup> 0.017	<sup>69</sup> 0.102	<sup>77</sup> 0.086	<sup>101</sup> 0.063	<sup>57</sup> 0.980	<sup>67</sup> 0.978	<sup>99</sup> 0.973	<sup>84</sup> 0.062	<sup>97</sup> 0.047			<sup>61</sup> 0.308	<sup>83</sup> 0.273		
111	MEGVII-001	<sup>161</sup> 0.210	<sup>137</sup> 0.072	<sup>141</sup> 0.037	<sup>81</sup> 0.119	<sup>98</sup> 0.097	<sup>94</sup> 0.061											
112	MEGVII-002	<sup>174</sup> 0.258	<sup>143</sup> 0.072	<sup>143</sup> 0.037	<sup>82</sup> 0.120	<sup>98</sup> 0.096	<sup>91</sup> 0.059	<sup>124</sup> 0.999	<sup>128</sup> 0.998	<sup>66</sup> 0.872								
113	MICROFOCUS-003	<sup>232</sup> 0.958	<sup>236</sup> 0.931	<sup>239</sup> 0.866	<sup>227</sup> 0.988	<sup>234</sup> 0.979	<sup>234</sup> 0.948				<sup>160</sup> 0.982	<sup>160</sup> 0.945			<sup>146</sup> 0.991	<sup>153</sup> 0.977		
114	MICROFOCUS-004	<sup>240</sup> 0.999	<sup>241</sup> 0.999	<sup>245</sup> 0.999	<sup>229</sup> 0.984	<sup>231</sup> 0.975	<sup>233</sup> 0.940				<sup>159</sup> 0.974	<sup>159</sup> 0.935			<sup>144</sup> 0.989	<sup>152</sup> 0.976		
115	MICROFOCUS-005	<sup>227</sup> 0.883	<sup>231</sup> 0.835	<sup>237</sup> 0.736	<sup>219</sup> 0.951	<sup>220</sup> 0.928	<sup>230</sup> 0.865				<sup>157</sup> 0.935	<sup>157</sup> 0.848			<sup>143</sup> 0.985	<sup>151</sup> 0.965		
116	MICROFOCUS-006	<sup>238</sup> 0.983	<sup>238</sup> 0.978	<sup>240</sup> 0.963	<sup>218</sup> 0.950	<sup>227</sup> 0.923	<sup>229</sup> 0.858				<sup>158</sup> 0.923	<sup>159</sup> 0.843			<sup>140</sup> 0.971	<sup>148</sup> 0.939		
117	MICROSOFT-003	<sup>61</sup> 0.049	<sup>76</sup> 0.028	<sup>75</sup> 0.012	<sup>76</sup> 0.117	<sup>85</sup> 0.091	<sup>88</sup> 0.056				<sup>58</sup> 0.036	<sup>64</sup> 0.019			<sup>45</sup> 0.233	<sup>50</sup> 0.176		
118	MICROSOFT-004	<sup>56</sup> 0.046	<sup>78</sup> 0.026	<sup>69</sup> 0.011	<sup>73</sup> 0.111	<sup>79</sup> 0.087	<sup>82</sup> 0.053				<sup>54</sup> 0.033	<sup>60</sup> 0.018			<sup>41</sup> 0.222	<sup>48</sup> 0.170		
119	MICROSOFT-005	<sup>58</sup> 0.047	<sup>68</sup> 0.026	<sup>68</sup> 0.010	<sup>57</sup> 0.090	<sup>68</sup> 0.070	<sup>62</sup> 0.041	<sup>132</sup> 0.999	<sup>22</sup> 0.587	<sup>22</sup> 0.354	<sup>42</sup> 0.027	<sup>43</sup> 0.013			<sup>32</sup> 0.180	<sup>32</sup> 0.134		
120	MICROSOFT-006	<sup>30</sup> 0.025	<sup>39</sup> 0.012	<sup>41</sup> 0.006	<sup>29</sup> 0.048	<sup>29</sup> 0.037	<sup>32</sup> 0.024	<sup>8</sup> 0.452	<sup>9</sup> 0.386	<sup>15</sup> 0.281	<sup>51</sup> 0.032	<sup>48</sup> 0.015			<sup>30</sup> 0.178	<sup>34</sup> 0.138		
121	NEC-000	<sup>109</sup> 0.113	<sup>144</sup> 0.079	<sup>158</sup> 0.047	<sup>116</sup> 0.171	<sup>128</sup> 0.140	<sup>135</sup> 0.093	<sup>60</sup> 0.983	<sup>68</sup> 0.979	<sup>94</sup> 0.969					<sup>88</sup> 0.474	<sup>106</sup> 0.377		
122	NEC-001	<sup>132</sup> 0.148	<sup>161</sup> 0.106	<sup>171</sup> 0.060	<sup>143</sup> 0.238	<sup>150</sup> 0.197	<sup>161</sup> 0.133	<sup>74</sup> 0.991	<sup>80</sup> 0.986	<sup>96</sup> 0.972	<sup>107</sup> 0.133	<sup>116</sup> 0.082			<sup>87</sup> 0.468	<sup>107</sup> 0.378		
123	NEC-002	<sup>20</sup> 0.018	<sup>18</sup> 0.003	<sup>8</sup> 0.002	<sup>15</sup> 0.029	<sup>13</sup> 0.020	<sup>11</sup> 0.013	<sup>139</sup> 1.000	<sup>144</sup> 0.999	<sup>144</sup> 0.995	<sup>15</sup> 0.008	<sup>17</sup> 0.005			<sup>108</sup> 0.676	<sup>90</sup> 0.292		
124	NEC-003	<sup>7</sup> 0.005	<sup>8</sup> 0.002	<sup>10</sup> 0.002	<sup>11</sup> 0.021	<sup>11</sup> 0.017	<sup>10</sup> 0.013	<sup>35</sup> 0.902	<sup>36</sup> 0.824	<sup>40</sup> 0.628	<sup>16</sup> 0.008	<sup>18</sup> 0.006	<sup>6</sup> 0.036	<sup>7</sup> 0.023	<sup>107</sup> 0.668	<sup>79</sup> 0.261		
125	NEC-004	<sup>3</sup> 0.003	<sup>3</sup> 0.002	<sup>4</sup> 0.002	<sup>3</sup> 0.015	<sup>4</sup> 0.013	<sup>7</sup> 0.010	<sup>19</sup> 0.654	<sup>24</sup> 0.622	<sup>36</sup> 0.575	<sup>3</sup> 0.004	<sup>6</sup> 0.004	<sup>1</sup> 0.019	<sup>1</sup> 0.012	<sup>6</sup> 0.100	<sup>6</sup> 0.088		
126	NEUROTECHNOLOGY-003	<sup>239</sup> 0.999	<sup>229</sup> 0.636	<sup>195</sup> 0.099	<sup>209</sup> 0.773	<sup>178</sup> 0.266	<sup>175</sup> 0.164	<sup>182</sup> 1.000	<sup>189</sup> 1.000	<sup>216</sup> 1.000								
127	NEUROTECHNOLOGY-004	<sup>111</sup> 0.120	<sup>131</sup> 0.063	<sup>127</sup> 0.028	<sup>108</sup> 0.146	<sup>109</sup> 0.117	<sup>113</sup> 0.073	<sup>99</sup> 0.996	<sup>108</sup> 0.994	<sup>121</sup> 0.990								
128	NEUROTECHNOLOGY-005	<sup>110</sup> 0.117	<sup>119</sup> 0.054	<sup>110</sup> 0.022	<sup>146</sup> 0.252	<sup>121</sup> 0.130	<sup>116</sup> 0.074	<sup>122</sup> 0.999	<sup>122</sup> 0.998	<sup>118</sup> 0.989								
129	NEUROTECHNOLOGY-006	<sup>237</sup> 0.987	<sup>199</sup> 0.249	<sup>200</sup> 0.121	<sup>241</sup> 1.000	<sup>199</sup> 0.418	<sup>191</sup> 0.206											
130	NEUROTECHNOLOGY-007	<sup>170</sup> 0.252	<sup>130</sup> 0.062	<sup>107</sup> 0.021	<sup>230</sup> 0.996	<sup>148</sup> 0.173	<sup>106</sup> 0.068	<sup>171</sup> 1.000	<sup>162</sup> 1.000	<sup>156</sup> 0.997	<sup>138</sup> 0.339	<sup>88</sup> 0.036			<sup>154</sup> 1.000	<sup>159</sup> 0.989		
131	NEUROTECHNOLOGY-008	<sup>230</sup> 0.797	<sup>114</sup> 0.053	<sup>79</sup> 0.012	<sup>71</sup> 0.110	<sup>79</sup> 0.080	<sup>70</sup> 0.047	<sup>157</sup> 1.000	<sup>168</sup> 1.000	<sup>191</sup> 1.000	<sup>57</sup> 0.035	<sup>56</sup> 0.017	<sup>48</sup> 0.293	<sup>49</sup> 0.149	<sup>37</sup> 0.203	<sup>39</sup> 0.152		
132	NEUROTECHNOLOGY-009	<sup>33</sup> 0.027	<sup>47</sup> 0.015	<sup>40</sup> 0.006	<sup>36</sup> 0.066	<sup>44</sup> 0.052	<sup>43</sup> 0.032	<sup>20</sup> 0.661	<sup>23</sup> 0.588	<sup>26</sup> 0.436	<sup>34</sup> 0.020	<sup>33</sup> 0.010	<sup>28</sup> 0.153	<sup>31</sup> 0.082	<sup>26</sup> 0.165	<sup>29</sup> 0.129		
133	NEWLAND-002	<sup>206</sup> 0.523	<sup>218</sup> 0.438	<sup>220</sup> 0.294	<sup>189</sup> 0.535	<sup>200</sup> 0.466	<sup>207</sup> 0.335	<sup>129</sup> 0.999	<sup>137</sup> 0.999	<sup>162</sup> 0.998								
134	NOBLIS-001	<sup>243</sup> 1.000	<sup>243</sup> 1.000	<sup>243</sup> 0.991	<sup>239</sup> 1.000	<sup>238</sup> 1.000		<sup>169</sup> 1.000	<sup>178</sup> 1.000	<sup>186</sup> 1.000								
135	NOBLIS-002	<sup>241</sup> 1.000	<sup>239</sup> 0.997	<sup>229</sup> 0.488	<sup>246</sup> 1.000	<sup>241</sup> 1.000	<sup>241</sup> 1.000	<sup>160</sup> 1.000	<sup>170</sup> 1.000	<sup>190</sup> 1.000								
136	NTECHLAB-003	<sup>86</sup> 0.080	<sup>111</sup> 0.054	<sup>125</sup> 0.028	<sup>105</sup> 0.148	<sup>110</sup> 0.118	<sup>118</sup> 0.075	<sup>32</sup> 0.873	<sup>38</sup> 0.837	<sup>55</sup> 0.752								
137	NTECHLAB-004	<sup>78</sup> 0.063	<sup>98</sup> 0.041	<sup>105</sup> 0.021	<sup>94</sup> 0.131	<sup>103</sup> 0.105	<sup>103</sup> 0.065	<sup>31</sup> 0.868	<sup>39</sup> 0.833	<sup>53</sup> 0.746	<sup>26</sup> 0.053	<sup>29</sup> 0.030			<sup>53</sup> 0.263	<sup>66</sup> 0.214		
138	NTECHLAB-005	<sup>77</sup> 0.062	<sup>94</sup> 0.042	<sup>106</sup> 0.021	<sup>99</sup> 0.130	<sup>100</sup> 0.102	<sup>102</sup> 0.063	<sup>29</sup> 0.816	<sup>34</sup> 0.771	<sup>45</sup> 0.661	<sup>50</sup> 0.073	<sup>51</sup> 0.039			<sup>58</sup> 0.294	<sup>70</sup> 0.227		

MISSES BELOW THRESHOLD, T		ENROL RECENT MUGSHOT, N = 1.6M									ENROL APPLICATION PORTRAIT, N = 1.6M					
		ENROL: MUGSHOT PROBE: MUGSHOT			ENROL: MUGSHOT PROBE: WEBCAM			ENROL: MUGSHOT PROBE: PROFILE			ENROL: VISA PROBE: BORDER		ENROL: BORDER PROBE: BORDER 10+YR		ENROL: VISA PROBE: KIOSK	
		FPIR=0.0003	FPIR=0.001	FPIR=0.01	FPIR=0.0003	FPIR=0.001	FPIR=0.01	FPIR=0.0003	FPIR=0.001	FPIR=0.01	FPIR=0.001	FPIR=0.01	FPIR=0.001	FPIR=0.01	FPIR=0.001	FPIR=0.01
139	NTECHLAB-006	<sup>74</sup> 0.056	<sup>88</sup> 0.037	<sup>95</sup> 0.018	<sup>85</sup> 0.121	<sup>88</sup> 0.094	<sup>90</sup> 0.059	<sup>27</sup> 0.802	<sup>31</sup> 0.754	<sup>41</sup> 0.635	<sup>29</sup> 0.057	<sup>83</sup> 0.032			<sup>52</sup> 0.260	<sup>64</sup> 0.207
140	NTECHLAB-007	<sup>49</sup> 0.040	<sup>67</sup> 0.026	<sup>76</sup> 0.012	<sup>58</sup> 0.085	<sup>59</sup> 0.067	<sup>64</sup> 0.041	<sup>28</sup> 0.796	<sup>30</sup> 0.750	<sup>44</sup> 0.642	<sup>52</sup> 0.032	<sup>59</sup> 0.017			<sup>48</sup> 0.223	<sup>49</sup> 0.176
141	NTECHLAB-008	<sup>28</sup> 0.024	<sup>41</sup> 0.014	<sup>48</sup> 0.007	<sup>38</sup> 0.057	<sup>35</sup> 0.045	<sup>39</sup> 0.029	<sup>18</sup> 0.601	<sup>19</sup> 0.529	<sup>23</sup> 0.391	<sup>35</sup> 0.033	<sup>61</sup> 0.018			<sup>39</sup> 0.183	<sup>35</sup> 0.140
142	NTECHLAB-009	<sup>12</sup> 0.010	<sup>19</sup> 0.005	<sup>19</sup> 0.003	<sup>14</sup> 0.028	<sup>15</sup> 0.022	<sup>19</sup> 0.014	<sup>10</sup> 0.522	<sup>11</sup> 0.430	<sup>17</sup> 0.311	<sup>25</sup> 0.015	<sup>26</sup> 0.008	<sup>20</sup> 0.109	<sup>21</sup> 0.061	<sup>19</sup> 0.142	<sup>17</sup> 0.114
143	NTECHLAB-010	<sup>9</sup> 0.005	<sup>9</sup> 0.003	<sup>6</sup> 0.002	<sup>8</sup> 0.018	<sup>9</sup> 0.015	<sup>8</sup> 0.011	<sup>7</sup> 0.334	<sup>7</sup> 0.252	<sup>10</sup> 0.169	<sup>9</sup> 0.007	<sup>10</sup> 0.004	<sup>11</sup> 0.059	<sup>13</sup> 0.031	<sup>3</sup> 0.098	<sup>3</sup> 0.077
144	PARAVISION-000	<sup>179</sup> 0.278	<sup>153</sup> 0.089	<sup>158</sup> 0.045	<sup>185</sup> 0.447	<sup>147</sup> 0.170	<sup>148</sup> 0.100	<sup>167</sup> 1.000	<sup>139</sup> 0.999	<sup>154</sup> 0.997	<sup>144</sup> 0.470	<sup>148</sup> 0.443			<sup>138</sup> 0.926	<sup>141</sup> 0.779
145	PARAVISION-001	<sup>127</sup> 0.140	<sup>107</sup> 0.049	<sup>108</sup> 0.020	<sup>138</sup> 0.207	<sup>120</sup> 0.128	<sup>118</sup> 0.074	<sup>168</sup> 1.000	<sup>131</sup> 0.999	<sup>138</sup> 0.994	<sup>141</sup> 0.444	<sup>147</sup> 0.428			<sup>111</sup> 0.739	<sup>123</sup> 0.573
146	PARAVISION-002	<sup>93</sup> 0.085	<sup>108</sup> 0.050	<sup>112</sup> 0.022	<sup>109</sup> 0.152	<sup>113</sup> 0.119	<sup>120</sup> 0.076	<sup>78</sup> 0.992	<sup>75</sup> 0.983	<sup>54</sup> 0.748	<sup>80</sup> 0.080	<sup>96</sup> 0.043			<sup>91</sup> 0.497	<sup>82</sup> 0.268
147	PARAVISION-003	<sup>79</sup> 0.063	<sup>86</sup> 0.035	<sup>86</sup> 0.016	<sup>88</sup> 0.124	<sup>92</sup> 0.096	<sup>93</sup> 0.060	<sup>105</sup> 0.997	<sup>101</sup> 0.994	<sup>49</sup> 0.733	<sup>80</sup> 0.058	<sup>86</sup> 0.034			<sup>59</sup> 0.296	<sup>72</sup> 0.232
148	PARAVISION-004	<sup>29</sup> 0.025	<sup>30</sup> 0.010	<sup>28</sup> 0.004	<sup>26</sup> 0.049	<sup>30</sup> 0.038	<sup>30</sup> 0.024	<sup>161</sup> 1.000	<sup>169</sup> 1.000	<sup>59</sup> 0.797	<sup>32</sup> 0.018	<sup>38</sup> 0.011			<sup>128</sup> 0.908	<sup>65</sup> 0.211
149	PARAVISION-005	<sup>19</sup> 0.014	<sup>15</sup> 0.004	<sup>15</sup> 0.002	<sup>16</sup> 0.031	<sup>16</sup> 0.024	<sup>17</sup> 0.016	<sup>103</sup> 0.997	<sup>69</sup> 0.980	<sup>11</sup> 0.181	<sup>20</sup> 0.011	<sup>27</sup> 0.008			<sup>15</sup> 0.132	<sup>22</sup> 0.120
150	PARAVISION-007	<sup>59</sup> 0.048	<sup>14</sup> 0.004	<sup>11</sup> 0.002	<sup>190</sup> 0.560	<sup>17</sup> 0.025	<sup>16</sup> 0.015	<sup>124</sup> 1.000	<sup>182</sup> 1.000	<sup>193</sup> 1.000	<sup>18</sup> 0.009	<sup>20</sup> 0.006	<sup>21</sup> 0.113	<sup>9</sup> 0.024	<sup>169</sup> 1.000	<sup>183</sup> 1.000
151	PIXELALL-002	<sup>214</sup> 0.664	<sup>160</sup> 0.105	<sup>134</sup> 0.030	<sup>224</sup> 0.974	<sup>195</sup> 0.388	<sup>124</sup> 0.083		<sup>174</sup> 1.000	<sup>181</sup> 1.000	<sup>147</sup> 0.602	<sup>48</sup> 0.047			<sup>225</sup> 1.000	<sup>161</sup> 1.000
152	PIXELALL-003	<sup>60</sup> 0.049	<sup>62</sup> 0.022	<sup>69</sup> 0.009	<sup>66</sup> 0.102	<sup>66</sup> 0.073	<sup>69</sup> 0.043		<sup>153</sup> 1.000	<sup>161</sup> 0.998	<sup>61</sup> 0.037	<sup>60</sup> 0.020			<sup>99</sup> 0.554	<sup>77</sup> 0.255
153	PIXELALL-004	<sup>112</sup> 0.120	<sup>54</sup> 0.018	<sup>49</sup> 0.007	<sup>210</sup> 0.783	<sup>72</sup> 0.079	<sup>59</sup> 0.037		<sup>166</sup> 1.000	<sup>168</sup> 0.999	<sup>72</sup> 0.051	<sup>49</sup> 0.015			<sup>147</sup> 0.994	<sup>149</sup> 0.942
154	PIXELALL-005	<sup>88</sup> 0.079	<sup>34</sup> 0.012	<sup>30</sup> 0.005	<sup>185</sup> 0.456	<sup>39</sup> 0.050	<sup>35</sup> 0.027		<sup>172</sup> 1.000	<sup>175</sup> 0.999	<sup>43</sup> 0.027	<sup>33</sup> 0.017	<sup>39</sup> 0.203	<sup>24</sup> 0.071	<sup>152</sup> 1.000	<sup>155</sup> 0.983
155	PTAKURATSATU-000	<sup>73</sup> 0.057	<sup>87</sup> 0.037	<sup>90</sup> 0.017	<sup>116</sup> 0.165	<sup>118</sup> 0.124	<sup>111</sup> 0.071	<sup>41</sup> 0.947	<sup>48</sup> 0.924	<sup>68</sup> 0.868	<sup>69</sup> 0.046	<sup>60</sup> 0.022	<sup>41</sup> 0.206	<sup>43</sup> 0.120	<sup>41</sup> 0.232	<sup>52</sup> 0.179
156	QNAP-000	<sup>235</sup> 0.972	<sup>191</sup> 0.129	<sup>164</sup> 0.052	<sup>232</sup> 0.998	<sup>167</sup> 0.238	<sup>156</sup> 0.117	<sup>181</sup> 1.000	<sup>188</sup> 1.000	<sup>194</sup> 1.000	<sup>121</sup> 0.191	<sup>109</sup> 0.068	<sup>56</sup> 0.539	<sup>88</sup> 0.263	<sup>149</sup> 0.998	<sup>157</sup> 0.985
157	QUANTASOFT-001	<sup>218</sup> 0.713	<sup>228</sup> 0.639	<sup>230</sup> 0.493												
158	RANKONE-002	<sup>146</sup> 0.184	<sup>164</sup> 0.118	<sup>178</sup> 0.071	<sup>162</sup> 0.308	<sup>174</sup> 0.261	<sup>188</sup> 0.190									
159	RANKONE-003	<sup>147</sup> 0.184	<sup>165</sup> 0.118	<sup>177</sup> 0.071	<sup>159</sup> 0.300	<sup>175</sup> 0.255	<sup>183</sup> 0.187									
160	RANKONE-004	<sup>169</sup> 0.250	<sup>191</sup> 0.193	<sup>201</sup> 0.124	<sup>187</sup> 0.482	<sup>199</sup> 0.426	<sup>205</sup> 0.324									
161	RANKONE-005	<sup>38</sup> 0.096	<sup>127</sup> 0.059	<sup>136</sup> 0.033	<sup>139</sup> 0.212	<sup>150</sup> 0.173	<sup>159</sup> 0.119	<sup>150</sup> 0.999	<sup>125</sup> 0.998	<sup>140</sup> 0.994						
162	RANKONE-006	<sup>74</sup> 0.061	<sup>89</sup> 0.037	<sup>98</sup> 0.020				<sup>68</sup> 0.987	<sup>65</sup> 0.977	<sup>79</sup> 0.937						
163	RANKONE-007	<sup>40</sup> 0.034	<sup>64</sup> 0.022	<sup>71</sup> 0.011	<sup>80</sup> 0.118	<sup>89</sup> 0.095	<sup>98</sup> 0.061	<sup>59</sup> 0.975	<sup>35</sup> 0.967	<sup>73</sup> 0.924						
164	RANKONE-009	<sup>37</sup> 0.031	<sup>50</sup> 0.018	<sup>58</sup> 0.008	<sup>62</sup> 0.098	<sup>68</sup> 0.076	<sup>69</sup> 0.045	<sup>59</sup> 0.983	<sup>57</sup> 0.969	<sup>64</sup> 0.859	<sup>82</sup> 0.062	<sup>78</sup> 0.029			<sup>68</sup> 0.328	<sup>63</sup> 0.206
165	RANKONE-010	<sup>24</sup> 0.023	<sup>39</sup> 0.014	<sup>38</sup> 0.007	<sup>48</sup> 0.077	<sup>52</sup> 0.058	<sup>54</sup> 0.036	<sup>36</sup> 0.905	<sup>34</sup> 0.802	<sup>44</sup> 0.652	<sup>75</sup> 0.052	<sup>36</sup> 0.027	<sup>42</sup> 0.208	<sup>42</sup> 0.119	<sup>50</sup> 0.259	<sup>58</sup> 0.194
166	RANKONE-011	<sup>107</sup> 0.109	<sup>24</sup> 0.009	<sup>26</sup> 0.004	<sup>31</sup> 0.079	<sup>37</sup> 0.048	<sup>39</sup> 0.029				<sup>60</sup> 0.037	<sup>38</sup> 0.017	<sup>35</sup> 0.182	<sup>35</sup> 0.092	<sup>141</sup> 0.977	<sup>114</sup> 0.465
167	REALNETWORKS-000	<sup>190</sup> 0.374	<sup>197</sup> 0.234	<sup>204</sup> 0.138	<sup>180</sup> 0.433	<sup>189</sup> 0.319	<sup>190</sup> 0.209									
168	REALNETWORKS-001	<sup>189</sup> 0.374	<sup>196</sup> 0.234	<sup>205</sup> 0.138	<sup>181</sup> 0.433	<sup>190</sup> 0.319	<sup>191</sup> 0.209									
169	REALNETWORKS-002	<sup>188</sup> 0.370	<sup>195</sup> 0.231	<sup>203</sup> 0.137	<sup>179</sup> 0.416	<sup>188</sup> 0.315	<sup>192</sup> 0.209									
170	REALNETWORKS-003	<sup>177</sup> 0.273	<sup>181</sup> 0.159	<sup>187</sup> 0.090	<sup>168</sup> 0.342	<sup>177</sup> 0.266	<sup>181</sup> 0.172	<sup>127</sup> 0.999	<sup>127</sup> 0.998	<sup>115</sup> 0.987	<sup>116</sup> 0.164	<sup>121</sup> 0.103			<sup>92</sup> 0.500	<sup>103</sup> 0.364
171	REALNETWORKS-004	<sup>169</sup> 0.242	<sup>180</sup> 0.158	<sup>188</sup> 0.090	<sup>172</sup> 0.353	<sup>175</sup> 0.263	<sup>178</sup> 0.169	<sup>142</sup> 1.000	<sup>140</sup> 0.999	<sup>132</sup> 0.992	<sup>117</sup> 0.170	<sup>122</sup> 0.103			<sup>103</sup> 0.613	<sup>104</sup> 0.370
172	REALNETWORKS-005	<sup>66</sup> 0.052	<sup>75</sup> 0.028	<sup>78</sup> 0.012	<sup>60</sup> 0.094	<sup>67</sup> 0.074	<sup>69</sup> 0.047	<sup>62</sup> 0.984	<sup>59</sup> 0.971	<sup>68</sup> 0.896	<sup>89</sup> 0.037	<sup>84</sup> 0.017	<sup>43</sup> 0.223	<sup>45</sup> 0.123	<sup>39</sup> 0.215	<sup>45</sup> 0.165
173	REMARKAI-000	<sup>156</sup> 0.197	<sup>169</sup> 0.128	<sup>170</sup> 0.059	<sup>151</sup> 0.263	<sup>156</sup> 0.203	<sup>159</sup> 0.123									
174	REMARKAI-000	<sup>116</sup> 0.125	<sup>120</sup> 0.055	<sup>117</sup> 0.023	<sup>117</sup> 0.173	<sup>114</sup> 0.120	<sup>108</sup> 0.070	<sup>131</sup> 0.999	<sup>138</sup> 0.999	<sup>141</sup> 0.995	<sup>89</sup> 0.069	<sup>85</sup> 0.033			<sup>109</sup> 0.717	<sup>96</sup> 0.315
175	REMARKAI-002	<sup>152</sup> 0.188	<sup>168</sup> 0.124	<sup>169</sup> 0.059	<sup>145</sup> 0.248	<sup>154</sup> 0.196	<sup>158</sup> 0.122	<sup>79</sup> 0.993	<sup>94</sup> 0.991	<sup>108</sup> 0.980						
176	RENDIP-000	<sup>25</sup> 0.023	<sup>33</sup> 0.012	<sup>34</sup> 0.005	<sup>138</sup> 0.189	<sup>33</sup> 0.059	<sup>49</sup> 0.034	<sup>48</sup> 0.945	<sup>45</sup> 0.894	<sup>52</sup> 0.744	<sup>36</sup> 0.022	<sup>41</sup> 0.013	<sup>37</sup> 0.185	<sup>32</sup> 0.089	<sup>29</sup> 0.167	<sup>30</sup> 0.130
177	S1-000	<sup>123</sup> 0.137	<sup>77</sup> 0.028	<sup>71</sup> 0.011	<sup>91</sup> 0.129	<sup>76</sup> 0.085	<sup>71</sup> 0.048	<sup>178</sup> 1.000	<sup>187</sup> 1.000	<sup>39</sup> 0.596	<sup>71</sup> 0.047	<sup>62</sup> 0.018	<sup>202</sup> 1.000	<sup>44</sup> 0.123	<sup>247</sup> 1.000	<sup>128</sup> 0.632
178	SCANOVATE-000	<sup>103</sup> 0.103	<sup>134</sup> 0.067	<sup>132</sup> 0.030	<sup>158</sup> 0.296	<sup>190</sup> 0.240	<sup>168</sup> 0.150	<sup>39</sup> 0.931	<sup>44</sup> 0.893	<sup>69</sup> 0.803	<sup>125</sup> 0.215	<sup>129</sup> 0.118			<sup>76</sup> 0.400	<sup>92</sup> 0.299
179	SCANOVATE-001	<sup>118</sup> 0.128	<sup>145</sup> 0.081	<sup>144</sup> 0.037	<sup>157</sup> 0.281	<sup>164</sup> 0.227	<sup>164</sup> 0.140	<sup>40</sup> 0.935	<sup>47</sup> 0.911	<sup>62</sup> 0.834	<sup>122</sup> 0.192	<sup>123</sup> 0.103			<sup>76</sup> 0.404	<sup>88</sup> 0.290
180	SENSETIME-000	<sup>44</sup> 0.036	<sup>60</sup> 0.021	<sup>61</sup> 0.009	<sup>48</sup> 0.078	<sup>56</sup> 0.063	<sup>58</sup> 0.040	<sup>235</sup> 1.000	<sup>231</sup> 1.000	<sup>116</sup> 0.988						
181	SENSETIME-001	<sup>45</sup> 0.036	<sup>63</sup> 0.022	<sup>61</sup> 0.010	<sup>57</sup> 0.080	<sup>57</sup> 0.064	<sup>61</sup> 0.041									
182	SENSETIME-002	<sup>46</sup> 0.037	<sup>42</sup> 0.015	<sup>38</sup> 0.014	<sup>87</sup> 0.124	<sup>21</sup> 0.028	<sup>28</sup> 0.023	<sup>102</sup> 0.997	<sup>99</sup> 0.994	<sup>109</sup> 0.979	<sup>50</sup> 0.032	<sup>55</sup> 0.017			<sup>94</sup> 0.523	<sup>44</sup> 0.160
183	SENSETIME-003	<sup>4</sup> 0.004	<sup>4</sup> 0.002	<sup>4</sup> 0.001	<sup>1</sup> 0.014	<sup>1</sup> 0.012	<sup>2</sup> 0.009	<sup>16</sup> 0.607	<sup>15</sup> 0.477	<sup>18</sup> 0.311	<sup>14</sup> 0.008	<sup>16</sup> 0.005			<sup>16</sup> 0.133	<sup>15</sup> 0.115
184	SENSETIME-004	<sup>2</sup> 0.003	<sup>1</sup> 0.002	<sup>3</sup> 0.001	<sup>2</sup> 0.015	<sup>3</sup> 0.013	<sup>6</sup> 0.010	<sup>6</sup> 0.301	<sup>6</sup> 0.229	<sup>8</sup> 0.149	<sup>7</sup> 0.006	<sup>7</sup> 0.004			<sup>11</sup> 0.113	<sup>13</sup> 0.100

Table 28

#	ALGORITHM	ENROL RECENT MUGSHOT, N = 1.6M									ENROL APPLICATION PORTRAIT, N = 1.6M					
		ENROL: MUGSHOT			ENROL: MUGSHOT			ENROL: MUGSHOT			ENROL: VISA		ENROL: BORDER		ENROL: VISA	
		PROBE: MUGSHOT			PROBE: WEBCAM			PROBE: PROFILE			PROBE: BORDER		PROBE: BORDER 10-YR		PROBE: KIOSK	
		FPIR=0.0003	FPIR=0.001	FPIR=0.01	FPIR=0.0003	FPIR=0.001	FPIR=0.01	FPIR=0.0003	FPIR=0.001	FPIR=0.01	FPIR=0.001	FPIR=0.01	FPIR=0.001	FPIR=0.01	FPIR=0.001	FPIR=0.01
185	SENSETIME-005	<sup>15</sup> 0.011	<sup>7</sup> 0.002	<sup>2</sup> 0.001	<sup>10</sup> 0.018	<sup>8</sup> 0.014	<sup>4</sup> 0.010	<sup>2</sup> 0.259	<sup>1</sup> 0.173	<sup>3</sup> 0.103	<sup>10</sup> 0.007	<sup>7</sup> 0.004	<sup>8</sup> 0.051	<sup>8</sup> 0.023	<sup>8</sup> 0.104	<sup>10</sup> 0.093
186	SENSETIME-006	<sup>6</sup> 0.005	<sup>7</sup> 0.002	<sup>1</sup> 0.001	<sup>5</sup> 0.016	<sup>6</sup> 0.012	<sup>1</sup> 0.009	<sup>120</sup> 0.999	<sup>120</sup> 0.998	<sup>46</sup> 0.680	<sup>1</sup> 0.004	<sup>1</sup> 0.002	<sup>4</sup> 0.034	<sup>3</sup> 0.016	<sup>2</sup> 0.093	<sup>4</sup> 0.079
187	SHAMAN-003	<sup>200</sup> 0.506	<sup>210</sup> 0.451	<sup>222</sup> 0.347	<sup>200</sup> 0.650	<sup>210</sup> 0.597	<sup>216</sup> 0.472									
188	SHAMAN-004	<sup>210</sup> 0.679	<sup>220</sup> 0.615	<sup>228</sup> 0.488	<sup>211</sup> 0.812	<sup>220</sup> 0.754	<sup>223</sup> 0.639									
189	SHAMAN-006	<sup>140</sup> 0.185	<sup>125</sup> 0.141	<sup>108</sup> 0.092	<sup>155</sup> 0.278	<sup>166</sup> 0.237	<sup>177</sup> 0.168	<sup>32</sup> 0.978	<sup>60</sup> 0.972	<sup>90</sup> 0.960						
190	SHAMAN-007	<sup>144</sup> 0.183	<sup>170</sup> 0.141	<sup>188</sup> 0.092	<sup>150</sup> 0.280	<sup>160</sup> 0.240	<sup>179</sup> 0.169									
191	SIAT-001	<sup>121</sup> 0.132	<sup>40</sup> 0.018	<sup>4</sup> 0.007	<sup>190</sup> 0.641	<sup>194</sup> 0.365	<sup>208</sup> 0.348				<sup>40</sup> 0.031	<sup>45</sup> 0.014				
192	SIAT-002	<sup>192</sup> 0.417	<sup>61</sup> 0.022	<sup>51</sup> 0.007	<sup>214</sup> 0.942	<sup>205</sup> 0.478	<sup>214</sup> 0.460				<sup>134</sup> 0.372	<sup>142</sup> 0.356			<sup>132</sup> 0.923	<sup>47</sup> 0.169
193	SMILART-004	<sup>234</sup> 0.970	<sup>230</sup> 0.968	<sup>241</sup> 0.965	<sup>224</sup> 0.977	<sup>230</sup> 0.976	<sup>235</sup> 0.973									
194	SMILART-005															
195	STAUQ-000	<sup>184</sup> 0.334	<sup>120</sup> 0.062	<sup>108</sup> 0.022	<sup>212</sup> 0.848	<sup>201</sup> 0.443	<sup>96</sup> 0.061	<sup>155</sup> 1.000	<sup>159</sup> 1.000	<sup>170</sup> 0.999	<sup>145</sup> 0.535	<sup>92</sup> 0.039	<sup>61</sup> 0.961	<sup>52</sup> 0.183	<sup>197</sup> 1.000	<sup>160</sup> 0.999
196	SYNESIS-003	<sup>214</sup> 0.648	<sup>224</sup> 0.582	<sup>227</sup> 0.443	<sup>204</sup> 0.708	<sup>216</sup> 0.646	<sup>218</sup> 0.524									
197	SYNESIS-003	<sup>100</sup> 0.111	<sup>130</sup> 0.065	<sup>133</sup> 0.032	<sup>110</sup> 0.155	<sup>117</sup> 0.123	<sup>121</sup> 0.078	<sup>47</sup> 0.973	<sup>53</sup> 0.960	<sup>70</sup> 0.911	<sup>91</sup> 0.075	<sup>90</sup> 0.039			<sup>63</sup> 0.314	<sup>74</sup> 0.235
198	SYNESIS-005	<sup>60</sup> 0.050	<sup>60</sup> 0.025	<sup>74</sup> 0.011	<sup>50</sup> 0.088	<sup>60</sup> 0.072	<sup>66</sup> 0.043	<sup>87</sup> 0.995	<sup>70</sup> 0.984	<sup>57</sup> 0.795	<sup>50</sup> 0.032	<sup>50</sup> 0.016			<sup>38</sup> 0.214	<sup>43</sup> 0.158
199	TECH5-001	<sup>222</sup> 0.807	<sup>120</sup> 0.057	<sup>94</sup> 0.018	<sup>229</sup> 0.994	<sup>220</sup> 0.935	<sup>87</sup> 0.055	<sup>184</sup> 1.000	<sup>186</sup> 1.000	<sup>181</sup> 1.000	<sup>120</sup> 0.244	<sup>77</sup> 0.028			<sup>148</sup> 0.994	<sup>144</sup> 0.817
200	TECH5-002	<sup>67</sup> 0.053	<sup>73</sup> 0.027	<sup>77</sup> 0.012	<sup>39</sup> 0.094	<sup>64</sup> 0.070	<sup>59</sup> 0.040	<sup>33</sup> 0.874	<sup>35</sup> 0.805	<sup>39</sup> 0.627	<sup>62</sup> 0.039	<sup>63</sup> 0.019	<sup>40</sup> 0.205	<sup>40</sup> 0.111	<sup>82</sup> 0.440	<sup>55</sup> 0.182
201	TEVIAN-003	<sup>160</sup> 0.239	<sup>180</sup> 0.177	<sup>194</sup> 0.096	<sup>168</sup> 0.346	<sup>180</sup> 0.298	<sup>187</sup> 0.198									
202	TEVIAN-004	<sup>141</sup> 0.170	<sup>160</sup> 0.117	<sup>174</sup> 0.063	<sup>140</sup> 0.216	<sup>151</sup> 0.176	<sup>155</sup> 0.115									
203	TEVIAN-005	<sup>120</sup> 0.129	<sup>150</sup> 0.087	<sup>135</sup> 0.045	<sup>122</sup> 0.180	<sup>131</sup> 0.144	<sup>132</sup> 0.089	<sup>69</sup> 0.988	<sup>54</sup> 0.962	<sup>58</sup> 0.796						
204	TEVIAN-006	<sup>21</sup> 0.024	<sup>20</sup> 0.010	<sup>33</sup> 0.005	<sup>23</sup> 0.041	<sup>24</sup> 0.032	<sup>24</sup> 0.021	<sup>12</sup> 0.562	<sup>10</sup> 0.425	<sup>16</sup> 0.291	<sup>35</sup> 0.016	<sup>29</sup> 0.009	<sup>16</sup> 0.093	<sup>18</sup> 0.050	<sup>136</sup> 0.951	<sup>20</sup> 0.117
205	TEVIAN-007	<sup>10</sup> 0.011	<sup>21</sup> 0.005	<sup>20</sup> 0.003	<sup>13</sup> 0.028	<sup>14</sup> 0.022	<sup>15</sup> 0.015	<sup>5</sup> 0.504	<sup>3</sup> 0.301	<sup>12</sup> 0.183	<sup>10</sup> 0.009	<sup>14</sup> 0.005	<sup>15</sup> 0.065	<sup>14</sup> 0.033	<sup>13</sup> 0.122	<sup>15</sup> 0.102
206	TIGER-000	<sup>190</sup> 0.462	<sup>210</sup> 0.390	<sup>216</sup> 0.261	<sup>191</sup> 0.565	<sup>200</sup> 0.500	<sup>209</sup> 0.366									
207	TIGER-002	<sup>138</sup> 0.158	<sup>140</sup> 0.086	<sup>147</sup> 0.039	<sup>135</sup> 0.202	<sup>140</sup> 0.158	<sup>139</sup> 0.095	<sup>135</sup> 0.999	<sup>135</sup> 0.999	<sup>104</sup> 0.975						
208	TIGER-003	<sup>130</sup> 0.158	<sup>140</sup> 0.086	<sup>146</sup> 0.039	<sup>134</sup> 0.202	<sup>141</sup> 0.158	<sup>138</sup> 0.095									
209	TONGYITRANS-000	<sup>100</sup> 0.107	<sup>130</sup> 0.074	<sup>145</sup> 0.038	<sup>102</sup> 0.141	<sup>108</sup> 0.112	<sup>108</sup> 0.069									
210	TONGYITRANS-001	<sup>110</sup> 0.124	<sup>130</sup> 0.066	<sup>134</sup> 0.032	<sup>90</sup> 0.128	<sup>90</sup> 0.101	<sup>99</sup> 0.062									
211	TOSHIBA-000	<sup>114</sup> 0.123	<sup>120</sup> 0.062	<sup>126</sup> 0.027	<sup>100</sup> 0.150	<sup>111</sup> 0.118	<sup>114</sup> 0.074	<sup>104</sup> 0.997	<sup>100</sup> 0.995	<sup>117</sup> 0.988						
212	TOSHIBA-001	<sup>160</sup> 0.225	<sup>120</sup> 0.058	<sup>90</sup> 0.019	<sup>90</sup> 0.133	<sup>86</sup> 0.092	<sup>86</sup> 0.054									
213	TRUEFACE-000	<sup>50</sup> 0.046	<sup>50</sup> 0.018	<sup>57</sup> 0.008	<sup>50</sup> 0.079	<sup>50</sup> 0.062	<sup>56</sup> 0.039	<sup>91</sup> 0.995	<sup>41</sup> 0.882	<sup>28</sup> 0.499	<sup>47</sup> 0.030	<sup>52</sup> 0.016	<sup>38</sup> 0.194	<sup>41</sup> 0.111	<sup>35</sup> 0.188	<sup>39</sup> 0.145
214	VD-000	<sup>231</sup> 0.950	<sup>235</sup> 0.917	<sup>238</sup> 0.827	<sup>222</sup> 0.968	<sup>231</sup> 0.946	<sup>231</sup> 0.871									
215	VD-001	<sup>170</sup> 0.278	<sup>190</sup> 0.201	<sup>190</sup> 0.116	<sup>163</sup> 0.331	<sup>181</sup> 0.281	<sup>184</sup> 0.188									
216	VD-002	<sup>130</sup> 0.144	<sup>140</sup> 0.079	<sup>140</sup> 0.036	<sup>127</sup> 0.188	<sup>138</sup> 0.148	<sup>133</sup> 0.092	<sup>112</sup> 0.998	<sup>112</sup> 0.996	<sup>114</sup> 0.987	<sup>97</sup> 0.095	<sup>100</sup> 0.048	<sup>32</sup> 0.367	<sup>50</sup> 0.220	<sup>72</sup> 0.372	<sup>84</sup> 0.280
217	VD-003	<sup>160</sup> 0.234	<sup>102</sup> 0.046	<sup>90</sup> 0.020	<sup>97</sup> 0.133	<sup>90</sup> 0.100	<sup>98</sup> 0.061	<sup>131</sup> 0.999	<sup>130</sup> 0.999	<sup>136</sup> 0.994	<sup>73</sup> 0.051	<sup>74</sup> 0.027	<sup>44</sup> 0.244	<sup>46</sup> 0.133	<sup>65</sup> 0.315	<sup>60</sup> 0.203
218	VERIDAS-001	<sup>90</sup> 0.080	<sup>90</sup> 0.037	<sup>89</sup> 0.016	<sup>69</sup> 0.106	<sup>70</sup> 0.082	<sup>74</sup> 0.051	<sup>77</sup> 0.993	<sup>82</sup> 0.987	<sup>80</sup> 0.938	<sup>66</sup> 0.044	<sup>71</sup> 0.023	<sup>45</sup> 0.266	<sup>47</sup> 0.146	<sup>55</sup> 0.264	<sup>61</sup> 0.204
219	VERIDAS-002	<sup>91</sup> 0.080	<sup>90</sup> 0.037	<sup>88</sup> 0.016	<sup>70</sup> 0.106	<sup>70</sup> 0.082	<sup>75</sup> 0.051	<sup>78</sup> 0.993	<sup>81</sup> 0.987	<sup>81</sup> 0.938	<sup>66</sup> 0.044	<sup>72</sup> 0.023	<sup>46</sup> 0.266	<sup>48</sup> 0.146	<sup>54</sup> 0.264	<sup>62</sup> 0.204
220	VIGILANTSOLUTIONS-003	<sup>202</sup> 0.482	<sup>210</sup> 0.408	<sup>218</sup> 0.282	<sup>207</sup> 0.730	<sup>210</sup> 0.660	<sup>220</sup> 0.526	<sup>128</sup> 0.999	<sup>132</sup> 0.999	<sup>145</sup> 0.995						
221	VIGILANTSOLUTIONS-004	<sup>210</sup> 0.624	<sup>223</sup> 0.549	<sup>226</sup> 0.422	<sup>211</sup> 0.858	<sup>223</sup> 0.817	<sup>223</sup> 0.709	<sup>116</sup> 0.998	<sup>114</sup> 0.996	<sup>126</sup> 0.991						
222	VIGILANTSOLUTIONS-005	<sup>230</sup> 0.936	<sup>210</sup> 0.388	<sup>149</sup> 0.043				<sup>166</sup> 1.000	<sup>170</sup> 1.000	<sup>187</sup> 1.000						
223	VIGILANTSOLUTIONS-006	<sup>230</sup> 0.959	<sup>200</sup> 0.353	<sup>152</sup> 0.043				<sup>158</sup> 1.000	<sup>172</sup> 1.000	<sup>188</sup> 1.000						
224	VIGILANTSOLUTIONS-007	<sup>87</sup> 0.076	<sup>70</sup> 0.028	<sup>73</sup> 0.011	<sup>74</sup> 0.113	<sup>80</sup> 0.088	<sup>81</sup> 0.053	<sup>109</sup> 0.997	<sup>113</sup> 0.996	<sup>129</sup> 0.991	<sup>94</sup> 0.081	<sup>98</sup> 0.047	<sup>53</sup> 0.371	<sup>56</sup> 0.242	<sup>75</sup> 0.391	<sup>91</sup> 0.295
225	VIGILANTSOLUTIONS-008	<sup>68</sup> 0.051	<sup>58</sup> 0.021	<sup>64</sup> 0.010	<sup>68</sup> 0.105	<sup>69</sup> 0.077	<sup>68</sup> 0.046	<sup>132</sup> 1.000	<sup>134</sup> 0.999	<sup>125</sup> 0.991	<sup>101</sup> 0.104	<sup>103</sup> 0.054	<sup>55</sup> 0.398	<sup>59</sup> 0.259	<sup>93</sup> 0.511	<sup>97</sup> 0.316
226	VISIONBOX-000	<sup>84</sup> 0.073	<sup>50</sup> 0.018	<sup>48</sup> 0.007	<sup>44</sup> 0.071	<sup>51</sup> 0.057	<sup>53</sup> 0.035	<sup>84</sup> 0.995	<sup>90</sup> 0.990	<sup>102</sup> 0.974	<sup>38</sup> 0.023	<sup>38</sup> 0.012	<sup>27</sup> 0.146	<sup>28</sup> 0.081	<sup>25</sup> 0.162	<sup>27</sup> 0.126
227	VISIONLABS-004	<sup>90</sup> 0.091	<sup>120</sup> 0.058	<sup>117</sup> 0.024	<sup>131</sup> 0.199	<sup>142</sup> 0.159	<sup>141</sup> 0.097	<sup>41</sup> 0.944	<sup>40</sup> 0.890	<sup>51</sup> 0.742						
228	VISIONLABS-005	<sup>94</sup> 0.080	<sup>100</sup> 0.050	<sup>101</sup> 0.020	<sup>125</sup> 0.183	<sup>132</sup> 0.147	<sup>130</sup> 0.087	<sup>42</sup> 0.945	<sup>42</sup> 0.888	<sup>50</sup> 0.736						
229	VISIONLABS-006	<sup>50</sup> 0.044	<sup>70</sup> 0.027	<sup>67</sup> 0.010	<sup>70</sup> 0.117	<sup>80</sup> 0.090	<sup>77</sup> 0.051	<sup>24</sup> 0.764	<sup>20</sup> 0.672	<sup>32</sup> 0.511						
230	VISIONLABS-007	<sup>50</sup> 0.044	<sup>70</sup> 0.027	<sup>66</sup> 0.010	<sup>72</sup> 0.117	<sup>80</sup> 0.090	<sup>76</sup> 0.051	<sup>23</sup> 0.764	<sup>20</sup> 0.672	<sup>31</sup> 0.511	<sup>40</sup> 0.031	<sup>46</sup> 0.014			<sup>34</sup> 0.185	<sup>38</sup> 0.145

Table 29: **Threshold-based accuracy.** Values are FNIR(N, T, L) with N = 1.6 million with thresholds set to produce FPIR = 0.0003, 0.001, and 0.01 in non-mate searches. Throughout blue superscripts indicate the rank of the algorithm for that column. Caution: The Power-low models are mostly intended to draw attention to the kind of behavior, not as a model to be used for prediction.

2021/10/28  
13:44:33

FNIR(N, R, T) =  
FPIR(N, T) =

False neg. identification rate  
False pos. identification rate

N = Num. enrolled subjects  
R = Num. candidates examined

T = Threshold

T = 0 → Investigation  
T > 0 → Identification

MISSES BELOW THRESHOLD, T		ENROL RECENT MUGSHOT, N = 1.6M									ENROL APPLICATION PORTRAIT, N = 1.6M					
		ENROL: MUGSHOT PROBE: MUGSHOT			ENROL: MUGSHOT PROBE: WEBCAM			ENROL: MUGSHOT PROBE: PROFILE			ENROL: VISA PROBE: BORDER		ENROL: BORDER PROBE: BORDER 10+YR		ENROL: VISA PROBE: KIOSK	
#	ALGORITHM	FPIR=0.0003	FPIR=0.001	FPIR=0.01	FPIR=0.0003	FPIR=0.001	FPIR=0.01	FPIR=0.0003	FPIR=0.001	FPIR=0.01	FPIR=0.001	FPIR=0.01	FPIR=0.001	FPIR=0.01	FPIR=0.001	FPIR=0.01
231	VISIONLABS-008	<sup>34</sup> 0.028	<sup>37</sup> 0.013	<sup>37</sup> 0.006	<sup>40</sup> 0.068	<sup>43</sup> 0.051	<sup>45</sup> 0.032	<sup>13</sup> 0.574	<sup>16</sup> 0.481	<sup>19</sup> 0.317	<sup>27</sup> 0.017	<sup>25</sup> 0.008			<sup>19</sup> 0.151	<sup>21</sup> 0.119
232	VISIONLABS-009	<sup>17</sup> 0.012	<sup>17</sup> 0.005	<sup>14</sup> 0.002	<sup>17</sup> 0.032	<sup>18</sup> 0.025	<sup>18</sup> 0.017	<sup>38</sup> 0.930	<sup>33</sup> 0.799	<sup>15</sup> 0.196	<sup>17</sup> 0.008	<sup>15</sup> 0.004			<sup>11</sup> 0.113	<sup>11</sup> 0.093
233	VISIONLABS-010	<sup>18</sup> 0.014	<sup>20</sup> 0.005	<sup>18</sup> 0.002	<sup>18</sup> 0.034	<sup>20</sup> 0.027	<sup>20</sup> 0.019			<sup>5</sup> 0.169	<sup>12</sup> 0.008	<sup>8</sup> 0.004	<sup>10</sup> 0.055	<sup>10</sup> 0.027	<sup>10</sup> 0.109	<sup>8</sup> 0.089
234	VOCORD-003	<sup>185</sup> 0.354	<sup>167</sup> 0.122	<sup>159</sup> 0.048	<sup>180</sup> 0.195	<sup>138</sup> 0.155	<sup>136</sup> 0.093	<sup>121</sup> 0.999	<sup>124</sup> 0.998	<sup>123</sup> 0.991	<sup>115</sup> 0.157	<sup>124</sup> 0.105			<sup>78</sup> 0.404	<sup>87</sup> 0.289
235	VOCORD-004	<sup>223</sup> 0.826	<sup>208</sup> 0.355	<sup>160</sup> 0.051	<sup>176</sup> 0.401	<sup>148</sup> 0.173	<sup>134</sup> 0.093	<sup>159</sup> 1.000	<sup>161</sup> 1.000	<sup>167</sup> 0.999	<sup>123</sup> 0.193	<sup>107</sup> 0.065			<sup>145</sup> 0.991	<sup>140</sup> 0.776
236	VOCORD-005	<sup>216</sup> 0.689	<sup>179</sup> 0.158	<sup>153</sup> 0.044	<sup>117</sup> 0.161	<sup>122</sup> 0.130	<sup>124</sup> 0.080	<sup>126</sup> 0.999	<sup>116</sup> 0.997	<sup>91</sup> 0.968	<sup>110</sup> 0.138	<sup>118</sup> 0.090			<sup>72</sup> 0.381	<sup>85</sup> 0.287
237	VOCORD-006	<sup>244</sup> 1.000	<sup>244</sup> 1.000	<sup>237</sup> 1.000	<sup>239</sup> 1.000	<sup>246</sup> 1.000	<sup>246</sup> 1.000	<sup>213</sup> 1.000	<sup>218</sup> 1.000	<sup>241</sup> 1.000	<sup>183</sup> 1.000	<sup>212</sup> 1.000			<sup>161</sup> 1.000	<sup>164</sup> 1.000
238	VTS-000	<sup>210</sup> 0.605	<sup>225</sup> 0.598	<sup>232</sup> 0.595	<sup>196</sup> 0.624	<sup>214</sup> 0.619	<sup>222</sup> 0.613	<sup>133</sup> 0.999	<sup>142</sup> 0.999	<sup>168</sup> 0.998	<sup>150</sup> 0.613	<sup>152</sup> 0.609	<sup>59</sup> 0.760	<sup>62</sup> 0.739	<sup>113</sup> 0.761	<sup>137</sup> 0.749
239	VTS-001	<sup>42</sup> 0.035	<sup>38</sup> 0.013	<sup>38</sup> 0.006	<sup>39</sup> 0.067	<sup>42</sup> 0.051	<sup>40</sup> 0.031	<sup>111</sup> 0.998	<sup>38</sup> 0.994	<sup>36</sup> 0.510	<sup>37</sup> 0.022	<sup>39</sup> 0.012	<sup>23</sup> 0.141	<sup>25</sup> 0.079	<sup>36</sup> 0.192	<sup>28</sup> 0.126
240	XFORWARDAI-000	<sup>36</sup> 0.029	<sup>45</sup> 0.015	<sup>48</sup> 0.006	<sup>48</sup> 0.070	<sup>47</sup> 0.053	<sup>51</sup> 0.034	<sup>28</sup> 0.698	<sup>12</sup> 0.440	<sup>14</sup> 0.250	<sup>35</sup> 0.021	<sup>34</sup> 0.011	<sup>30</sup> 0.159	<sup>30</sup> 0.082	<sup>28</sup> 0.169	<sup>31</sup> 0.134
241	XFORWARDAI-001	<sup>14</sup> 0.010	<sup>18</sup> 0.005	<sup>21</sup> 0.003	<sup>20</sup> 0.036	<sup>22</sup> 0.028	<sup>21</sup> 0.020	<sup>30</sup> 0.838	<sup>13</sup> 0.448	<sup>6</sup> 0.143	<sup>15</sup> 0.008	<sup>15</sup> 0.005	<sup>12</sup> 0.062	<sup>12</sup> 0.030	<sup>14</sup> 0.123	<sup>14</sup> 0.102
242	XFORWARDAI-002	<sup>10</sup> 0.007	<sup>12</sup> 0.003	<sup>15</sup> 0.002	<sup>9</sup> 0.018	<sup>10</sup> 0.016	<sup>14</sup> 0.014	<sup>49</sup> 0.975	<sup>17</sup> 0.525	<b>0.095</b>	<sup>6</sup> 0.005	<sup>5</sup> 0.003	<sup>7</sup> 0.041	<sup>5</sup> 0.018	<sup>4</sup> 0.099	<sup>7</sup> 0.089
243	YISHENG-001	<sup>196</sup> 0.452	<sup>205</sup> 0.346	<sup>211</sup> 0.206	<sup>225</sup> 0.983	<sup>221</sup> 0.808	<sup>201</sup> 0.269				<sup>151</sup> 0.666	<sup>146</sup> 0.396			<sup>131</sup> 0.919	<sup>131</sup> 0.695
244	YITU-002	<sup>38</sup> 0.031	<sup>49</sup> 0.018	<sup>52</sup> 0.008	<sup>38</sup> 0.063	<sup>38</sup> 0.049	<sup>38</sup> 0.028									
245	YITU-003	<sup>39</sup> 0.032	<sup>56</sup> 0.019	<sup>60</sup> 0.009	<sup>37</sup> 0.067	<sup>45</sup> 0.052	<sup>48</sup> 0.033									
246	YITU-004	<sup>21</sup> 0.019	<sup>26</sup> 0.010	<sup>27</sup> 0.004	<sup>19</sup> 0.035	<sup>19</sup> 0.027	<sup>19</sup> 0.017	<sup>45</sup> 0.948	<sup>49</sup> 0.936	<sup>71</sup> 0.913						
247	YITU-005	<sup>23</sup> 0.022	<sup>29</sup> 0.010	<sup>36</sup> 0.005	<sup>27</sup> 0.039	<sup>25</sup> 0.032	<sup>27</sup> 0.023									

Table 30: **Threshold-based accuracy.** Values are FNIR(N, T, L) with N = 1.6 million with thresholds set to produce FPIR = 0.0003, 0.001, and 0.01 in non-mate searches. Throughout blue superscripts indicate the rank of the algorithm for that column. Caution: The Power-low models are mostly intended to draw attention to the kind of behavior, not as a model to be used for prediction.

2021/10/28  
13:44:33

FNIR(N, R, T) =  
FPIR(N, T) =

False neg. identification rate  
False pos. identification rate

N = Num. enrolled subjects  
R = Num. candidates examined

T = Threshold

T = 0 → Investigation  
T > 0 → Identification

# Appendices

## Appendix A Accuracy on large-population FRVT 2018 mugshots

This publication is available free of charge from: <https://doi.org/10.6028/NIST.IR.8271>

---

2021/10/28 FNIR(N, R, T) = False neg. identification rate N = Num. enrolled subjects T = Threshold T = 0 → Investigation  
13:44:33 FPIR(N, T) = False pos. identification rate R = Num. candidates examined T > 0 → Identification

2021/10/28  
 FNIR(N, R, T) =  
 FPR(N, T) =  
 False neg. identification rate  
 False pos. identification rate  
 N = Num. enrolled subjects  
 R = Num. candidates examined  
 T = Threshold  
 T = 0 → Investigation  
 T > 0 → Identification

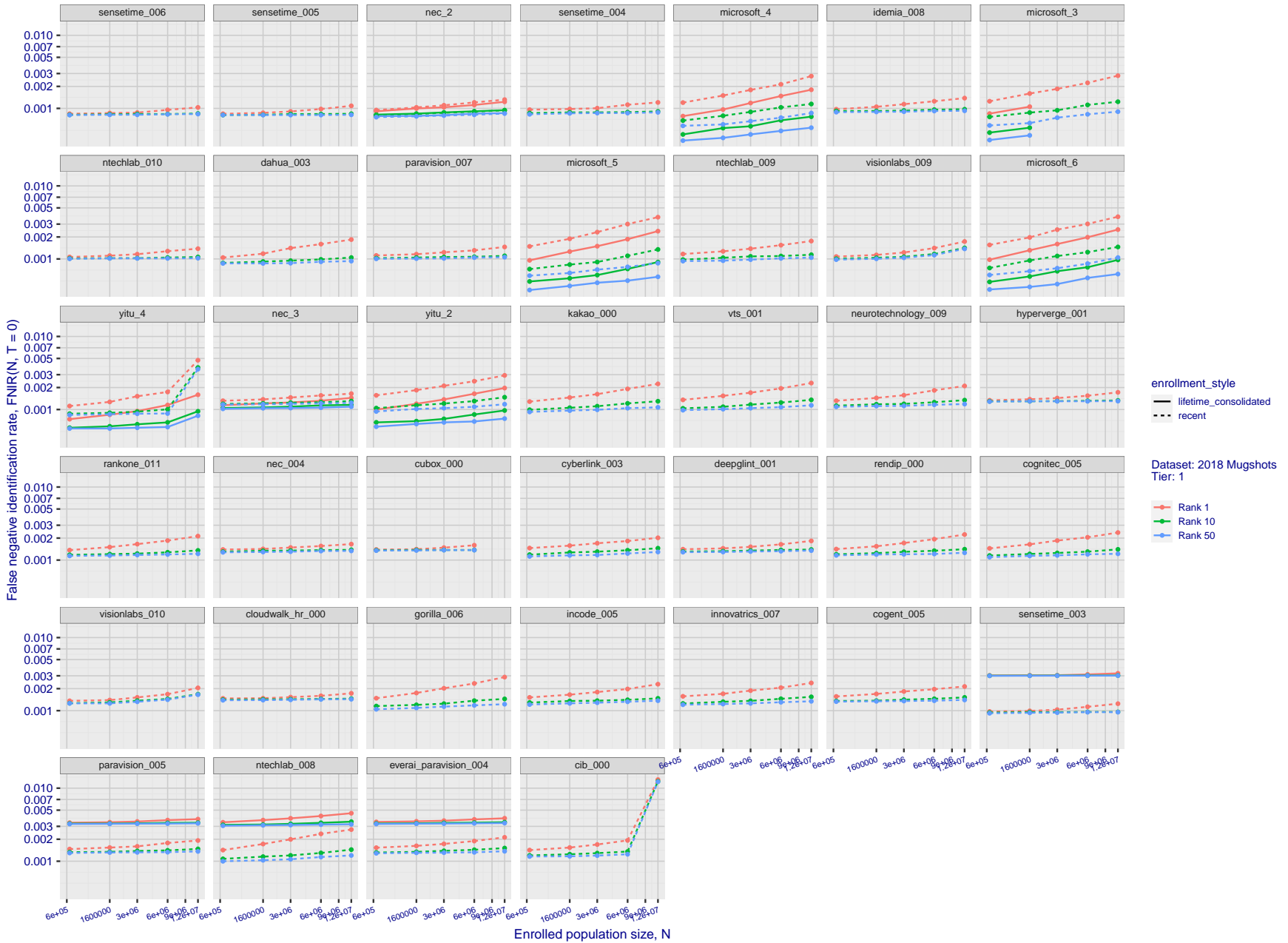


Figure 20: [FRVT-2018 Mugshot Dataset] Rank-based identification miss rates vs. number of enrolled subjects. The figure shows false negative identification rates,  $FNIR(N, R)$ , across various gallery sizes and ranks 1, 10 and 50. The threshold is set to zero, so this metric rewards even weak scoring rank 1 mates. This also means  $FPIR = 1$ , so any search without an enrolled mate will return non-mated candidates. For clarity, results are sorted and reported into tiers spanning multiple pages, the tiering criteria being rank 1 hit rate on a gallery size of 640 000.

2021/10/28  
13:44:33

FNIR(N, R, T) =  
FPIR(N, T) =

False neg. identification rate  
False pos. identification rate

N = Num. enrolled subjects  
R = Num. candidates examined

T = Threshold

T = 0 → Investigation  
T > 0 → Identification

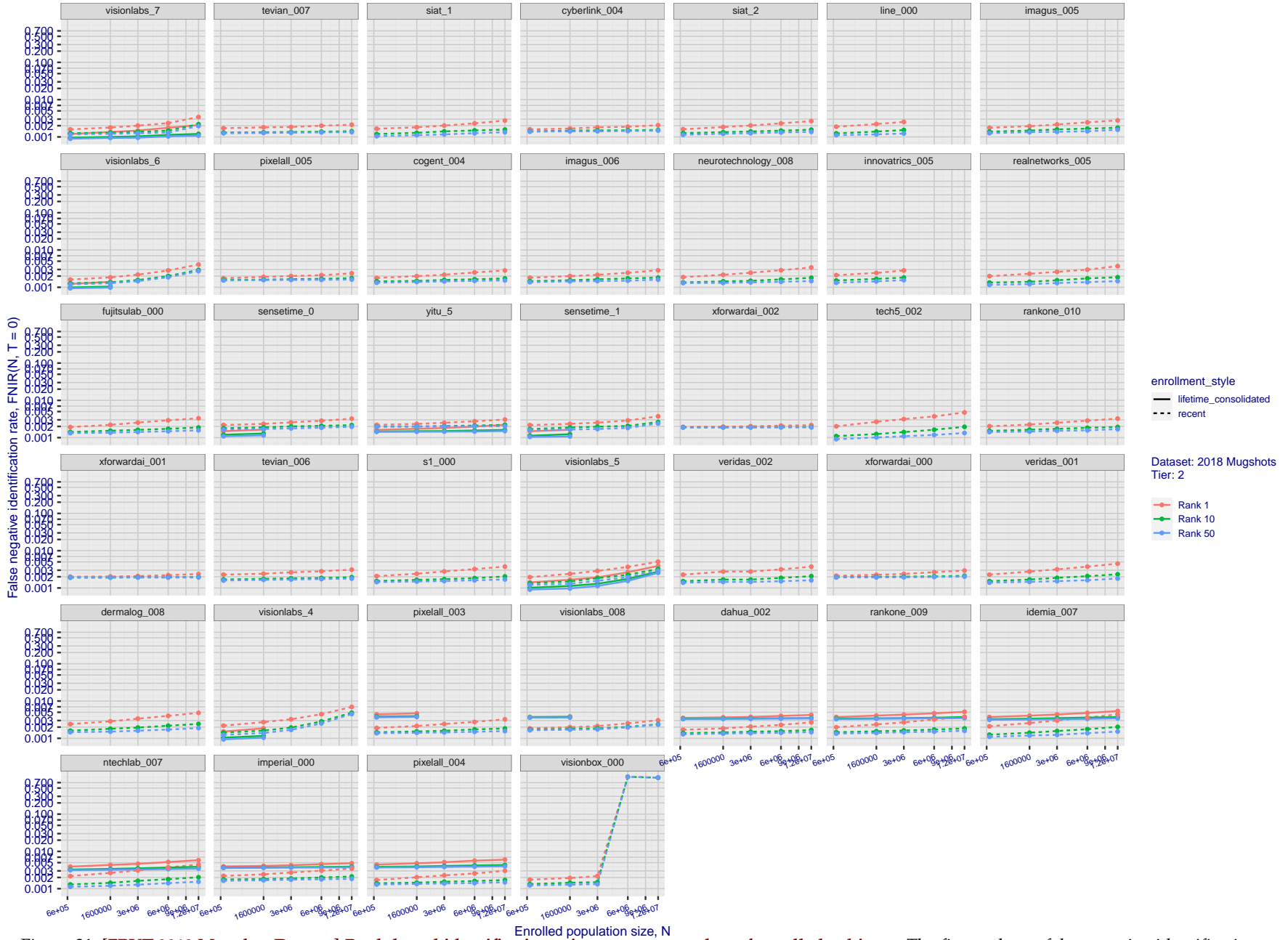


Figure 21: [FRVT-2018 Mugshot Dataset] Rank-based identification miss rates vs. number of enrolled subjects. The figure shows false negative identification rates,  $FNIR(N, R)$ , across various gallery sizes and ranks 1, 10 and 50. The threshold is set to zero, so this metric rewards even weak scoring rank 1 mates. This also means  $FPIR = 1$ , so any search without an enrolled mate will return non-mated candidates. For clarity, results are sorted and reported into tiers spanning multiple pages, the tiering criteria being rank 1 hit rate on a gallery size of 640 000.

2021/10/28  
13:44:33

FNIR(N, R, T) =  
FPIR(N, T) =

False neg. identification rate  
False pos. identification rate

N = Num. enrolled subjects  
R = Num. candidates examined

T = Threshold

T = 0 → Investigation  
T > 0 → Identification

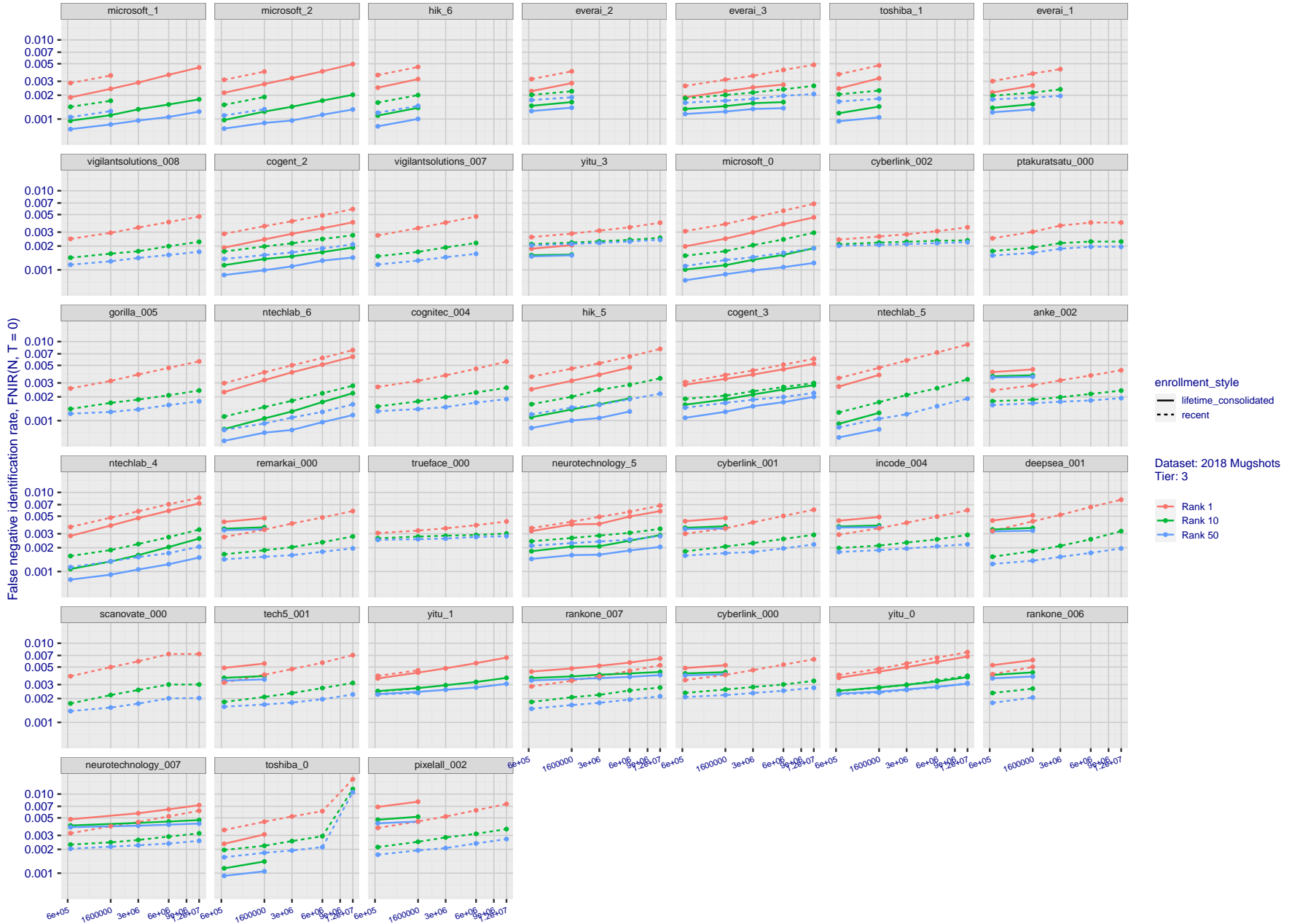


Figure 22: [FRVT-2018 Mugshot Dataset] Rank-based identification miss rates vs. number of enrolled subjects. The figure shows false negative identification rates,  $FNIR(N, R)$ , across various gallery sizes and ranks 1, 10 and 50. The threshold is set to zero, so this metric rewards even weak scoring rank 1 mates. This also means  $FPIR = 1$ , so any search without an enrolled mate will return non-mated candidates. For clarity, results are sorted and reported into tiers spanning multiple pages, the tiering criteria being rank 1 hit rate on a gallery size of 640 000.

2021/10/28  
13:44:33

FNIR(N, R, T) =  
FPIR(N, T) =

False neg. identification rate  
False pos. identification rate

N = Num. enrolled subjects  
R = Num. candidates examined

T = Threshold

T = 0 → Investigation  
T > 0 → Identification

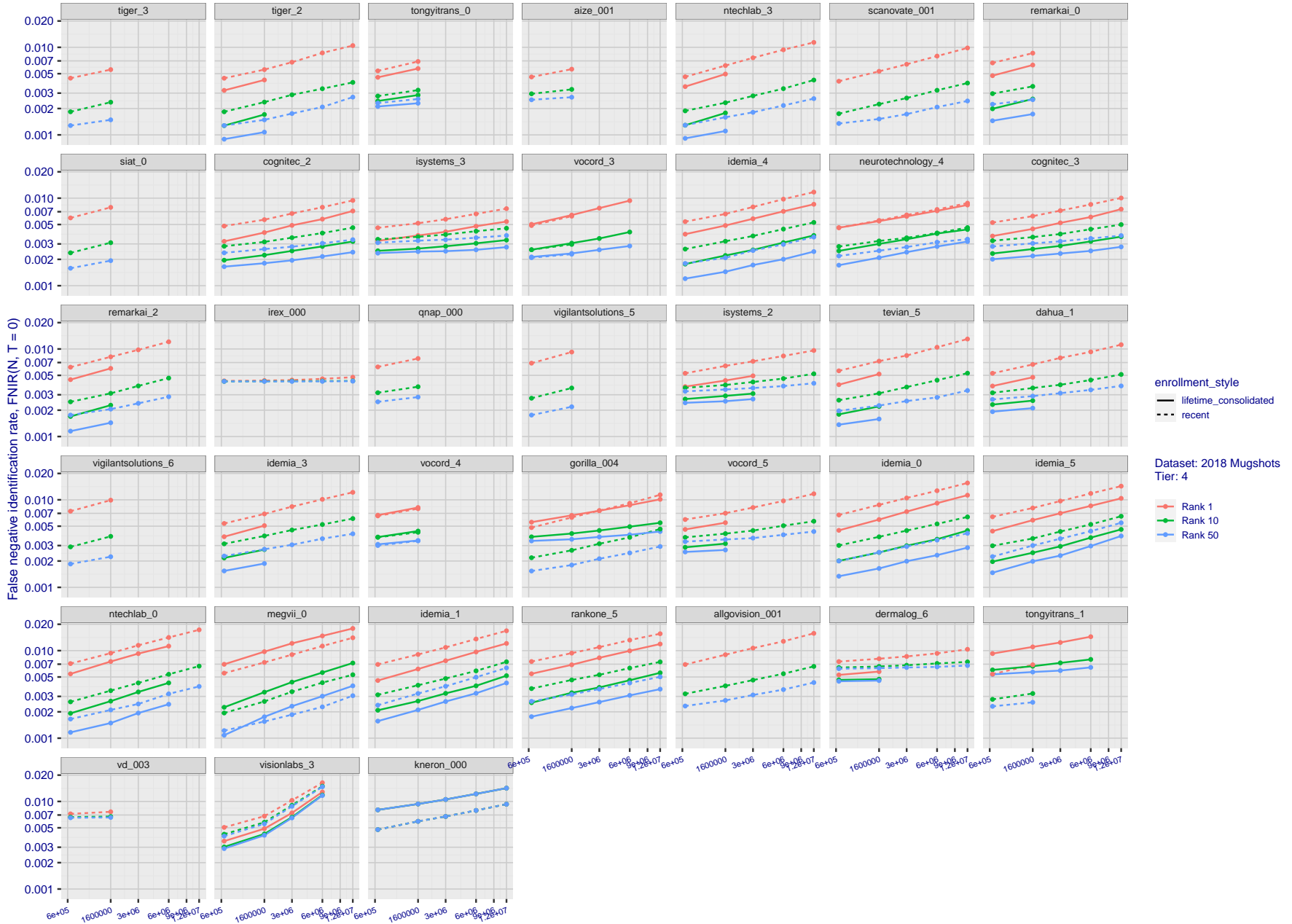


Figure 23: [FRVT-2018 Mugshot Dataset] Rank-based identification miss rates vs. number of enrolled subjects. The figure shows false negative identification rates, FNIR(N, R), across various gallery sizes and ranks 1, 10 and 50. The threshold is set to zero, so this metric rewards even weak scoring rank 1 mates. This also means FPIR = 1, so any search without an enrolled mate will return non-mated candidates. For clarity, results are sorted and reported into tiers spanning multiple pages, the tiering criteria being rank 1 hit rate on a gallery size of 640 000.

2021/10/28  
13:44:33

FNIR(N, R, T) =  
FPIR(N, T) =

False neg. identification rate  
False pos. identification rate

N = Num. enrolled subjects  
R = Num. candidates examined

T = Threshold

T = 0 → Investigation  
T > 0 → Identification

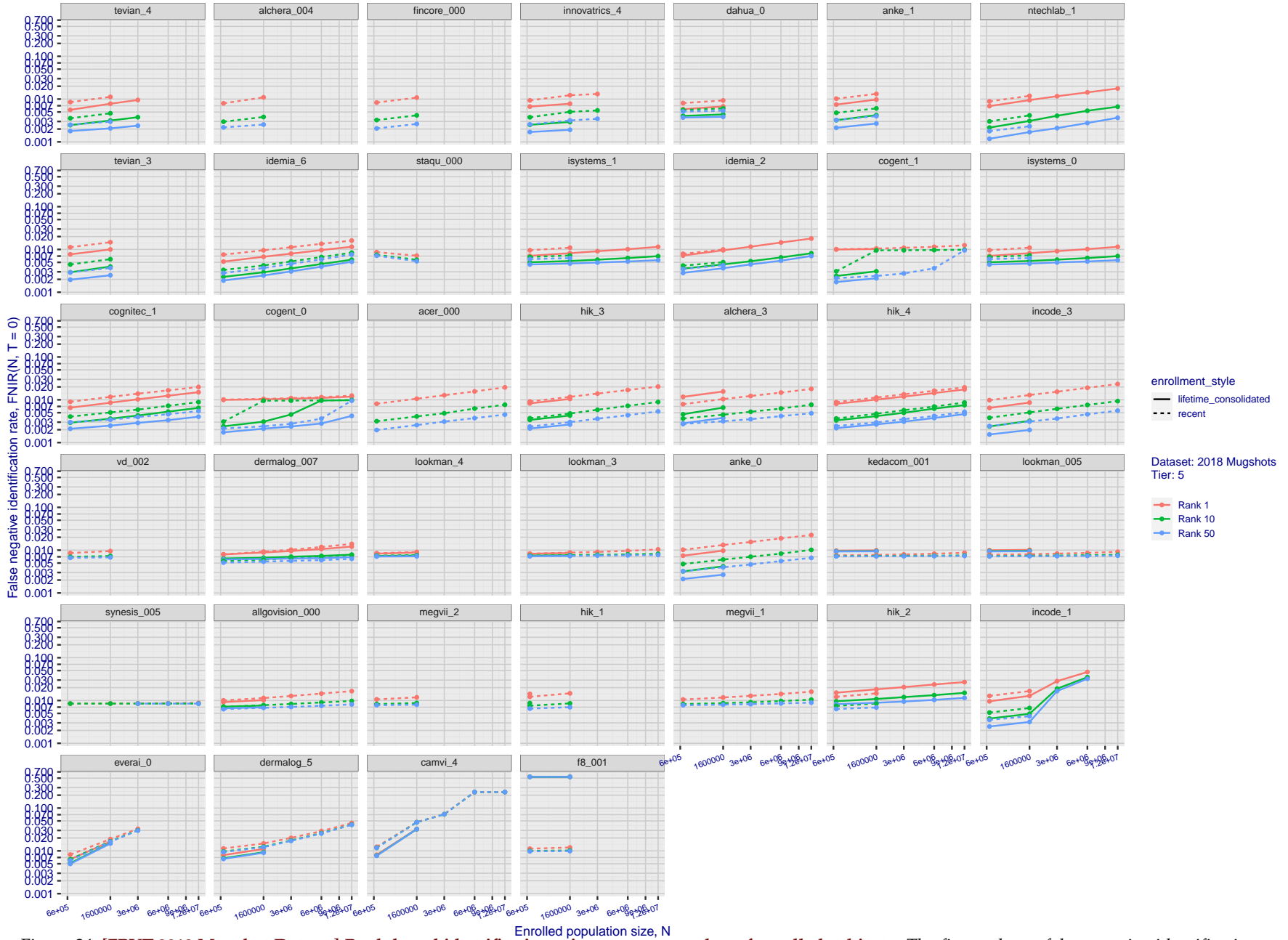


Figure 24: [FRVT-2018 Mugshot Dataset] Rank-based identification miss rates vs. number of enrolled subjects. The figure shows false negative identification rates,  $FNIR(N, R)$ , across various gallery sizes and ranks 1, 10 and 50. The threshold is set to zero, so this metric rewards even weak scoring rank 1 mates. This also means  $FPIR = 1$ , so any search without an enrolled mate will return non-mated candidates. For clarity, results are sorted and reported into tiers spanning multiple pages, the tiering criteria being rank 1 hit rate on a gallery size of 640 000.

2021/10/28  
13:44:33

FNIR(N, R, T) =  
FPIR(N, T) =

False neg. identification rate  
False pos. identification rate

N = Num. enrolled subjects  
R = Num. candidates examined

T = Threshold

T = 0 → Investigation  
T > 0 → Identification

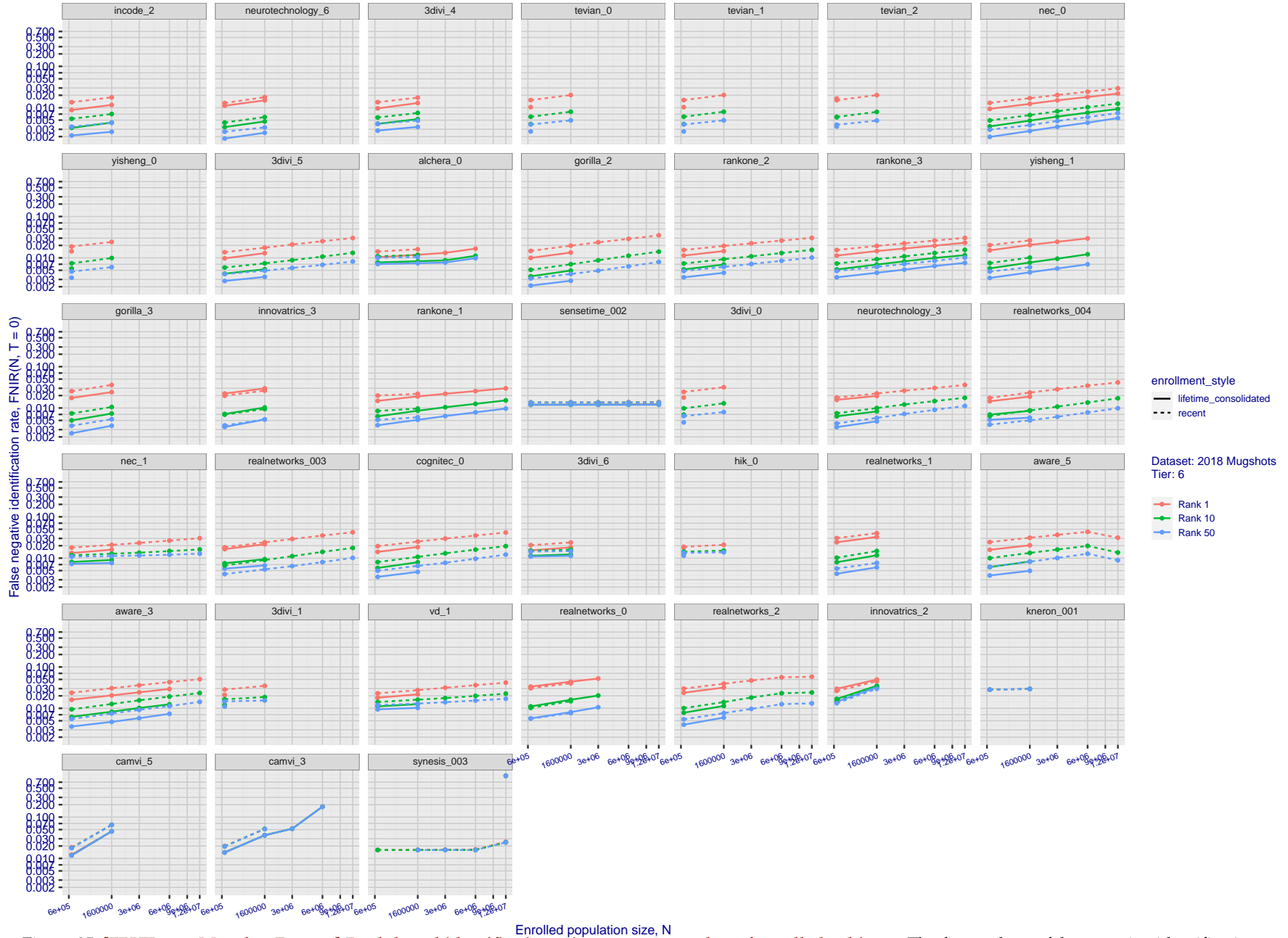


Figure 25: [FRVT-2018 Mugshot Dataset] Rank-based identification miss rates vs. number of enrolled subjects. The figure shows false negative identification rates,  $FNIR(N, R)$ , across various gallery sizes and ranks 1, 10 and 50. The threshold is set to zero, so this metric rewards even weak scoring rank 1 mates. This also means  $FPIR = 1$ , so any search without an enrolled mate will return non-mated candidates. For clarity, results are sorted and reported into tiers spanning multiple pages, the tiering criteria being rank 1 hit rate on a gallery size of 640 000.

2021/10/28  
13:44:33

FNIR(N, R, T) =  
FPIR(N, T) =

False neg. identification rate  
False pos. identification rate

N = Num. enrolled subjects  
R = Num. candidates examined

T = Threshold

T = 0 → Investigation  
T > 0 → Identification

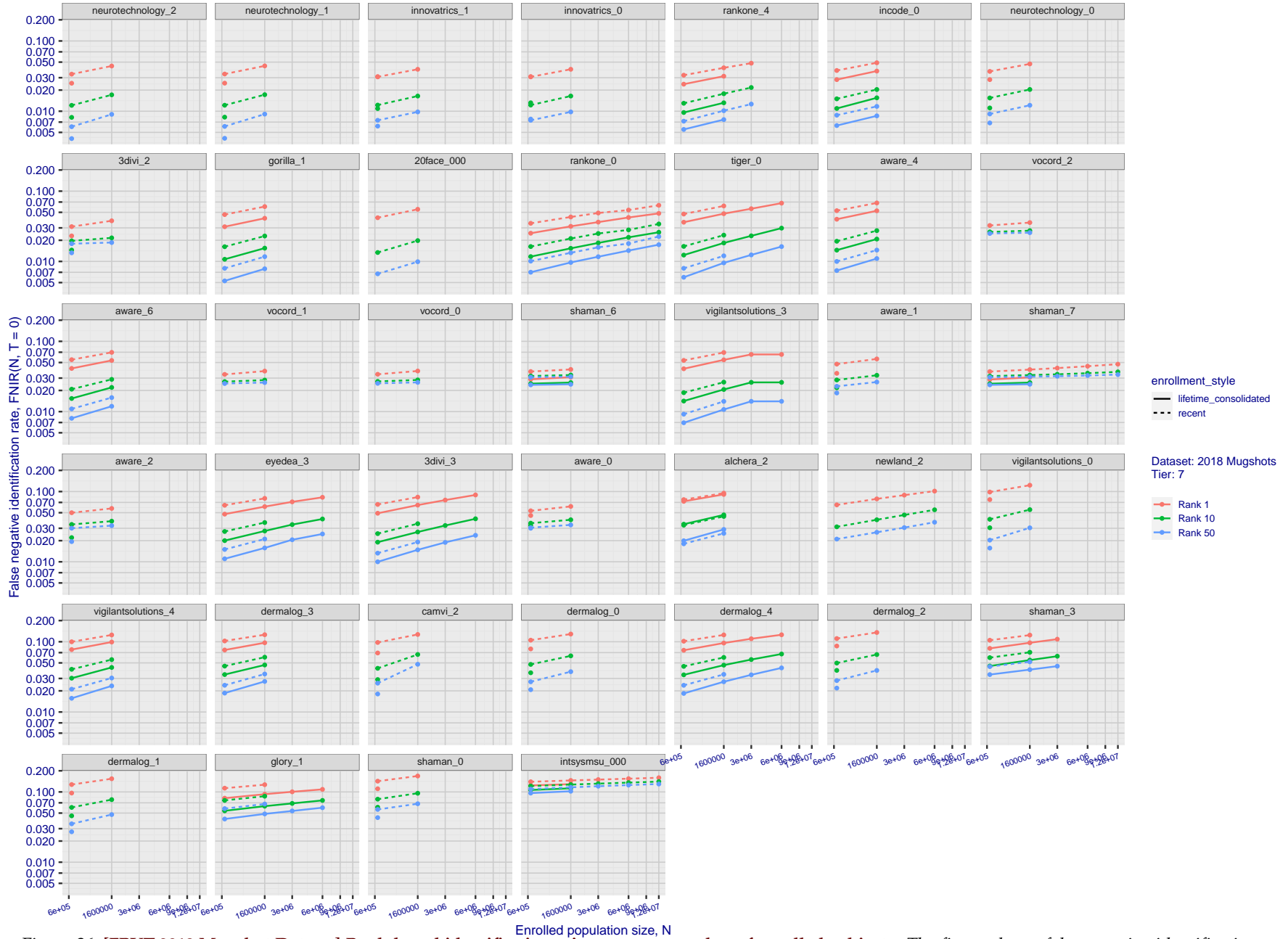


Figure 26: [FRVT-2018 Mugshot Dataset] Rank-based identification miss rates vs. number of enrolled subjects. The figure shows false negative identification rates,  $FNIR(N, R)$ , across various gallery sizes and ranks 1, 10 and 50. The threshold is set to zero, so this metric rewards even weak scoring rank 1 mates. This also means  $FPIR = 1$ , so any search without an enrolled mate will return non-mated candidates. For clarity, results are sorted and reported into tiers spanning multiple pages, the tiering criteria being rank 1 hit rate on a gallery size of 640 000.

2021/10/28  
 FNIR(N, R, T) =  
 FP(R, T) =  
 False neg. identification rate  
 False pos. identification rate  
 N = Num. enrolled subjects  
 R = Num. candidates examined  
 T = Threshold  
 T = 0 → Investigation  
 T > 0 → Identification

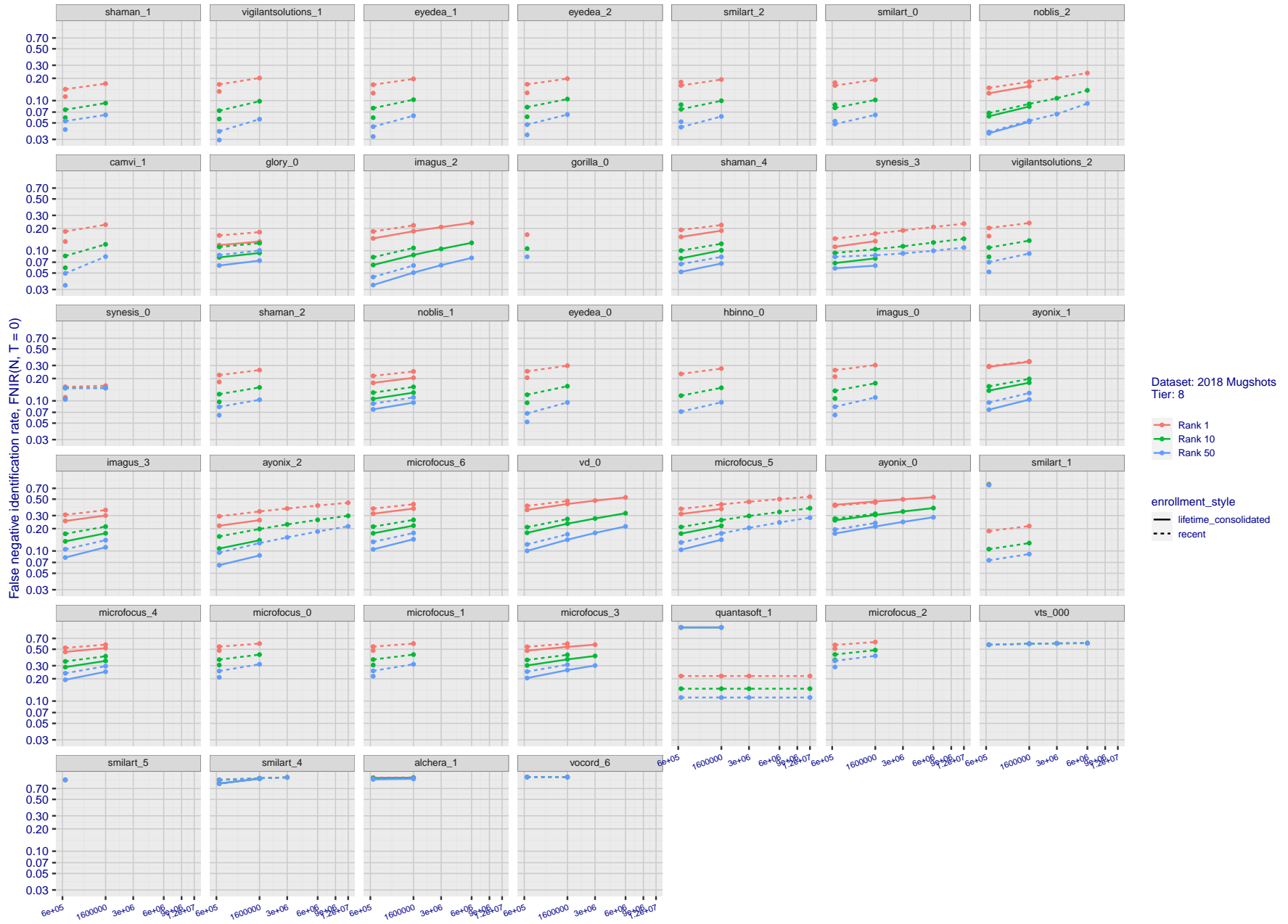


Figure 27: [FRVT-2018 Mugshot Dataset] Rank-based identification miss rates vs. number of enrolled subjects. The figure shows false negative identification rates, FNIR(N, R), across various gallery sizes and ranks 1, 10 and 50. The threshold is set to zero, so this metric rewards even weak scoring rank 1 mates. This also means FPIR = 1, so any search without an enrolled mate will return non-mated candidates. For clarity, results are sorted and reported into tiers spanning multiple pages, the tiering criteria being rank 1 hit rate on a gallery size of 640 000.

---

2021/10/28 FNIR(N, R, T) = False neg. identification rate N = Num. enrolled subjects T = Threshold T = 0 → Investigation  
13:44:33 FPIR(N, T) = False pos. identification rate R = Num. candidates examined T > 0 → Identification

2021/10/28  
 13:44:33  
 FNIR(N, R, T) =  
 FP(R, T) =  
 False neg. identification rate  
 False pos. identification rate  
 N = Num. enrolled subjects  
 R = Num. candidates examined  
 T = Threshold  
 T = 0 → Investigation  
 T > 0 → Identification

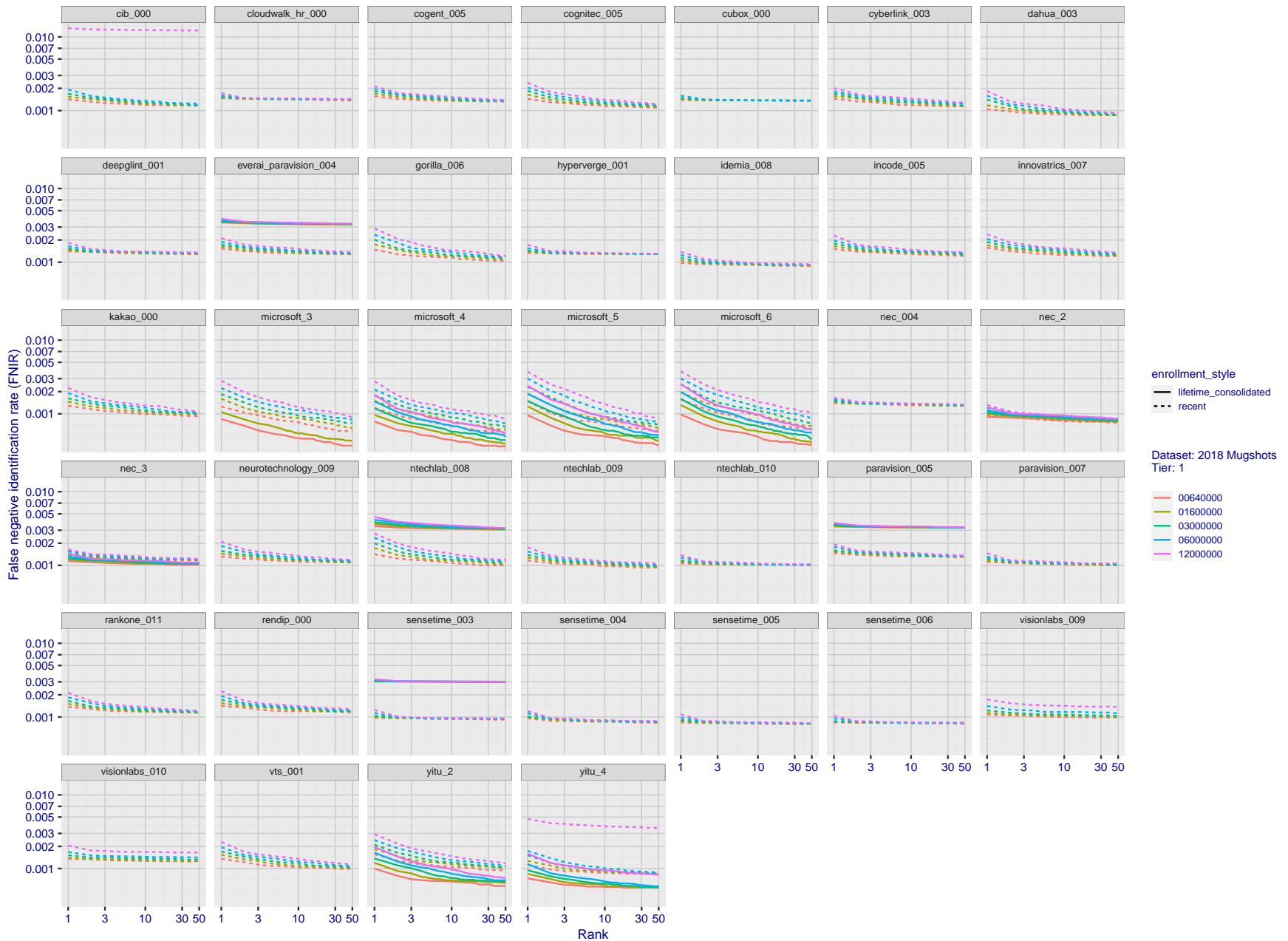


Figure 28: [FRVT-2018 Mugshot Dataset] Rank-based identification miss rates vs. rank. The figure shows false negative identification rates (FNIR) for ranks up to 50. This metric is appropriate to investigational applications where human reviewers will adjudicate sorted candidate lists. Note that with threshold set to zero, FPIR = 1, i.e. any search without an enrolled mate will return non-mated candidates. Results are sorted and reported into tiers for clarity, with the tiering criteria being rank 1 hit rate on a gallery size of  $N = 640\,000$  subjects.

2021/10/28  
13:44:33

FNIR(N, R, T) =  
FPIR(N, T) =

False neg. identification rate  
False pos. identification rate

N = Num. enrolled subjects  
R = Num. candidates examined

T = Threshold

T = 0 → Investigation  
T > 0 → Identification

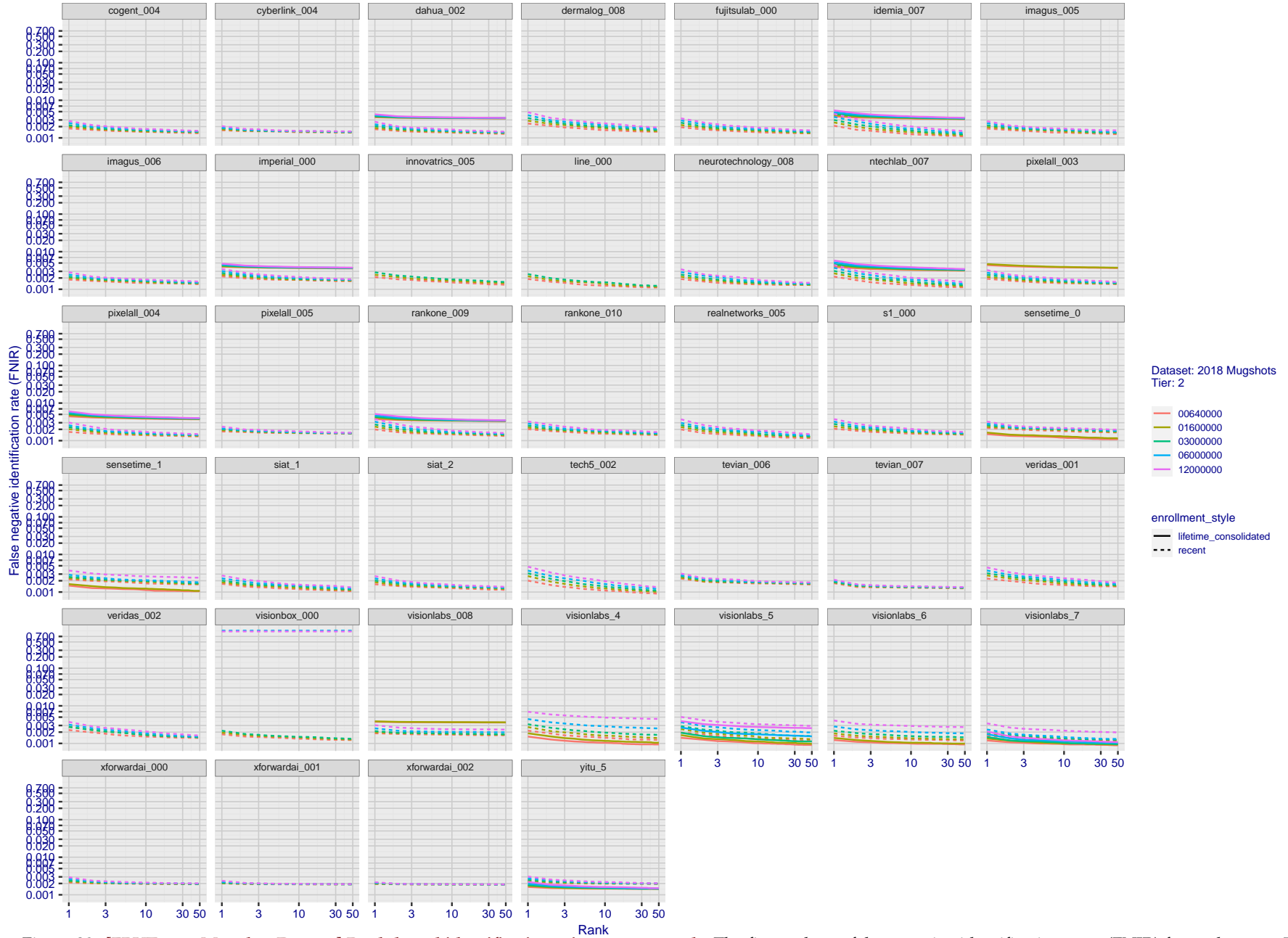


Figure 29: [FRVT-2018 Mugshot Dataset] Rank-based identification miss rates vs. rank. The figure shows false negative identification rates (FNIR) for ranks up to 50. This metric is appropriate to investigational applications where human reviewers will adjudicate sorted candidate lists. Note that with threshold set to zero, FPIR = 1, i.e. any search without an enrolled mate will return non-mated candidates. Results are sorted and reported into tiers for clarity, with the tiering criteria being rank 1 hit rate on a gallery size of  $N = 640\,000$  subjects.

2021/10/28  
 FNIR(N, R, T) =  
 FPR(N, T) =  
 False neg. identification rate  
 False pos. identification rate  
 N = Num. enrolled subjects  
 R = Num. candidates examined  
 T = Threshold  
 T = 0 → Investigation  
 T > 0 → Identification

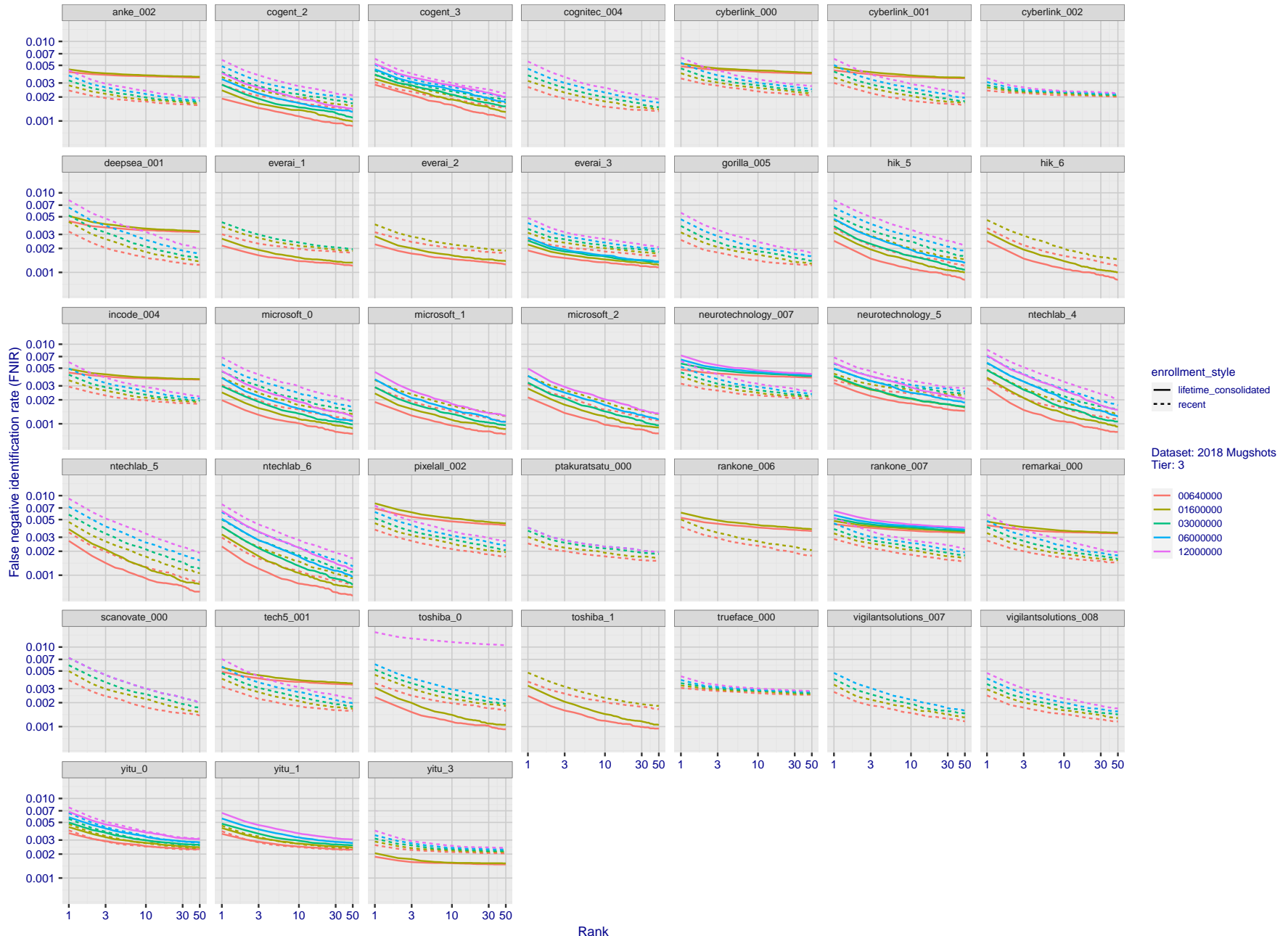


Figure 30: [FRVT-2018 Mugshot Dataset] Rank-based identification miss rates vs. rank. The figure shows false negative identification rates (FNIR) for ranks up to 50. This metric is appropriate to investigational applications where human reviewers will adjudicate sorted candidate lists. Note that with threshold set to zero, FPIR = 1, i.e. any search without an enrolled mate will return non-mated candidates. Results are sorted and reported into tiers for clarity, with the tiering criteria being rank 1 hit rate on a gallery size of  $N = 640\,000$  subjects.

2021/10/28  
 13:44:33  
 FNIR(N, R, T) =  
 FPR(N, T) =  
 False neg. identification rate  
 False pos. identification rate  
 N = Num. enrolled subjects  
 R = Num. candidates examined  
 T = Threshold  
 T = 0 → Investigation  
 T > 0 → Identification

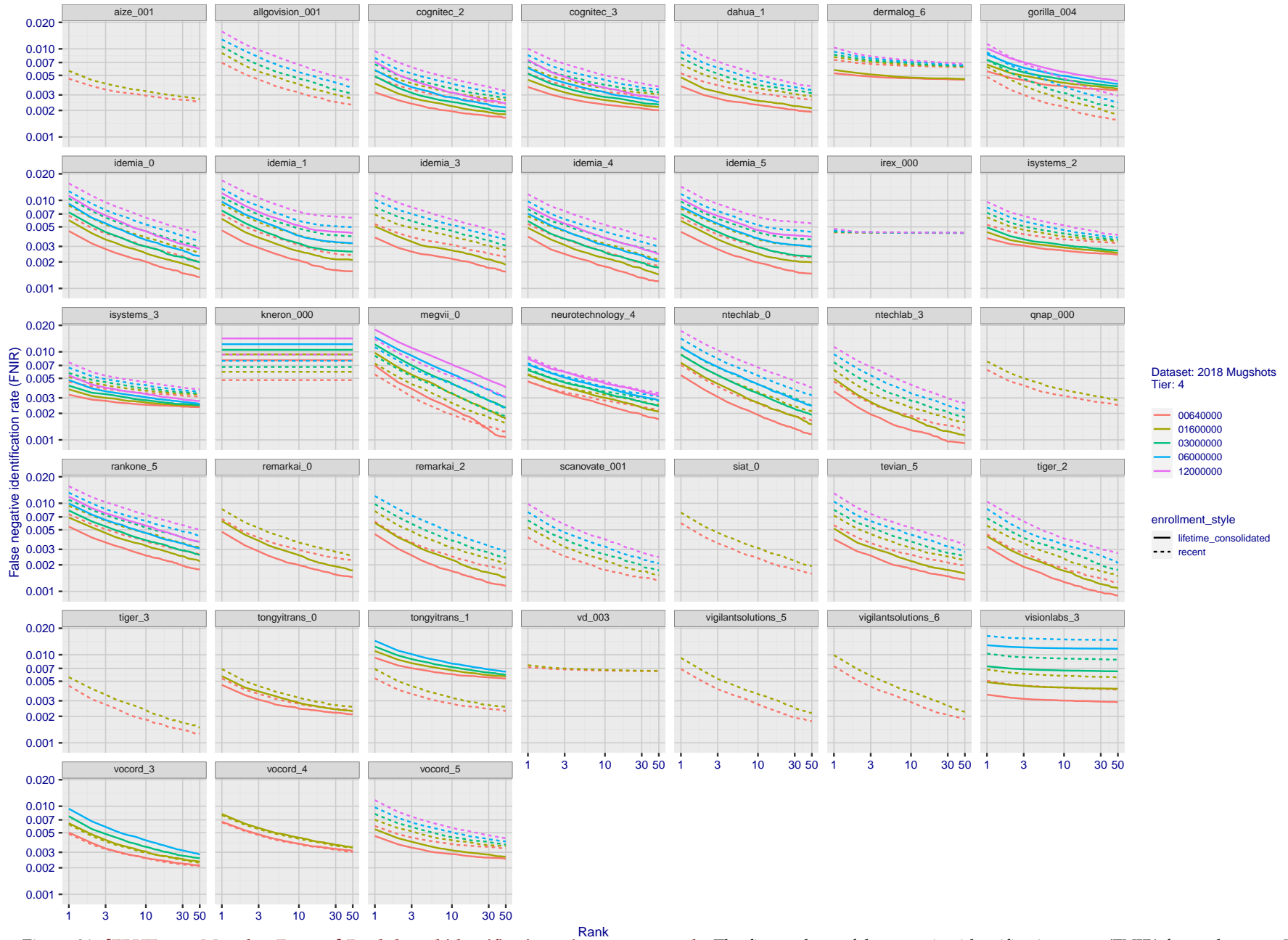


Figure 31: [FRVT-2018 Mugshot Dataset] Rank-based identification miss rates vs. rank. The figure shows false negative identification rates (FNIR) for ranks up to 50. This metric is appropriate to investigational applications where human reviewers will adjudicate sorted candidate lists. Note that with threshold set to zero, FPIR = 1, i.e. any search without an enrolled mate will return non-mated candidates. Results are sorted and reported into tiers for clarity, with the tiering criteria being rank 1 hit rate on a gallery size of  $N = 640\,000$  subjects.

2021/10/28  
13:44:33

FNIR(N, R, T) =  
FPIR(N, T) =

False neg. identification rate  
False pos. identification rate

N = Num. enrolled subjects  
R = Num. candidates examined

T = Threshold

T = 0 → Investigation  
T > 0 → Identification

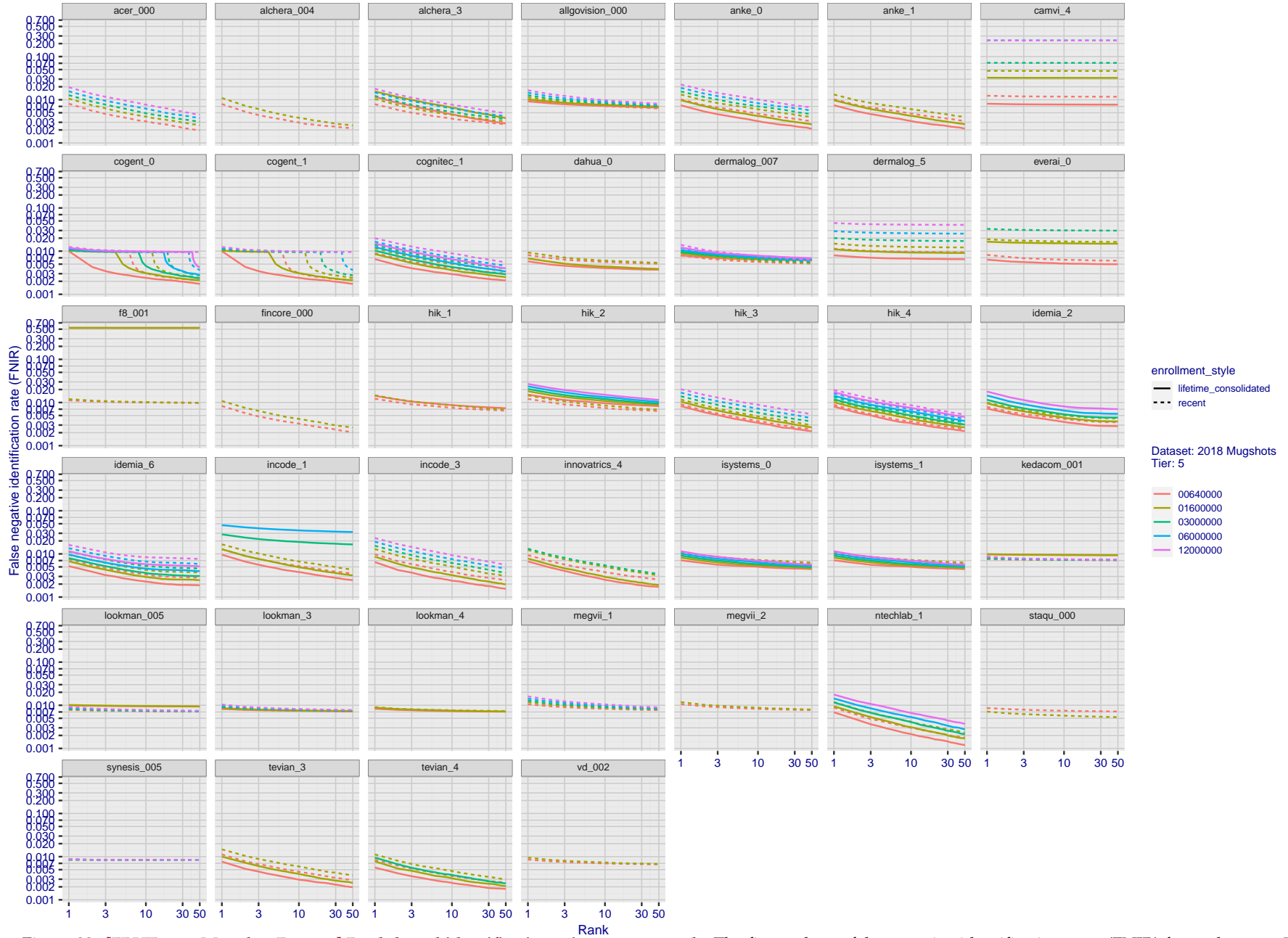


Figure 32: [FRVT-2018 Mugshot Dataset] Rank-based identification miss rates vs. rank. The figure shows false negative identification rates (FNIR) for ranks up to 50. This metric is appropriate to investigational applications where human reviewers will adjudicate sorted candidate lists. Note that with threshold set to zero, FPIR = 1, i.e. any search without an enrolled mate will return non-mated candidates. Results are sorted and reported into tiers for clarity, with the tiering criteria being rank 1 hit rate on a gallery size of  $N = 640\,000$  subjects.

2021/10/28  
 FNIR(N, R, T) =  
 FP(R, T) =  
 False neg. identification rate  
 False pos. identification rate  
 N = Num. enrolled subjects  
 R = Num. candidates examined  
 T = Threshold  
 T = 0 → Investigation  
 T > 0 → Identification

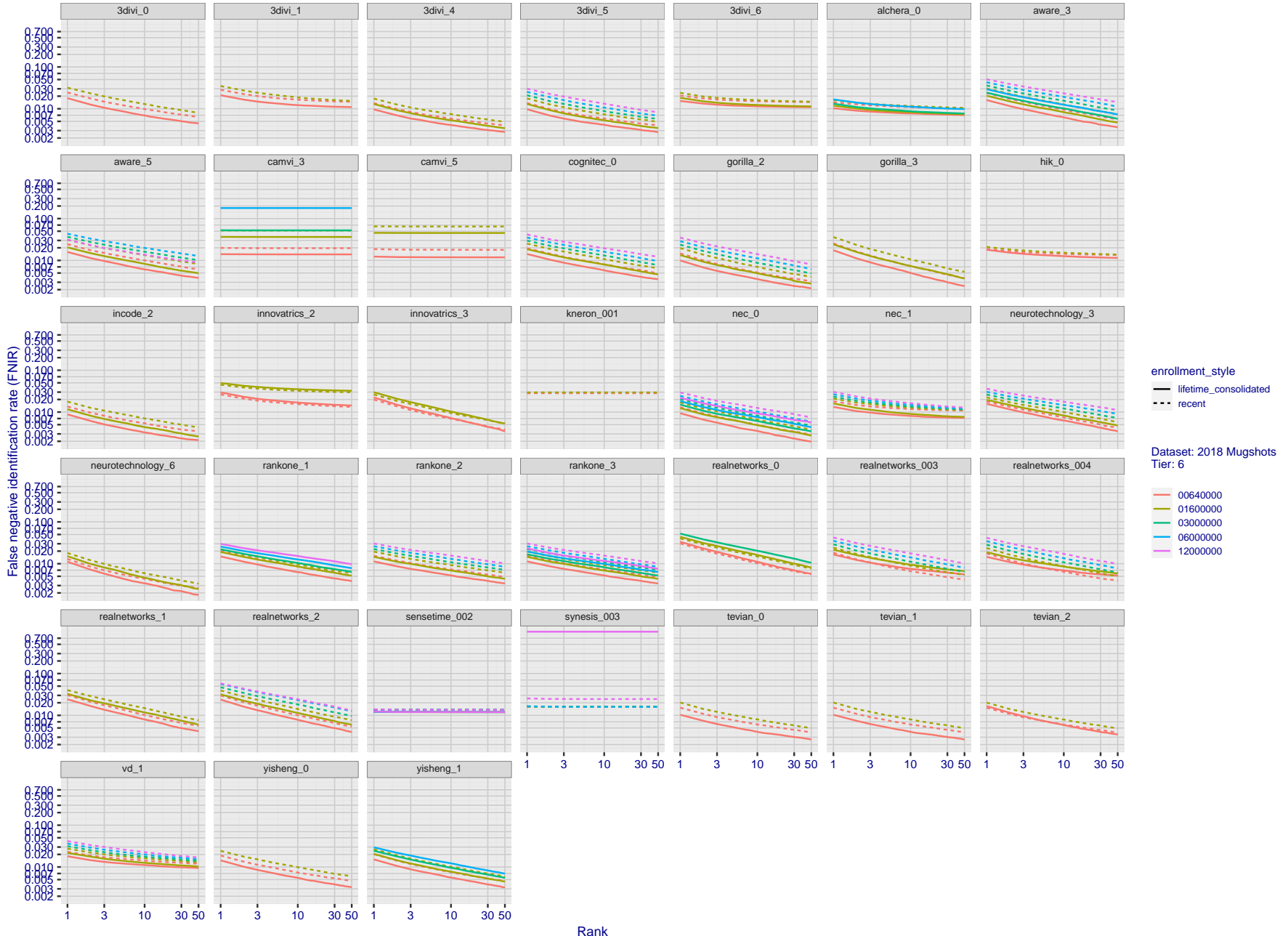


Figure 33: [FRVT-2018 Mugshot Dataset] Rank-based identification miss rates vs. rank. The figure shows false negative identification rates (FNIR) for ranks up to 50. This metric is appropriate to investigational applications where human reviewers will adjudicate sorted candidate lists. Note that with threshold set to zero, FPIR = 1, i.e. any search without an enrolled mate will return non-mated candidates. Results are sorted and reported into tiers for clarity, with the tiering criteria being rank 1 hit rate on a gallery size of  $N = 640\,000$  subjects.

2021/10/28  
 FNIR(N, R, T) =  
 FP(R(N, T) =  
 False neg. identification rate  
 False pos. identification rate  
 N = Num. enrolled subjects  
 R = Num. candidates examined  
 T = Threshold  
 T = 0 → Investigation  
 T > 0 → Identification

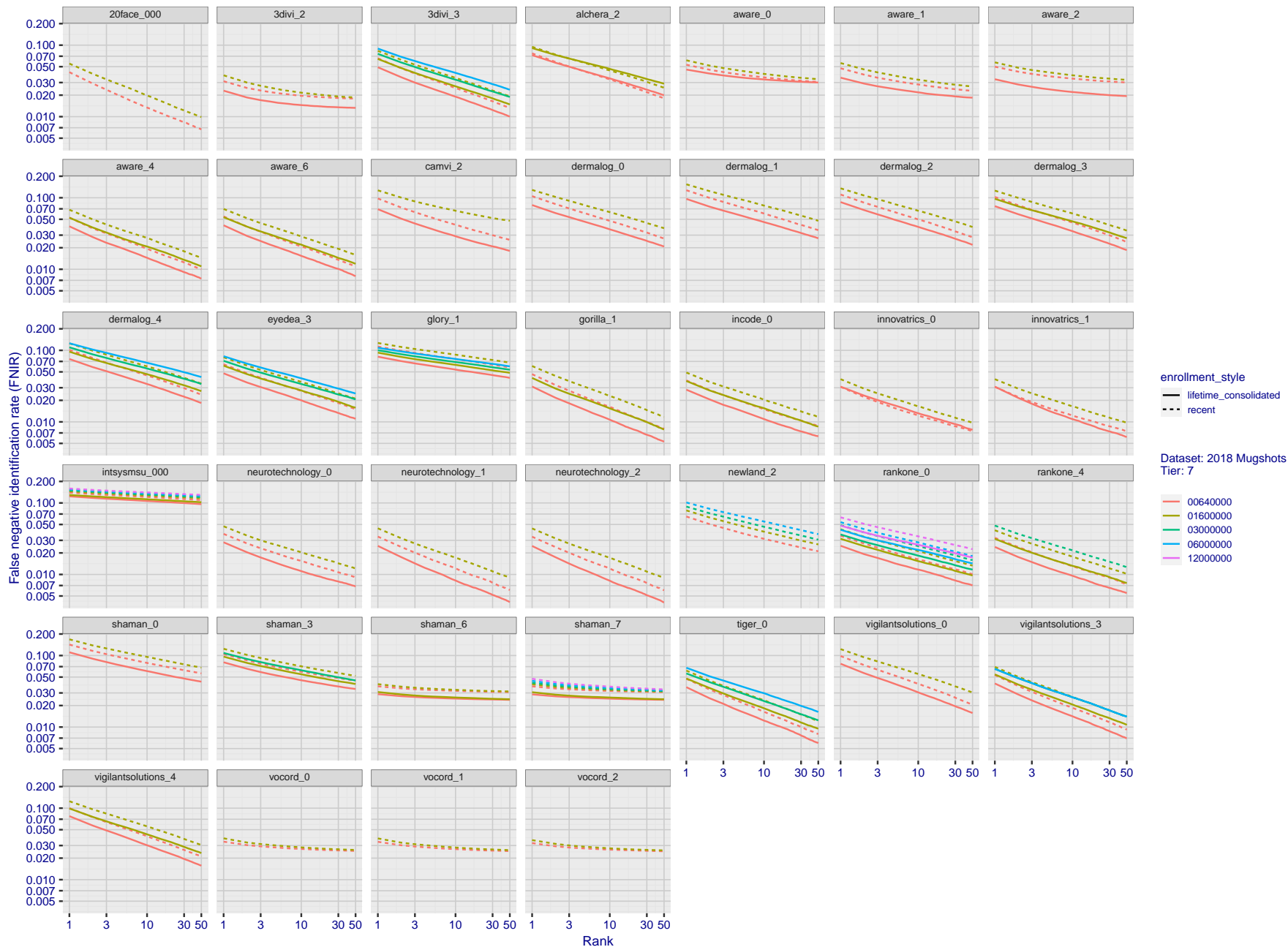


Figure 34: [FRVT-2018 Mugshot Dataset] Rank-based identification miss rates vs. rank. The figure shows false negative identification rates (FNIR) for ranks up to 50. This metric is appropriate to investigational applications where human reviewers will adjudicate sorted candidate lists. Note that with threshold set to zero, FPIR = 1, i.e. any search without an enrolled mate will return non-mated candidates. Results are sorted and reported into tiers for clarity, with the tiering criteria being rank 1 hit rate on a gallery size of  $N = 640\,000$  subjects.

2021/10/28  
 FNIR(N, R, T) =  
 FPR(N, T) =  
 False neg. identification rate  
 False pos. identification rate  
 N = Num. enrolled subjects  
 R = Num. candidates examined  
 T = Threshold  
 T = 0 → Investigation  
 T > 0 → Identification

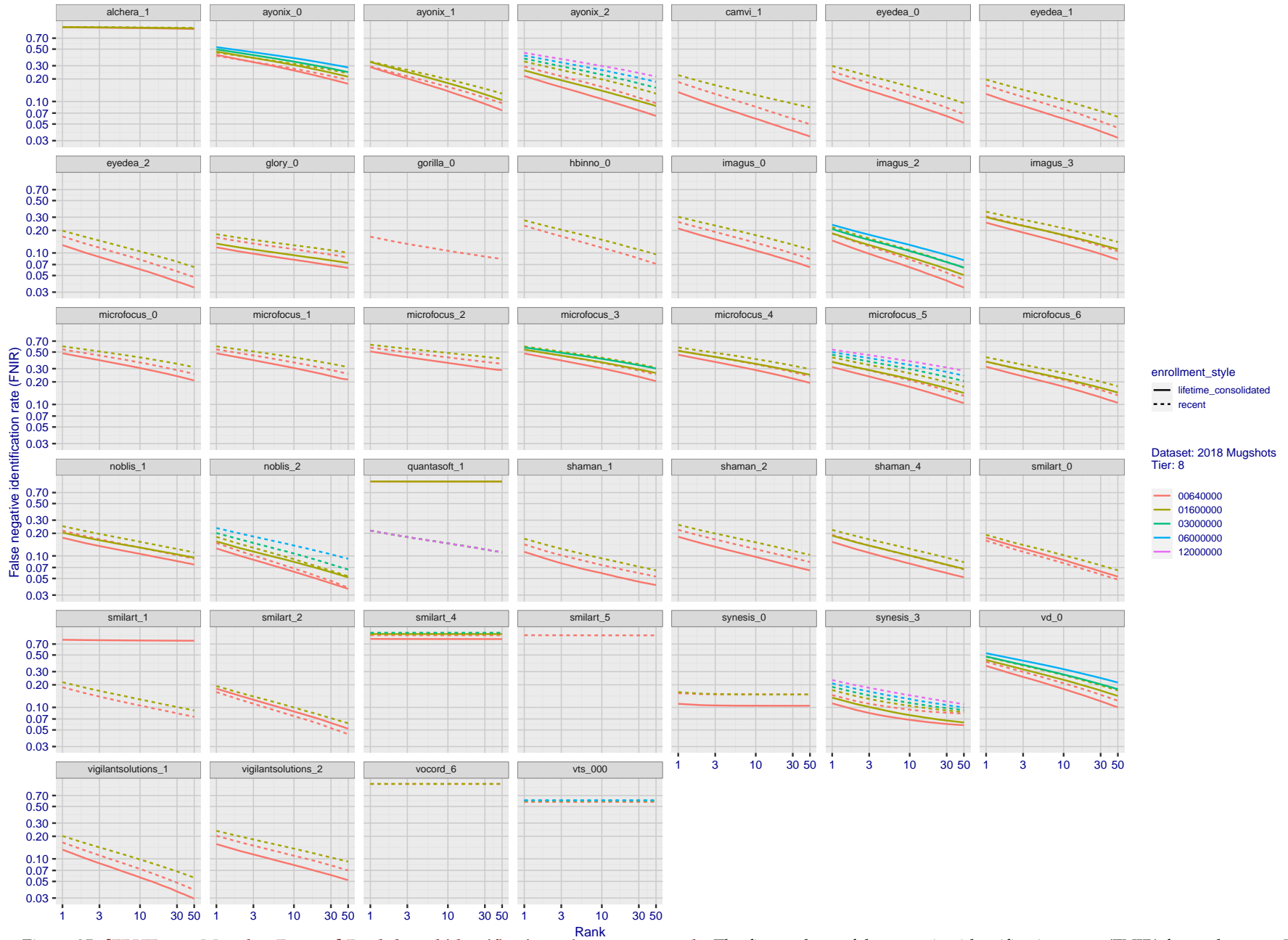


Figure 35: [FRVT-2018 Mugshot Dataset] Rank-based identification miss rates vs. rank. The figure shows false negative identification rates (FNIR) for ranks up to 50. This metric is appropriate to investigational applications where human reviewers will adjudicate sorted candidate lists. Note that with threshold set to zero, FPIR = 1, i.e. any search without an enrolled mate will return non-mated candidates. Results are sorted and reported into tiers for clarity, with the tiering criteria being rank 1 hit rate on a gallery size of  $N = 640\,000$  subjects.

---

2021/10/28 FNIR(N, R, T) = False neg. identification rate N = Num. enrolled subjects T = Threshold T = 0 → Investigation  
13:44:33 FPIR(N, T) = False pos. identification rate R = Num. candidates examined T > 0 → Identification

2021/10/28  
13:44:33

FNIR(N, T) =  
FPIR(N, T) =

False neg. identification rate  
False pos. identification rate

N = Num. enrolled subjects  
R = Num. candidates examined

T = Threshold

T = 0 → Investigation  
T > 0 → Identification

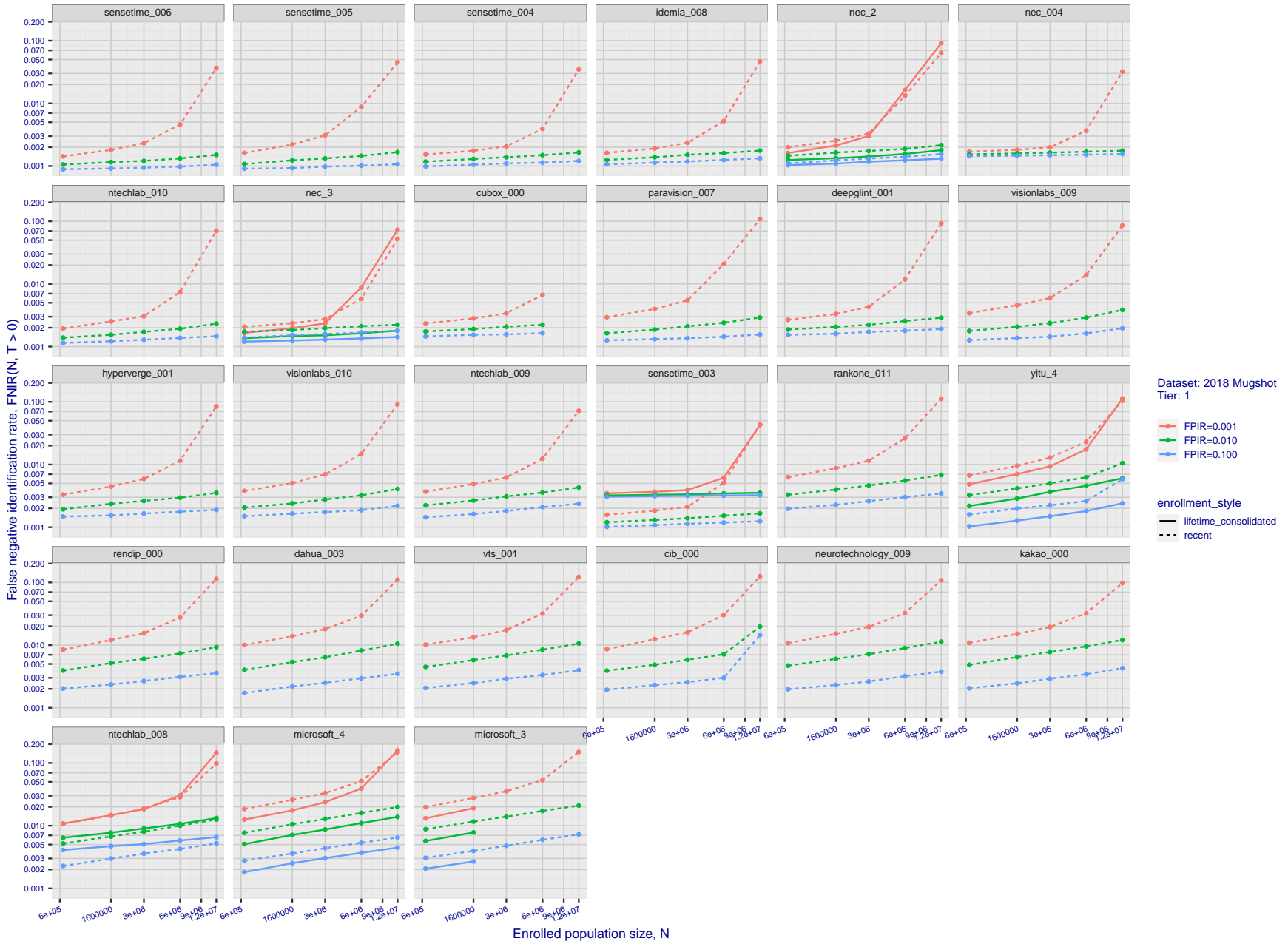


Figure 36: [FRVT-2018 Mugshot Dataset] Threshold-based identification miss rates vs. number of enrolled subjects. The figure shows FNIR(N, T) across various gallery sizes when the threshold is set to achieve the given FPIRs. The rank criterion is irrelevant at high thresholds as mates are always at rank 1. The results are computed from the trials listed in rows 1-10 of Table 1. Less accurate algorithms were not run on large N, so results are missing. For clarity, results are sorted and reported into tiers spanning multiple pages. The tiering criteria is complicated: First paging by FNIR(N<sub>b</sub>, 1, 0), then sorting by median FNIR(N<sub>b</sub>, T), N<sub>b</sub> = 640 000.

2021/10/28  
13:44:33

FNIR(N, T) =  
FPR(N, T) =

False neg. identification rate  
False pos. identification rate

N = Num. enrolled subjects  
R = Num. candidates examined

T = Threshold

T > 0 → Investigation  
T = 0 → Identification

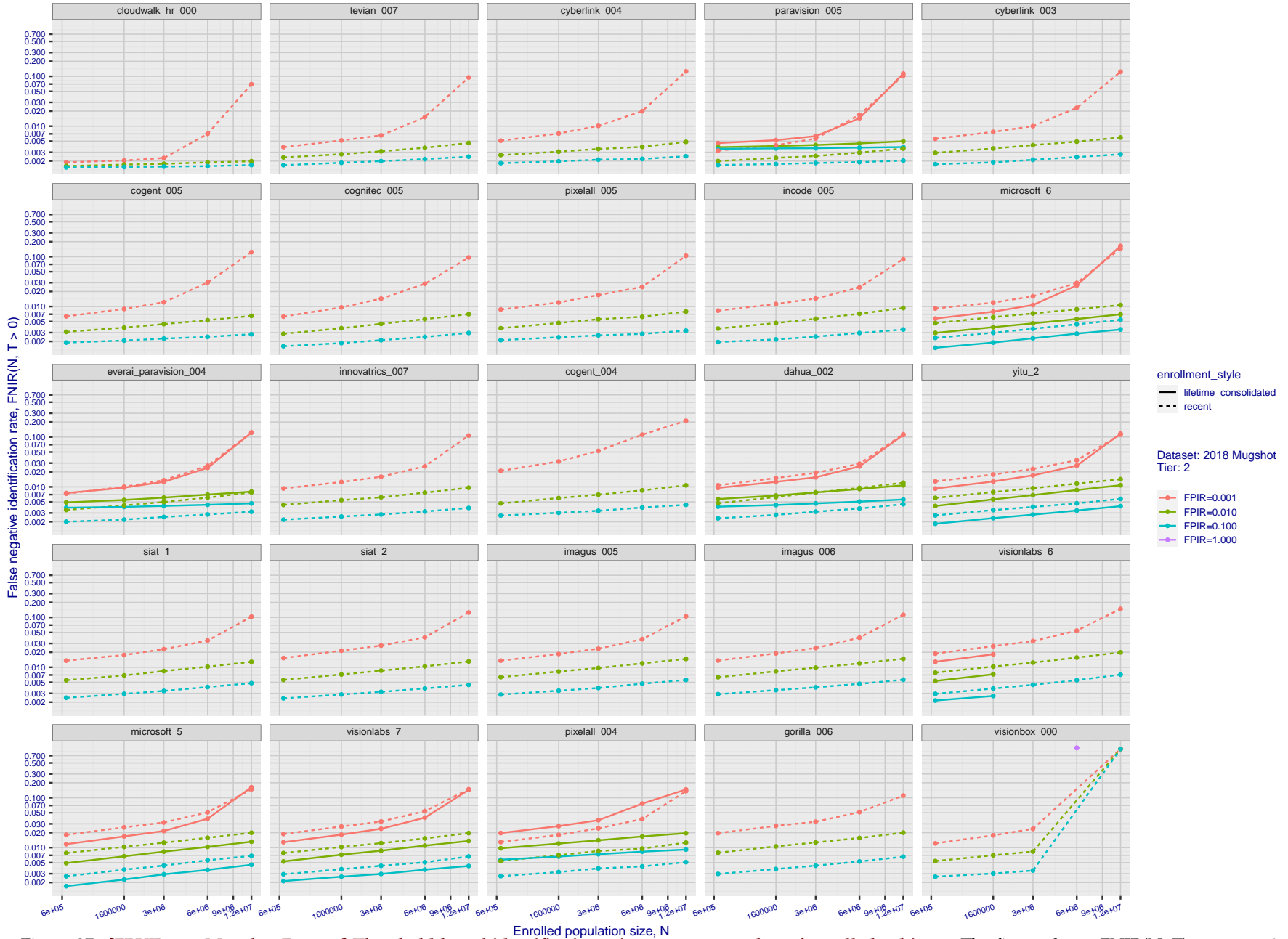


Figure 37: [FRVT-2018 Mugshot Dataset] Threshold-based identification miss rates vs. number of enrolled subjects. The figure shows FNIR(N, T) across various gallery sizes when the threshold is set to achieve the given FPIRs. The rank criterion is irrelevant at high thresholds as mates are always at rank 1. The results are computed from the trials listed in rows 1-10 of Table 1. Less accurate algorithms were not run on large N, so results are missing. For clarity, results are sorted and reported into tiers spanning multiple pages. The tiering criteria is complicated: First paging by FNIR(N<sub>b</sub>, 1, 0), then sorting by median FNIR(N<sub>b</sub>, T), N<sub>b</sub> = 640 000.

2021/10/28  
13:44:33

FNIR(N, T) = False neg. identification rate  
FPIR(N, T) = False pos. identification rate  
N = Num. enrolled subjects  
R = Num. candidates examined

T = Threshold

T = 0 → Investigation  
T > 0 → Identification

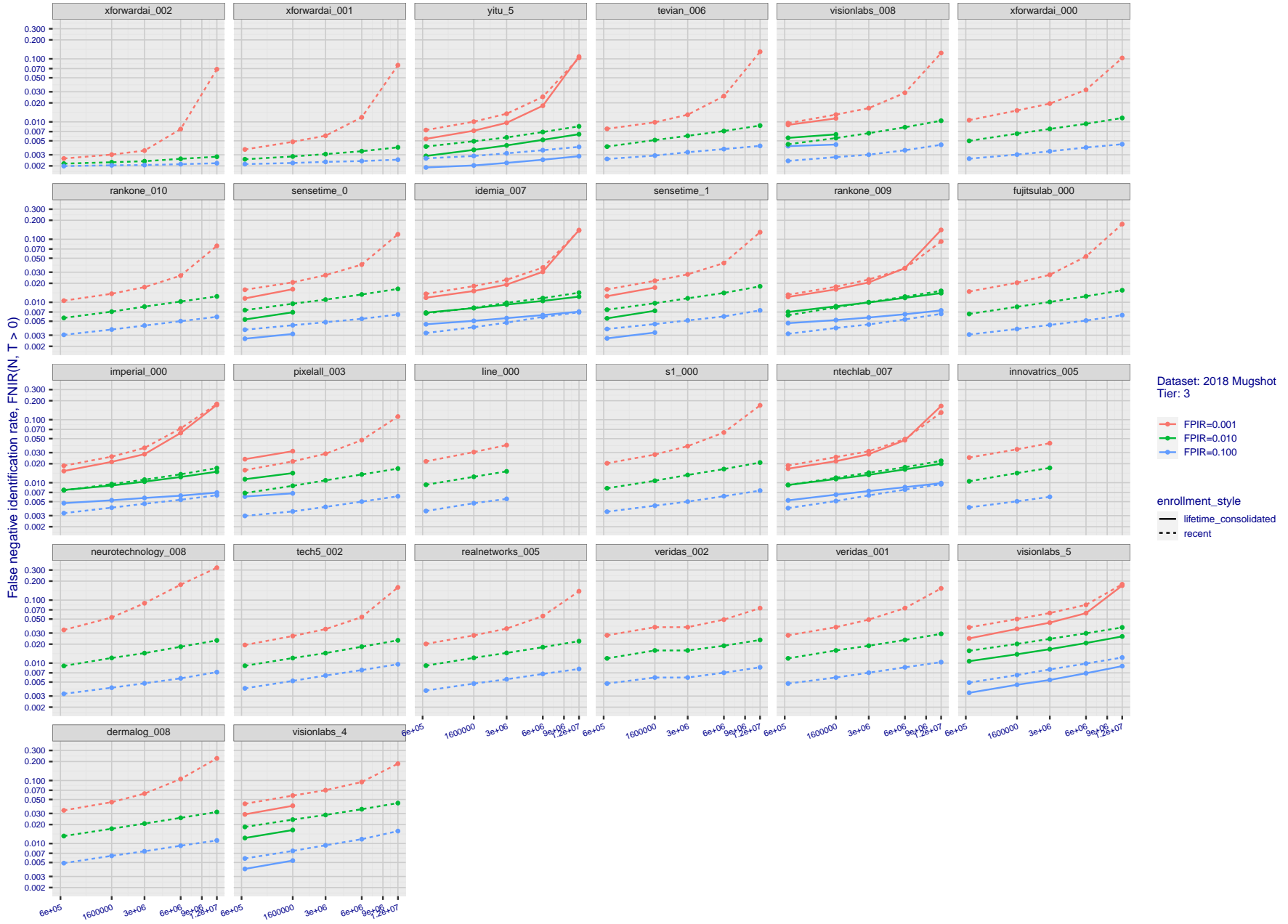


Figure 38: [FRVT-2018 Mugshot Dataset] Threshold-based enrollment miss rates vs. number of enrolled subjects. The figure shows FNIR(N, T) across various gallery sizes when the threshold is set to achieve the given FPIRs. The rank criterion is irrelevant at high thresholds as mates are always at rank 1. The results are computed from the trials listed in rows 1-10 of Table 1. Less accurate algorithms were not run on large N, so results are missing. For clarity, results are sorted and reported into tiers spanning multiple pages. The tiering criteria is complicated: First paging by FNIR(N<sub>b</sub>, 1, 0), then sorting by median FNIR(N<sub>b</sub>, T), N<sub>b</sub> = 640 000.

2021/10/28  
13:44:33

FNIR(N, T) =  
FPNR(N, T) =

False neg. identification rate  
False pos. identification rate

N = Num. enrolled subjects  
R = Num. candidates examined

T = Threshold

T = 0 → Investigation  
T > 0 → Identification

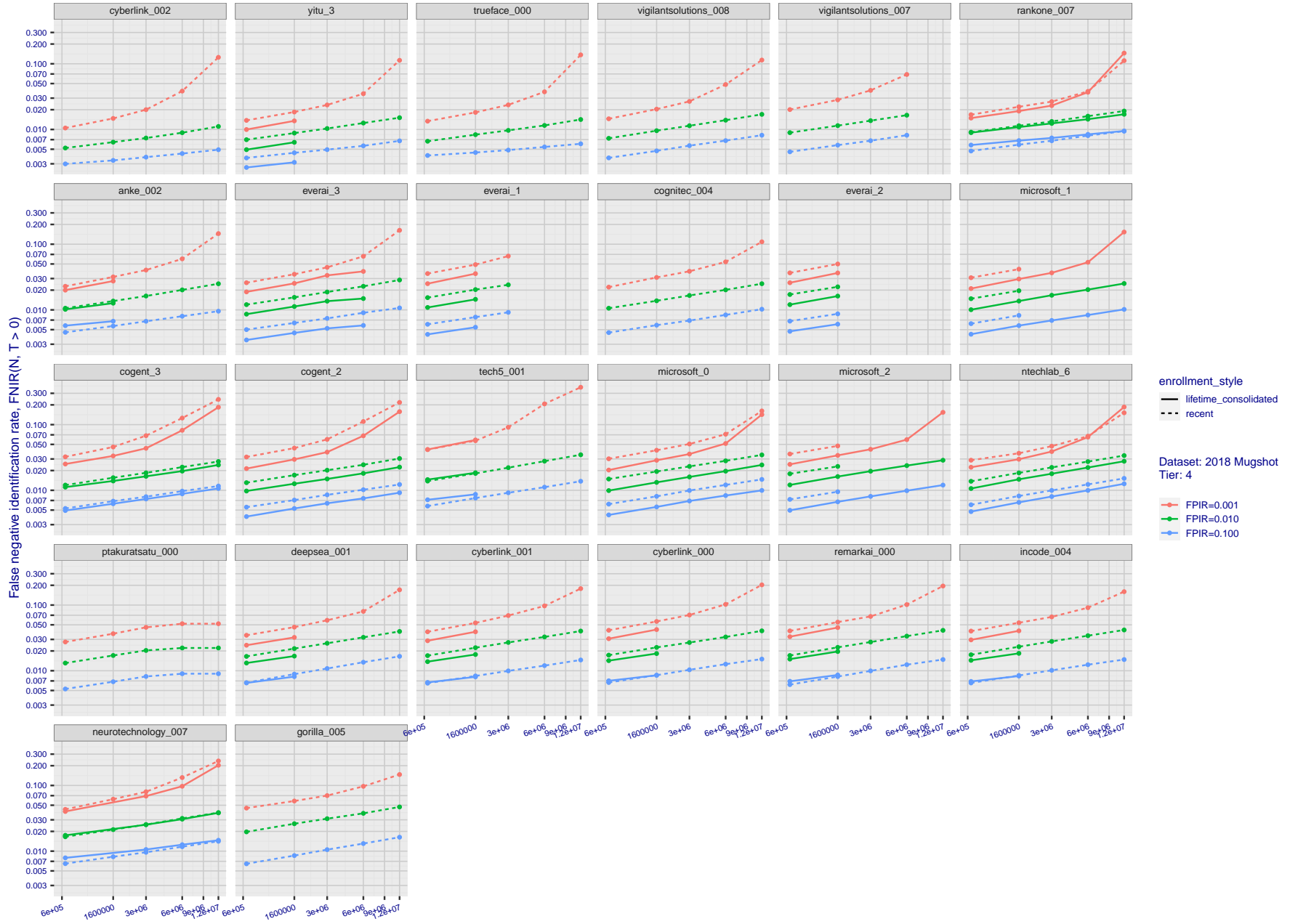


Figure 39: [FRVT-2018 Mugshot Dataset] Threshold-based enrollment miss rates vs. number of enrolled subjects. The figure shows FNIR(N, T) across various gallery sizes when the threshold is set to achieve the given FPIRs. The rank criterion is irrelevant at high thresholds as mates are always at rank 1. The results are computed from the trials listed in rows 1-10 of Table 1. Less accurate algorithms were not run on large N, so results are missing. For clarity, results are sorted and reported into tiers spanning multiple pages. The tiering criteria is complicated: First paging by FNIR(N<sub>b</sub>, 1, 0), then sorting by median FNIR(N<sub>b</sub>, T), N<sub>b</sub> = 640 000.

2021/10/28  
13:44:33

FNIR(N, R, T) =  
FPR(N, T) =

False neg. identification rate  
False pos. identification rate

N = Num. enrolled subjects  
R = Num. candidates examined

T = Threshold

T = 0 → Investigation  
T > 0 → Identification

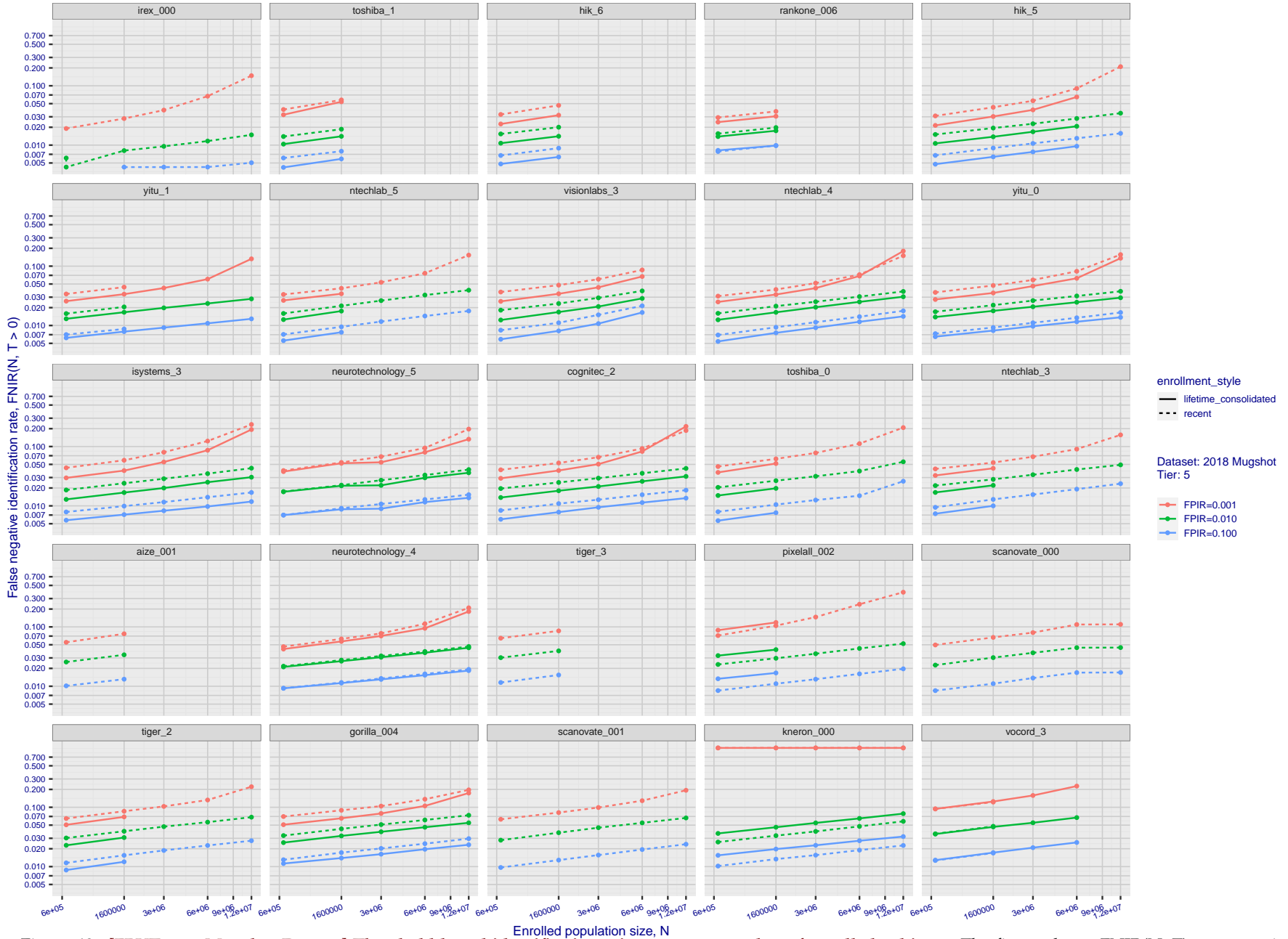


Figure 40: [FRVT-2018 Mugshot Dataset] Threshold-based identification miss rates vs. number of enrolled subjects. The figure shows FNIR(N, T) across various gallery sizes when the threshold is set to achieve the given FPIRs. The rank criterion is irrelevant at high thresholds as mates are always at rank 1. The results are computed from the trials listed in rows 1-10 of Table 1. Less accurate algorithms were not run on large N, so results are missing. For clarity, results are sorted and reported into tiers spanning multiple pages. The tiering criteria is complicated: First paging by FNIR(N<sub>b</sub>, 1, 0), then sorting by median FNIR(N<sub>b</sub>, T), N<sub>b</sub> = 640 000.

2021/10/28  
13:44:33

FNIR(N, R, T) =  
FPR(N, T) =

False neg. identification rate  
False pos. identification rate

N = Num. enrolled subjects  
R = Num. candidates examined

T = Threshold

T = 0 → Investigation  
T > 0 → Identification

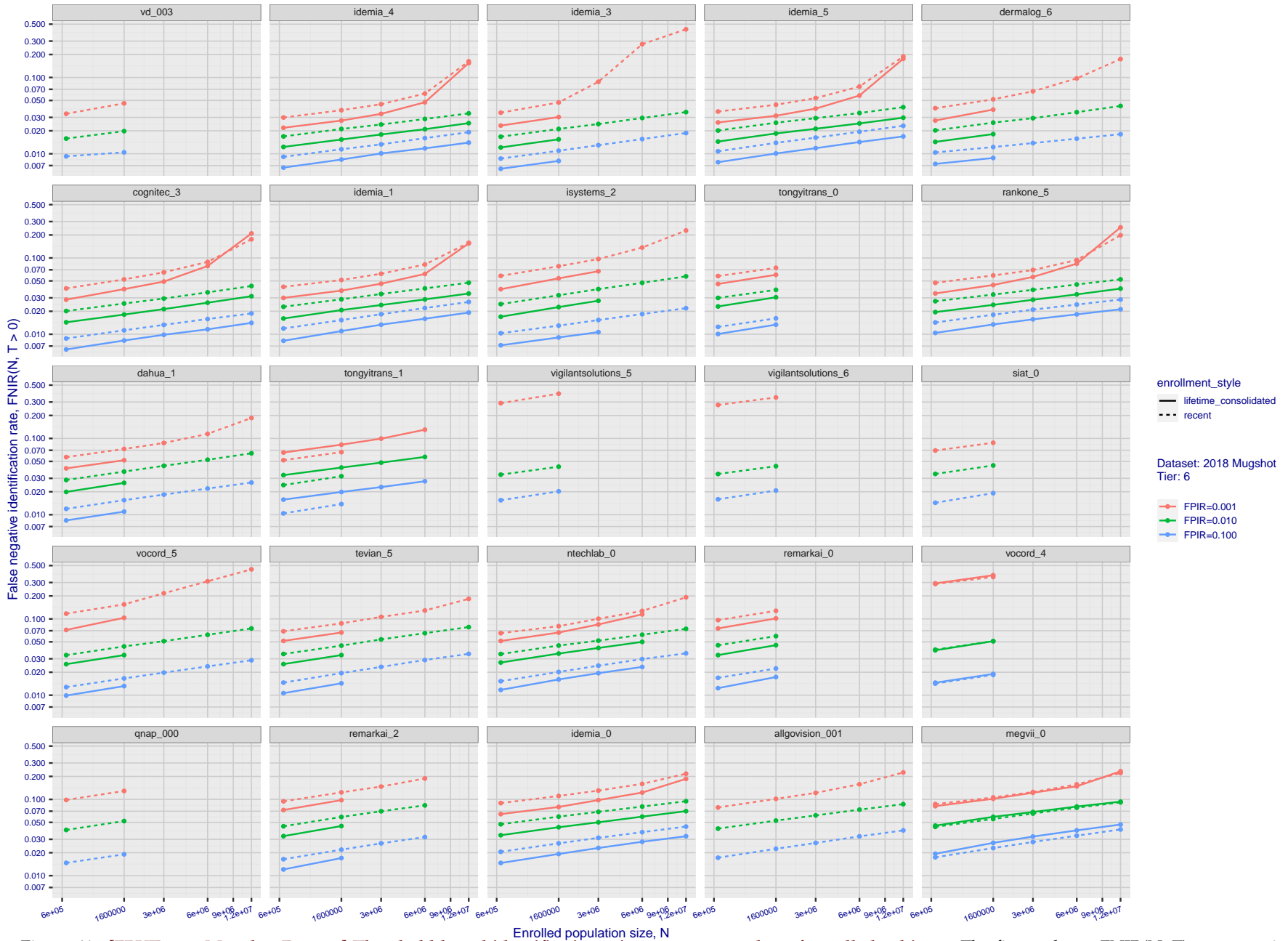


Figure 41: [FRVT-2018 Mugshot Dataset] Threshold-based identification miss rates vs. number of enrolled subjects. The figure shows FNIR(N, T) across various gallery sizes when the threshold is set to achieve the given FPIRs. The rank criterion is irrelevant at high thresholds as mates are always at rank 1. The results are computed from the trials listed in rows 1-10 of Table 1. Less accurate algorithms were not run on large N, so results are missing. For clarity, results are sorted and reported into tiers spanning multiple pages. The tiering criteria is complicated: First paging by FNIR(N<sub>b</sub>, 1, 0), then sorting by median FNIR(N<sub>b</sub>, T), N<sub>b</sub> = 640 000.

2021/10/28  
13:44:33

FNIR(N, T) =  
FPR(N, T) =

False neg. identification rate  
False pos. identification rate

N = Num. enrolled subjects  
R = Num. candidates examined

T = Threshold

T = 0 → Investigation  
T > 0 → Identification

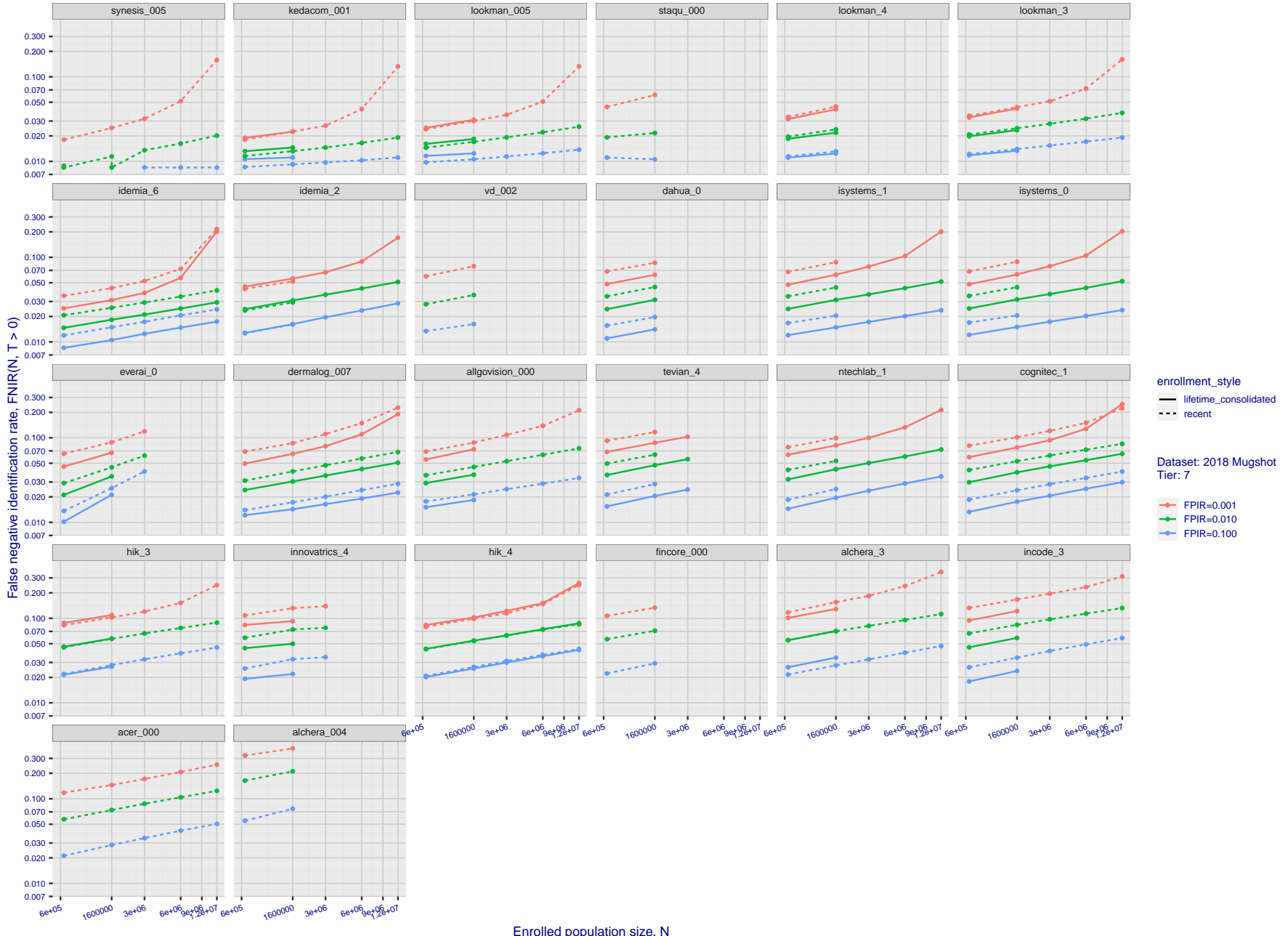


Figure 42: [FRVT-2018 Mugshot Dataset] Threshold-based identification miss rates vs. number of enrolled subjects. The figure shows  $FNIR(N, T)$  across various gallery sizes when the threshold is set to achieve the given FPIRs. The rank criterion is irrelevant at high thresholds as mates are always at rank 1. The results are computed from the trials listed in rows 1-10 of Table 1. Less accurate algorithms were not run on large  $N$ , so results are missing. For clarity, results are sorted and reported into tiers spanning multiple pages. The tiering criteria is complicated: First paging by  $FNIR(N_b, 1, 0)$ , then sorting by median  $FNIR(N_b, T)$ ,  $N_b = 640\,000$ .

2021/10/28  
13:44:33

FNIR(N, R, T) =  
FPIR(N, T) =

False neg. identification rate  
False pos. identification rate

N = Num. enrolled subjects  
R = Num. candidates examined

T = Threshold

T = 0 → Investigation  
T > 0 → Identification

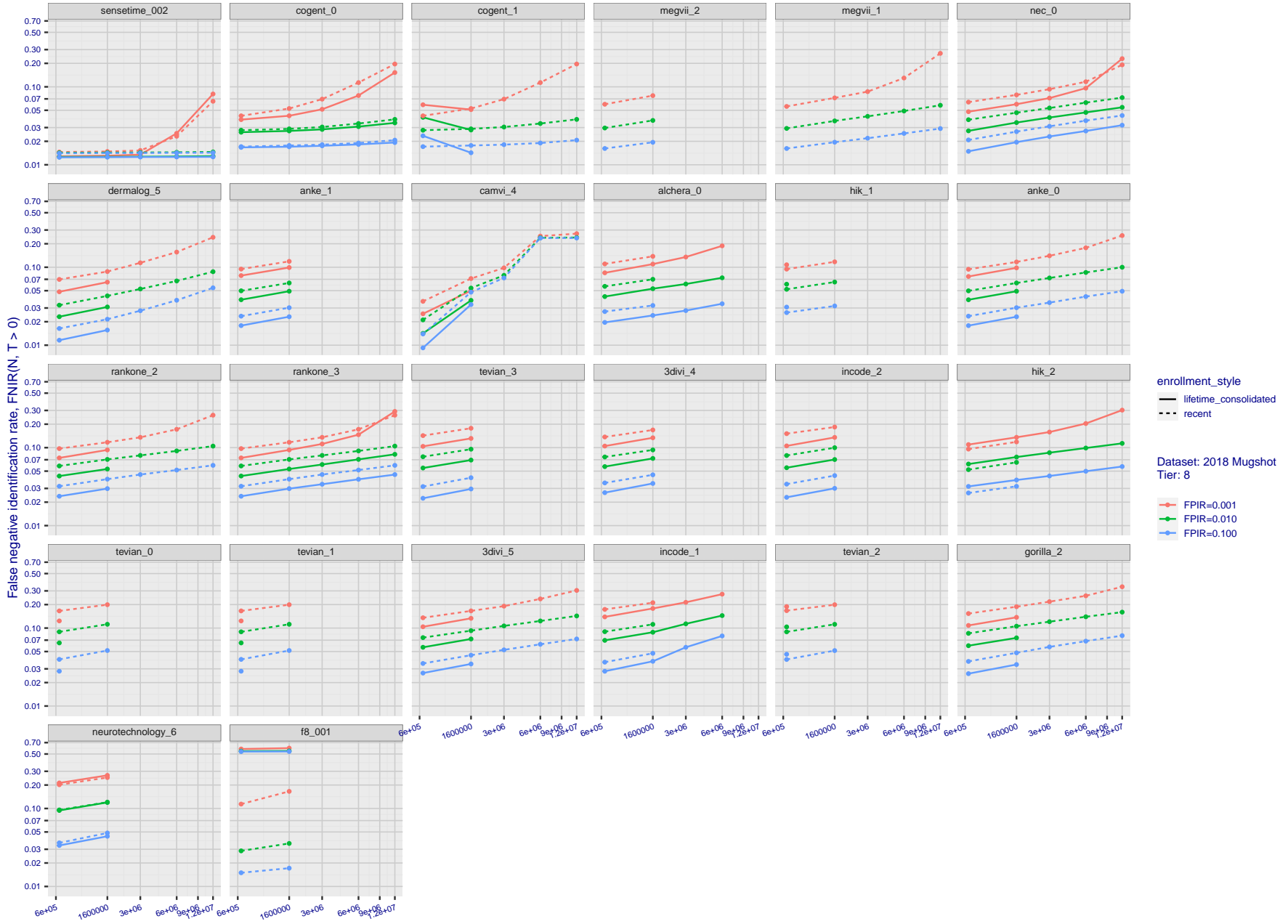


Figure 43: [FRVT-2018 Mugshot Dataset] Threshold-based identification miss rates vs. number of enrolled subjects. The figure shows  $FNIR(N, T)$  across various gallery sizes when the threshold is set to achieve the given FPIRs. The rank criterion is irrelevant at high thresholds as mates are always at rank 1. The results are computed from the trials listed in rows 1-10 of Table 1. Less accurate algorithms were not run on large  $N$ , so results are missing. For clarity, results are sorted and reported into tiers spanning multiple pages. The tiering criteria is complicated: First paging by  $FNIR(N_b, 1, 0)$ , then sorting by median  $FNIR(N_b, T)$ ,  $N_b = 640\,000$ .

2021/10/28  
13:44:33

FNIR(N, R, T) =  
FPNR(N, T) =

False neg. identification rate  
False pos. identification rate

N = Num. enrolled subjects  
R = Num. candidates examined

T = Threshold

T = 0 → Investigation  
T > 0 → Identification

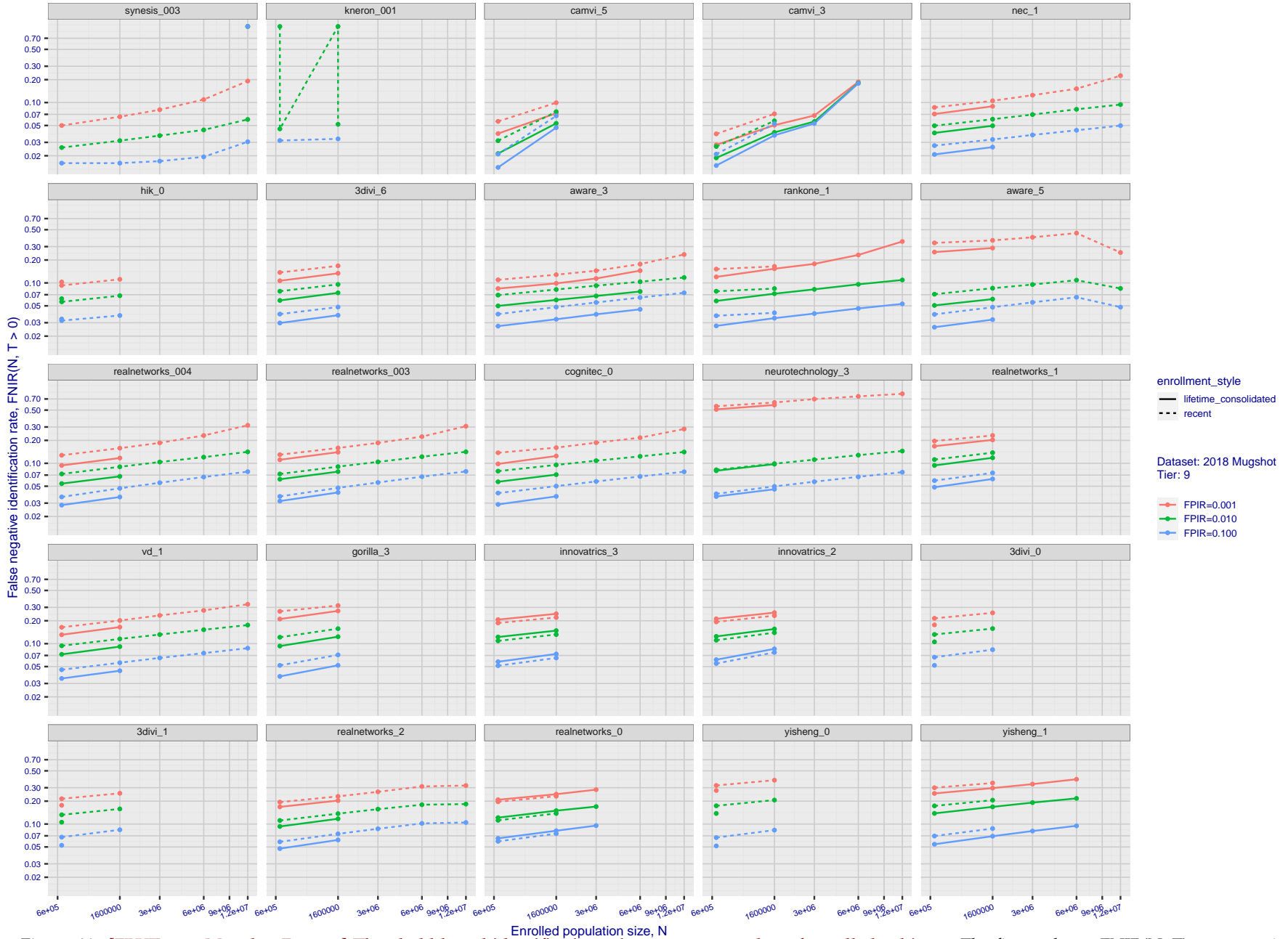


Figure 44: [FRVT-2018 Mugshot Dataset] Threshold-based identification miss rates vs. number of enrolled subjects. The figure shows FNIR(N, T) across various gallery sizes when the threshold is set to achieve the given FPIRs. The rank criterion is irrelevant at high thresholds as mates are always at rank 1. The results are computed from the trials listed in rows 1-10 of Table 1. Less accurate algorithms were not run on large N, so results are missing. For clarity, results are sorted and reported into tiers spanning multiple pages. The tiering criteria is complicated: First paging by FNIR(N<sub>b</sub>, 1, 0), then sorting by median FNIR(N<sub>b</sub>, T), N<sub>b</sub> = 640 000.

2021/10/28  
13:44:33

FNIR(N, R, T) = False neg. identification rate  
FPIR(N, T) = False pos. identification rate  
N = Num. enrolled subjects  
R = Num. candidates examined

T = Threshold

T = 0 → Investigation  
T > 0 → Identification

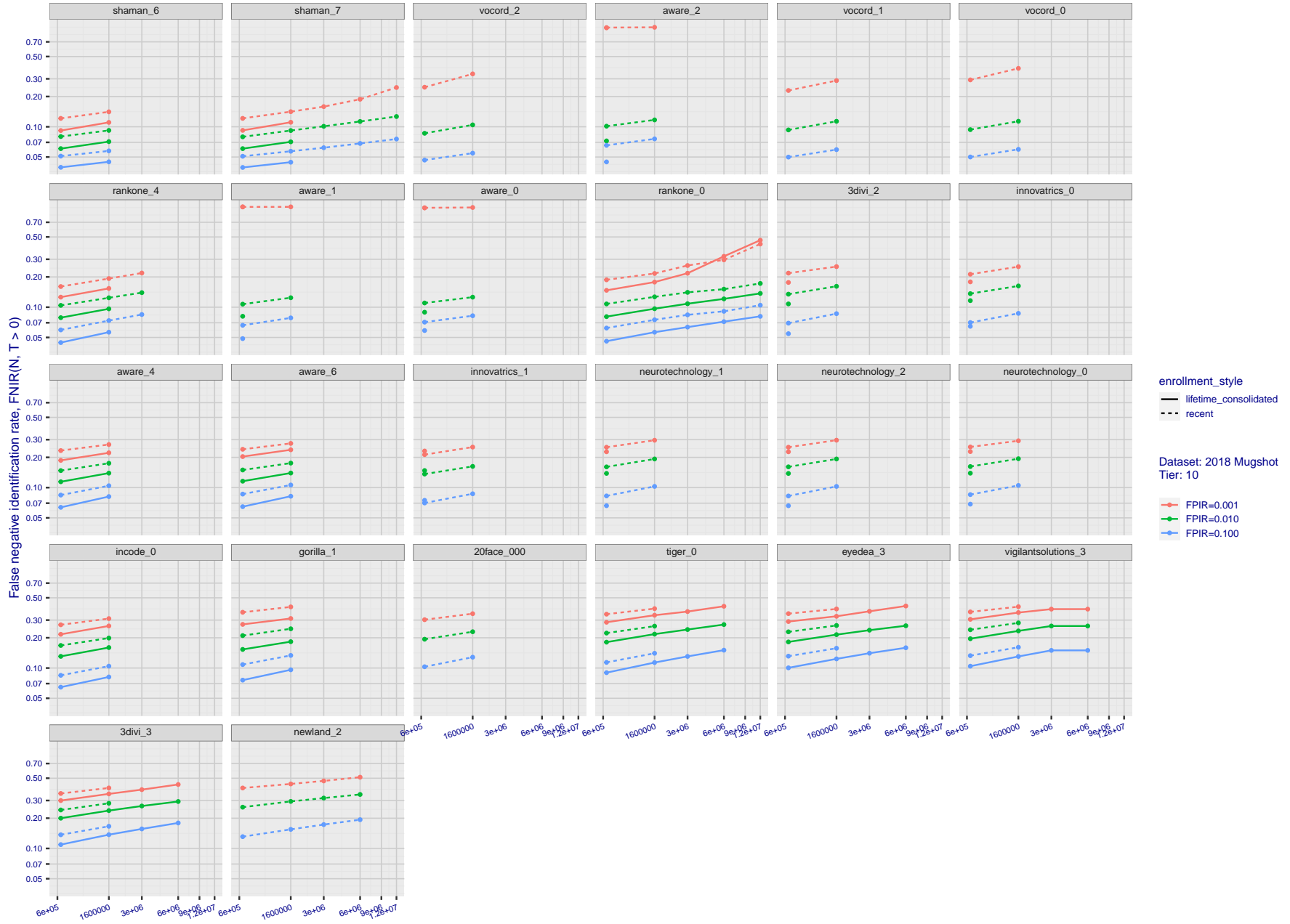


Figure 45: [FRVT-2018 Mugshot Dataset] Threshold-based identification miss rates vs. number of enrolled subjects. The figure shows FNIR(N, T) across various gallery sizes when the threshold is set to achieve the given FPIRs. The rank criterion is irrelevant at high thresholds as mates are always at rank 1. The results are computed from the trials listed in rows 1-10 of Table 1. Less accurate algorithms were not run on large N, so results are missing. For clarity, results are sorted and reported into tiers spanning multiple pages. The tiering criteria is complicated: First paging by FNIR(N<sub>b</sub>, 1, 0), then sorting by median FNIR(N<sub>b</sub>, T), N<sub>b</sub> = 640 000.

2021/10/28  
13:44:33

FNIR(N, R, T) = False neg. identification rate  
FPIR(N, T) = False pos. identification rate  
N = Num. enrolled subjects  
R = Num. candidates examined

T = Threshold

T = 0 → Investigation  
T > 0 → Identification

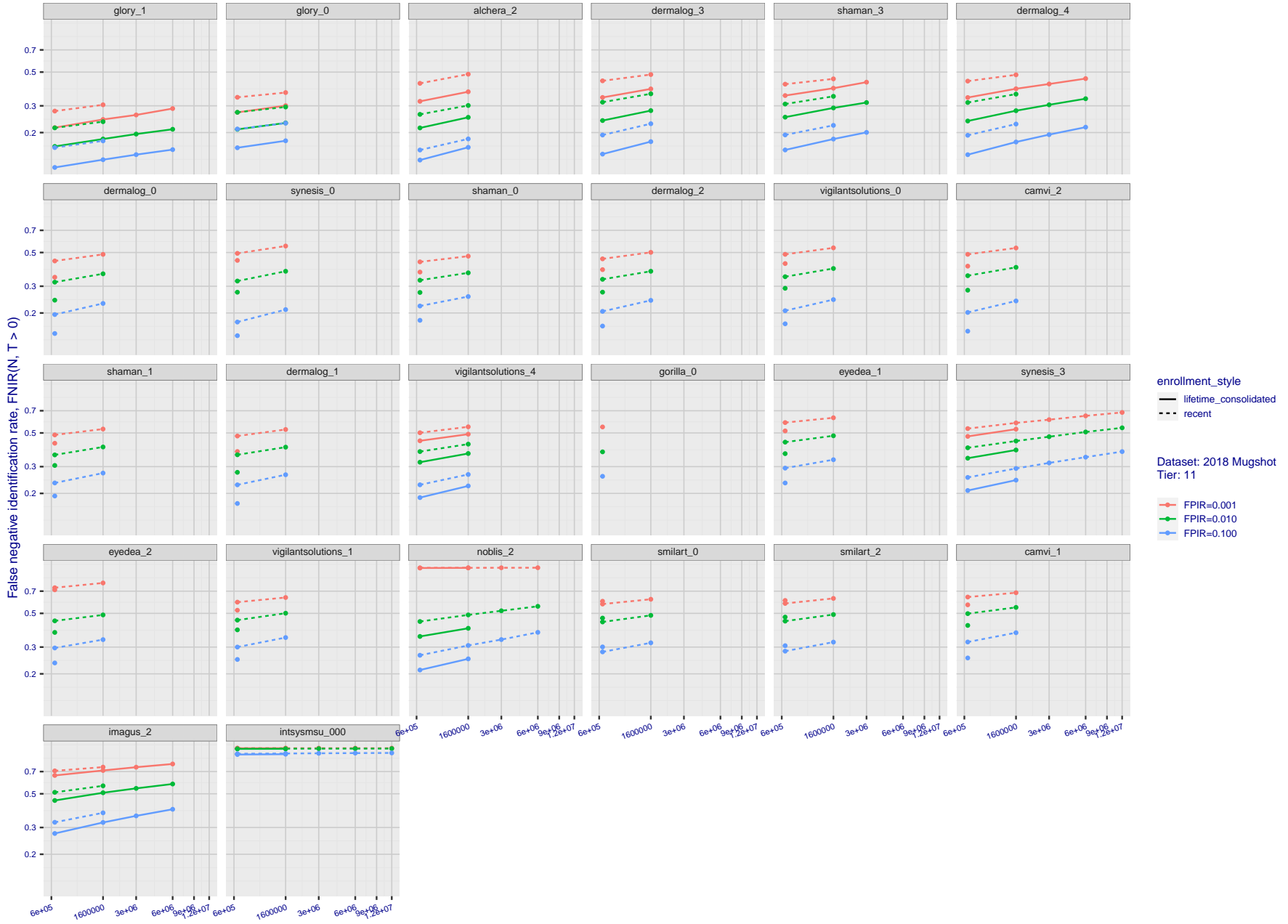


Figure 46: [FRVT-2018 Mugshot Dataset] Threshold-based identification miss rates vs. number of enrolled subjects. The figure shows FNIR(N, T) across various gallery sizes when the threshold is set to achieve the given FPIRs. The rank criterion is irrelevant at high thresholds as mates are always at rank 1. The results are computed from the trials listed in rows 1-10 of Table 1. Less accurate algorithms were not run on large N, so results are missing. For clarity, results are sorted and reported into tiers spanning multiple pages. The tiering criteria is complicated: First paging by FNIR(N<sub>b</sub>, 1, 0), then sorting by median FNIR(N<sub>b</sub>, T), N<sub>b</sub> = 640 000.

2021/10/28  
13:44:33

FNIR(N, R, T) =  
FPIR(N, T) =

False neg. identification rate  
False pos. identification rate

N = Num. enrolled subjects  
R = Num. candidates examined

T = Threshold

T = 0 → Investigation  
T > 0 → Identification

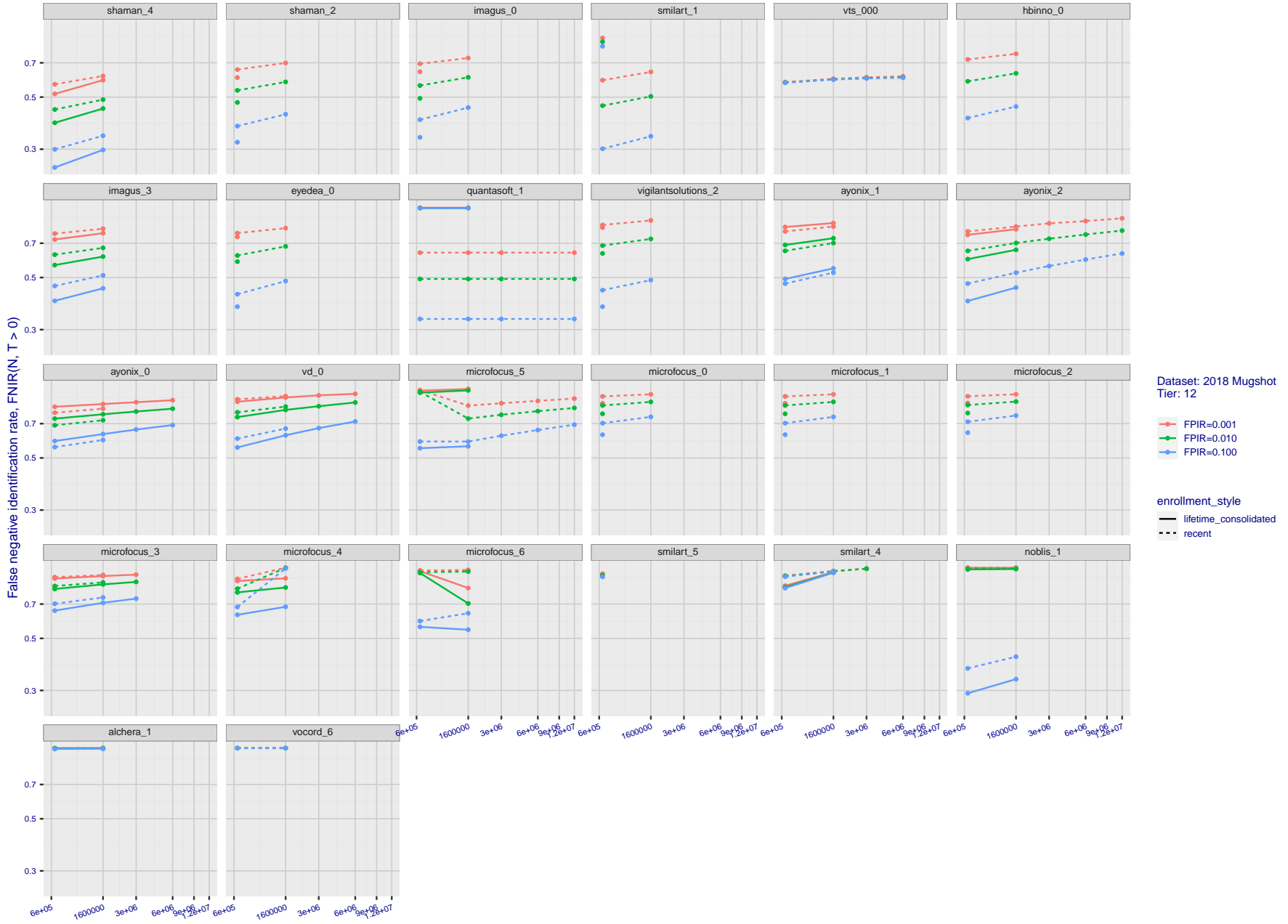


Figure 47: [FRVT-2018 Mugshot Dataset] Threshold-based identification miss rates vs. number of enrolled subjects. The figure shows FNIR(N, T) across various gallery sizes when the threshold is set to achieve the given FPIRs. The rank criterion is irrelevant at high thresholds as mates are always at rank 1. The results are computed from the trials listed in rows 1-10 of Table 1. Less accurate algorithms were not run on large N, so results are missing. For clarity, results are sorted and reported into tiers spanning multiple pages. The tiering criteria is complicated: First paging by FNIR(N<sub>b</sub>, 1, 0), then sorting by median FNIR(N<sub>b</sub>, T), N<sub>b</sub> = 640 000.

---

2021/10/28	FNIR(N, R, T) =	False neg. identification rate	N = Num. enrolled subjects	T = Threshold	T = 0 → Investigation
13:44:33	FPIR(N, T) =	False pos. identification rate	R = Num. candidates examined		T > 0 → Identification

2021/10/28  
13:44:33

FNIR(N, R, T) =  
FPIR(N, T) =

False neg. identification rate  
False pos. identification rate

N = Num. enrolled subjects  
R = Num. candidates examined

T = Threshold

T = 0 → Investigation  
T > 0 → Identification

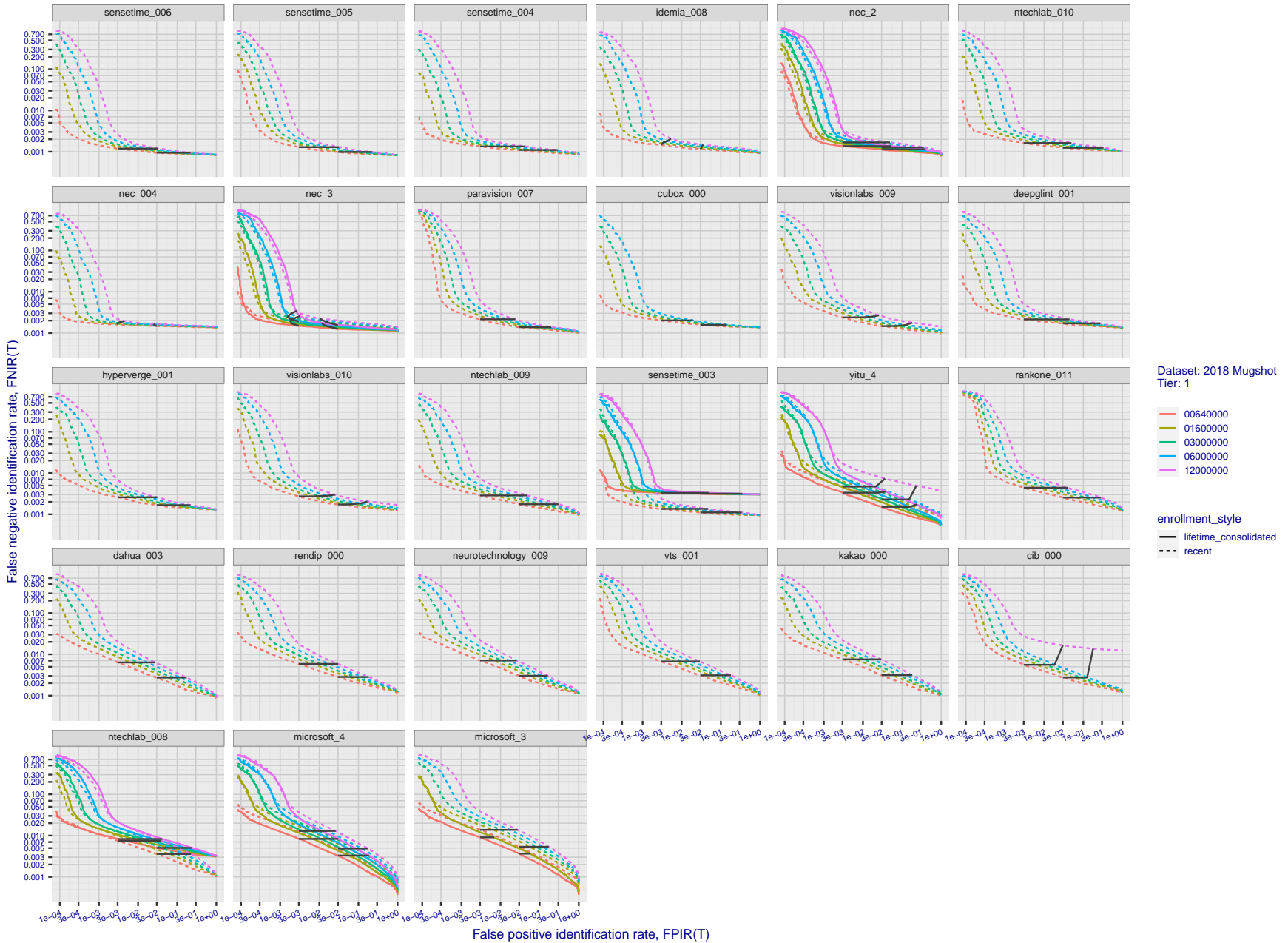


Figure 48: [FRVT-2018 Mugshot Dataset] Identification miss rates vs. false positive rates. The figure shows miss rates  $FNIR(N, L, T)$  as a function of  $FPIR(N, T)$ , with  $N$  ranging from 640 000 to 12 000 000 as noted in rows 1-10 of Table 1. These error tradeoff characteristics are useful for applications where a threshold must be elevated to limit false positives, such as when human reviewer labor is not matched to the volume of searches. Dark lines join points of equal threshold: If horizontal,  $FPIR(T)$  rises with  $N$ , and mate scores are independent of  $N$ . Other algorithms adjust scores in an attempt to make  $FPIR(T)$  independent of  $N$ .

2021/10/28  
13:44:33

FNIR(N, R, T) =  
FPIR(N, T) =

False neg. identification rate  
False pos. identification rate

N = Num. enrolled subjects  
R = Num. candidates examined

T = Threshold

T = 0 → Investigation  
T > 0 → Identification

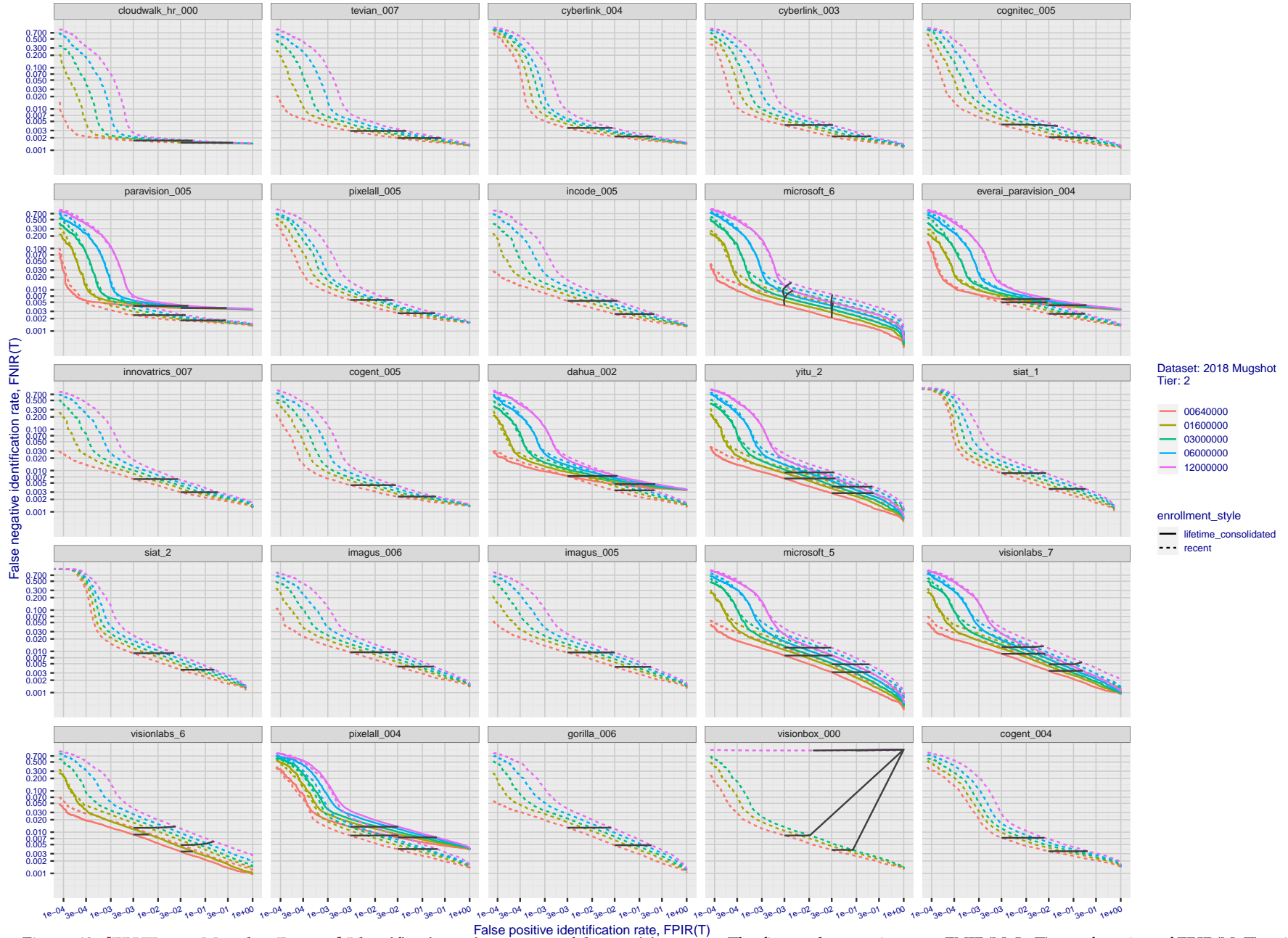


Figure 49: [FRVT-2018 Mugshot Dataset] Identification miss rates vs. false positive rates. The figure shows miss rates  $FNIR(N, L, T)$  as a function of  $FPIR(N, T)$ , with  $N$  ranging from 640 000 to 12 000 000 as noted in rows 1-10 of Table 1. These error tradeoff characteristics are useful for applications where a threshold must be elevated to limit false positives, such as when human reviewer labor is not matched to the volume of searches. Dark lines join points of equal threshold: If horizontal,  $FPIR(N, T)$  rises with  $N$ , and mate scores are independent of  $N$ . Other algorithms adjust scores in an attempt to make  $FPIR$  independent of  $N$ .

2021/10/28  
13:44:33

FNIR(N, R, T) = False neg. identification rate  
FPIR(N, T) = False pos. identification rate  
N = Num. enrolled subjects  
R = Num. candidates examined

T = Threshold

T = 0 → Investigation  
T > 0 → Identification

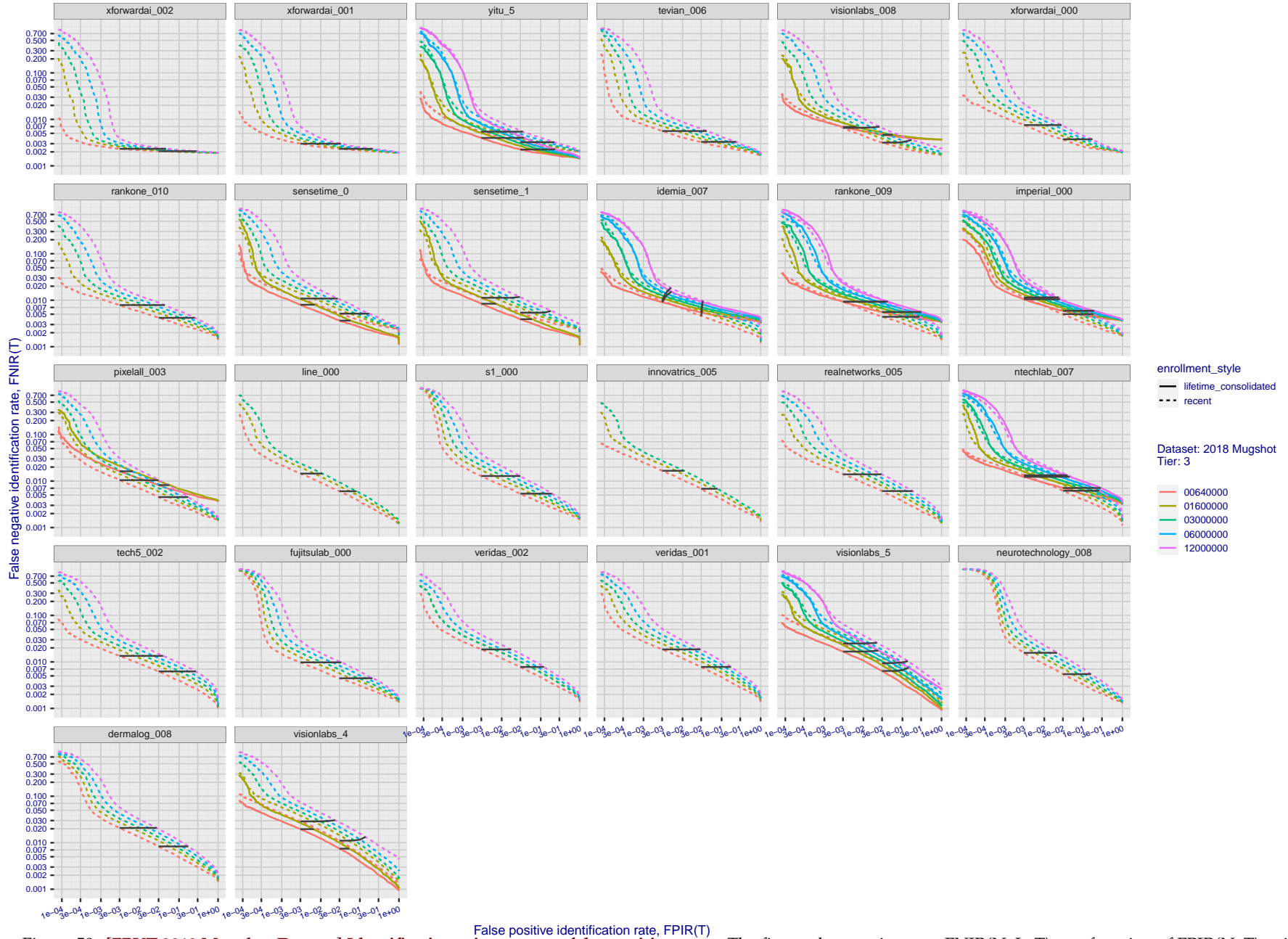


Figure 50: [FRVT-2018 Mugshot Dataset] Identification miss rates vs. false positive rates. The figure shows miss rates  $FNIR(N, L, T)$  as a function of  $FPIR(N, T)$ , with  $N$  ranging from 640 000 to 12 000 000 as noted in rows 1-10 of Table 1. These error tradeoff characteristics are useful for applications where a threshold must be elevated to limit false positives, such as when human reviewer labor is not matched to the volume of searches. Dark lines join points of equal threshold: If horizontal,  $FPIR(T)$  rises with  $N$ , and mate scores are independent of  $N$ . Other algorithms adjust scores in an attempt to make  $FPIR(T)$

2021/10/28  
13:44:33

FNIR(N, R, T) =  
FPIR(N, T) =

False neg. identification rate  
False pos. identification rate

N = Num. enrolled subjects  
R = Num. candidates examined

T = Threshold

T = 0 → Investigation  
T > 0 → Identification

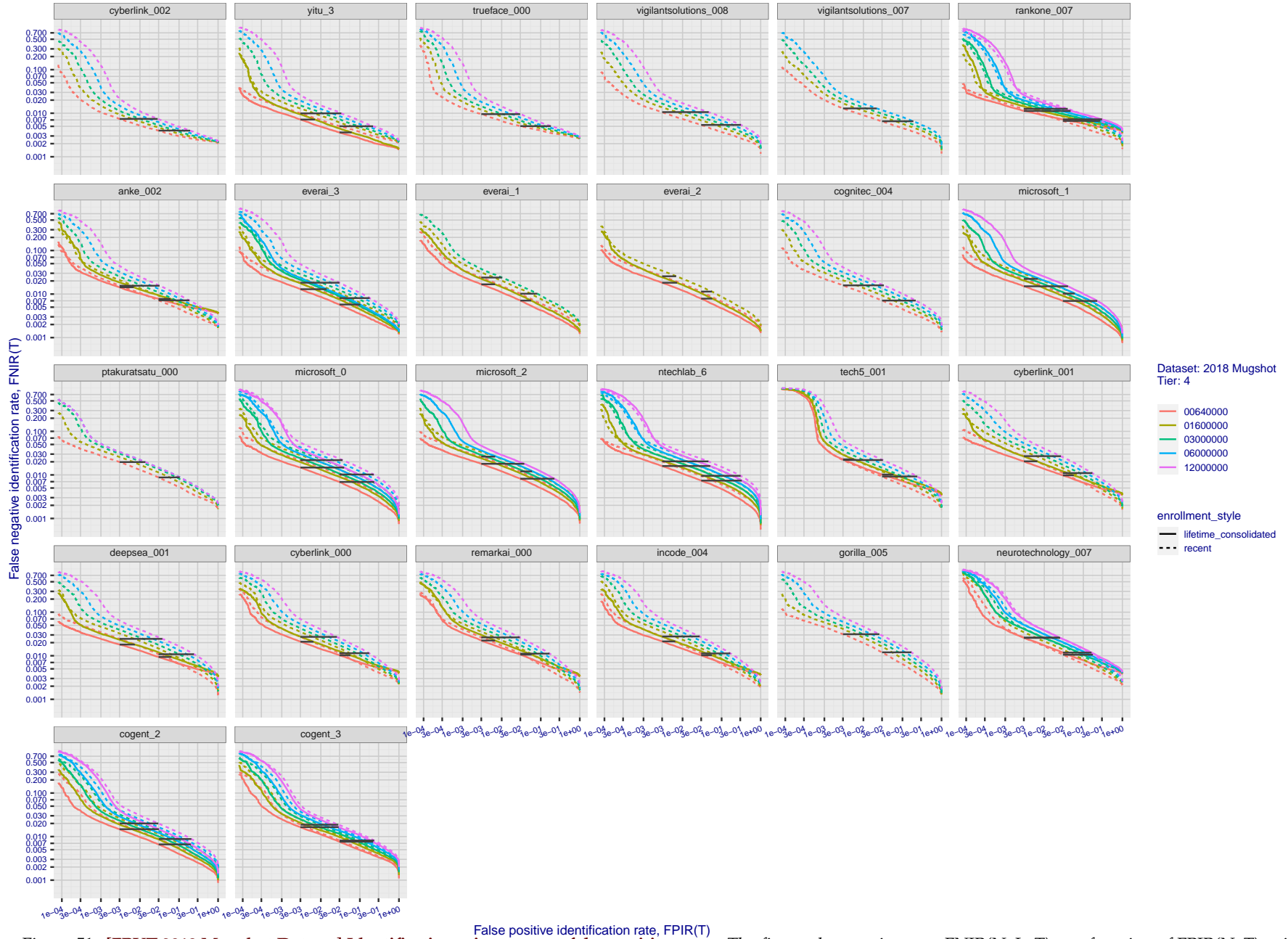


Figure 51: [FRVT-2018 Mugshot Dataset] Identification miss rates vs. false positive rates. The figure shows miss rates  $FNIR(N, L, T)$  as a function of  $FPIR(N, T)$ , with  $N$  ranging from 640 000 to 12 000 000 as noted in rows 1-10 of Table 1. These error tradeoff characteristics are useful for applications where a threshold must be elevated to limit false positives, such as when human reviewer labor is not matched to the volume of searches. Dark lines join points of equal threshold: If horizontal,  $FPIR(T)$  rises with  $N$ , and mate scores are independent of  $N$ . Other algorithms adjust scores in an attempt to make  $FPIR(T)$  independent of  $N$ .

2021/10/28  
13:44:33

FNIR(N, R, T) =  
FPIR(N, T) =

False neg. identification rate  
False pos. identification rate

N = Num. enrolled subjects  
R = Num. candidates examined

T = Threshold

T = 0 → Investigation  
T > 0 → Identification

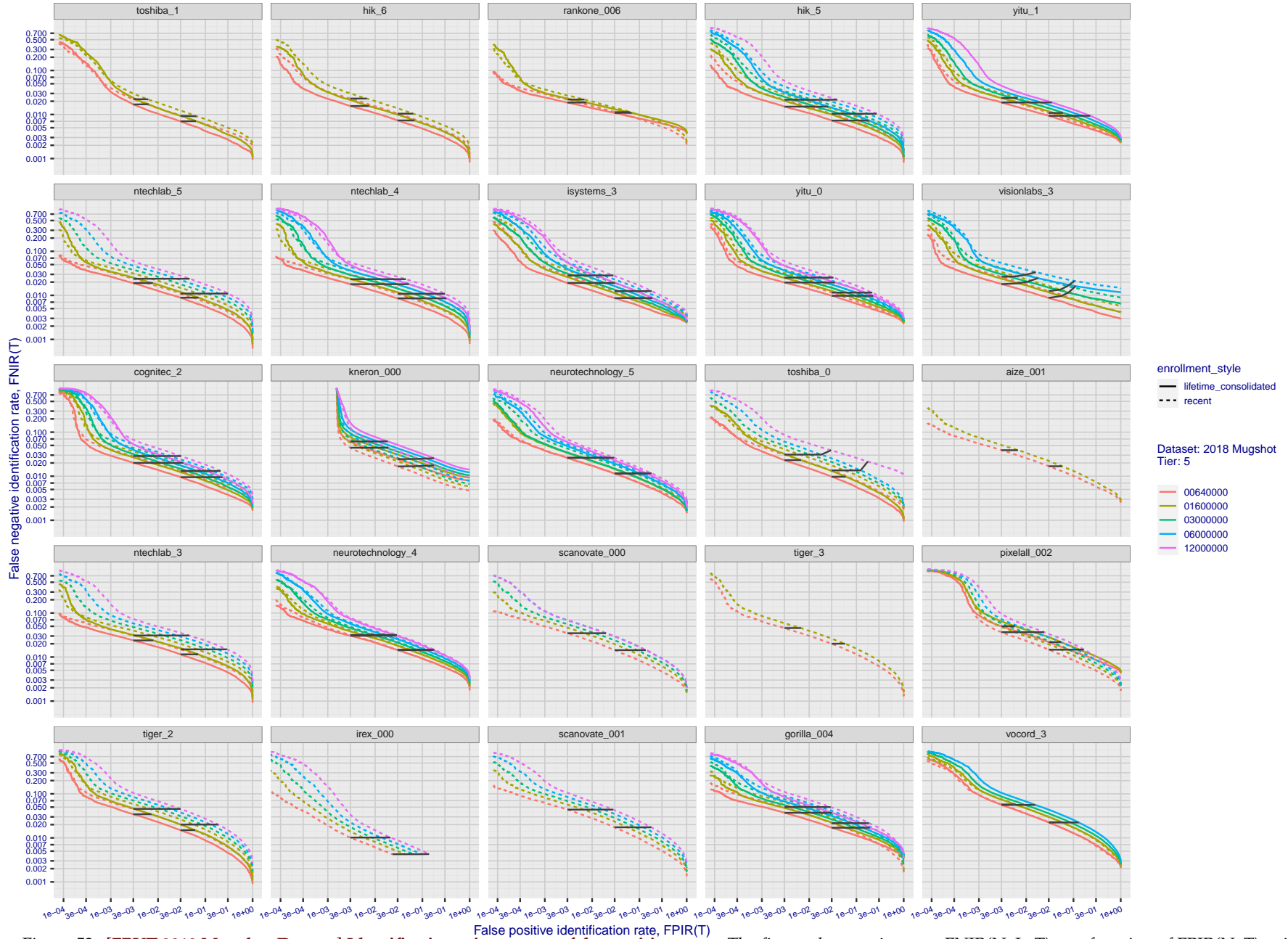


Figure 52: [FRVT-2018 Mugshot Dataset] Identification miss rates vs. false positive rates. The figure shows miss rates  $FNIR(N, L, T)$  as a function of  $FPIR(N, T)$ , with  $N$  ranging from 640 000 to 12 000 000 as noted in rows 1-10 of Table 1. These error tradeoff characteristics are useful for applications where a threshold must be elevated to limit false positives, such as when human reviewer labor is not matched to the volume of searches. Dark lines join points of equal threshold: If horizontal,  $FPIR(T)$  rises with  $N$ , and mate scores are independent of  $N$ . Other algorithms adjust scores in an attempt to make  $FPIR$  independent of  $N$ .

2021/10/28  
13:44:33

FNIR(N, R, T) =  
FPR(N, T) =

False neg. identification rate  
False pos. identification rate

N = Num. enrolled subjects  
R = Num. candidates examined

T = Threshold

T = 0 → Investigation  
T > 0 → Identification

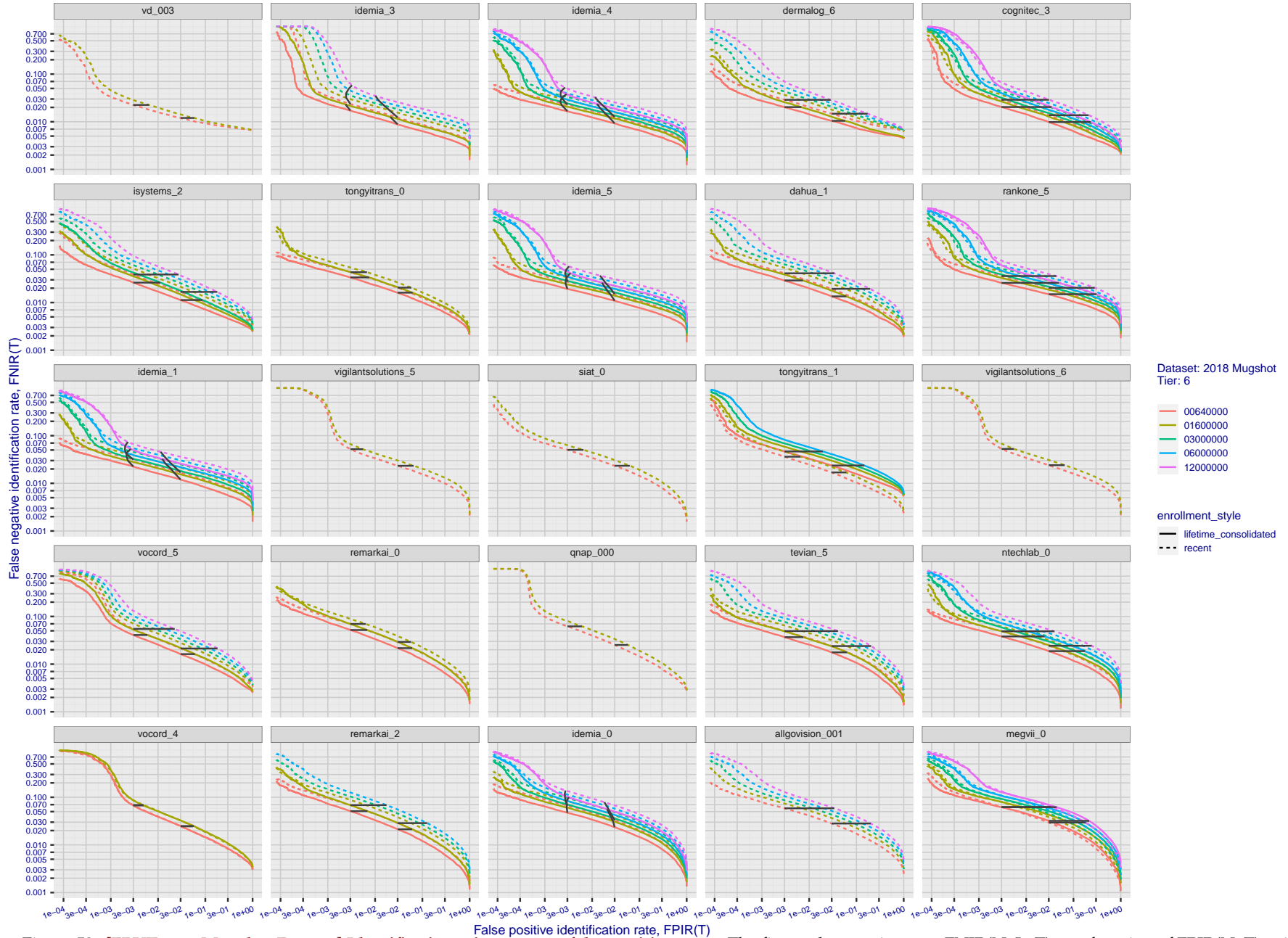


Figure 53: [FRVT-2018 Mugshot Dataset] Identification miss rates vs. false positive rates. The figure shows miss rates  $FNIR(N, L, T)$  as a function of  $FPIR(N, T)$ , with  $N$  ranging from 640 000 to 12 000 000 as noted in rows 1-10 of Table 1. These error tradeoff characteristics are useful for applications where a threshold must be elevated to limit false positives, such as when human reviewer labor is not matched to the volume of searches. Dark lines join points of equal threshold: If horizontal,  $FPIR(T)$  rises with  $N$ , and mate scores are independent of  $N$ . Other algorithms adjust scores in an attempt to make  $FPIR$  independent of  $N$ .

2021/10/28  
13:44:33

FNIR(N, T) =  
FPIR(N, T) =

False neg. identification rate  
False pos. identification rate

N = Num. enrolled subjects  
R = Num. candidates examined

T = Threshold

T = 0 → Investigation  
T > 0 → Identification

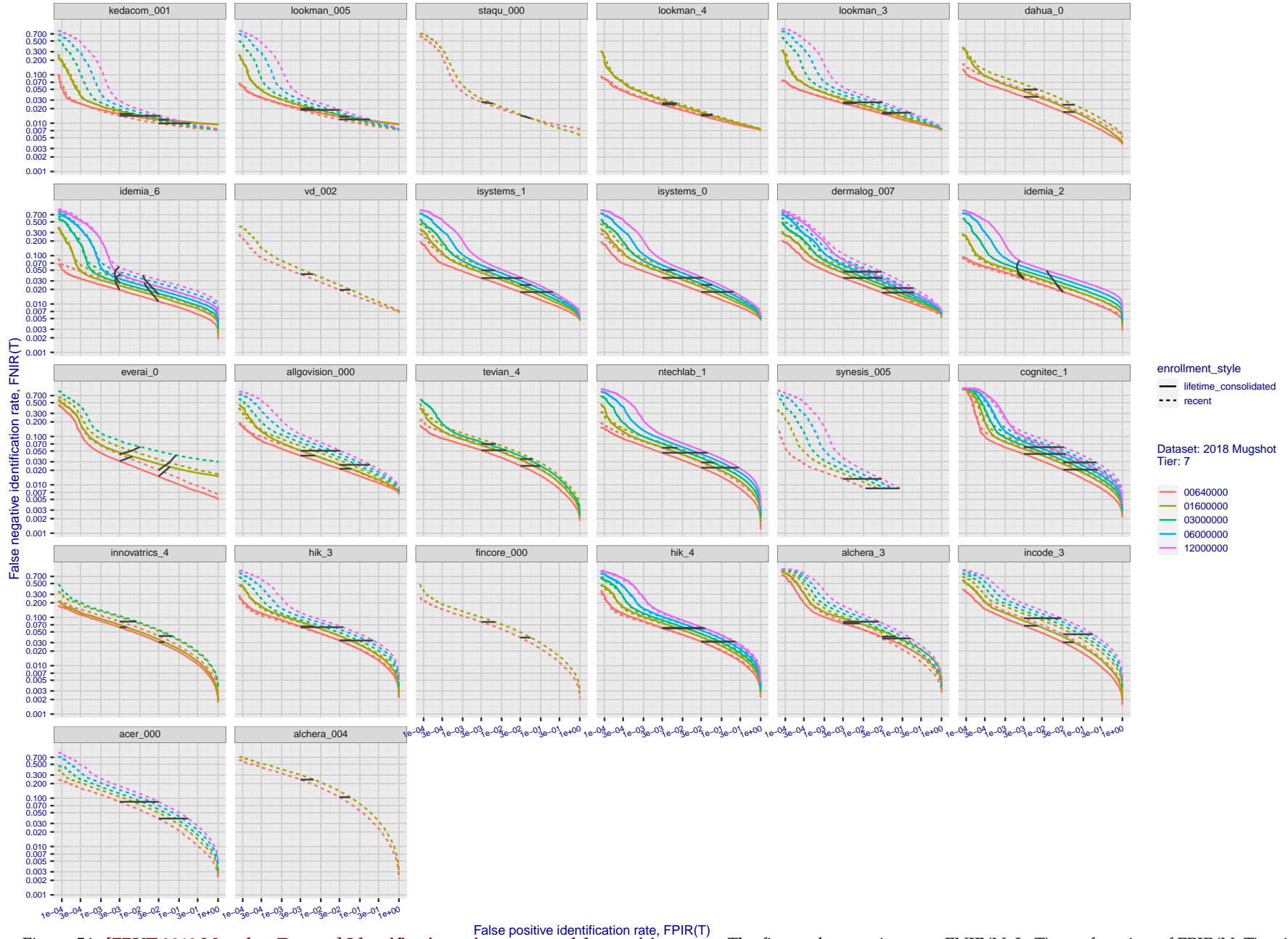


Figure 54: [FRVT-2018 Mugshot Dataset] Identification miss rates vs. false positive rates. The figure shows miss rates  $FNIR(N, L, T)$  as a function of  $FPIR(N, T)$ , with  $N$  ranging from 640 000 to 12 000 000 as noted in rows 1-10 of Table 1. These error tradeoff characteristics are useful for applications where a threshold must be elevated to limit false positives, such as when human reviewer labor is not matched to the volume of searches. Dark lines join points of equal threshold: If horizontal,  $FPIR(T)$  rises with  $N$ , and mate scores are independent of  $N$ . Other algorithms adjust scores in an attempt to make  $FPIR(T)$  independent of  $N$ .

2021/10/28  
13:44:33

FNIR(N, R, T) = False neg. identification rate  
FPIR(N, T) = False pos. identification rate  
N = Num. enrolled subjects  
R = Num. candidates examined

T = Threshold

T = 0 → Investigation  
T > 0 → Identification

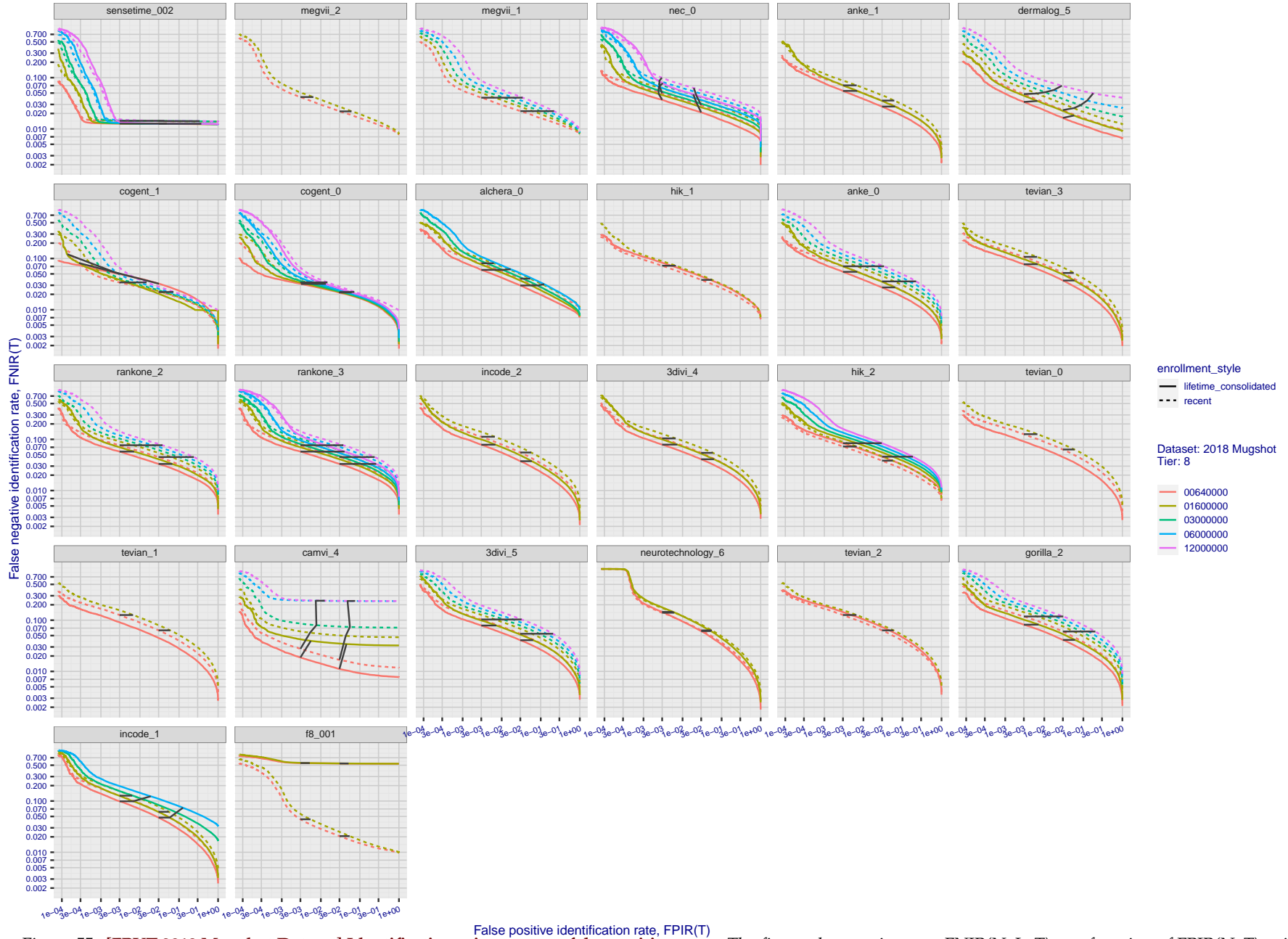


Figure 55: [FRVT-2018 Mugshot Dataset] Identification miss rates vs. false positive rates. The figure shows miss rates  $FNIR(N, L, T)$  as a function of  $FPIR(N, T)$ , with  $N$  ranging from 640 000 to 12 000 000 as noted in rows 1-10 of Table 1. These error tradeoff characteristics are useful for applications where a threshold must be elevated to limit false positives, such as when human reviewer labor is not matched to the volume of searches. Dark lines join points of equal threshold: If horizontal,  $FPIR(T)$  rises with  $N$ , and mate scores are independent of  $N$ . Other algorithms adjust scores in an attempt to make  $FPIR(T)$  independent of  $N$ .

2021/10/28  
13:44:33

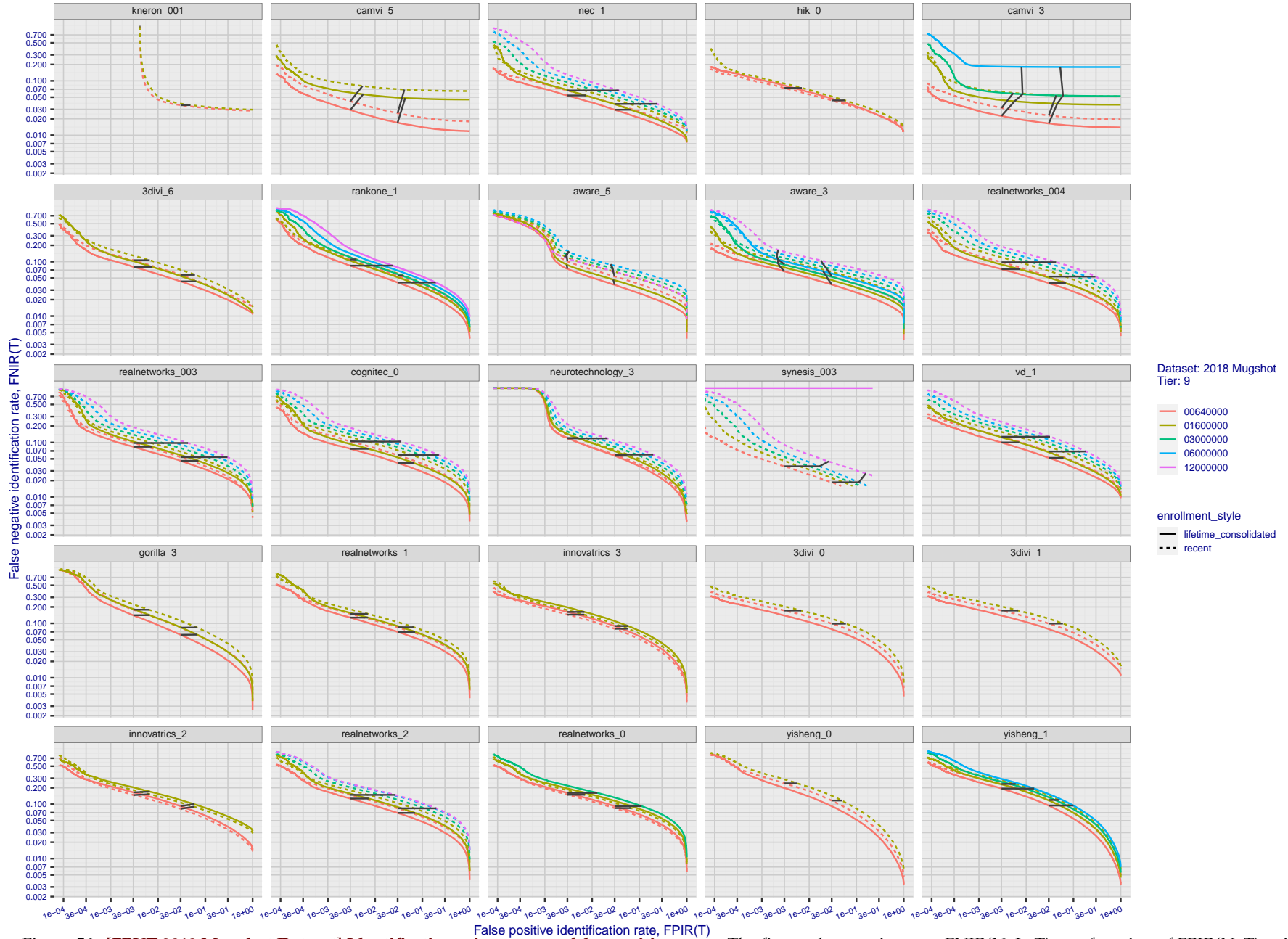
FNIR(N, R, T) =  
FPIR(N, T) =

False neg. identification rate  
False pos. identification rate

N = Num. enrolled subjects  
R = Num. candidates examined

T = Threshold

T = 0 → Investigation  
T > 0 → Identification



Dataset: 2018 Mugshot  
Tier: 9

00640000  
01600000  
03000000  
06000000  
12000000

enrollment\_style  
— lifetime\_consolidated  
- - - recent

Figure 56: [FRVT-2018 Mugshot Dataset] Identification miss rates vs. false positive rates. The figure shows miss rates  $FNIR(N, L, T)$  as a function of  $FPIR(N, T)$ , with  $N$  ranging from 640 000 to 12 000 000 as noted in rows 1-10 of Table 1. These error tradeoff characteristics are useful for applications where a threshold must be elevated to limit false positives, such as when human reviewer labor is not matched to the volume of searches. Dark lines join points of equal threshold: If horizontal,  $FPIR(T)$  rises with  $N$ , and mate scores are independent of  $N$ . Other algorithms adjust scores in an attempt to make  $FPIR$  independent of  $N$ .

2021/10/28  
13:44:33

FNIR(N, R, T) =  
FPIR(N, T) =

False neg. identification rate  
False pos. identification rate

N = Num. enrolled subjects  
R = Num. candidates examined

T = Threshold

T = 0 → Investigation  
T > 0 → Identification

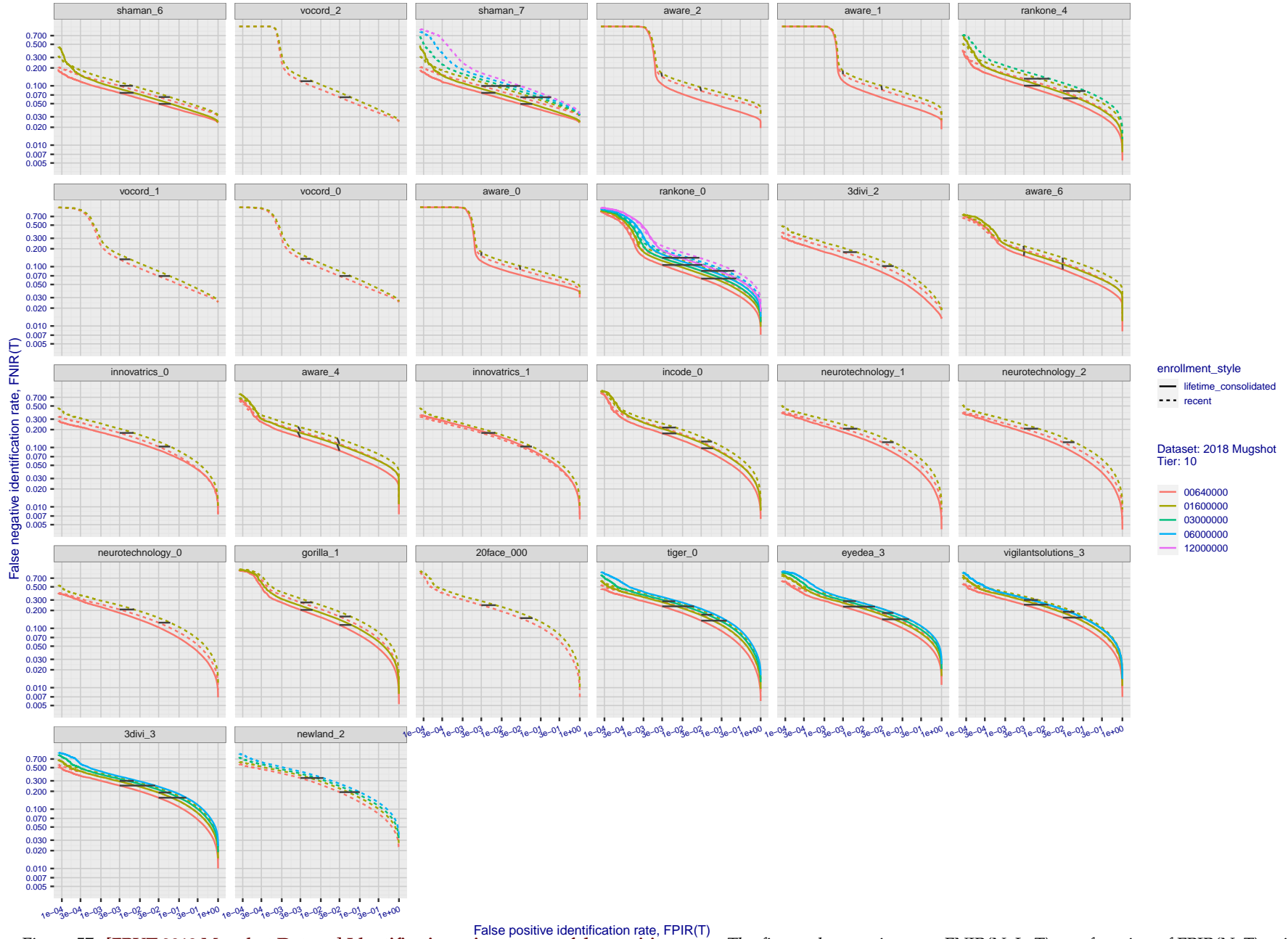


Figure 57: [FRVT-2018 Mugshot Dataset] Identification miss rates vs. false positive rates. The figure shows miss rates  $FNIR(N, L, T)$  as a function of  $FPIR(N, T)$ , with  $N$  ranging from 640 000 to 12 000 000 as noted in rows 1-10 of Table 1. These error tradeoff characteristics are useful for applications where a threshold must be elevated to limit false positives, such as when human reviewer labor is not matched to the volume of searches. Dark lines join points of equal threshold: If horizontal,  $FPIR(T)$  rises with  $N$ , and mate scores are independent of  $N$ . Other algorithms adjust scores in an attempt to make  $FPIR(T)$  independent of  $N$ .

2021/10/28  
13:44:33

FNIR(N, R, T) =  
FPIR(N, T) =

False neg. identification rate  
False pos. identification rate

N = Num. enrolled subjects  
R = Num. candidates examined

T = Threshold

T = 0 → Investigation  
T > 0 → Identification

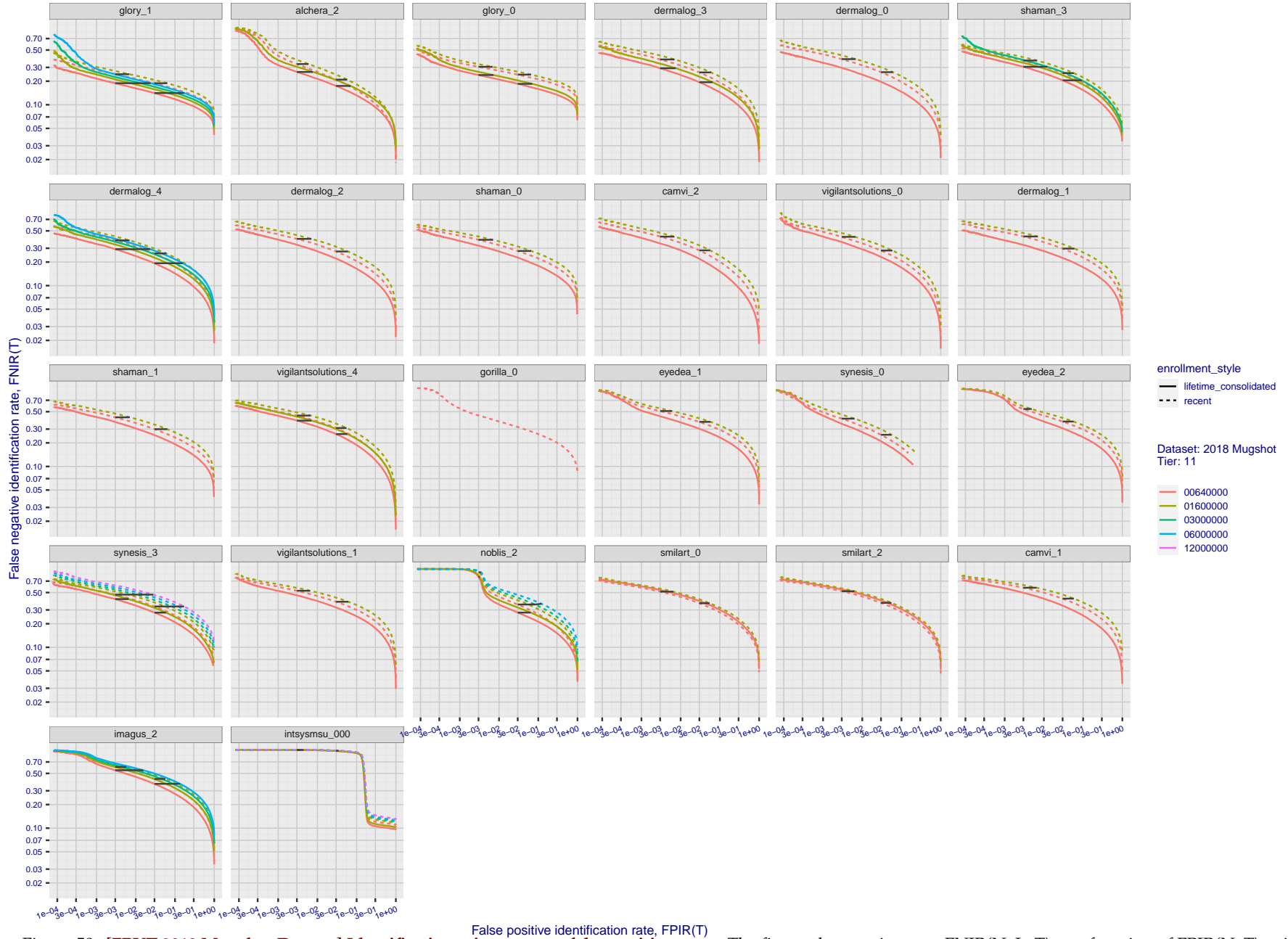


Figure 58: [FRVT-2018 Mugshot Dataset] Identification miss rates vs. false positive rates. The figure shows miss rates  $FNIR(N, L, T)$  as a function of  $FPIR(N, T)$ , with  $N$  ranging from 640 000 to 12 000 000 as noted in rows 1-10 of Table 1. These error tradeoff characteristics are useful for applications where a threshold must be elevated to limit false positives, such as when human reviewer labor is not matched to the volume of searches. Dark lines join points of equal threshold: If horizontal,  $FPIR(T)$  rises with  $N$ , and mate scores are independent of  $N$ . Other algorithms adjust scores in an attempt to make  $FPIR$  independent of  $N$ .

2021/10/28  
13:44:33

FNIR(N, R, T) =  
FPIR(N, T) =

False neg. identification rate  
False pos. identification rate

N = Num. enrolled subjects  
R = Num. candidates examined

T = Threshold

T = 0 → Investigation  
T > 0 → Identification

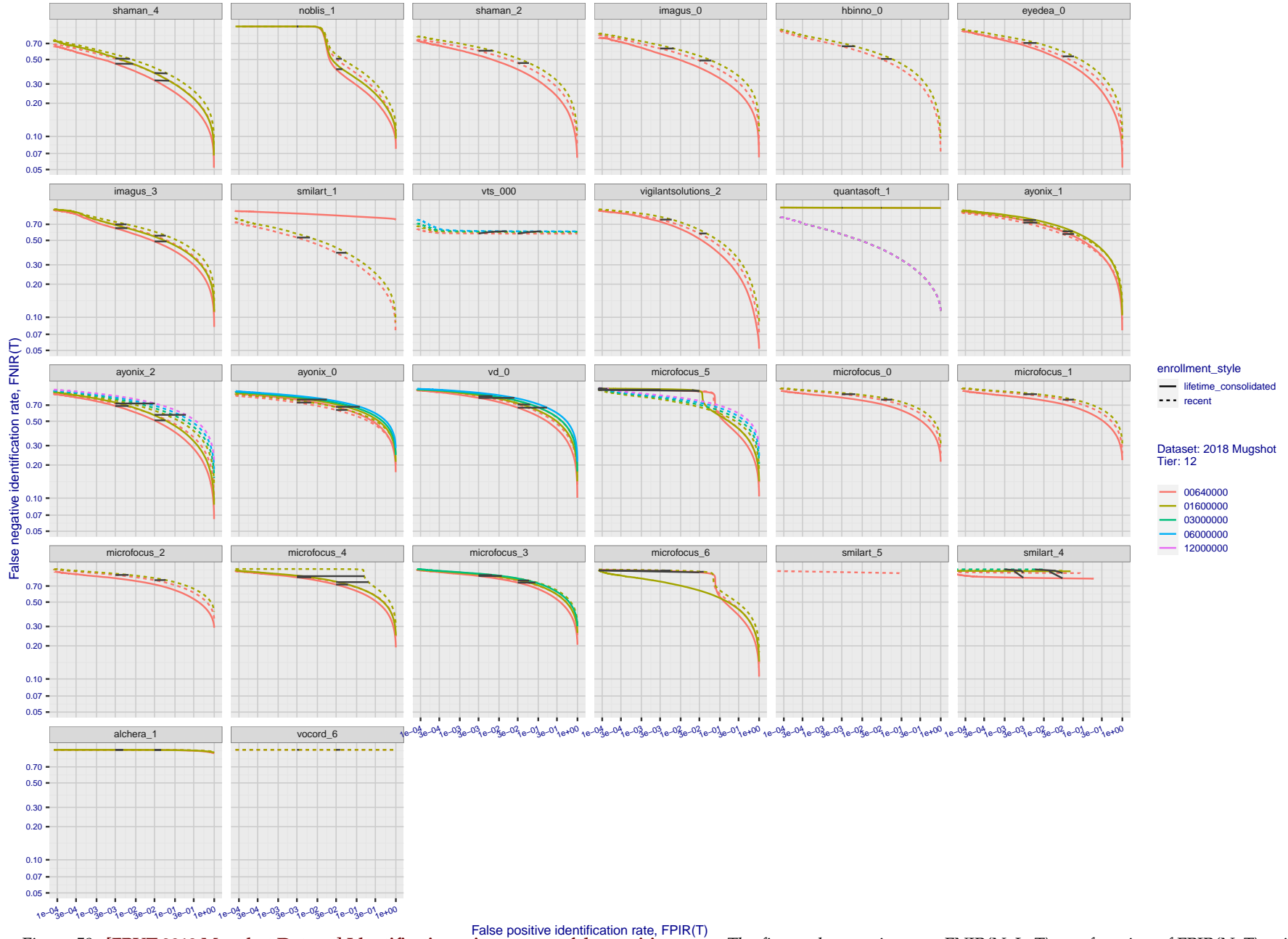


Figure 59: [FRVT-2018 Mugshot Dataset] Identification miss rates vs. false positive rates. The figure shows miss rates  $FNIR(N, L, T)$  as a function of  $FPIR(N, T)$ , with  $N$  ranging from 640 000 to 12 000 000 as noted in rows 1-10 of Table 1. These error tradeoff characteristics are useful for applications where a threshold must be elevated to limit false positives, such as when human reviewer labor is not matched to the volume of searches. Dark lines join points of equal threshold: If horizontal,  $FPIR(T)$  rises with  $N$ , and mate scores are independent of  $N$ . Other algorithms adjust scores in an attempt to make  $FPIR$  independent of  $N$ .

## Appendix B Effect of time-lapse: Accuracy after face ageing

This publication is available free of charge from: <https://doi.org/10.6028/NIST.IR.8271>

2021/10/28  
 FNIR(N, R, T) =  
 FPR(N, T) =  
 False neg. identification rate  
 False pos. identification rate  
 N = Num. enrolled subjects  
 R = Num. candidates examined  
 T = Threshold  
 T = 0 → Investigation  
 T > 0 → Identification

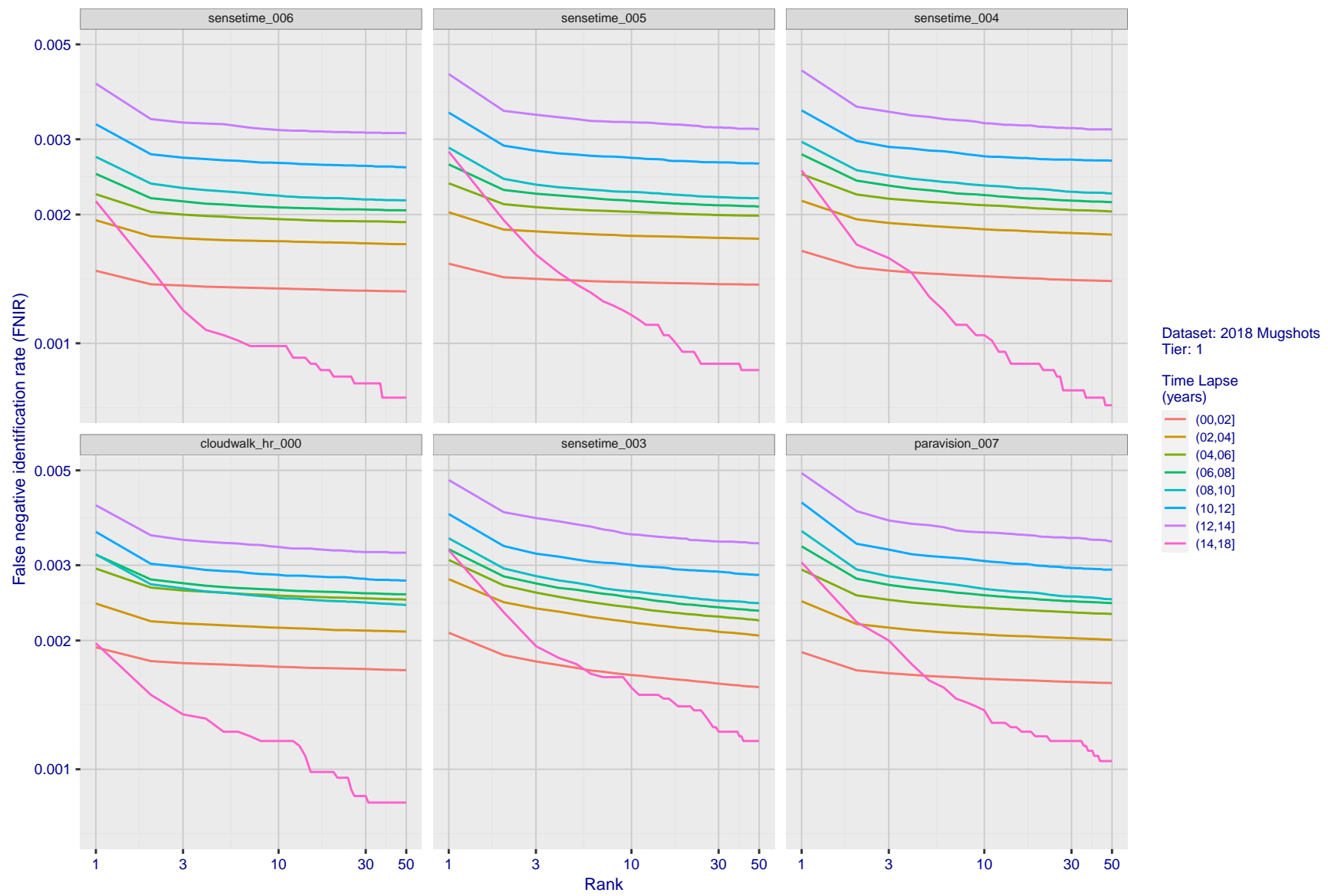


Figure 60: [FRVT-2018 Mugshot Ageing Dataset] Identification miss rates vs. rank by time-elapsed. The oldest image of each individual is enrolled. Thereafter, all more recent images are searched. Miss rates are computed over all searches noted in row 17 of Table 1 and binned by number of years between search and initial enrollment.

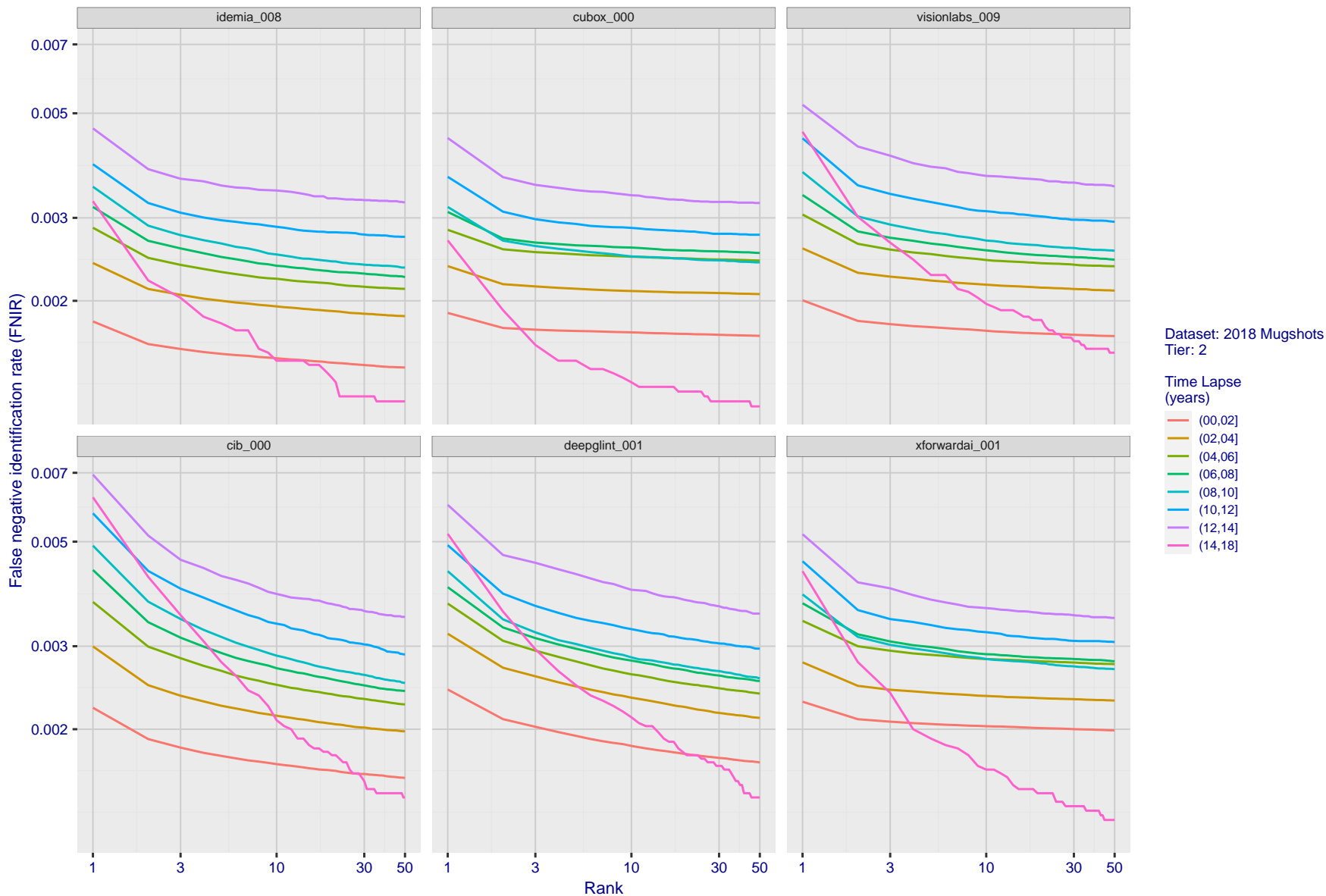


Figure 61: [FRVT-2018 Mugshot Ageing Dataset] Identification miss rates vs. rank by time-elapsd. The oldest image of each individual is enrolled. Thereafter, all more recent images are searched. Miss rates are computed over all searches noted in row 17 of Table 1 and binned by number of years between search and initial enrollment.

2021/10/28  
 FNIR(N, R, T) = False neg. identification rate  
 FPR(N, T) = False pos. identification rate  
 N = Num. enrolled subjects  
 R = Num. candidates examined  
 T = Threshold  
 T = 0 → Investigation  
 T > 0 → Identification

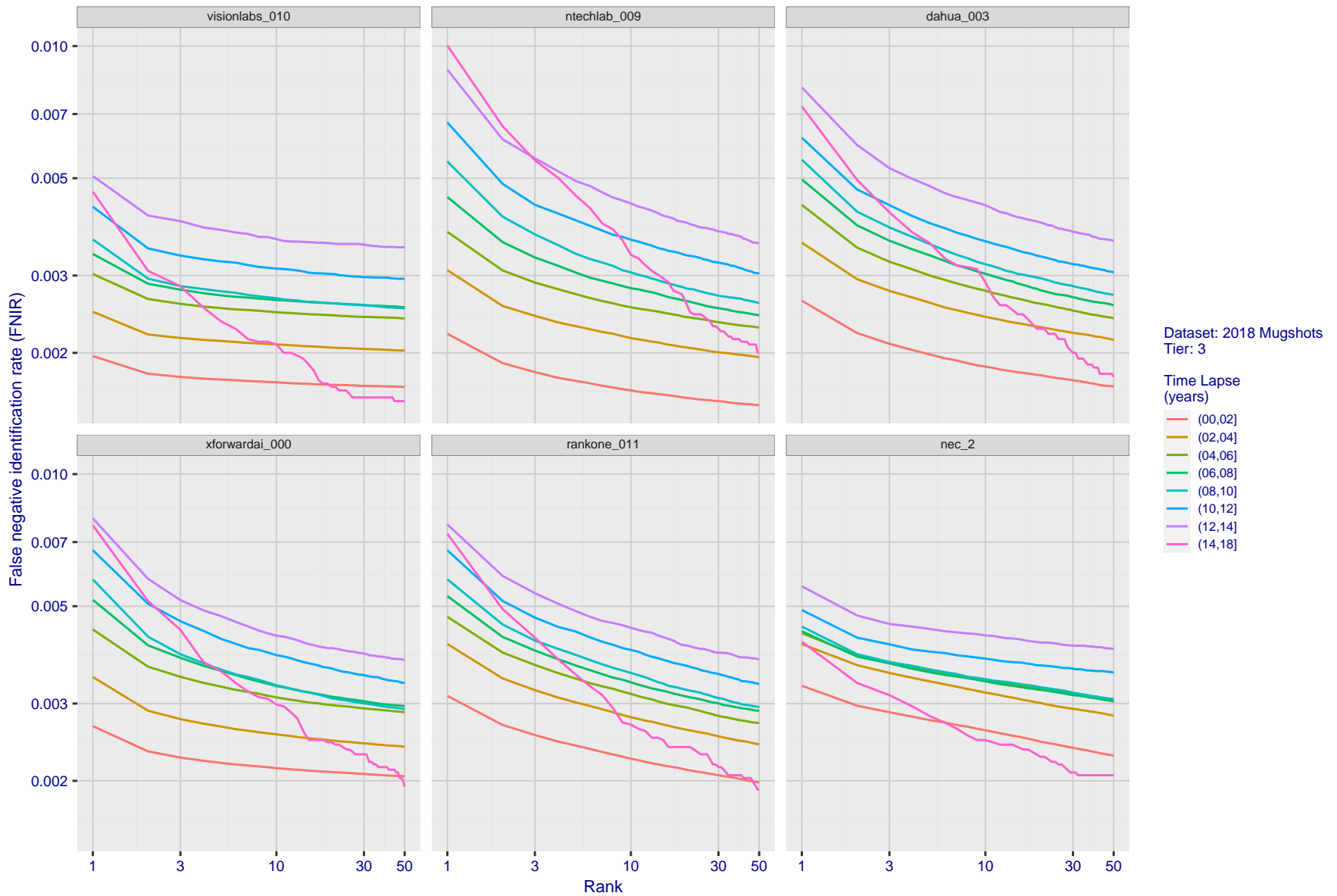


Figure 62: [FRVT-2018 Mugshot Ageing Dataset] Identification miss rates vs. rank by time-elapsd. The oldest image of each individual is enrolled. Thereafter, all more recent images are searched. Miss rates are computed over all searches noted in row 17 of Table 1 and binned by number of years between search and initial enrollment.

2021/10/28  
13:44:33

FNIR(N, R, T) =  
FPR(N, T) =

False neg. identification rate  
False pos. identification rate

N = Num. enrolled subjects  
R = Num. candidates examined

T = Threshold

T = 0 → Investigation  
T > 0 → Identification

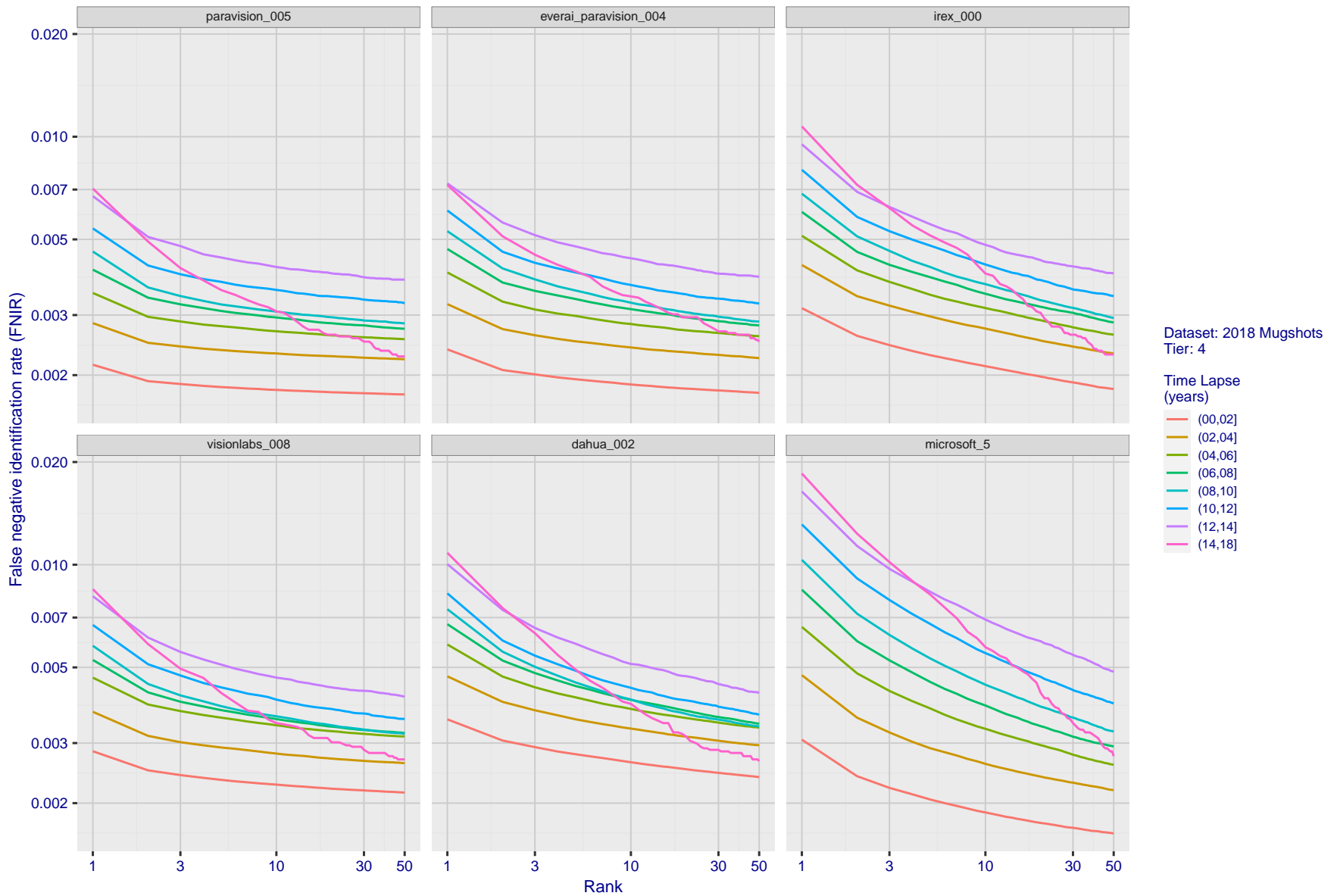


Figure 63: [FRVT-2018 Mugshot Ageing Dataset] Identification miss rates vs. rank by time-elapsd. The oldest image of each individual is enrolled. Thereafter, all more recent images are searched. Miss rates are computed over all searches noted in row 17 of Table 1 and binned by number of years between search and initial enrollment.

2021/10/28  
13:44:33

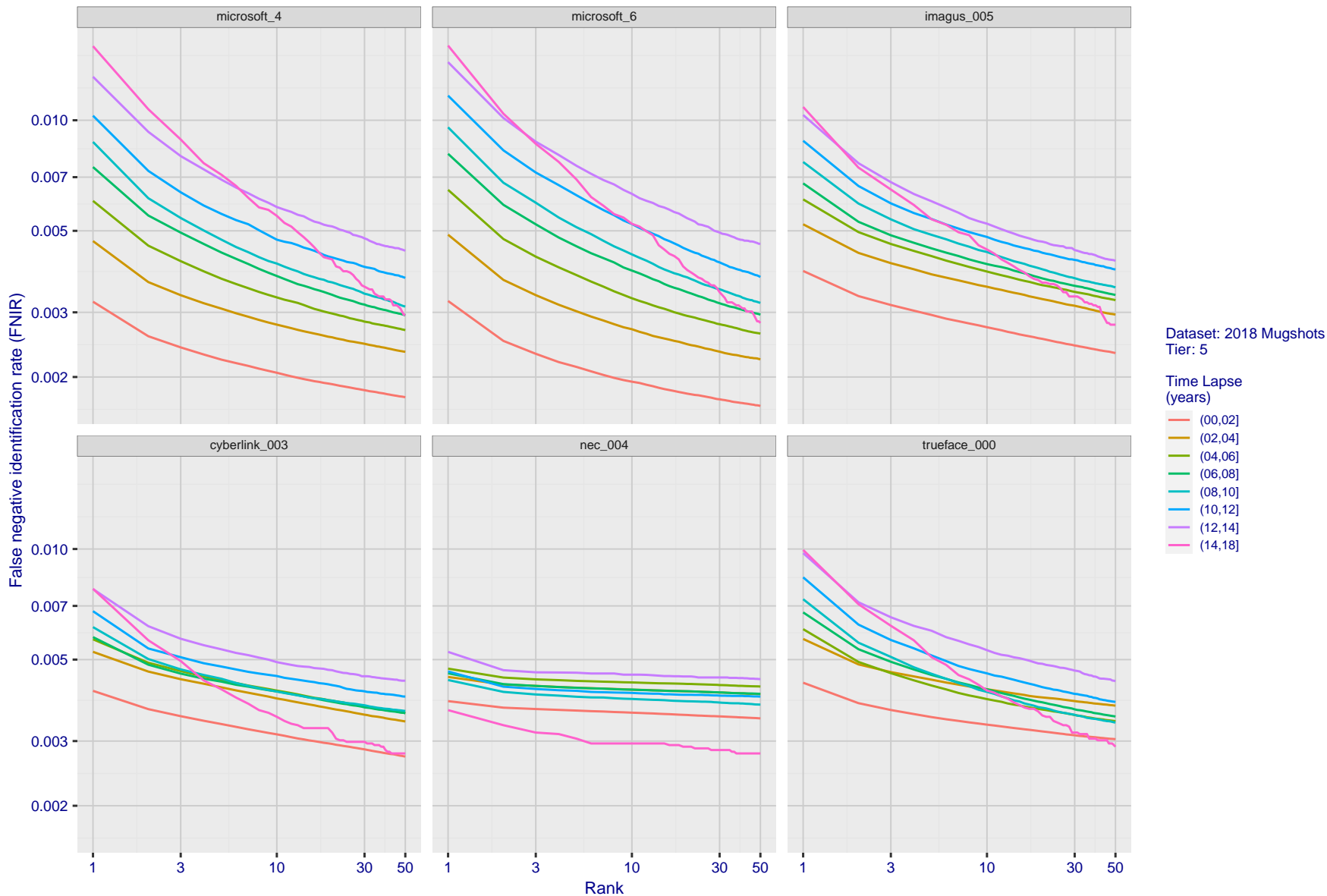
FNIR(N, R, T) =  
FPR(N, T) =

False neg. identification rate  
False pos. identification rate

N = Num. enrolled subjects  
R = Num. candidates examined

T = Threshold

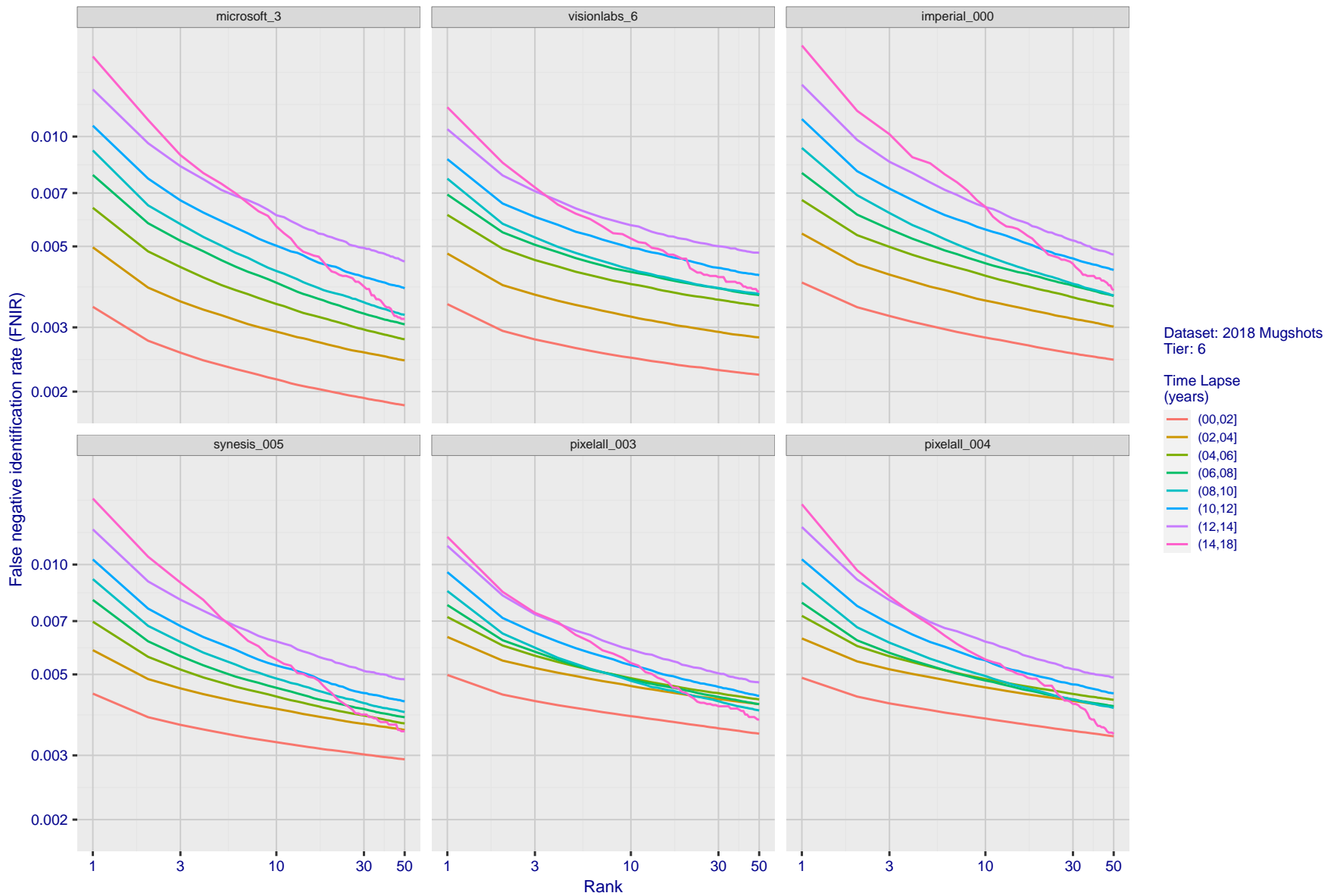
T = 0 → Investigation  
T > 0 → Identification



Dataset: 2018 Mugshots  
Tier: 5  
Time Lapse (years)  
(00,02]  
(02,04]  
(04,06]  
(06,08]  
(08,10]  
(10,12]  
(12,14]  
(14,18]

Figure 64: [FRVT-2018 Mugshot Ageing Dataset] Identification miss rates vs. rank by time-elapsd. The oldest image of each individual is enrolled. Thereafter, all more recent images are searched. Miss rates are computed over all searches noted in row 17 of Table 1 and binned by number of years between search and initial enrollment.

2021/10/28 13:44:33 FNIR(N, R, T) = False neg. identification rate N = Num. enrolled subjects T = Threshold  
FPR(N, T) = False pos. identification rate R = Num. candidates examined T > 0 → Investigation  
T > 0 → Identification



Dataset: 2018 Mugshots  
Tier: 6

Time Lapse (years)

- (00,02]
- (02,04]
- (04,06]
- (06,08]
- (08,10]
- (10,12]
- (12,14]
- (14,18]

Figure 65: [FRVT-2018 Mugshot Ageing Dataset] Identification miss rates vs. rank by time-elapsd. The oldest image of each individual is enrolled. Thereafter, all more recent images are searched. Miss rates are computed over all searches noted in row 17 of Table 1 and binned by number of years between search and initial enrollment.

2021/10/28  
13:44:33  
FNIR(N, R, T) = False neg. identification rate  
FPR(N, T) = False pos. identification rate  
N = Num. enrolled subjects  
R = Num. candidates examined  
T = Threshold  
T = 0 → Investigation  
T > 0 → Identification

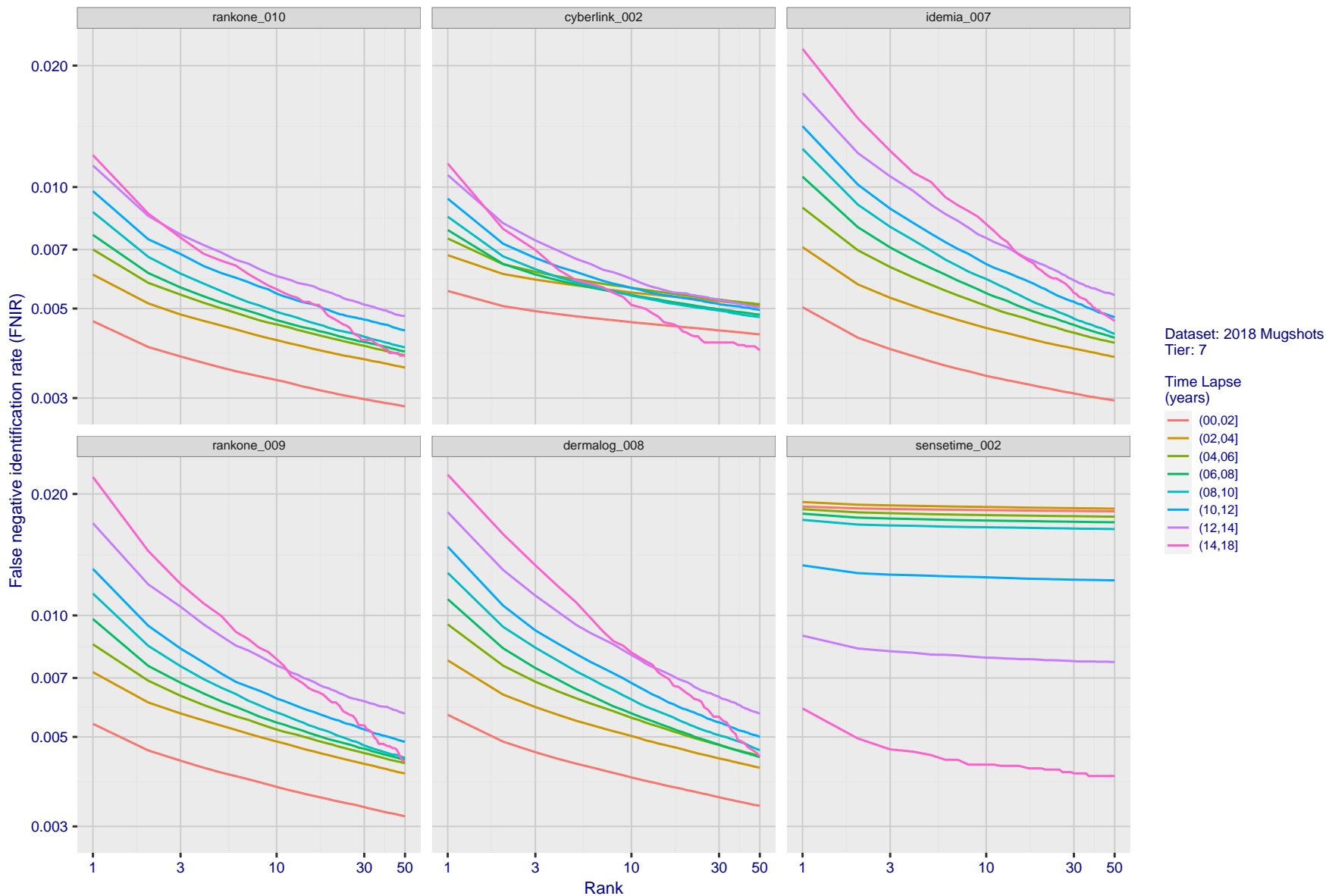


Figure 66: [FRVT-2018 Mugshot Ageing Dataset] Identification miss rates vs. rank by time-elapsd. The oldest image of each individual is enrolled. Thereafter, all more recent images are searched. Miss rates are computed over all searches noted in row 17 of Table 1 and binned by number of years between search and initial enrollment.

2021/10/28 13:44:33  
FNIR(N, R, T) = False neg. identification rate  
FPR(N, T) = False pos. identification rate  
N = Num. enrolled subjects  
R = Num. candidates examined  
T = Threshold  
T = 0 → Investigation  
T > 0 → Identification

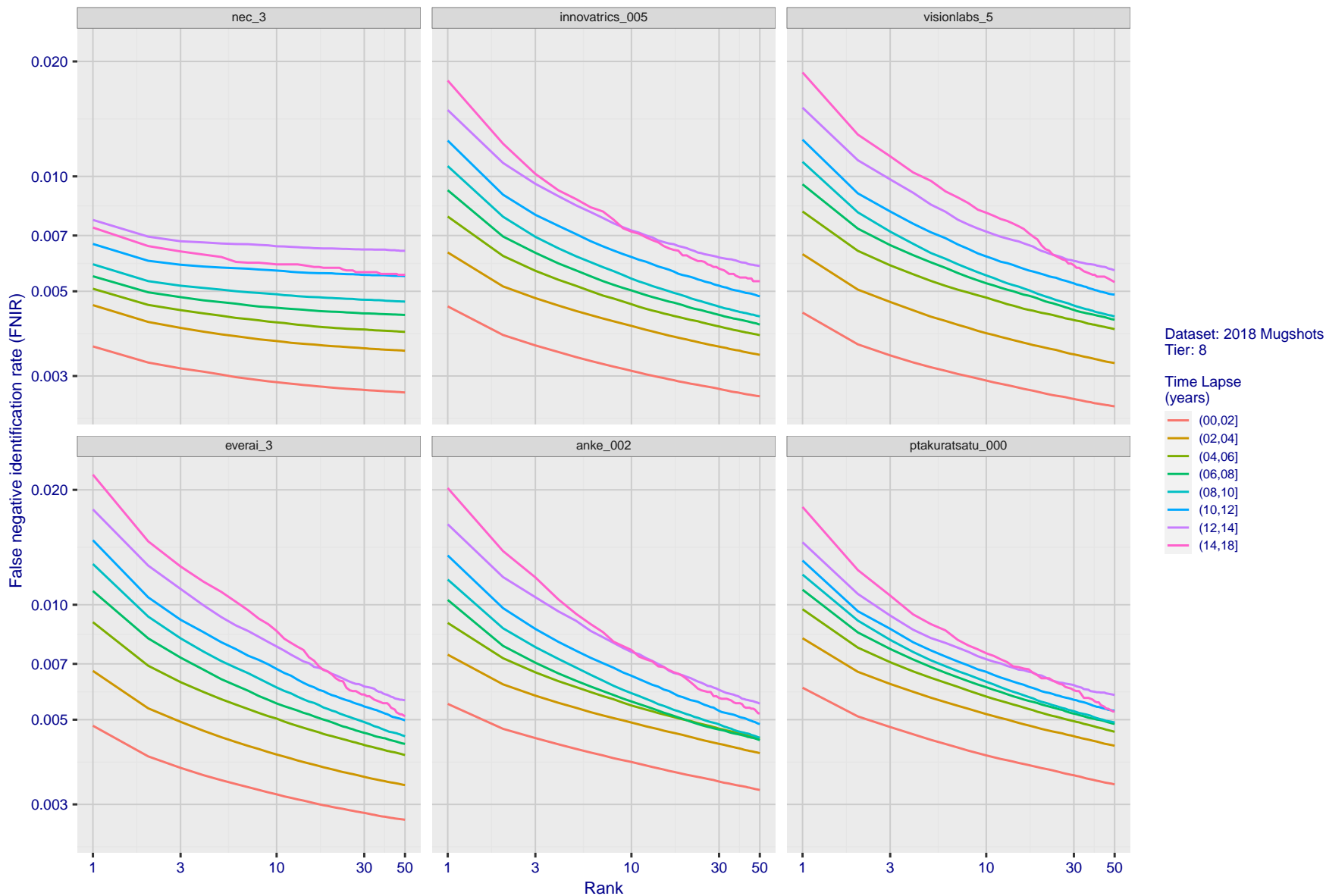


Figure 67: [FRVT-2018 Mugshot Ageing Dataset] Identification miss rates vs. rank by time-elapsd. The oldest image of each individual is enrolled. Thereafter, all more recent images are searched. Miss rates are computed over all searches noted in row 17 of Table 1 and binned by number of years between search and initial enrollment.

2021/10/28  
 13:44:33  
 FNIR(N, R, T) = False neg. identification rate  
 FPR(N, T) = False pos. identification rate  
 N = Num. enrolled subjects  
 R = Num. candidates examined  
 T = Threshold  
 T = 0 → Investigation  
 T > 0 → Identification

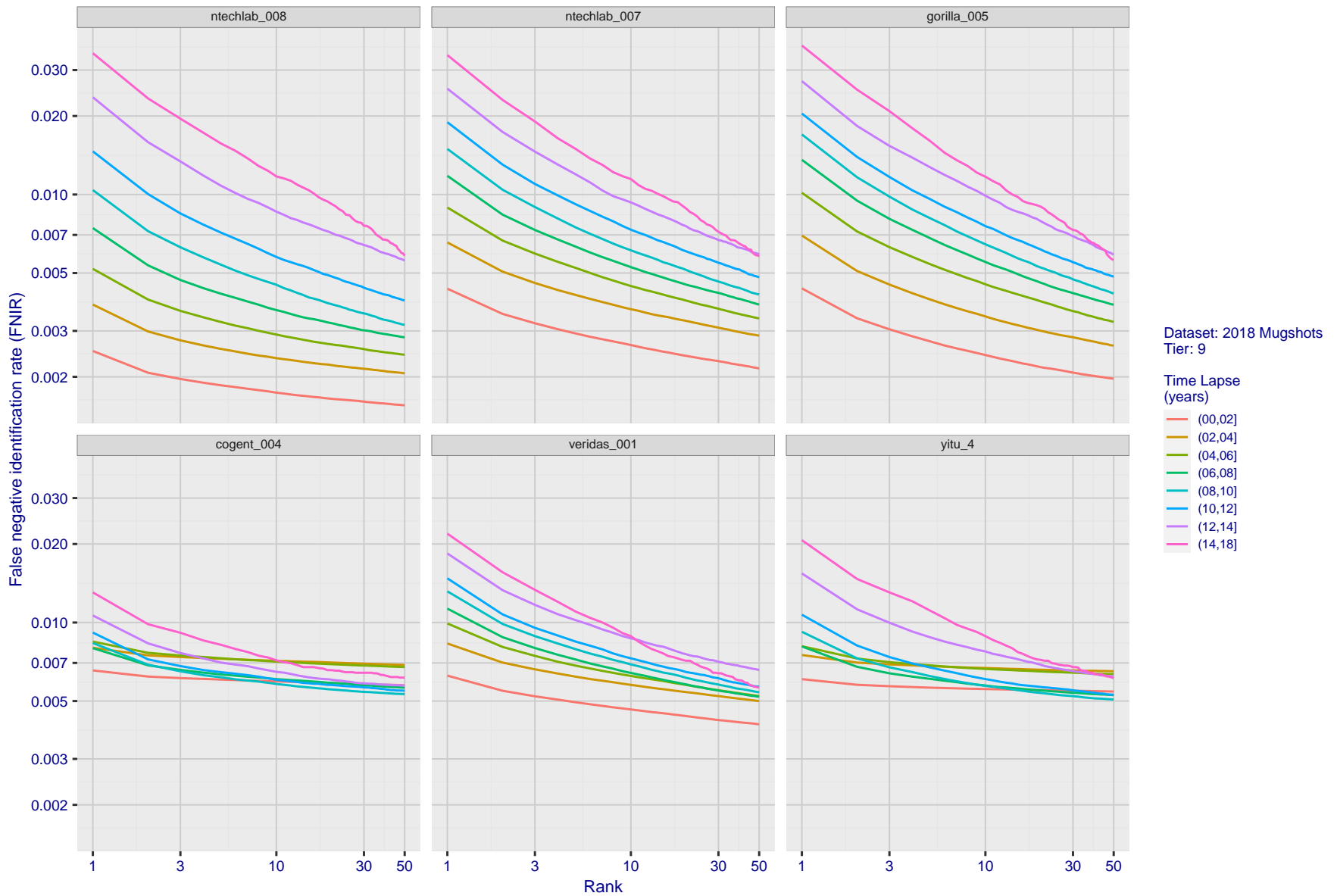


Figure 68: [FRVT-2018 Mugshot Ageing Dataset] Identification miss rates vs. rank by time-elapsd. The oldest image of each individual is enrolled. Thereafter, all more recent images are searched. Miss rates are computed over all searches noted in row 17 of Table 1 and binned by number of years between search and initial enrollment.

2021/10/28  
13:44:33  
FNIR(N, R, T) = False neg. identification rate  
FPIR(N, T) = False pos. identification rate  
N = Num. enrolled subjects  
R = Num. candidates examined  
T = Threshold  
T = 0 → Investigation  
T > 0 → Identification

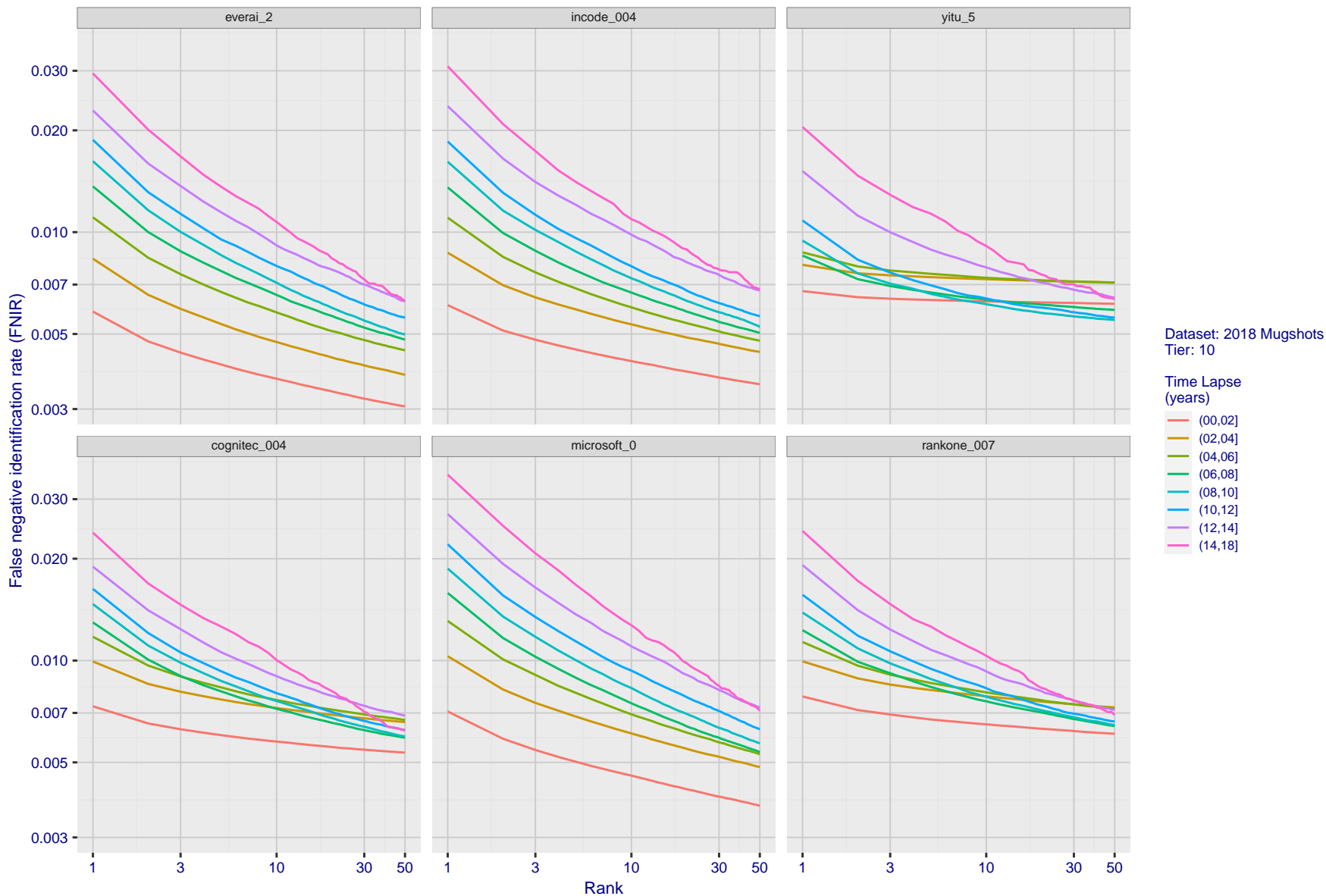


Figure 69: [FRVT-2018 Mugshot Ageing Dataset] Identification miss rates vs. rank by time-elapsd. The oldest image of each individual is enrolled. Thereafter, all more recent images are searched. Miss rates are computed over all searches noted in row 17 of Table 1 and binned by number of years between search and initial enrollment.

2021/10/28  
 13:44:33  
 FNIR(N, R, T) = False neg. identification rate  
 FPR(N, T) = False pos. identification rate  
 N = Num. enrolled subjects  
 R = Num. candidates examined  
 T = Threshold  
 T = 0 → Investigation  
 T > 0 → Identification

2021/10/28  
 13:44:33  
 FNIR(N, R, T) = False neg. identification rate  
 FPR(N, T) = False pos. identification rate  
 N = Num. enrolled subjects  
 R = Num. candidates examined  
 T = Threshold  
 T = 0 → Investigation  
 T > 0 → Identification

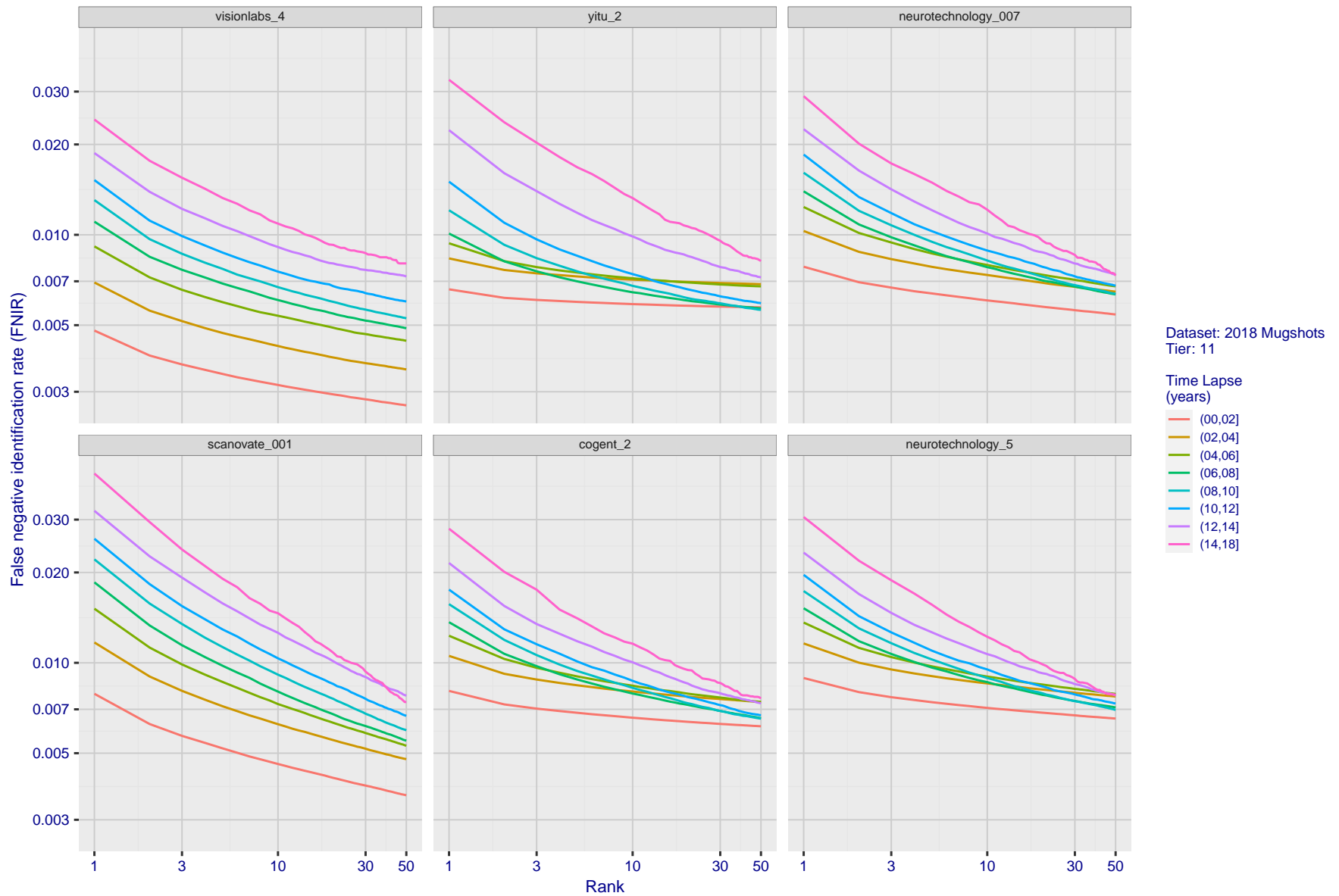


Figure 70: [FRVT-2018 Mugshot Ageing Dataset] Identification miss rates vs. rank by time-elapsd. The oldest image of each individual is enrolled. Thereafter, all more recent images are searched. Miss rates are computed over all searches noted in row 17 of Table 1 and binned by number of years between search and initial enrollment.

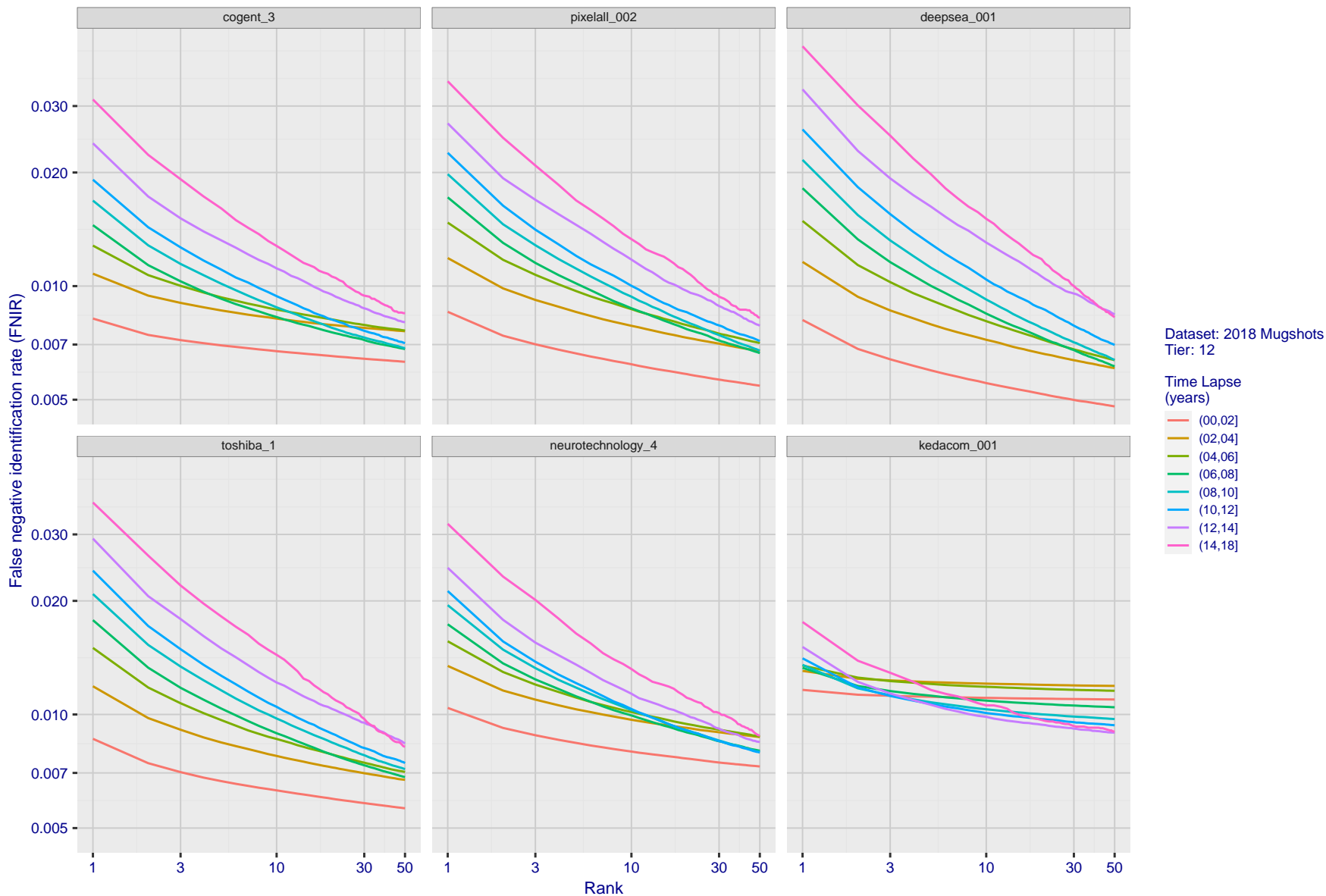


Figure 71: [FRVT-2018 Mugshot Ageing Dataset] Identification miss rates vs. rank by time-elapsd. The oldest image of each individual is enrolled. Thereafter, all more recent images are searched. Miss rates are computed over all searches noted in row 17 of Table 1 and binned by number of years between search and initial enrollment.

2021/10/28  
 13:44:33  
 FNIR(N, R, T) = False neg. identification rate  
 FPR(N, T) = False pos. identification rate  
 N = Num. enrolled subjects  
 R = Num. candidates examined  
 T = Threshold  
 T = 0 → Investigation  
 T > 0 → Identification

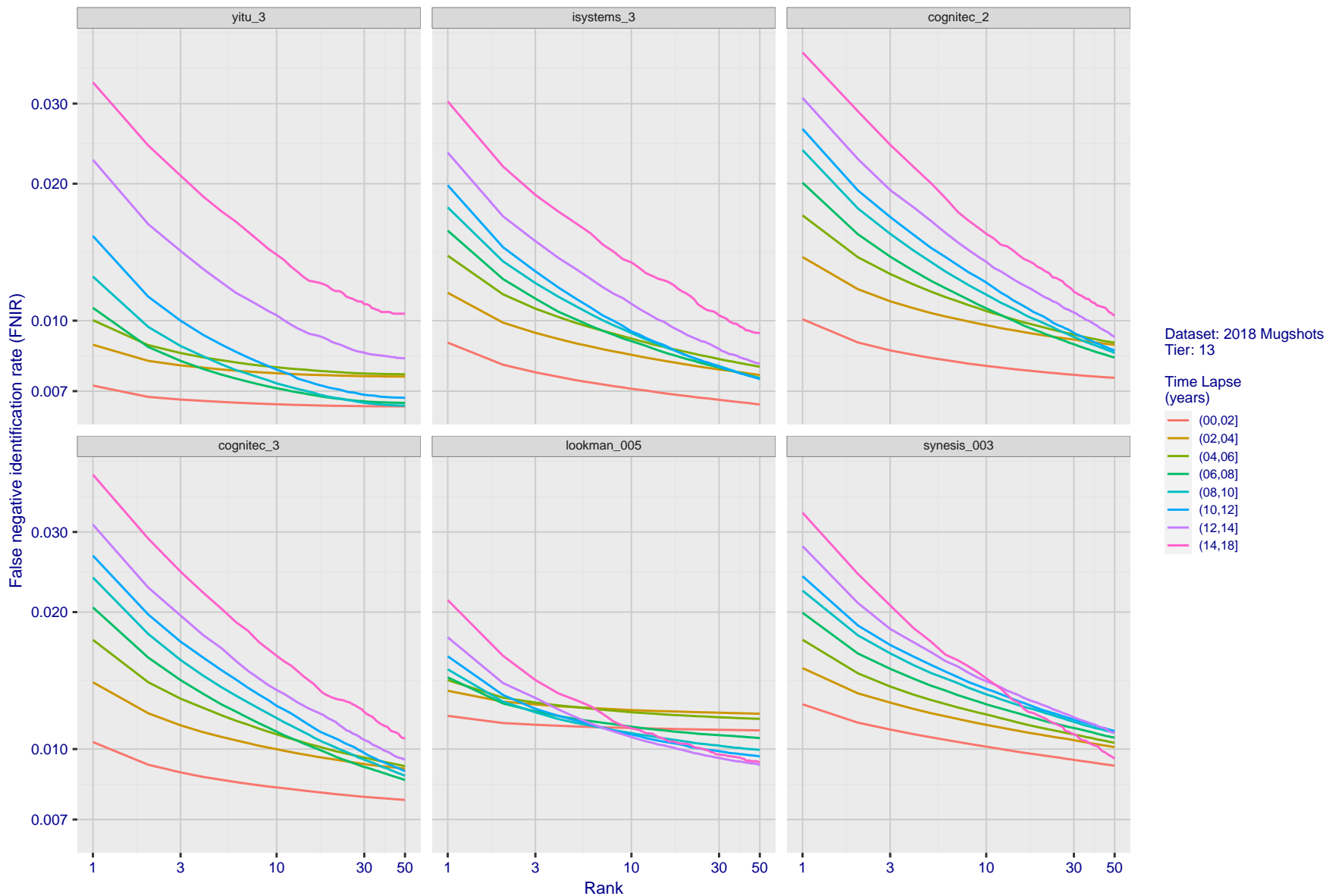


Figure 72: [FRVT-2018 Mugshot Ageing Dataset] Identification miss rates vs. rank by time-elapsd. The oldest image of each individual is enrolled. Thereafter, all more recent images are searched. Miss rates are computed over all searches noted in row 17 of Table 1 and binned by number of years between search and initial enrollment.

2021/10/28  
13:44:33

FNIR(N, R, T) =  
FPR(N, T) =

False neg. identification rate  
False pos. identification rate

N = Num. enrolled subjects  
R = Num. candidates examined

T = Threshold

T = 0 → Investigation  
T > 0 → Identification

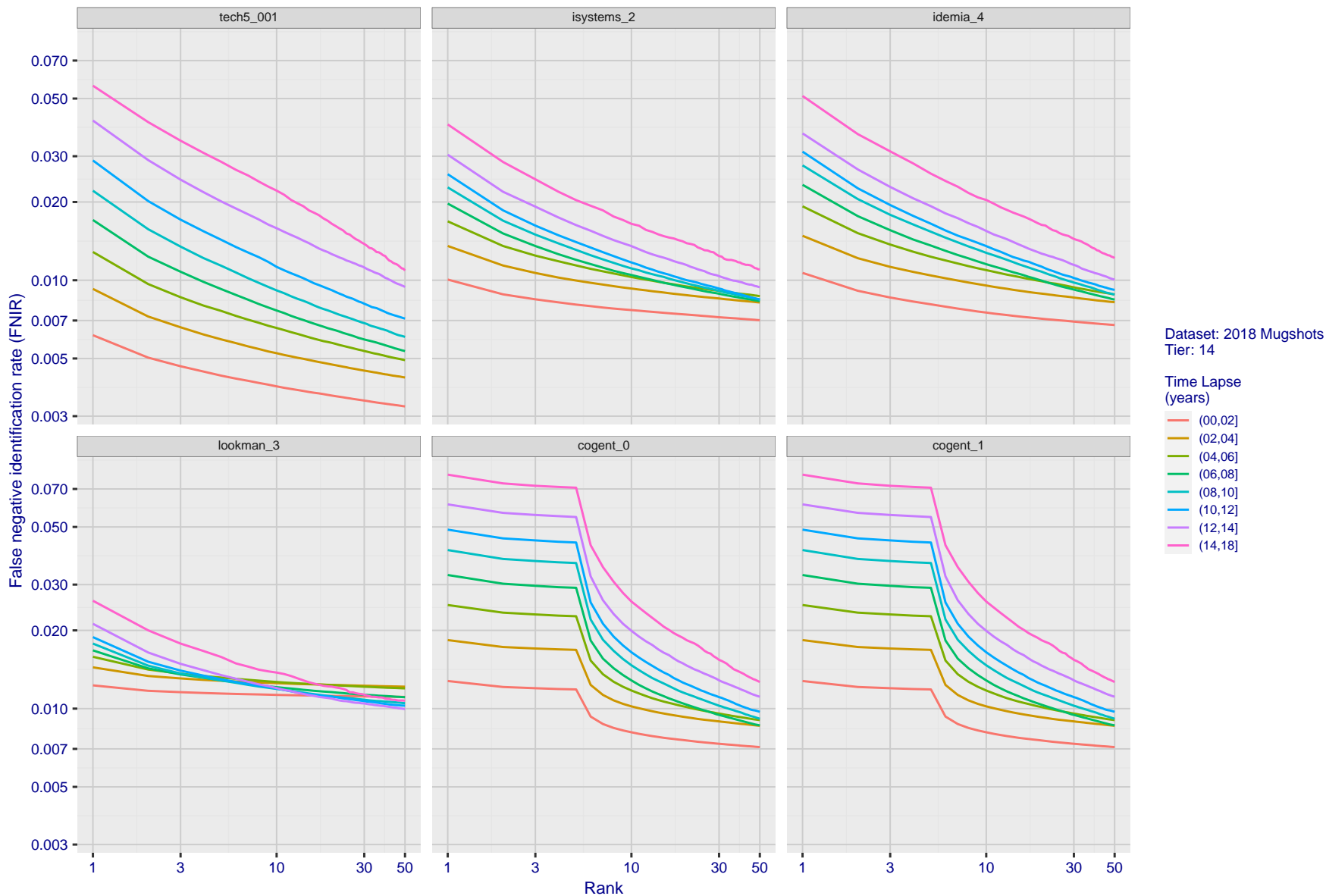


Figure 73: [FRVT-2018 Mugshot Ageing Dataset] Identification miss rates vs. rank by time-elapsd. The oldest image of each individual is enrolled. Thereafter, all more recent images are searched. Miss rates are computed over all searches noted in row 17 of Table 1 and binned by number of years between search and initial enrollment.

2021/10/28  
13:44:33  
FNIR(N, R, T) = False neg. identification rate  
FPR(N, T) = False pos. identification rate  
N = Num. enrolled subjects  
R = Num. candidates examined  
T = Threshold  
T = 0 → Investigation  
T > 0 → Identification

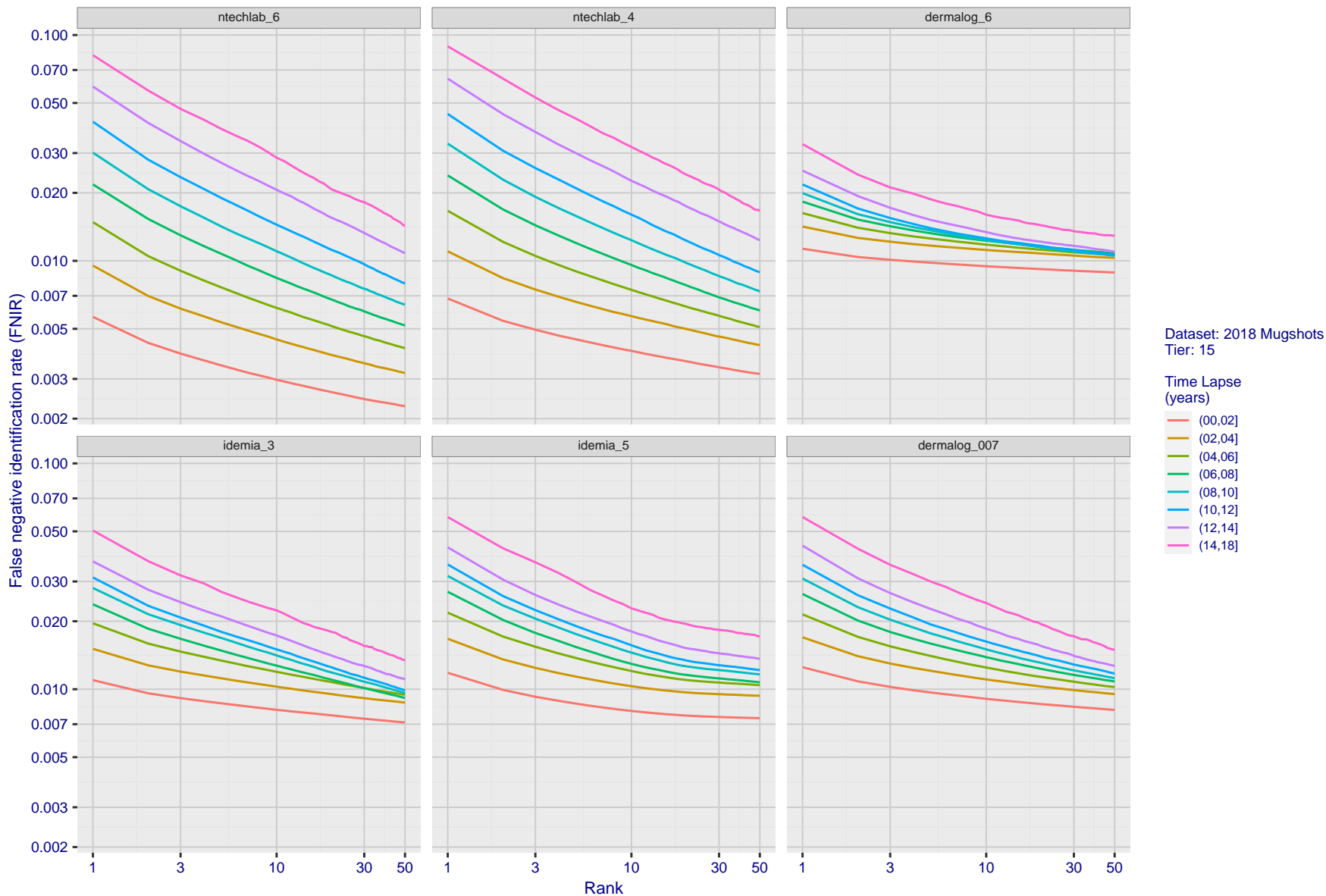


Figure 74: [FRVT-2018 Mugshot Ageing Dataset] Identification miss rates vs. rank by time-elapsd. The oldest image of each individual is enrolled. Thereafter, all more recent images are searched. Miss rates are computed over all searches noted in row 17 of Table 1 and binned by number of years between search and initial enrollment.

2021/10/28  
13:44:33

FNIR(N, R, T) =  
FPIR(N, T) =

False neg. identification rate  
False pos. identification rate

N = Num. enrolled subjects  
R = Num. candidates examined

T = Threshold

T = 0 → Investigation  
T > 0 → Identification

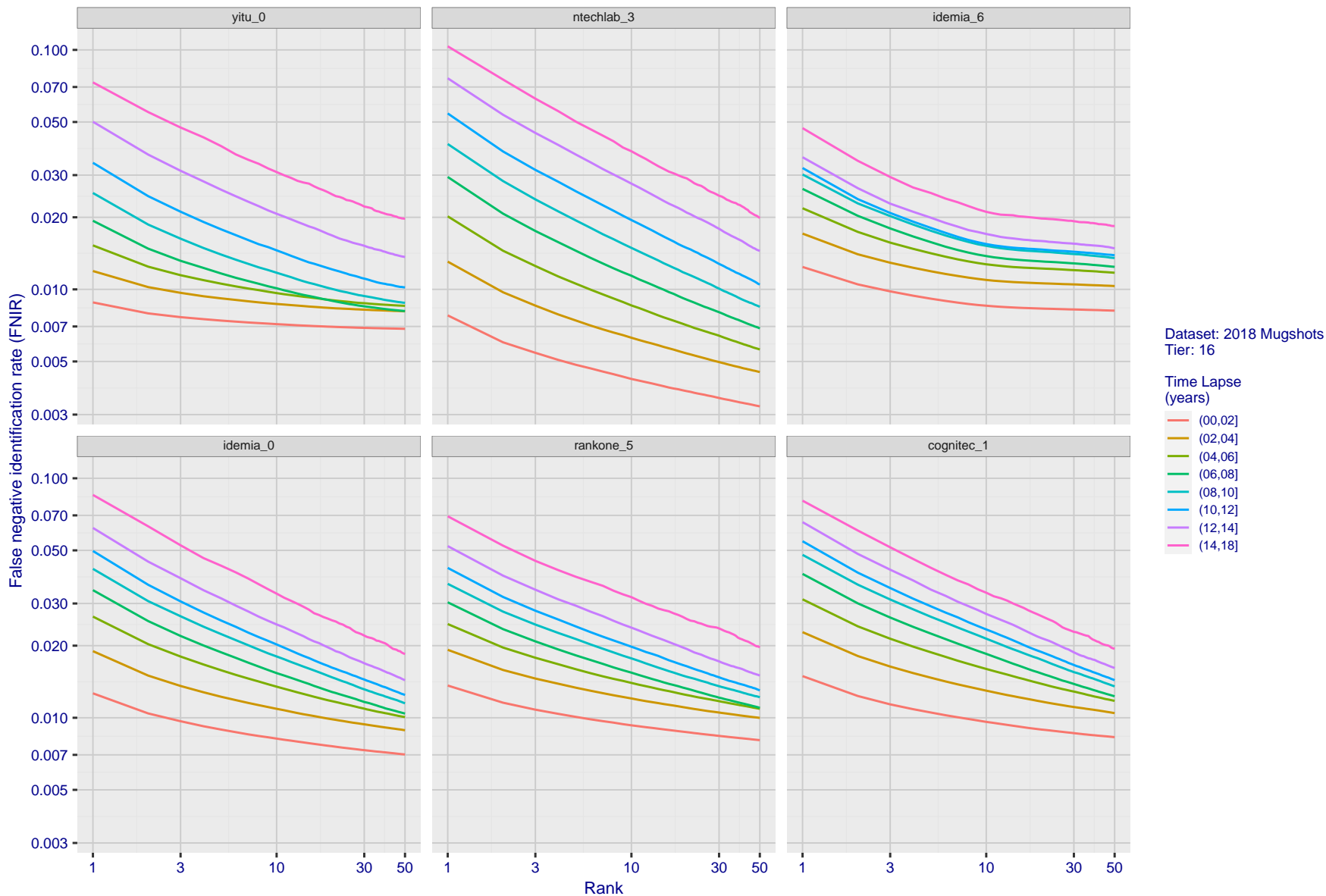


Figure 75: [FRVT-2018 Mugshot Ageing Dataset] Identification miss rates vs. rank by time-elapsd. The oldest image of each individual is enrolled. Thereafter, all more recent images are searched. Miss rates are computed over all searches noted in row 17 of Table 1 and binned by number of years between search and initial enrollment.

2021/10/28  
13:44:33

FNIR(N, R, T) =  
FPR(N, T) =

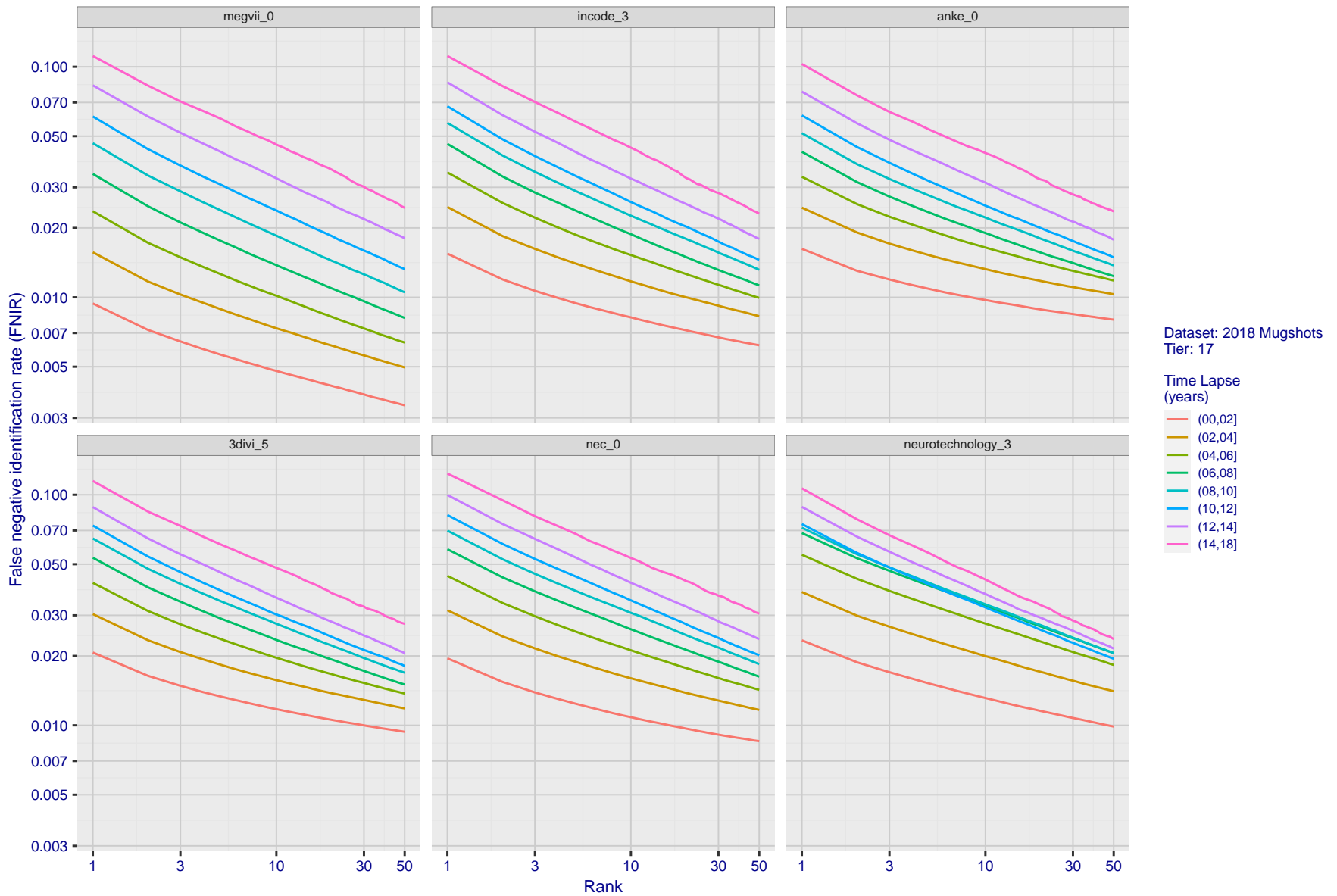
False neg. identification rate  
False pos. identification rate

N = Num. enrolled subjects  
R = Num. candidates examined

T = Threshold

T = 0 → Investigation  
T > 0 → Identification

2021/10/28  
 13:44:33  
 FNIR(N, R, T) =  
 FPR(N, T) =  
 False neg. identification rate  
 False pos. identification rate  
 N = Num. enrolled subjects  
 R = Num. candidates examined  
 T = Threshold  
 T = 0 → Investigation  
 T > 0 → Identification



Dataset: 2018 Mugshots  
 Tier: 17  
 Time Lapse (years)  
 (00,02]  
 (02,04]  
 (04,06]  
 (06,08]  
 (08,10]  
 (10,12]  
 (12,14]  
 (14,18]

Figure 76: [FRVT-2018 Mugshot Ageing Dataset] Identification miss rates vs. rank by time-elapsd. The oldest image of each individual is enrolled. Thereafter, all more recent images are searched. Miss rates are computed over all searches noted in row 17 of Table 1 and binned by number of years between search and initial enrollment.

2021/10/28  
 13:44:33  
 FNIR(N, R, T) = False neg. identification rate  
 FPR(N, T) = False pos. identification rate  
 N = Num. enrolled subjects  
 R = Num. candidates examined  
 T = Threshold  
 T = 0 → Investigation  
 T > 0 → Identification

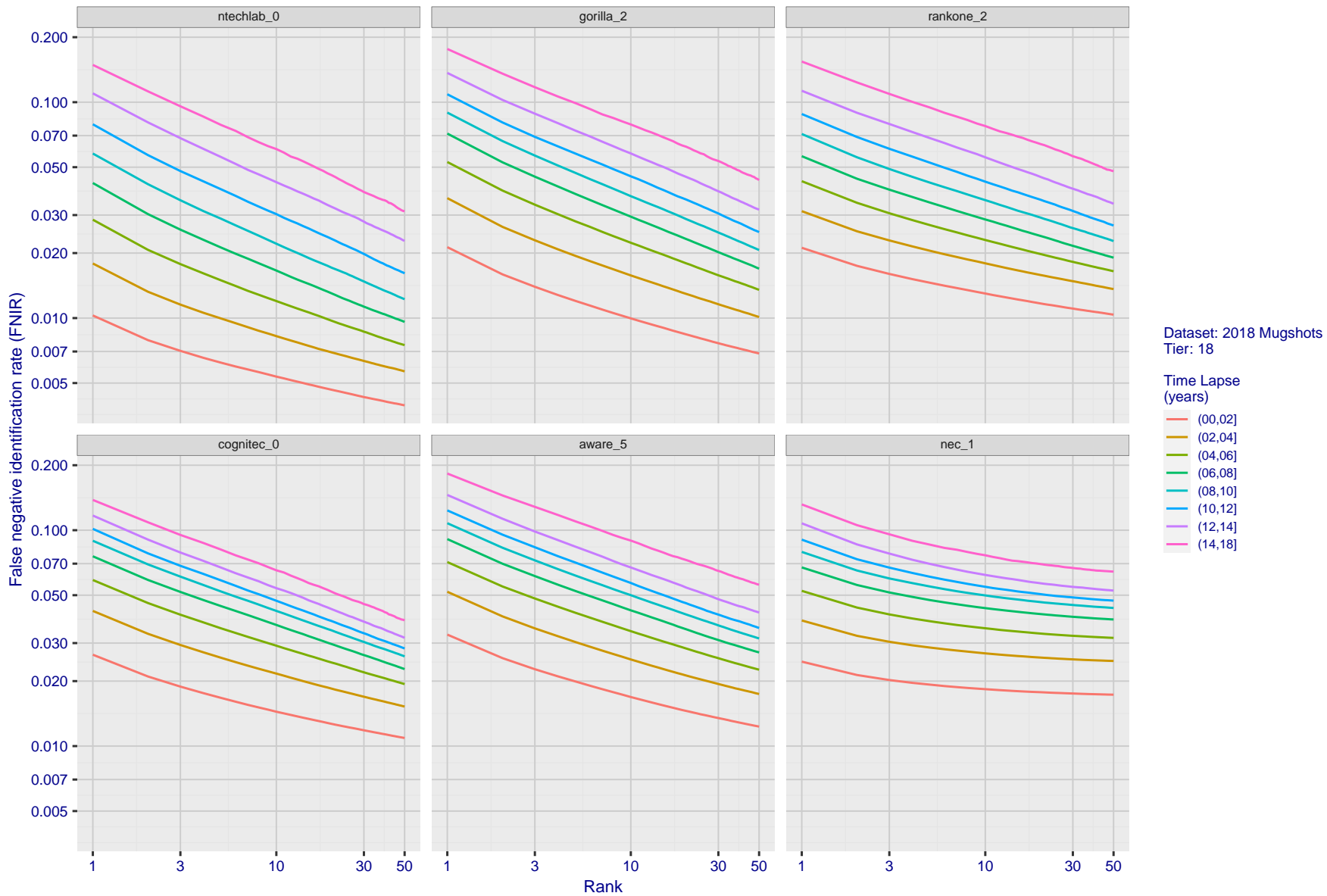


Figure 77: [FRVT-2018 Mugshot Ageing Dataset] Identification miss rates vs. rank by time-elapsd. The oldest image of each individual is enrolled. Thereafter, all more recent images are searched. Miss rates are computed over all searches noted in row 17 of Table 1 and binned by number of years between search and initial enrollment.

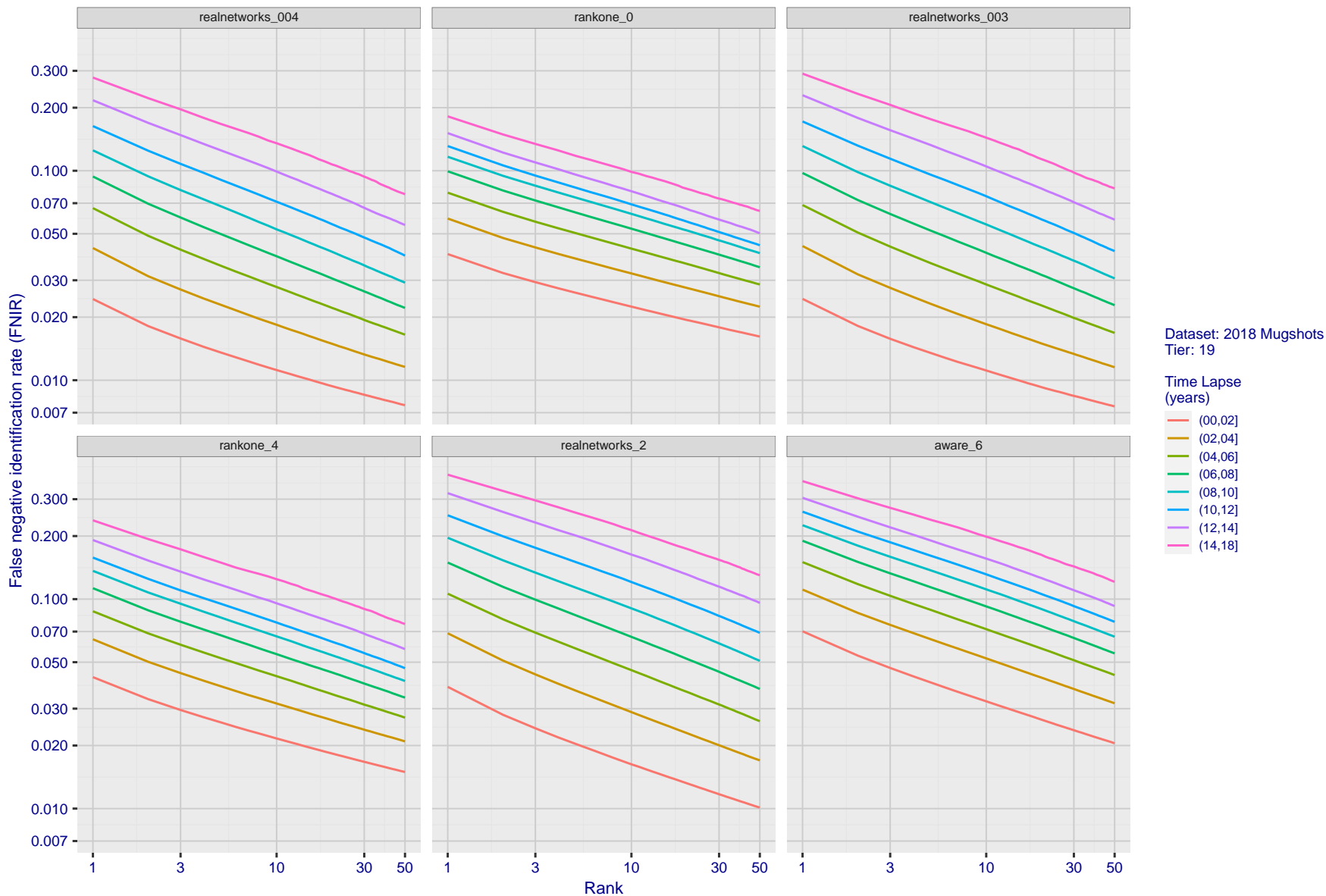


Figure 78: [FRVT-2018 Mugshot Ageing Dataset] Identification miss rates vs. rank by time-elapsd. The oldest image of each individual is enrolled. Thereafter, all more recent images are searched. Miss rates are computed over all searches noted in row 17 of Table 1 and binned by number of years between search and initial enrollment.

2021/10/28  
13:44:33

FNIR(N, R, T) =  
FPNR(N, T) =

False neg. identification rate  
False pos. identification rate

N = Num. enrolled subjects  
R = Num. candidates examined

T = Threshold

T = 0 → Investigation  
T > 0 → Identification

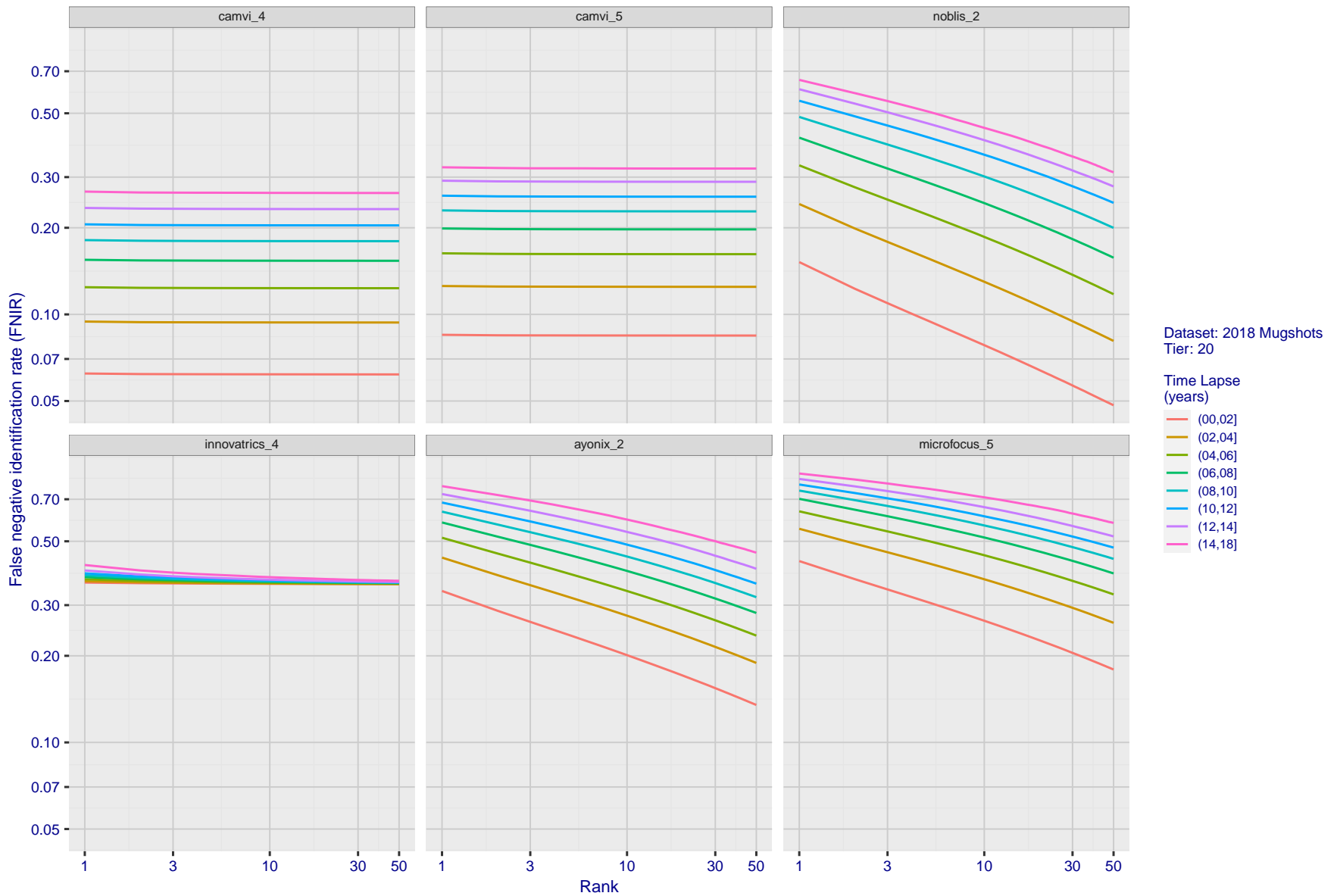


Figure 79: [FRVT-2018 Mugshot Ageing Dataset] Identification miss rates vs. rank by time-elapsd. The oldest image of each individual is enrolled. Thereafter, all more recent images are searched. Miss rates are computed over all searches noted in row 17 of Table 1 and binned by number of years between search and initial enrollment.

2021/10/28  
 13:44:33  
 FNIR(N, R, T) = False neg. identification rate  
 FPR(N, T) = False pos. identification rate  
 N = Num. enrolled subjects  
 R = Num. candidates examined  
 T = Threshold  
 T = 0 → Investigation  
 T > 0 → Identification

2021/10/28  
13:44:33

FNIR(N, R, T) =  
FPR(N, T) =

False neg. identification rate  
False pos. identification rate

N = Num. enrolled subjects  
R = Num. candidates examined

T = Threshold

T = 0 → Investigation  
T > 0 → Identification

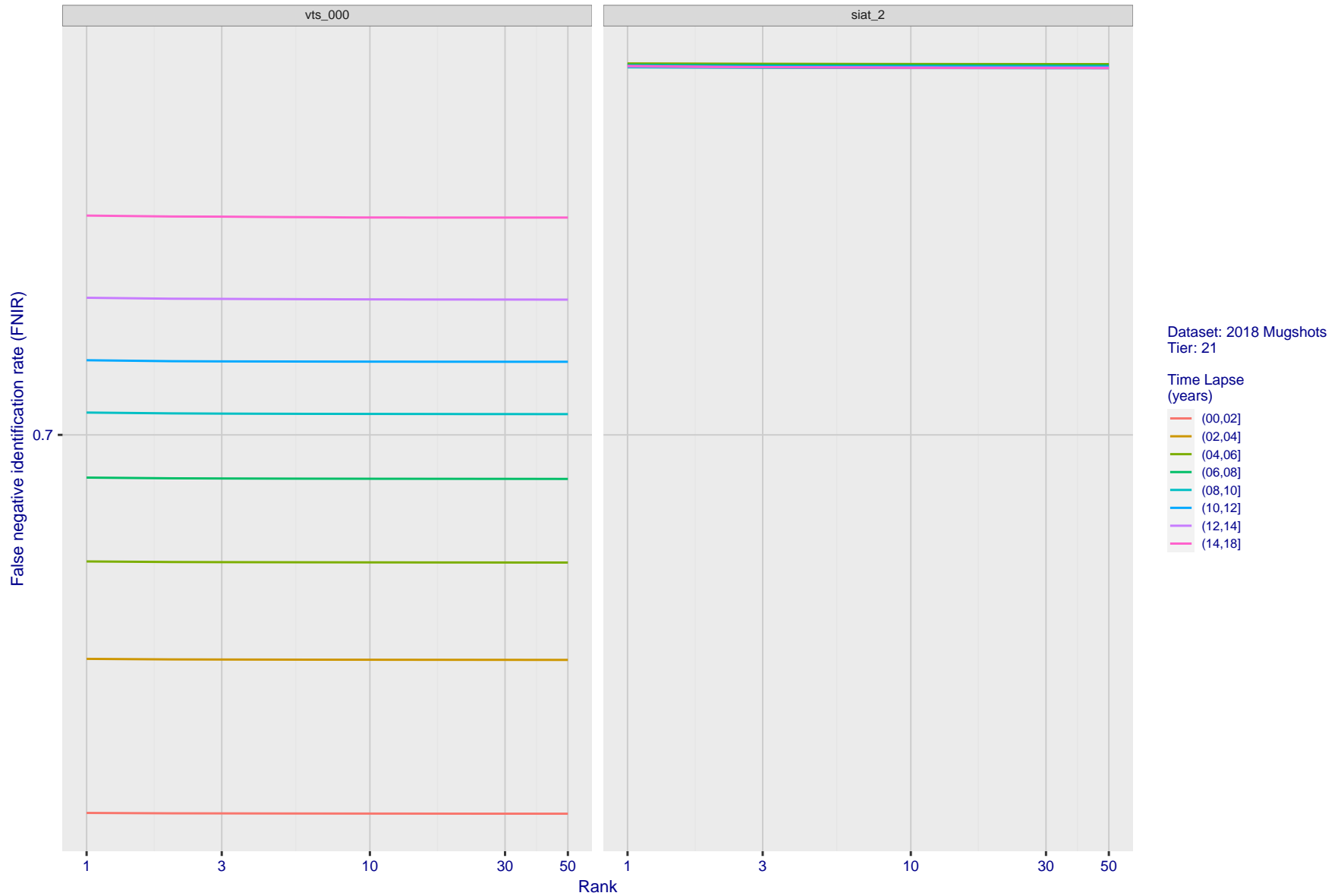


Figure 80: [FRVT-2018 Mugshot Ageing Dataset] Identification miss rates vs. rank by time-elapsd. The oldest image of each individual is enrolled. Thereafter, all more recent images are searched. Miss rates are computed over all searches noted in row 17 of Table 1 and binned by number of years between search and initial enrollment.

---

2021/10/28 FNIR(N, R, T) = False neg. identification rate N = Num. enrolled subjects T = Threshold T = 0 → Investigation  
13:44:33 FPIR(N, T) = False pos. identification rate R = Num. candidates examined T > 0 → Identification

---

2021/10/28  
 13:44:33  
 FNIR(N, R, T) =  
 FPIR(N, T) =  
 False neg. identification rate  
 False pos. identification rate  
 N = Num. enrolled subjects  
 R = Num. candidates examined  
 T = Threshold  
 T = 0 → Investigation  
 T > 0 → Identification

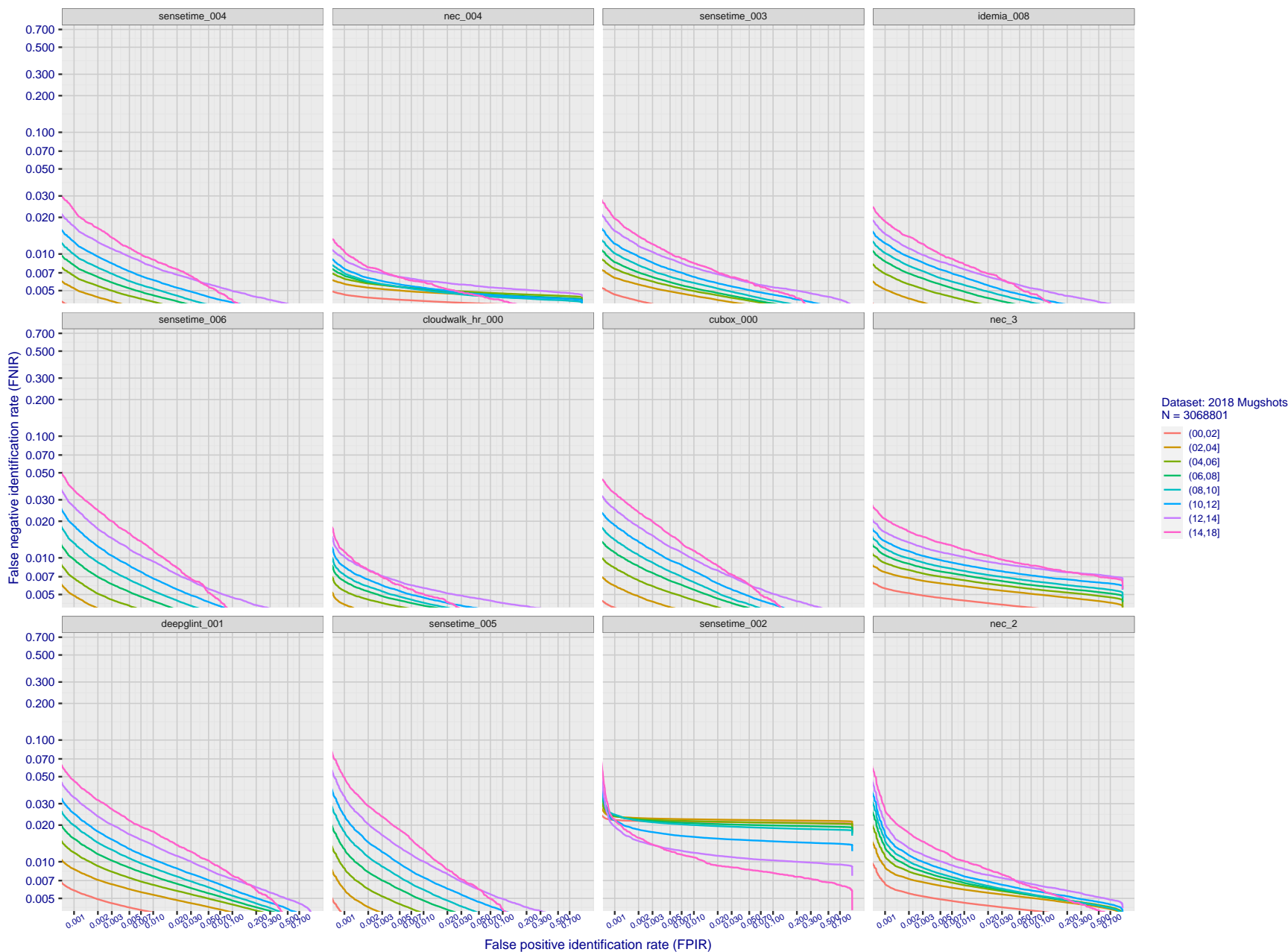


Figure 81: [FRVT-2018 Mugshot Ageing Dataset] Identification miss rates vs. FPIR by time-elapsd. The oldest image of each individual is enrolled. Thereafter, all more recent images are searched. Miss rates are computed over all searches noted in row 17 of Table 1 and binned by number of years between search and initial enrollment. FPIR is computed from the same FRVT 2018 non-mates noted in row 3 of Table 1 with  $N = 3\,000\,000$ .

2021/10/28  
 13:44:33  
 FNIR(N, R, T) =  
 FPIR(N, T) =  
 False neg. identification rate  
 False pos. identification rate  
 N = Num. enrolled subjects  
 R = Num. candidates examined  
 T = Threshold  
 T = 0 → Investigation  
 T > 0 → Identification

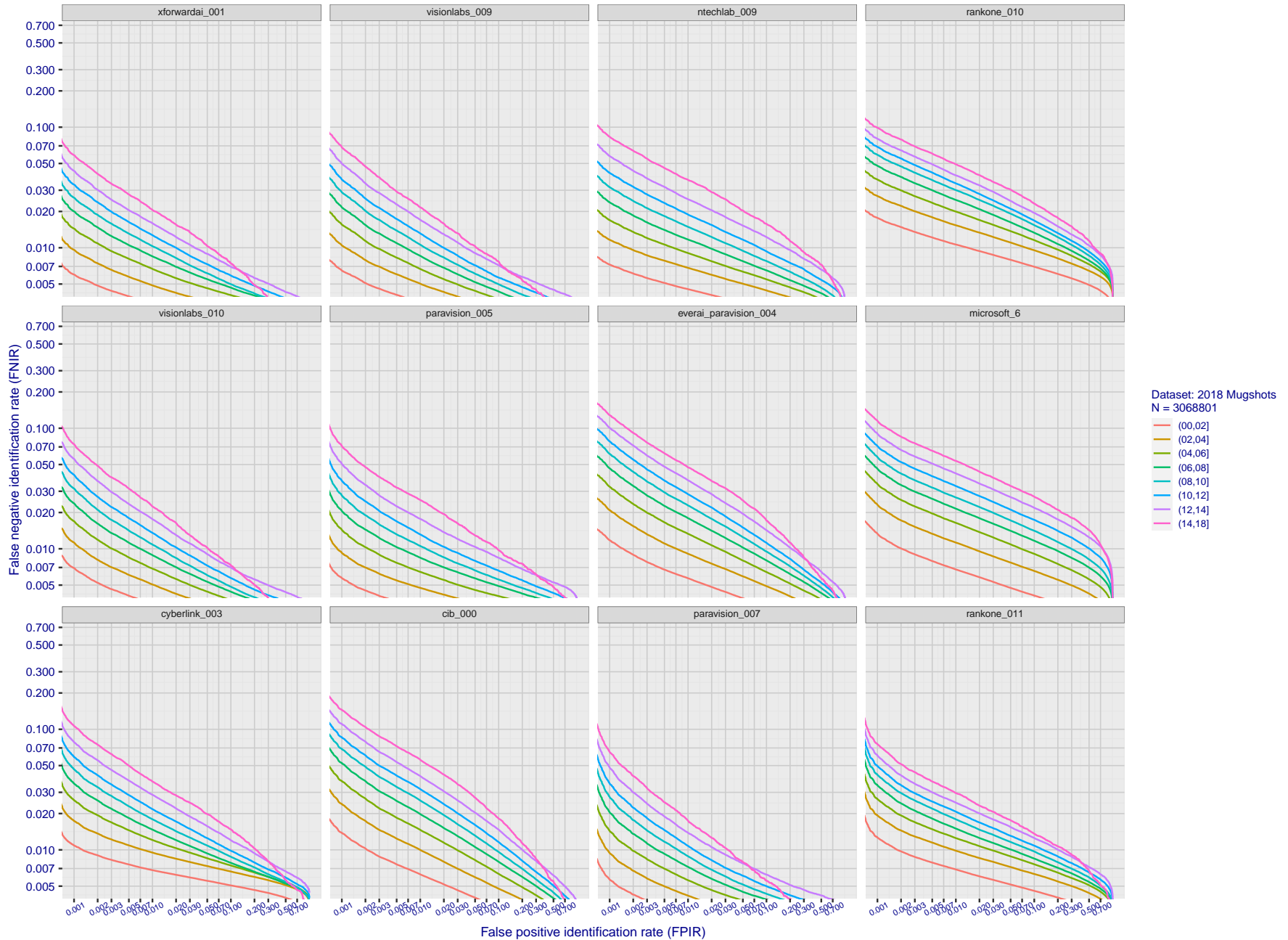


Figure 82: [FRVT-2018 Mugshot Ageing Dataset] Identification miss rates vs. FPIR by time-elapsed. The oldest image of each individual is enrolled. Thereafter, all more recent images are searched. Miss rates are computed over all searches noted in row 17 of Table 1 and binned by number of years between search and initial enrollment. FPIR is computed from the same FRVT 2018 non-mates noted in row 3 of Table 1 with  $N = 3\,000\,000$ .

2021/10/28  
 13:44:33  
 FNIR(N, R, T) =  
 FPIR(N, T) =  
 False neg. identification rate  
 False pos. identification rate  
 N = Num. enrolled subjects  
 R = Num. candidates examined  
 T = Threshold  
 T = 0 → Investigation  
 T > 0 → Identification

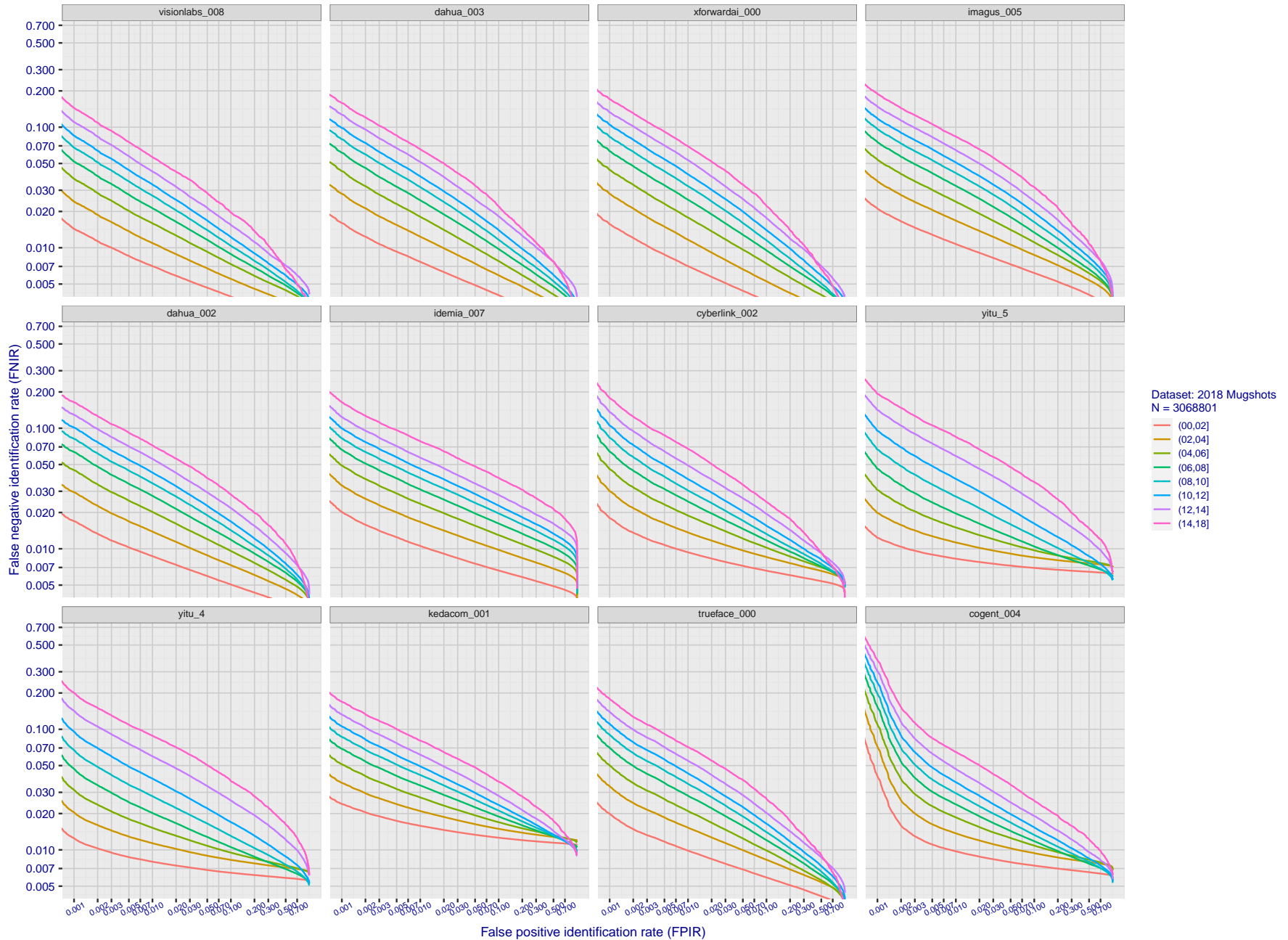


Figure 83: [FRVT-2018 Mugshot Ageing Dataset] Identification miss rates vs. FPIR by time-elapsd. The oldest image of each individual is enrolled. Thereafter, all more recent images are searched. Miss rates are computed over all searches noted in row 17 of Table 1 and binned by number of years between search and initial enrollment. FPIR is computed from the same FRVT 2018 non-mates noted in row 3 of Table 1 with  $N = 3\,000\,000$ .

2021/10/28  
 13:44:33  
 FNIR(N, R, T) =  
 FPIR(N, T) =  
 False neg. identification rate  
 False pos. identification rate  
 N = Num. enrolled subjects  
 R = Num. candidates examined  
 T = Threshold  
 T = 0 → Investigation  
 T > 0 → Identification

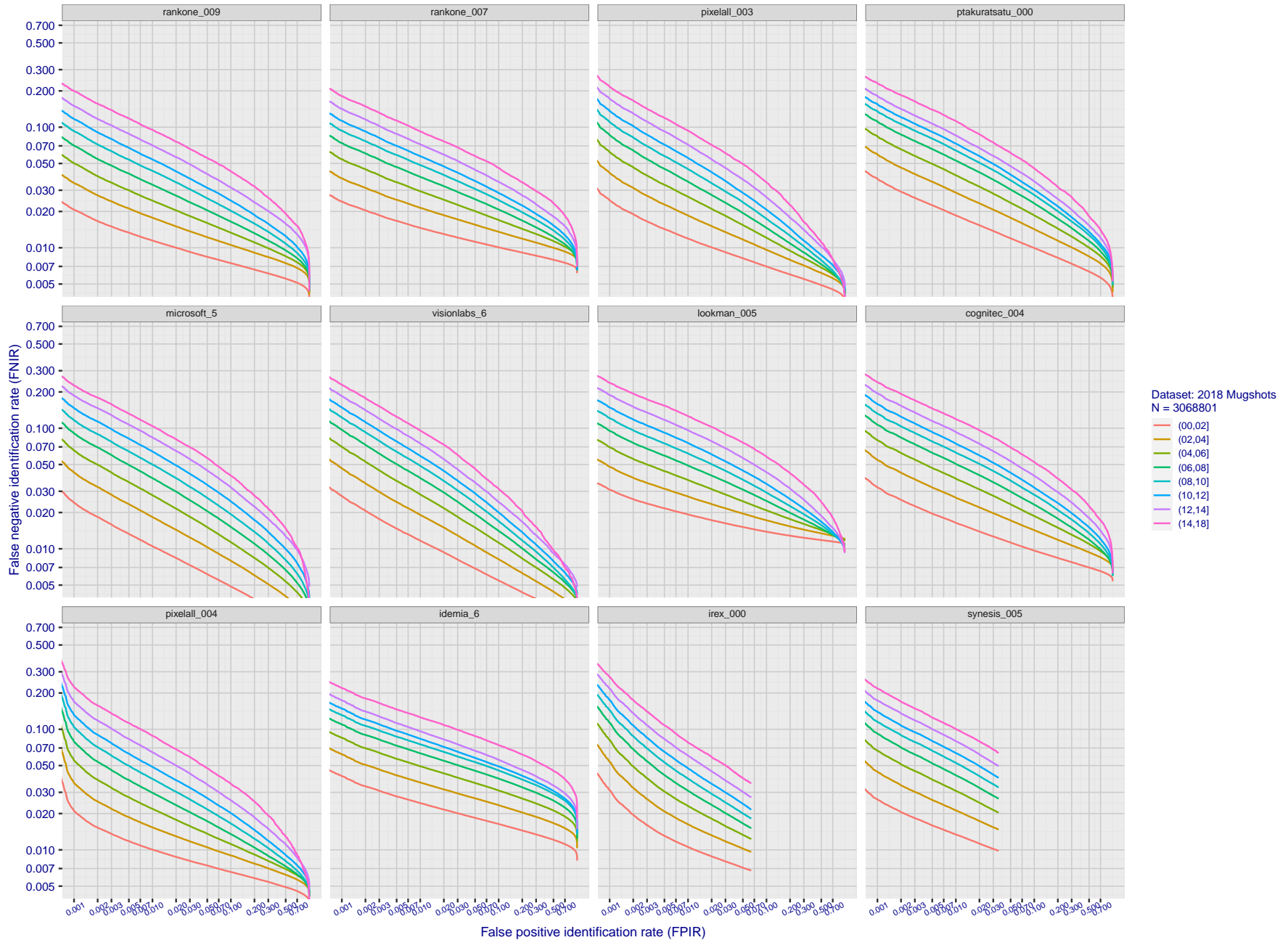


Figure 84: [FRVT-2018 Mugshot Ageing Dataset] Identification miss rates vs. FPIR by time-elapsd. The oldest image of each individual is enrolled. Thereafter, all more recent images are searched. Miss rates are computed over all searches noted in row 17 of Table 1 and binned by number of years between search and initial enrollment. FPIR is computed from the same FRVT 2018 non-mates noted in row 3 of Table 1 with  $N = 3\,000\,000$ .

2021/10/28  
 FNIR(N, R, T) =  
 FPIR(N, T) =  
 False neg. identification rate  
 False pos. identification rate  
 N = Num. enrolled subjects  
 R = Num. candidates examined  
 T = Threshold  
 T = 0 → Investigation  
 T > 0 → Identification

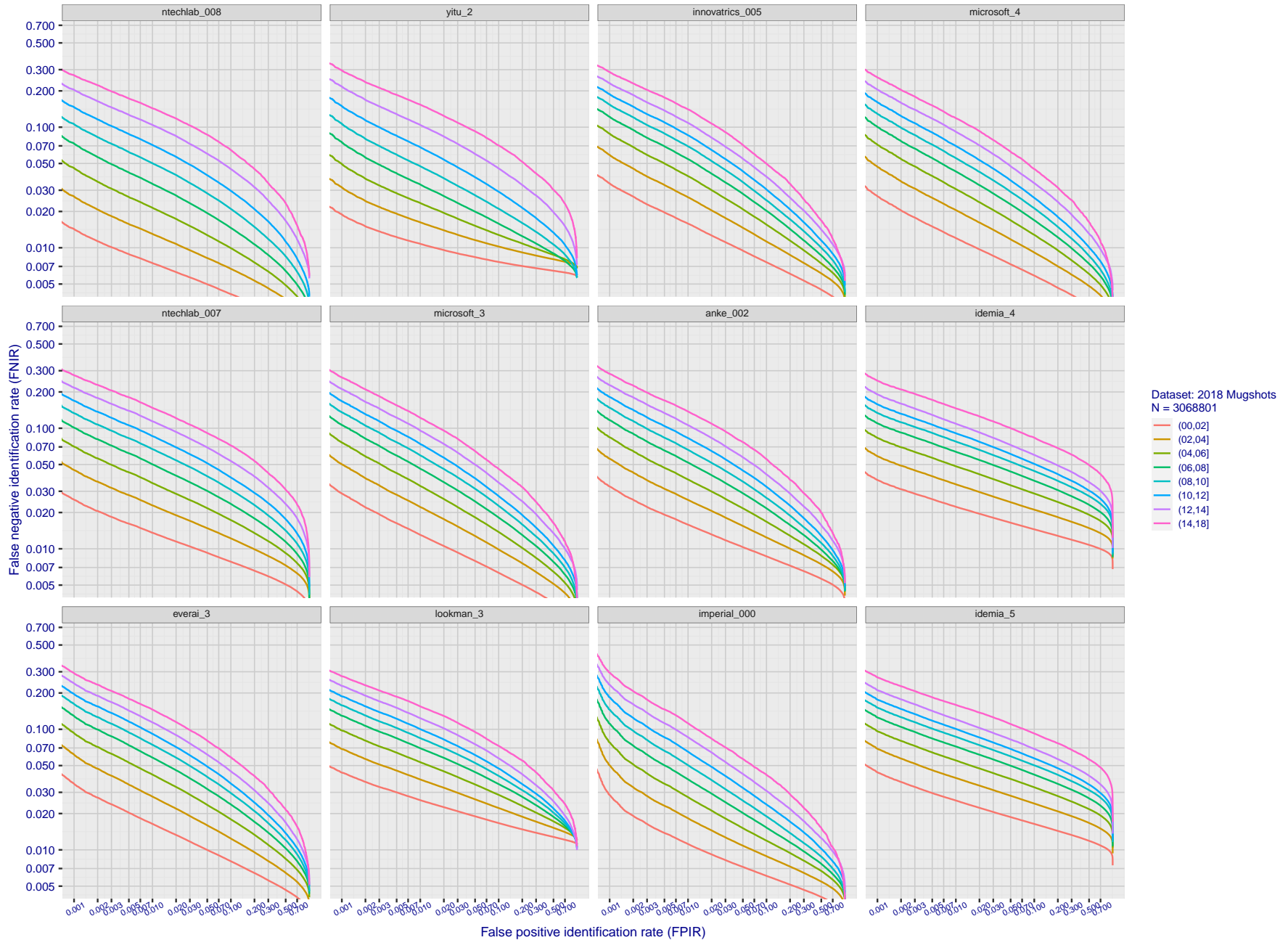


Figure 85: [FRVT-2018 Mugshot Ageing Dataset] Identification miss rates vs. FPIR by time-elapsd. The oldest image of each individual is enrolled. Thereafter, all more recent images are searched. Miss rates are computed over all searches noted in row 17 of Table 1 and binned by number of years between search and initial enrollment. FPIR is computed from the same FRVT 2018 non-mates noted in row 3 of Table 1 with  $N = 3\,000\,000$ .

2021/10/28  
 13:44:33  
 FNIR(N, R, T) =  
 FPIR(N, T) =  
 False neg. identification rate  
 False pos. identification rate  
 N = Num. enrolled subjects  
 R = Num. candidates examined  
 T = Threshold  
 T = 0 → Investigation  
 T > 0 → Identification

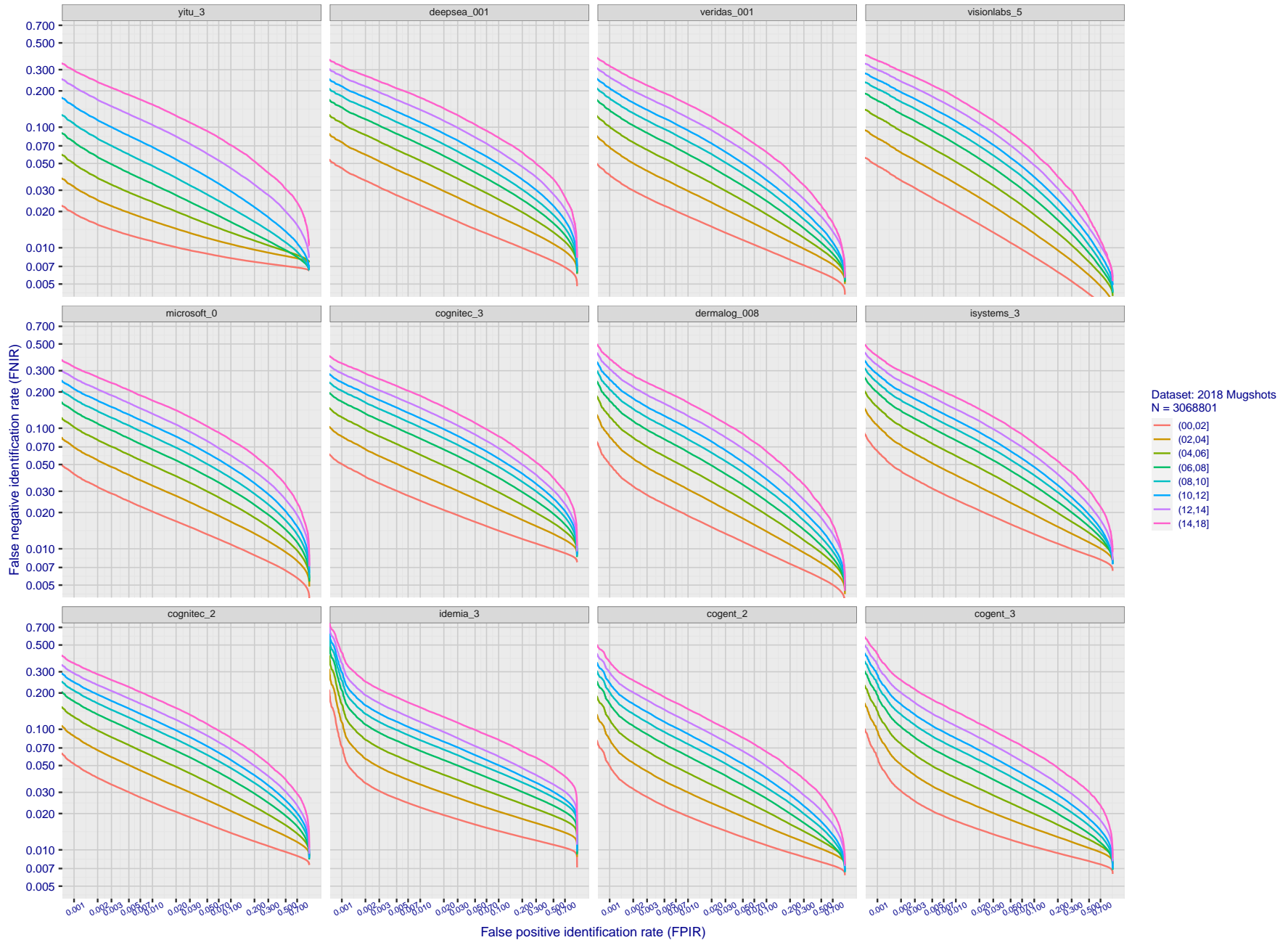


Figure 86: [FRVT-2018 Mugshot Ageing Dataset] Identification miss rates vs. FPIR by time-elapsd. The oldest image of each individual is enrolled. Thereafter, all more recent images are searched. Miss rates are computed over all searches noted in row 17 of Table 1 and binned by number of years between search and initial enrollment. FPIR is computed from the same FRVT 2018 non-mates noted in row 3 of Table 1 with N = 3 000 000.

2021/10/28  
 13:44:33  
 FNIR(N, R, T) =  
 FPR(N, T) =  
 False neg. identification rate  
 False pos. identification rate  
 N = Num. enrolled subjects  
 R = Num. candidates examined  
 T = Threshold  
 T = 0 → Investigation  
 T > 0 → Identification

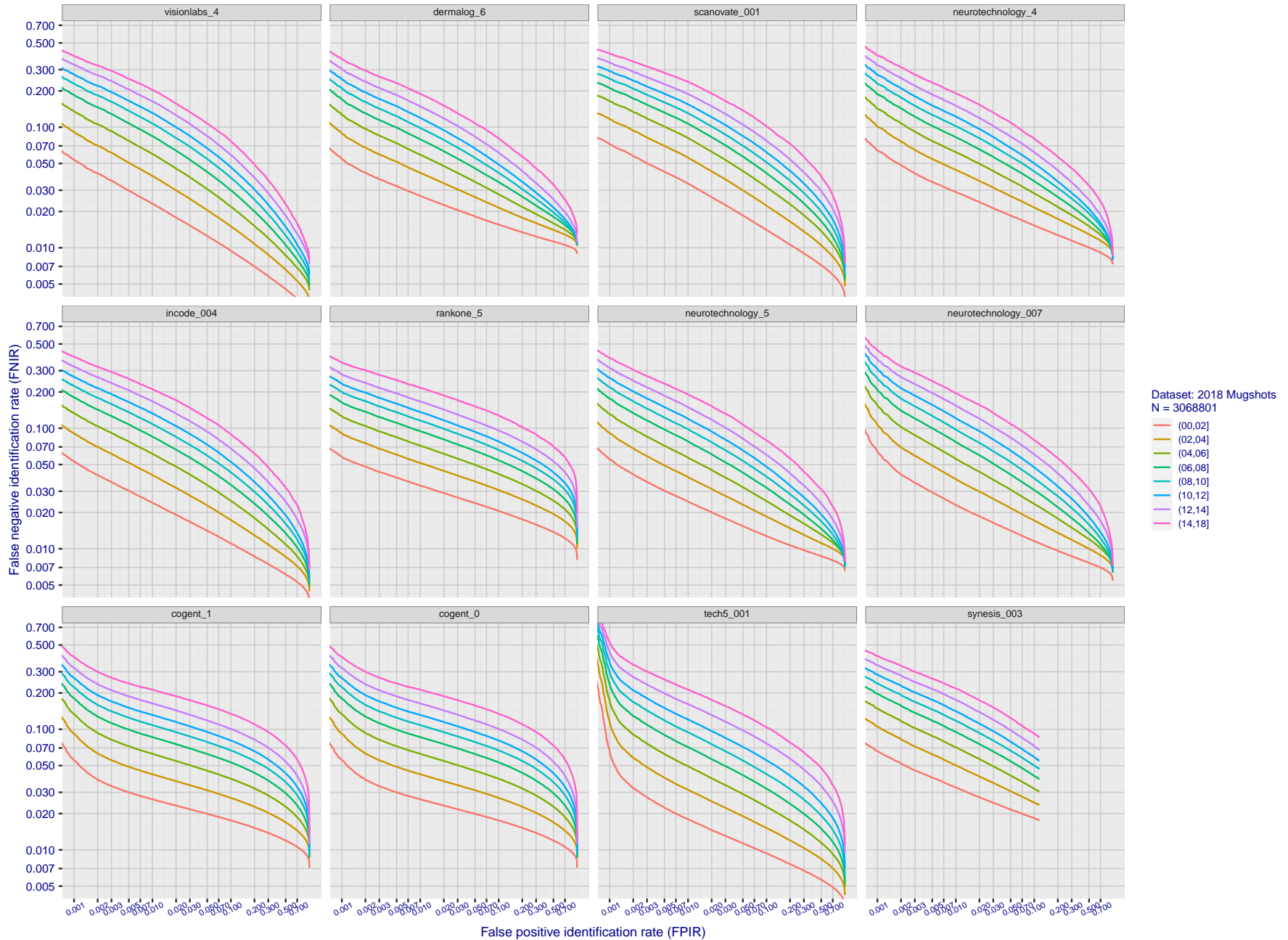


Figure 87: [FRVT-2018 Mugshot Ageing Dataset] Identification miss rates vs. FPIR by time-elapsd. The oldest image of each individual is enrolled. Thereafter, all more recent images are searched. Miss rates are computed over all searches noted in row 17 of Table 1 and binned by number of years between search and initial enrollment. FPIR is computed from the same FRVT 2018 non-mates noted in row 3 of Table 1 with  $N = 3\,000\,000$ .

2021/10/28  
 13:44:33  
 FNIR(N, R, T) =  
 FPR(N, T) =  
 False neg. identification rate  
 False pos. identification rate  
 N = Num. enrolled subjects  
 R = Num. candidates examined  
 T = Threshold  
 T = 0 → Investigation  
 T > 0 → Identification

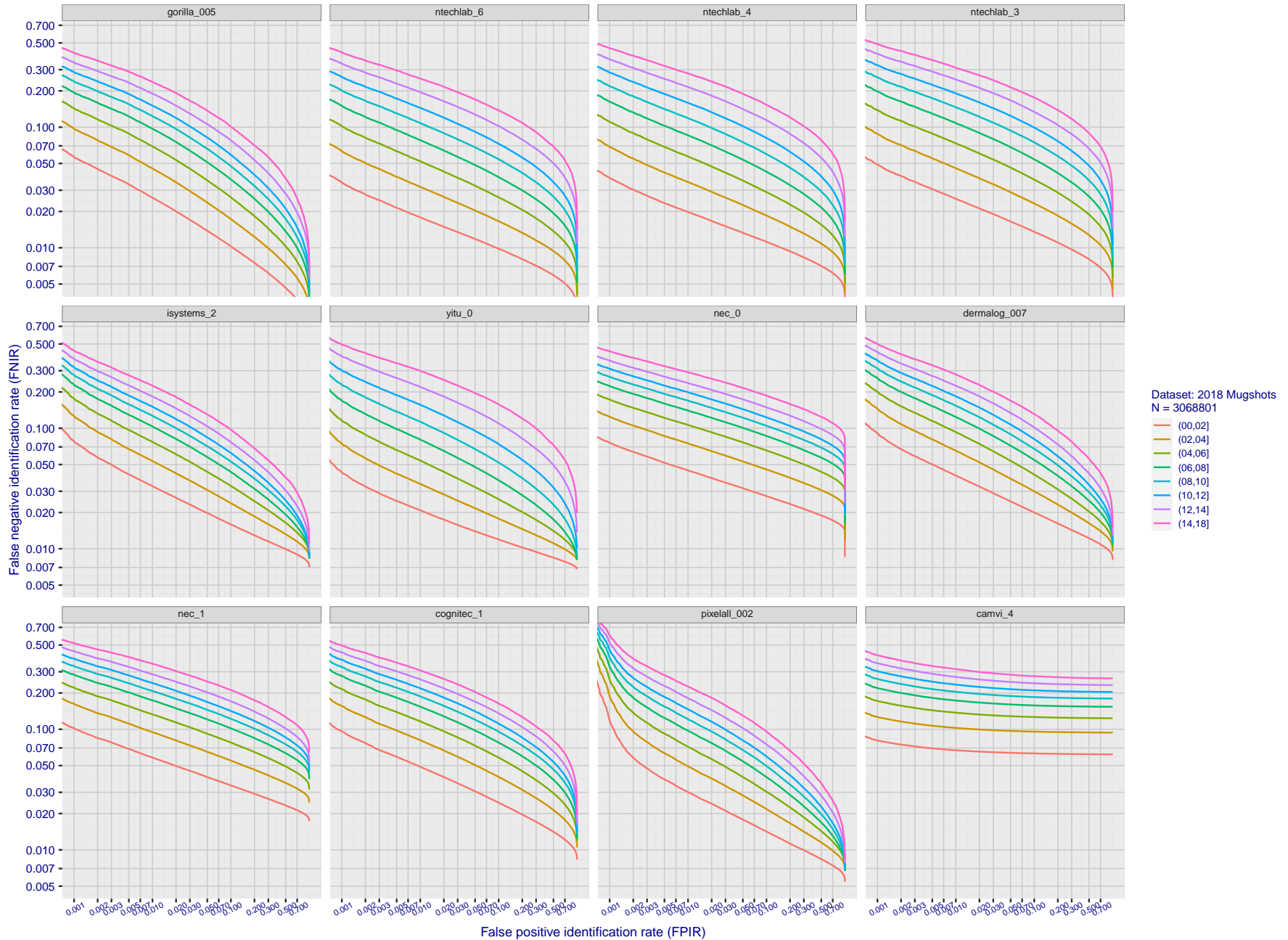


Figure 88: [FRVT-2018 Mugshot Ageing Dataset] Identification miss rates vs. FPIR by time-elapsd. The oldest image of each individual is enrolled. Thereafter, all more recent images are searched. Miss rates are computed over all searches noted in row 17 of Table 1 and binned by number of years between search and initial enrollment. FPIR is computed from the same FRVT 2018 non-mates noted in row 3 of Table 1 with  $N = 3\,000\,000$ .

2021/10/28  
 13:44:33  
 FNIR(N, R, T) =  
 FPR(N, T) =  
 False neg. identification rate  
 False pos. identification rate  
 N = Num. enrolled subjects  
 R = Num. candidates examined  
 T = Threshold  
 T = 0 → Investigation  
 T > 0 → Identification

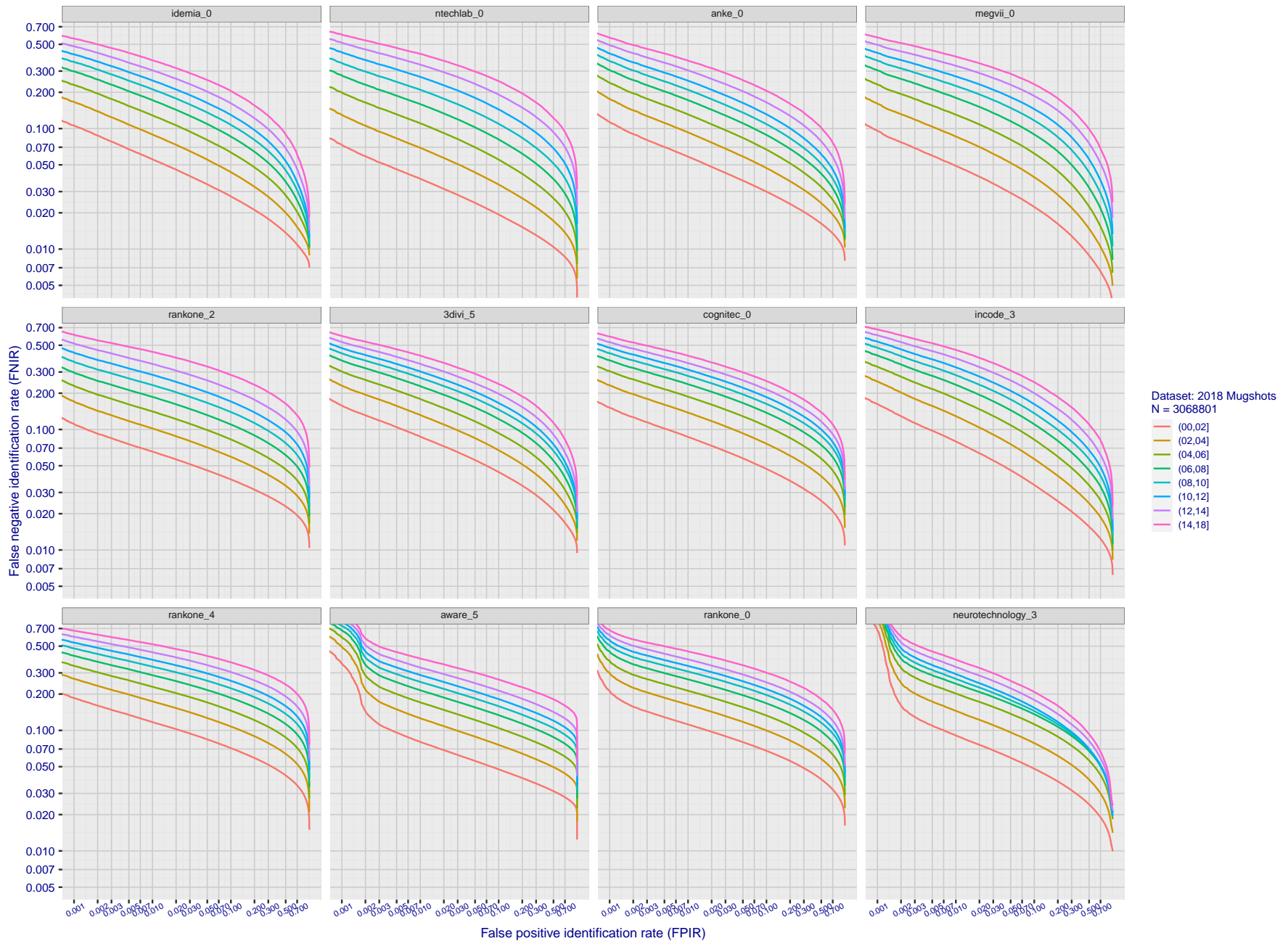


Figure 89: [FRVT-2018 Mugshot Ageing Dataset] Identification miss rates vs. FPIR by time-elapsing. The oldest image of each individual is enrolled. Thereafter, all more recent images are searched. Miss rates are computed over all searches noted in row 17 of Table 1 and binned by number of years between search and initial enrollment. FPIR is computed from the same FRVT 2018 non-mates noted in row 3 of Table 1 with  $N = 3\,000\,000$ .

2021/10/28  
 13:44:33  
 FNIR(N, R, T) =  
 FPR(N, T) =  
 False neg. identification rate  
 False pos. identification rate  
 N = Num. enrolled subjects  
 R = Num. candidates examined  
 T = Threshold  
 T = 0 → Investigation  
 T > 0 → Identification

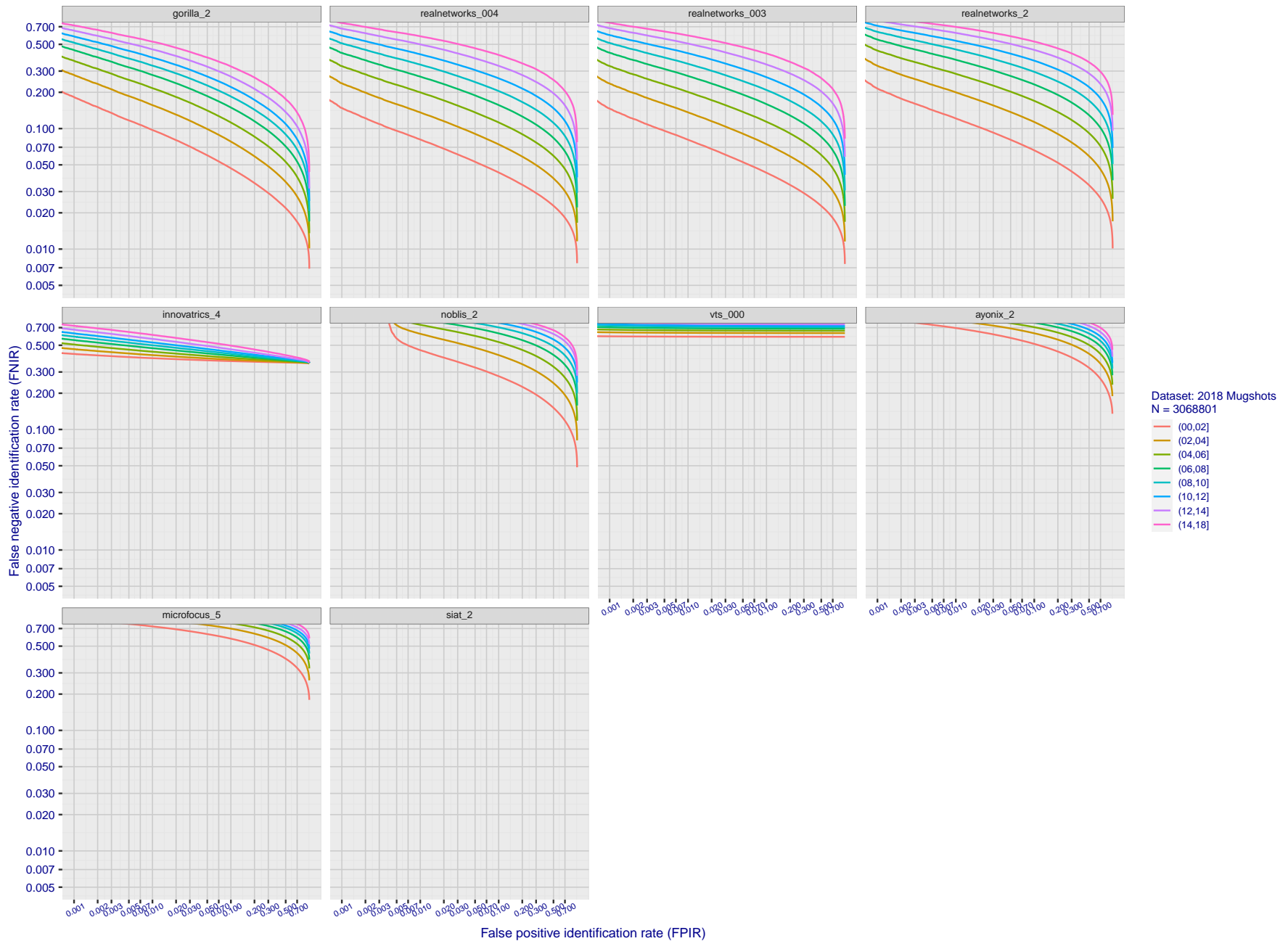


Figure 90: [FRVT-2018 Mugshot Ageing Dataset] Identification miss rates vs. FPIR by time-elapsed. The oldest image of each individual is enrolled. Thereafter, all more recent images are searched. Miss rates are computed over all searches noted in row 17 of Table 1 and binned by number of years between search and initial enrollment. FPIR is computed from the same FRVT 2018 non-mates noted in row 3 of Table 1 with  $N = 3\,000\,000$ .

---

2021/10/28 FNIR(N, R, T) = False neg. identification rate N = Num. enrolled subjects T = Threshold T = 0 → Investigation  
13:44:33 FPIR(N, T) = False pos. identification rate R = Num. candidates examined T > 0 → Identification

2021/10/28 13:44:33  
 FNIR(N, R, T) = False neg. identification rate  
 FPIR(N, T) = False pos. identification rate  
 N = Num. enrolled subjects  
 R = Num. candidates examined  
 T = Threshold  
 T = 0 → Investigation  
 T > 0 → Identification

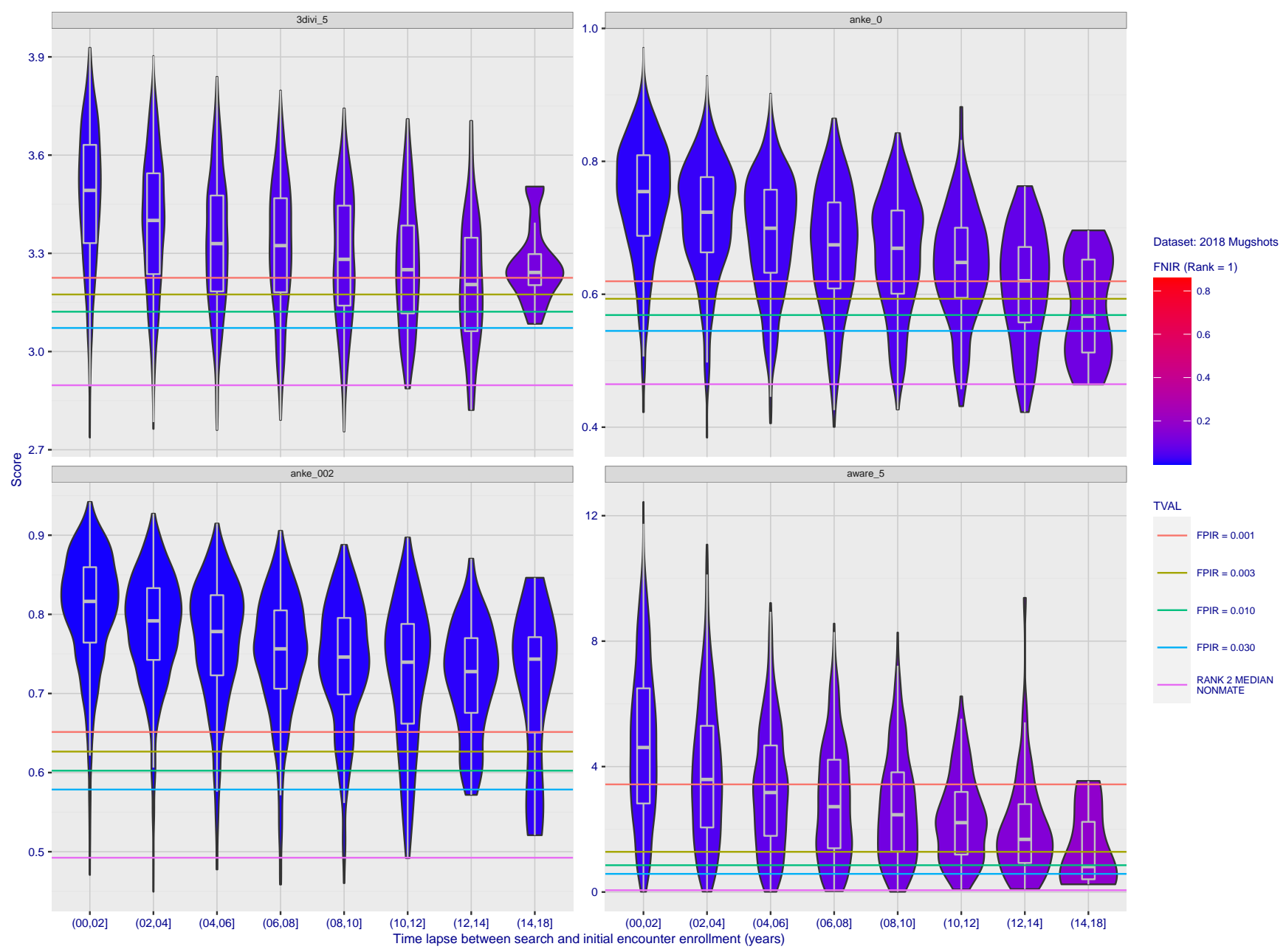


Figure 91: [FRVT-2018 Mugshot Ageing Dataset] Native mate scores vs. time-elapsed. The oldest image of each individual is enrolled. Thereafter, all more recent images are searched. Mated score distributions are computed over all searches noted in row 17 of Table 1 binned by number of years between search and initial enrollment.

2021/10/28  
13:44:33

FNIR(N, R, T) = False neg. identification rate  
FPIR(N, T) = False pos. identification rate

N = Num. enrolled subjects  
R = Num. candidates examined

T = Threshold

T = 0 → Investigation  
T > 0 → Identification

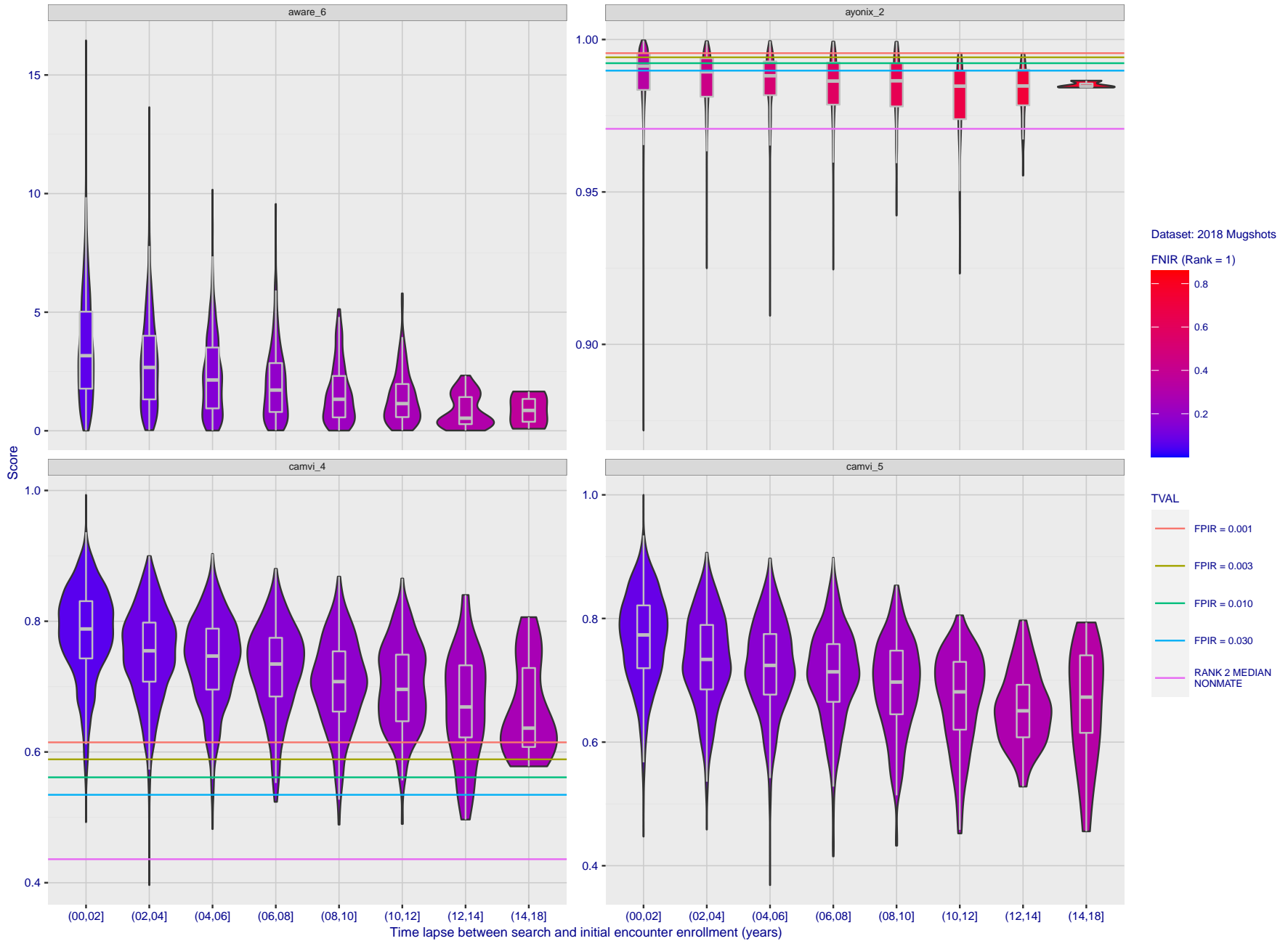


Figure 92: [FRVT-2018 Mugshot Ageing Dataset] Native mate scores vs. time-elapsed. The oldest image of each individual is enrolled. Thereafter, all more recent images are searched. Mated score distributions are computed over all searches noted in row 17 of Table 1 binned by number of years between search and initial enrollment.

2021/10/28 13:44:33  
 FNIR(N, R, T) = False neg. identification rate  
 FPIR(N, T) = False pos. identification rate  
 N = Num. enrolled subjects  
 R = Num. candidates examined  
 T = Threshold  
 T = 0 → Investigation  
 T > 0 → Identification

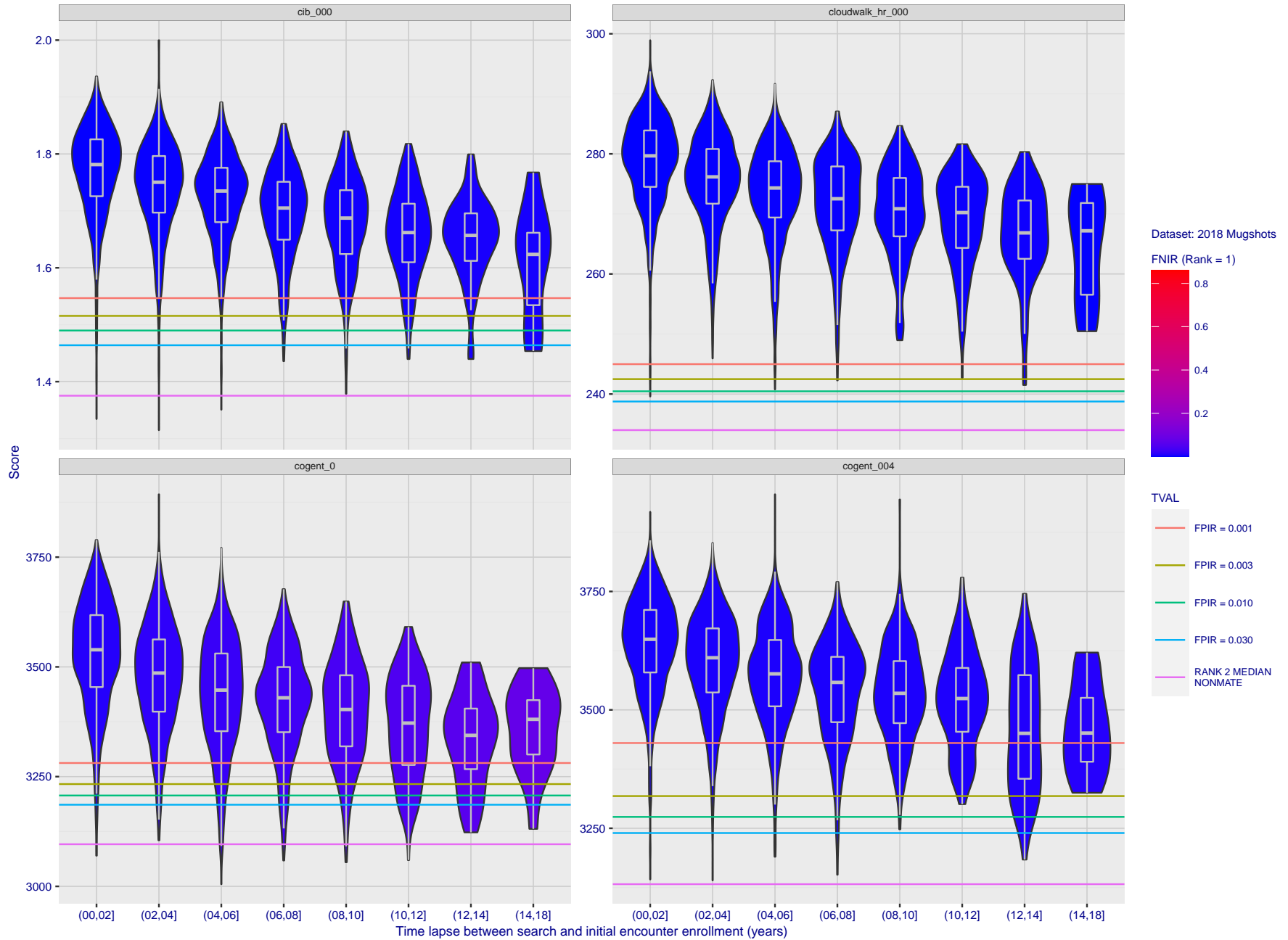


Figure 93: [FRVT-2018 Mugshot Ageing Dataset] Native mate scores vs. time-elapsed. The oldest image of each individual is enrolled. Thereafter, all more recent images are searched. Mated score distributions are computed over all searches noted in row 17 of Table 1 binned by number of years between search and initial enrollment.

2021/10/28 13:44:33  
 FNIR(N, R, T) = False neg. identification rate  
 FPIR(N, T) = False pos. identification rate  
 N = Num. enrolled subjects  
 R = Num. candidates examined  
 T = Threshold  
 T = 0 → Investigation  
 T > 0 → Identification

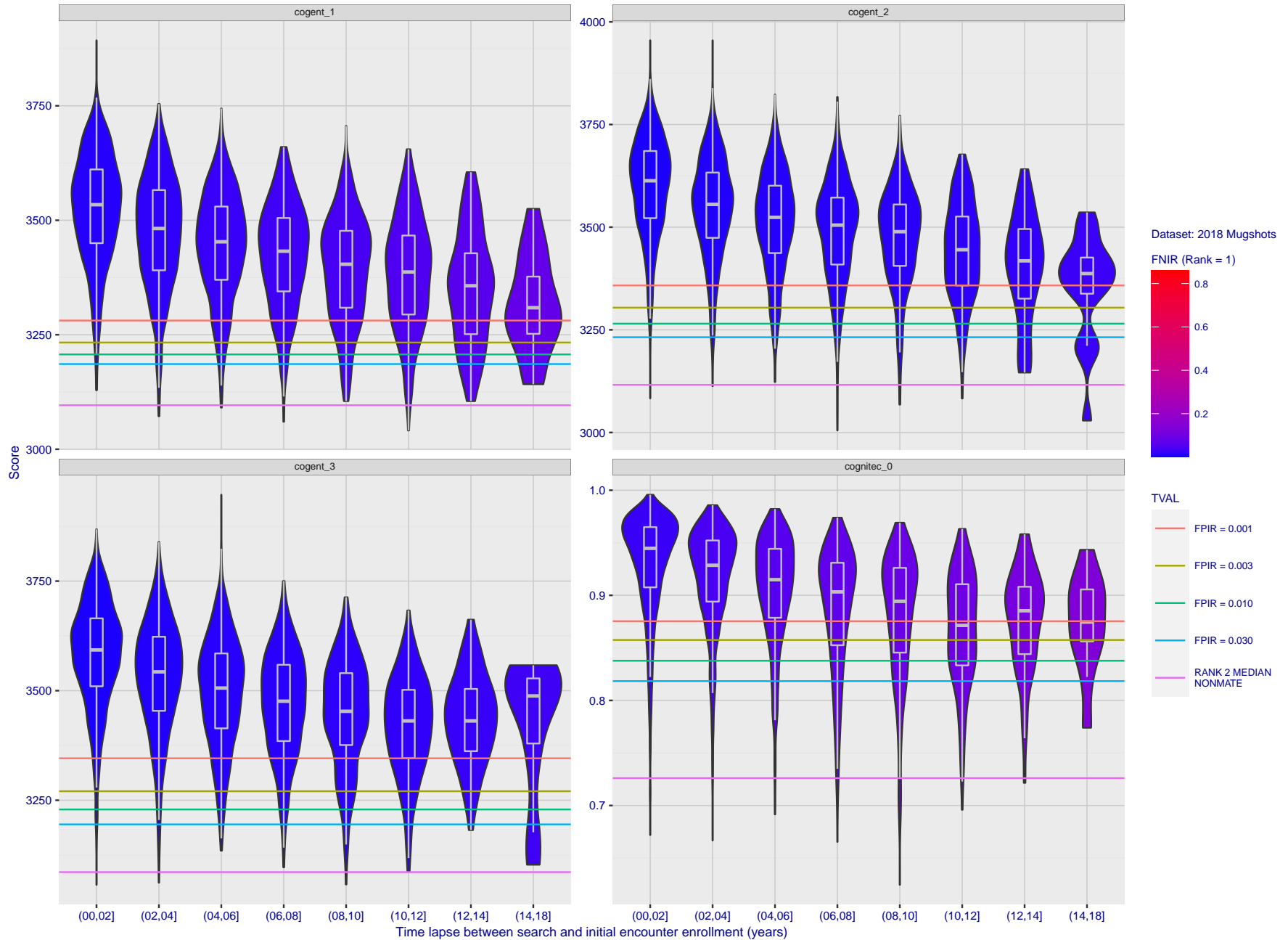


Figure 94: [FRVT-2018 Mugshot Ageing Dataset] Native mate scores vs. time-elapsed. The oldest image of each individual is enrolled. Thereafter, all more recent images are searched. Mated score distributions are computed over all searches noted in row 17 of Table 1 binned by number of years between search and initial enrollment.

2021/10/28  
13:44:33

FNIR(N, R, T) = False neg. identification rate  
FPIR(N, T) = False pos. identification rate

N = Num. enrolled subjects  
R = Num. candidates examined

T = Threshold

T = 0 → Investigation  
T > 0 → Identification

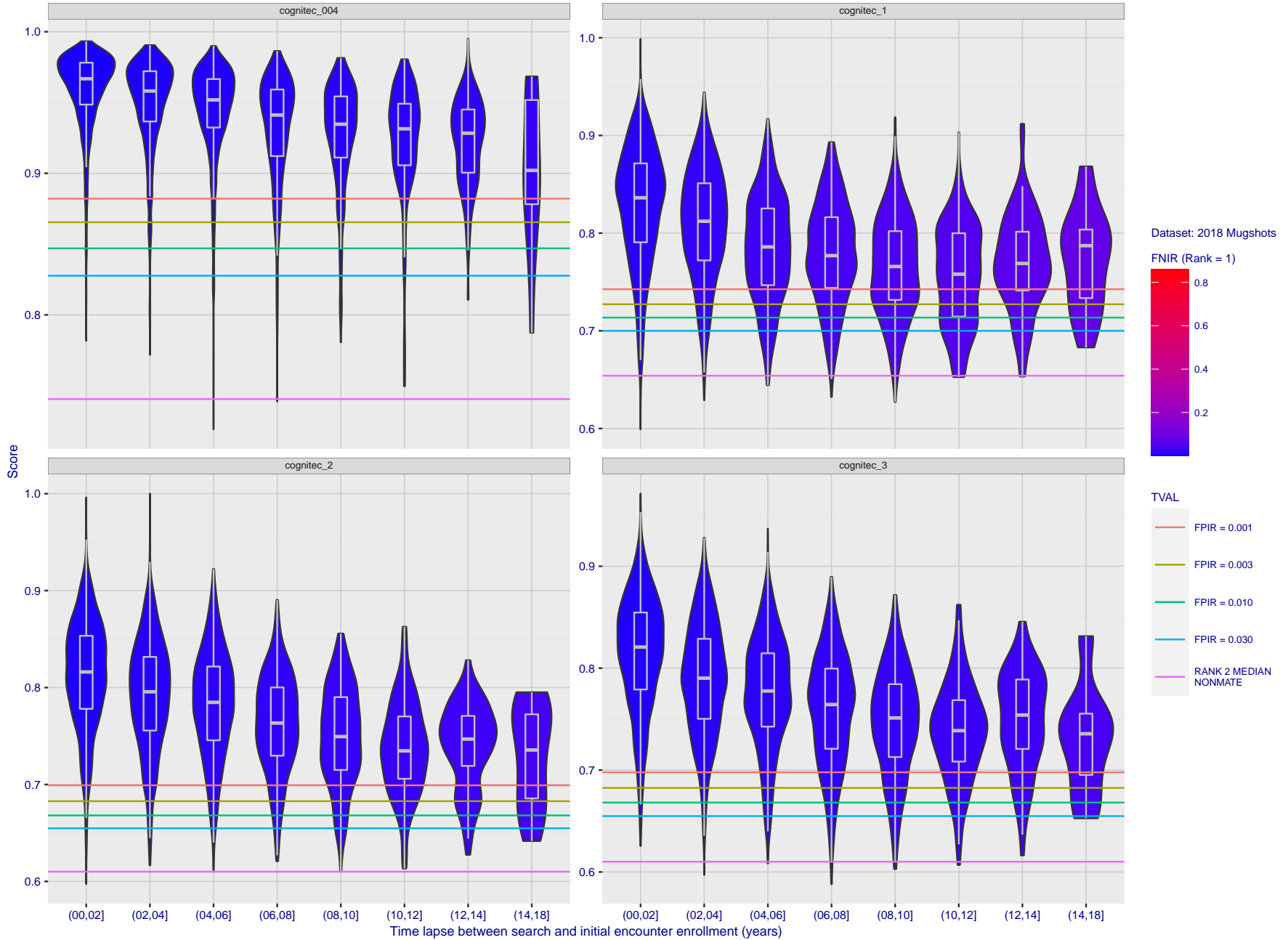


Figure 95: [FRVT-2018 Mugshot Ageing Dataset] Native mate scores vs. time-elapsed. The oldest image of each individual is enrolled. Thereafter, all more recent images are searched. Mated score distributions are computed over all searches noted in row 17 of Table 1 binned by number of years between search and initial enrollment.

2021/10/28 13:44:33  
 FNIR(N, R, T) = False neg. identification rate  
 FPIR(N, T) = False pos. identification rate  
 N = Num. enrolled subjects  
 R = Num. candidates examined  
 T = Threshold  
 T = 0 → Investigation  
 T > 0 → Identification

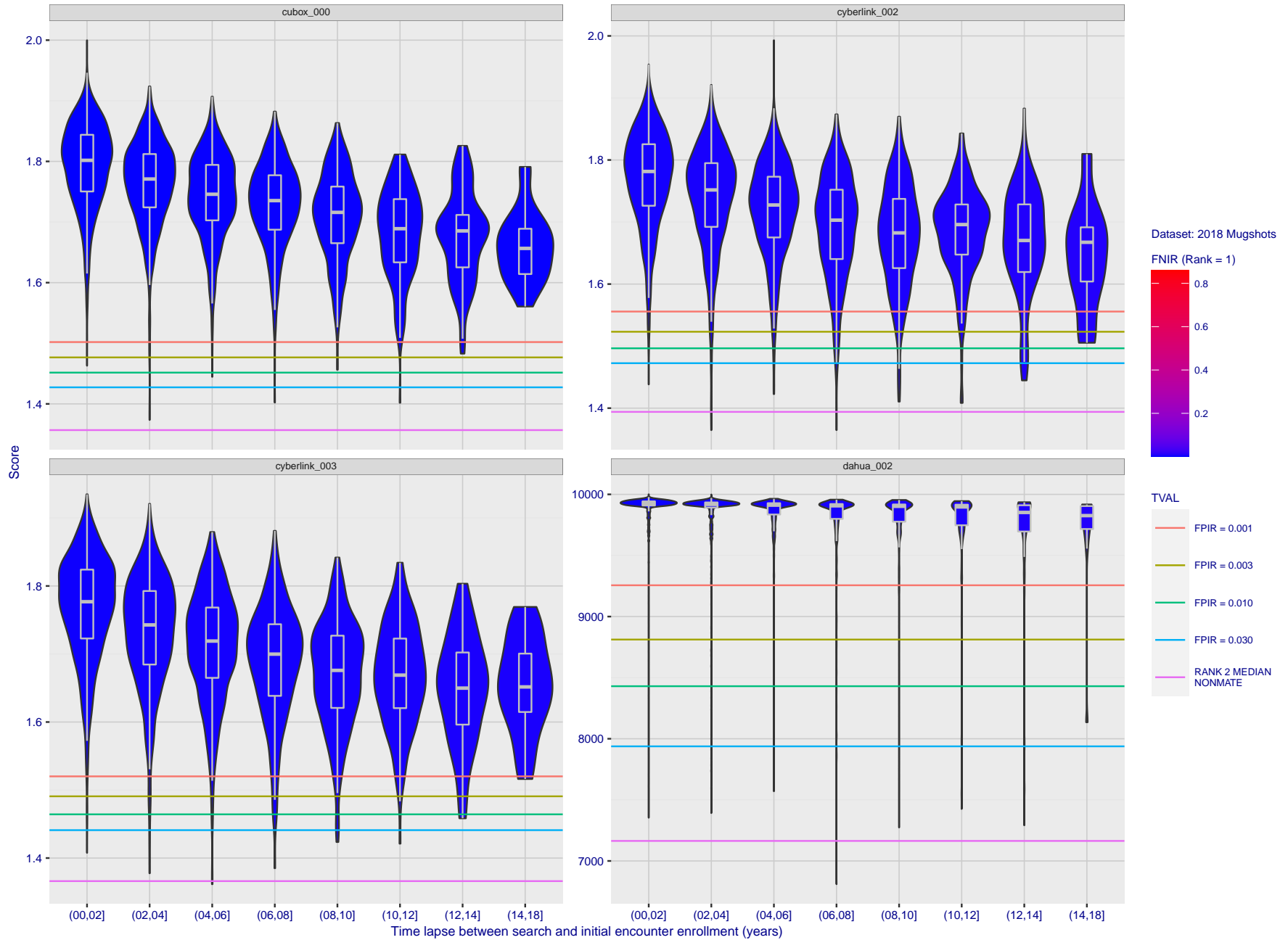


Figure 96: [FRVT-2018 Mugshot Ageing Dataset] Native mate scores vs. time-elapsed. The oldest image of each individual is enrolled. Thereafter, all more recent images are searched. Mated score distributions are computed over all searches noted in row 17 of Table 1 binned by number of years between search and initial enrollment.

2021/10/28 13:44:33  
 FNIR(N, R, T) = False neg. identification rate  
 FPR(N, T) = False pos. identification rate  
 N = Num. enrolled subjects  
 R = Num. candidates examined  
 T = Threshold  
 T = 0 → Investigation  
 T > 0 → Identification

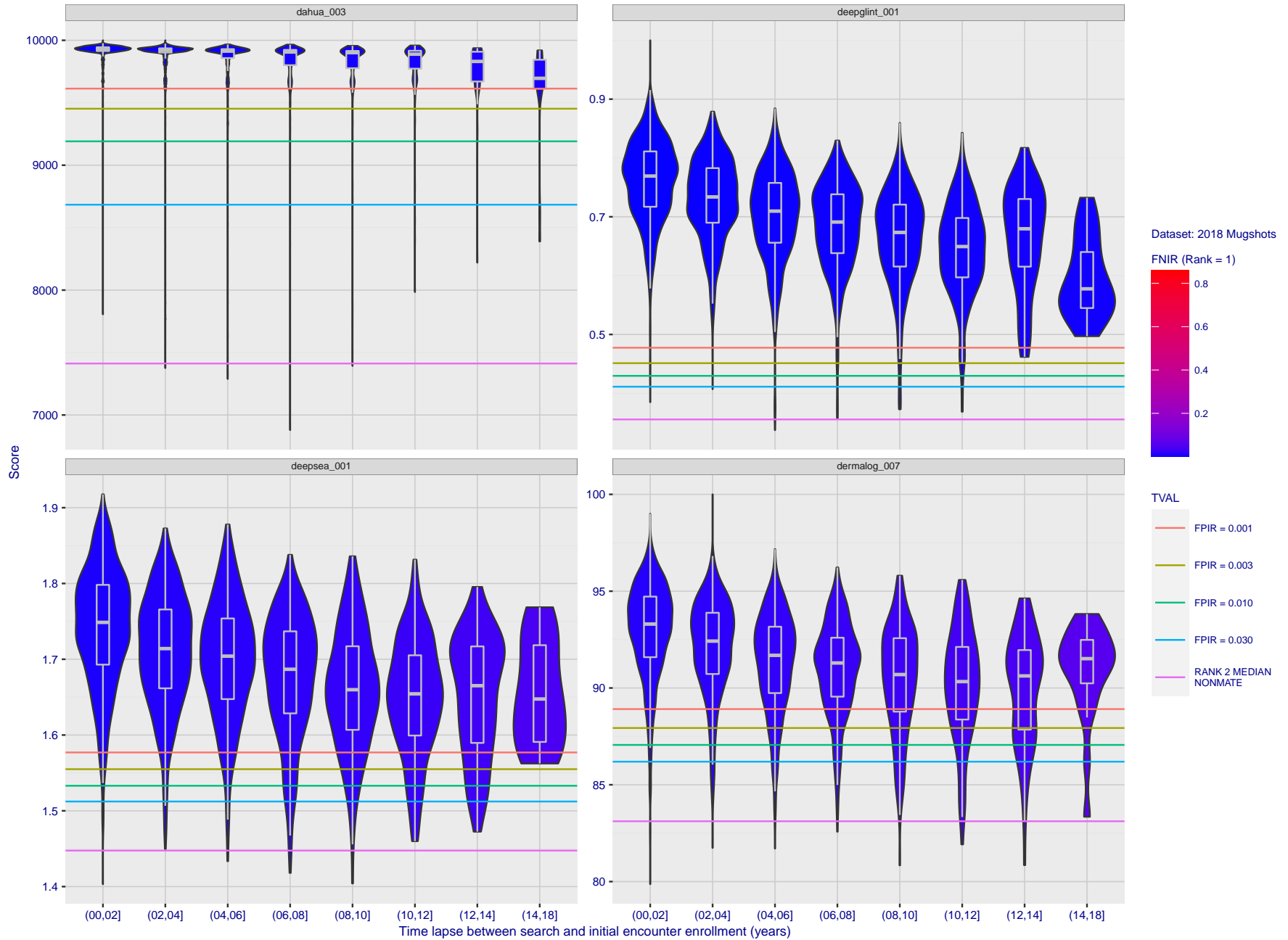


Figure 97: [FRVT-2018 Mugshot Ageing Dataset] Native mate scores vs. time-elapsed. The oldest image of each individual is enrolled. Thereafter, all more recent images are searched. Mated score distributions are computed over all searches noted in row 17 of Table 1 binned by number of years between search and initial enrollment.

2021/10/28  
 13:44:33  
 FNIR(N, R, T) =  
 FPIR(N, T) =  
 False neg. identification rate  
 False pos. identification rate  
 N = Num. enrolled subjects  
 R = Num. candidates examined  
 T = Threshold  
 T = 0 → Investigation  
 T > 0 → Identification

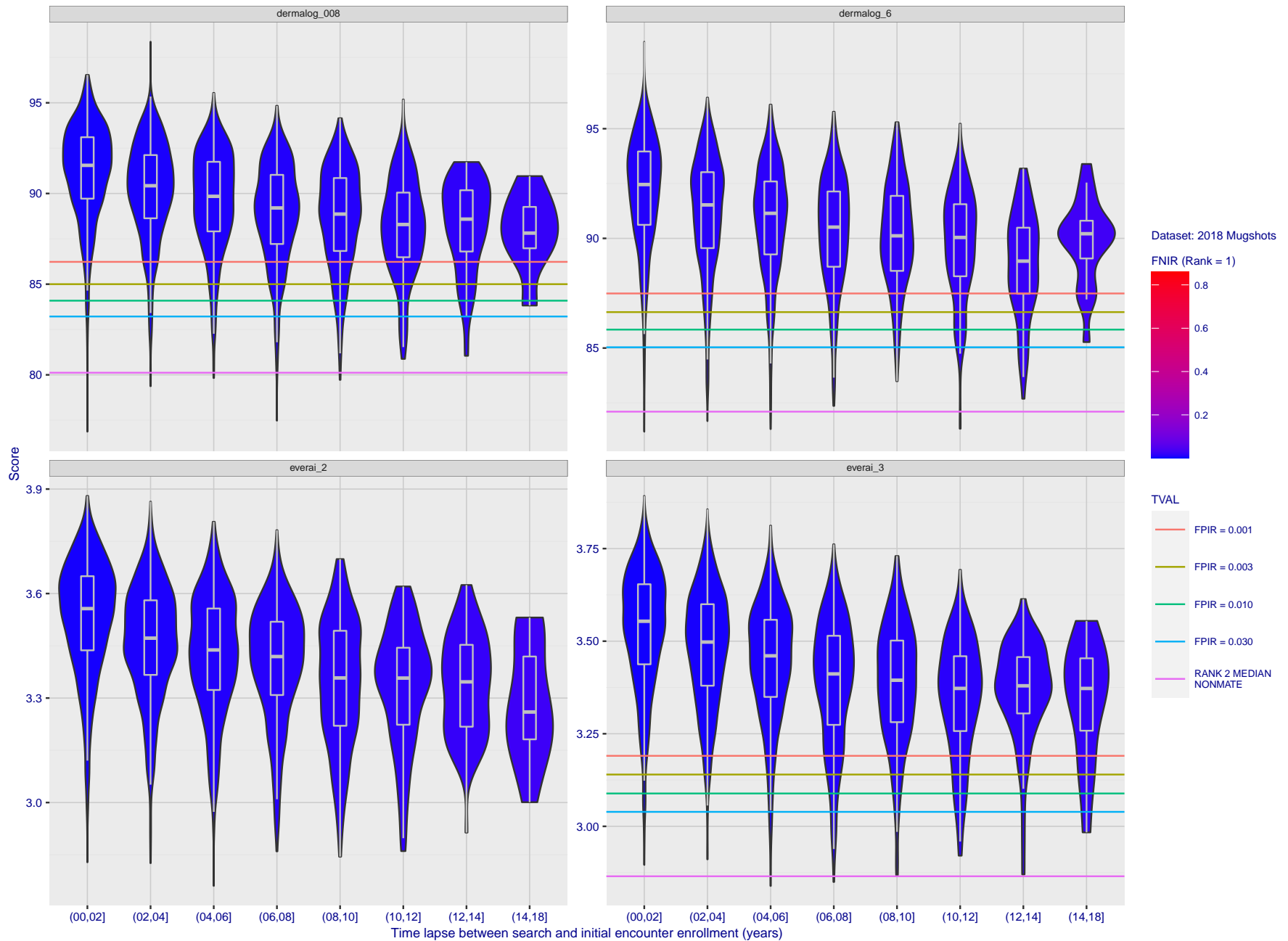


Figure 98: [FRVT-2018 Mugshot Ageing Dataset] Native mate scores vs. time-elapsed. The oldest image of each individual is enrolled. Thereafter, all more recent images are searched. Mated score distributions are computed over all searches noted in row 17 of Table 1 binned by number of years between search and initial enrollment.

2021/10/28  
 13:44:33  
 FNIR(N, R, T) =  
 FPIR(N, T) =  
 False neg. identification rate  
 False pos. identification rate  
 N = Num. enrolled subjects  
 R = Num. candidates examined  
 T = Threshold  
 T = 0 → Investigation  
 T > 0 → Identification

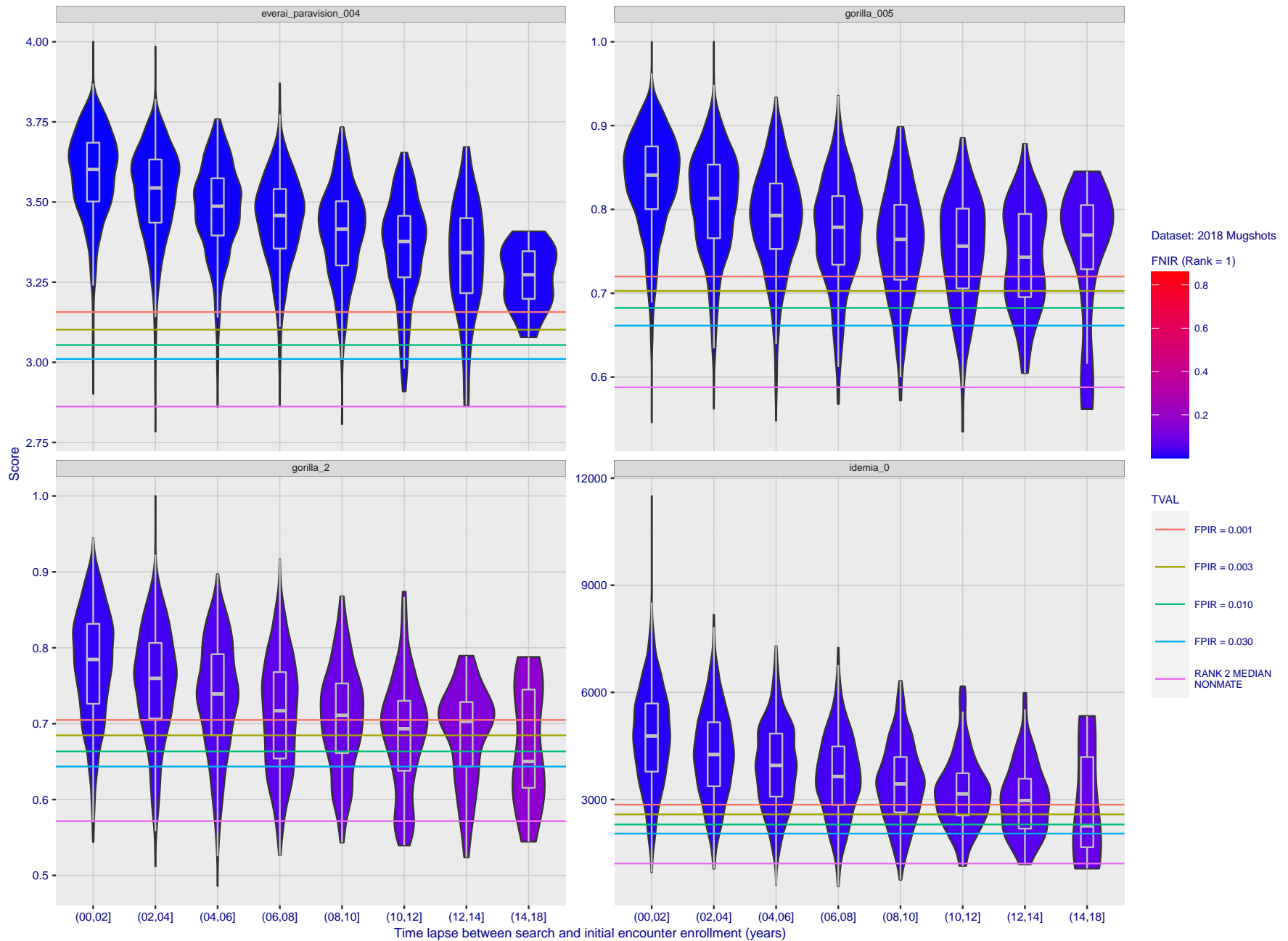


Figure 99: [FRVT-2018 Mugshot Ageing Dataset] Native mate scores vs. time-elapsed. The oldest image of each individual is enrolled. Thereafter, all more recent images are searched. Mated score distributions are computed over all searches noted in row 17 of Table 1 binned by number of years between search and initial enrollment.

2021/10/28  
13:44:33

FNIR(N, R, T) = False neg. identification rate  
FPIR(N, T) = False pos. identification rate

N = Num. enrolled subjects  
R = Num. candidates examined

T = Threshold

T = 0 → Investigation  
T > 0 → Identification

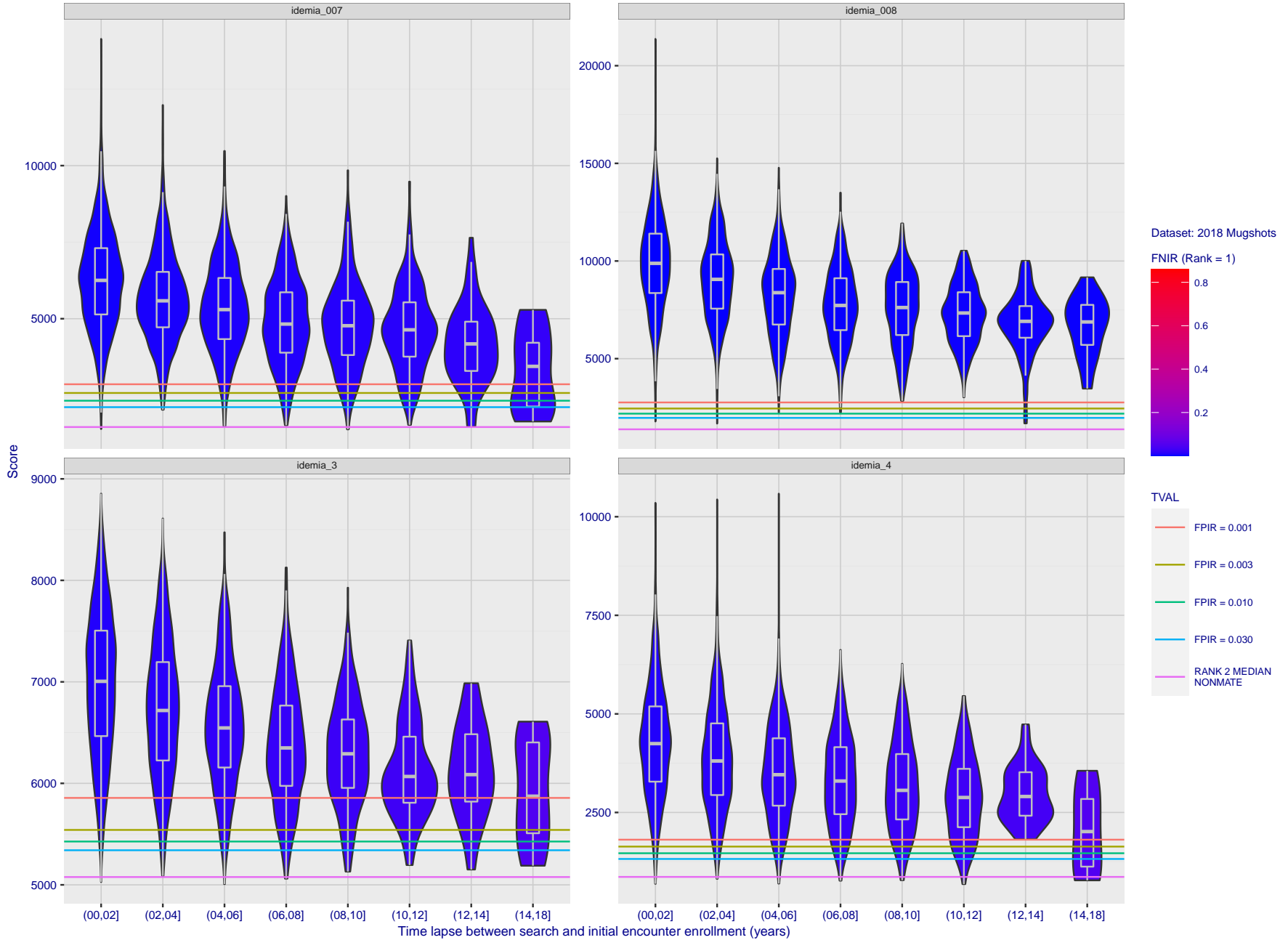


Figure 100: [FRVT-2018 Mugshot Ageing Dataset] Native mate scores vs. time-elapsed. The oldest image of each individual is enrolled. Thereafter, all more recent images are searched. Mated score distributions are computed over all searches noted in row 17 of Table 1 binned by number of years between search and initial enrollment.

2021/10/28 13:44:33  
 FNIR(N, R, T) = False neg. identification rate  
 FPIR(N, T) = False pos. identification rate  
 N = Num. enrolled subjects  
 R = Num. candidates examined  
 T = Threshold  
 T = 0 → Investigation  
 T > 0 → Identification

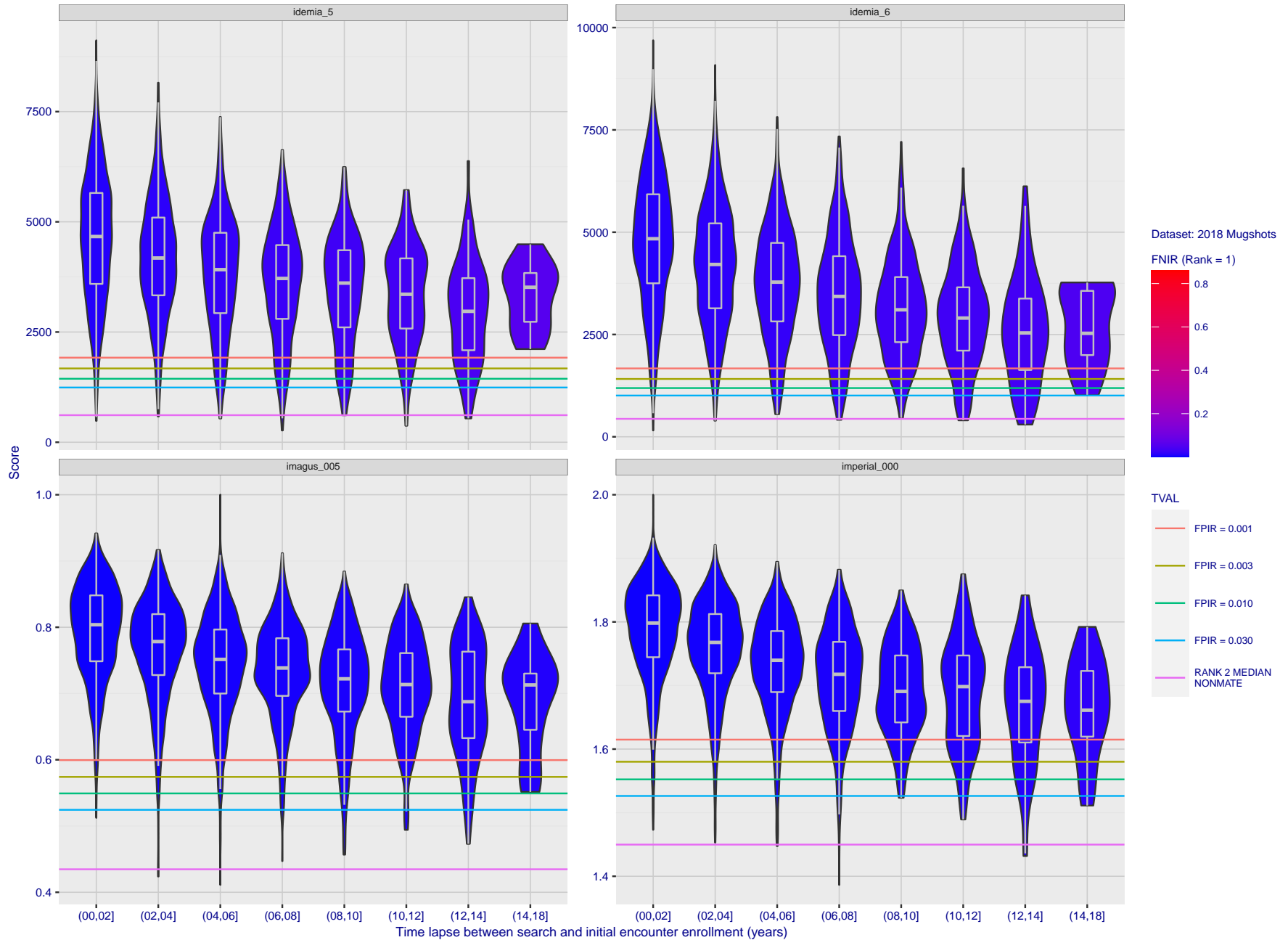


Figure 101: [FRVT-2018 Mugshot Ageing Dataset] Native mate scores vs. time-elapsed. The oldest image of each individual is enrolled. Thereafter, all more recent images are searched. Mated score distributions are computed over all searches noted in row 17 of Table 1 binned by number of years between search and initial enrollment.

2021/10/28  
 13:44:33  
 FNIR(N, R, T) =  
 FPIR(N, T) =  
 False neg. identification rate  
 False pos. identification rate  
 N = Num. enrolled subjects  
 R = Num. candidates examined  
 T = Threshold  
 T = 0 → Investigation  
 T > 0 → Identification

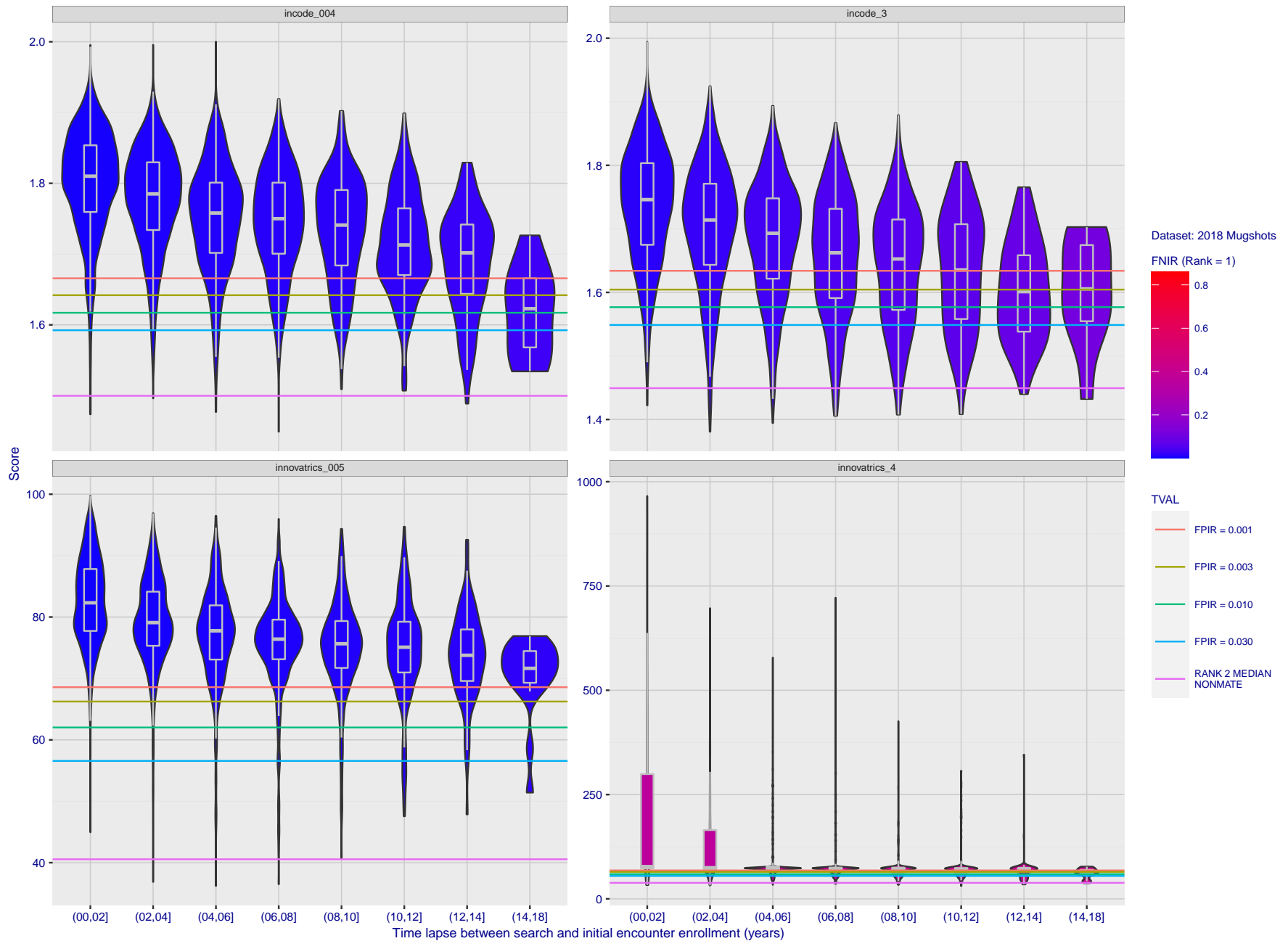


Figure 102: [FRVT-2018 Mugshot Ageing Dataset] Native mate scores vs. time-elapsed. The oldest image of each individual is enrolled. Thereafter, all more recent images are searched. Mated score distributions are computed over all searches noted in row 17 of Table 1 binned by number of years between search and initial enrollment.

2021/10/28  
13:44:33

FNIR(N, R, T) = False neg. identification rate  
FPIR(N, T) = False pos. identification rate

N = Num. enrolled subjects  
R = Num. candidates examined

T = Threshold

T = 0 → Investigation  
T > 0 → Identification

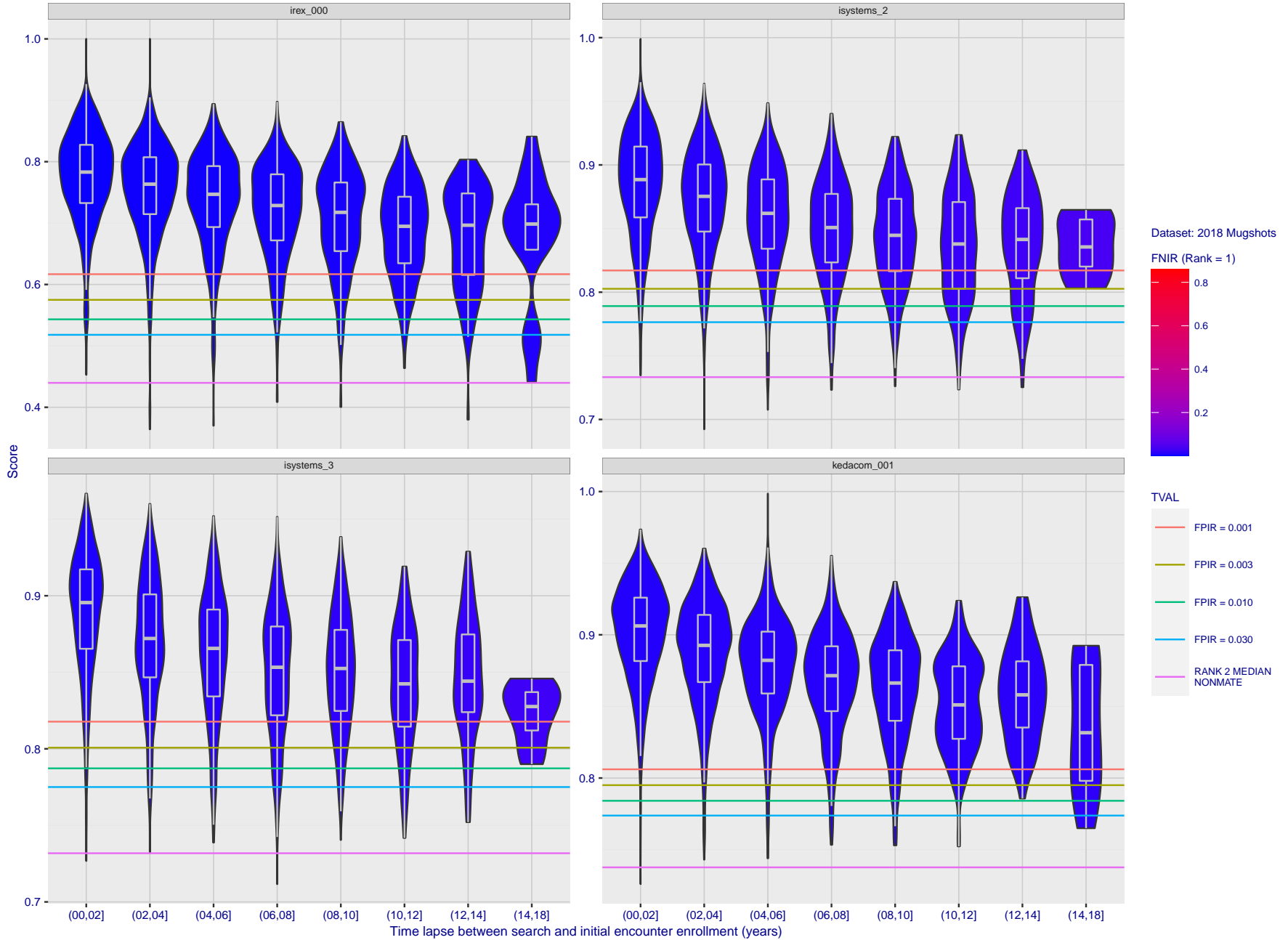


Figure 103: [FRVT-2018 Mugshot Ageing Dataset] Native mate scores vs. time-elapsed. The oldest image of each individual is enrolled. Thereafter, all more recent images are searched. Mated score distributions are computed over all searches noted in row 17 of Table 1 binned by number of years between search and initial enrollment.

2021/10/28 13:44:33  
 FNIR(N, R, T) = False neg. identification rate  
 FPIR(N, T) = False pos. identification rate  
 N = Num. enrolled subjects  
 R = Num. candidates examined  
 T = Threshold  
 T = 0 → Investigation  
 T > 0 → Identification

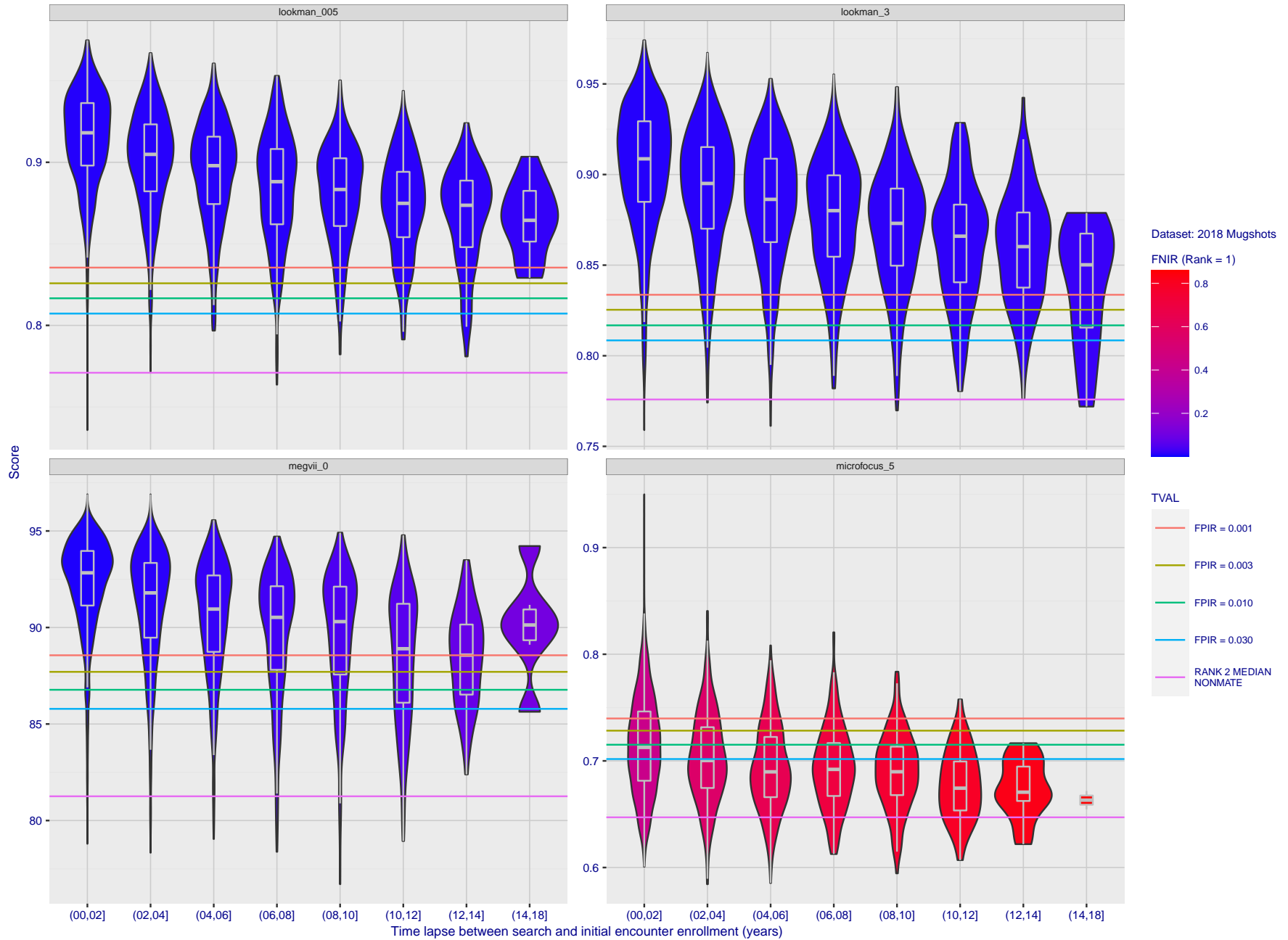


Figure 104: [FRVT-2018 Mugshot Ageing Dataset] Native mate scores vs. time-elapsed. The oldest image of each individual is enrolled. Thereafter, all more recent images are searched. Mated score distributions are computed over all searches noted in row 17 of Table 1 binned by number of years between search and initial enrollment.

2021/10/28 13:44:33 FNIR(N, R, T) = False neg. identification rate N = Num. enrolled subjects T = Threshold T = 0 → Investigation  
 FPIR(N, T) = False pos. identification rate R = Num. candidates examined T > 0 → Identification

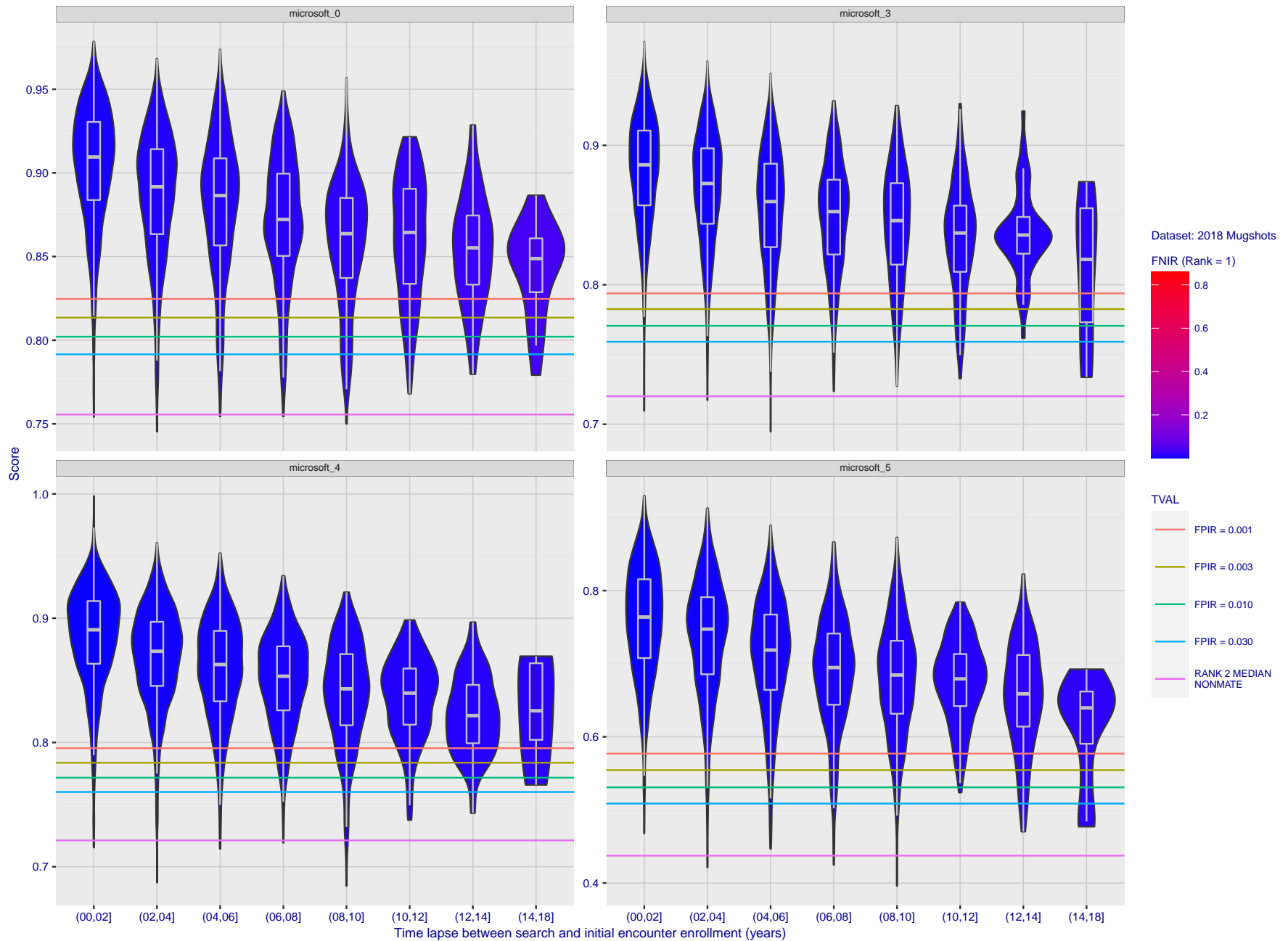


Figure 105: [FRVT-2018 Mugshot Ageing Dataset] Native mate scores vs. time-elapsed. The oldest image of each individual is enrolled. Thereafter, all more recent images are searched. Mated score distributions are computed over all searches noted in row 17 of Table 1 binned by number of years between search and initial enrollment.

2021/10/28  
 13:44:33  
 FNIR(N, R, T) =  
 FPR(N, T) =  
 False neg. identification rate  
 False pos. identification rate  
 N = Num. enrolled subjects  
 R = Num. candidates examined  
 T = Threshold  
 T = 0 → Investigation  
 T > 0 → Identification

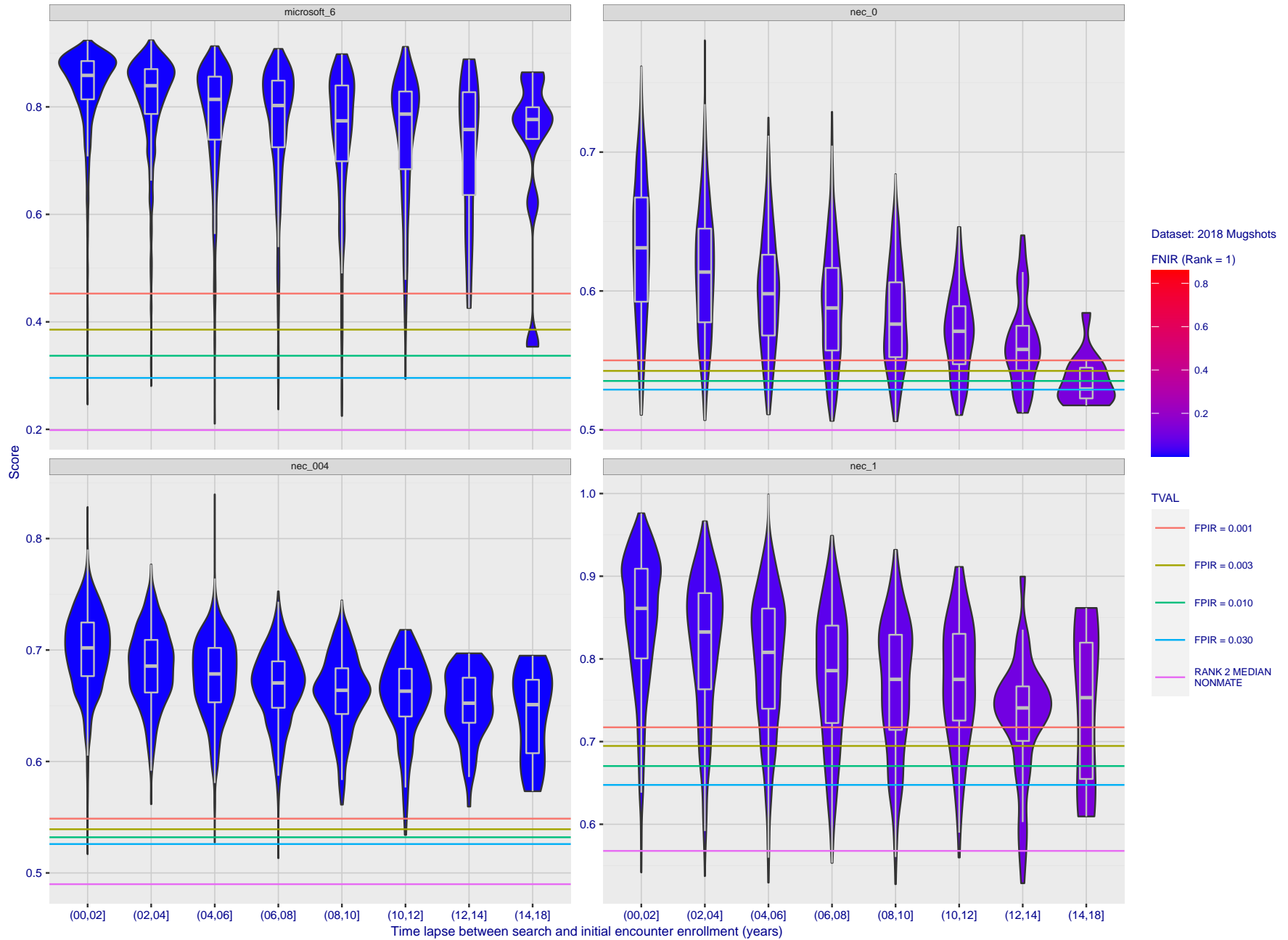


Figure 106: [FRVT-2018 Mugshot Ageing Dataset] Native mate scores vs. time-elapsed. The oldest image of each individual is enrolled. Thereafter, all more recent images are searched. Mated score distributions are computed over all searches noted in row 17 of Table 1 binned by number of years between search and initial enrollment.

2021/10/28 13:44:33 FNIR(N, R, T) = False neg. identification rate  
 FPIR(N, T) = False pos. identification rate  
 N = Num. enrolled subjects  
 R = Num. candidates examined  
 T = Threshold  
 T = 0 → Investigation  
 T > 0 → Identification

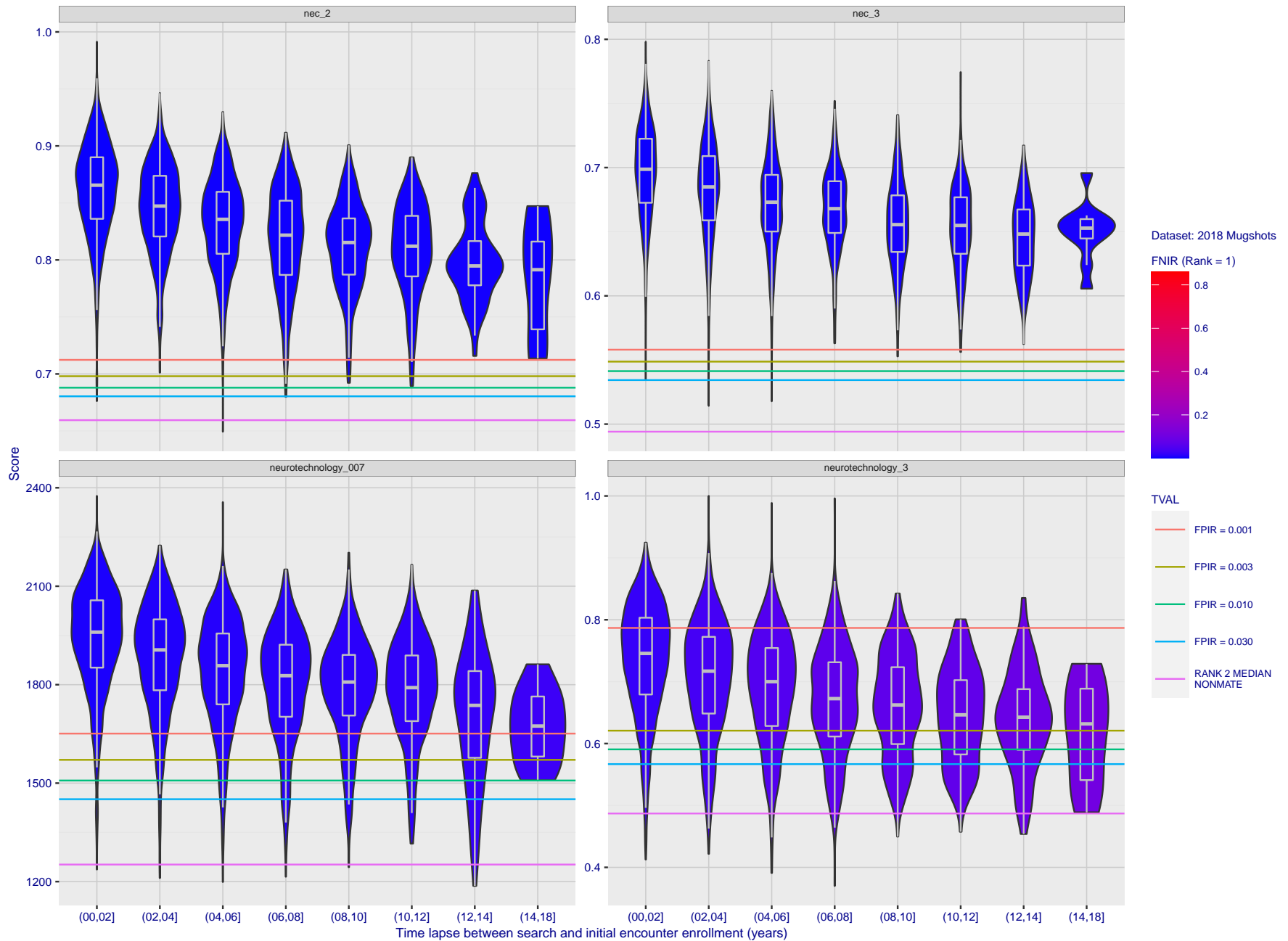


Figure 107: [FRVT-2018 Mugshot Ageing Dataset] Native mate scores vs. time-elapsed. The oldest image of each individual is enrolled. Thereafter, all more recent images are searched. Mated score distributions are computed over all searches noted in row 17 of Table 1 binned by number of years between search and initial enrollment.

2021/10/28  
 13:44:33  
 FNIR(N, R, T) =  
 FPR(N, T) =  
 False neg. identification rate  
 False pos. identification rate  
 N = Num. enrolled subjects  
 R = Num. candidates examined  
 T = Threshold  
 T = 0 → Investigation  
 T > 0 → Identification

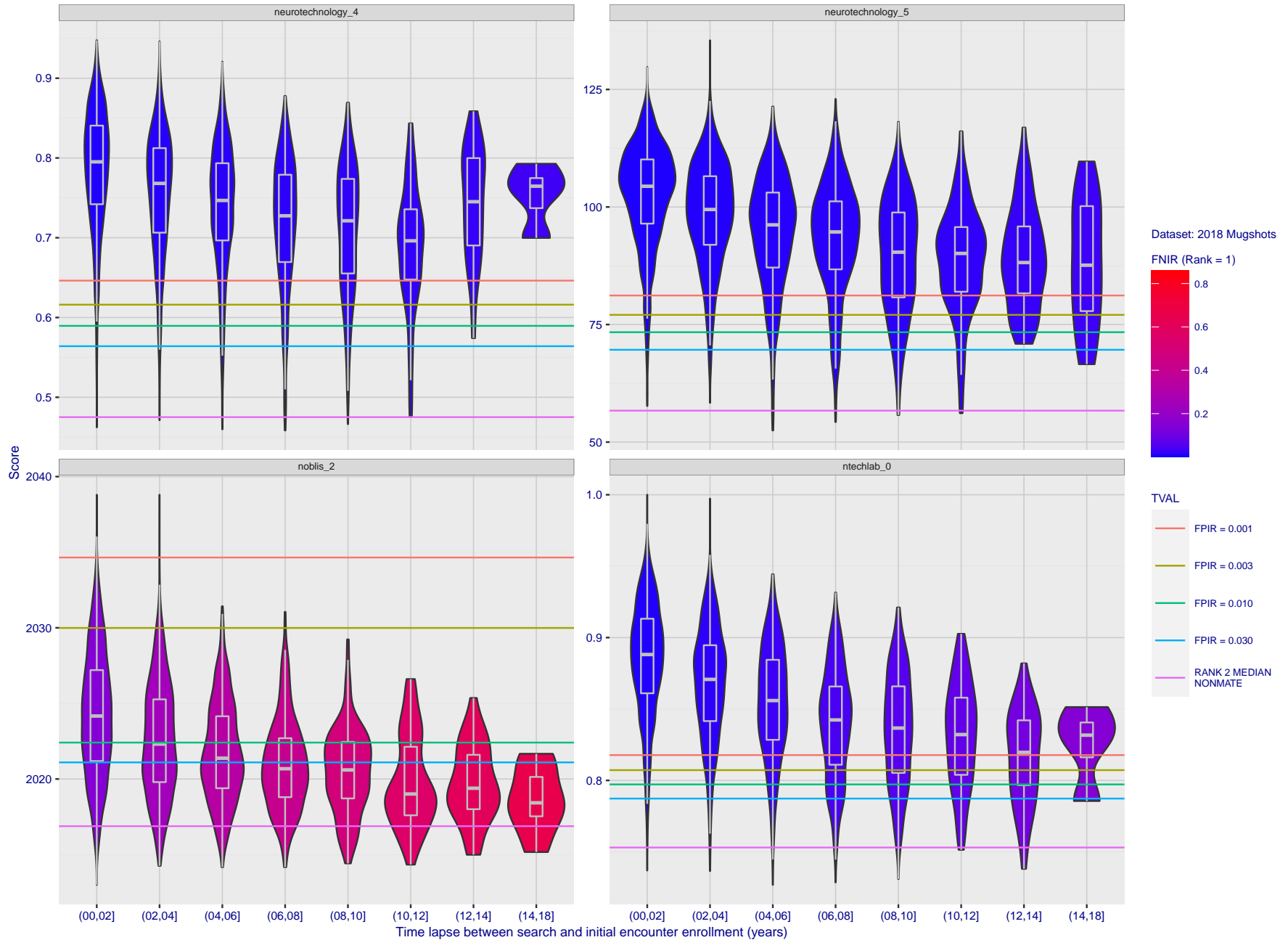


Figure 108: [FRVT-2018 Mugshot Ageing Dataset] Native mate scores vs. time-elapsed. The oldest image of each individual is enrolled. Thereafter, all more recent images are searched. Mated score distributions are computed over all searches noted in row 17 of Table 1 binned by number of years between search and initial enrollment.

2021/10/28  
 13:44:33  
 FNIR(N, R, T) =  
 FPIR(N, T) =  
 False neg. identification rate  
 False pos. identification rate  
 N = Num. enrolled subjects  
 R = Num. candidates examined  
 T = Threshold  
 T = 0 → Investigation  
 T > 0 → Identification

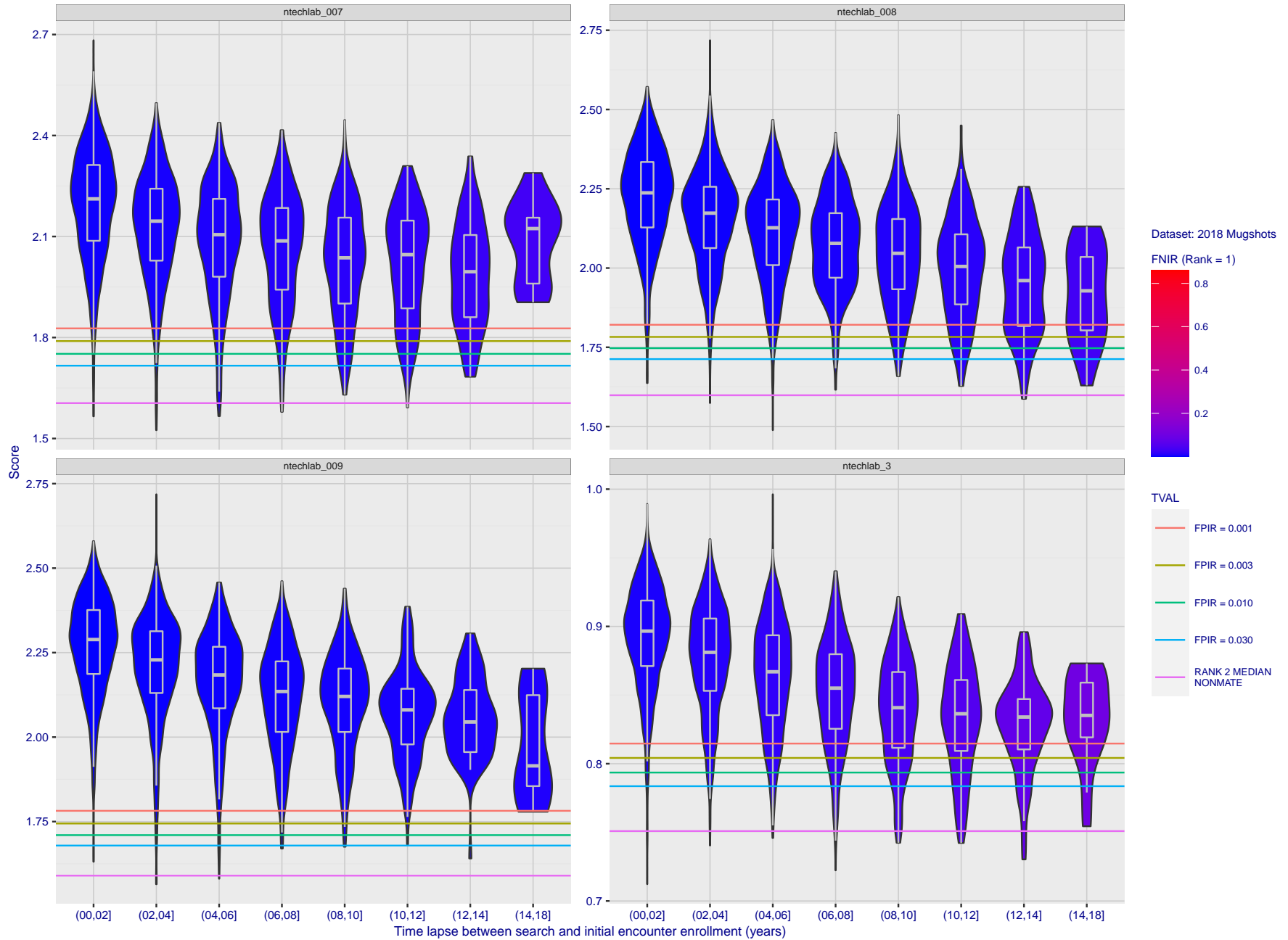


Figure 109: [FRVT-2018 Mugshot Ageing Dataset] Native mate scores vs. time-elapsed. The oldest image of each individual is enrolled. Thereafter, all more recent images are searched. Mated score distributions are computed over all searches noted in row 17 of Table 1 binned by number of years between search and initial enrollment.

2021/10/28  
13:44:33

FNIR(N, R, T) =  
FPIR(N, T) =

False neg. identification rate  
False pos. identification rate

N = Num. enrolled subjects  
R = Num. candidates examined

T = Threshold

T = 0 → Investigation  
T > 0 → Identification

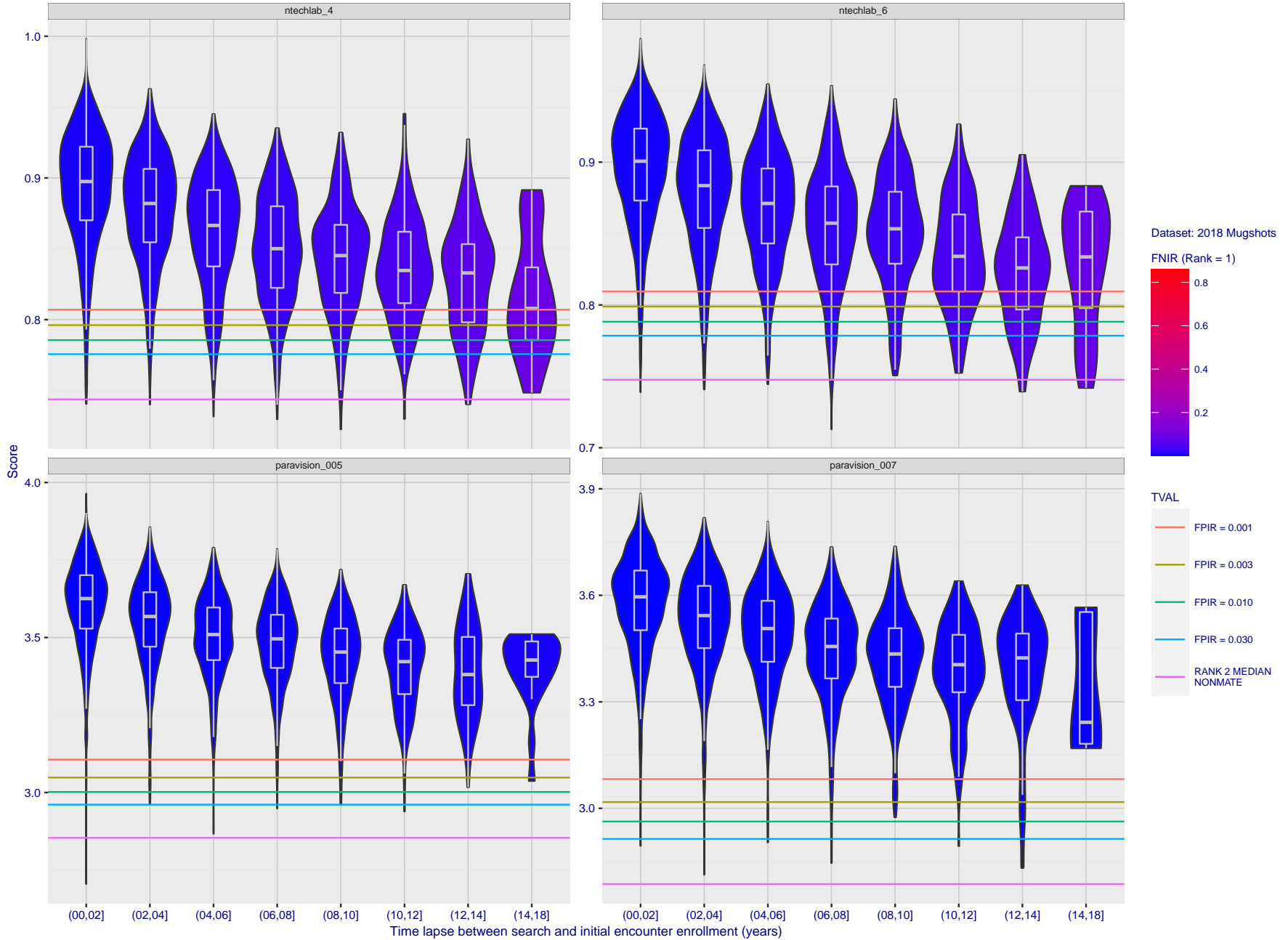


Figure 110: [FRVT-2018 Mugshot Ageing Dataset] Native mate scores vs. time-elapsed. The oldest image of each individual is enrolled. Thereafter, all more recent images are searched. Mated score distributions are computed over all searches noted in row 17 of Table 1 binned by number of years between search and initial enrollment.

2021/10/28  
13:44:33

FNIR(N, R, T) = False neg. identification rate  
FPIR(N, T) = False pos. identification rate

N = Num. enrolled subjects  
R = Num. candidates examined

T = Threshold

T = 0 → Investigation  
T > 0 → Identification

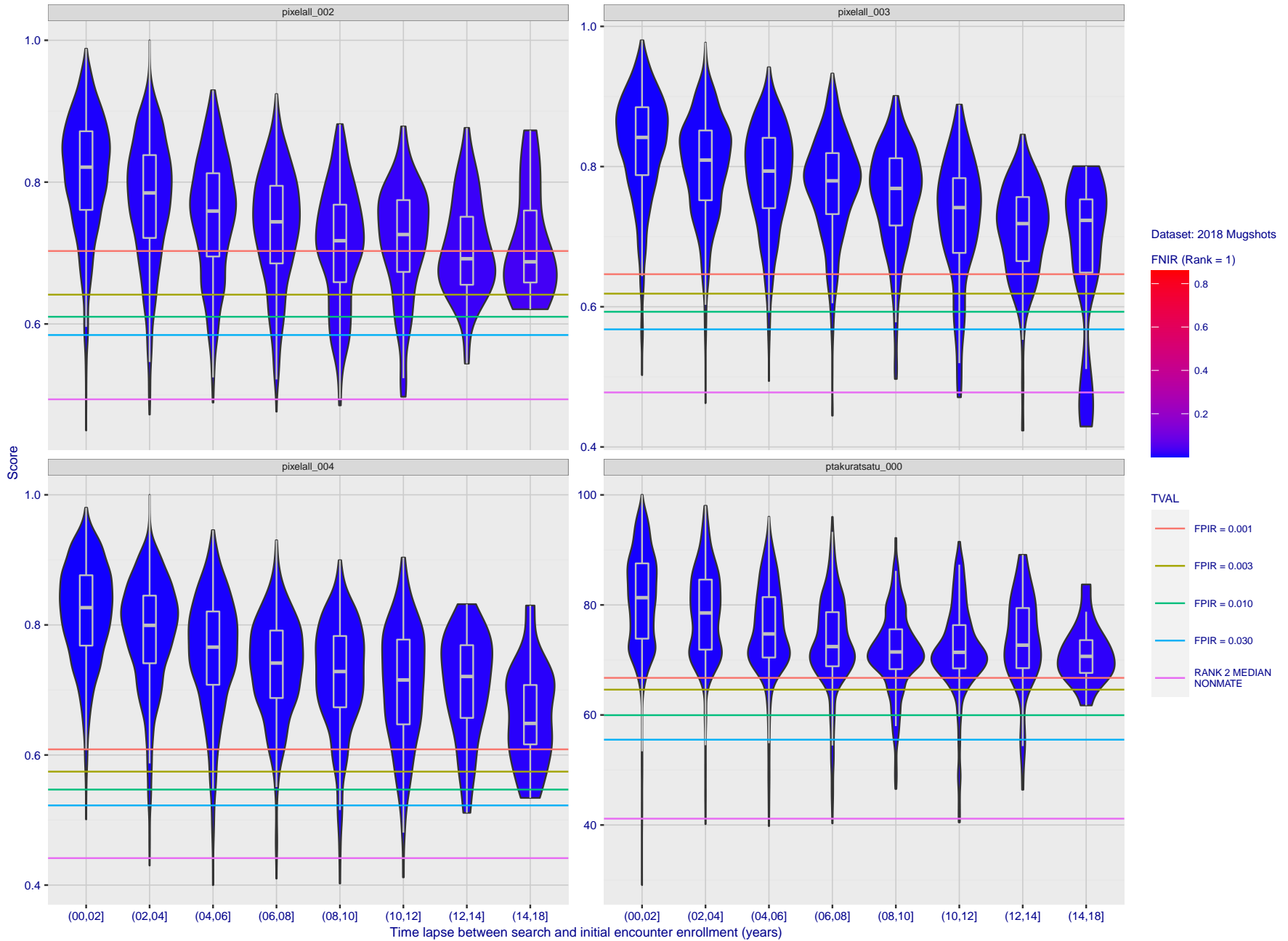


Figure 111: [FRVT-2018 Mugshot Ageing Dataset] Native mate scores vs. time-elapsed. The oldest image of each individual is enrolled. Thereafter, all more recent images are searched. Mated score distributions are computed over all searches noted in row 17 of Table 1 binned by number of years between search and initial enrollment.

2021/10/28 13:44:33  
 FNIR(N, R, T) = False neg. identification rate  
 FPIR(N, T) = False pos. identification rate  
 N = Num. enrolled subjects  
 R = Num. candidates examined  
 T = Threshold  
 T = 0 → Investigation  
 T > 0 → Identification

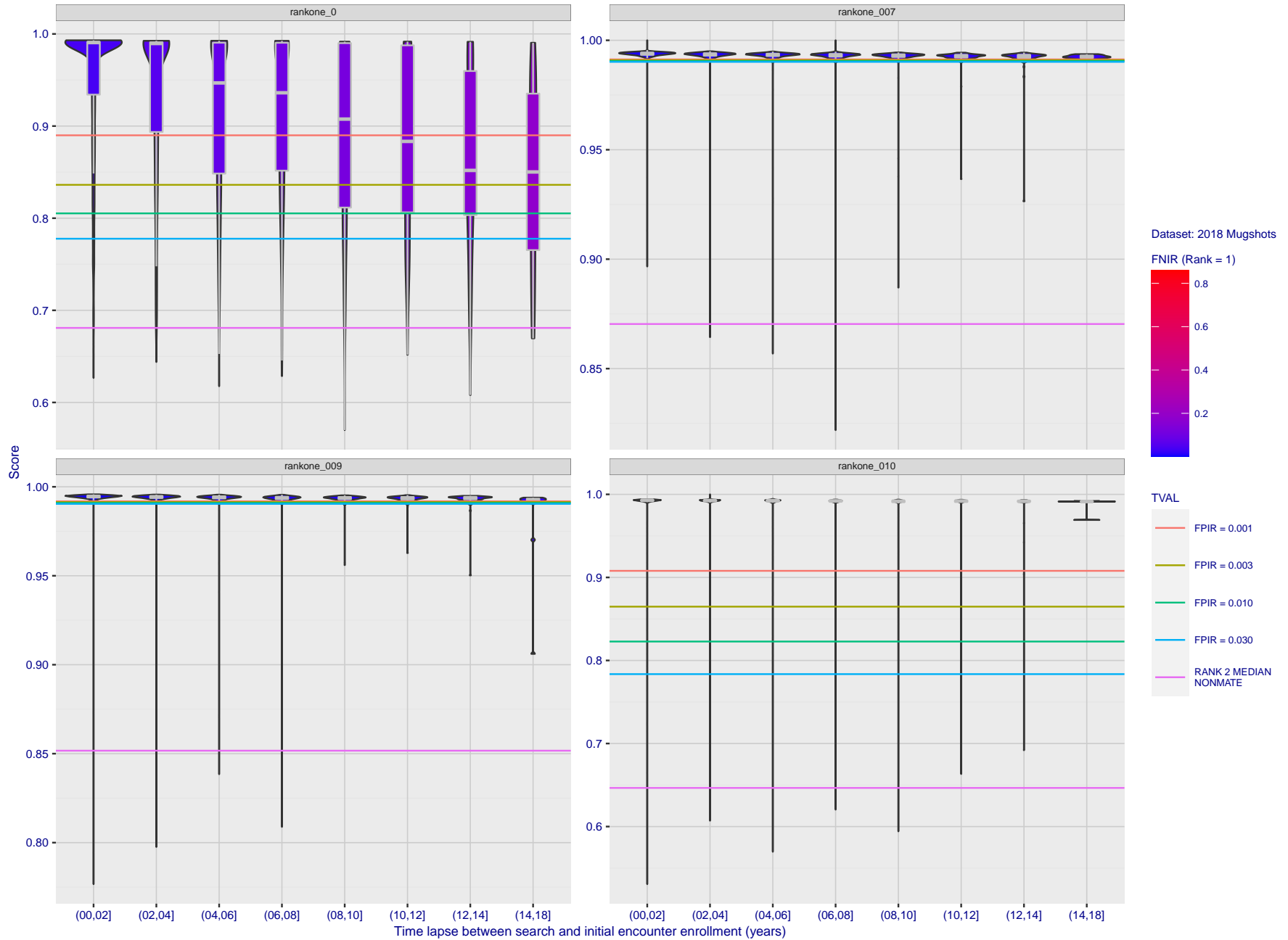


Figure 112: [FRVT-2018 Mugshot Ageing Dataset] Native mate scores vs. time-elapsed. The oldest image of each individual is enrolled. Thereafter, all more recent images are searched. Mated score distributions are computed over all searches noted in row 17 of Table 1 binned by number of years between search and initial enrollment.

2021/10/28 13:44:33  
 FNIR(N, R, T) = False neg. identification rate  
 FPIR(N, T) = False pos. identification rate  
 N = Num. enrolled subjects  
 R = Num. candidates examined  
 T = Threshold  
 T = 0 → Investigation  
 T > 0 → Identification

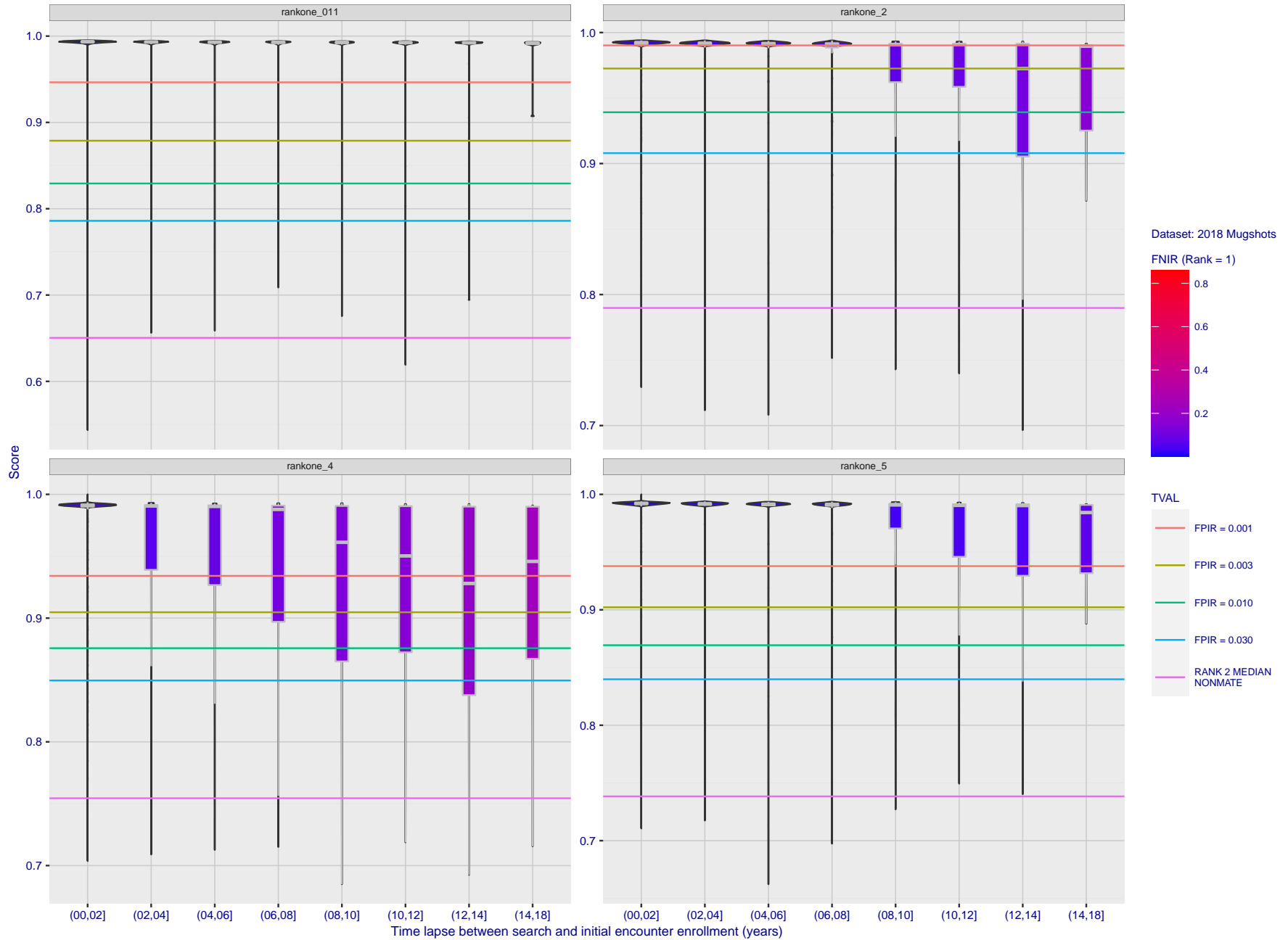


Figure 113: [FRVT-2018 Mugshot Ageing Dataset] Native mate scores vs. time-elapsed. The oldest image of each individual is enrolled. Thereafter, all more recent images are searched. Mated score distributions are computed over all searches noted in row 17 of Table 1 binned by number of years between search and initial enrollment.

2021/10/28  
13:44:33

FNIR(N, R, T) = False neg. identification rate  
FPIR(N, T) = False pos. identification rate

N = Num. enrolled subjects  
R = Num. candidates examined

T = Threshold

T = 0 → Investigation  
T > 0 → Identification

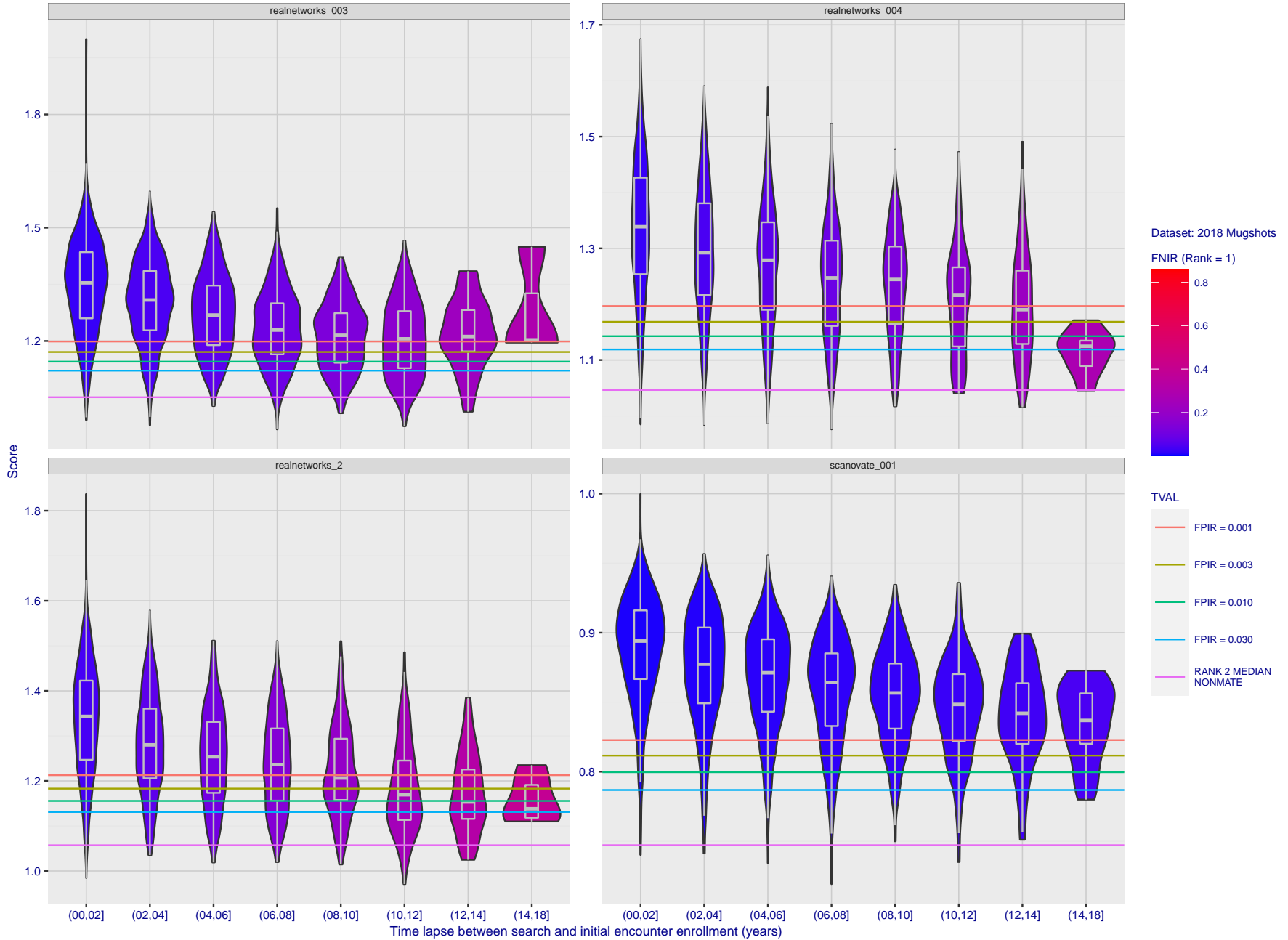


Figure 114: [FRVT-2018 Mugshot Ageing Dataset] Native mate scores vs. time-elapsed. The oldest image of each individual is enrolled. Thereafter, all more recent images are searched. Mated score distributions are computed over all searches noted in row 17 of Table 1 binned by number of years between search and initial enrollment.

2021/10/28  
 13:44:33  
 FNIR(N, R, T) =  
 FPIR(N, T) =  
 False neg. identification rate  
 False pos. identification rate  
 N = Num. enrolled subjects  
 R = Num. candidates examined  
 T = Threshold  
 T = 0 → Investigation  
 T > 0 → Identification

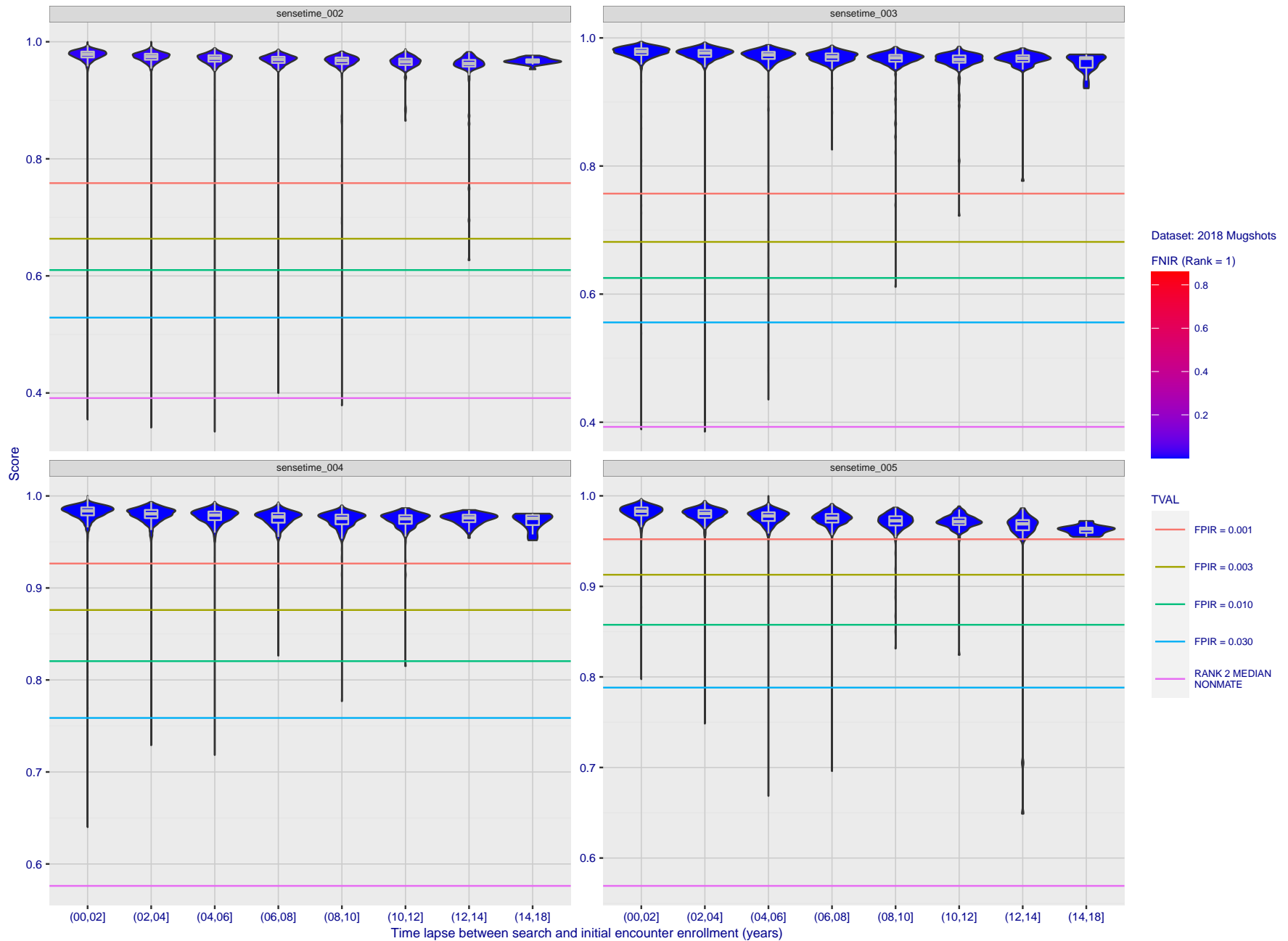


Figure 115: [FRVT-2018 Mugshot Ageing Dataset] Native mate scores vs. time-elapsed. The oldest image of each individual is enrolled. Thereafter, all more recent images are searched. Mated score distributions are computed over all searches noted in row 17 of Table 1 binned by number of years between search and initial enrollment.

2021/10/28  
13:44:33

FNIR(N, R, T) = False neg. identification rate  
FPIR(N, T) = False pos. identification rate

N = Num. enrolled subjects  
R = Num. candidates examined

T = Threshold

T = 0 → Investigation  
T > 0 → Identification

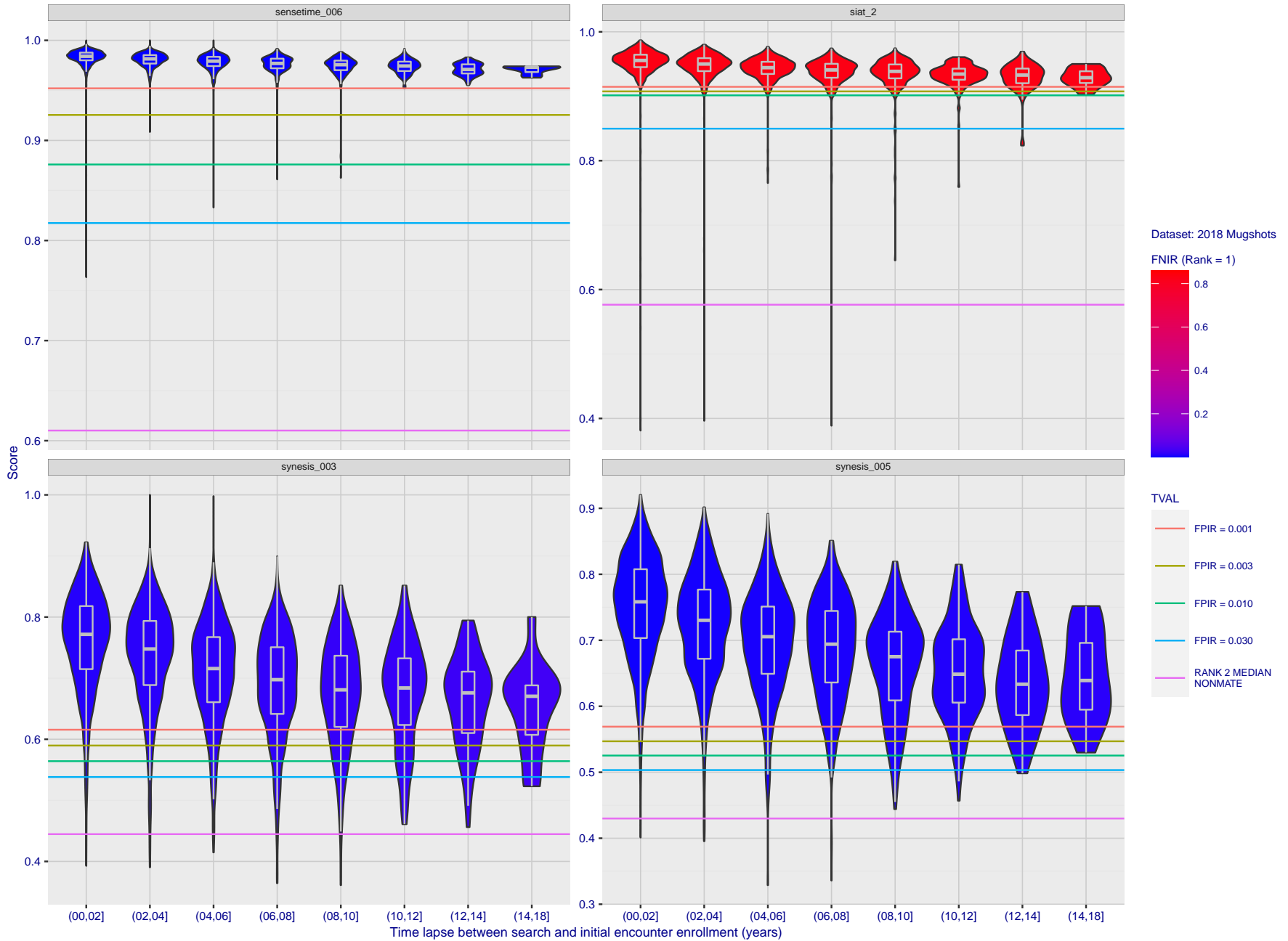


Figure 116: [FRVT-2018 Mugshot Ageing Dataset] Native mate scores vs. time-elapsed. The oldest image of each individual is enrolled. Thereafter, all more recent images are searched. Mated score distributions are computed over all searches noted in row 17 of Table 1 binned by number of years between search and initial enrollment.

2021/10/28  
13:44:33

FNIR(N, R, T) = False neg. identification rate  
FPIR(N, T) = False pos. identification rate

N = Num. enrolled subjects  
R = Num. candidates examined

T = Threshold

T = 0 → Investigation  
T > 0 → Identification

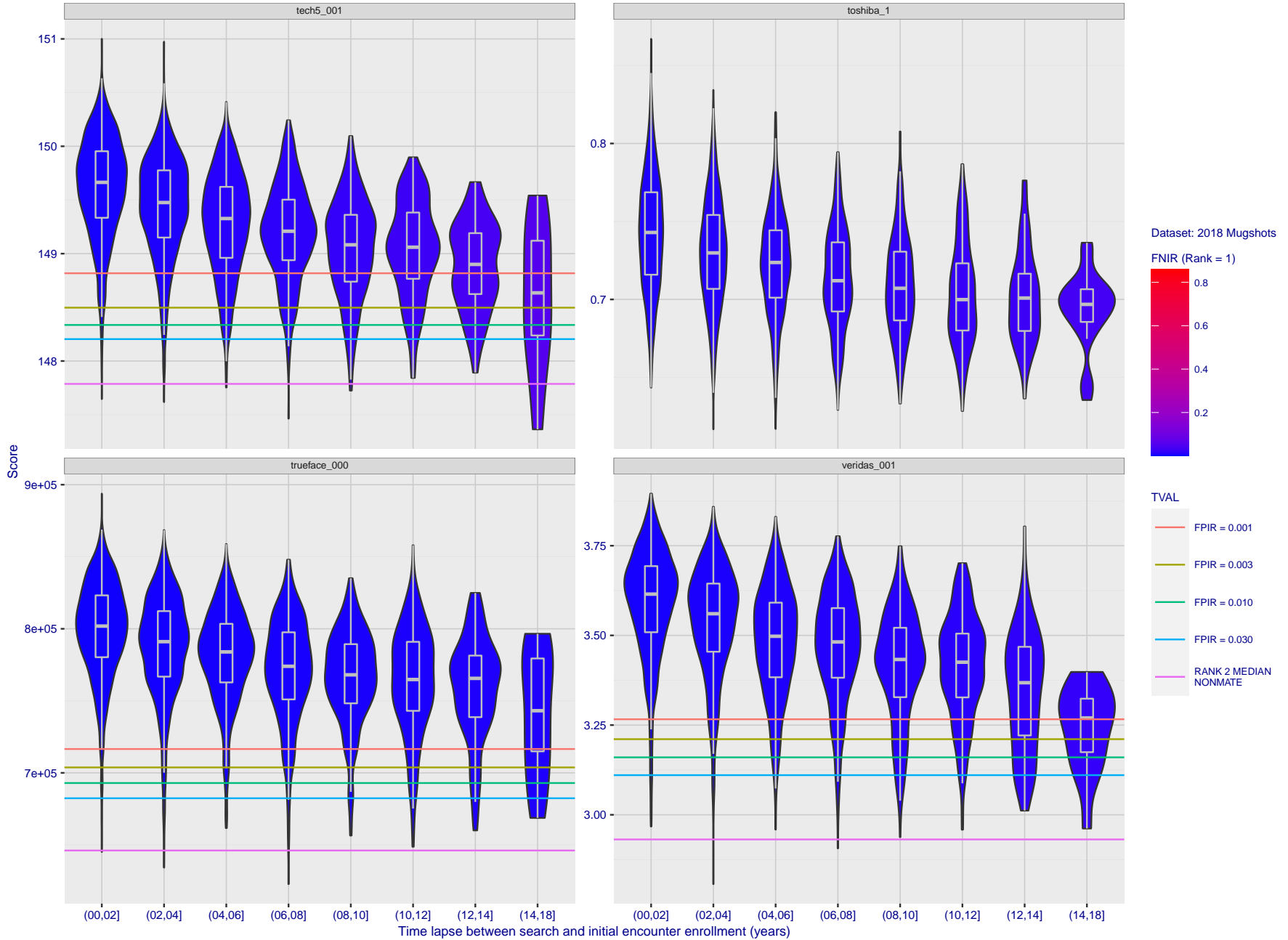


Figure 117: [FRVT-2018 Mugshot Ageing Dataset] Native mate scores vs. time-elapsed. The oldest image of each individual is enrolled. Thereafter, all more recent images are searched. Mated score distributions are computed over all searches noted in row 17 of Table 1 binned by number of years between search and initial enrollment.

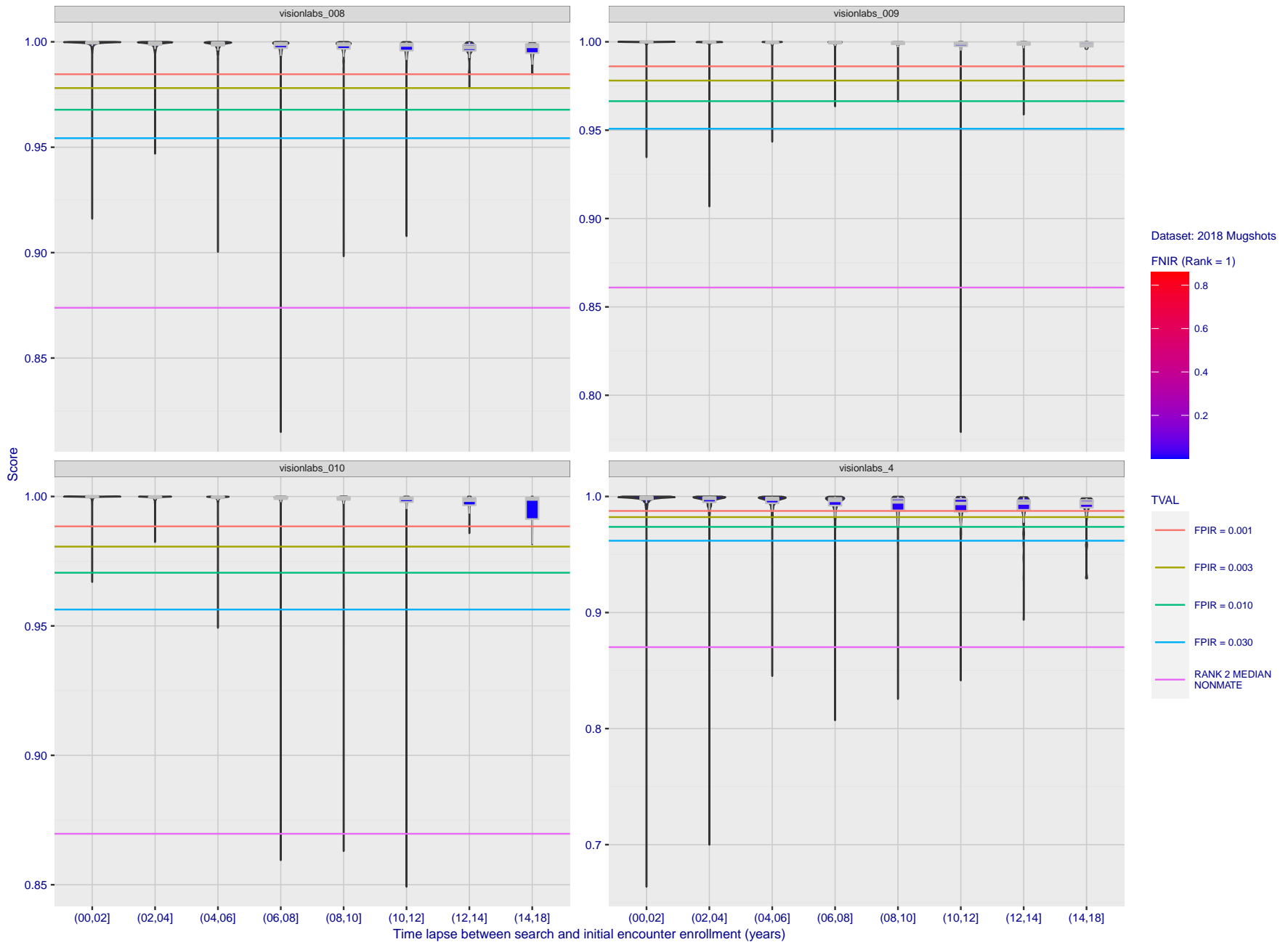


Figure 118: [FRVT-2018 Mugshot Ageing Dataset] Native mate scores vs. time-elapsed. The oldest image of each individual is enrolled. Thereafter, all more recent images are searched. Mated score distributions are computed over all searches noted in row 17 of Table 1 binned by number of years between search and initial enrollment.

2021/10/28  
13:44:33

FNIR(N, R, T) = False neg. identification rate  
FPIR(N, T) = False pos. identification rate

N = Num. enrolled subjects  
R = Num. candidates examined

T = Threshold

T = 0 → Investigation  
T > 0 → Identification

2021/10/28  
 13:44:33  
 FNIR(N, R, T) =  
 FPR(N, T) =  
 False neg. identification rate  
 False pos. identification rate  
 N = Num. enrolled subjects  
 R = Num. candidates examined  
 T = Threshold  
 T = 0 → Investigation  
 T > 0 → Identification

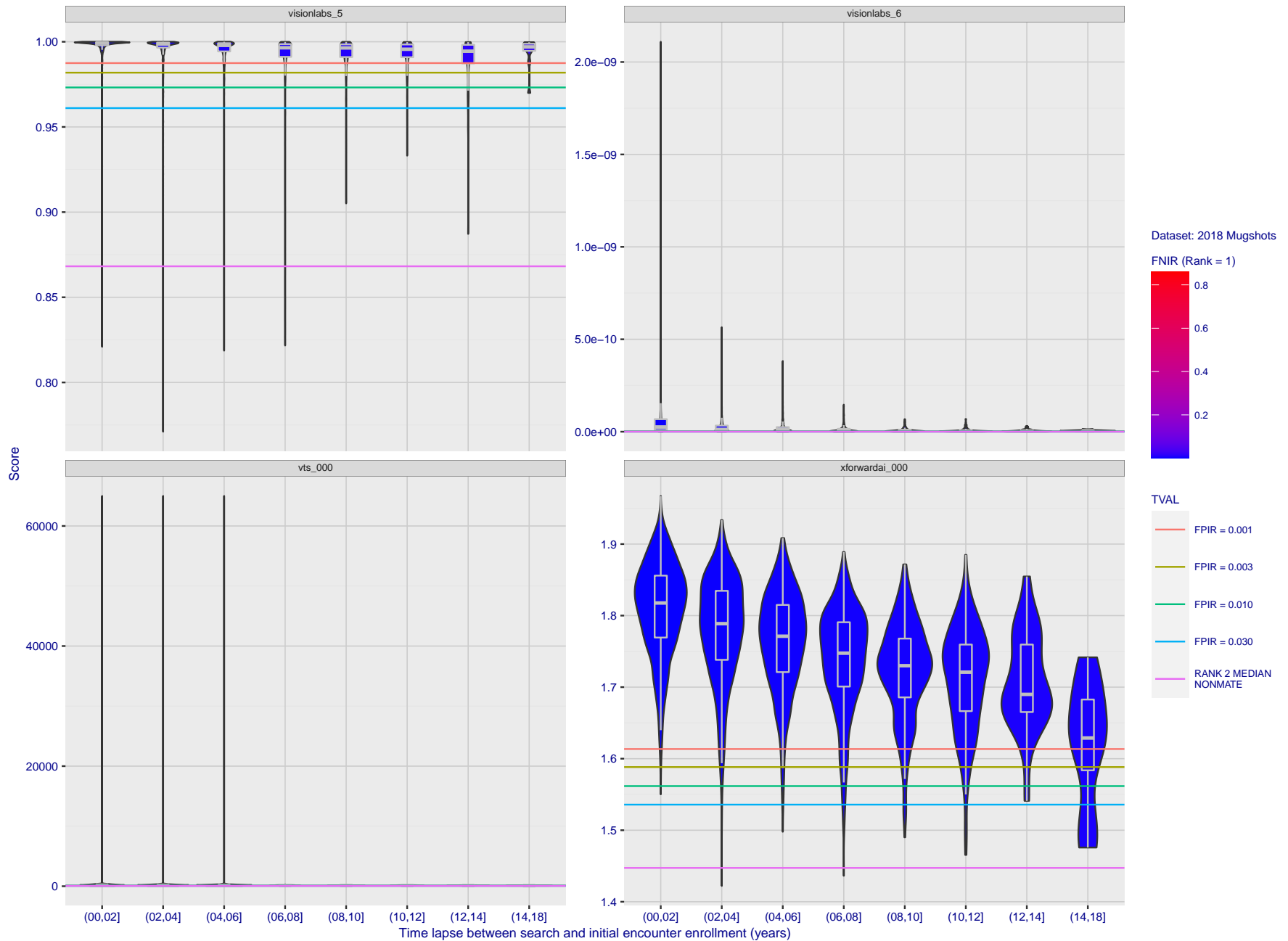


Figure 119: [FRVT-2018 Mugshot Ageing Dataset] Native mate scores vs. time-elapsed. The oldest image of each individual is enrolled. Thereafter, all more recent images are searched. Mated score distributions are computed over all searches noted in row 17 of Table 1 binned by number of years between search and initial enrollment.

2021/10/28 13:44:33  
 FNIR(N, R, T) = False neg. identification rate  
 FPIR(N, T) = False pos. identification rate  
 N = Num. enrolled subjects  
 R = Num. candidates examined  
 T = Threshold  
 T = 0 → Investigation  
 T > 0 → Identification

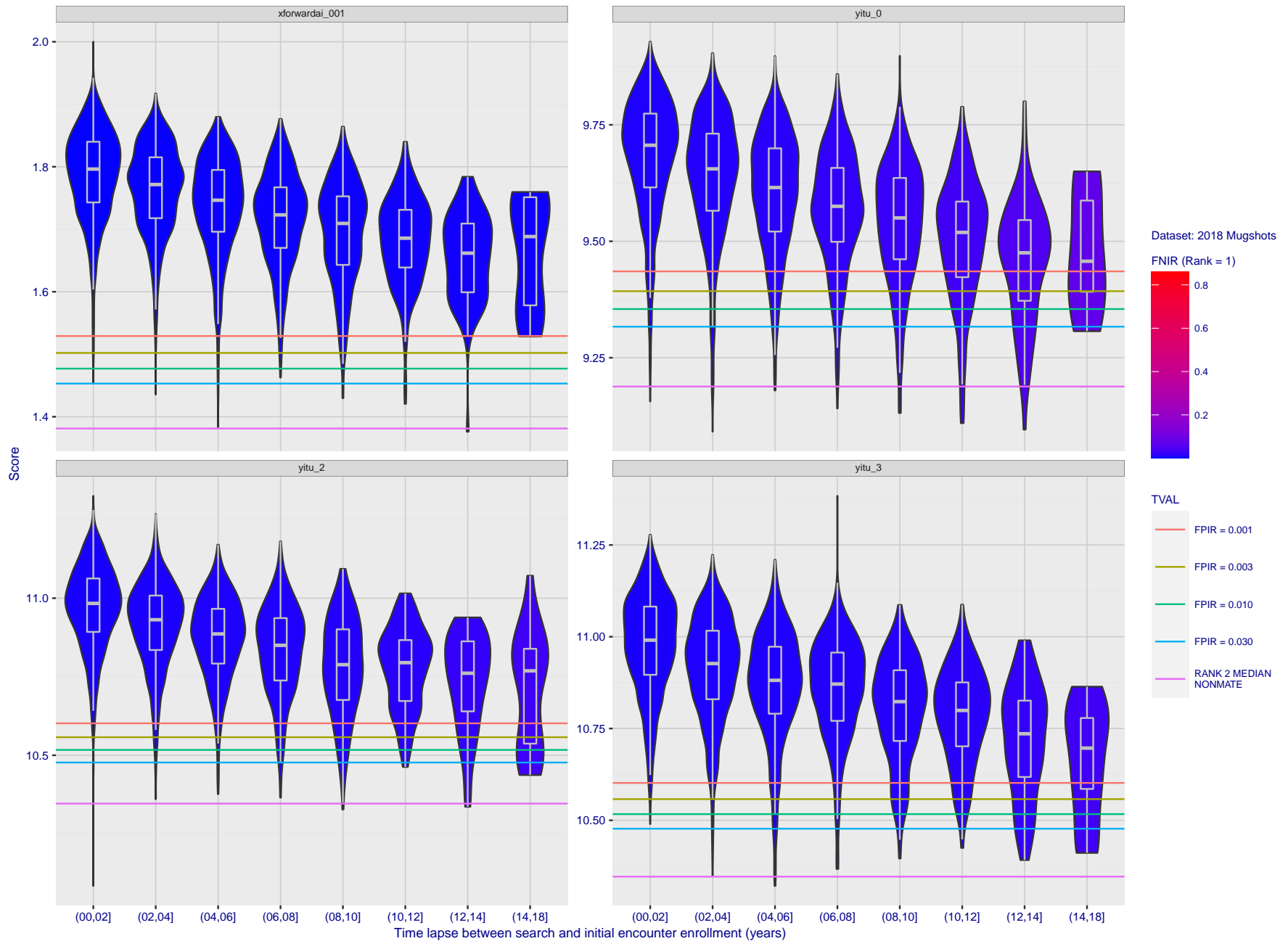


Figure 120: [FRVT-2018 Mugshot Ageing Dataset] Native mate scores vs. time-elapsed. The oldest image of each individual is enrolled. Thereafter, all more recent images are searched. Mated score distributions are computed over all searches noted in row 17 of Table 1 binned by number of years between search and initial enrollment.

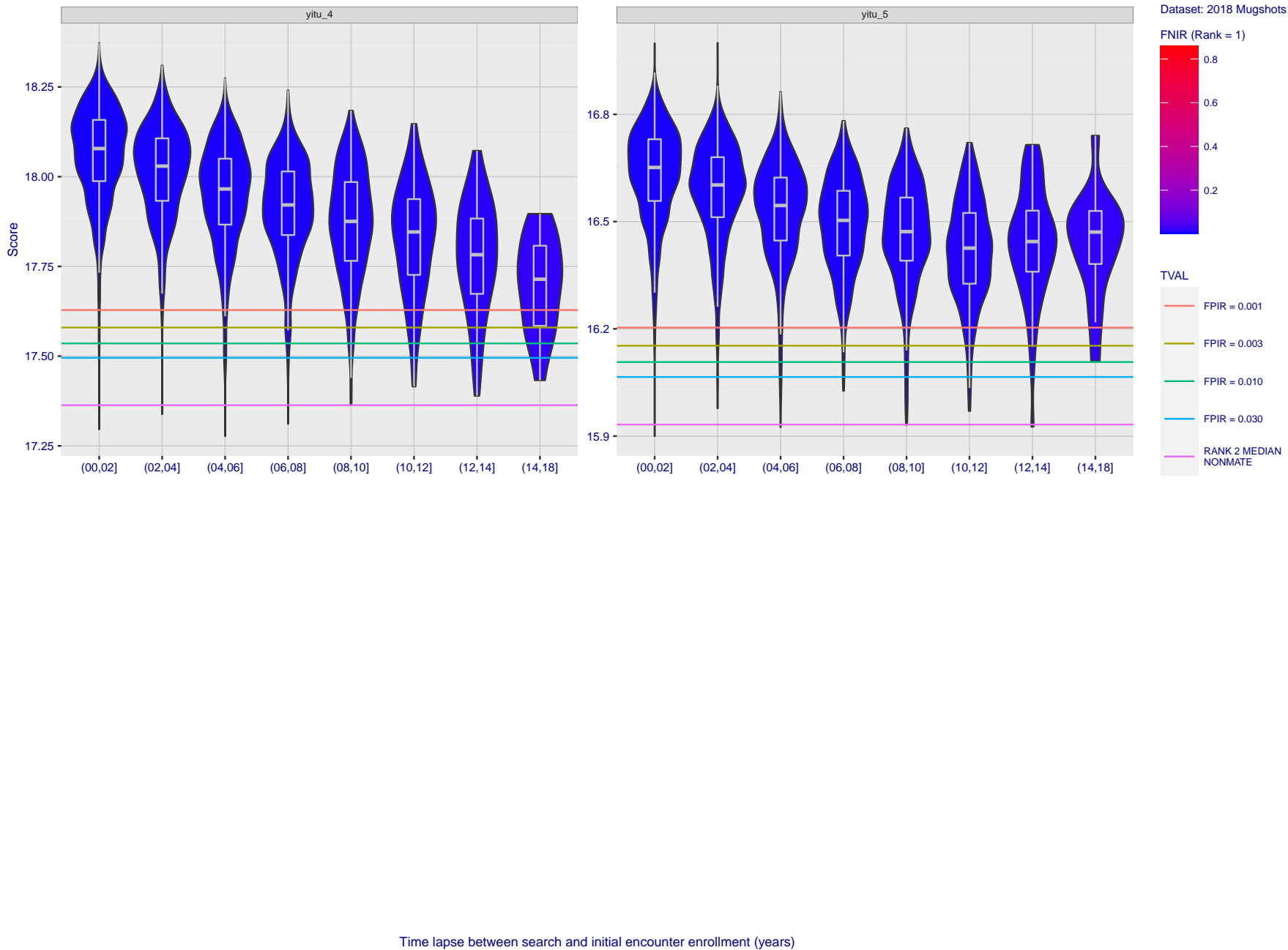


Figure 121: [FRVT-2018 Mugshot Ageing Dataset] Native mate scores vs. time-elapsed. The oldest image of each individual is enrolled. Thereafter, all more recent images are searched. Mated score distributions are computed over all searches noted in row 17 of Table 1 binned by number of years between search and initial enrollment.

2021/10/28  
 13:44:33

FNIR(N, R, T) =  
 FPIR(N, T) =  
 False neg. identification rate  
 False pos. identification rate

N = Num. enrolled subjects  
 R = Num. candidates examined

T = Threshold

T = 0 → Investigation  
 T > 0 → Identification

2021/10/28 13:44:33  
 FNIR(N, R, T) = False neg. identification rate  
 FPIR(N, T) = False pos. identification rate  
 N = Num. enrolled subjects  
 R = Num. candidates examined  
 T = Threshold  
 T = 0 → Investigation  
 T > 0 → Identification

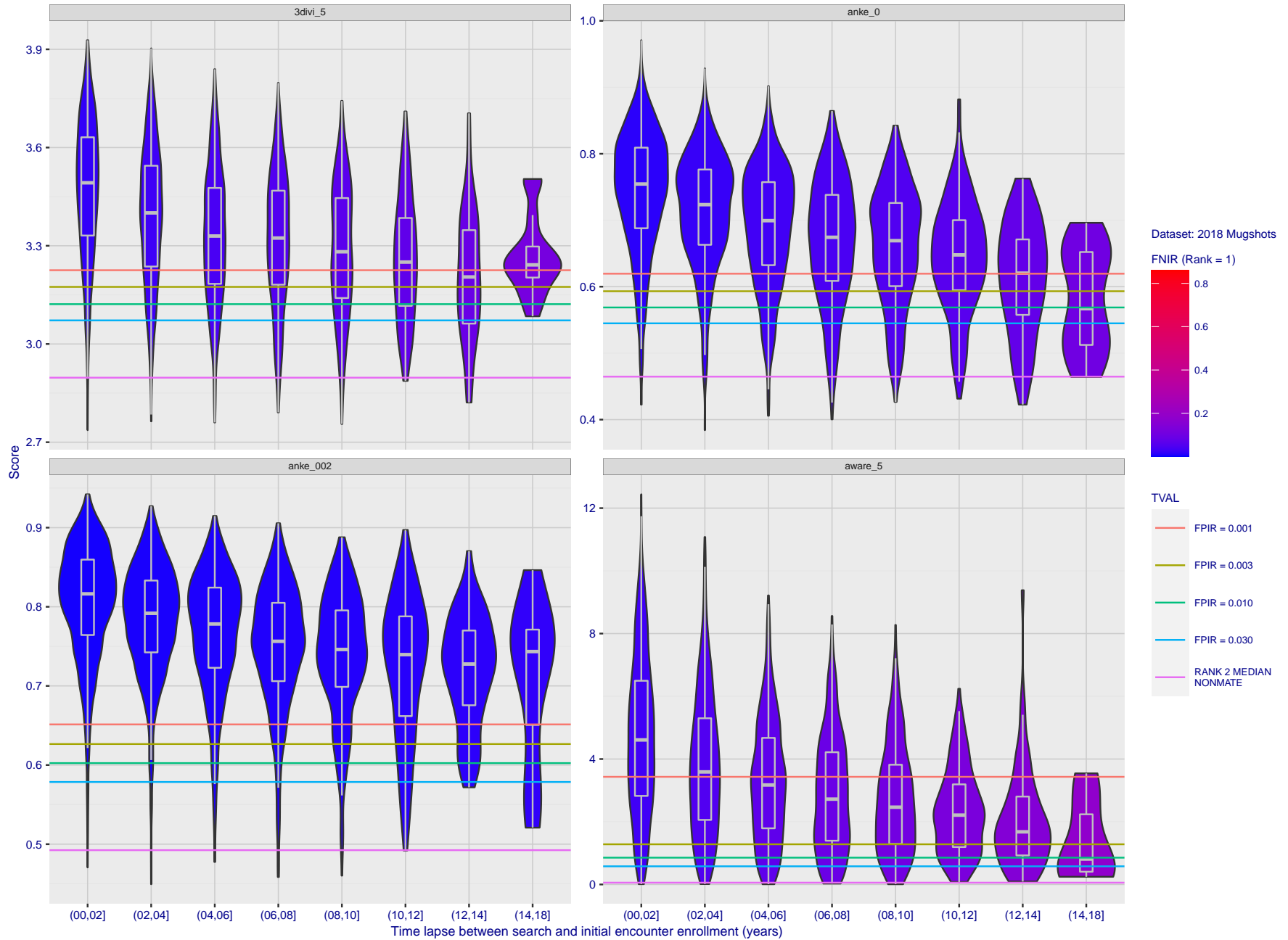


Figure 122: [FRVT-2018 Mugshot Ageing Dataset] Native mate scores vs. time-elapsed. The oldest image of each individual is enrolled. Thereafter, all more recent images are searched. Mated score distributions are computed over all searches noted in row 17 of Table 1 binned by number of years between search and initial enrollment.

2021/10/28 13:44:33  
 FNIR(N, R, T) = False neg. identification rate  
 FPR(N, T) = False pos. identification rate  
 N = Num. enrolled subjects  
 R = Num. candidates examined  
 T = Threshold  
 T = 0 → Investigation  
 T > 0 → Identification

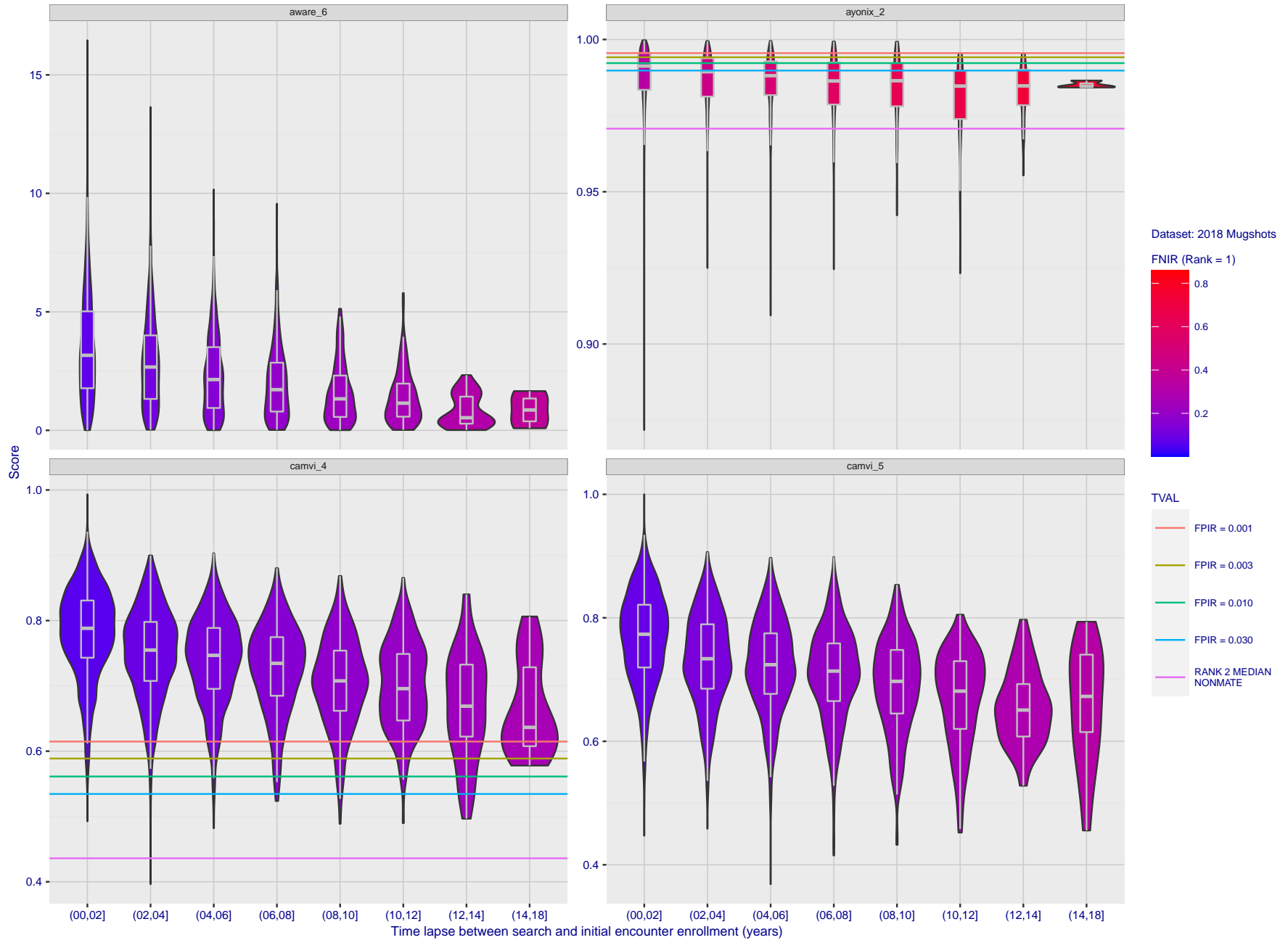


Figure 123: [FRVT-2018 Mugshot Ageing Dataset] Native mate scores vs. time-elapsed. The oldest image of each individual is enrolled. Thereafter, all more recent images are searched. Mated score distributions are computed over all searches noted in row 17 of Table 1 binned by number of years between search and initial enrollment.

2021/10/28 13:44:33  
 FNIR(N, R, T) = False neg. identification rate  
 FPIR(N, T) = False pos. identification rate  
 N = Num. enrolled subjects  
 R = Num. candidates examined  
 T = Threshold  
 T = 0 → Investigation  
 T > 0 → Identification

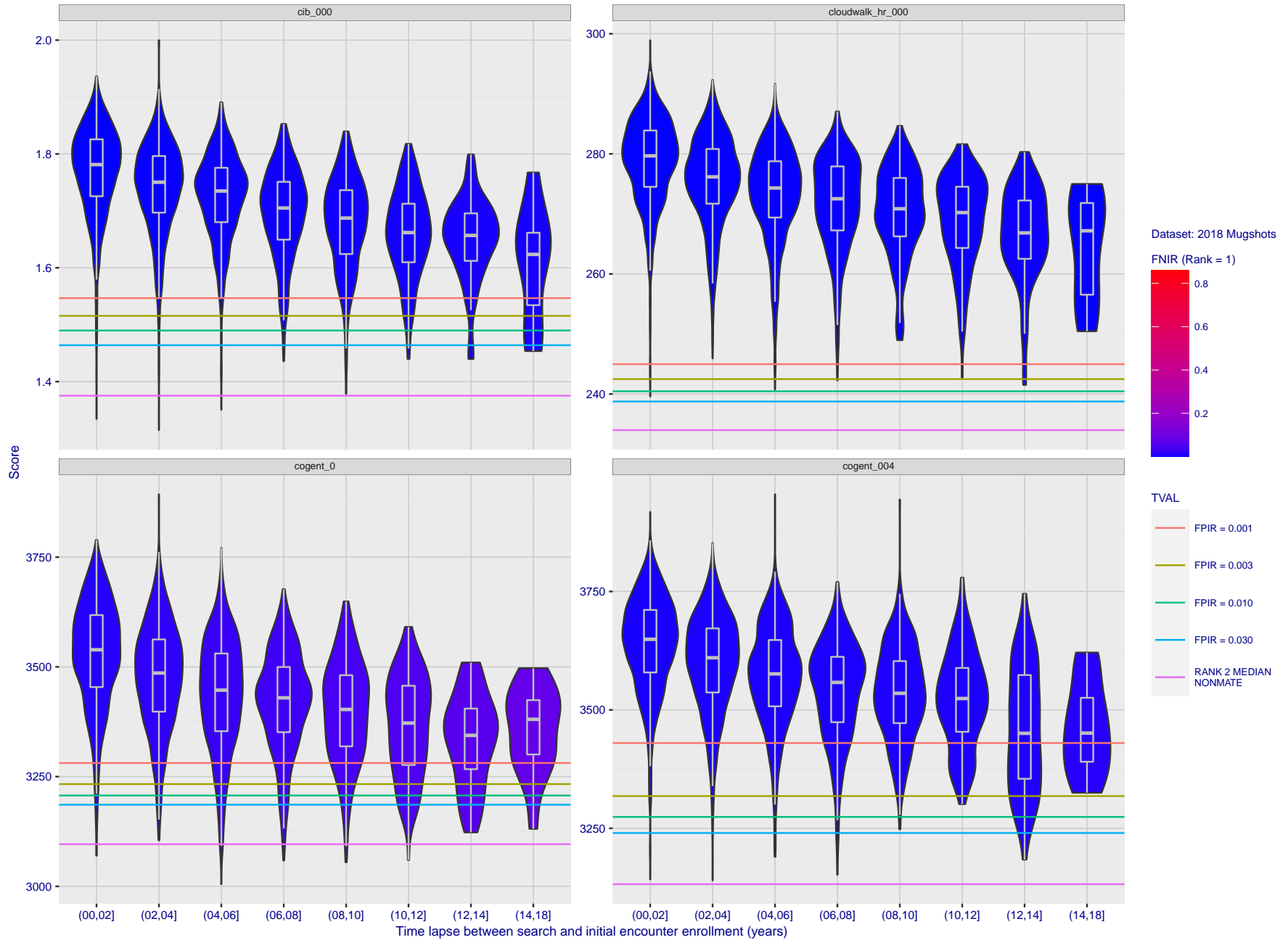


Figure 124: [FRVT-2018 Mugshot Ageing Dataset] Native mate scores vs. time-elapsed. The oldest image of each individual is enrolled. Thereafter, all more recent images are searched. Mated score distributions are computed over all searches noted in row 17 of Table 1 binned by number of years between search and initial enrollment.

2021/10/28 13:44:33  
 FNIR(N, R, T) = False neg. identification rate  
 FPIR(N, T) = False pos. identification rate  
 N = Num. enrolled subjects  
 R = Num. candidates examined  
 T = Threshold  
 T = 0 → Investigation  
 T > 0 → Identification

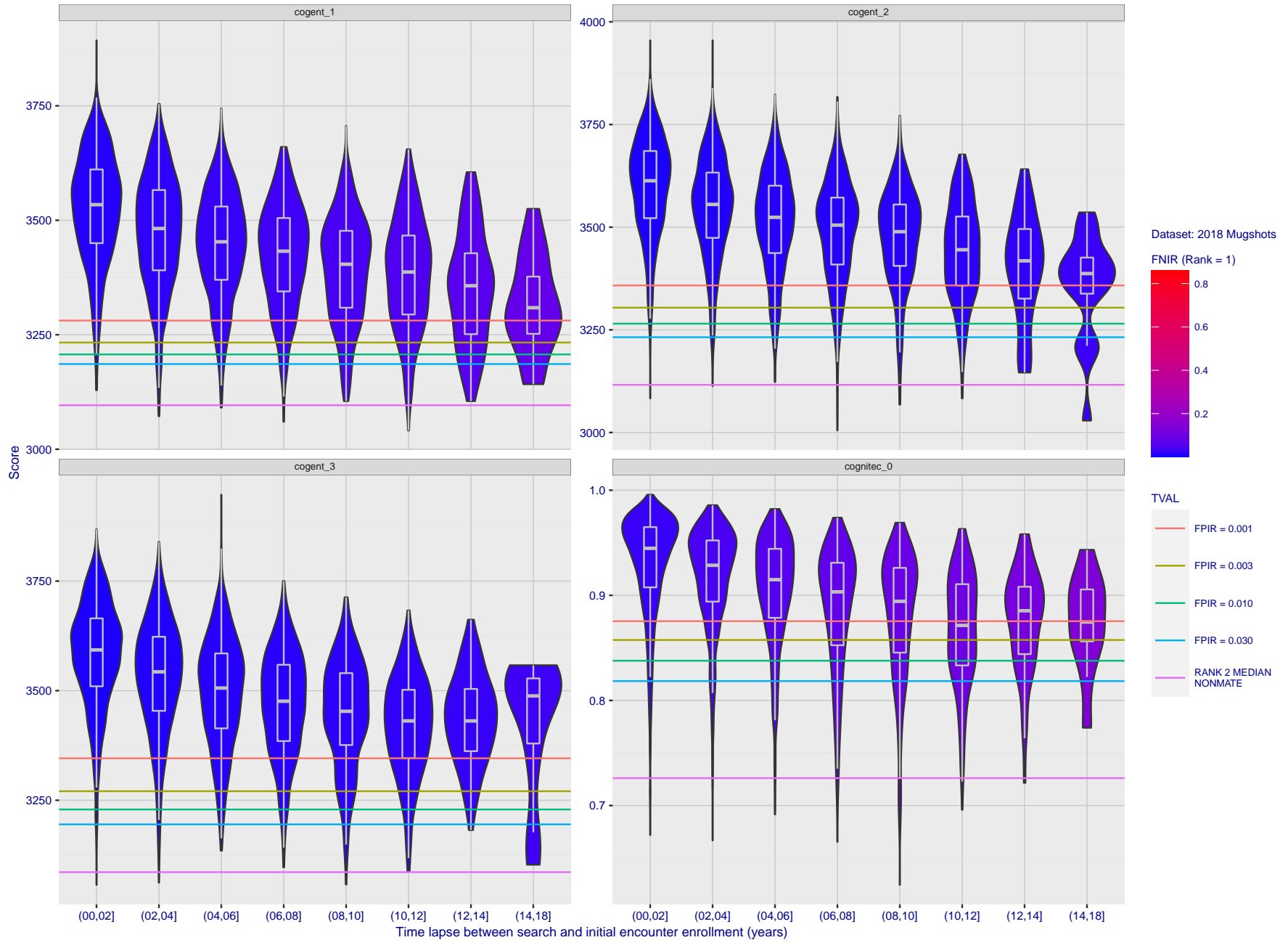


Figure 125: [FRVT-2018 Mugshot Ageing Dataset] Native mate scores vs. time-elapsed. The oldest image of each individual is enrolled. Thereafter, all more recent images are searched. Mated score distributions are computed over all searches noted in row 17 of Table 1 binned by number of years between search and initial enrollment.

2021/10/28 13:44:33  
 FNIR(N, R, T) = False neg. identification rate  
 FPIR(N, T) = False pos. identification rate  
 N = Num. enrolled subjects  
 R = Num. candidates examined  
 T = Threshold  
 T = 0 → Investigation  
 T > 0 → Identification

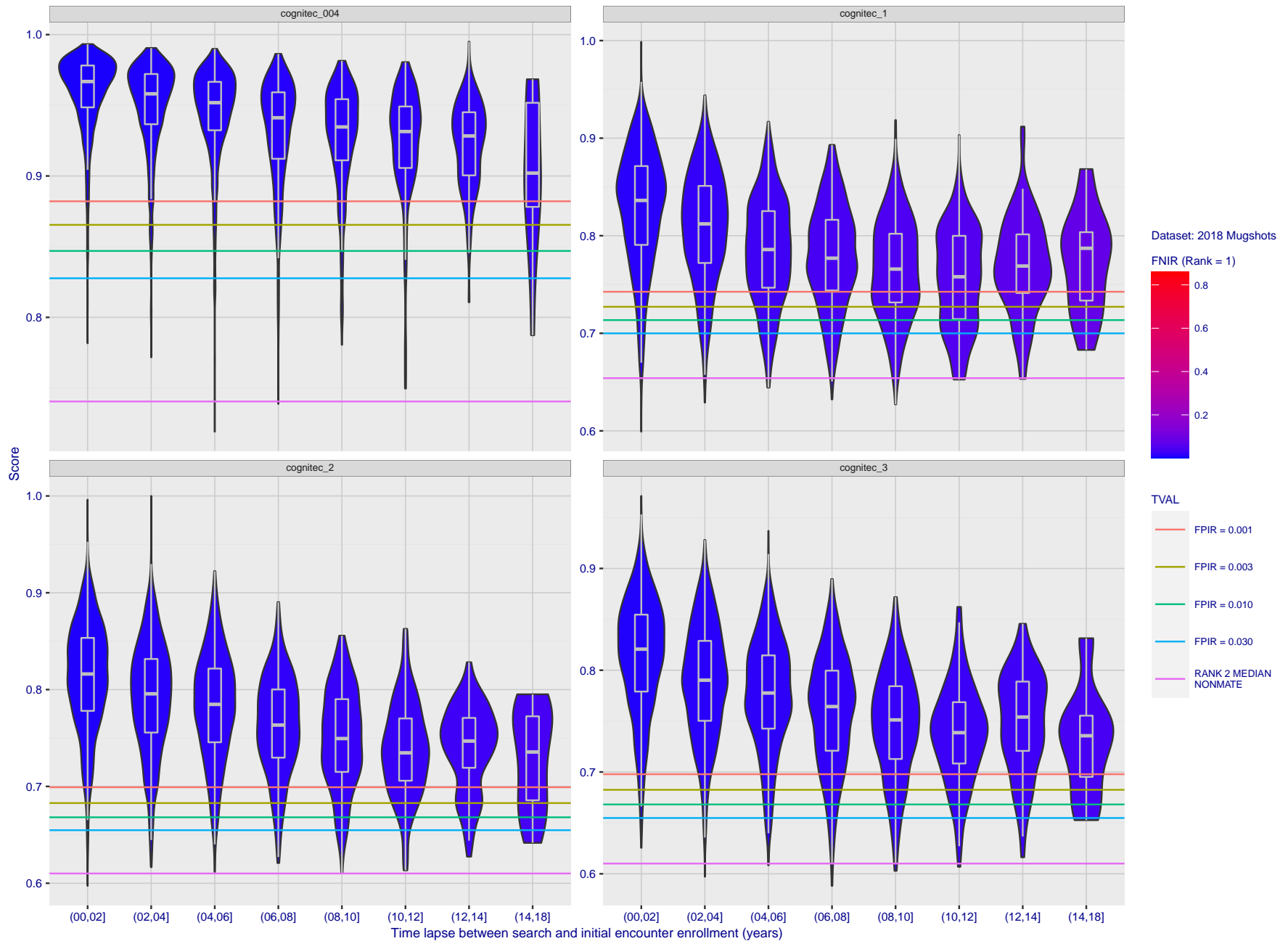


Figure 126: [FRVT-2018 Mugshot Ageing Dataset] Native mate scores vs. time-elapsed. The oldest image of each individual is enrolled. Thereafter, all more recent images are searched. Mated score distributions are computed over all searches noted in row 17 of Table 1 binned by number of years between search and initial enrollment.

2021/10/28 13:44:33  
 FNIR(N, R, T) = False neg. identification rate  
 FPIR(N, T) = False pos. identification rate  
 N = Num. enrolled subjects  
 R = Num. candidates examined  
 T = Threshold  
 T = 0 → Investigation  
 T > 0 → Identification

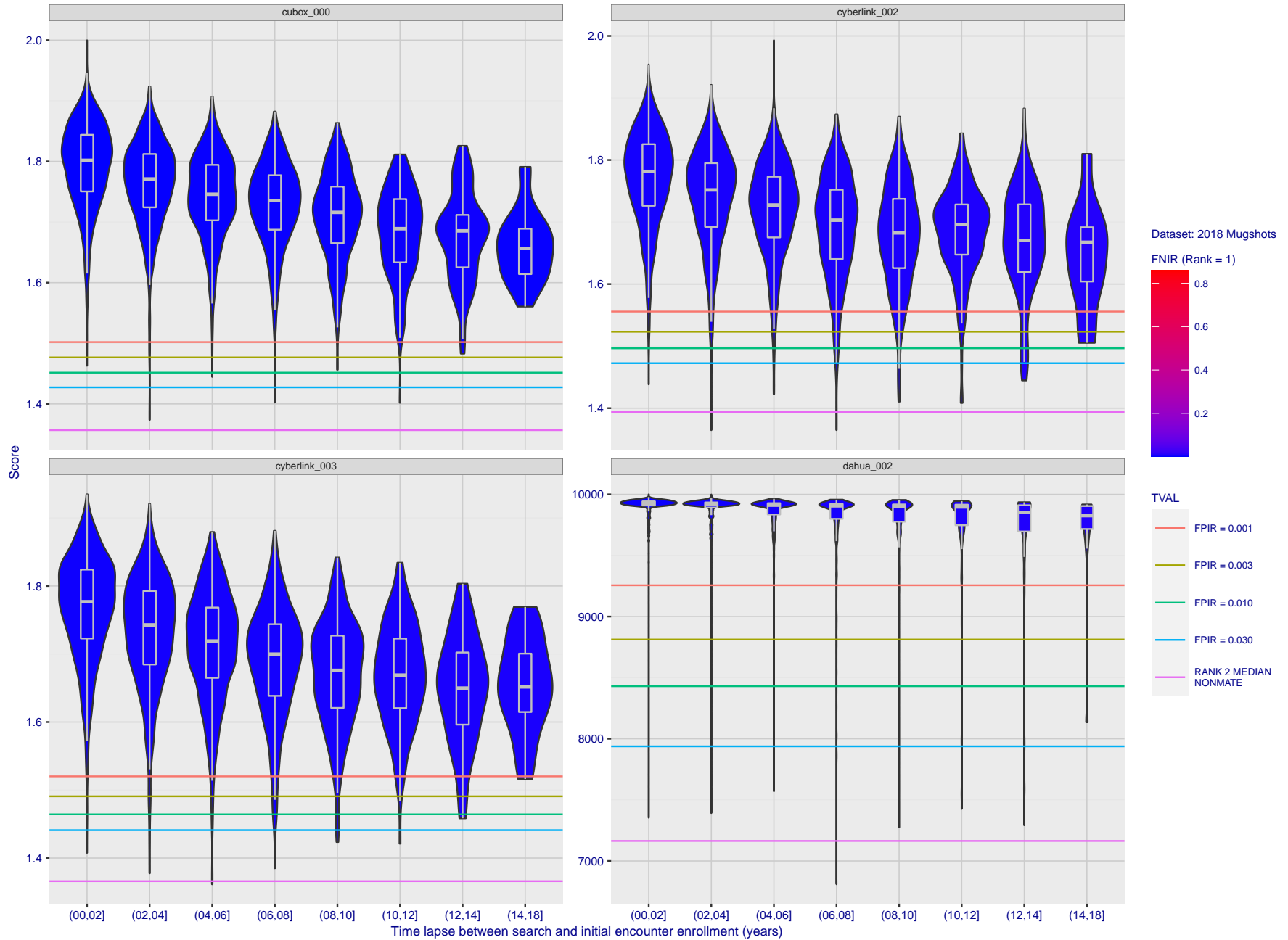


Figure 127: [FRVT-2018 Mugshot Ageing Dataset] Native mate scores vs. time-elapsed. The oldest image of each individual is enrolled. Thereafter, all more recent images are searched. Mated score distributions are computed over all searches noted in row 17 of Table 1 binned by number of years between search and initial enrollment.

2021/10/28 13:44:33  
 FNIR(N, R, T) = False neg. identification rate  
 FPR(N, T) = False pos. identification rate  
 N = Num. enrolled subjects  
 R = Num. candidates examined  
 T = Threshold  
 T = 0 → Investigation  
 T > 0 → Identification

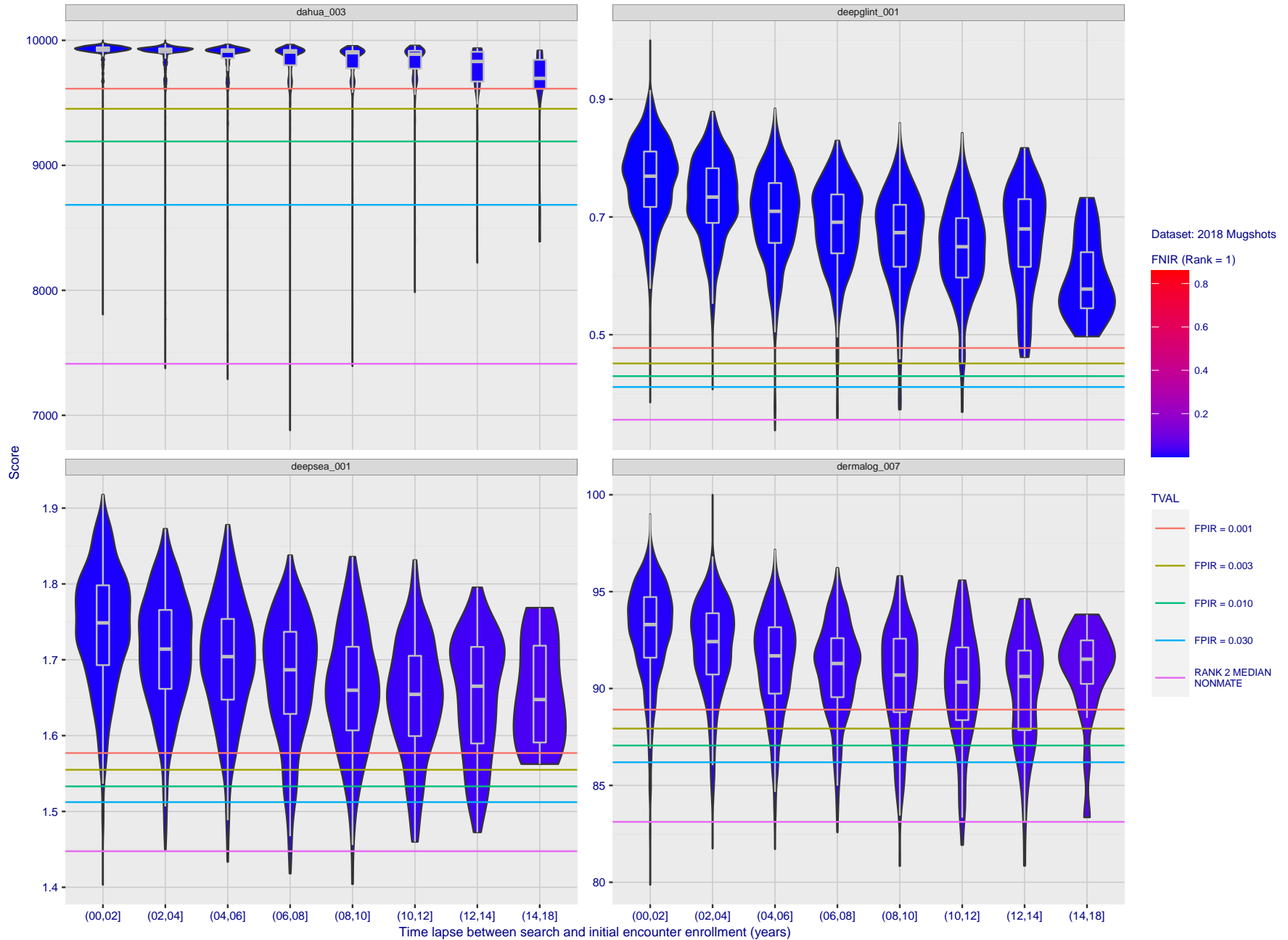


Figure 128: [FRVT-2018 Mugshot Ageing Dataset] Native mate scores vs. time-elapsed. The oldest image of each individual is enrolled. Thereafter, all more recent images are searched. Mated score distributions are computed over all searches noted in row 17 of Table 1 binned by number of years between search and initial enrollment.

2021/10/28  
 13:44:33  
 FNIR(N, R, T) =  
 FPIR(N, T) =  
 False neg. identification rate  
 False pos. identification rate  
 N = Num. enrolled subjects  
 R = Num. candidates examined  
 T = Threshold  
 T = 0 → Investigation  
 T > 0 → Identification

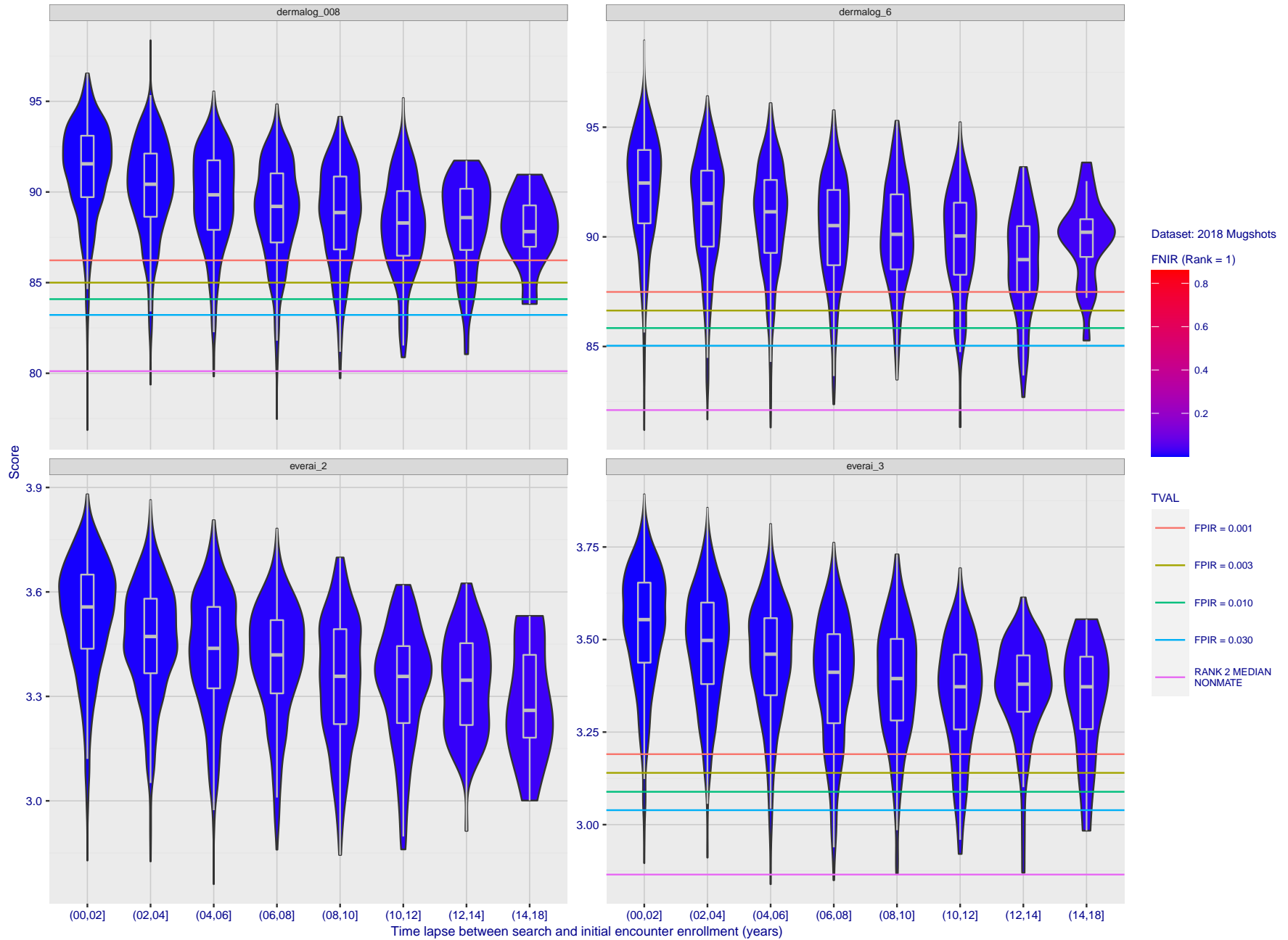


Figure 129: [FRVT-2018 Mugshot Ageing Dataset] Native mate scores vs. time-elapsed. The oldest image of each individual is enrolled. Thereafter, all more recent images are searched. Mated score distributions are computed over all searches noted in row 17 of Table 1 binned by number of years between search and initial enrollment.

2021/10/28  
 13:44:33  
 FNIR(N, R, T) =  
 FPIR(N, T) =  
 False neg. identification rate  
 False pos. identification rate  
 N = Num. enrolled subjects  
 R = Num. candidates examined  
 T = Threshold  
 T = 0 → Investigation  
 T > 0 → Identification

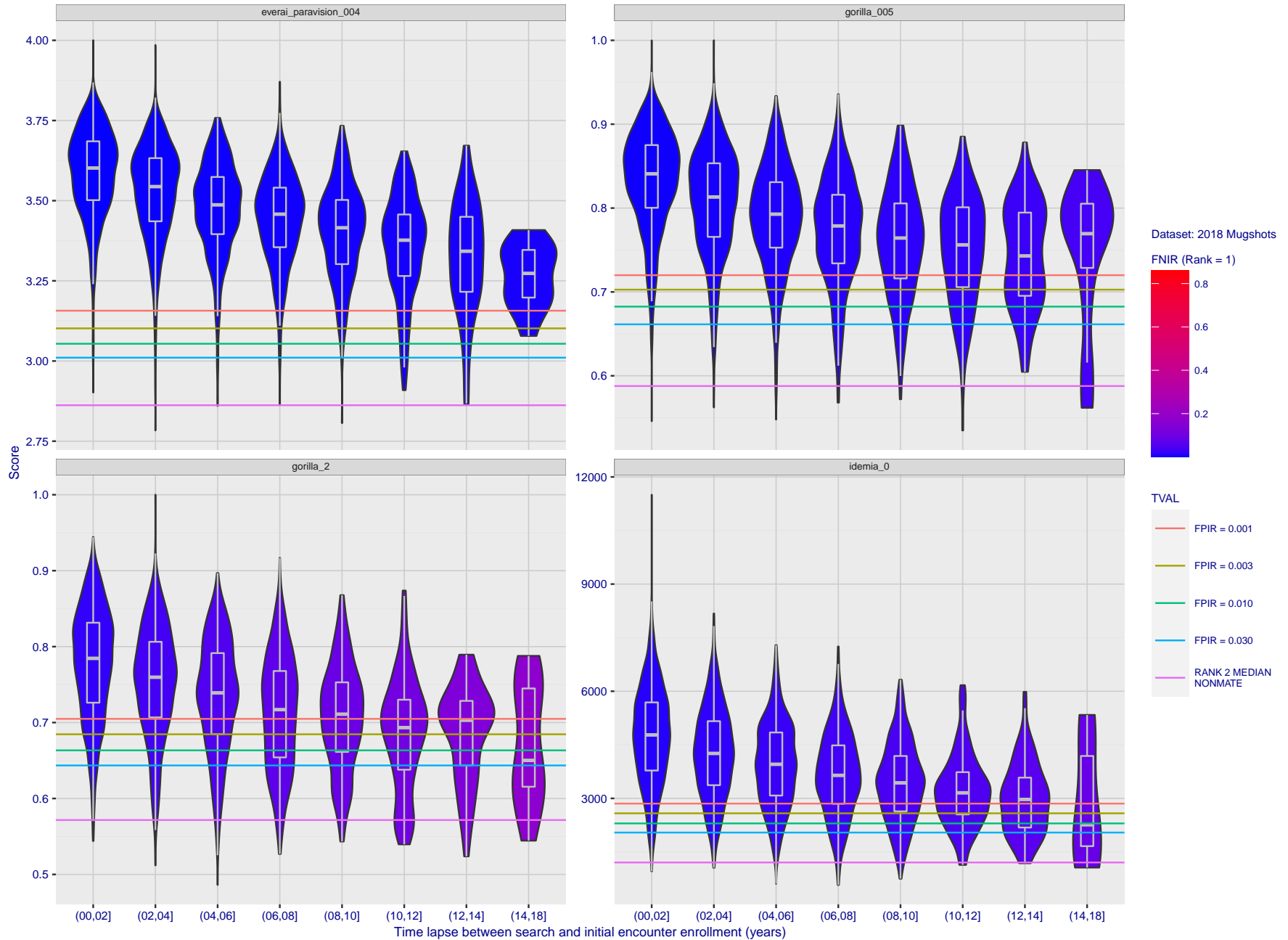


Figure 130: [FRVT-2018 Mugshot Ageing Dataset] Native mate scores vs. time-elapsed. The oldest image of each individual is enrolled. Thereafter, all more recent images are searched. Mated score distributions are computed over all searches noted in row 17 of Table 1 binned by number of years between search and initial enrollment.

2021/10/28  
 13:44:33  
 FNIR(N, R, T) = False neg. identification rate  
 FPIR(N, T) = False pos. identification rate  
 N = Num. enrolled subjects  
 R = Num. candidates examined  
 T = Threshold  
 T = 0 → Investigation  
 T > 0 → Identification

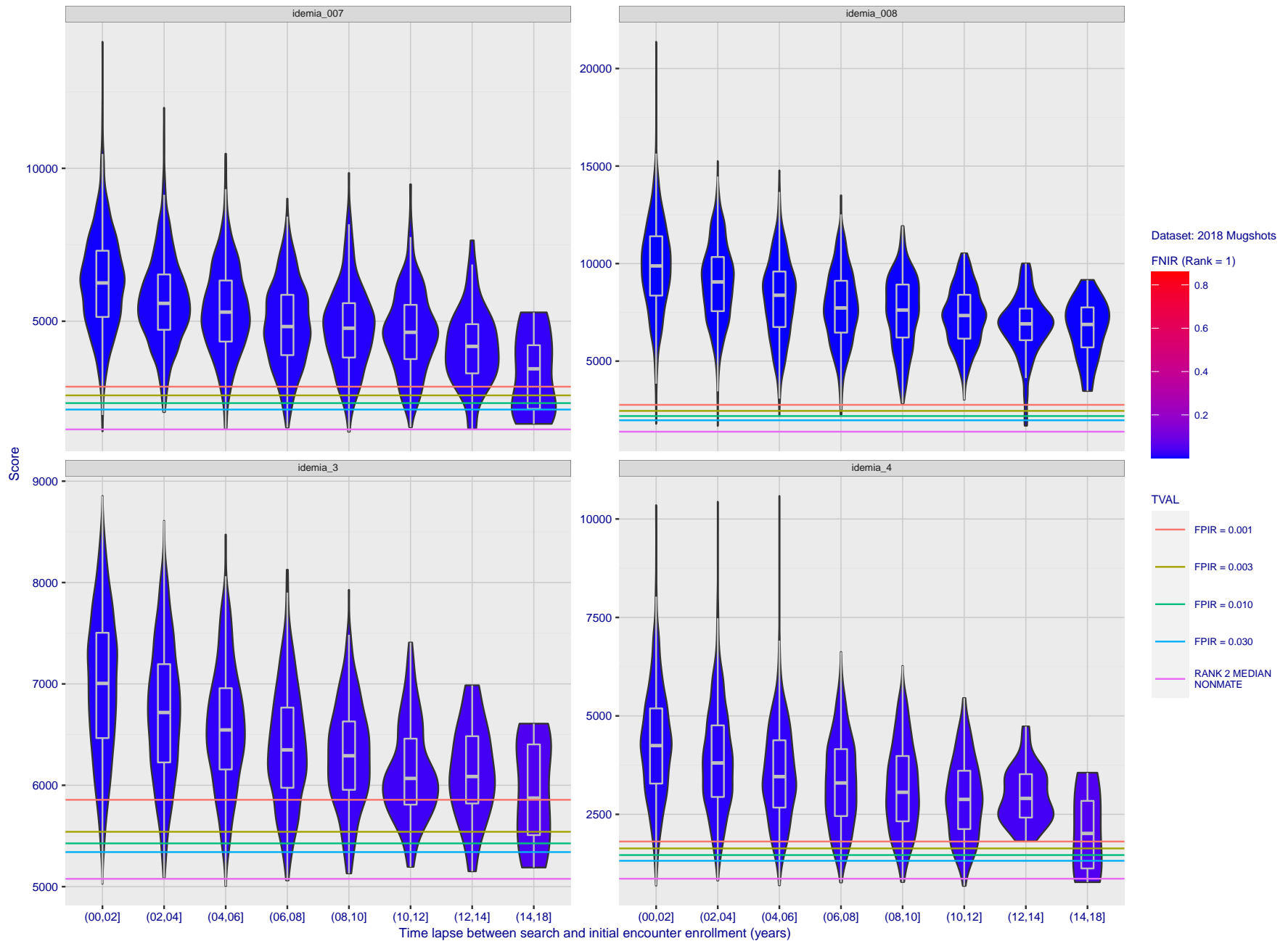


Figure 131: [FRVT-2018 Mugshot Ageing Dataset] Native mate scores vs. time-elapsed. The oldest image of each individual is enrolled. Thereafter, all more recent images are searched. Mated score distributions are computed over all searches noted in row 17 of Table 1 binned by number of years between search and initial enrollment.

2021/10/28 13:44:33  
 FNIR(N, R, T) = False neg. identification rate  
 FPIR(N, T) = False pos. identification rate  
 N = Num. enrolled subjects  
 R = Num. candidates examined  
 T = Threshold  
 T = 0 → Investigation  
 T > 0 → Identification

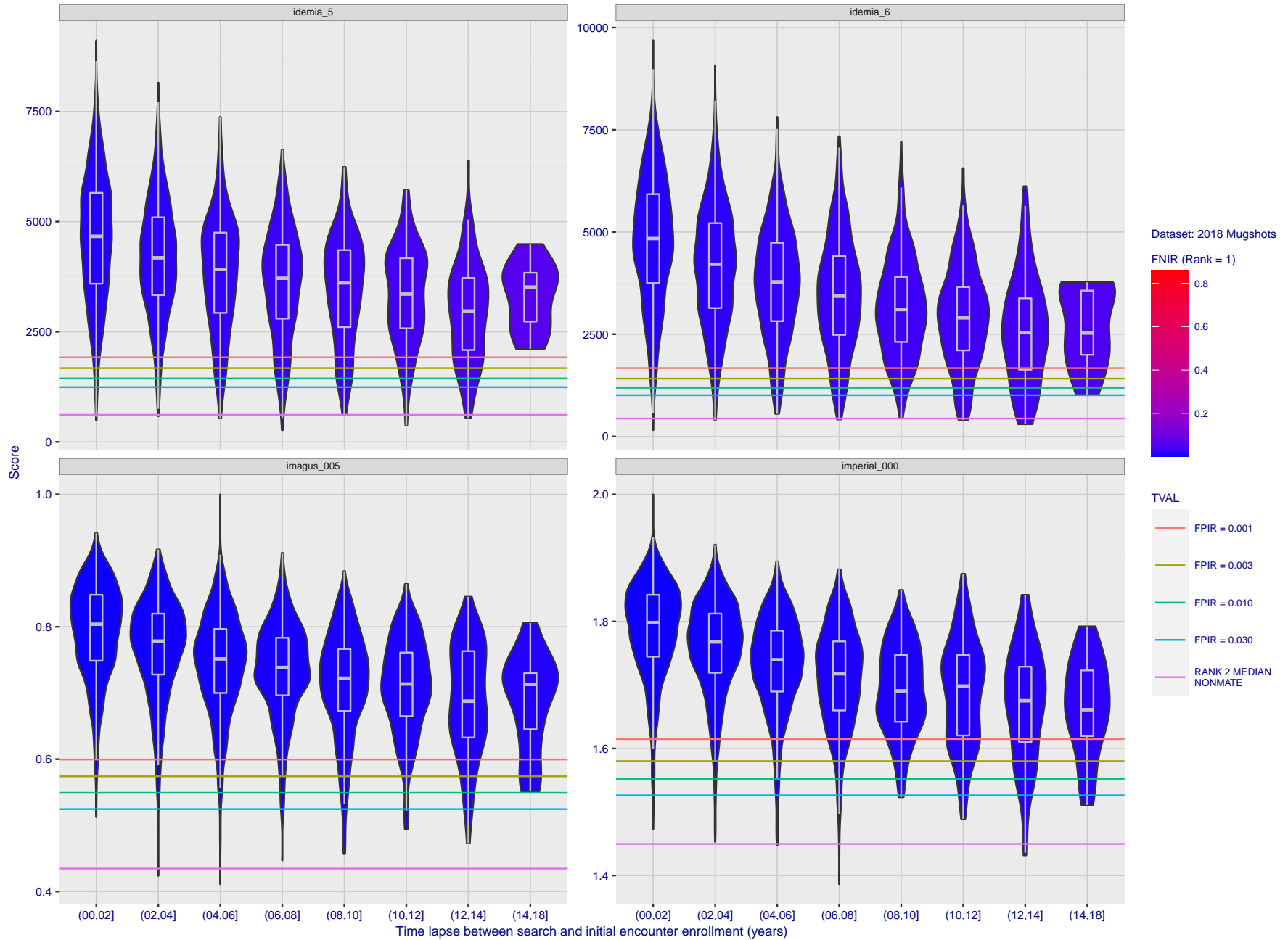


Figure 132: [FRVT-2018 Mugshot Ageing Dataset] Native mate scores vs. time-elapsed. The oldest image of each individual is enrolled. Thereafter, all more recent images are searched. Mated score distributions are computed over all searches noted in row 17 of Table 1 binned by number of years between search and initial enrollment.

2021/10/28  
13:44:33

FNIR(N, R, T) = False neg. identification rate  
FPIR(N, T) = False pos. identification rate

N = Num. enrolled subjects  
R = Num. candidates examined

T = Threshold

T = 0 → Investigation  
T > 0 → Identification

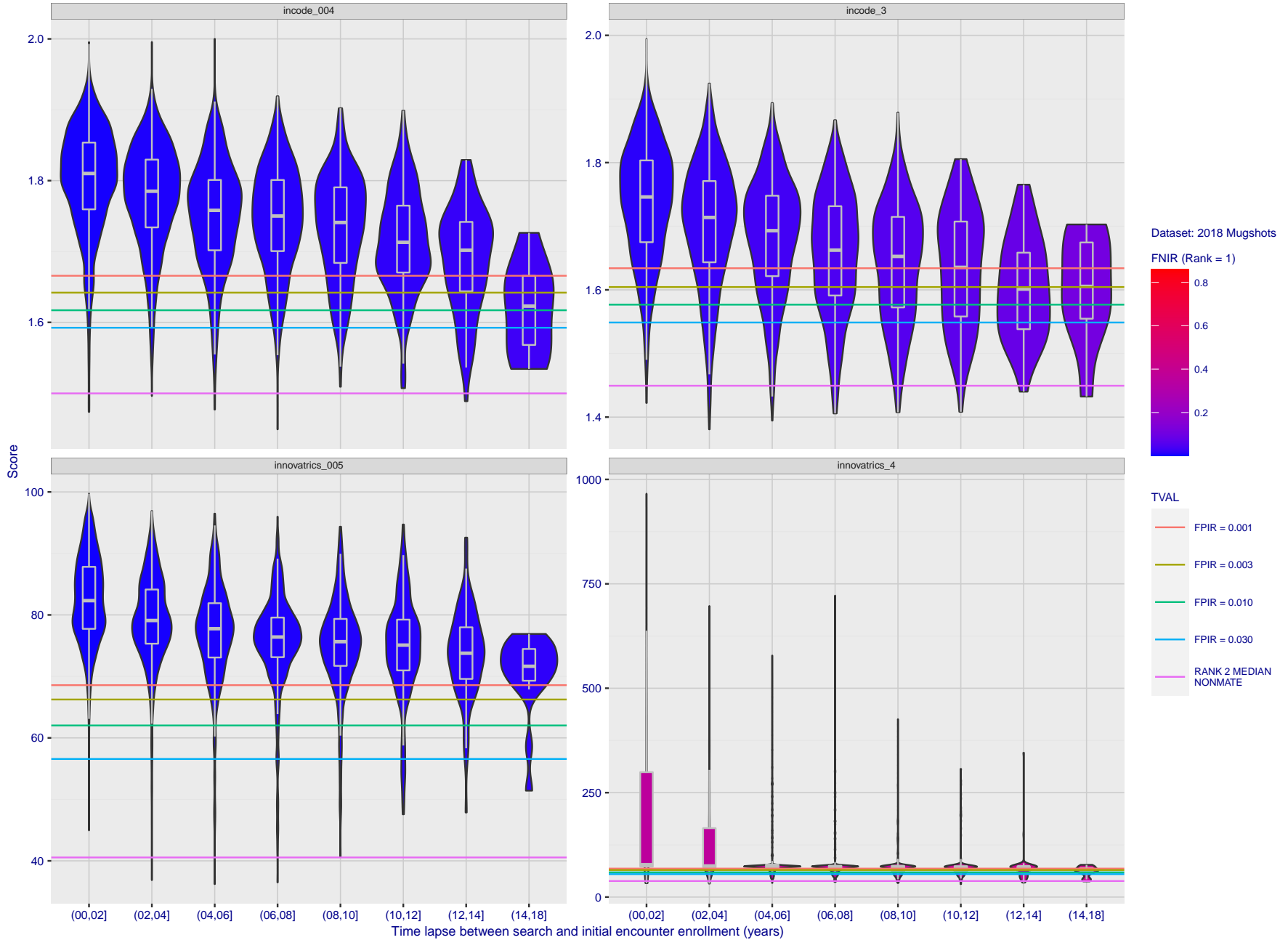


Figure 133: [FRVT-2018 Mugshot Ageing Dataset] Native mate scores vs. time-elapsed. The oldest image of each individual is enrolled. Thereafter, all more recent images are searched. Mated score distributions are computed over all searches noted in row 17 of Table 1 binned by number of years between search and initial enrollment.

2021/10/28  
13:44:33

FNIR(N, R, T) = False neg. identification rate  
FPIR(N, T) = False pos. identification rate

N = Num. enrolled subjects  
R = Num. candidates examined

T = Threshold

T = 0 → Investigation  
T > 0 → Identification

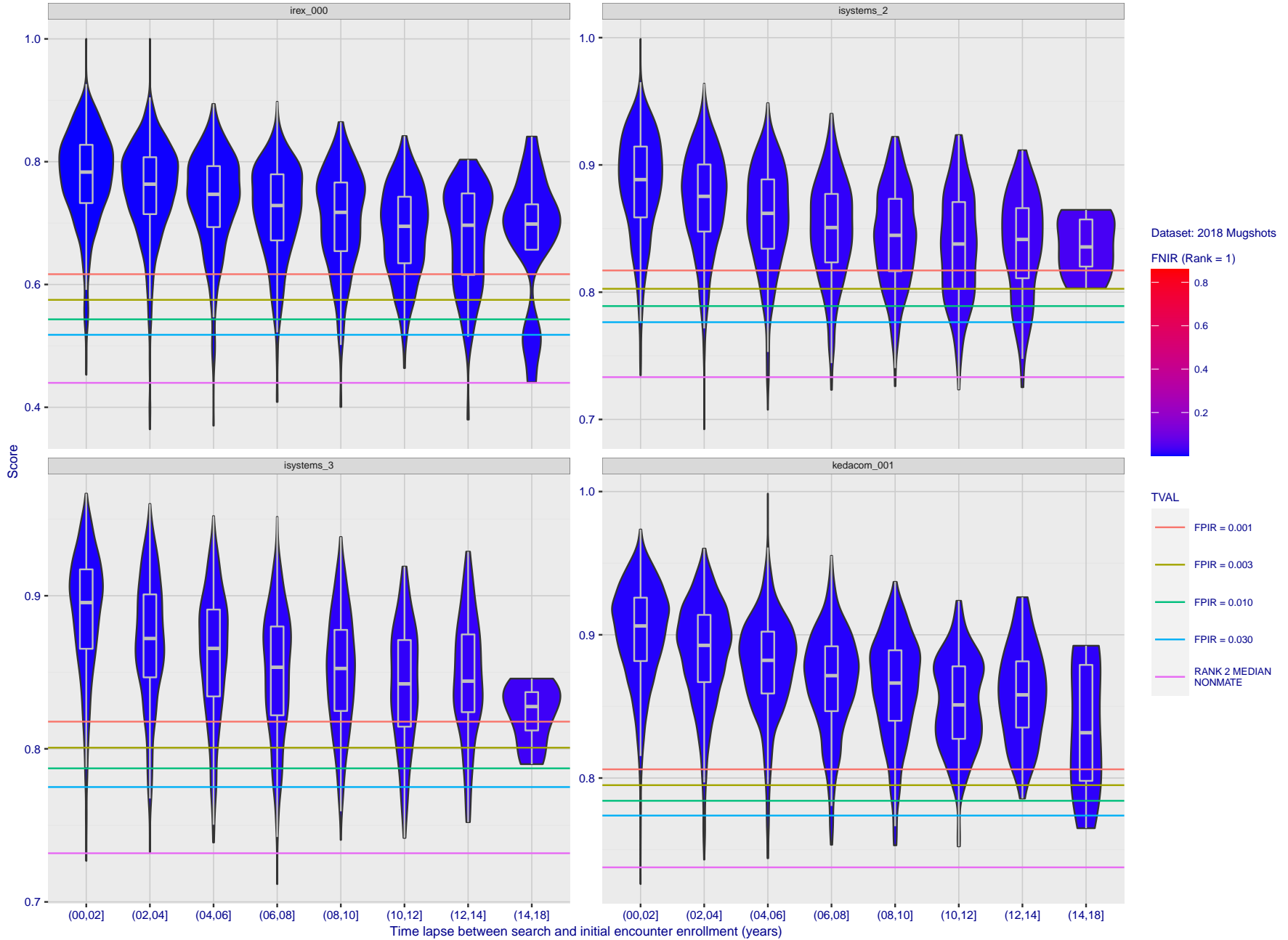


Figure 134: [FRVT-2018 Mugshot Ageing Dataset] Native mate scores vs. time-elapsed. The oldest image of each individual is enrolled. Thereafter, all more recent images are searched. Mated score distributions are computed over all searches noted in row 17 of Table 1 binned by number of years between search and initial enrollment.

2021/10/28  
 13:44:33  
 FNIR(N, R, T) =  
 FPIR(N, T) =  
 False neg. identification rate  
 False pos. identification rate  
 N = Num. enrolled subjects  
 R = Num. candidates examined  
 T = Threshold  
 T = 0 → Investigation  
 T > 0 → Identification

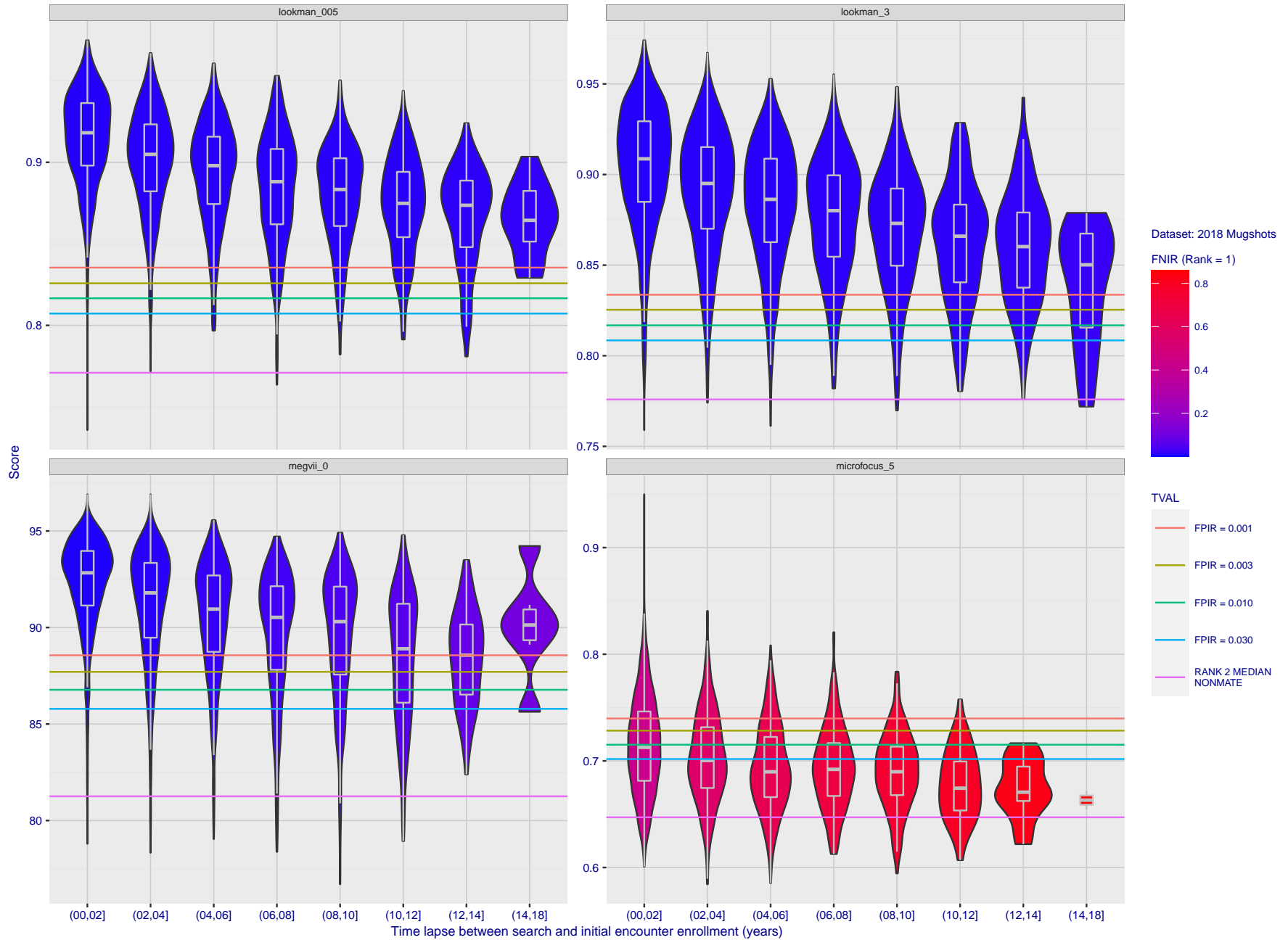


Figure 135: [FRVT-2018 Mugshot Ageing Dataset] Native mate scores vs. time-elapsed. The oldest image of each individual is enrolled. Thereafter, all more recent images are searched. Mated score distributions are computed over all searches noted in row 17 of Table 1 binned by number of years between search and initial enrollment.

2021/10/28 13:44:33 FNIR(N, R, T) = False neg. identification rate N = Num. enrolled subjects T = Threshold T = 0 → Investigation  
 FPIR(N, T) = False pos. identification rate R = Num. candidates examined T > 0 → Identification

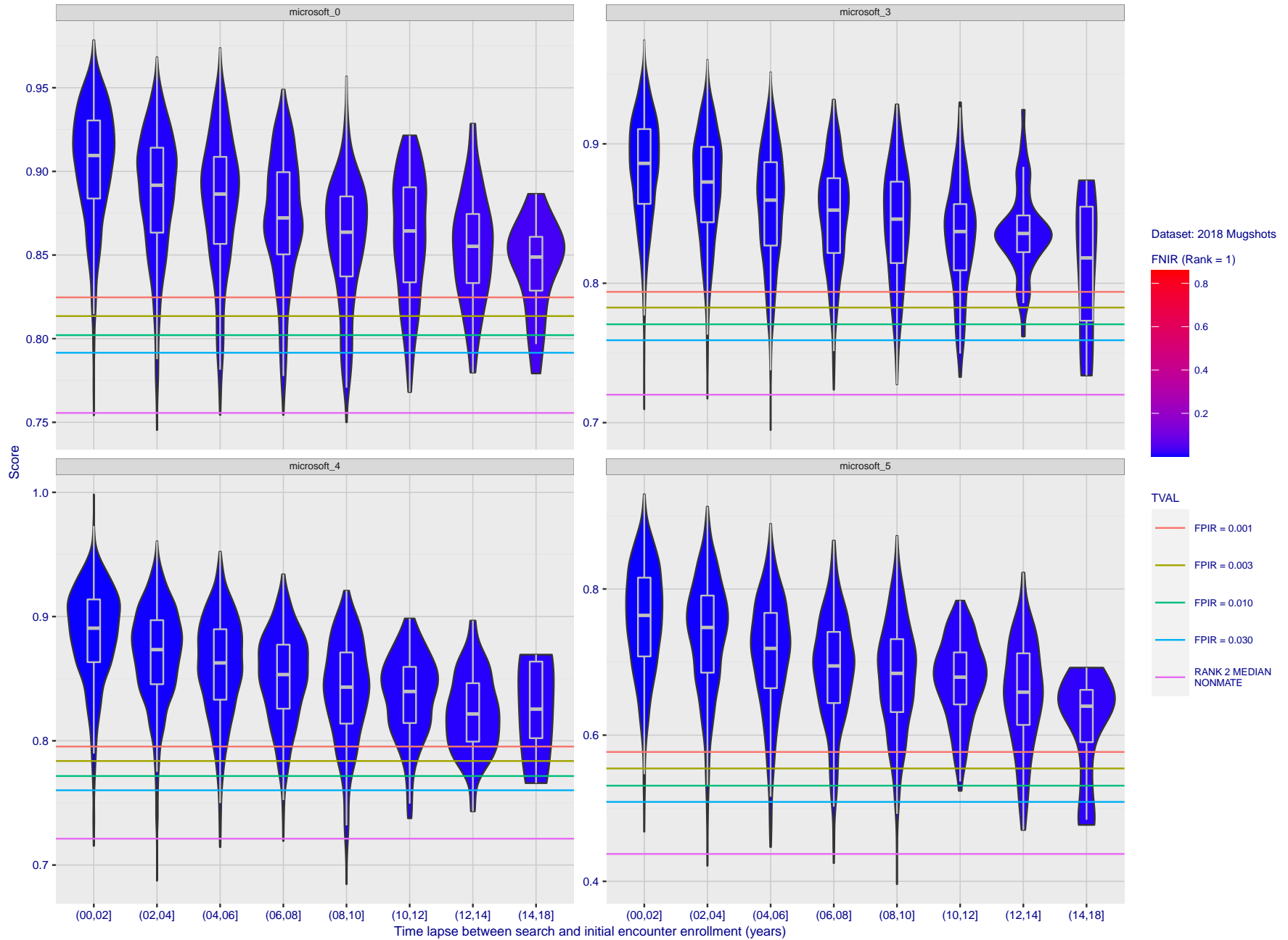


Figure 136: [FRVT-2018 Mugshot Ageing Dataset] Native mate scores vs. time-elapsed. The oldest image of each individual is enrolled. Thereafter, all more recent images are searched. Mated score distributions are computed over all searches noted in row 17 of Table 1 binned by number of years between search and initial enrollment.

2021/10/28  
 13:44:33  
 FNIR(N, R, T) =  
 FPIR(N, T) =  
 False neg. identification rate  
 False pos. identification rate  
 N = Num. enrolled subjects  
 R = Num. candidates examined  
 T = Threshold  
 T = 0 → Investigation  
 T > 0 → Identification

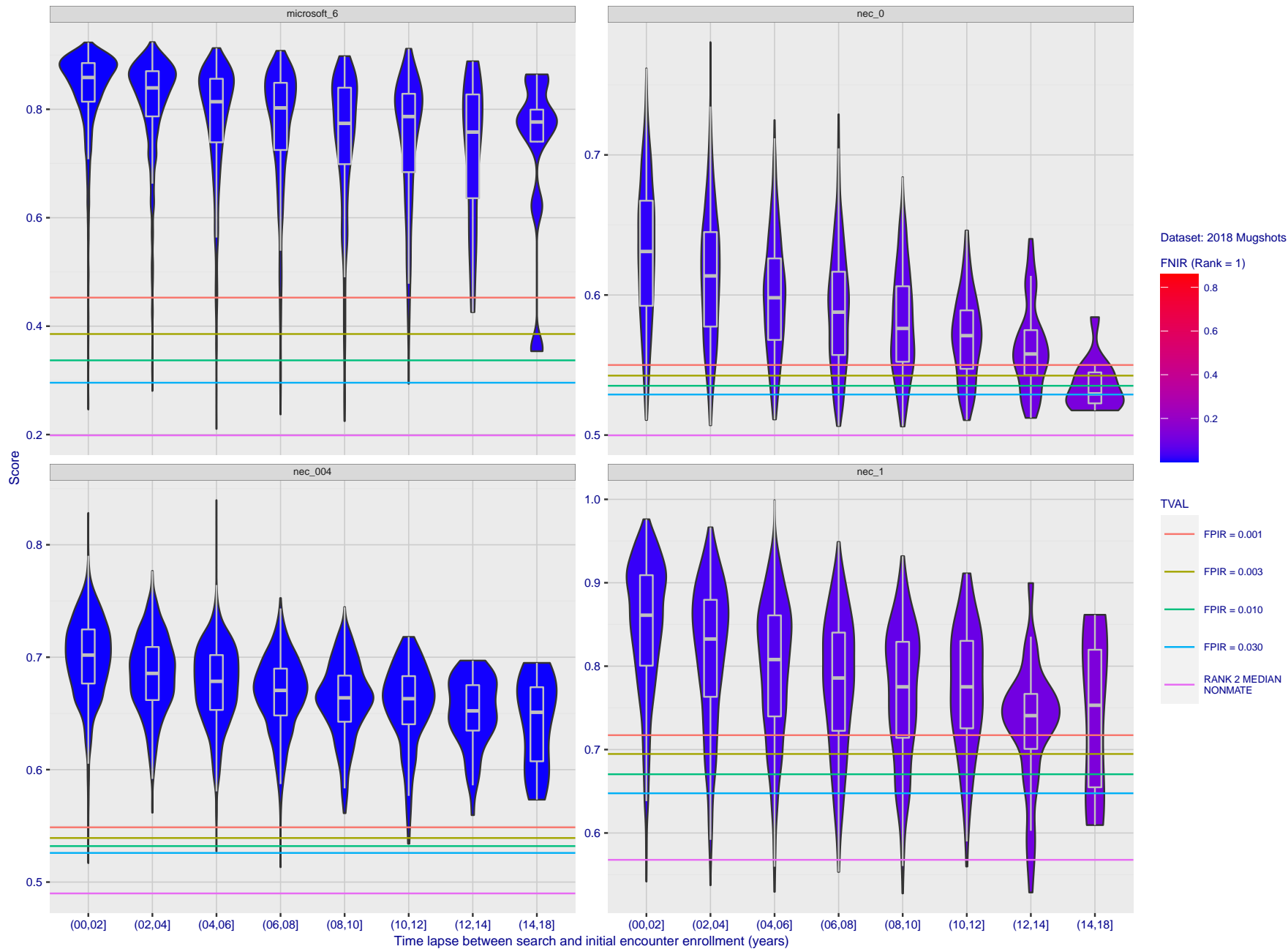


Figure 137: [FRVT-2018 Mugshot Ageing Dataset] Native mate scores vs. time-elapsed. The oldest image of each individual is enrolled. Thereafter, all more recent images are searched. Mated score distributions are computed over all searches noted in row 17 of Table 1 binned by number of years between search and initial enrollment.

2021/10/28 13:44:33 FNIR(N, R, T) = False neg. identification rate N = Num. enrolled subjects T = Threshold  
 FPIR(N, T) = False pos. identification rate R = Num. candidates examined T > 0 → Investigation  
 T > 0 → Identification

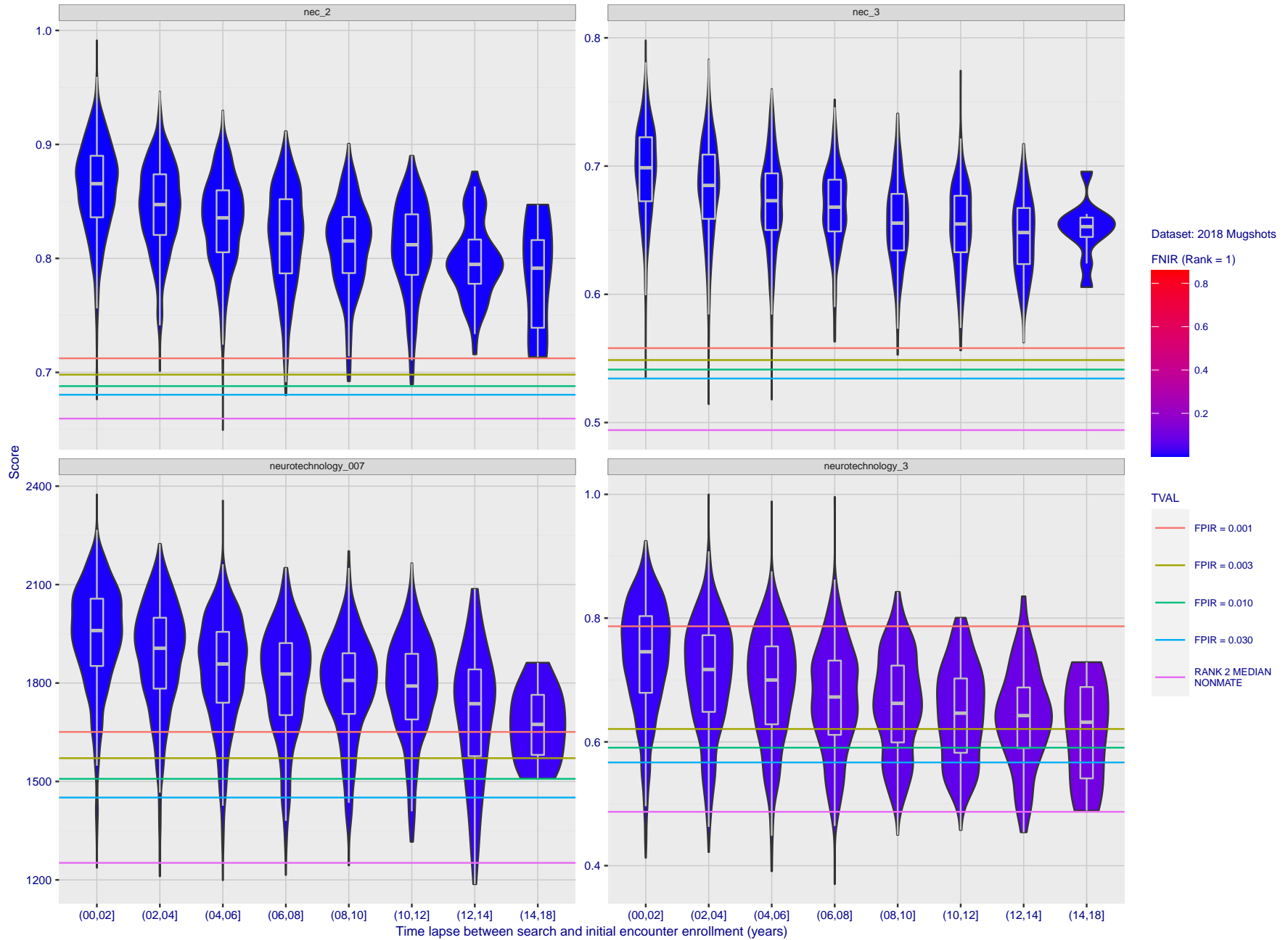


Figure 138: [FRVT-2018 Mugshot Ageing Dataset] Native mate scores vs. time-elapsed. The oldest image of each individual is enrolled. Thereafter, all more recent images are searched. Mated score distributions are computed over all searches noted in row 17 of Table 1 binned by number of years between search and initial enrollment.

2021/10/28  
 13:44:33  
 FNIR(N, R, T) =  
 FPR(N, T) =  
 False neg. identification rate  
 False pos. identification rate  
 N = Num. enrolled subjects  
 R = Num. candidates examined  
 T = Threshold  
 T = 0 → Investigation  
 T > 0 → Identification

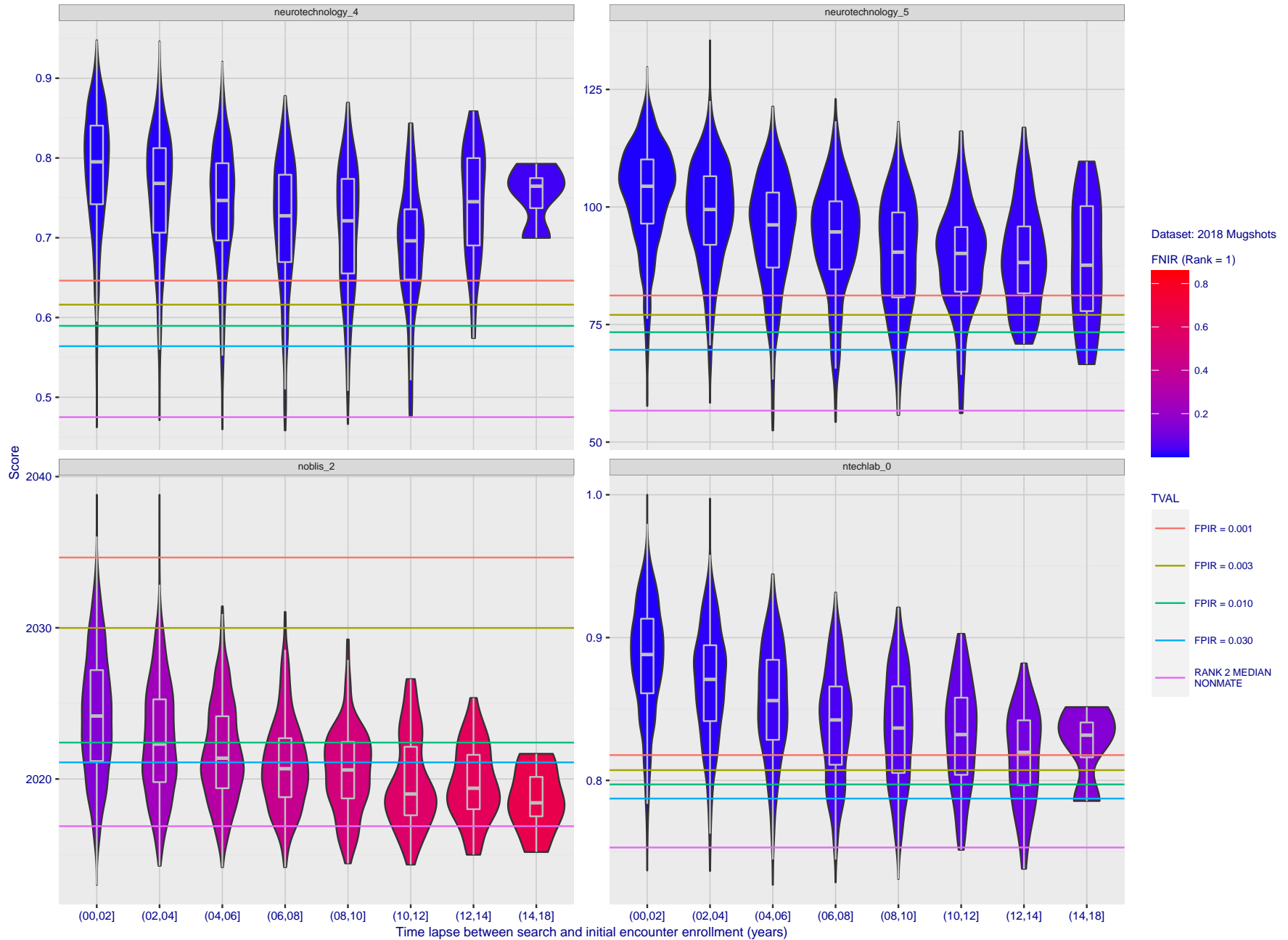


Figure 139: [FRVT-2018 Mugshot Ageing Dataset] Native mate scores vs. time-elapsed. The oldest image of each individual is enrolled. Thereafter, all more recent images are searched. Mated score distributions are computed over all searches noted in row 17 of Table 1 binned by number of years between search and initial enrollment.

2021/10/28  
 13:44:33  
 FNIR(N, R, T) =  
 FPIR(N, T) =  
 False neg. identification rate  
 False pos. identification rate  
 N = Num. enrolled subjects  
 R = Num. candidates examined  
 T = Threshold  
 T = 0 → Investigation  
 T > 0 → Identification

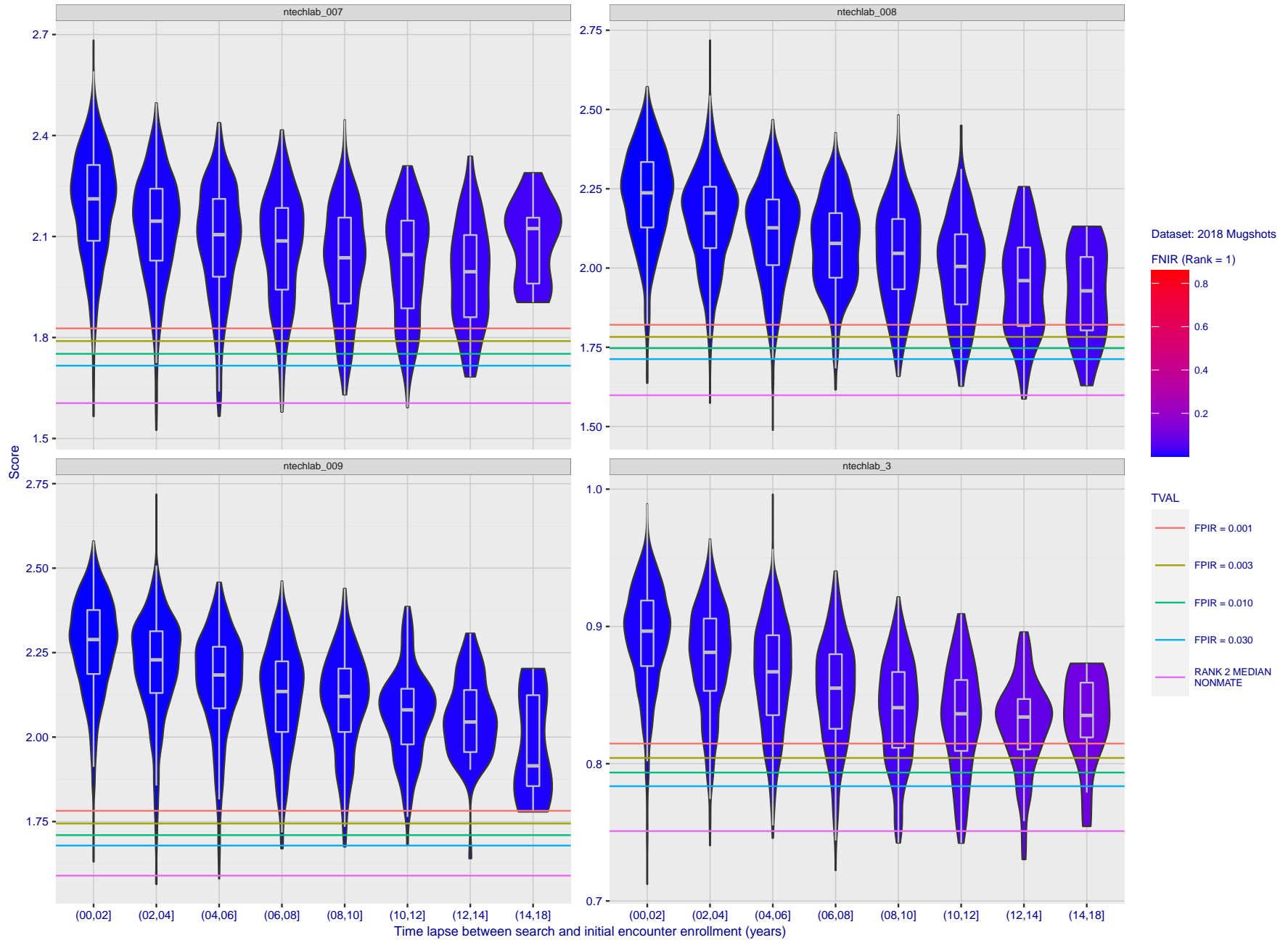


Figure 140: [FRVT-2018 Mugshot Ageing Dataset] Native mate scores vs. time-elapsed. The oldest image of each individual is enrolled. Thereafter, all more recent images are searched. Mated score distributions are computed over all searches noted in row 17 of Table 1 binned by number of years between search and initial enrollment.

2021/10/28  
13:44:33

FNIR(N, R, T) = False neg. identification rate  
FPIR(N, T) = False pos. identification rate

N = Num. enrolled subjects  
R = Num. candidates examined

T = Threshold

T = 0 → Investigation  
T > 0 → Identification

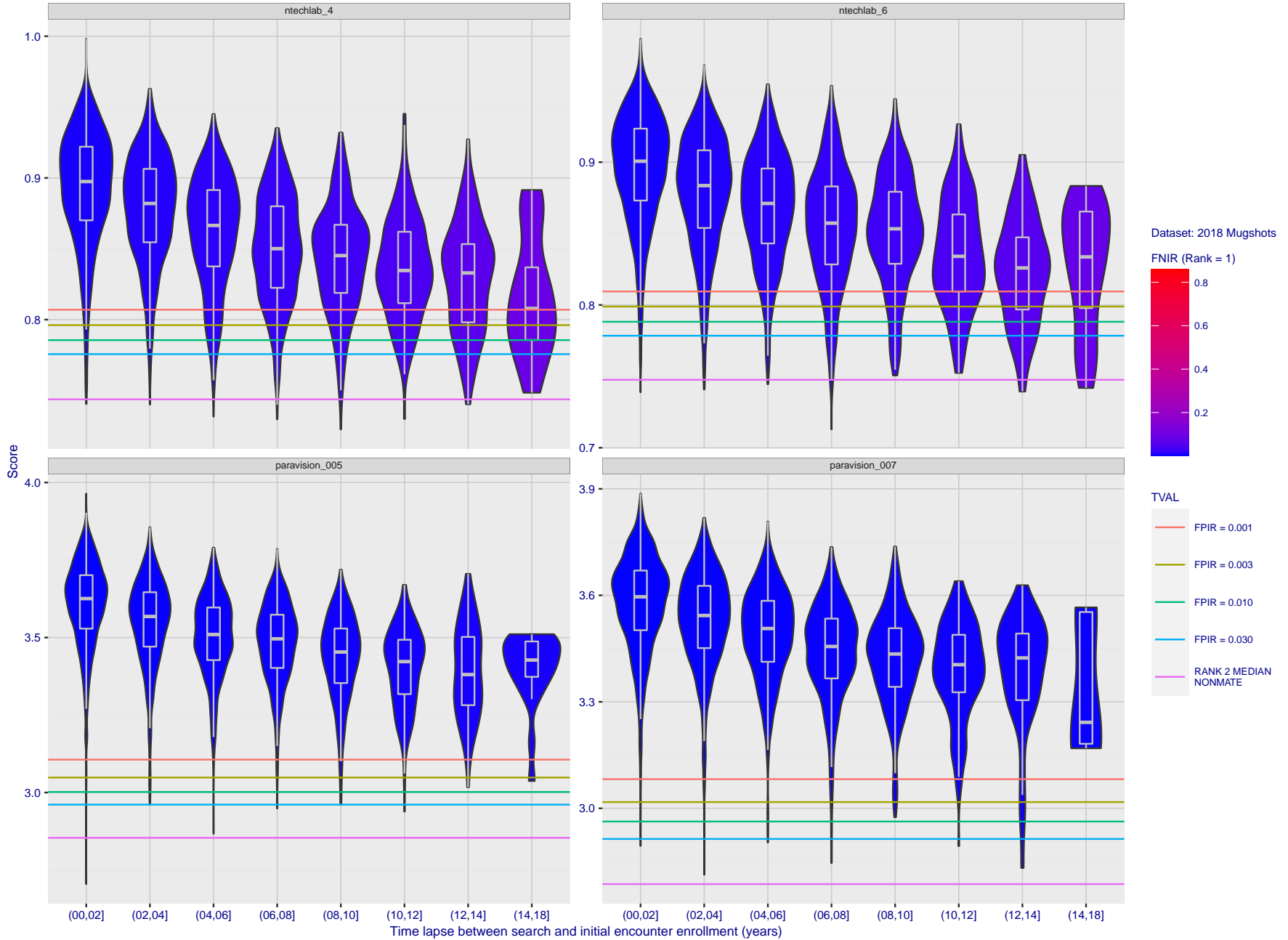


Figure 141: [FRVT-2018 Mugshot Ageing Dataset] Native mate scores vs. time-elapsed. The oldest image of each individual is enrolled. Thereafter, all more recent images are searched. Mated score distributions are computed over all searches noted in row 17 of Table 1 binned by number of years between search and initial enrollment.

2021/10/28 13:44:33 FNIR(N, R, T) = False neg. identification rate  
 FPIR(N, T) = False pos. identification rate  
 N = Num. enrolled subjects  
 R = Num. candidates examined  
 T = Threshold  
 T = 0 → Investigation  
 T > 0 → Identification

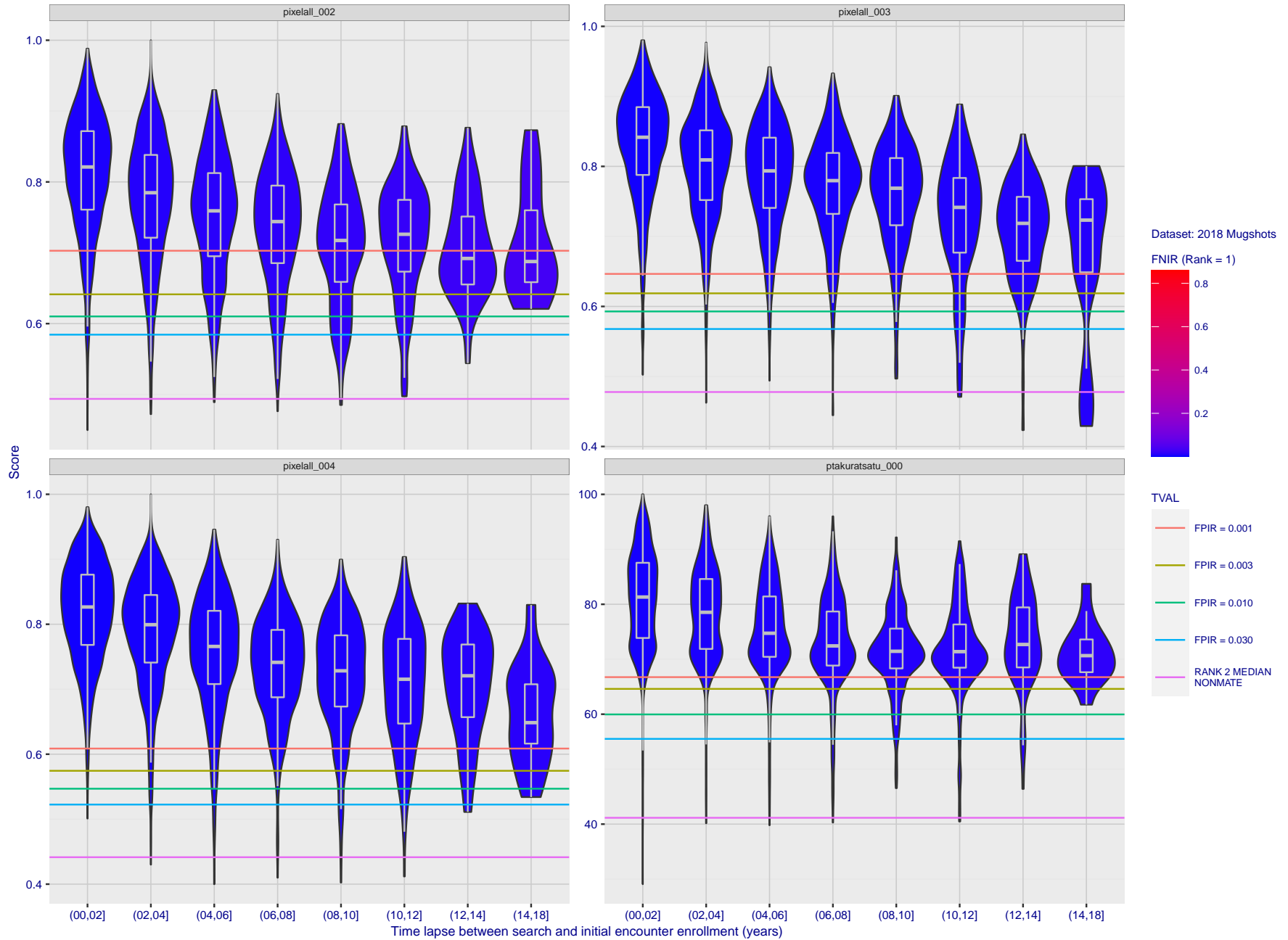


Figure 142: [FRVT-2018 Mugshot Ageing Dataset] Native mate scores vs. time-elapsed. The oldest image of each individual is enrolled. Thereafter, all more recent images are searched. Mated score distributions are computed over all searches noted in row 17 of Table 1 binned by number of years between search and initial enrollment.

2021/10/28  
13:44:33

FNIR(N, R, T) = False neg. identification rate  
FPIR(N, T) = False pos. identification rate

N = Num. enrolled subjects  
R = Num. candidates examined

T = Threshold

T = 0 → Investigation  
T > 0 → Identification

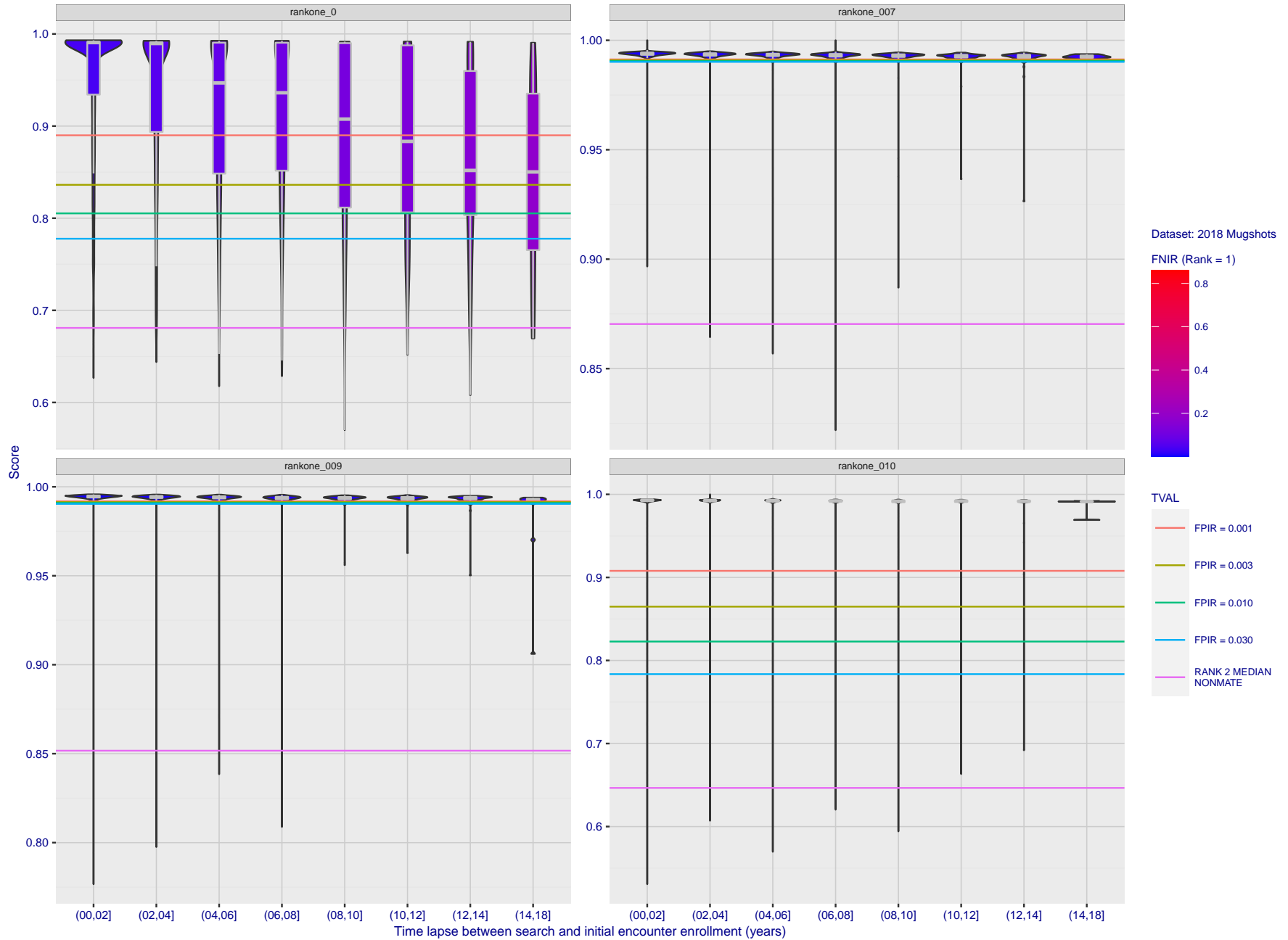


Figure 143: [FRVT-2018 Mugshot Ageing Dataset] Native mate scores vs. time-elapsed. The oldest image of each individual is enrolled. Thereafter, all more recent images are searched. Mated score distributions are computed over all searches noted in row 17 of Table 1 binned by number of years between search and initial enrollment.

2021/10/28 13:44:33 FNIR(N, R, T) = False neg. identification rate N = Num. enrolled subjects T = Threshold  
 FPIR(N, T) = False pos. identification rate R = Num. candidates examined T > 0 → Investigation  
 T > 0 → Identification

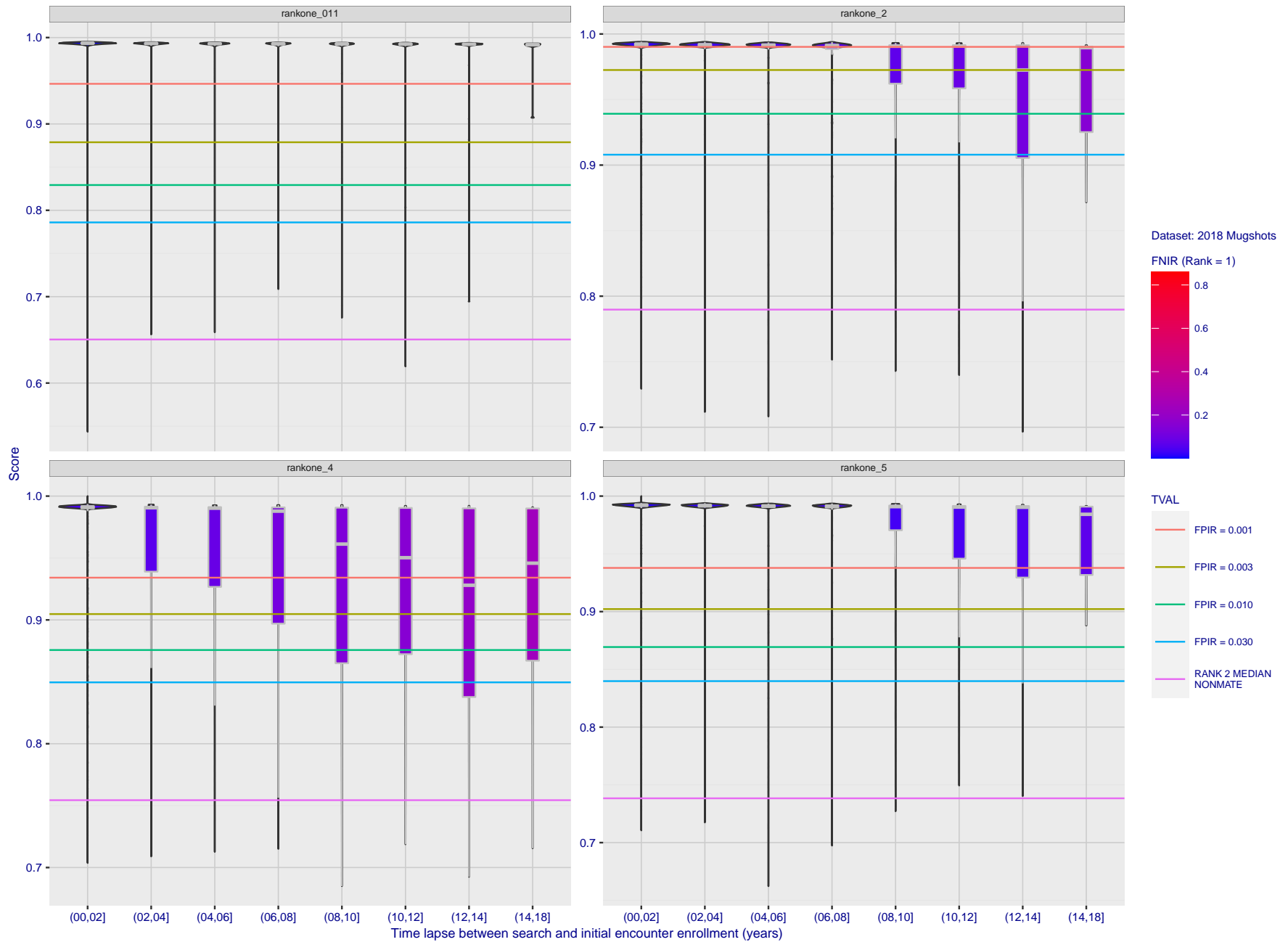


Figure 144: [FRVT-2018 Mugshot Ageing Dataset] Native mate scores vs. time-elapsed. The oldest image of each individual is enrolled. Thereafter, all more recent images are searched. Mated score distributions are computed over all searches noted in row 17 of Table 1 binned by number of years between search and initial enrollment.

2021/10/28  
13:44:33

FNIR(N, R, T) = False neg. identification rate  
FPIR(N, T) = False pos. identification rate

N = Num. enrolled subjects  
R = Num. candidates examined

T = Threshold

T = 0 → Investigation  
T > 0 → Identification

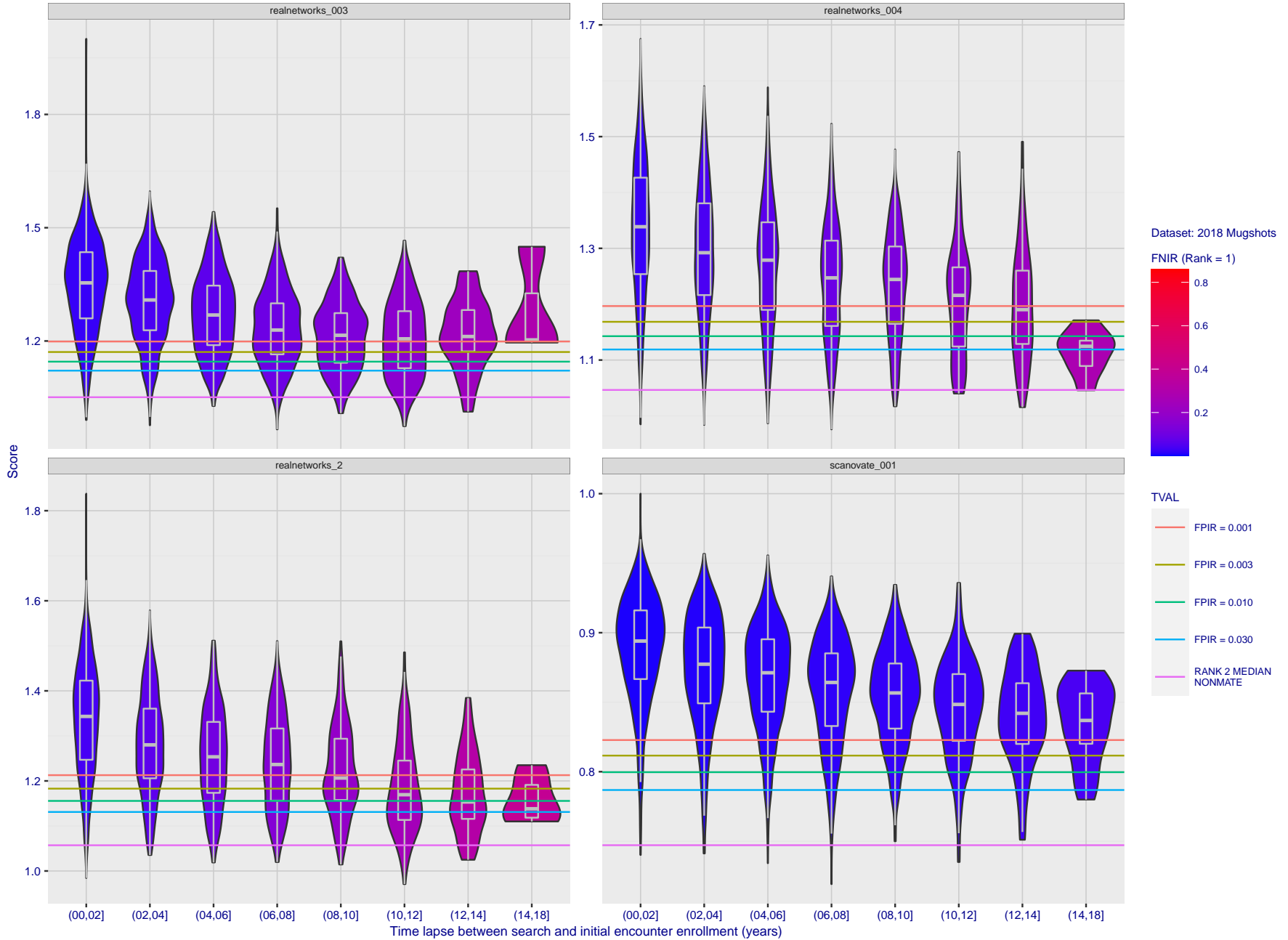


Figure 145: [FRVT-2018 Mugshot Ageing Dataset] Native mate scores vs. time-elapsed. The oldest image of each individual is enrolled. Thereafter, all more recent images are searched. Mated score distributions are computed over all searches noted in row 17 of Table 1 binned by number of years between search and initial enrollment.

2021/10/28  
 13:44:33  
 FNIR(N, R, T) =  
 FPIR(N, T) =  
 False neg. identification rate  
 False pos. identification rate  
 N = Num. enrolled subjects  
 R = Num. candidates examined  
 T = Threshold  
 T = 0 → Investigation  
 T > 0 → Identification

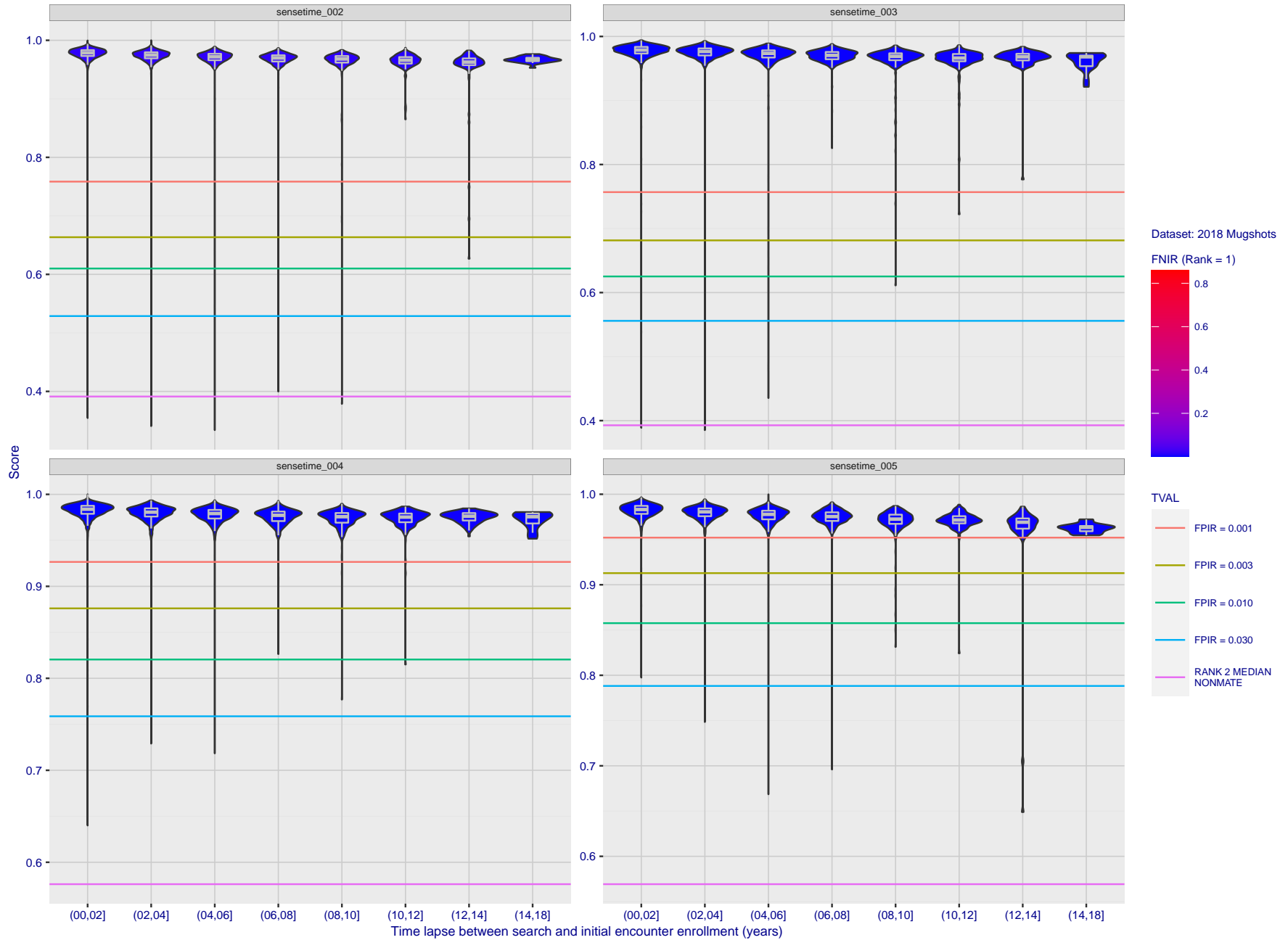


Figure 146: [FRVT-2018 Mugshot Ageing Dataset] Native mate scores vs. time-elapsed. The oldest image of each individual is enrolled. Thereafter, all more recent images are searched. Mated score distributions are computed over all searches noted in row 17 of Table 1 binned by number of years between search and initial enrollment.

2021/10/28  
13:44:33

FNIR(N, R, T) = False neg. identification rate  
FPIR(N, T) = False pos. identification rate

N = Num. enrolled subjects  
R = Num. candidates examined

T = Threshold

T = 0 → Investigation  
T > 0 → Identification

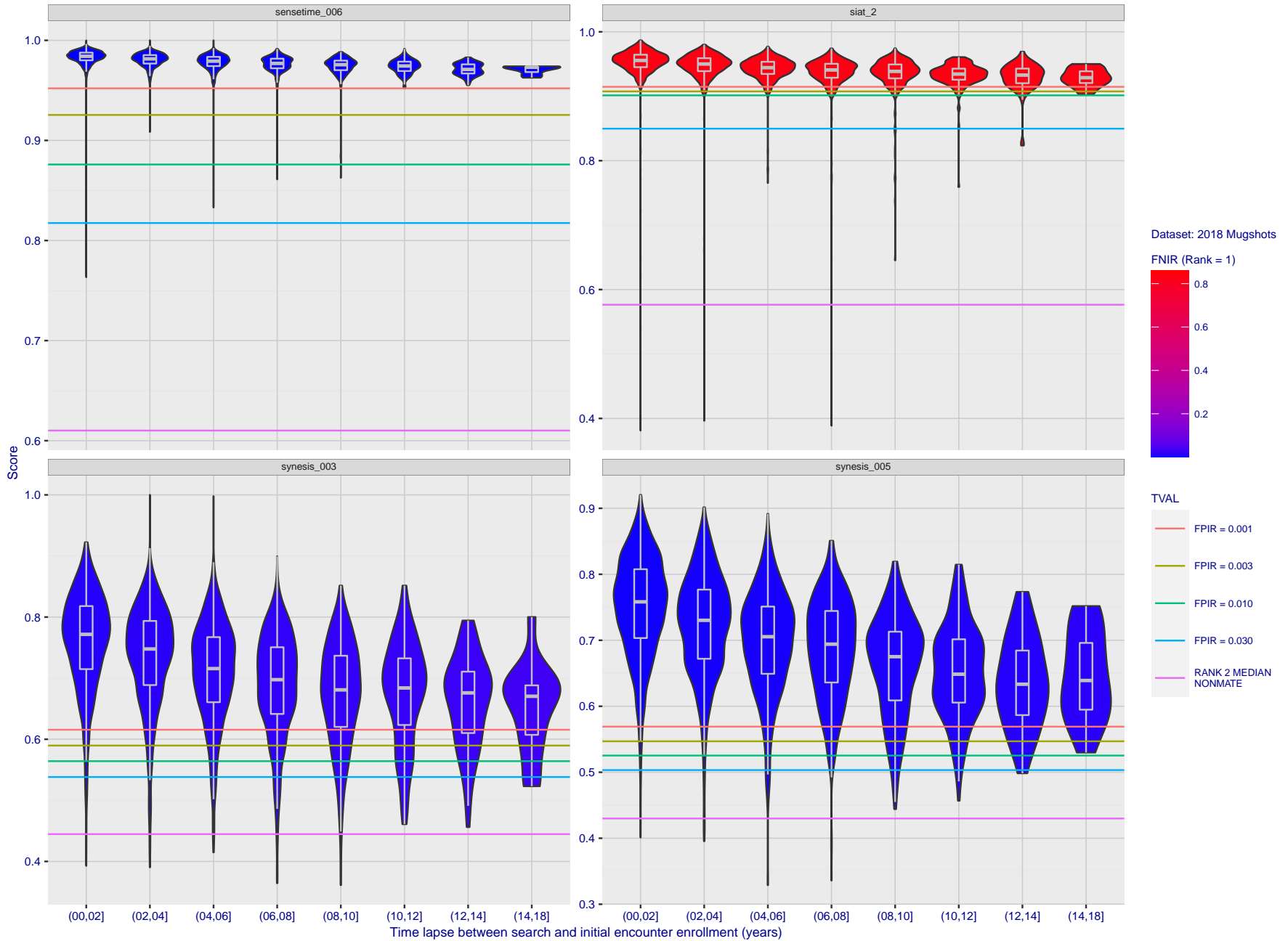


Figure 147: [FRVT-2018 Mugshot Ageing Dataset] Native mate scores vs. time-elapsed. The oldest image of each individual is enrolled. Thereafter, all more recent images are searched. Mated score distributions are computed over all searches noted in row 17 of Table 1 binned by number of years between search and initial enrollment.

2021/10/28  
13:44:33

FNIR(N, R, T) =  
FPIR(N, T) =  
False neg. identification rate  
False pos. identification rate

N = Num. enrolled subjects  
R = Num. candidates examined

T = Threshold

T = 0 → Investigation  
T > 0 → Identification

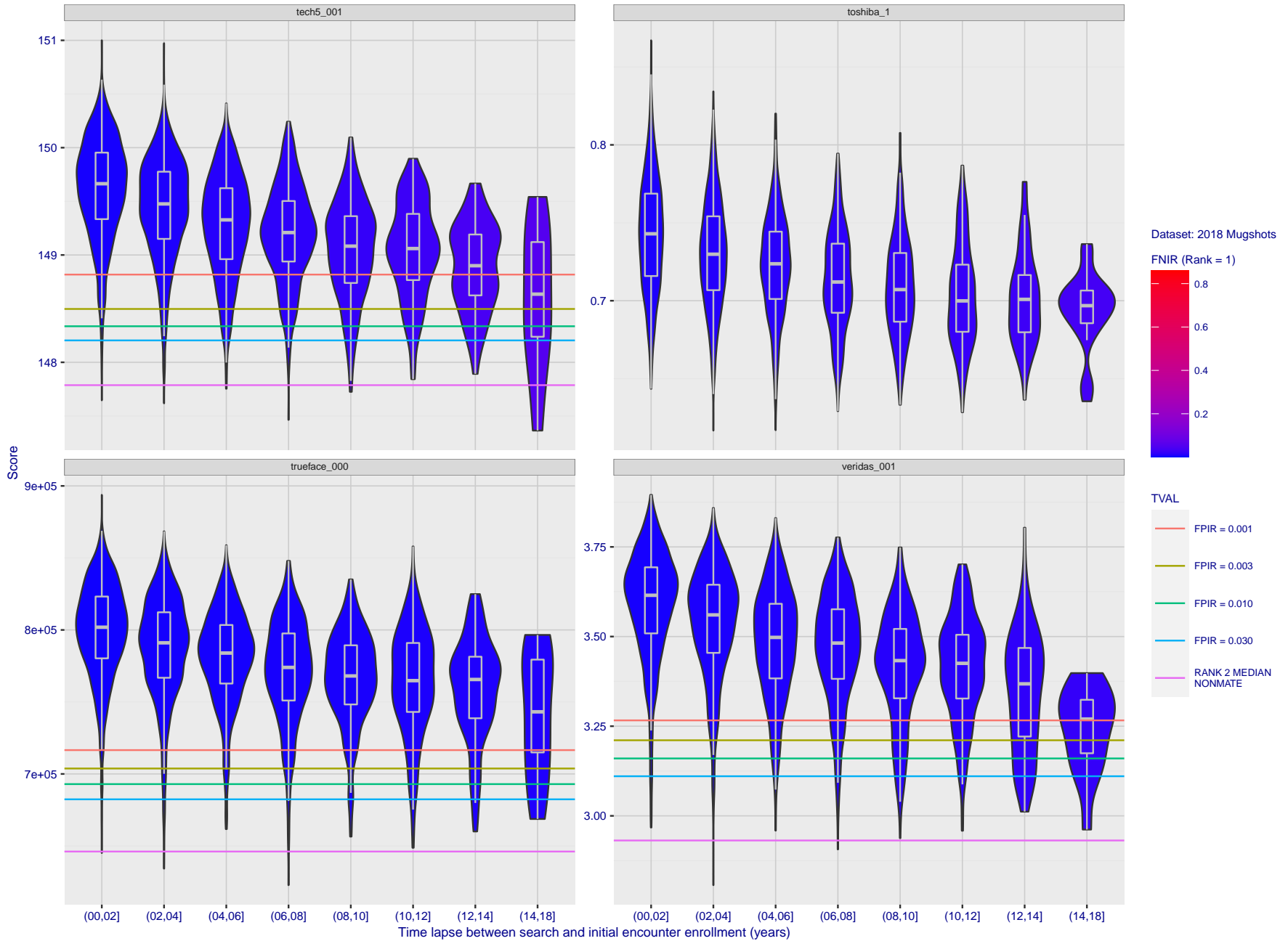


Figure 148: [FRVT-2018 Mugshot Ageing Dataset] Native mate scores vs. time-elapsed. The oldest image of each individual is enrolled. Thereafter, all more recent images are searched. Mated score distributions are computed over all searches noted in row 17 of Table 1 binned by number of years between search and initial enrollment.

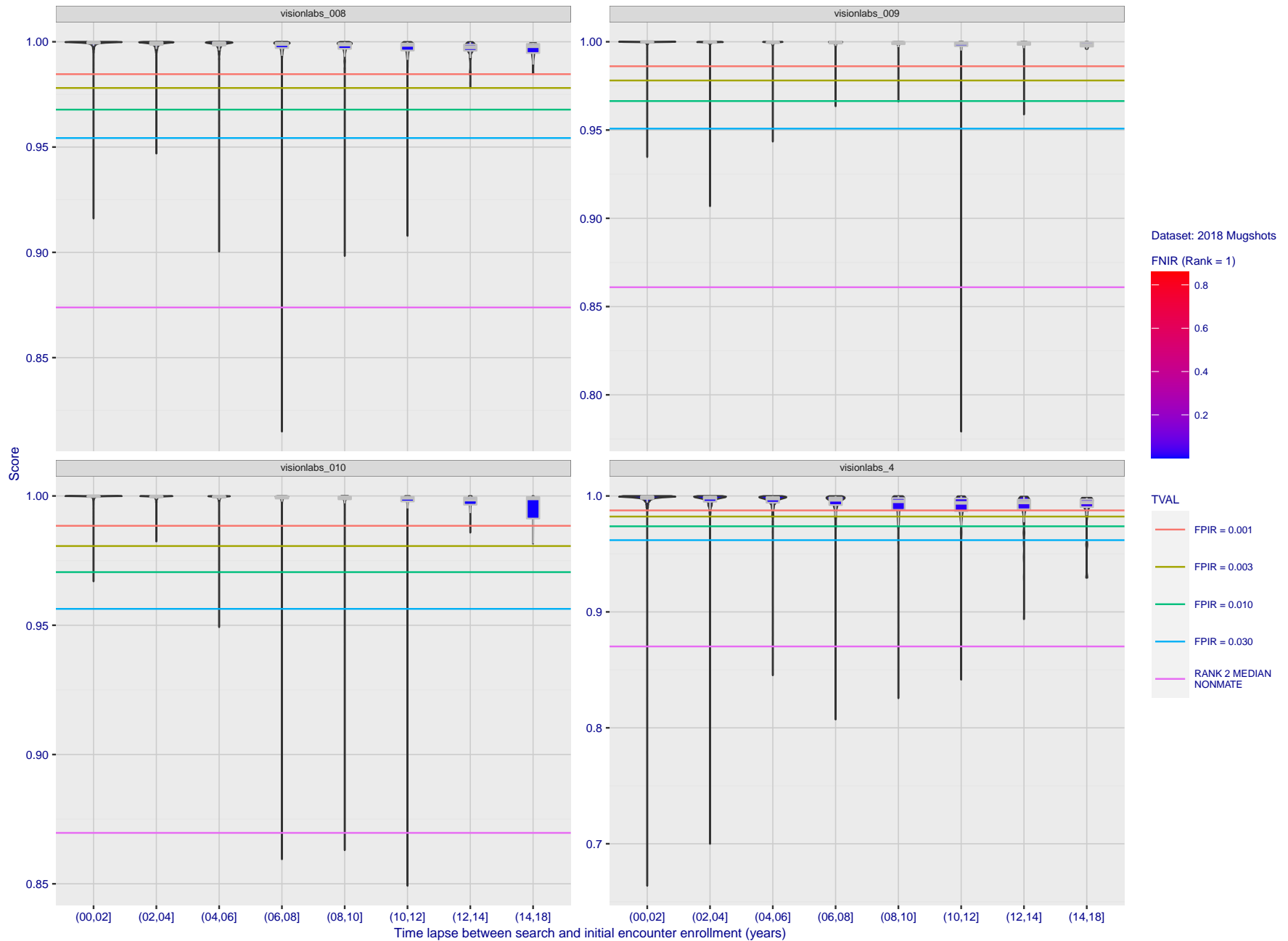


Figure 149: [FRVT-2018 Mugshot Ageing Dataset] Native mate scores vs. time-elapsed. The oldest image of each individual is enrolled. Thereafter, all more recent images are searched. Mated score distributions are computed over all searches noted in row 17 of Table 1 binned by number of years between search and initial enrollment.

2021/10/28  
13:44:33

FNIR(N, R, T) = False neg. identification rate  
FPIR(N, T) = False pos. identification rate

N = Num. enrolled subjects  
R = Num. candidates examined

T = Threshold

T = 0 → Investigation  
T > 0 → Identification

2021/10/28  
 13:44:33  
 FNIR(N, R, T) =  
 FPR(N, T) =  
 False neg. identification rate  
 False pos. identification rate  
 N = Num. enrolled subjects  
 R = Num. candidates examined  
 T = Threshold  
 T = 0 → Investigation  
 T > 0 → Identification

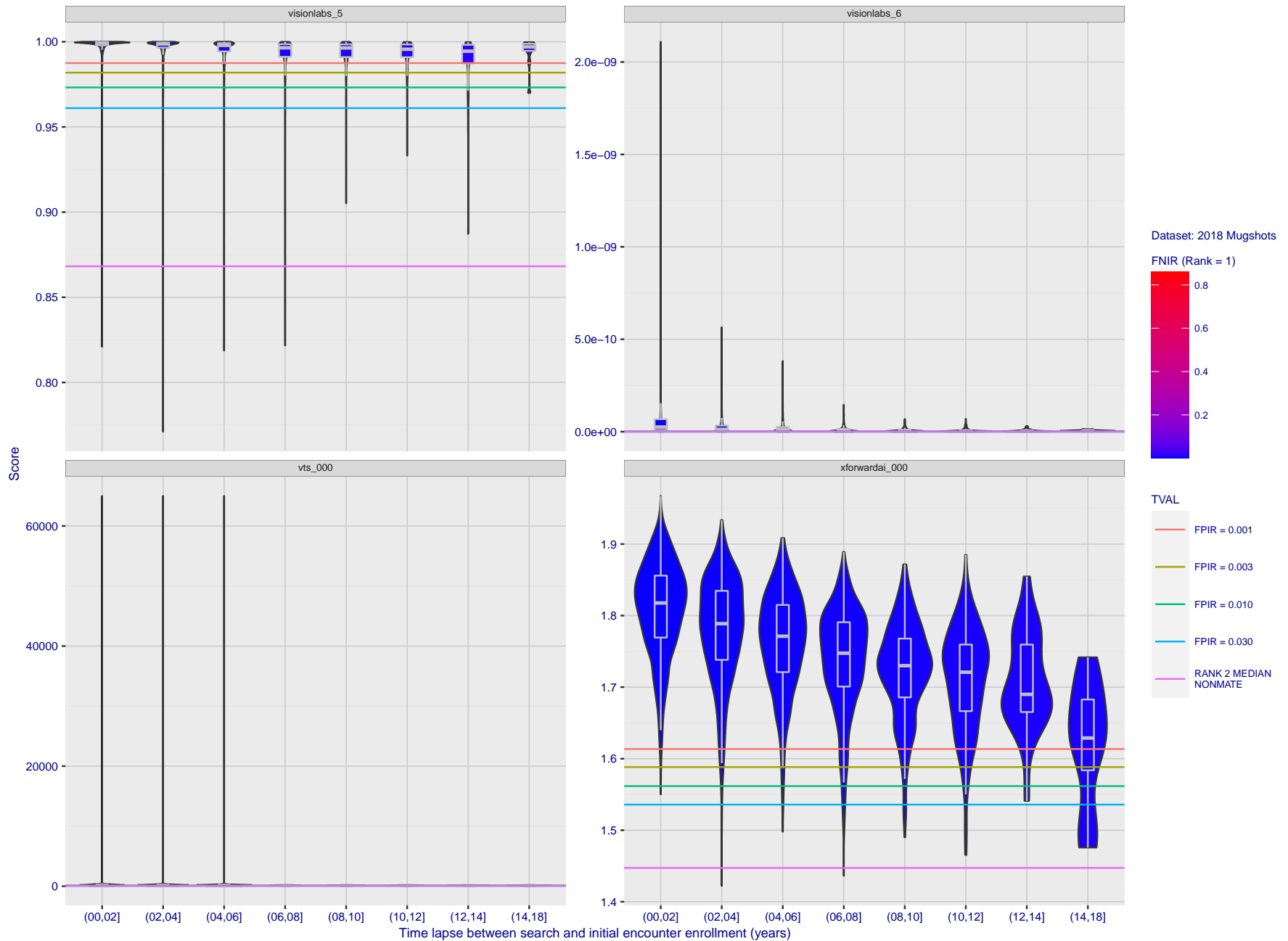


Figure 150: [FRVT-2018 Mugshot Ageing Dataset] Native mate scores vs. time-elapsed. The oldest image of each individual is enrolled. Thereafter, all more recent images are searched. Mated score distributions are computed over all searches noted in row 17 of Table 1 binned by number of years between search and initial enrollment.

2021/10/28 13:44:33  
 FNIR(N, R, T) = False neg. identification rate  
 FPIR(N, T) = False pos. identification rate  
 N = Num. enrolled subjects  
 R = Num. candidates examined  
 T = Threshold  
 T = 0 → Investigation  
 T > 0 → Identification

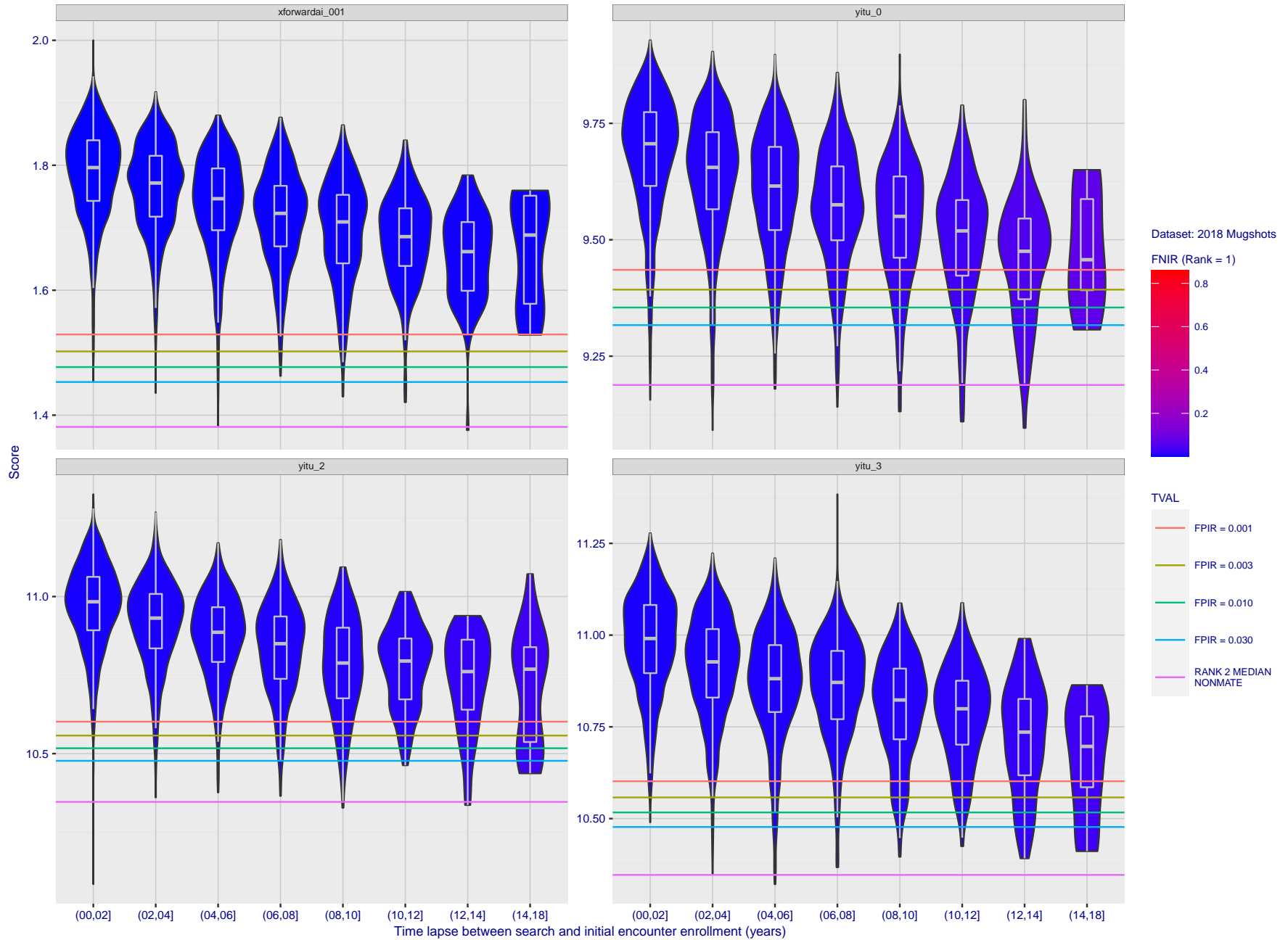


Figure 151: [FRVT-2018 Mugshot Ageing Dataset] Native mate scores vs. time-elapsed. The oldest image of each individual is enrolled. Thereafter, all more recent images are searched. Mated score distributions are computed over all searches noted in row 17 of Table 1 binned by number of years between search and initial enrollment.

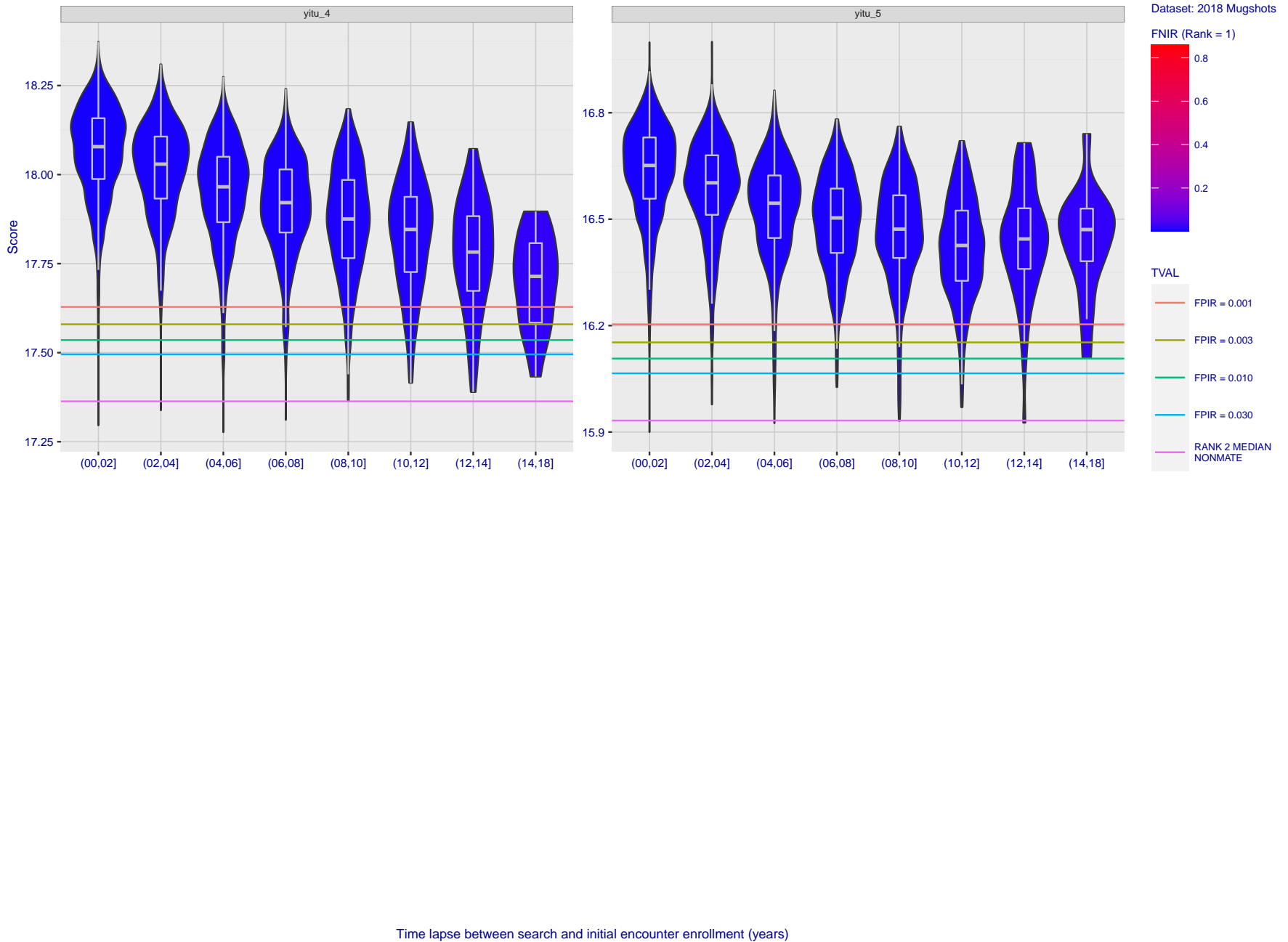


Figure 152: [FRVT-2018 Mugshot Ageing Dataset] Native mate scores vs. time-elapsed. The oldest image of each individual is enrolled. Thereafter, all more recent images are searched. Mated score distributions are computed over all searches noted in row 17 of Table 1 binned by number of years between search and initial enrollment.

2021/10/28  
 13:44:33

FNIR(N, R, T) =  
 FPIR(N, T) =  
 False neg. identification rate  
 False pos. identification rate

N = Num. enrolled subjects  
 R = Num. candidates examined

T = Threshold

T = 0 → Investigation  
 T > 0 → Identification

## Appendix C Effect of enrolling multiple images

This publication is available free of charge from: <https://doi.org/10.6028/NIST.IR.8271>

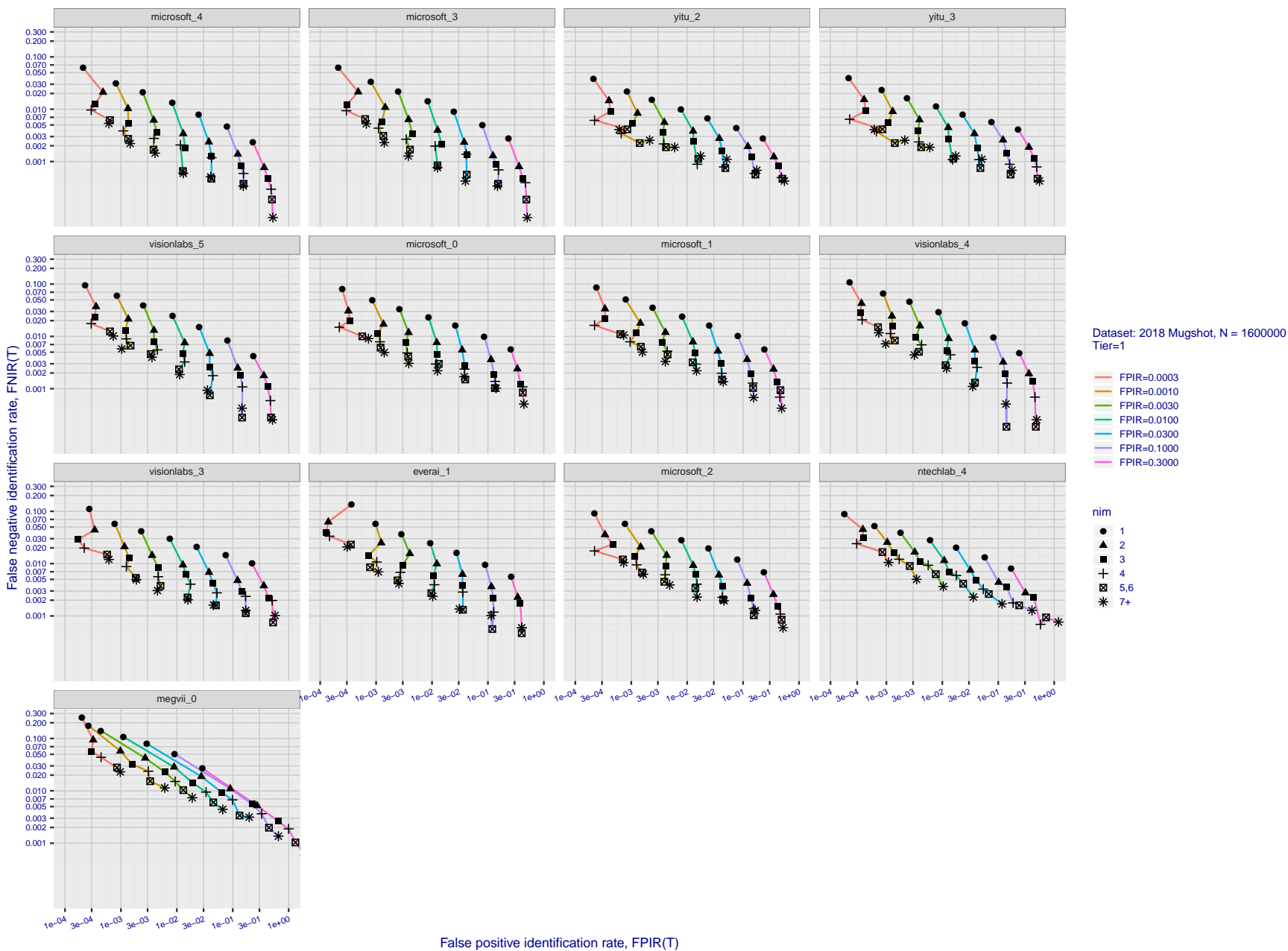


Figure 153: [FRVT-2018 Mugshot Dataset] Effect of enrolling multiple images for each identity. The plot shows an identification miss rates vs. false positive rates, at seven operating thresholds. The enrolled population size is fixed. The images are enrolled with lifetime-consolidation - see section 2.3.

2021/10/28  
13:44:33

FNIR(N, R, T) = False neg. identification rate  
FPIR(N, T) = False pos. identification rate  
N = Num. enrolled subjects  
R = Num. candidates examined

T = Threshold  
T = 0 → Investigation  
T > 0 → Identification

2021/10/28  
13:44:33

FNIR(N, R, T) =  
FPIR(N, T) =

False neg. identification rate  
False pos. identification rate

N = Num. enrolled subjects  
R = Num. candidates examined

T = Threshold

T = 0 → Investigation  
T > 0 → Identification

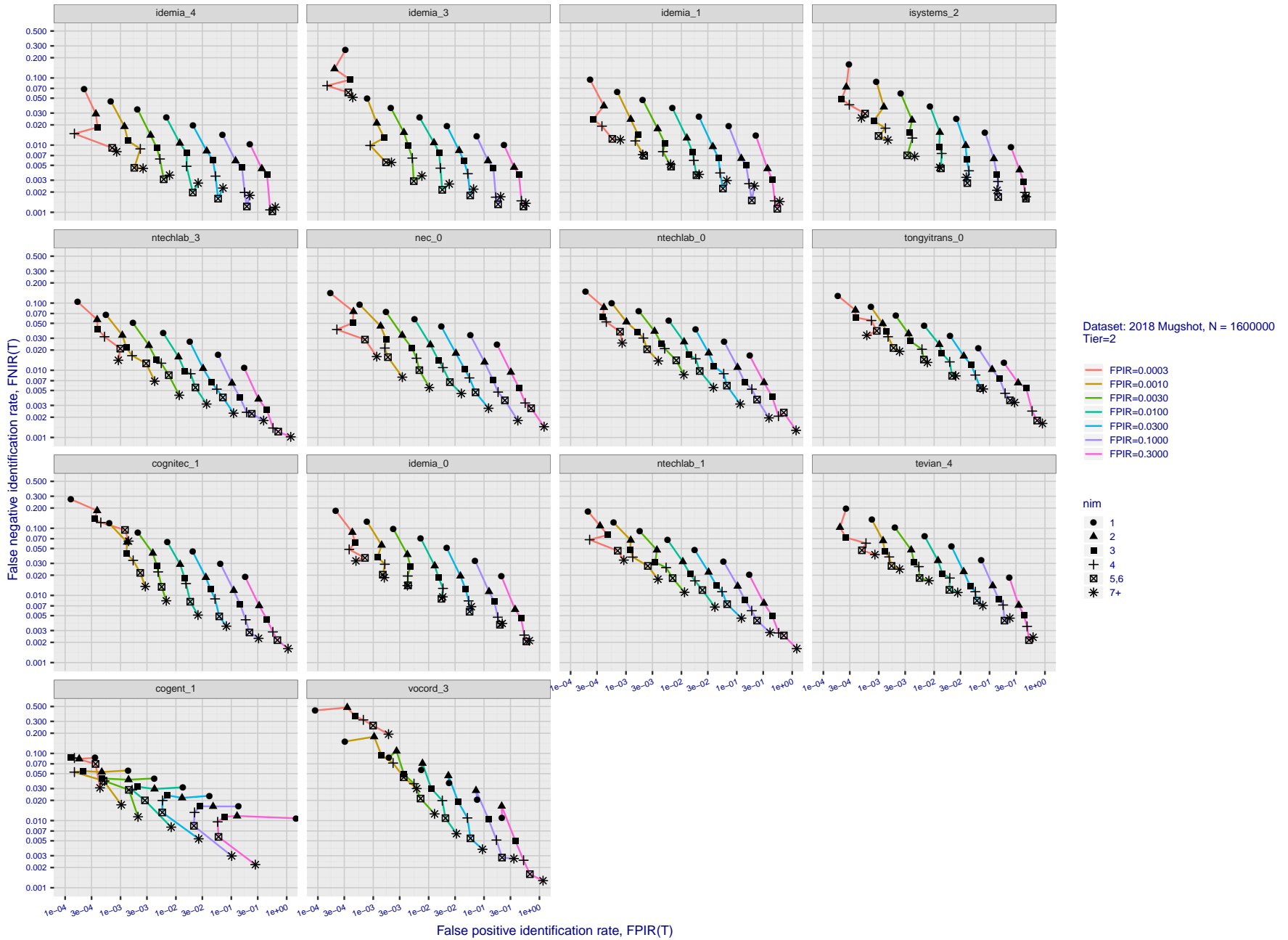


Figure 154: [FRVT-2018 Mugshot Dataset] Effect of enrolling multiple images for each identity. The plot shows an identification miss rates vs. false positive rates, at seven operating thresholds. The enrolled population size is fixed. The images are enrolled with lifetime-consolidation - see section 2.3.

2021/10/28  
13:44:33

FNIR(N, R, T) =  
FPIR(N, T) =

False neg. identification rate  
False pos. identification rate

N = Num. enrolled subjects  
R = Num. candidates examined

T = Threshold

T = 0 → Investigation  
T > 0 → Identification

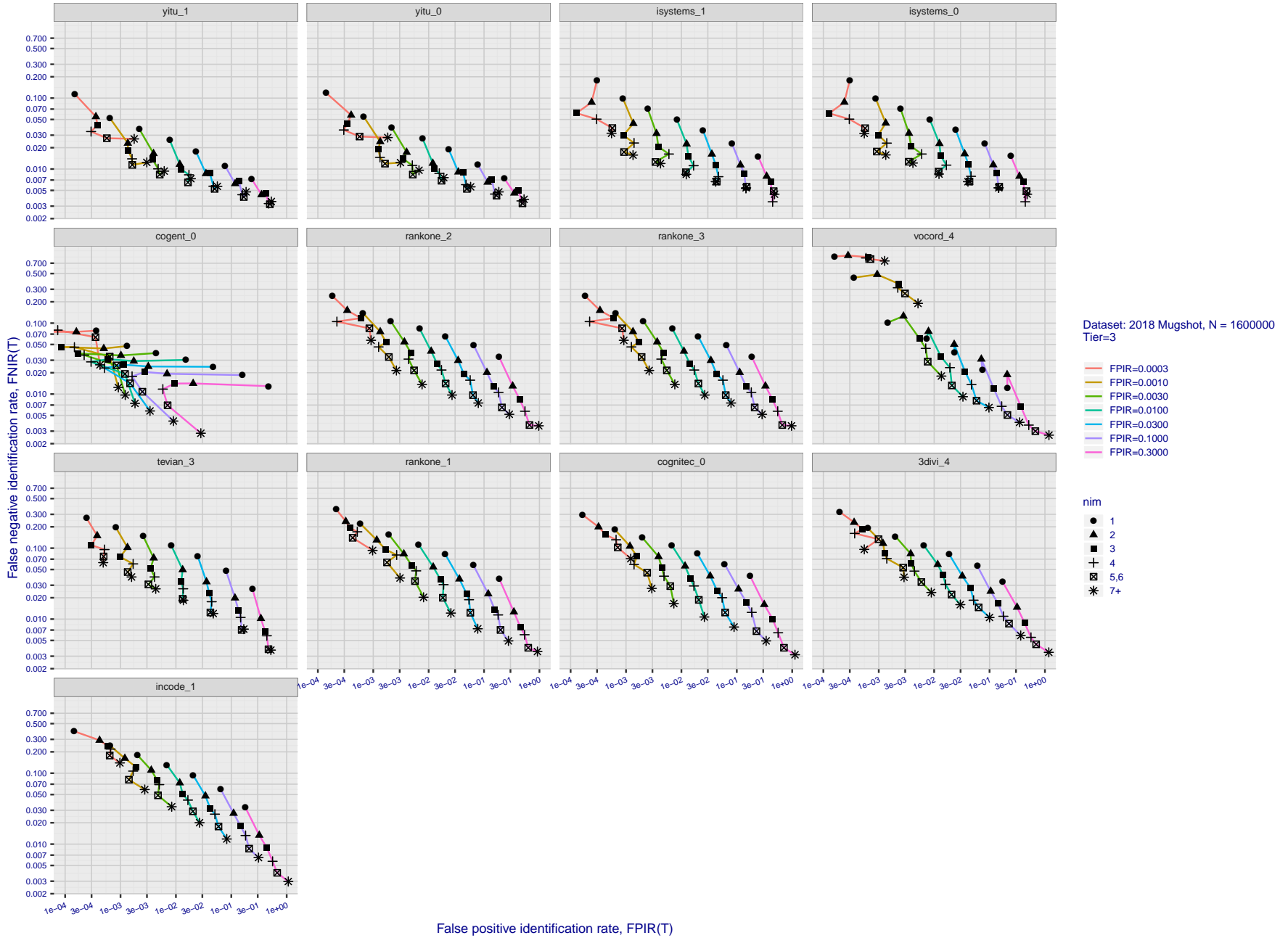


Figure 155: [FRVT-2018 Mugshot Dataset] Effect of enrolling multiple images for each identity. The plot shows an identification miss rates vs. false positive rates, at seven operating thresholds. The enrolled population size is fixed. The images are enrolled with lifetime-consolidation - see section 2.3.

2021/10/28  
13:44:33

FNIR(N, R, T) =  
FPIR(N, T) =

False neg. identification rate  
False pos. identification rate

N = Num. enrolled subjects  
R = Num. candidates examined

T = Threshold

T = 0 → Investigation  
T > 0 → Identification

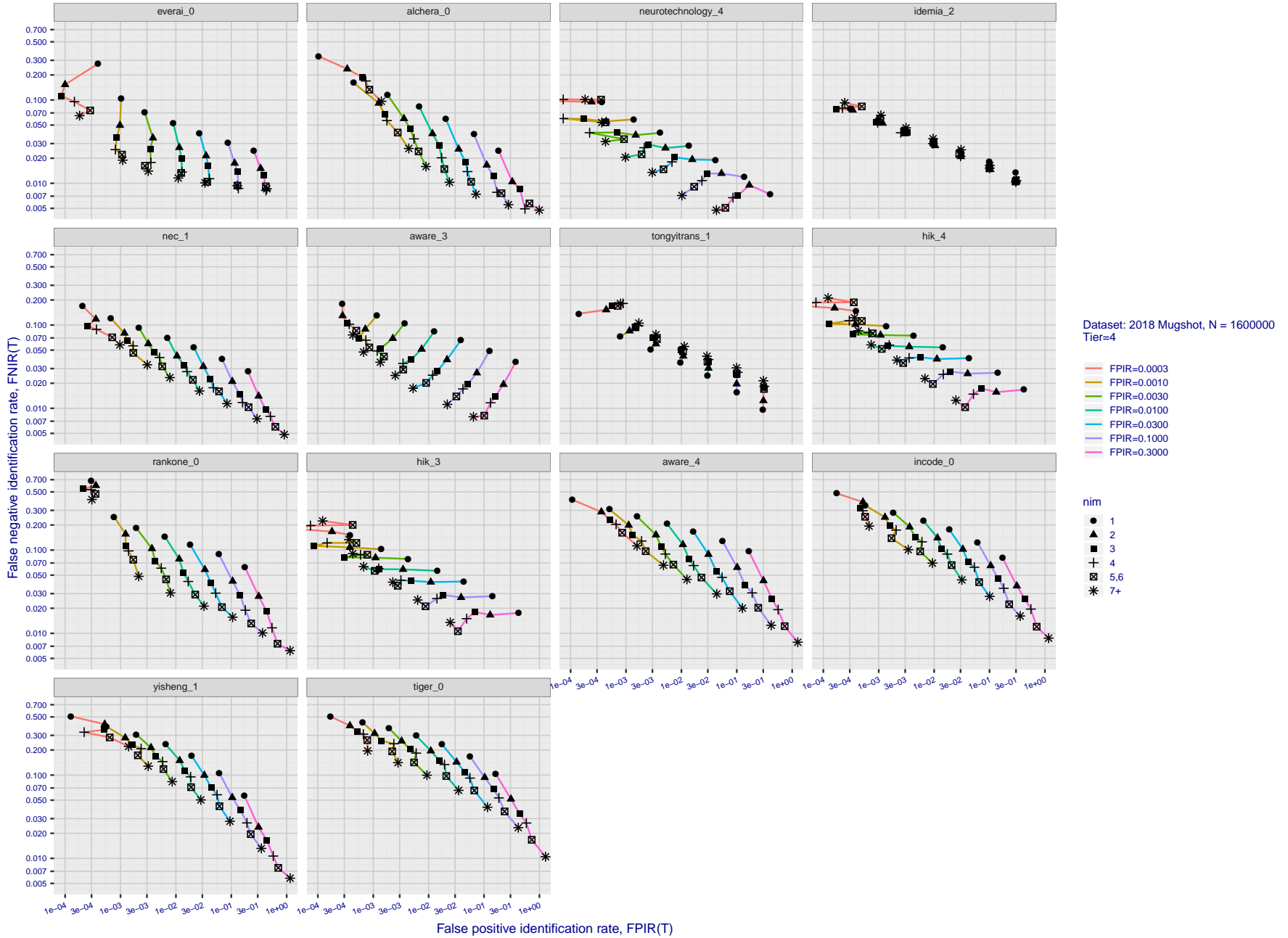


Figure 156: [FRVT-2018 Mugshot Dataset] Effect of enrolling multiple images for each identity. The plot shows an identification miss rates vs. false positive rates, at seven operating thresholds. The enrolled population size is fixed. The images are enrolled with lifetime-consolidation - see section 2.3.

2021/10/28  
13:44:33

FNIR(N, R, T) =  
FPIR(N, T) =

False neg. identification rate  
False pos. identification rate

N = Num. enrolled subjects  
R = Num. candidates examined

T = Threshold

T = 0 → Investigation  
T > 0 → Identification

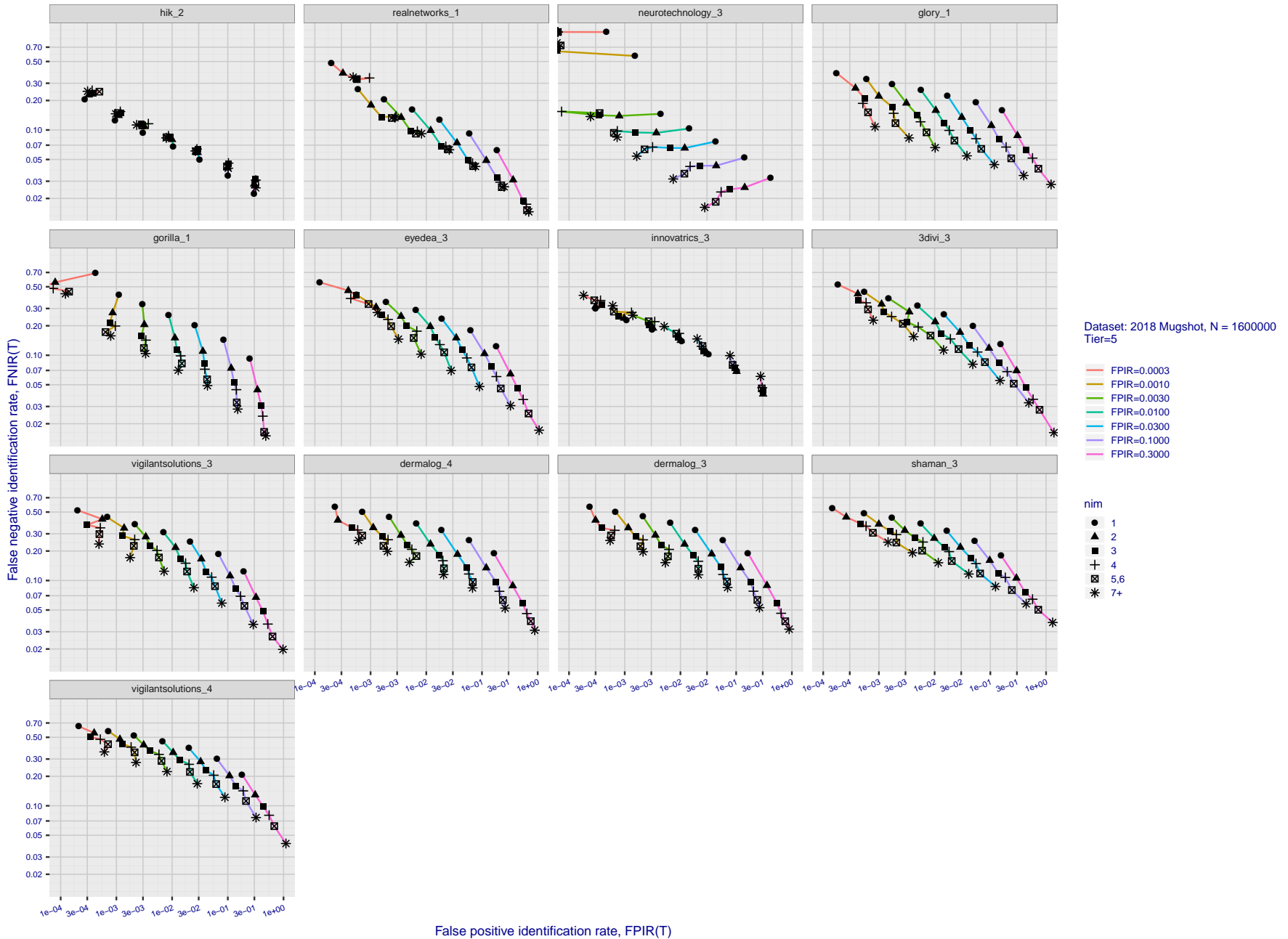


Figure 157: [FRVT-2018 Mugshot Dataset] Effect of enrolling multiple images for each identity. The plot shows an identification miss rates vs. false positive rates, at seven operating thresholds. The enrolled population size is fixed. The images are enrolled with lifetime-consolidation - see section 2.3.

2021/10/28  
13:44:33

FNIR(N, R, T) =  
FPIR(N, T) =

False neg. identification rate  
False pos. identification rate

N = Num. enrolled subjects  
R = Num. candidates examined

T = Threshold

T = 0 → Investigation  
T > 0 → Identification

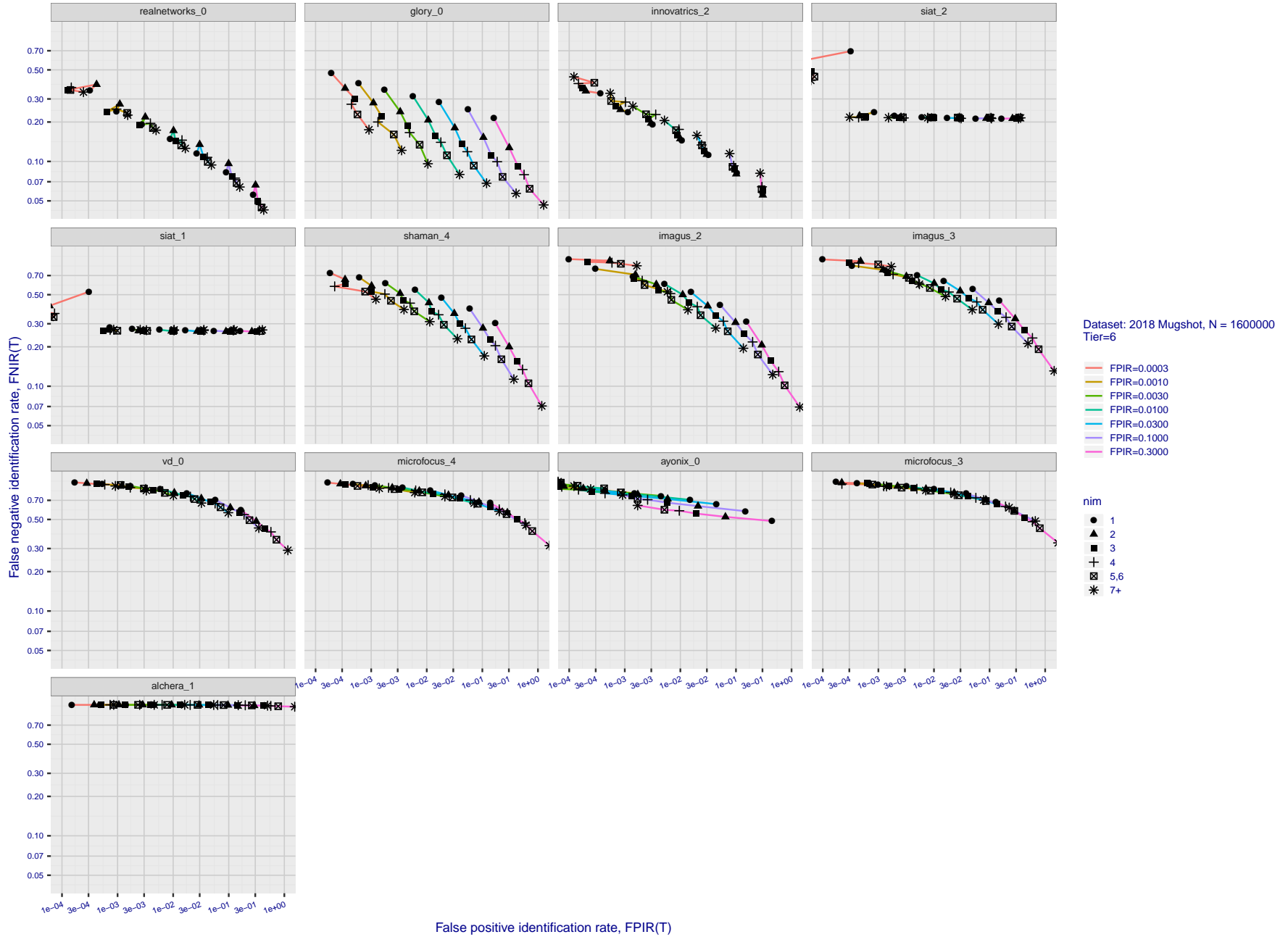


Figure 158: [FRVT-2018 Mugshot Dataset] Effect of enrolling multiple images for each identity. The plot shows an identification miss rates vs. false positive rates, at seven operating thresholds. The enrolled population size is fixed. The images are enrolled with lifetime-consolidation - see section 2.3.

## Appendix D Accuracy with poor quality webcam images

This publication is available free of charge from: <https://doi.org/10.6028/NIST.IR.8271>

---

2021/10/28 FNIR(N, R, T) = False neg. identification rate N = Num. enrolled subjects T = Threshold T = 0 → Investigation  
13:44:33 FPIR(N, T) = False pos. identification rate R = Num. candidates examined T > 0 → Identification

2021/10/28  
 13:44:33  
 FNIR(N, R, T) =  
 FPR(N, T) =  
 False neg. identification rate  
 False pos. identification rate  
 N = Num. enrolled subjects  
 R = Num. candidates examined  
 T = Threshold  
 T = 0 → Investigation  
 T > 0 → Identification

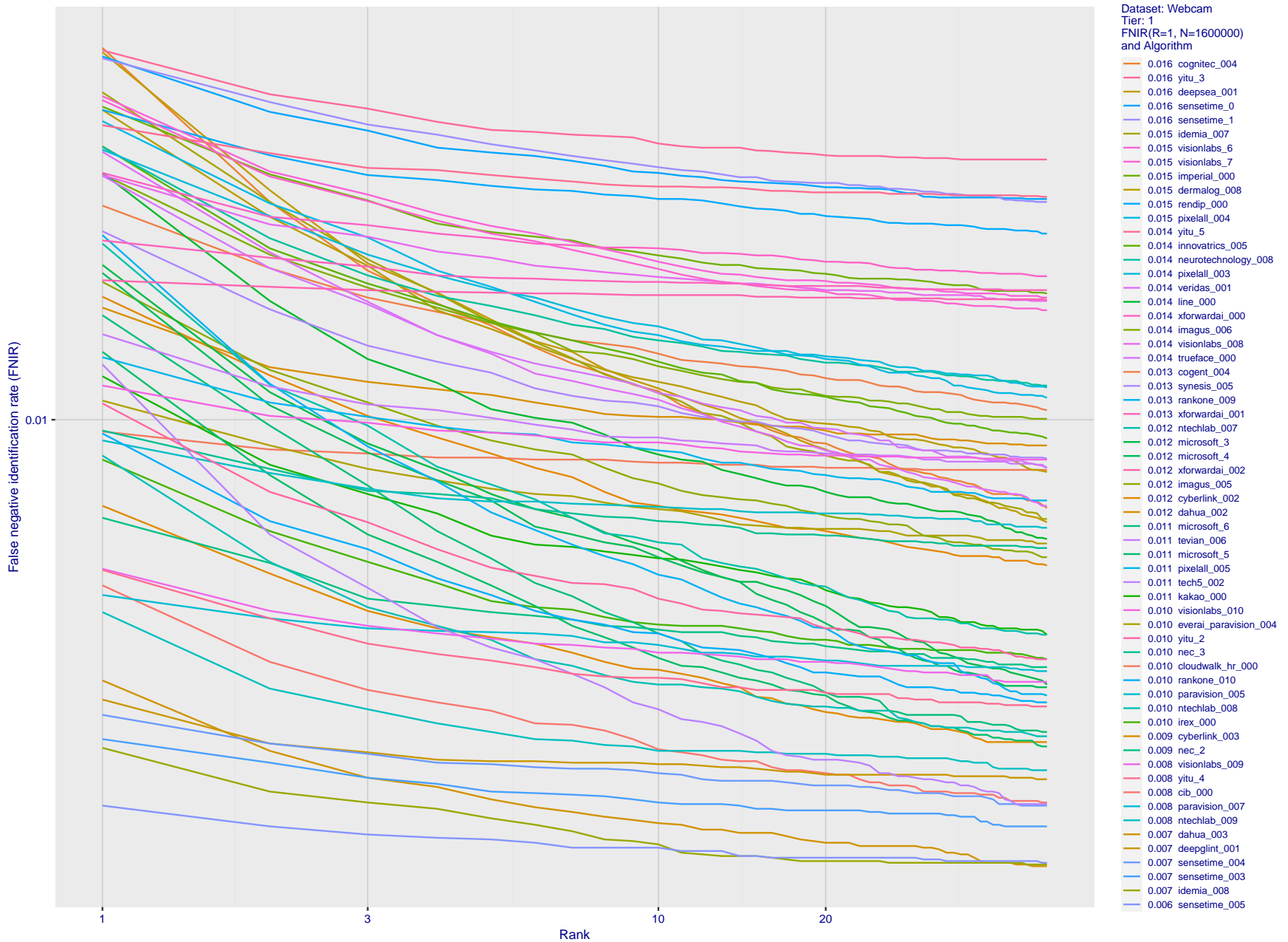


Figure 159: [Webcam Dataset] Identification miss rates vs. rank. The results apply to cross-domain recognition in which webcams are searched against enrolled mugshots. The FNIR values are higher than those for mugshot-mugshot identification due to low image resolution, lighting and less constrained subject pose in webcam images - see Figure 6.

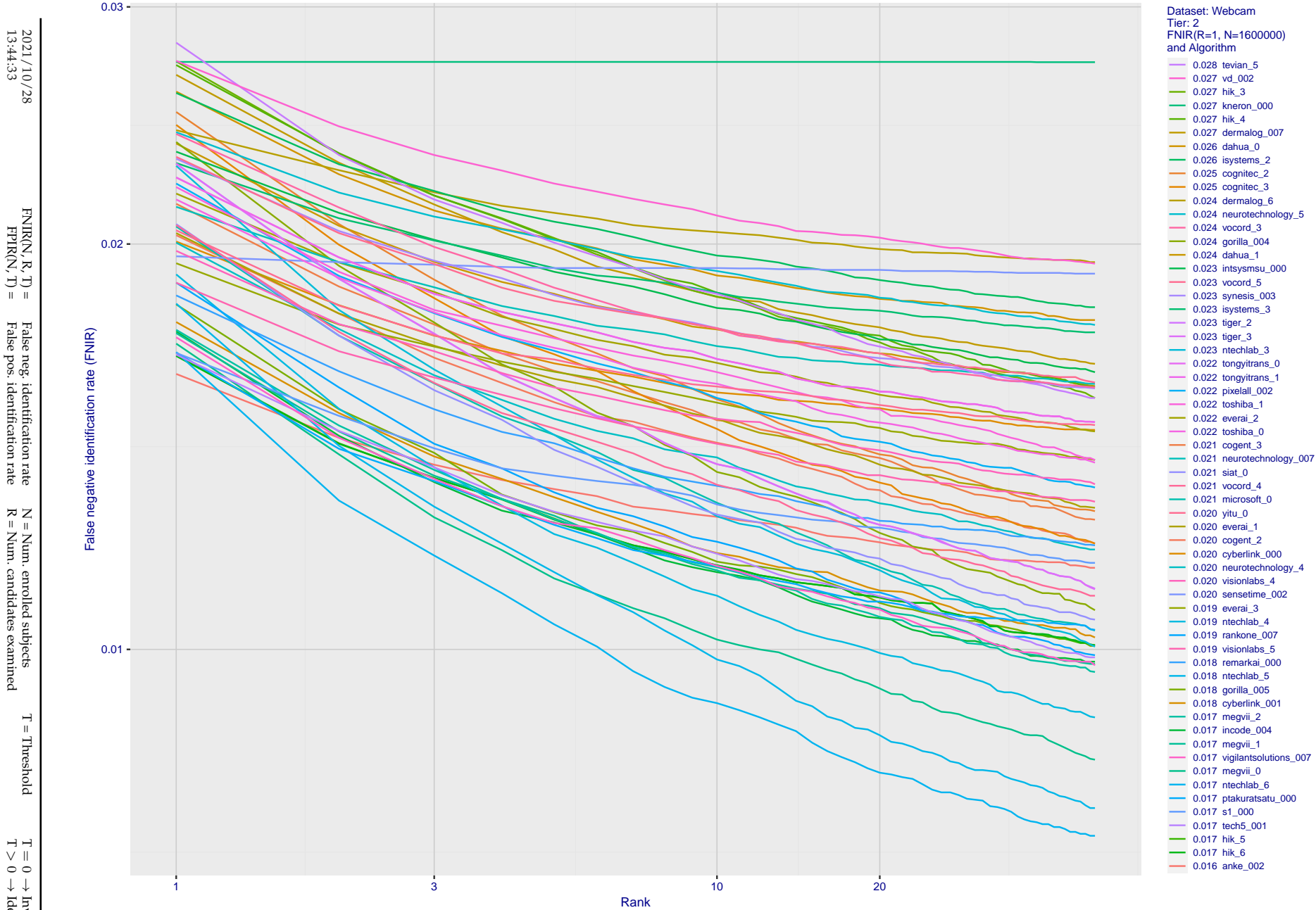


Figure 160: [Webcam Dataset] Identification miss rates vs. rank. The results apply to cross-domain recognition in which webcams are searched against enrolled mugshots. The FNIR values are higher than those for mugshot-mugshot identification due to low image resolution, lighting and less constrained subject pose in webcam images - see Figure 6.

2021/10/28  
13:44:33

FNIR(N, R, T) =  
FPR(N, T) =

False neg. identification rate  
False pos. identification rate

N = Num. enrolled subjects  
R = Num. candidates examined

T = Threshold

T = 0 → Investigation  
T > 0 → Identification

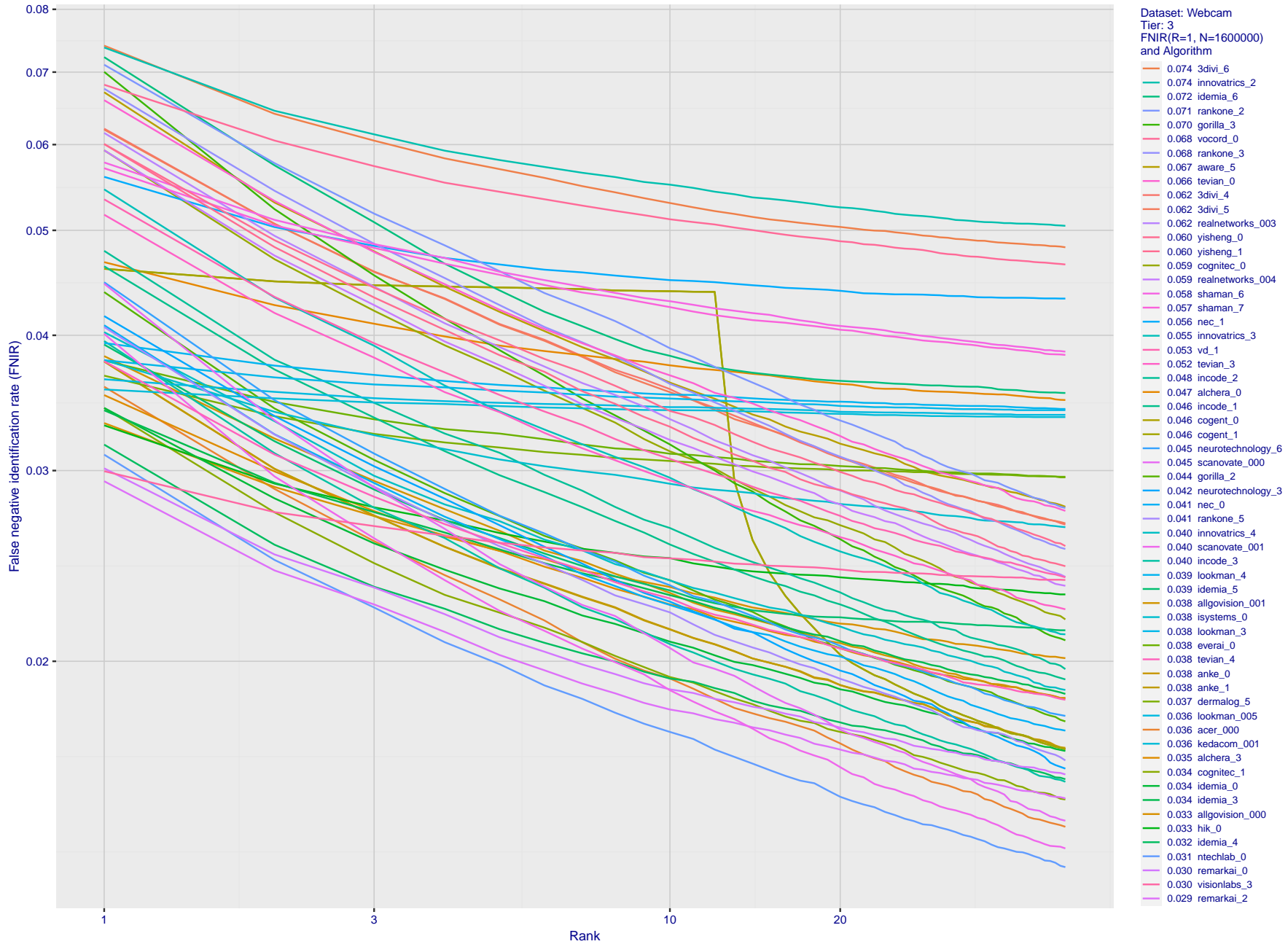


Figure 161: [Webcam Dataset] Identification miss rates vs. rank. The results apply to cross-domain recognition in which webcams are searched against enrolled mugshots. The FNIR values are higher than those for mugshot-mugshot identification due to low image resolution, lighting and less constrained subject pose in webcam images - see Figure 6.

2021/10/28  
 FNIR(N, R, T) =  
 FPR(N, T) =  
 False neg. identification rate  
 False pos. identification rate  
 N = Num. enrolled subjects  
 R = Num. candidates examined  
 T = Threshold  
 T = 0 → Investigation  
 T > 0 → Identification

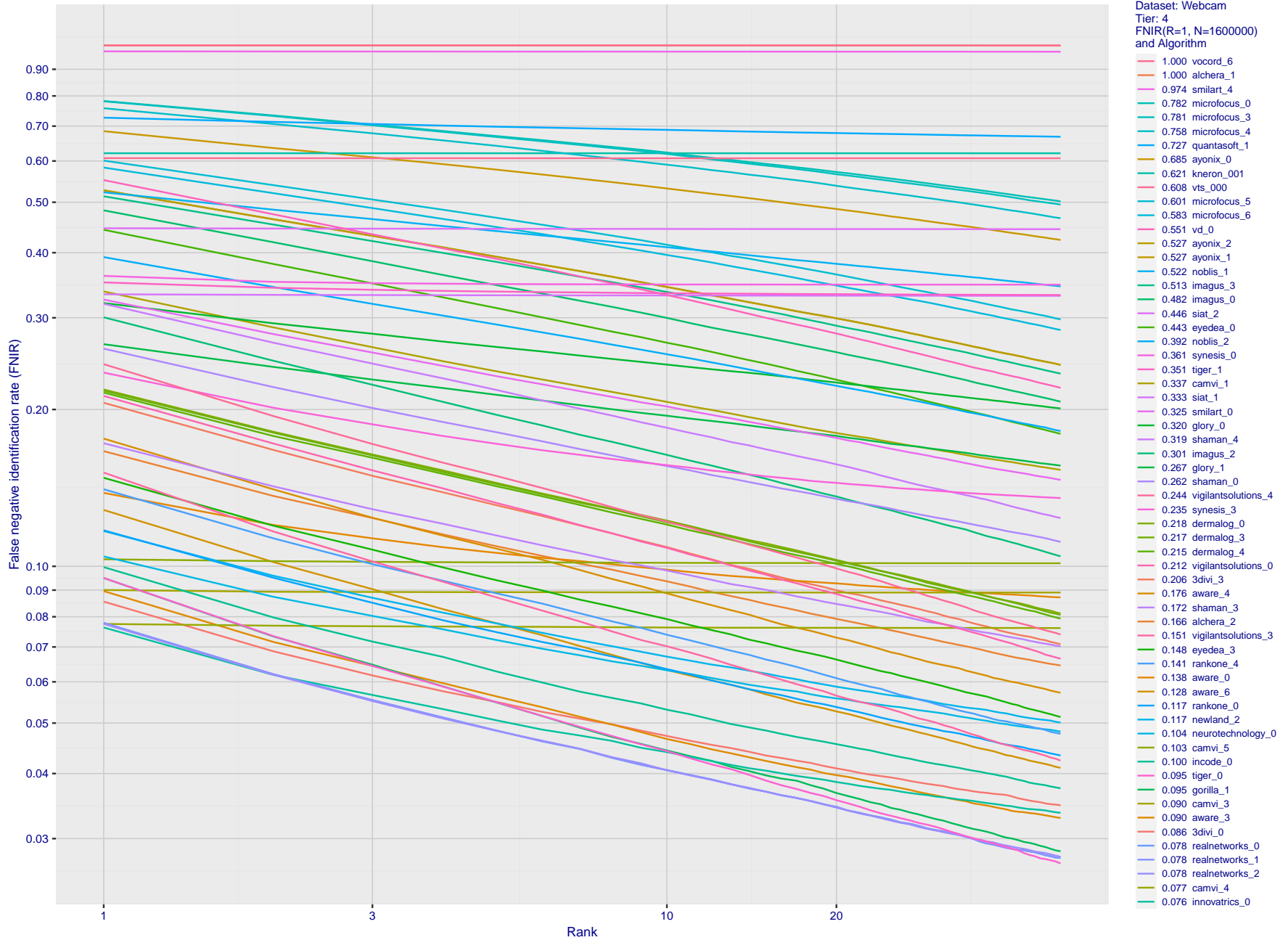


Figure 162: [Webcam Dataset] Identification miss rates vs. rank. The results apply to cross-domain recognition in which webcams are searched against enrolled mugshots. The FNIR values are higher than those for mugshot-mugshot identification due to low image resolution, lighting and less constrained subject pose in webcam images - see Figure 6.

---

2021/10/28 FNIR(N, R, T) = False neg. identification rate N = Num. enrolled subjects T = Threshold T = 0 → Investigation  
13:44:33 FPIR(N, T) = False pos. identification rate R = Num. candidates examined T > 0 → Identification

---

2021/10/28  
 13:44:33  
 FNIR(N, R, T) = False neg. identification rate  
 FPIR(N, T) = False pos. identification rate  
 N = Num. enrolled subjects  
 R = Num. candidates examined  
 T = Threshold  
 T = 0 → Investigation  
 T > 0 → Identification

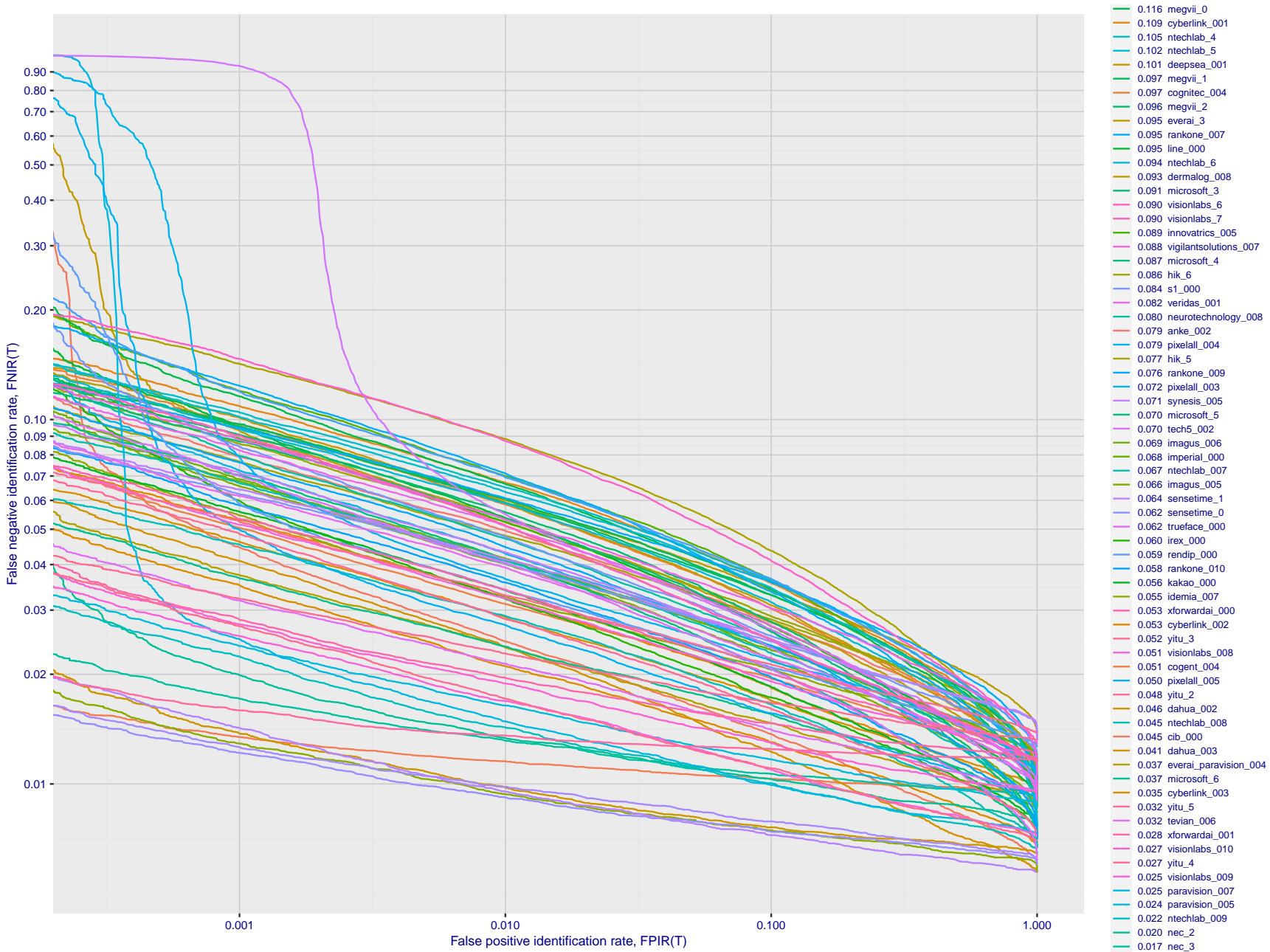


Figure 163: [Webcam Dataset] Identification miss rates vs. false positive rates. The results apply to cross-domain recognition in which webcams are searched against enrolled mugshots. The FNIR values are higher than those for mugshot-mugshot identification due to low image resolution, lighting and less constrained subject pose in webcam images - see Figure 6.

2021/10/28  
13:44:33

FNIR(N, R, T) =  
FPIR(N, T) =

False neg. identification rate  
False pos. identification rate

N = Num. enrolled subjects  
R = Num. candidates examined

T = Threshold

T = 0 → Investigation  
T > 0 → Identification

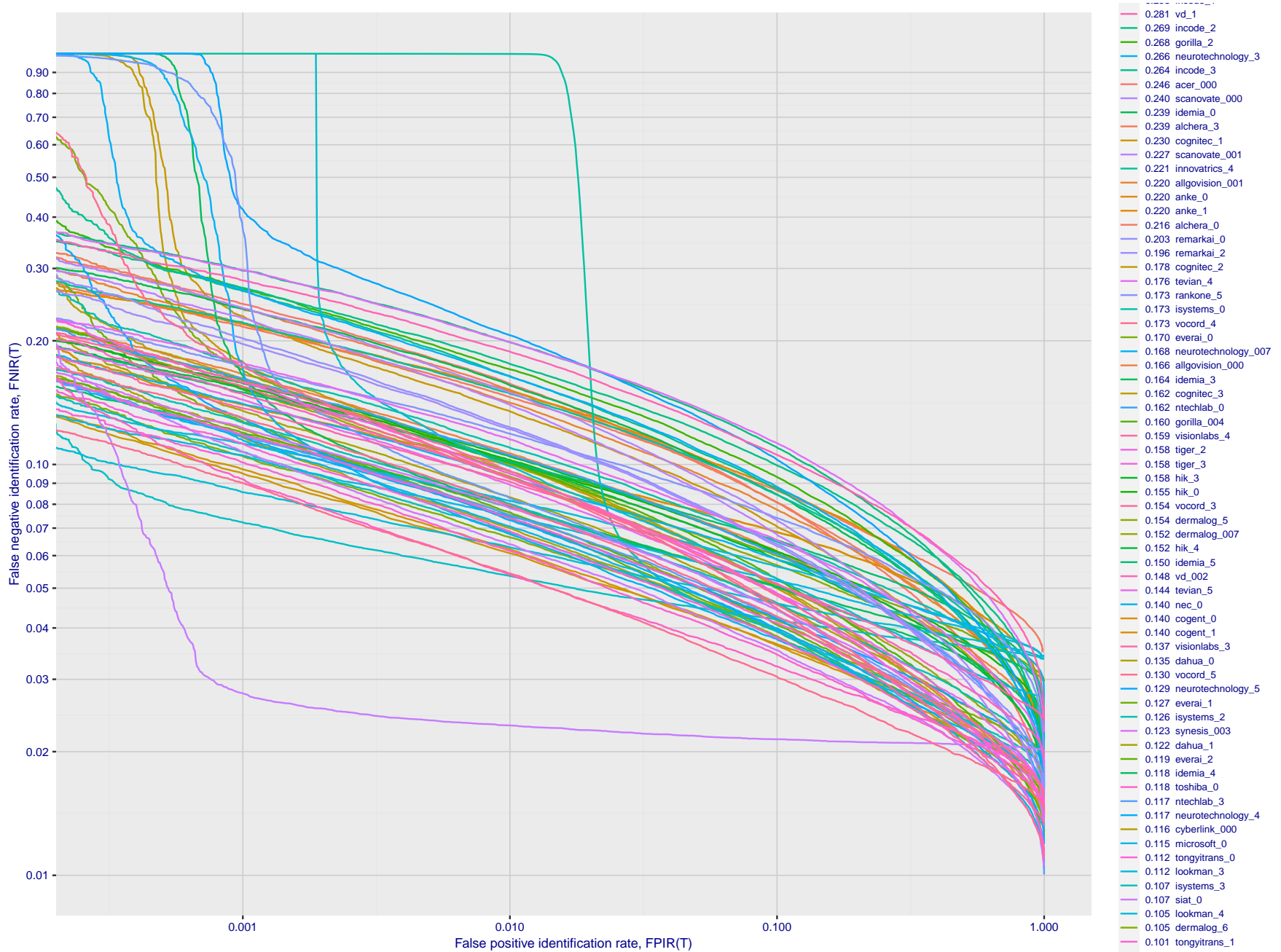


Figure 164: [Webcam Dataset] Identification miss rates vs. false positive rates. The results apply to cross-domain recognition in which webcams are searched against enrolled mugshots. The FNIR values are higher than those for mugshot-mugshot identification due to low image resolution, lighting and less constrained subject pose in webcam images - see Figure 6.

2021/10/28  
 13:44:33  
 FNIR(N, R, T) = False neg. identification rate  
 FPIR(N, T) = False pos. identification rate  
 N = Num. enrolled subjects  
 R = Num. candidates examined  
 T = Threshold  
 T = 0 → Investigation  
 T > 0 → Identification

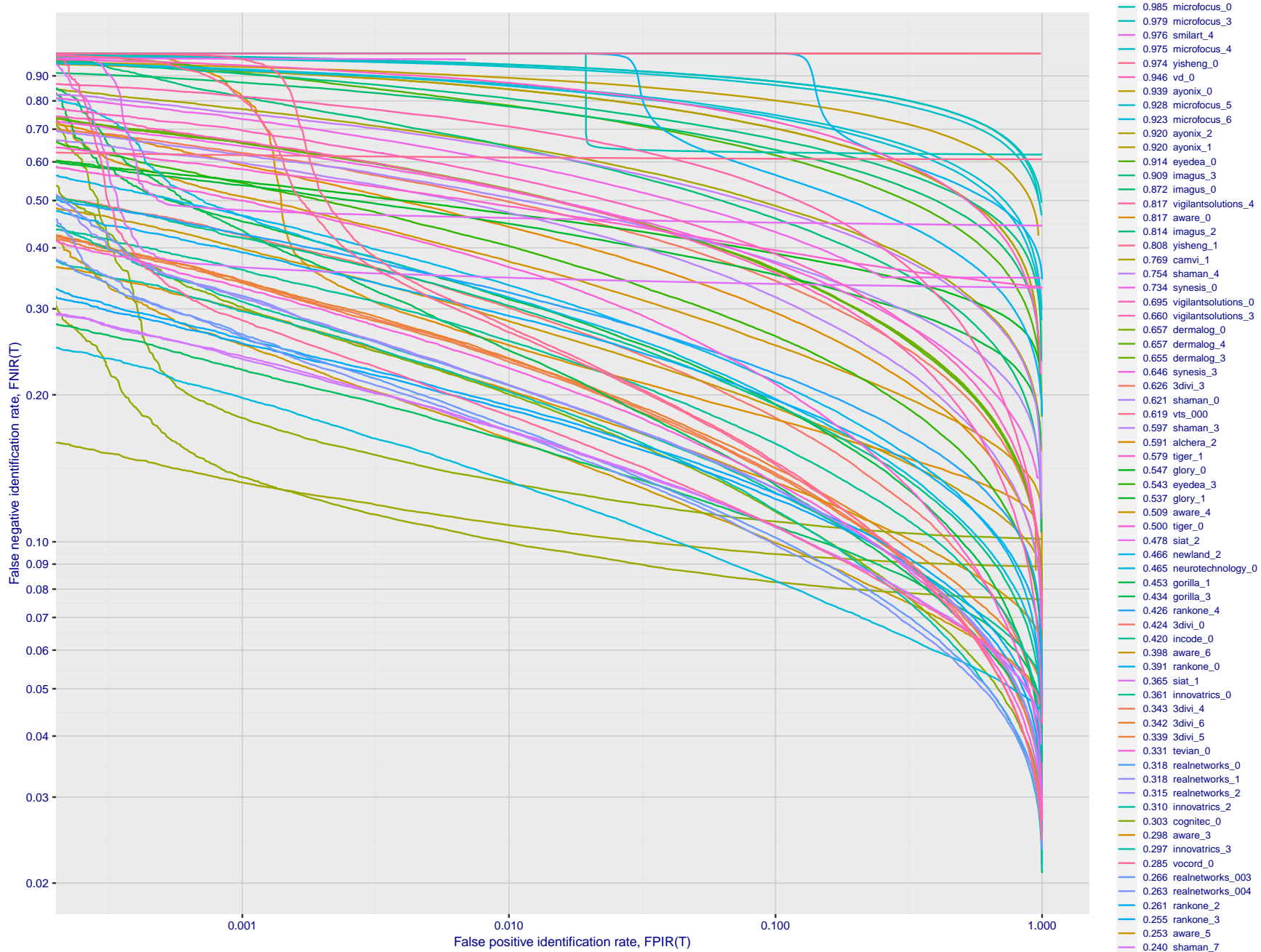


Figure 165: [Webcam Dataset] Identification miss rates vs. false positive rates. The results apply to cross-domain recognition in which webcams are searched against enrolled mugshots. The FNIR values are higher than those for mugshot-mugshot identification due to low image resolution, lighting and less constrained subject pose in webcam images - see Figure 6.

## Appendix E Accuracy for profile-view to frontal recognition

Figures 166 - 168 gives accuracy results for searching 100 000 mated and 100 000 non-mated profile-view images against the same FRVT 2018 frontal enrollment dataset,  $N = 1\,600\,000$ , used in the main mugshot trials. This experiment corresponds to row-13 of Table 1. An example of profile-view image is given in Figure 7.

2021/10/28  
13:44:33

FNIR(N, R, T) =  
FPR(N, T) =

False neg. identification rate  
False pos. identification rate

N = Num. enrolled subjects  
R = Num. candidates examined

T = Threshold

T = 0 → Investigation  
T > 0 → Identification

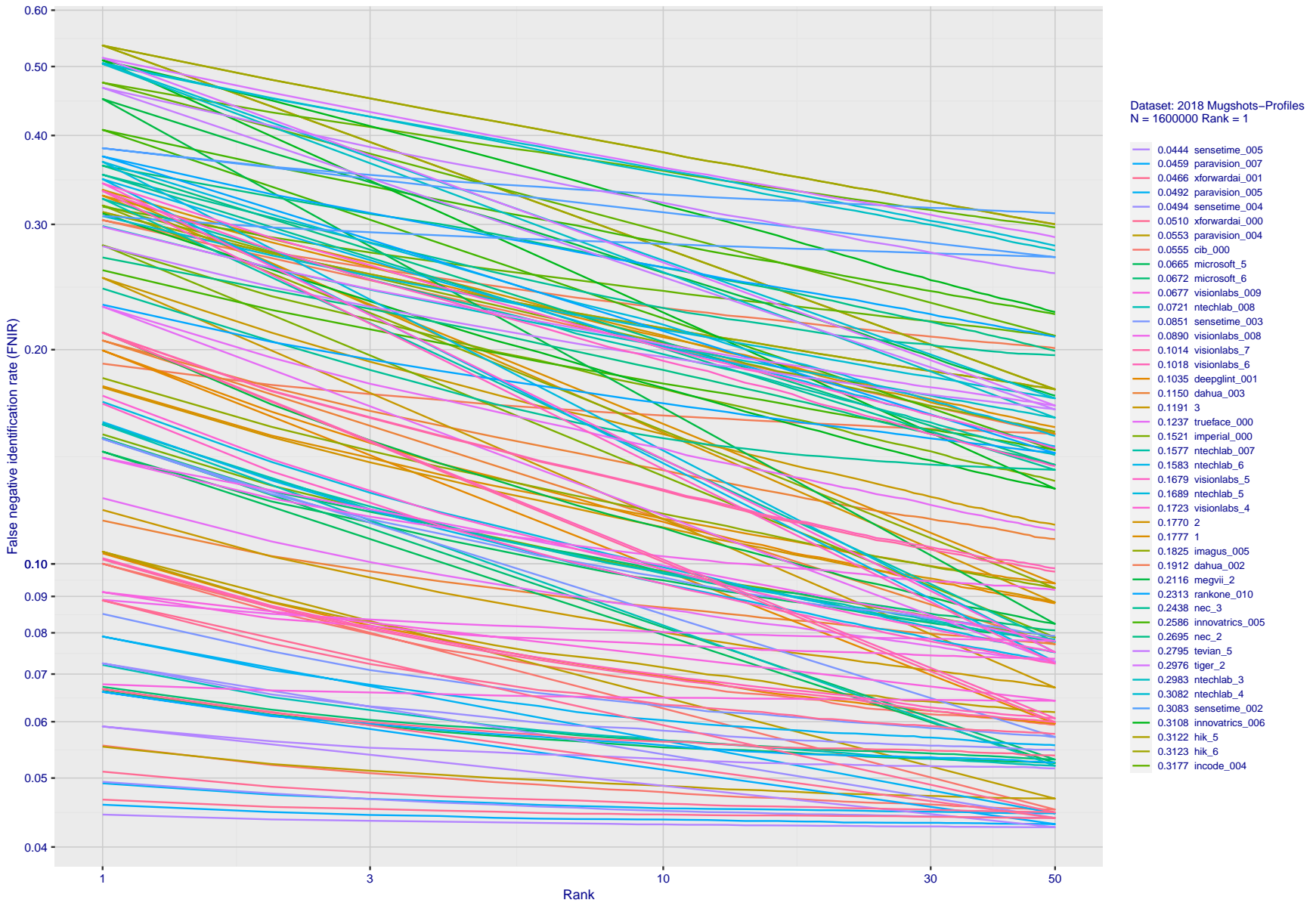


Figure 166: [Mugshot and profile-view dataset] Rank-based accuracy. For some of the more accurate Phase 3 algorithms the figure plots error tradeoff characteristics for frontal and profile-view searches into an enrolled set of  $N = 1\,600\,000$  frontal images. Note that some algorithms fail on profile-view images with  $FNIR \rightarrow 1$  - this evaluation did not ask developers to provide profile-view capability. Some algorithms, on the other hand, give  $FNIR$  approaching that for frontal-view searches using c. 2010 algorithms. The best result is that 91% of profile-view searches yield the correct mate at rank 1, and better than 94% in the top-50 candidates.

2021/10/28  
 13:44:33  
 FNIR(N, R, T) =  
 FPIR(N, T) =  
 False neg. identification rate  
 False pos. identification rate  
 N = Num. enrolled subjects  
 R = Num. candidates examined  
 T = Threshold  
 T = 0 → Investigation  
 T > 0 → Identification

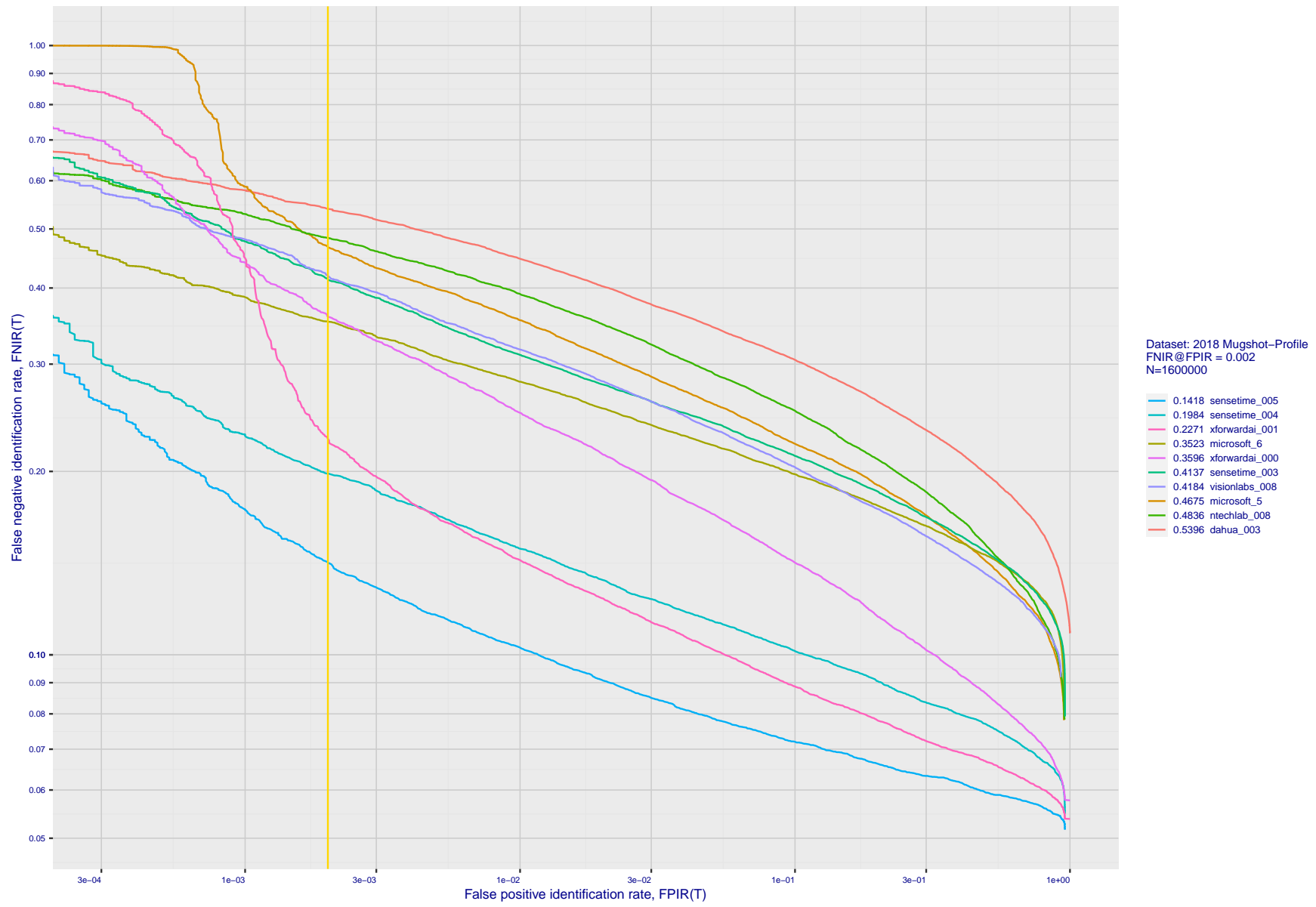


Figure 167: [Mugshot and profile-view dataset] Threshold-based accuracy. For some of the more accurate Phase 3 algorithms the figure plots error tradeoff characteristics for frontal and profile-view searches into an enrolled set of  $N = 1\,600\,000$  frontal images. Note that some algorithms fail on profile-view images with  $FNIR \rightarrow 1$  - this evaluation did not ask developers to provide profile-view capability. Some algorithms, on the other hand, give  $FNIR$  approaching that for frontal-view searches using c. 2010 algorithms.

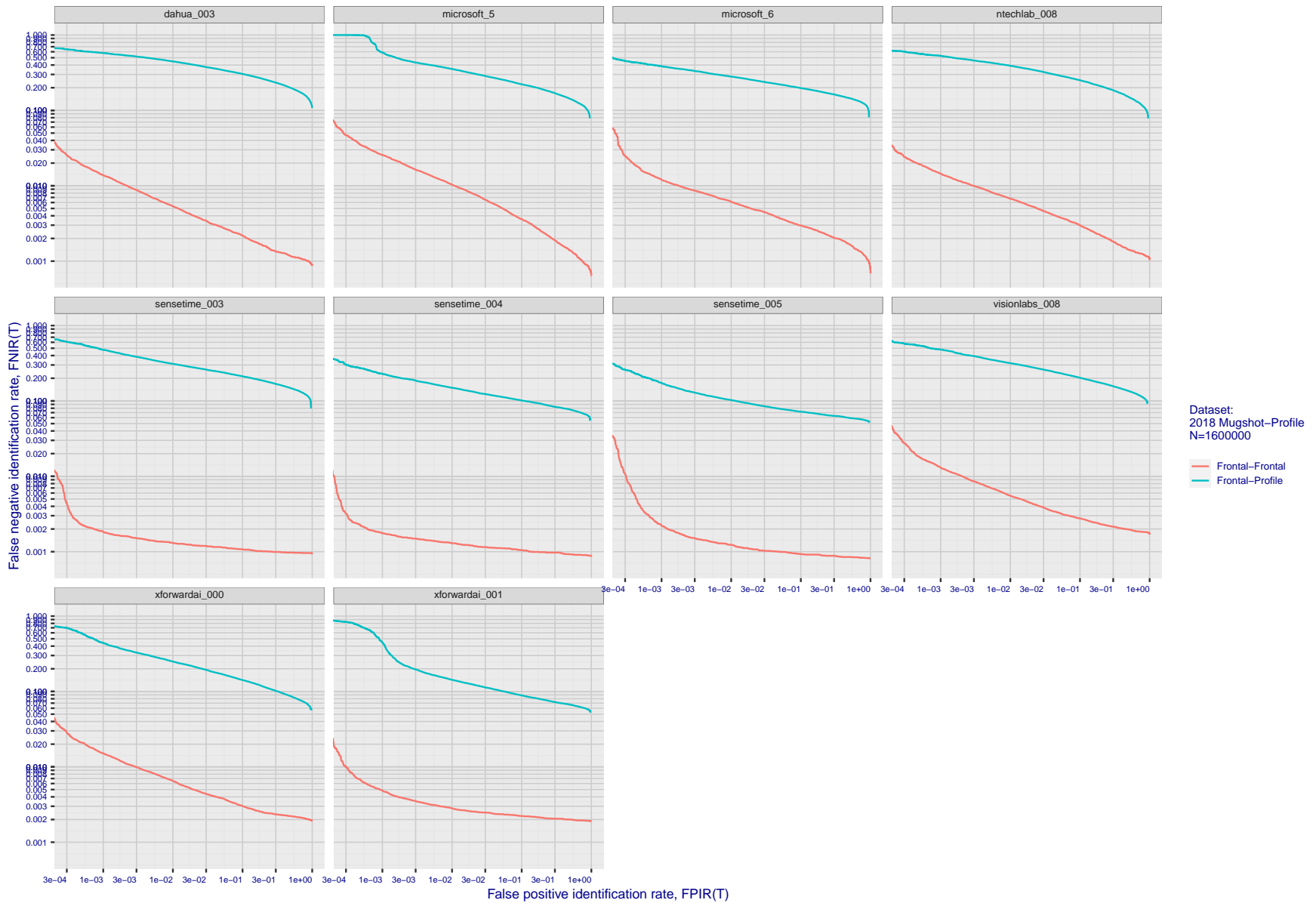


Figure 168: [Mugshot and profile-view dataset] Speed-accuracy tradeoff. For some of the more accurate Phase 3 algorithms the figure plots error tradeoff characteristics for frontal and profile-view searches into an enrolled set of  $N = 1\,600\,000$  frontal images. Some algorithms fail on profile-view images with  $FNIR \rightarrow 1$  - this evaluation did not ask developers to provide profile-view capability. Some algorithms, on the other hand, give  $FNIR$  approaching that for frontal-view searches using c. 2010 algorithms. Blue lines connect points of equal threshold from which it is evident that some algorithms would give markedly higher false positive outcomes if profile-view images were searched in a system configured for frontal searches. This would be a vulnerability in an access control system.

2021/10/28  
13:44:33

FNIR(N, R, T) =  
FPIR(N, T) =

False neg. identification rate  
False pos. identification rate

N = Num. enrolled subjects  
R = Num. candidates examined

T = Threshold

T = 0 → Investigation  
T > 0 → Identification

## Appendix F Search duration

As in and prior tests, this section documents search speeds spanning three orders of magnitude. In applications where search volumes are high enough, this will have implications for hardware requirements especially for large  $N$  or when search duration is appreciably larger than the time it takes to prepare a template from the search image(s). Further, given very large (and growing) operational databases, the scalability of algorithms is important. It has been reported previously [8] that search duration can scale sublinearly with enrolled population size  $N$ . Further there has been considerable recent research on indexing, exact [13] and approximate nearest neighbor search [1,13] and fast-search [14,16].

Figure 169 charts the search duration measurements presented earlier in Tables 2 - 4.

- ▷ Most algorithms scale linearly. For those in that category, there is a wide range in speed with search durations ranging from 82 milliseconds for a 12 million gallery (for NEC-3) to more than 40 seconds (for Yitu-3, Toshiba-2) and even higher for less accurate algorithms.
- ▷ Some developers (Camvi, Dermalog, EverAI, Innvovetrics, and Visionlabs) provide algorithms whose template search durations grow approximately logarithmically i.e.  $T(N) \sim a \log N$  with the constant  $a$  varying between implementations. In the figure this model is fit using the point  $T(1) = 0$ , and  $T(640\,000)$ . This very sublinear behaviour affords extremely fast search times in very large galleries. One caveat for the sublinear algorithms is that their fast-search data structures can require considerable computation time - on the order of hours - for  $N$  in the millions, and this scales mildly super-linearly, i.e.  $O(N^b)$ ,  $b > 1$ . There are exceptions: the Camvi algorithms take minutes; and Innvovetrics' scale sublinearly.

---

2021/10/28	FNIR(N, R, T) =	False neg. identification rate	N = Num. enrolled subjects	T = Threshold	T = 0 → Investigation
13:44:33	FPIR(N, T) =	False pos. identification rate	R = Num. candidates examined		T > 0 → Identification

2021/10/28  
 13:44:33  
 FN(R,N,R,T) =  
 FP(R,N,T) =  
 False neg. identification rate  
 False pos. identification rate  
 N = Num. enrolled subjects  
 R = Num. candidates examined  
 T = Threshold  
 T = 0 → Investigation  
 T > 0 → Identification

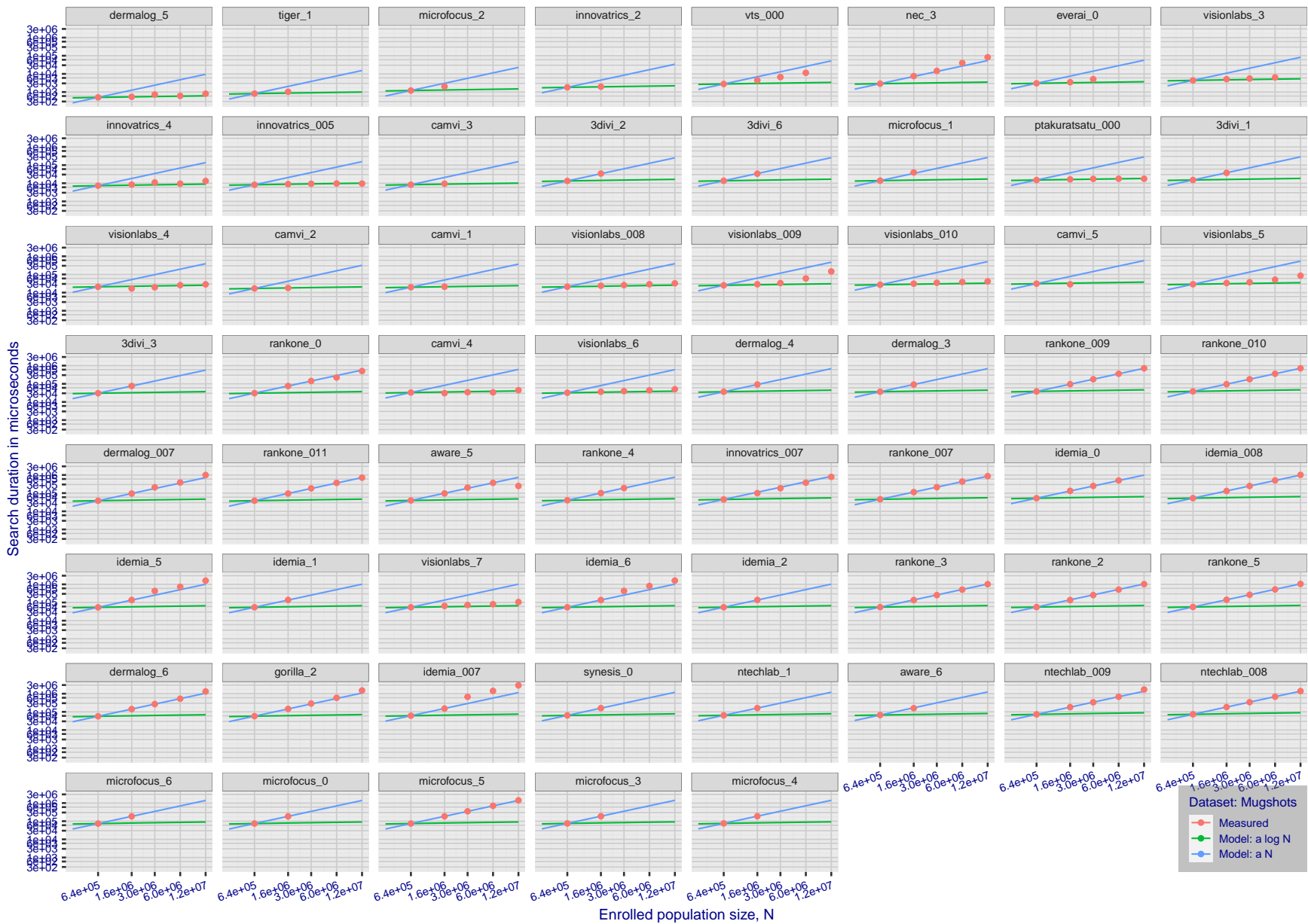


Figure 169: [Mugshot Dataset] Search duration vs. enrolled population size. In red are the actual point durations measured on a single c. 2016 core. The blue shows linear growth from  $N = 640\,000$ . The green line shows logarithmic growth from that point to  $N = 1\,600\,000$ . Note the sublinear growth from algorithms from Camvi, Dermalog, EverAI, Innovatrics, and Visionlabs. The tiger\_1 algorithm is also sublinear, but inaccurate and inoperable at  $N \geq 3\,000\,000$ . This capability sometimes comes at the additional expense of converting a linear gallery data structure into whatever fast-search data structure is used. Note that search times are sometimes dominated by the template generation times shown in Table 21.

2021/10/28  
13:44:33

FN(R,N,R,T) =  
FP(R,N,T) =

False neg. identification rate  
False pos. identification rate

N = Num. enrolled subjects  
R = Num. candidates examined

T = Threshold

T = 0 → Investigation  
T > 0 → Identification

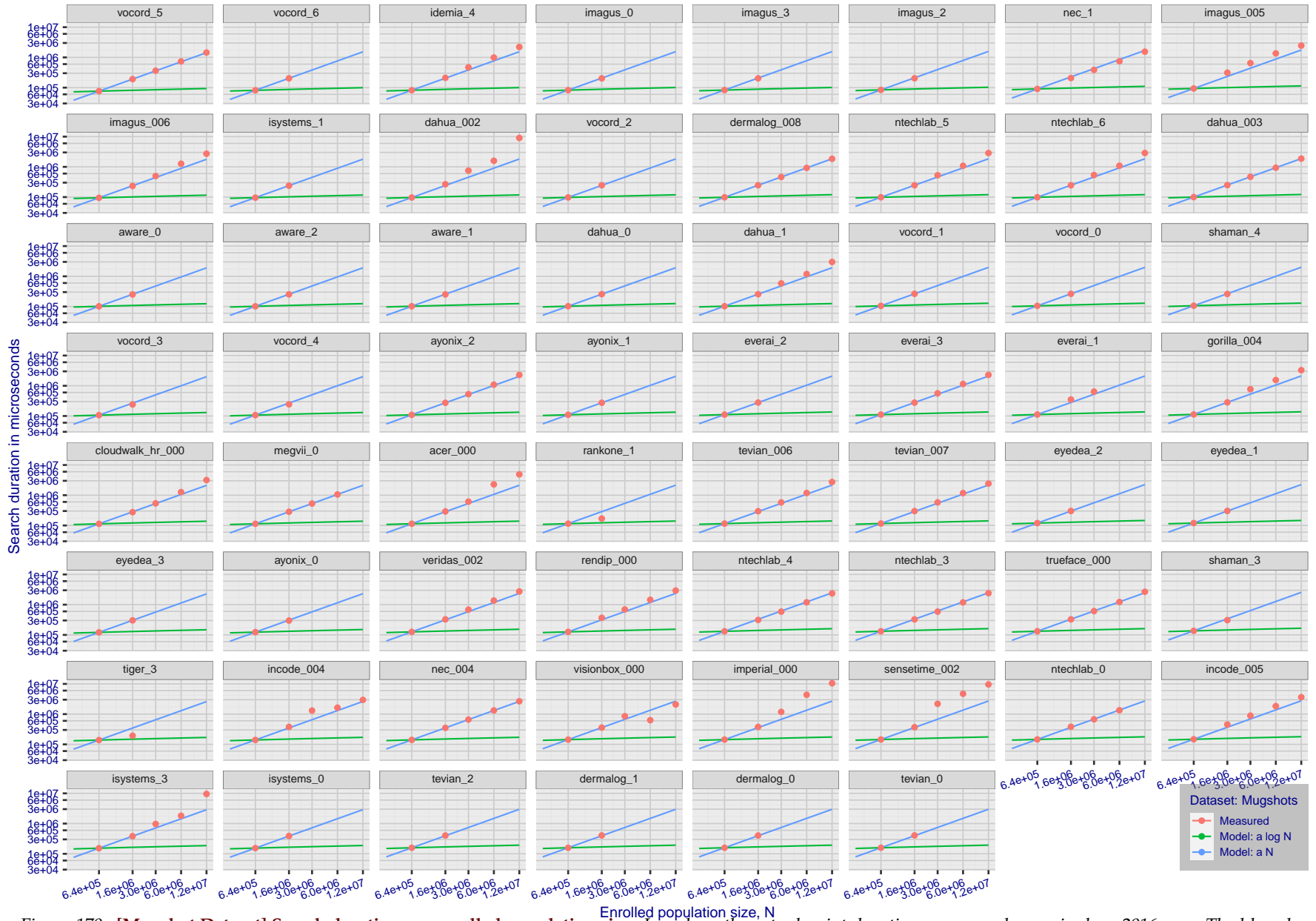


Figure 170: [Mugshot Dataset] Search duration vs. enrolled population size. In red are the actual point durations measured on a single c. 2016 core. The blue shows linear growth from  $N = 640\,000$ . The green line shows logarithmic growth from that point to  $N = 1\,600\,000$ . Note the sublinear growth from algorithms from Camvi, Dermalog, EverAI, Innovatrics, and Visionlabs. The tiger.1 algorithm is also sublinear, but inaccurate and inoperable at  $N \geq 3\,000\,000$ . This capability sometimes comes at the additional expense of converting a linear gallery data structure into whatever fast-search data structure is used. Note that search times are sometimes dominated by the template generation times shown in Table 21.

2021/10/28  
13:44:33

FN(R,N,R,T) =  
FP(R,N,T) =

False neg. identification rate  
False pos. identification rate

N = Num. enrolled subjects  
R = Num. candidates examined

T = Threshold

T = 0 → Investigation  
T > 0 → Identification

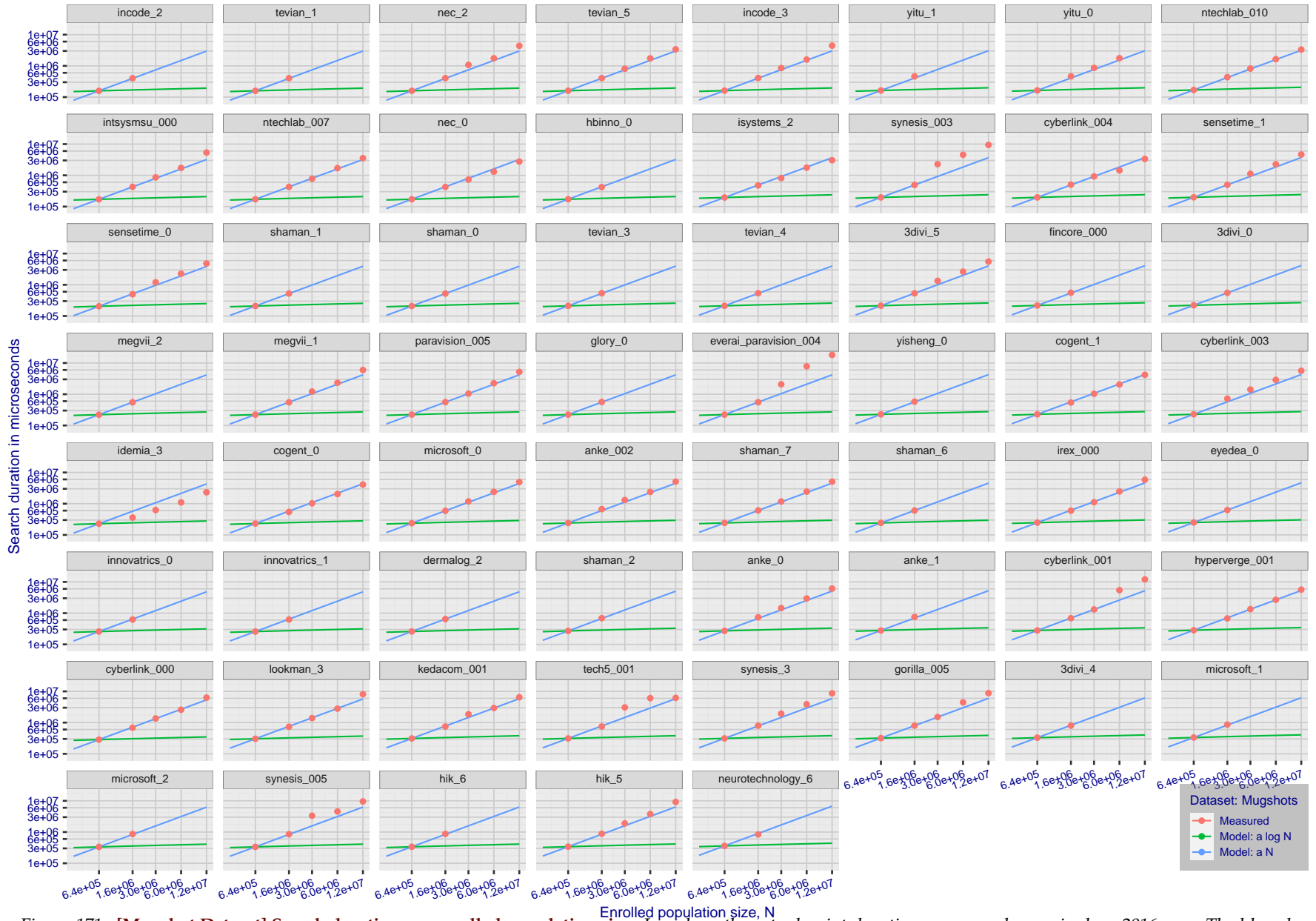


Figure 171: [Mugshot Dataset] Search duration vs. enrolled population size. In red are the actual point durations measured on a single c. 2016 core. The blue shows linear growth from  $N = 640\,000$ . The green line shows logarithmic growth from that point to  $N = 1\,600\,000$ . Note the sublinear growth from algorithms from Camvi, Dermalog, EverAI, Innovatrics, and Visionlabs. The tiger.1 algorithm is also sublinear, but inaccurate and inoperable at  $N \geq 3\,000\,000$ . This capability sometimes comes at the additional expense of converting a linear gallery data structure into whatever fast-search data structure is used. Note that search times are sometimes dominated by the template generation times shown in Table 21.

2021/10/28  
13:44:33

FNIR(N, R, T) =  
FP(R, T) =

False neg. identification rate  
False pos. identification rate

N = Num. enrolled subjects  
R = Num. candidates examined

T = Threshold

T = 0 → Investigation  
T > 0 → Identification

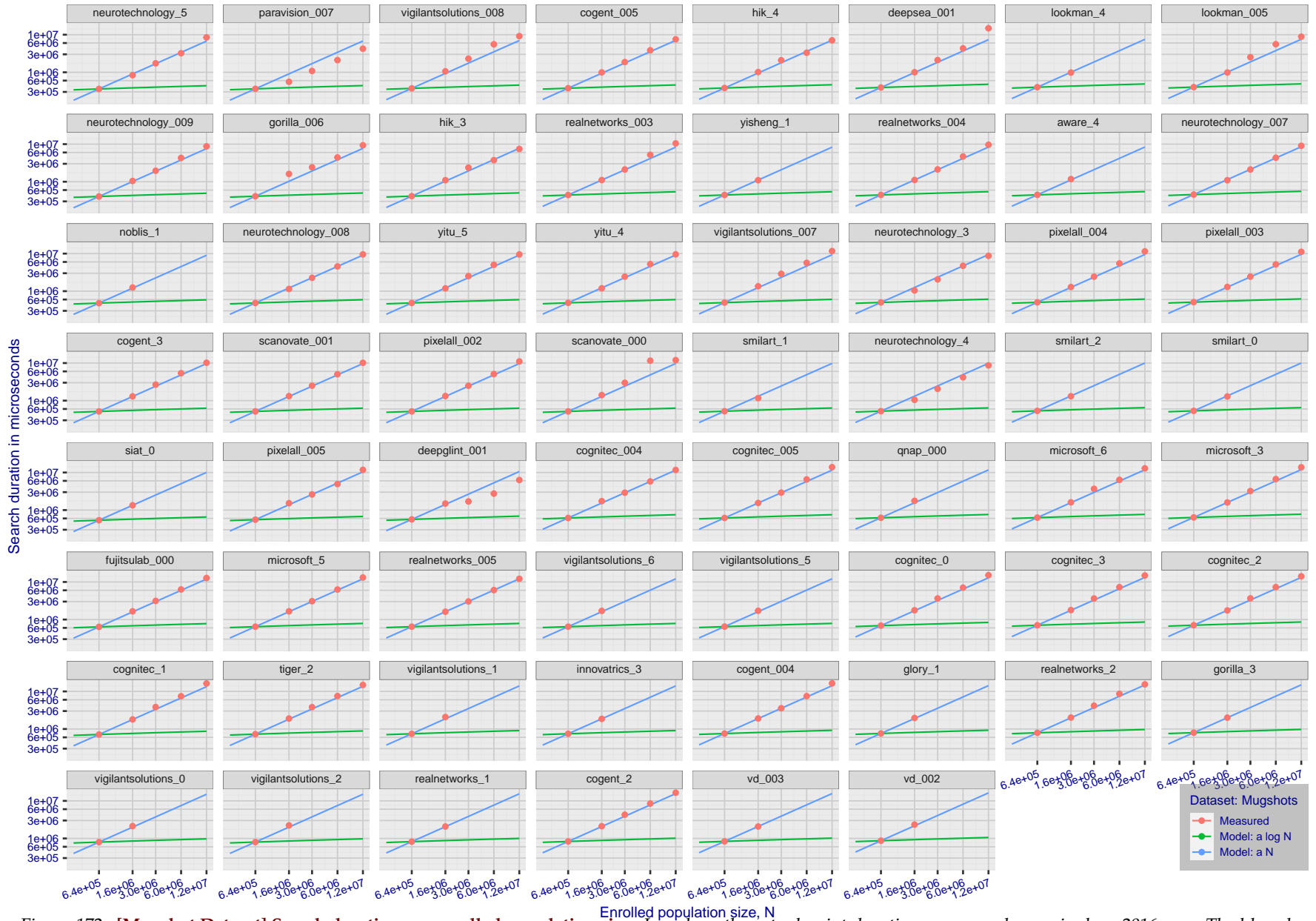


Figure 172: [Mugshot Dataset] Search duration vs. enrolled population size. In red are the actual point durations measured on a single c. 2016 core. The blue shows linear growth from  $N = 640\,000$ . The green line shows logarithmic growth from that point to  $N = 1\,600\,000$ . Note the sublinear growth from algorithms from Camvi, Dermalog, EverAI, Innovatrics, and Visionlabs. The tiger.1 algorithm is also sublinear, but inaccurate and inoperable at  $N \geq 3\,000\,000$ . This capability sometimes comes at the additional expense of converting a linear gallery data structure into whatever fast-search data structure is used. Note that search times are sometimes dominated by the template generation times shown in Table 21.

2021/10/28  
13:44:33

FNIR(N, R, T) =  
FP(R, T) =

False neg. identification rate  
False pos. identification rate

N = Num. enrolled subjects  
R = Num. candidates examined

T = Threshold

T = 0 → Investigation  
T > 0 → Identification

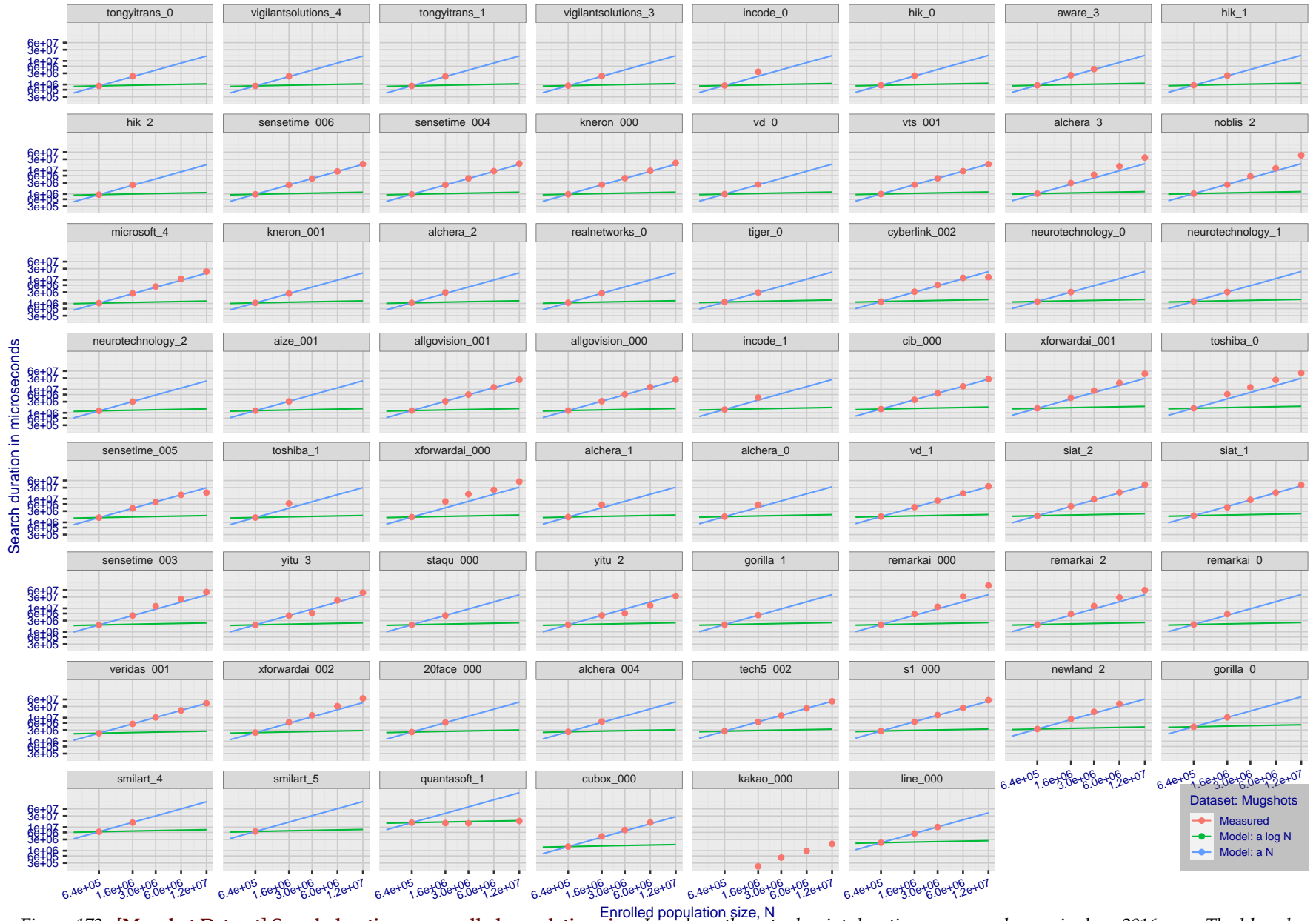


Figure 173: [Mugshot Dataset] Search duration vs. enrolled population size. In red are the actual point durations measured on a single c. 2016 core. The blue shows linear growth from  $N = 640\,000$ . The green line shows logarithmic growth from that point to  $N = 1\,600\,000$ . Note the sublinear growth from algorithms from Camvi, Dermalog, EverAI, Innovatrics, and Visionlabs. The tiger\_1 algorithm is also sublinear, but inaccurate and inoperable at  $N \geq 3\,000\,000$ . This capability sometimes comes at the additional expense of converting a linear gallery data structure into whatever fast-search data structure is used. Note that search times are sometimes dominated by the template generation times shown in Table 21.

## Appendix G Gallery Insertion Timing

This publication is available free of charge from: <https://doi.org/10.6028/NIST.IR.8271>

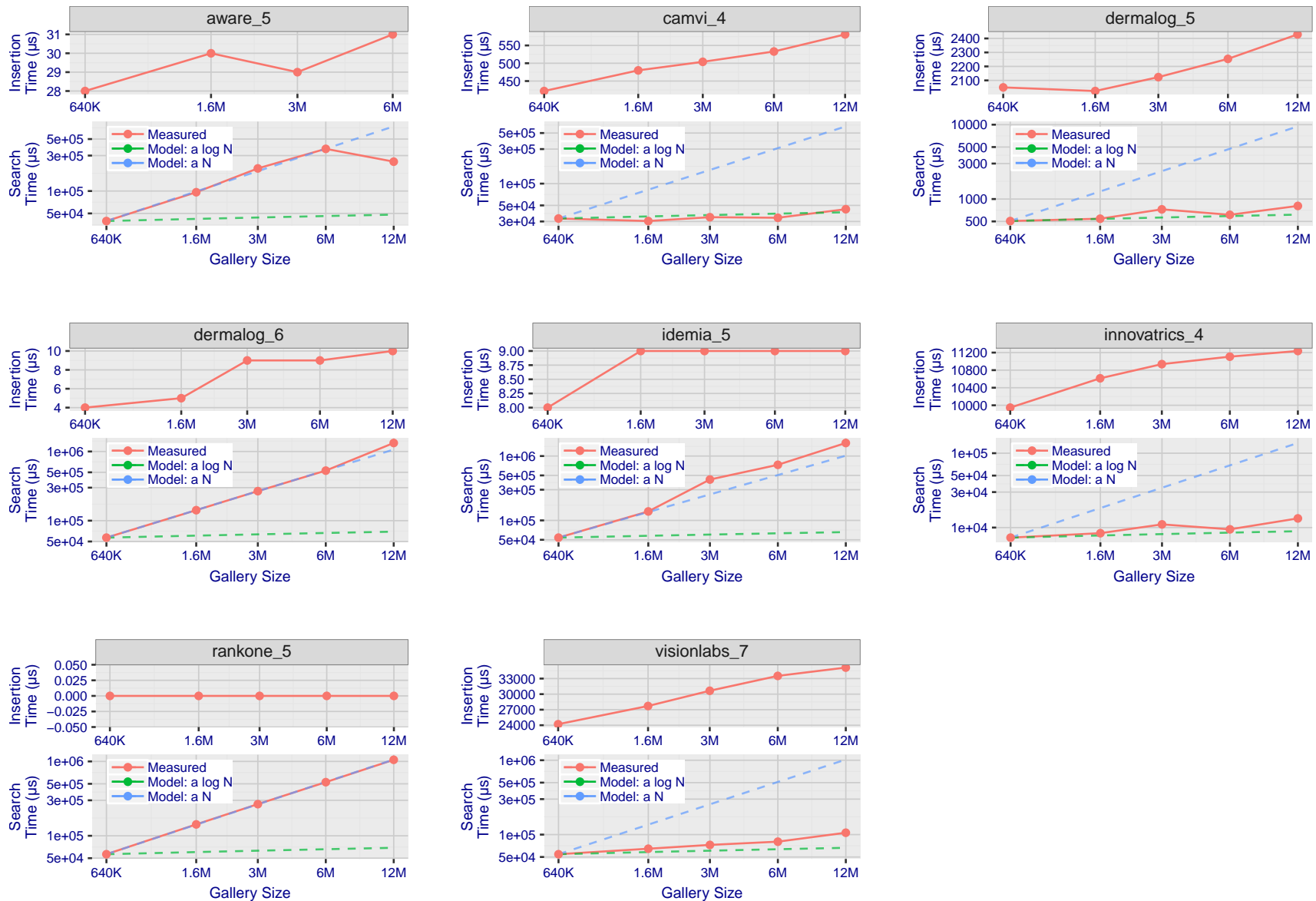


Figure 174: [Mugshot Dataset] Gallery insertion duration vs. enrolled population size. This chart plots the time it takes to insert a single template into a finalized gallery, illustrated over increasing gallery sizes. For reference, search times on finalized galleries of corresponding sizes are plotted right underneath. Gallery insertion time plots were generated on algorithms that 1) successfully implemented gallery insertion with no errors and 2) that were run on galleries with  $N$  up to 12 000 000. Generally, only the more accurate algorithms were run on galleries with  $N$  up to 12 000 000.

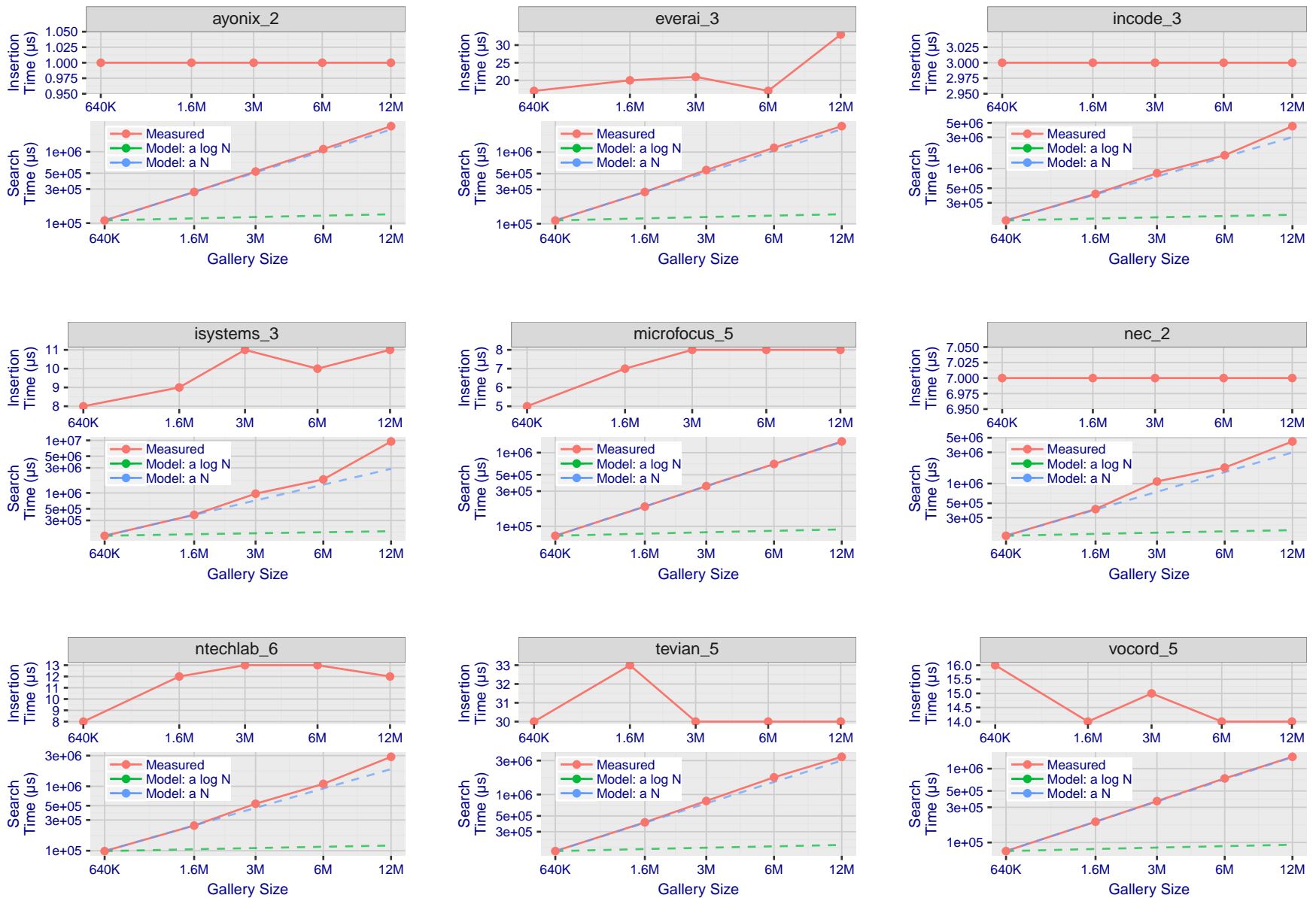


Figure 175: [Mugshot Dataset] Gallery insertion duration vs. enrolled population size. This chart plots the time it takes to insert a single template into a finalized gallery, illustrated over increasing gallery sizes. For reference, search times on finalized galleries of corresponding sizes are plotted right underneath. Gallery insertion time plots were generated on algorithms that 1) successfully implemented gallery insertion with no errors and 2) that were run on galleries with  $N$  up to 12 000 000. Generally, only the more accurate algorithms were run on galleries with  $N$  up to 12 000 000.

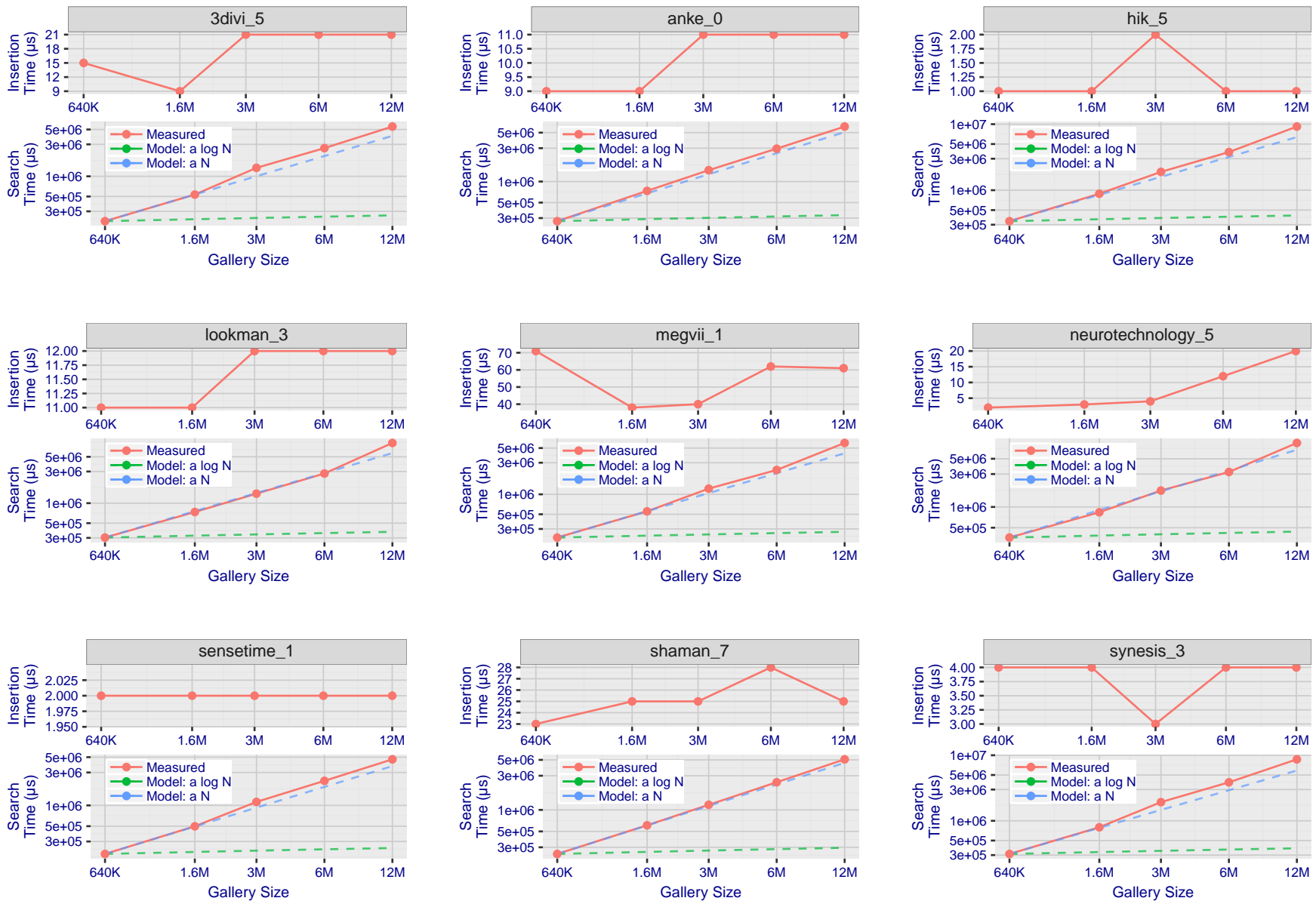


Figure 176: [Mugshot Dataset] Gallery insertion duration vs. enrolled population size. This chart plots the time it takes to insert a single template into a finalized gallery, illustrated over increasing gallery sizes. For reference, search times on finalized galleries of corresponding sizes are plotted right underneath. Gallery insertion time plots were generated on algorithms that 1) successfully implemented gallery insertion with no errors and 2) that were run on galleries with  $N$  up to 12 000 000. Generally, only the more accurate algorithms were run on galleries with  $N$  up to 12 000 000.

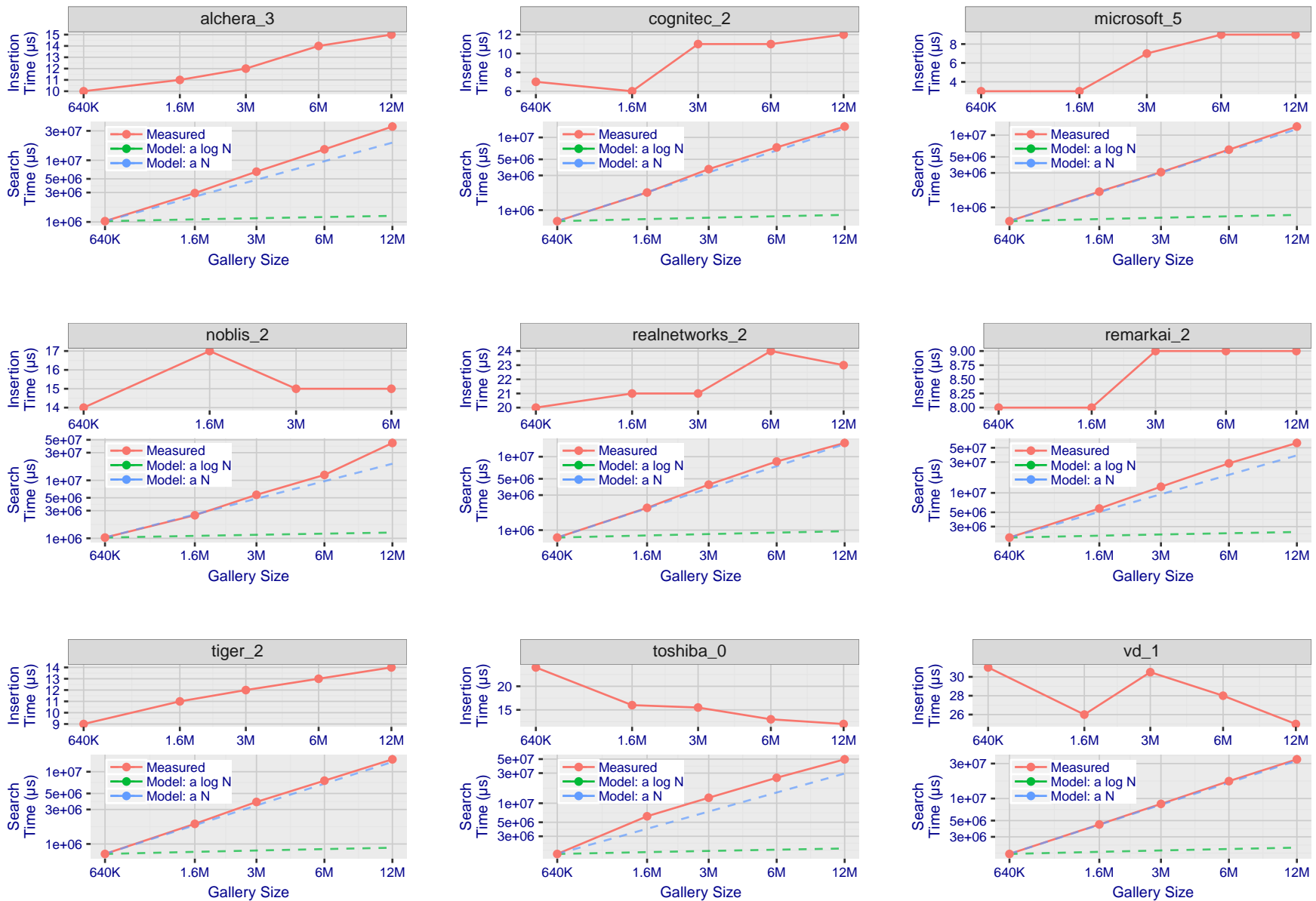


Figure 177: [Mugshot Dataset] Gallery insertion duration vs. enrolled population size. This chart plots the time it takes to insert a single template into a finalized gallery, illustrated over increasing gallery sizes. For reference, search times on finalized galleries of corresponding sizes are plotted right underneath. Gallery insertion time plots were generated on algorithms that 1) successfully implemented gallery insertion with no errors and 2) that were run on galleries with  $N$  up to 12 000 000. Generally, only the more accurate algorithms were run on galleries with  $N$  up to 12 000 000.

## References

- [1] Artem Babenko and Victor Lempitsky. Efficient indexing of billion-scale datasets of deep descriptors. In *The IEEE Conference on Computer Vision and Pattern Recognition (CVPR)*, June 2016.
- [2] L. Best-Rowden and A. K. Jain. Longitudinal study of automatic face recognition. *IEEE Transactions on Pattern Analysis and Machine Intelligence*, 40(1):148–162, Jan 2018.
- [3] Blumstein, Cohen, Roth, and Visser, editors. *Random parameter stochastic models of criminal careers*. National Academy of Sciences Press, 1986.
- [4] Thomas P. Bonczar and Lauren E. Glaze. Probation and parole in the united statesm 2007, statistical tables. Technical report, Bureau of Justice Statistics, December 2008.
- [5] White D., Kemp R. I., Jenkins R., Matheson M, and Burton A. M. Passport officers’ errors in face matching. *PLoS ONE*, 9(8), 2014. e103510. doi:10.1371/journal.pone.0103510.
- [6] P. Grother, G. W. Quinn, and P. J. Phillips. Evaluation of 2d still-image face recognition algorithms. NIST Interagency Report 7709, National Institute of Standards and Technology, 8 2010. <http://face.nist.gov/mbeas/MBE2010FRVT2010>.
- [7] P. J. Grother, R. J. Micheals, and P. J. Phillips. Performance metrics for the frvt 2002 evaluation. In *Proceedings of Audio and Video Based Person Authentication Conference (AVBPA)*, June 2003.
- [8] Patrick Grother and Mei Ngan. Interagency report 8009, performance of face identification algorithms. *Face Recognition Vendor Test (FRVT)*, May 2014.
- [9] Patrick Grother, George Quinn, and Mei Ngan. Face in video evaluation (five) face recognition of non-cooperative subjects. Interagency Report 8173, National Institute of Standards and Technology, March 2017. <https://doi.org/10.6028/NIST.IR.8173>.
- [10] Patrick Grother, George W. Quinn, and Mei Ngan. Face recognition vendor test - still face image and video concept, evaluation plan and api. Technical report, National Institute of Standards and Technology, 7 2013. [http://biometrics.nist.gov/cs\\_links/face/frvt/frvt2012/NIST\\_FRVT2012\\_api\\_Aug15.pdf](http://biometrics.nist.gov/cs_links/face/frvt/frvt2012/NIST_FRVT2012_api_Aug15.pdf).
- [11] K. He, X. Zhang, S. Ren, and J. Sun. Deep residual learning for image recognition. In *2016 IEEE Conference on Computer Vision and Pattern Recognition (CVPR)*, pages 770–778, June 2016.
- [12] Gary B. Huang, Manu Ramesh, Tamara Berg, and Erik Learned-Miller. Labeled faces in the wild: A database for studying face recognition in unconstrained environments. Technical Report 07-49, University of Massachusetts, Amherst, October 2007.
- [13] Masato Ishii, Hitoshi Imaoka, and Atsushi Sato. Fast k-nearest neighbor search for face identification using bounds of residual score. In *2017 12th IEEE International Conference on Automatic Face & Gesture Recognition (FG 2017)*, pages 194–199, Los Alamitos, CA, USA, May 2017. IEEE Computer Society.
- [14] Jeff Johnson, Matthijs Douze, and Hervé Jégou. Billion-scale similarity search with gpus. *CoRR*, abs/1702.08734, 2017.

- [15] Ira Kemelmacher-Shlizerman, Steven M. Seitz, Daniel Miller, and Evan Brossard. The megaface benchmark: 1 million faces for recognition at scale. *CoRR*, abs/1512.00596, 2015.
- [16] Yury A. Malkov and D. A. Yashunin. Efficient and robust approximate nearest neighbor search using hierarchical navigable small world graphs. *CoRR*, abs/1603.09320, 2016.
- [17] Joyce A. Martin, Brady E. Hamilton, Michelle J.K. Osterman, Anne K. Driscoll, , and Patrick Drake. National vital statistics reports. Technical Report 8, Centers for Disease Control and Prevention, National Center for Health Statistics, National Vital Statistics System, Division of Vital Statistics, November 2018.
- [18] O. M. Parkhi, A. Vedaldi, and A. Zisserman. Deep face recognition. In *British Machine Vision Conference*, 2015.
- [19] P. Jonathon Phillips, Amy N. Yates, Ying Hu, Carina A. Hahn, Eilidh Noyes, Kelsey Jackson, Jacqueline G. Cavazos, Géraldine Jeckeln, Rajeev Ranjan, Swami Sankaranarayanan, Jun-Cheng Chen, Carlos D. Castillo, Rama Chellappa, David White, and Alice J. O’Toole. Face recognition accuracy of forensic examiners, superrecognizers, and face recognition algorithms. *Proceedings of the National Academy of Sciences*, 115(24):6171–6176, 2018.
- [20] Florian Schroff, Dmitry Kalenichenko, and James Philbin. Facenet: A unified embedding for face recognition and clustering. *CoRR*, abs/1503.03832, 2015.
- [21] Jeroen Smits and Christiaan Monden. Twinning across the developing world. *PLOS ONE*, 6(9):1–5, 09 2011.
- [22] Yaniv Taigman, Ming Yang, Marc’Aurelio Ranzato, and Lior Wolf. Deepface: Closing the gap to human-level performance in face verification. In *Proceedings of the 2014 IEEE Conference on Computer Vision and Pattern Recognition, CVPR ’14*, pages 1701–1708, Washington, DC, USA, 2014. IEEE Computer Society.
- [23] A. Towler, R. I. Kemp, and D White. *Unfamiliar face matching systems in applied settings*. Nova Science, 2017.
- [24] Working Group 3. Ed. M. Werner. *ISO/IEC 19794-5 Information Technology - Biometric Data Interchange Formats - Part 5: Face image data*. JTC1 :: SC37, 2 edition, 2011. <http://webstore.ansi.org>.
- [25] David White, James D. Dunn, Alexandra C. Schmid, and Richard I. Kemp. Error rates in users of automatic face recognition software. *PLoS ONE*, 10:1–14, October 2015.
- [26] Bradford Wing and R. Michael McCabe. Special publication 500-271: American national standard for information systems data format for the interchange of fingerprint, facial, and other biometric information part 1. Technical report, NIST, September 2015. ANSI/NIST ITL 1-2015.
- [27] Andreas Wolf. Portrait quality - (reference facial images for mrtd). Technical report, ICAO, April 2018.
- [28] D. Yadav, N. Kohli, P. Pandey, R. Singh, M. Vatsa, and A. Noore. Effect of illicit drug abuse on face recognition. In *2016 IEEE Winter Conference on Applications of Computer Vision (WACV)*, pages 1–7, Los Alamitos, CA, USA, mar 2016. IEEE Computer Society.